Water Quality Study

for the

Pelton Round Butte Project and the Lower Deschutes River:

Monitoring & Modeling

Report prepared for Portland General Electric &

The Confederated Tribes of the Warm Springs Reservation of Oregon

by Joseph Eilers and Kellie Vache

MaxDepth Aquatics, Inc.

Bend, Oregon

March 2021

CONTENTS

Executive Summary i

1 Introduction 1

1.1 Objectives of the Water Quality Study 2

1.2 Water Quality and Regulatory Context 3

2 Study Area 6

2.1 The Deschutes River Basin 6

2.1.1 Geology 8

2.1.2 Land Cover 14

2.2 Project Operations 16

2.3 Hydrology and Climate Overview 19

2.3.1 Meteorological Data 19

2.3.2 Water Flow Data 21

3 Water Quality Monitoring Methods 28

3.1 Fixed Site Sampling 28

3.2 72-Hour Monitoring 33

3.3 ReReg Dam Tailrace Monitoring 33

3.4 River Float 34

3.5 Impoundments and Tributaries to Impoundments 34

3.6 Data Review 39

3.7 Data Analysis 48

4 Reservoir Water Quality Data Results 49

4.1 Tributaries to Lake Billy Chinook 49

4.1.1 Hydrology 49

4.1.2 Temperature 52

4.1.3 Ambient Water Quality Monitoring Data 54

4.1.4 2015–2017 Water Quality Data 57

4.1.5 Periphyton 67
4.2 Project Impoundments 70
4.2.1 Lake Billy Chinook 70
4.2.1.1 Temperature 70
4.2.1.2 Conductivity 77
4.2.1.3 Dissolved Oxygen 79
4.2.1.4 pH 81
4.2.1.5 Transparency and Light Attenuation 82
4.2.1.6 Turbidity 84
4.2.1.7 Total Phosphorus 86
4.2.1.8 Phosphate 88
4.2.1.9 Total Nitrogen 90
4.2.1.10 Nitrate 92
4.2.1.11 Ammonia 94
4.2.1.12 Total Nitrogen:Total Phosphorus Ratio 96
4.2.1.13 Nitrate:Phosphate Ratio 98
4.2.1.14 Chloride 101
4.2.1.15 Total Chlorophyll 103
4.2.1.16 Cyanobacterial Pigment 105
4.2.1.17 Phytoplankton Community Composition 107
4.2.1.18 Zooplankton 113
4.2.2 Lake Simtustus 114
4.2.2.1 Temperature 115
4.2.2.2 Conductivity 120
4.2.2.3 Dissolved Oxygen 122
4.2.2.4 pH 124
4.2.2.5 Transparency and Light Attenuation 125
4.2.2.6 Turbidity 127
4.2.2.7 Total Phosphorus 128

4.2.2.8 Phosphate 129
4.2.2.9 Total Nitrogen 130
4.2.2.10 Nitrate 131
4.2.2.11 Ammonia 133
4.2.2.12 Total Nitrogen:Total Phosphorus Ratio 134
4.2.2.13 Nitrate:Phosphate Ratio 135
4.2.2.14 Chloride 137
4.2.2.15 Total Chlorophyll 138
4.2.2.16 Cyanobacteria 140
4.2.2.17 Phytoplankton Community Composition 141
4.2.2.18 Zooplankton 146
4.2.3 Transitions and Transformations between Impoundments 147
4.3 Comparison with Other Impoundments 154
5 Water Quality Changes in the Reservoirs 156
5.1 Lake Billy Chinook 157
5.1.1 Temperature Regime 157
5.1.2 Conductivity 169
5.1.3 pH 171
5.1.4 Dissolved Oxygen 172
5.1.5 Transparency 174
5.1.6 Nutrients 175
5.1.7 Chlorophyll a 177
5.1.8 Phytoplankton Community Composition 179
5.1.9 Zooplankton 181
5.2 Lake Simtustus 186
5.2.1 Temperature Regime 186
5.2.2 Conductivity 188
5.2.3 pH 189
5.2.4 Dissolved Oxygen 191

5.2.5 Transparency 192
5.2.6 Nutrients 193
5.2.7 Chlorophyll a 195
5.2.8 Phytoplankton Community Composition 196
5.2.9 Zooplankton 198
6 Water Quality in the Lower Deschutes River 199
6.1 River Morphometry 199
6.2 Water Temperature and Quality 203
6.2.1 Temperature 203
6.2.2 pH 206
6.2.3 Dissolved Oxygen 210
6.2.4 Turbidity 215
6.2.5 Nutrient Chemistry 219
6.2.6 Other Chemical Constituents 227
6.2.7 Chlorophyll and Phycocyanin 229
6.2.8 Periphyton 235
6.2.8.1 N-Fixing Periphyton 244
6.2.8.2 Planktonic Algae Attached to Periphyton 247
6.2.9 Volatile Solids 249
6.2.10 Periphyton Chlorophyll 250
6.2.11 Seston (Floating Algae) 252
6.3 Comparison with Other Oregon Rivers 256
7 Changes in Water Quality in the Lower Deschutes River 265
7.1 River Temperature 265
7.2 1997 Survey 266
7.3 ODEQ AWQMP Data 272
8 Discussion 281
8.1 Tributaries 281

8.2 Lake Billy Chinook 282
8.3 Lake Simtustus 285
8.4 Lower Deschutes River 286
8.4.1 Water Chemistry 286
8.4.2 Nutrient Contributions 288
8.4.3 Eutrophication 295
8.4.4 Algal Community 300
8.4.5 Cladophora 303
8.4.6 Turbidity 304
8.4.7 Flow Regimes 306
8.4.8 Pesticide Use 313
8.4.9 Urbanization and Climate Change 316
8.5 Limitations of the Water Quality Monitoring Portion of the Study 317
8.6 Summary of Major Findings Regarding Water Quality Monitoring 320
8.6.1 Tributaries to the Project 320
8.6.2 Lake Billy Chinook 321
8.6.3 Lake Simtustus 323
8.6.4 ReReg Dam Release 325
8.6.5 Lower Deschutes River 325
9 Water Quality Modeling in Project Reservoirs 328
9.1 CE-QUAL-W2 Model 328
9.2 Water Quality Modeling and Calibration 329
9.3 Data Sources 332
9.3.1 Geometry 332
9.3.2 Meteorological Data 332
9.3.3 Observed Data 333
9.3.4 Tributary Flow Data 333
9.3.5 Discharge from Reservoirs 333
9.3.6 Reservoir Stage Data 334

9.4 Water Temperature Data 334
9.4.1 Tributary Data 334
9.4.2 Discharge from Dams 334
9.4.3 In-Reservoir Temperature Data 334
9.5 Water Quality Data 335
9.5.1 Tributary Data 335
9.5.2 Discharge from Dams 336
9.5.3 In-Reservoir Water Quality Data 336
9.6 Pelton Round Butte Model Development and Calibration 336
9.6.1 Model Setup 336
9.6.1.1 Input data and initial conditions 336
9.6.1.2 Meteorological inputs 336
9.6.2 Model Calibration 337
9.6.2.1 Hydrology/ELWS/balance flows 337
9.6.2.2 Water temperature 339
9.6.2.3 Conservative tracers 344
9.6.2.4 Nutrients 350
9.6.3 Dissolved Oxygen and pH 355
9.6.3.1 Biological components 357
9.7 Lake Simtustus Model Development and Calibration 361
9.7.1 Model Setup 361
9.7.1.1 Input data and initial conditions 361
9.7.1.2 Meteorological inputs 361
9.7.2 Model Calibration 361
9.7.2.1 Hydrology/ELWS/balance flows 361
9.7.2.2 Water temperature 363
9.7.2.3 Conservative tracers 369

9.7.2.4 Nutrients 374
9.7.2.5 Dissolved Oxygen and pH 381
9.7.2.6 Biological components 383
9.8 ReReg Reservoir Model Development and Calibration 386
9.8.1 Model Setup 386
9.8.1.1 Input data and initial conditions 386
9.8.1.2 Meteorological inputs 386
9.8.2 Model Calibration 386
9.8.2.1 Hydrology/ELWS/balance flows 386
9.8.2.2 Water temperature 388
9.8.2.3 Conservative tracers 389
9.8.2.4 Nutrients 390
9.8.2.5 Biological components 393
9.9 Conclusions 394
10 Water Quality Modeling in the Lower Deschutes River 395
10.1 Introduction 395
10.2 Study Area 395
10.3 Background 395
10.4 QUAL2Kw Model 396
10.5 Data Sources 398
10.5.1 Climate Data 398
10.5.2 Discharge Data 399
10.5.3 Water Quality Data 399
10.6 Model Setup 400
10.6.1 Geometry and Ttools 401
10.6.2 Model Input Data 402
10.6.3 Effective Shade 407
10.6.4 Boundary Conditions 408

10.7 Model Analysis 409
10.7.1 Hydrology 410
10.7.2 Water Temperature 411
10.7.2.1 Calibration 411
10.7.2.2 Short term simulations and longitudinal profile 416
10.7.3 Water Quality Model 418
10.7.3.1 Dissolved Oxygen and pH 419
10.7.3.2 Nitrogen and Phosphorus 426
10.7.3.3 Conductivity, alkalinity, and chloride 434
10.7.3.4 Phytoplankton and Periphyton 440
10.8 Conclusions 445
11 Scenario Analysis: Integrated Modeling of Project Reservoirs and the Lower Deschutes River 446
11.1 Model Limitations 448
11.2 SWW 100/40 Scenario 454
11.3 SWW 40 Scenario 464
11.4 No SWW Scenario 474
11.5 Night Blend Scenario 482
11.6 NO_3 Decrease Scenario 492
11.7 Nitrogen and Phosphorus Decrease Scenario 496
11.8 Curtain Scenario 500
11.9 Cold Flush Scenario 512
11.10 Flushing Flow Scenario 517
11.11 Future Climate Scenario 525
11.12 Future Tributary Temperature Scenario 533
11.13 Statistical Comparison of Scenario Results 541
11.14 Scenarios Conclusion 556
11.15 Areas for Future Research 559

11.15.1 Data Collection 559
11.15.2 Modeling 560
12 Study Conclusions 561
12.1 Overview 561
12.2 Current Status 561
12.2.1 Water Quality Status in the Tributaries to Lake Billy Chinook 561
12.2.2 Water Quality Status in the Impoundments 562
12.2.3 Water Quality Status in the Lower Deschutes River 563
12.3 Historical Changes in Water Quality 565
12.3.1 Water Quality Changes in the Major Tributaries to Lake Billy Chinook 565
12.3.2 Water Quality Changes in the Reservoirs 565
12.3.3 Water Quality Changes in the Lower Deschutes River 566
12.4 Model Development and Calibration of the Pelton Round Butte Reservoirs 567
12.5 Model Development and Calibration of the Lower Deschutes River 568
12.6 Scenario Analysis 569
12.7 Recommendations 570
12.7.1 Nutrient Reduction 570
12.7.2 Operational Considerations 571
12.7.3 Research Considerations 572
13 Acknowledgments 575
14 Literature Cited 576

Figures

Figure 2-1. The division of the Deschutes River basin and its topographic relief..... 7
Figure 2-2. Geologic map units of the Deschutes River basin. 10
Figure 2-3. Locations of the phosphorus sampling sites summarized in Table 2-1. 13
Figure 2-4. Land-cover types in the Deschutes River basin 15
Figure 2-5. The Pelton Round Butte Project area. 18
Figure 2-6. LDR cumulative flow for June 1 and September 1, 2015. 22
Figure 2-7. Daily discharge at the Moody (RM 1) and Madras (RM 100) USGS stream gages for water years 2015–2017. 24
Figure 2-8. Differences in daily flows between the Moody (RM 1) and Madras (RM 100) USGS stream gages for WY 2015–2017. 24
Figure 2-9. Warm Springs River flow from January to November for 2015–2017 26
Figure 2-10. Daily snowpack at the Hogg Pass SNOTEL site 26
Figure 2-11. Peak annual flow for the LDR at Moody USGS Stream Gage #14103000 27
Figure 3-1. Sample sites along the LDR and its tributaries. 30
Figure 3-2. Monitoring sites in LBC, Lake Simtustus, and the tributaries of LBC. 36
Figure 4-1. Daily average flow for the three major tributaries to LBC for WY2015–2017 51
Figure 4-2. Daily average river temperature for the three major tributaries to LBC 53
Figure 4-3. Discharge in the Crooked River above and below Opal Springs 54
Figure 4-4. Time-series plots of water quality data for the three major tributaries to LBC. 55
Figure 4-5. Distributions of turbidity, PO_4, biochemical oxygen demand (BOD_5), and NO_3 for the three tributaries monitored by the ODEQ AWQMP. 56
Figure 4-6. Conductivity values collected by field staff for the three tributaries in 2016. 58
Figure 4-7. pH measured at the three tributaries to LBC in 2015 and 2016. 59
Figure 4-8. DO concentrations measured at the three tributaries to LBC in 2015 and 2016 59
Figure 4-9. Concentrations of TN in the tributaries to LBC for 2015 (left) and 2016 (right). 61
Figure 4-10. Concentrations of NO_3 at the three tributaries to LBC measured during the study. 61
Figure 4-11. TP concentrations for the tributaries to LBC for 2015 (left) and 2016 (right). 63
Figure 4-12. PO_4 concentrations for the tributaries to LBC for 2015 (left) and 2016 (right) 63
Figure 4-13. Mass ratios of TN:TP for the three inlets for 2015 (top) and 2016 (bottom) 65
Figure 4-14. Mass ratio of NO_3 to PO_4 in the three tributaries to LBC in 2015 (top) and 2016 . 66
Figure 4-15. Benthic chlorophyll values at the three inlets to LBC. 67

Figure 4-16. Periphyton biovolume for the major taxonomic groups from the three sites tributary to LBC in August and October 2015 and May 2016. 69

Figure 4-17. Temperature contours for Round Butte forebay (RES07) (top) and the Common Pool (RES08) (bottom). 72

Figure 4-18. Selected temperature profiles in LBC for Round Butte forebay (RES07) in 2016. 73

Figure 4-19. Temperature data for thermistors deployed in Round Butte forebay (RES07) July 16, 2016..... 74

Figure 4-20. RTR at Round Butte forebay (RES07) on June 9, 2015 (left) and July 29, 2015 (right). 75

Figure 4-21. Total RTR for Round Butte forebay (RES07) (top) and the Common Pool (RES08) (bottom) during the study..... 76

Figure 4-22. Conductivity contours for Round Butte forebay (RES07) (top) and the Common Pool (RES08) (bottom). 78

Figure 4-23. DO saturation contours for Round Butte forebay (RES07) (top) and the Common Pool (RES08) (bottom) in 2015. 80

Figure 4-24. Contours of pH in Round Butte forebay (RES07) (top) and the Common Pool (RES08) (bottom)..... 81

Figure 4-25. Secchi disk transparency for Round Butte forebay (RES07) and the Common Pool (RES08) in 2015 (left) and 2016 (right). 82

Figure 4-26. Contours of light attenuation in Round Butte forebay (RES07) (top) and the Common Pool (RES08) (bottom). 83

Figure 4-27. Turbidity contours in Round Butte forebay (RES07) (top) and the Common Pool (RES08) (bottom)..... 85

Figure 4-28. TP concentrations for Round Butte forebay (RES07) (top) and the Common Pool (RES08) (bottom)..... 87

Figure 4-29. PO_4 concentrations at Round Butte forebay (RES07) (top) and the Common Pool (RES08) (bottom)..... 89

Figure 4-30. TN concentrations at Round Butte forebay (RES07) (top) and the Common Pool (RES08) (bottom)..... 91

Figure 4-31. NO_3 concentrations in Round Butte forebay (RES07) (top) and the Common Pool (RES08) (bottom)..... 93

Figure 4-32. NH_3 concentrations in Round Butte forebay (RES07) (left) and the Common Pool (RES08) (right) from 2015 to 2017. 95

Figure 4-33. Mass ratio of TN:TP in Round Butte forebay (RES07) (top) and the Common Pool (RES08) (bottom)..... 97

Figure 4-34. Mass ratio of NO3:PO4 in Round Butte forebay (RES07) (top) and the Common Pool (RES08) (bottom). 99

Figure 4-35. Concentrations of DIN (top) and PO_4 (bottom) in the surface waters of LBC at Round Butte forebay (RES07). 100

Figure 4-36. Mass ratio of DIN to PO4 in the surface waters of LBC at Round Butte forebay (RES07)..... 100

Figure 4-37. Cl^- concentrations in Round Butte forebay (RES07) (top) and the Common Pool (RES08) (bottom)..... 102

Figure 4-38. Chlorophyll concentration contours in Round Butte forebay (RES07) (top) and the Common Pool (RES08) (bottom). 104

Figure 4-39. Cyanobacteria pigment density contours in the Round Butte forebay (RES07) (top) and the Common Pool (RES08) (bottom)..... 106

Figure 4-40. Total algal biovolume in Round Butte forebay (RES07) at 1 m during the study.108

Figure 4-41. Boxplot of the cumulative algal biovolume of dominant phytoplankton taxa for all phytoplankton samples from 2016. 109

Figure 4-42. Dominant phytoplankton taxa in Round Butte forebay (RES07) in 2016. 110

Figure 4-43. Dominant phytoplankton taxa in the Common Pool (RES08) in 2016. 110

Figure 4-44. The three dominant phytoplankton taxa for each sampling date in 2016 in the upper 1 m of Round Butte forebay (RES07)..... 111

Figure 4-45. The three dominant phytoplankton taxa for each sampling date in 2016 in the upper 1 m of the Common Pool (RES08). 111

Figure 4-46. Comparison of dominant phytoplankton taxa from surface samples collected at Round Butte forebay (RES07) and the Common Pool (RES08) in LBC in 2016. 112

Figure 4-47. Abundance of the major zooplankton divisions collected in the upper 10 m at Round Butte forebay (RES07) in 2016. 113

Figure 4-48. Density of the three species of Daphnia present in the upper 10 m tows from Round Butte forebay (RES07) in 2016..... 114

Figure 4-49. Temperature contours at Pelton forebay (RES04) (top) and Mid-Lake site (RES25) (bottom)..... 117

Figure 4-50. Dye signal strength measured at Pelton Dam tailrace following the addition of dye at Round Butte Dam tailrace in August 2016. 118

Figure 4-51. RTR in the Pelton forebay (RES04) on two summer dates. 119

Figure 4-52. Total RTR at Pelton forebay (RES04) and Mid-Lake site (RES25) during the study. 119

Figure 4-53. Conductivity contours for Pelton forebay (RES04) (top) and Mid-Lake site (RES25) (bottom)..... 121

Figure 4-54. DO saturation contours for Pelton forebay (RES04) (top) and Mid-Lake site (RES25) (bottom)..... 123

Figure 4-55. pH contours for Pelton forebay (RES04) (top) and Mid-Lake site (RES25) (bottom)..... 124

Figure 4-56. Secchi disk transparency in Lake Simtustus in 2015 (top) and 2016 (bottom). ... 125

Figure 4-57. Light attenuation contours for Pelton forebay (RES04) (top) and Mid-Lake site (RES25) (bottom)..... 126

Figure 4-58. Turbidity contours for Pelton forebay (RES04) (top) and Mid-Lake site (RES25)(bottom)..... 127

Figure 4-59. TP concentrations at Pelton forebay (RES04) (top) and Mid-Lake site (RES25) (bottom)..... 128

Figure 4-60. PO_4 concentrations at Pelton forebay (RES04) (top) and Mid-Lake site (RES25) (bottom)..... 129

Figure 4-61. TN concentrations at Pelton forebay (RES04) (top) and Mid-Lake site (RES25) (bottom)..... 131

Figure 4-62. NO_3 concentrations at Pelton forebay (RES04) (top) and Mid-Lake site (RES25) (bottom)..... 132

Figure 4-63. NH_3 concentrations at Pelton forebay (RES04) (top) and Mid-Lake site (RES25) (bottom)..... 133

Figure 4-64. Mass ratio of TN:TP at Pelton forebay (RES04) (top) and Mid-Lake site (RES25) (bottom)..... 135

Figure 4-65. Mass ratio of NO_3:PO_4 at Pelton forebay (RES04) (top) and Mid-Lake site (RES25) (bottom)..... 136

Figure 4-66. Cl^- concentrations at Pelton forebay (RES04) (top) and Mid-Lake site (RES25) (bottom)..... 137

Figure 4-67. Chlorophyll pigment concentrations (µg/L) at Pelton forebay (RES04) (top) and Mid-Lake site (RES25) (bottom). 139

Figure 4-68. Cyanobacteria pigment levels (µg/L) at Pelton forebay (RES04) (top) and Mid-Lake site (RES25) (bottom). 141

Figure 4-69. Total algal biovolume at Pelton forebay (RES04) 142

Figure 4-70. The three dominant algal taxa groups at Pelton forebay (RES04) at 1 m 2015–2017. 143

Figure 4-71. Comparison of dominant phytoplankton taxa at Pelton forebay (RES04) and Mid-Lake site (RES25) for 2016. 145

Figure 4-72. Density of zooplankton groups at Pelton forebay (RES04) (10 m tow) in 2016. . 146

Figure 4-73. Density of Daphnia species at Pelton forebay (RES04) (10 m tow) in 2016..... 147

Figure 4-74. Nutrient chemistry measured at Round Butte tailrace (RES09), Pelton tailrace (RES10), and ReReg site (LDR01) in 2015–2016. LDR01 is immediately downstream of Reregulating Dam. 148

Figure 4-75. Concentrations of dissolved inorganic nitrogen (DIN) at Round Butte tailrace (RES09), Pelton tailrace (RES10), and ReReg site (LDR01) (top) 150

Figure 4-76. Conductivity measured in 2016 at the Crooked River and Metolius River sample sites and measurements at the three tailraces shown in the middle. 151

Figure 4-77. Average biovolume of the major phyla in the three tailraces of the Project from 2015–2016..... 152

Figure 4-78. Phytoplankton biovolume by phyla for Round Butte tailrace (RES09, upstream), Pelton tailrace (RES10), and ReReg site (LDR01, downstream) from 2015–2016. 153

Figure 4-79. Boxplots of water quality results for surface water samples from the Project and other impoundments in central and eastern Oregon. 155

Figure 5-1. Mean daily temperature in the three tributaries to LBC. 158

Figure 5-2. Temperature of tailrace water from Round Butte Dam for 2015–2017. 160

Figure 5-3. Mean monthly temperature of tailrace water from Round Butte Dam 161

Figure 5-4. Temperature contours for Round Butte forebay (RES07) from 1994–1996 (Raymond et al. 1997). 162

Figure 5-5. Temperature patterns in Round Butte forebay (RES07) for 1995 (left) and 2016 (right). 163

Figure 5-6. Water temperature at Round Butte forebay (RES07) collected by PGE from January 2005 through 2017. 164

Figure 5-7. Temperature at Round Butte forebay (RES07) in 2006 and 2016 165

Figure 5-8. Temperature patterns at Round Butte forebay (RES07) measured in 2006 (top) and 2016 (bottom)..... 166

Figure 5-9. Cross sections of the three arms of LBC showing conductivity (µS/cm) contours on July 23, 2018. 168

Figure 5-10. Conductivity patterns at Round Butte forebay (RES07) from 1994–1996. 170

Figure 5-11. Conductivity at Round Butte forebay (RES07) for 1995 (left) and 2016 (right).. 170

Figure 5-12. pH patterns at Round Butte forebay (RES07) from 1994–1996. 171

Figure 5-13. pH patterns at Round Butte forebay (RES 07) from 1995 (left) and 2016 (right). 172

Figure 5-14. DO patterns at Round Butte forebay (RES07) in 1994–1996. 173

Figure 5-15. DO patterns at Round Butte forebay (RES07) in 1995 (left) and in 2016 (right). 173

Figure 5-16. Secchi disk transparency at Round Butte forebay (RES07) from 1994 to 1996... 174

Figure 5-17. Concentrations of chlorophyll a (pheophytin corrected) at Round Butte forebay (RES07) for 1994–1996. 177

Figure 5-18. Monthly average chlorophyll a concentrations measured at Round Butte forebay in 1994–96 and 2015–17. 178

Figure 5-19. Dominant phytoplankton at Round Butte forebay (RES07) from 2006 and 2015.181

Figure 5-20. Density of zooplankton groups at Round Butte forebay (RES07) and Pelton forebay (RES04) comparing data collected by Raymond et al. (1997) and this study. 182

Figure 5-21. Density of Daphnia pulicaria at Round Butte forebay (RES07) 184

Figure 5-22. Species of Daphnia present in 2006 and 2016 at Round Butte forebay (RES07). 184

Figure 5-23. Fish population estimates for LBC conducted using hydroacoustic methodology186

Figure 5-24. Temperature patterns at Pelton forebay (RES04) 1994–1996. 187

Figure 5-25. Temperature patterns at Pelton forebay (RES04) for 1995 (left) and 2016 187

Figure 5-26. Conductivity patterns at Pelton forebay (RES04) from 1994–1996. 188

Figure 5-27. Conductivity patterns at Pelton forebay (RES04) in 1995 (left) and 2016 (right).189

Figure 5-28. pH patterns at Pelton forebay (RES04) from 1994–1996. 190

Figure 5-29. pH patterns at Pelton forebay (RES04) in 1995 (left) and 2016 (right). 190

Figure 5-30. DO patterns at Pelton forebay (RES04) from 1994–1996. 191

Figure 5-31. DO patterns at Pelton forebay (RES04) in 1995 (left) and 2016 (right). 192

Figure 5-32. Secchi disk transparency at Pelton forebay (RES04) for 1994–1996. The blue line is the LOESS fit of the observed data. 193

Figure 5-33. Concentrations of chlorophyll a (pheophytin corrected) at Pelton forebay (RES04) at 1-m depth from 1994–1996 196

Figure 5-34. Epilimnetic algal biovolume at Pelton forebay (RES04) in 2006 and 2015. 197

Figure 5-35. Major zooplankton groups at Pelton forebay (RES04) in 1994–1996 compared to 2015 and 2016. 199

Figure 6-1. Summary of physical attributes for the LDR. 201

Figure 6-2. LiDAR images of the LDR at Maupin. 202

Figure 6-3. Water temperature measured below the ReReg Dam (RM 100.1) from 2015 through 2017 203

Figure 6-4. River temperatures below the ReReg Dam (RM 100.1) and at Moody (RM 1) of the LDR for WY2015–2017 using 15-min data from USGS (n.d) 204

Figure 6-5. River temperature measured at six sites on the LDR during July 2016 (top) and August 2016 (bottom). 205

Figure 6-6. River temperature recorded during a float of the river in July 2016. 206

Figure 6-7. pH measured at the ReReg site (LDR01) from 2015 through 2017. 207
Figure 6-8. pH measured at the 72-hr monitoring sites in July 2016. 208
Figure 6-9. pH measured at the 72-hr monitoring sites in August 2016..... 209
Figure 6-10. pH measured during the river float of July 2016. 209
Figure 6-11. DO concentration (top) and DO percent saturation (bottom) measured at the ReReg site (LDR01) from 2015 through 2017. 211
Figure 6-12. DO concentration (top) and DO percent saturation (bottom) of at the four diurnal monitoring sites on the LDR for July 2016. 213
Figure 6-13. DO concentration (top) and DO percent saturation (bottom) in the LDR measured during a river float in July 2016..... 214
Figure 6-14. DO measurements (solid line) and water temperature (dashed line) during stationary conditions in the LDR in 2016. 215
Figure 6-15. Daily average turbidity measured at the ReReg site (LDR01) for WY2016–2017 measured by the ZAPS LiquID unit..... 216
Figure 6-16. Turbidity measured at the 72-hr study sites in July 2016. 218
Figure 6-17. Turbidity measured during the river float in July 2016. 218
Figure 6-18. Mean and standard error of nutrient concentrations, DIN:PO4 ratio, and Cl^- in the LDR from 2015–2017. 220
Figure 6-19. Mean TP concentrations by river mile for 2015 and 2016..... 222
Figure 6-20. Mean concentrations of PO_4 by river mile for 2015 and 2016. 223
Figure 6-21. Mean concentrations of TN in the LDR for 2015 and 2016. 224
Figure 6-22. TDN versus TN for samples collected from the LDR in 2015. 225
Figure 6-23. Concentrations of NH_3 in the LDR for 2015 and 2016..... 226
Figure 6-24. Concentrations of NO_3 in the LDR for 2015 and 2016 226
Figure 6-25. Concentrations of TOC measured in the LDR during 2016. 227
Figure 6-26. Relative measurements of FDOM measured using the ZAPS LiquID unit at ReReg site (LDR01) in WY2016–2017..... 228
Figure 6-27. Concentrations of chloride in the LDR during 2015 and 2016. Different analytical laboratories were used in the two years. 228
Figure 6-28. Measurements of algal pigments using the AlgaeTorch in the LDR for 2015, coded by month. 230
Figure 6-29. AlgaeTorch pigment measurements from 2015 at ReReg site (LDR01), Whitehorse (LDR07), Wreck (LDR14), and River Mouth (LDR21), coded by month. 231

Figure 6-30. Chlorophyll measured at the ReReg site (LDR01) for green algae and blue-green algae using the Algae Torch in 2016. 232

Figure 6-31. Chlorophyll from green algae measured with the Algae Torch at the ReReg site (LDR01), Lower Wapinitia (LDR11), and River Mouth (LDR21) for 2016. 233

Figure 6-32. Chlorophyll (upper) and phycocyanin (lower) measured with the ZAPS LiquID unit at the ReReg site (LDR01) for WY2016–2017. 234

Figure 6-33. Analytical laboratory measurements of chlorophyll a for samples collected at the ReReg site (LDR01). 235

Figure 6-34. Periphyton biovolume by season for 2015–2017 for the study sites. 236

Figure 6-35. Average periphyton biovolume by river mile in 2016. 237

Figure 6-36. Average periphyton biovolume and chlorophyll a in the LDR for 2016 by month. The vertical bars are standard errors of the mean. 238

Figure 6-37. Average periphyton biovolume in the LDR for 2015–2017 for each of the three major groups. 239

Figure 6-38. Average biovolume of major groups of periphyton by river mile for 2015–2017.240

Figure 6-39 Average seasonal biovolume for the three major periphyton groups in the LDR for 2016..... 241

Figure 6-40. Dominant genera in each of the three major periphyton groups from 2015–2017. 242

Figure 6-41. Average biovolume of Cladophora in the LDR for 2015-2017. 243

Figure 6-42. Biovolume of Cladophora by sample date in 2016. 243

Figure 6-43. Average biovolume of Ulothrix spp. by RM for April to June 2016. 244

Figure 6-44. Average biovolume of heterocystous (N-fixing) and non-heterocystous (non N-fixing) periphyton by year in the LDR for the 7 sites sampled in the summers of 2015–2017.. 245

Figure 6-45. Biovolume of heterocystous (N-fixing) and non-heterocystous (non N-fixing) periphyton in the LDR by season in 2016. 245

Figure 6-46. Average periphyton biovolume of N-fixing (heterocystous) and non N-fixing (non-heterocystous) periphyton in the LDR by river mile for 2016..... 246

Figure 6-47. Average biovolume of Calothrix by month for 2016 (left) and by river mile (right). 246

Figure 6-48. Average biovolume of Epithemia spp. by river mile for 2015–2017. 247

Figure 6-49. Average biovolume of Epithemia spp. by month for 2016. 247

Figure 6-50. Average biovolume of benthic periphyton taxa compared with planktonic taxa present in the periphyton in the LDR for 2016. 248

Figure 6-51. Average biovolume of Stephanodiscus spp. by RM for spring, summer, fall 2016. 249
Figure 6-52. Volatile solids in periphyton by river mile for 2015 (left) and 2016 (right). 250
Figure 6-53. Volatile solids in periphyton for 2015 (left) and 2016 (right) by month. 250
Figure 6-54. Periphyton chlorophyll content by river mile in 2015 (left) and 2016 (right). 251
Figure 6-55. Periphyton chlorophyll content by month in 2015 (left) and 2016 (right). 251
Figure 6-56. Partitioning of seston from LDR samples in 2016. 253
Figure 6-57. Average biovolume of Stephanodiscus spp. by RM for spring, summer, and fall 254
Figure 6-58. Algal biovolume of Stephanodiscus niagarae and Dolichospermum in Round Butte forebay (RES07) from surface samples (left) compared to biovolume of same taxa from seston samples in the LDR (right) in 2016. 255
Figure 6-59. Average biovolume of Dolichospermum present in the seston of the LDR in 2016 compared to that of Stephanodiscus niagarae. 256
Figure 6-60. Location of the six rivers used in the LDR water quality comparison. 257
Figure 6-61. Boxplots of pH distributions for the two ODEQ sites on the LDR and several other rivers in the ODEQ AWQMP database. 259
Figure 6-62. Boxplots of DO saturation for the two ODEQ sites on the LDR and other selected Oregon rivers. 260
Figure 6-63. Boxplots of conductivity for the two ODEQ sites on the LDR and other selected Oregon rivers. 260
Figure 6-64. Boxplots of PO_4 concentrations for the two ODEQ sites on the LDR and other selected Oregon rivers. 261
Figure 6-65. Boxplots of NO_3 for the two ODEQ sites on the LDR and other selected Oregon rivers. 262
Figure 6-66. Boxplots of chlorophyll a for the two ODEQ sites on the LDR and other selected Oregon rivers. 263
Figure 6-67. Boxplots of BOD_5 for the two ODEQ sites on the LDR and other selected Oregon rivers. 264
Figure 7-1. Daily average temperature of the LDR at the USGS Madras gage (RM 100.1) for the periods 2006–2008 and 2015–2017. 266
Figure 7-2. Concentrations of TP by river mile and year (1997, 2015, 2016, and 2017) for May (top), July (middle), and September (bottom). 268
Figure 7-3. Concentrations of NO_3 by river mile and year (1997, 2015, 2016, and 2017). 270
Figure 7-4. ODEQ AWQMP pH results at the Hwy 26 bridge site (RM 97.6) (top) and the LDR Mouth (RM 0.1) (bottom). 272

Figure 7-5. ODEQ AWQMP DO results at the Hwy 26 bridge site (RM 97.6) (top) and the LDR Mouth (RM 0.1) (bottom). 273

Figure 7-6. ODEQ AWQMP NO_3 results at the Hwy 26 bridge site (RM 97.6) (top) and the LDR Mouth (RM 0.1) (bottom). 274

Figure 7-7. NO_3 concentrations at the LDR Mouth (RM 0.1) shown by month based on ODEQ AWQMP data. 275

Figure 7-8. ODEQ AWQMP TP results at the Hwy 26 bridge site (RM 97.6) (top) and the LDR Mouth (RM 0.1) (bottom). 276

Figure 7-9. ODEQ AWQMP PO_4 results at the Hwy 26 bridge site (RM 97.6) (top) and the LDR Mouth (RM 0.1) (bottom). 277

Figure 7-10. ODEQ AWQMP BOD results at the Hwy 26 bridge site (RM 97.6) (top) and the LDR Mouth (RM 0.1) (bottom). 278

Figure 7-11. ODEQ AWQMP chlorophyll a results at the Hwy 26 bridge site (RM 97.6) (top) and the LDR Mouth (RM 0.1) (bottom). 279

Figure 7-12. Data from the ODEQ AWQMP for pH (upper left), DO (upper right), PO_4 (middle left), NO_3 (middle right), chlorophyll (lower left), and BOD (lower right) at the Hwy 26 bridge site (RM 97.6). 280

Figure 8-1. Boxplot of the ratio of DIN to PO_4 (mass) for all sites in the LDR grouped by sampling date (2016). 289

Figure 8-2. Boxplot of the ratio of DIN to PO_4 (mass) for all samples collected in 2016 in the LDR grouped by sample site. 289

Figure 8-3. NO_3 concentrations at the ReReg site (LDR01) and the River Mouth (LDR21) for 2015 (top) and 2016 (bottom). 290

Figure 8-4. Average NO3 concentrations by month for all ODEQ AWQMP data collected at the Hwy 26 bridge site (RM 97.6) and the Deschutes River SRA site at the mouth (RM 0.1). 291

Figure 8-5. Number of sample events with concentrations reported at less than 0.055 mg/L (top) and 0.075 mg/L (bottom) for 2015 and 2016. 293

Figure 8-6. Average seasonal nitrate concentrations in the LDR for 2015–2016. 293

Figure 8-7. Distribution of cropland along the LDR based on satellite imagery from 2016. 295

Figure 8-8. Cumulative storage behind major dams constructed in the Deschutes Basin. 307

Figure 8-9. The proportions of monthly peak flows measured at Moody (USGS # 14103000) from 1907 to 2017. 308

Figure 8-10. Average daily discharge at Moody for 1907–1948 and 1949–2017. 309

Figure 8-11. Peak streamflow at Moody during April from 1907–2017. 310

Figure 8-12. Biovolume of Cladophora during the summer from 2015 to 2017. Systematic sampling of periphyton was not initiated until August 2015. 311

Figure 8-13. Generalized relationship between stream velocity and transport of particles of various diameters. 312

Figure 8-14. Stream velocity in the LDR based on QUAL2Kw model estimates at a specific discharge. 313

Figure 8-15. Measurements of FDOM at ReReg site (LDR01) using the ZAPS LiquID unit in WY2016–2017 (top) and a comparison of discharge at the ReReg site (LDR01) to FDOM measurements in WY2017 (bottom). 315

Figure 8-16. Population growth from 1960 to 2017 in the four primary counties bordering the Deschutes River. 316

Figure 9-1. Daily balance flows for LBC. 337

Figure 9-2. Simulated and observed reservoir ELWSs from January 1, 2015, to January 1, 2018. 338

Figure 9-3. Simulated and observed water temperature at the outlet of LBC. 339

Figure 9-4. Simulated and observed water temperatures at different depths in LBC. 340

Figure 9-5. Observed temperature profiles (blue dots) and simulated temperature profiles (orange lines) at Round Butte forebay (RES07) (April 3, 2015–April 25, 2016). 341

Figure 9-6. Observed temperature profiles (blue dots) and simulated temperature profiles (orange lines) at Round Butte forebay (RES07) (May 10, 2016–September 12, 2016). 342

Figure 9-7. Observed temperature profiles (blue dots) and simulated temperature profiles (orange lines) at the Common Pool (RES08) (April 3, 2015–April 25, 2016). 343

Figure 9-8. Observed temperature profiles (blue dots) and simulated temperature profiles (orange lines) at the Common Pool (RES08) (May 10, 2016–September 12, 2016). 344

Figure 9-9. Simulated values at Round Butte forebay (RES07) showing the percentage of different water sources and estimated contribution of groundwater. 346

Figure 9-10. Simulated values at the Common Pool (RES08) showing the percentage of different water sources and estimated contribution of groundwater. 347

Figure 9-11. Simulated values at Round Butte tailrace showing the percentage of different water sources and estimated contribution of groundwater. 349

Figure 9-12. Simulated and observed nutrient dynamics at Round Butte forebay (RES07). 351

Figure 9-13. Simulated and observed nutrient dynamics at the Common Pool (RES08). 352

Figure 9-14. Simulated and observed nutrient dynamics in the Round Butte tailrace. 354

Figure 9-15. Simulated DO and pH dynamics at the Round Butte forebay (RES07). 355

Figure 9-16. Simulated DO and pH dynamics at the Common Pool (RES08). 356

Figure 9-17. Simulated and observed pH and DO in the Round Butte tailrace. 357

Figure 9-18. Simulated dynamics related to key biological components at Round Butte forebay (RES07)..... 358

Figure 9-19. Simulated dynamics of the biological components of the system at the Common Pool (RES08). 359

Figure 9-20. Dynamics outlining key features of the biological system in the Round Butte tailrace. 360

Figure 9-21. Daily balance flows for Lake Simtustus. 362

Figure 9-22. Observed and simulated hourly ELWS s for Lake Simtustus. 362

Figure 9-23. Simulated and observed temperature at Pelton forebay (RES04) at 0 m, 4 m, 9 m, and 40 m depth. 364

Figure 9-24. Simulated and observed water temperature profiles at the Common Pool (RES08) (April 2, 2015–April 27, 2016). 365

Figure 9-25. Simulated and observed water temperature profiles at the Common Pool (RES08) (May 11, 2016–September 12, 2017). 366

Figure 9-26. Simulated and observed water temperature profiles at the Mid-Lake site (RES25) (April 2, 2015–April 27, 2016). 367

Figure 9-27. Simulated and observed water temperature profiles at the Mid-Lake site (RES25) (May 11, 2016–August 10, 2016). 368

Figure 9-28. Simulated and observed water temperature profiles at the Pelton tailrace. 368

Figure 9-29. Simulated values at Pelton forebay (RES04). 370

Figure 9-30. Simulated values at the Mid-Lake site (RES25). 372

Figure 9-31. Simulated values at the Pelton tailrace..... 373

Figure 9-32. Simulated dynamics related to key biological components at Pelton forebay (RES04)..... 375

Figure 9-33. Simulated dynamics related to key biological components at Mid-Lake site (RES25)..... 376

Figure 9-34. Simulated and observed nutrient dynamics at Pelton forebay (RES04). 378

Figure 9-35. Simulated and observed nutrient dynamics at the Mid-Lake site (RES25). 379

Figure 9-36. Simulated and observed nutrient dynamics in the Pelton tailrace..... 380

Figure 9-37. Simulated DO and pH dynamics at Pelton forebay (RES04). 381

Figure 9-38. Simulated DO and pH dynamics at the Mid-Lake site (RES25). 382

Figure 9-39. Simulated and observed pH and DO in the Pelton tailrace. 383

Figure 9-40. Simulated biological components in the Pelton tailrace. 385

Figure 9-41. Simulated and observed elevation at the ReReg Reservoir. 387

Figure 9-42. Calculated daily balance flows needed to capture observed surface elevations at the ReReg Reservoir. 387
Figure 9-43. Simulated and observed temperatures downstream of the ReReg Reservoir. 388
Figure 9-44. Simulated values for conservative tracers in the ReReg tailrace. 389
Figure 9-45. Simulated and observed nutrient dynamics in the ReReg tailrace. 391
Figure 9-46. Simulated and observed DO and pH dynamics in the ReReg Reservoir tailrace. 392
Figure 9-47. Tailrace time series for biological components in the ReReg Reservoir. 393
Figure 10-1. Comparison of air temperature at Pelton Dam and the Madras AgriMet mrso station. 398
Figure 10-2. A longitudinal profile derived from LiDAR data representing the LDR. 402
Figure 10-3. These maps depict each of the 204 individual model segments, as implemented by Ttools. 406
Figure 10-4. Effective shade for one day at four locations. 407
Figure 10-5. Comparison of observed stream discharge at Moody (RM 1) and Madras (RM 100), with simulated stream discharge at Moody for the 2015 study period. 410
Figure 10-6. Diel time series of measured versus modeled temperature for the five locations in the LDR during summer 2015. 413
Figure 10-7. Hourly time series of measured versus modeled temperature at the five locations in the LDR during summer 2016. 415
Figure 10-8. Combined Eulerian and Lagrangian viewpoints of simulated and observed temperature dynamics in the LDR. 417
Figure 10-9. Simulated and observed DO during 2015. 420
Figure 10-10. Simulated and observed DO during 2016. 421
Figure 10-11. Combined Eulerian and Lagrangian viewpoints of simulated and observed DO dynamics in the LDR. 422
Figure 10-12. Simulated and observed pH during 2015. 423
Figure 10-13. Simulated and observed pH during 2016. 424
Figure 10-14. Combined Eulerian and Lagrangian viewpoints of simulated and observed pH dynamics in the LDR. 425
Figure 10-15. Simulated and observed NO_3 during 2015. 427
Figure 10-16. Simulated and observed NO_3 during 2016. 428
Figure 10-17. Simulated and observed ammonium during 2015. 429
Figure 10-18. Simulated and observed ammonium during 2016. 430
Figure 10-19. Simulated and observed TN during 2015. 431

Figure 10-20. Simulated and observed TN during 2016. 432
Figure 10-21. Simulated and observed TP during 2015. 433
Figure 10-22. Simulated and observed TP during 2016. 434
Figure 10-23. Simulated and observed conductivity during 2015. 435
Figure 10-24. Simulated and observed conductivity during 2016. 436
Figure 10-25. Simulated and observed Cl^- during 2015. 437
Figure 10-26. Simulated and observed Cl^- during 2016. 438
Figure 10-27. Simulated and observed alkalinity during 2015. 439
Figure 10-28. Simulated and observed alkalinity during 2016. 440
Figure 10-29. Simulated and observed phytoplankton during 2015. 441
Figure 10-30. Simulated and observed phytoplankton during 2016. 442
Figure 10-31. Simulated and observed periphyton (as chlorophyll a) during 2015. 444
Figure 10-32. Simulated and observed periphyton (as chlorophyll a) during 2016. 445
Figure 11-1. A simple assumed relationship between maximum growth rate and the difference between average spring temperatures at ReReg site (LDR01). 451
Figure 11-2. NO_3 concentration in the ReReg tailrace from April–September 2015 (top) and 2016 (bottom) 453
Figure 11-3. Gate flows for the SWW100/40 scenario with 100% surface withdrawals during the spring and 60% bottom release the rest of the year. 454
Figure 11-4. Time series of daily model results for the SWW100/40 scenario in the surface water of Round Butte forebay (RES07). 456
Figure 11-5. A comparison of the differences between baseline and SWW100/40 scenario daily values in the tailraces of the reservoirs across four seasons. 458
Figure 11-6. Time series of daily model results in the ReReg tailrace for the SWW100/40 scenario. 459
Figure 11-7. A comparison of daily results at RM 96 on the LDR for the SWW100/40 scenario. 461
Figure 11-8. A comparison of daily results at Moody (RM 1) on the LDR for the SWW100/40 scenario. 462
Figure 11-9. Water quality profiles from immediately below ReReg Dam to the LDR mouth for the SWW 100/40 scenario. 463
Figure 11-10. Gate flows for the SWW 40 scenario. 464
Figure 11-11. Time series of daily model results for the SWW40 scenario in the surface water of Round Butte forebay (RES07). 466

Figure 11-12. A comparison of the difference between baseline and SWW40 scenario daily values in the tailraces of the reservoirs across four seasons. 468

Figure 11-13. Time series of daily model results at ReReg tailrace for the SWW40 scenario. 469

Figure 11-14. A comparison of daily results at RM 96 on the LDR for the SWW40 scenario. 470

Figure 11-15. A comparison of daily results at Moody (RM 1) on the LDR for the SWW40 scenario. 472

Figure 11-16. Water quality profiles from immediately below ReReg Dam at RM 100.1 to the LDR mouth at RM 0. 474

Figure 11-17. Gate flows for the No SWW scenario assuming 100% bottom water withdrawal. The top figure shows the scenario gate flows, and the bottom figure shows the baseline gate flows. 475

Figure 11-18. Time series of daily model results for the No SWW scenario in the surface water of Round Butte forebay (RES07). 477

Figure 11-19. A comparison of the differences between baseline and No SWW scenario daily values in the tailraces of the reservoirs across four seasons. 478

Figure 11-20. Time series of daily model results in ReReg tailrace for the No SWW scenario. 479

Figure 11-21. A comparison of daily results at RM 96 on the LDR for the No SWW scenario. 480

Figure 11-22. A comparison of daily results at Moody (RM 1) on the LDR for the No SWW scenario. 481

Figure 11-23. Longitudinal water quality profiles for the No SWW scenario, from ReReg Dam (RM 100.1) to the LDR mouth (RM 0). 482

Figure 11-24. Gate flows associated with the Night Blend scenario. 483

Figure 11-25. Temperature profiles (°C) comparing results for the Night Blend scenario to the baseline in Round Butte forebay (RES07). 484

Figure 11-26. Time series of daily model results for the Night Blend scenario in the surface water of Round Butte forebay (RES07). 485

Figure 11-27. Time series of daily model results in the Round Butte tailrace with the baseline results in blue and the Night Blend scenario results in orange. 487

Figure 11-28. Time series of daily model results in the ReReg tailrace, with the baseline results in blue and the Night Blend scenario results in orange. 488

Figure 11-29. A comparison of the differences between baseline and scenario daily values across four seasons in the reservoirs. 489

Figure 11-30. A comparison of daily results for the Night Blend scenario and the baseline at RM 96. 491

Figure 11-31. A comparison of daily results for the Night Blend scenario and the baseline on the LDR at Moody (RM 1). 492

Figure 11-32. A comparison of daily results at RM 96 on the LDR for the NO_3 Decrease scenario. 494

Figure 11-33. A comparison of daily results at Moody (RM 1) on the LDR for the NO_3 Decrease scenario. 495

Figure 11-34. A comparison of daily results at RM 96 on the LDR for the Nitrogen and Phosphorus Decrease scenario. 497

Figure 11-35. A comparison of daily results at Moody (RM 1) on the LDR for the Nitrogen and Phosphorus Decrease scenario. 498

Figure 11-36. A time series figure outlining the proportion of total periphyton growth limitation attributed to each limiting variable. 500

Figure 11-37. The curtain is represented as a skimmer weir in the Curtain scenario 501

Figure 11-38. Time series of daily model results in the surface water in the Round Butte forebay (RES07) for the Curtain scenario. 503

Figure 11-39. A set of cross sections representing algal concentrations in LBC with a 40-ft curtain in place for the Curtain scenario. 504

Figure 11-40. Time series of daily model results in the surface water of LBC in the Common Pool (RES08) for the Curtain scenario. 506

Figure 11-41. Time series of daily model results in the ReReg tailrace for the Curtain scenario. 508

Figure 11-42. A comparison of daily results for the Curtain scenario at RM 96 on the LDR... 510

Figure 11-43. A comparison of daily results for the Curtain scenario on the LDR at Moody (RM 1). 511

Figure 11-44. Gate flows for the Cold Flush scenario. 513

Figure 11-45. Time series of daily modeled water temperature in the surface water of Round Butte forebay (RES07) and Round Butte tailrace for summer 2015 for the Cold Flush scenario. 515

Figure 11-46. Daily time series representing key water quality variables for the Cold Flush scenario at RM 96 on the LDR. 517

Figure 11-47. Average daily results of the Flushing Flow scenario at RM 96 on the LDR. 520

Figure 11-48. Average daily results of the Flushing Flow scenario at Moody (RM 1) on the LDR. 521

Figure 11-49. Longitudinal profiles of model results from ReReg Dam (RM 100.1) to the LDR's mouth (RM 0). 522

Figure 11-50. Results from a sensitivity run that included limited periphyton development.... 524

Figure 11-51. Daily average values for a simple model run with limited periphyton development from ReReg Dam (RM 100.1) to the LDR's mouth (RM 0). 525

Figure 11-52. Projected mean yearly air temperatures for the area around Round Butte Dam from 2006 to 2099. 526

Figure 11-53. Time series of daily model results for the HadGEM 8.5 climate scenario in the surface water of Round Butte forebay (RES07). 528

Figure 11-54. A comparison of the differences between the baseline and HadGEM 8.5 scenario daily values in the tailraces of the reservoirs across four seasons. 530

Figure 11-55. Time series of daily model results in for the HadGEM RCP 8.5 (years 2089–2091) climate scenario at ReReg tailrace. 531

Figure 11-56. A comparison of daily results at Moody (RM 1) on the LDR from the HadGEM 8.5 scenario. 532

Figure 11-57. Hourly baseline water temperatures with the Isaak et al. (2017) projected temperature delta applied during the summer months. 535

Figure 11-58. Time series of daily model results of the 2040 and 2080 Future Tributary Temperature scenarios in the surface water of Round Butte forebay (RES07). 537

Figure 11-59. Time series of daily model results for the 2040 and 2080 Future Tributary Temperature scenarios in the tailrace water of the ReReg Reservoir. 539

Figure 11-60. A comparison of daily results from the 2040 and 2080 Future Tributary Temperature scenarios on the LDR at RM 96. 540

Figure 11-61. A comparison of daily results from the 2040 and 2080 Future Tributary Temperature scenarios on the LDR at Moody (RM 1). 541

Figure 11-62. Boxplots presenting the subdaily modeled data from RM 96 used in developing the statistical tests. 543

Figure 11-63. Boxplots presenting statistical summaries of the subdaily modeled data at Moody (RM 1). 544

Figure 11-64. Radar plots outlining the differences in mean values between the scenarios and baseline model. 548

Figure 11-65. Longitudinal profiles of water temperature taken at three different points in time on June 15, 2015. 549

Figure 11-66. Mean water temperature and comparison intervals for each scenario and the baseline. 551

Figure 11-67. Mean DO concentrations and comparison intervals for each scenario and the baseline. 552

Figure 11-68. Mean pH values and comparison intervals for each scenario and the baseline. . 553

Figure 11-69. Mean NO_3 concentrations and comparison intervals for each scenario and the baseline. 554

Figure 11-70. Mean phytoplankton concentrations and comparison intervals for each scenario and the baseline. 555

Figure 11-71. Mean periphyton densities and comparison intervals for each scenario and the baseline. 556

Tables

Table 1-1. A summary of water bodies on the 2012 303(d) list relevant to the LDR. 5

Table 2-1. Average phosphate (PO_4) and total phosphorous (TP) concentrations in springs, lakes, rivers, and wells in the Deschutes River basin. Locations are shown in Figure 2-3. 11

Table 2-2. PGE weather stations and data available for model configuration. 20

Table 2-3. Discharge statistics for the Madras and Moody USGS stream gages on the LDR. ... 25

Table 3-1. Sample site locations on the LDR for the monitoring component of the Water Quality Study. 31

Table 3-2. The data collected and analysis methods used at the LDR and tributary sampling sites. 32

Table 3-3. Monitoring sites and locations in the impoundments and tributaries 37

Table 3-4. The data collected and analysis methods used at LBC and Lake Simtustus sampling sites. 38

Table 3-5. Summary of the quality assurance analysis. 41

Table 3-6. Analysis of replicate samples from 2015–2017. 45

Table 4-1. Daily average discharge statistics for the three primary tributaries to LBC for the water years of the study (2015–17) and for the PoR. 50

Table 4-2. Daily average discharge statistics for the three primary tributaries to LBC (WR2015–2017) from May through September 52

Table 4-3. Daily average water temperature statistics (in ˚C) for the three primary tributaries to LBC (WY2015–2017) from May through September and for the entire period. 53

Table 4-4. Nutrient concentrations measured in the three principal tributaries to LBC for 2015–2016 64

Table 4-5. Water chemistry of Willow Creek measured in 2015 and 2016. 115

Table 4-6. Summary statistics for concentrations of nutrients from the three tailraces for 2015–2016 149

Table 5-1. Comparison of nutrient concentrations at Round Butte forebay (RES07) in 1994–1996 to 2015–2017 for four depth classes. 176

Table 5-2. Comparison of nutrient concentration at Pelton forebay (RES04) in 1994–1996 to 2015–2017 for three depth classes. 194

Table 6-1. Mean and standard error of nutrients concentrations measured in the LDR. 221

Table 6-2. Phytoplankton total biovolume (10^8 µm3/mL) in the epilimnion of the two impoundments and the LDR in 2016 253

Table 6-3. River sites in Oregon used for comparison with the two ODEQ sites on the Deschutes 258

Table 7-1. Significant actions and events upstream of the ODEQ monitoring sites. 271

Table 8-1. Cropland downstream of Pelton Round Butte based on 2016 satellite imagery. 294

Table 8-2. Suggested values and ranges for maximum benthic biomass (as chlorophyll) levels to avoid problems for recreational and aesthetic use 302

Table 8-3. Percentage of periphyton samples from the LDR that would be classified as eutrophic based on a threshold. 303

Table 9-1. A listing of key categories and parameters outlined in the report. 330

Table 9-2. Average AME values for locations in the Project with thermistor and profile observations. 332

Table 9-3. Proportions used to allocate balance flows to the different arms. 338

Table 10-1. State variables captured by the 2Kw modeling framework 397

Table 10-2. Key boundary conditions developed as input for the 2015 and 2016 2Kw models. 408

Table 10-3. Mapping between required 2Kw water quality variables and available data. 409

Table 10-4. River temperature (°C) AME values for the diel data, 7-day running maximums, and 7-day running minimums for each of five locations within the LDR during 2015. 412

Table 10-5. River temperature (°C) AME values during model validation for the diel data, 7-day running maximums, and 7-day running minimums for the five locations within the LDR during 2016 414

Table 11-1. Key assumptions behind the scenario definitions. 447

Table 11-2. Estimated temperature differences and maximum periphyton growth rate parameter. 451

Table 11-3. A summary of the monthly stream temperatures for 2040 and 2080 taken from Isaak et al. (2017). 534

Table 11-4. Summary statistics for the subdaily model results from each scenario. 545

Appendices

Appendix A Water Quality Study Procedures
Appendix B Review of ZAPS Technologies LiquID Data
Appendix C Evaluation of Phytoplankton and Periphyton Data
Appendix D Selected Water Quality Profiles for Impoundment Sampling Sites
Appendix E Phytoplankton Community Composition at Reservoir Sampling Sites
Appendix F CE-QUAL-W2 Modeling Parameters
Appendix G CE-QUAL-W2 Grids
Appendix H Model Output
Appendix I QUAL2Kw Modeling Parameters

Acronyms and Abbreviations

˚C	degrees Celsius
µg/L	micrograms per liter
$\mu m^3/mL$	cubic micrometers per milliliter
µmhos	micromhos
µS	microsiemens
1-D	one-dimensional
2-D	two-dimensional
2Kw	QUAL2Kw
Ac	acre(s)
AFDW	ash-free dry weight
AME	absolute mean error (of model prediction)
ATU	attenuation units
AWQMP	Ambient Water Quality Monitoring Program
BOD	biochemical or biological oxygen demand
$CaCO_3$	calcium carbonate
CBOD	carbonaceous biochemical oxygen demand
CCAL	Cooperative Chemical Analytical Laboratory
cf.	consult
cfs	cubic feet per second, measure of streamflow
cfu	colony-forming unit
Cl^-	chloride
cm	centimeter(s)
cm/km	centimeter(s) per kilometer
cms	cubic meters per second, measure of streamflow
CO_2	carbon dioxide
CTWSRO	Confederated Tribes of the Warm Springs Reservation of Oregon
CWA	Clean Water Act
df	degrees of freedom
DIN	dissolved inorganic nitrogen

DL	detection limit
DO	dissolved oxygen
ELWS	water surface elevation
EPA	U.S. Environmental Protection Agency
F	Fisher's statistic
FDOM	fluorescent dissolved organic matter
FERC	Federal Energy Regulatory Commission
ft	foot, feet
FTU	Formazin turbidity units
GCM	Global Climate Model
$gD/m^2/d$	grams dry weight per meter squared per day
HadGEM	Hadley Center Global Environment
hr	hour(s)
IEH	IEH Laboratories & Consulting Group
km	kilometer(s)
kWh	kilowatt-hour(s)
LBC	Lake Billy Chinook
LDR	Lower Deschutes River
LiDAR	Light Detection and Ranging
LOESS	locally estimated scatterplot smoothing
m	meter
m/s	meter(s) per second
mg/L	milligrams per liter
mg/m^2	milligrams per square meter
n	sample size
NH_3	ammonia
NH_x	reduced forms of inorganic nitrogen
NO_2	nitrite
NO_3	nitrate
ns	not significant (at $p \leq 0.05$)
NTU	Nephelometric Turbidity Unit

ODEQ	Oregon Department of Environmental Quality
ODFW	Oregon Department of Fish and Wildlife
OHA	Oregon Health Authority
OWRD	Oregon Water Resources Department
p	*p* value
PGE	Portland General Electric
PNW	Pacific Northwest
PO_4	phosphate
PoR	period of record
PRB	Pelton Round Butte
Project	Pelton Round Butte Hydroelectric Project
RCP	Reference Concentration Pathway
ReReg	Reregulating Dam, ReRegulating Reservoir
RM	river mile
RTR	relative thermal resistance
sd	standard deviation
se	standard error (of the mean)
SNOTEL	Snow Telemetry
SNTEMP	Stream Network Temperature model
SRA	State Recreation Area
SWW	Selective Water Withdrawal
TDN	total dissolved nitrogen
TIC	total inorganic carbon
TKN	total Kjeldahl nitrogen
TN	total nitrogen
TOC	total organic carbon
TP	total phosphorus
USBR	U.S. Bureau of Reclamation
USGS	U.S. Geological Survey
W2	CE-QUAL-W2
WY	water year

Executive Summary

In December 2009, Portland General Electric (PGE) and the Confederated Tribes of the Warm Springs Reservation of Oregon (CTWSRO) (the Licensees) began operating a new structure in Lake Billy Chinook (LBC) called the Selective Water Withdrawal (SWW). The purpose of the SWW is to create an attractant flow to encourage salmonids to enter the fish collection facility. It also enables operators to control the temperature of water leaving LBC by mixing warmer surface water with the colder deep-water intake previously used. The SWW was designed to provide warmer river temperatures during the spring and cooler river temperatures in the late summer and fall, mimicking a more natural temperature regime in the Lower Deschutes River (LDR). The warmer spring temperatures support optimal emergence timing and growth conditions for fall Chinook and trout.

The Licensees initiated a multiyear study of the LDR and the water feeding the river from the Pelton Round Butte Hydroelectric Project (the Project) to better understand water quality in the LDR. The Water Quality Study consists of two components:

1. A water quality monitoring effort to determine the current status of the LDR and impoundments and to serve as a basis for assessing historical changes in the system. The monitoring was conducted from 2015 to 2017 and included sampling water quality in the three tributaries to LBC, two sites LBC and Lake Simtustus, and numerous sites along the LDR and its tributaries. Monitoring included measuring real-time conditions for temperature, pH, dissolved oxygen (DO), and other parameters with discrete sampling for nutrients (total phosphorus, phosphate, total nitrogen, nitrate and ammonia), algae attached to the substrate (periphyton), and algae present in the water column (seston).
2. Developing numerical models of the impoundments and LDR, which enable investigators to forecast possible changes to the LDR that might result from changes in nutrient inputs, Project operations, and other potential measures to mitigate water quality response in the LDR. A two-dimensional (2-D) model, CE-QUAL-W2 (W2), was applied to the impoundments and was used to generate inputs to the one-dimensional (1-D) QUAL2Kw

(2Kw) model for the LDR. The models were calibrated to data collected in 2015, and the output was compared to measured water quality data in 2016–2017. The models were used to test 11 hypothetical scenarios involving changes to Project operations, watershed management, and climate.

Monitoring Component LBC and Lake Simtustus are highly productive (or eutrophic), with high concentrations of chlorophyll and high pH and DO values in the surface waters during the warmer months. LBC has high densities of the centric diatom, *Stephanodiscus* spp., from fall through spring and moderately high densities of blue-green algae (cyanobacteria *Dolichospermum/Anabaena*) in the summer. Lake Simtustus is largely dominated by diatoms year-round, in part, because of nitrogen inputs from Willow Creek entering the lake from the east. Water quality data from LBC collected for this study were compared with data from a previous study conducted as part of the licensing activities for the Project in 1994–1996 and another study conducted by the Oregon Department of Environmental Quality (ODEQ) in 2006.

The monitoring data showed that the Crooked River contributes nearly one-half of the dissolved phosphorus to LBC and over 86% of the dissolved nitrate (NO_3) to the impoundment. The Metolius River provides about one-third of the dissolved phosphorus and only 4% of the NO_3 to LBC. The Deschutes River provides about 18% of the dissolved phosphorus and 10% of the NO_3 to the impoundment. The Metolius River represented 39.5% of the mean annual surface flow into LBC during the study compared to 38.3% for the Crooked River and 22.2% for the Deschutes River. Thus, the Crooked River provides a disproportionately high percentage of NO_3 to LBC. The vast majority of the phosphorus entering LBC is derived from natural weathering of the volcanic rocks in the Deschutes River basin, whereas most of the inorganic nitrogen entering LBC is derived from anthropogenic sources.

LDR is also productive and has about the same density of suspended algae as the surface waters of LBC. The periphyton (attached algae and cyanobacteria) on the rocky substrate in the river was dominated by *Cladophora* spp., a filamentous green algae, in 2015 and 2016, but its biovolume declined dramatically in summer 2017. During 2015 and 2016, the periphyton group with the highest biovolume was chlorophytes (green algae) followed by cyanophytes (blue-green

algae), followed by diatoms. However, in summer 2017, with the decline of *Cladophora*, all three periphyton groups had similar biovolumes. The dramatic change in periphyton community composition from 2016 to 2017 may be related to the higher flows in spring 2017, which could have dislodged a high proportion of the filamentous green algae. There was also a considerable amount of entrained phytoplankton transported to the LDR from the Project that was largely comprised of centric diatoms (*Stephanodiscus* spp.) and cyanobacteria (*Dolichospermum/Anabaena*). The LDR is generally nitrogen-limited, indicating that reducing nitrogen inputs likely would yield the greatest reduction in periphyton in the river. Concentrations of phosphorus exhibited a minor decline throughout the length of the LDR, whereas concentrations of NO_3 (the dominant inorganic, available form of nitrogen) exhibited considerable uptake proceeding down the river.

Data collected in this study on the LDR were compared with data from the pre-licensing investigation and with ODEQ data collected on the river since the 1960s. The historical data on the LDR are subject to more uncertainty than the data on the impoundments, but the available data indicate that the river also has become more productive, with higher measurements of daytime pH and DO observed in recent years.

The most significant contributor to current conditions in the impoundments and the LDR appears to be associated with nutrient inputs from the three major tributaries. The operation of the SWW has resulted in a greater proportion of the discharge from Round Butte Dam being comprised of water from the Crooked River. Travel time from the Crooked River inlet to the SWW intake structure is about three weeks, which is more than sufficient to have the nitrate contributions from the Crooked River assimilated by phytoplankton. Consequently, the nitrate in LBC forebay is likely derived from decomposition of algae and oxidation of reduced forms of nitrogen. The nitrogen-rich water appears to promote increased primary production, at least at the locations in the reservoir from which samples were collected, a conclusion supported by the fact that the phytoplankton population has increased in those locations. This highly productive epilimnetic water containing phytoplankton is then transported down the LDR. Primary production has increased in the LDR likely from increased temperature and availability of nitrogen. However, the SWW allows the Project to release water that more closely matches the temperature the river

would have just below the ReReg Dam if the Project were not in place: warmer spring temperatures and cooler late summer, early fall temperatures. This more natural thermal pattern in the LDR is intended to facilitate spawning, emergence, and growth of anadromous fish.

An examination of peak flows in the LDR suggests that the construction of dams throughout the Deschutes River basin has resulted in a decline in peak river flows during the spring. Peak river flows now are more common in winter, which may be caused, in part, by increasing winter temperatures and a reduction of the snowpack in the Cascade Range. More precise work on the contributions of dam construction and operation and climate change is needed to establish their role in changes in flows for the LDR.

Modeling Component The model software selected for the study are widely used and available to the public, and they offer a range of options for testing various scenarios. CE-QUAL-W2 was applied to all three impoundments, and the model output was used as input for QUAL2Kw. The reservoir model was calibrated to water temperature, pH, DO, nutrients, and chlorophyll. Two functional groups of algae (diatoms and cyanobacteria) were also included in the reservoir model. The river model included interactions between the water column and periphyton (attached algae) in addition to the normal water column chemistry. The calibrations were in close agreement with water temperature, but agreement between measured and modeled values decreased with the chemical and biological parameters.

The reservoir and river models were linked for analysis of 11 scenarios that explored how potential changes in Project operations, watershed management, and climate might influence water quality in the LDR. The modeling results indicated that water quality in the LDR is a complex function of climate, watershed inputs, and release-induced mixing within the impoundments. Nutrient inputs from the Crooked River into LBC are transported downstream to the LDR and contribute to the river's productivity. Operational changes to the SWW might improve LDR water quality; however, it is important to preserve the smolt-attraction flows at critical times. Also, cold water in LBC will become an increasingly scarce resource in late summer if forecasted changes in climate are realized. Increased temperatures in the reservoirs could lead to further changes in water quality within the reservoirs and in the LDR.

1 Introduction

The Lower Deschutes River (LDR) extends from the Reregulating (ReReg) Dam at river mile (RM) 100.1 to the mouth of the river at its confluence with the Columbia River. Because most of the flow to this reach of the river is controlled by releases from the Portland General Electric (PGE) and Confederated Tribes of the Warm Springs Reservation of Oregon (CTWSRO) (the Licensees) co-owned Pelton Round Butte Hydroelectric Project (the Project), it is logical that questions about water quality in the LDR often refer to the Project and its operation. In recent years, there has been increased attention on water quality in the LDR as various groups have questioned the effect of operational changes to the Project. Most of the inquiries focus on the Selective Water Withdrawal (SWW), a fish collection facility in Lake Billy Chinook (LBC) that became operational on December 3, 2009. The purpose of the SWW is to create an attractant flow in the surface water of LBC to encourage smolts to enter the fish collection facility, while enabling operators to create a blend of waters that more closely reproduces the temperature in the LDR that would occur naturally if the Project was not in place (Huntington et al. 1999). The Licensees anticipated that restoration of a more natural thermal pattern in the LDR waters would facilitate spawning, emergence, and growth of anadromous fish. Operation of the SWW is a condition of the Project's Federal Energy Regulatory Commission (FERC) license.

The SWW blends water from the hypolimnion and the epilimnion of LBC. The original intake structure at Round Butte Dam was positioned in the hypolimnion with a mid-point depth of 75 meters (m) (246 feet [ft]). With the SWW, a maximum of only 60% of hypolimnetic water passes through the lower intake while allowing 40%–100% of the flow from the upper 12.2 m (40 ft) of the impoundment.

The SWW has been successful in meeting its two intended purposes: creating an attractant flow to the dam for collection of smolts and providing cooler river temperatures in the late summer and fall and warmer river temperatures during the spring. Changes to the intake structure, however, have raised questions about the addition of surface waters from LBC to the LDR having adversely altered water quality in other ways. LBC is a highly productive reservoir and

transport of the surface water might carry additional nutrients and/or phytoplankton from the impoundment downstream, which could enrich the waters of the LDR and promote undesirable conditions.

The Licensees have sought to address these concerns by initiating a study of the LDR and its impoundments to determine the status of water quality in the river.

1.1 Objectives of the Water Quality Study

The primary objective of studying the water quality of the LDR was to characterize the current water quality in the river from the terminus of the Project immediately below the ReReg Dam to its confluence with the Columbia River. The specific water quality aspects defined for this study were the nutrient status of the waters, the temperature regime, diel fluctuations in pH and dissolved oxygen (DO), and the biovolume and composition of attached and suspended algal communities. The field measurements encompassed all seasons and extended over multiple years to help characterize temporal variability in water quality. Sites were distributed along the length of the river to define longitudinal conditions and to help clarify processes that might alter water quality throughout the length of the river. To the maximum extent practical, sites were co-located with those in a previous study by Raymond et al. (1998) to help quantify possible water quality changes over the last 20 years. The monitoring results were also intended to facilitate comparisons with historical data, including data collected by Raymond et al. and the Oregon Department of Environmental Quality (ODEQ) through its Ambient Water Quality Monitoring program (AWQMP).

Both major impoundments in the Project, LBC and Lake Simtustus, were also monitored. The goal for that effort was to characterize water entering the LDR, rather than to fully characterize water quality throughout the impoundments. Each impoundment was monitored at its respective forebay. Monitoring was also conducted at a Mid-Lake site for Lake Simtustus and at the Common Pool near the confluence of the Deschutes River and Crooked River arms for LBC.

The monitoring data were used to calibrate a two-dimensional (2-D) hydrodynamic model—CE-QUAL-W2 (W2)—for both major reservoirs and the ReReg Reservoir. The output from the W2 model for the ReReg Reservoir was used as input for a one-dimensional (1-D) model—

QUAL2Kw (2Kw)— to explore how potential changes in watershed management, climate, and Project operations may influence water quality in the LDR.

The report issued in June 2019 included periphyton data for the LDR provided by a contract laboratory that was determined to be incorrect after the final report was published. The report has been revised to reflect the corrected periphyton data provided by the laboratory in 2020.

1.2 Water Quality and Regulatory Context

The ODEQ regulates water quality in Oregon pursuant to the Clean Water Act (CWA) and state law. The Oregon Environmental Quality Commission, ODEQ's governing body, promulgates water quality standards, and ODEQ identifies water bodies that do not meet those standards. A detailed description of Deschutes River basin-specific standards is available online (ODEQ 2018). The water bodies determined by ODEQ not to meet water quality standards are identified in ODEQ's CWA subsection 303(d) list and are available online (ODEQ 2012). The LDR and its tributary, Trout Creek, do not meet Oregon water quality standards for temperature (Table 1-1). Two of the three major tributaries to the Project, the Upper Deschutes River and the Crooked River, are also listed as not meeting water quality standards for several parameters, including temperature, pH, DO and turbidity. Although chlorophyll is listed in the state standards, it is used as a guideline and not as an enforceable standard. The Crooked River is notable for its number of exceedances, the duration of those exceedances, and the geographic extent of the 303(d) listings throughout the Crooked River basin.

The two principal impoundments in the Project, LBC and Lake Simtustus, are also on the 303(d) list for pH and chlorophyll. ODEQ expects that LBC will also be listed for aquatic weeds and algae under the Harmful Algal Blooms category on the updated 303(d) listing (Becky Anthony, ODEQ, pers. comm., February 4, 2019). The Oregon Health Authority (OHA) posted advisories for the reservoir in 2015–2017 for recreational exceedances of the cyanobacterial toxin, microcystin. The OHA health advisory level for recreational contact with waters containing microcystin is 4 micrograms per liter (µg/L) and LBC had reported values of 225 µg/L (June 25, 2015); 10,450 µg/L (July 1, 2016); 135 µg/L (July 8, 2016); and 27.1 µg/L (June 30, 2017).

Numerical analyses of microcystin and other cyanotoxins were generally not available on a routine basis in Oregon prior to 2015.

Table 1-1. A summary of water bodies on the 2012 303(d) list relevant to the LDR. These water bodies are Category 5 listings, which represent instances in which water quality standards are not met, and which require the establishment of a total maximum daily load under the CWA.

Water Body	Site #	River Mile[b]	Parameter	Season – Criteria
Lower Deschutes River[a]	1209151456389	0–46.4	Temperature	Sep 1–Jun 30 – Spawning Summer – Rearing
			pH	Summer
		46.4–99.8	Temperature	Sep 1–Jun 30 – Spawning
			pH	Fall/winter/spring
		83.8–99.8	DO	Oct 15–Jun 15 – Spawning
Trout Creek	1210877448214	0–13.6	Biocriteria[c]	Year round
		0–50.7	Temperature	Year round Includes its tributaries
Lake Simtustus	1212585446551	--	pH	Summer
			Chlorophyll	Summer
Lake Billy Chinook[d]	1212653445438	--	pH	Summer
			Chlorophyll	Summer
Crooked River	1212676445778	0–51	E. coli	Summer
			pH	Fall/winter/spring/summer
			Temperature	Summer – Rearing Includes most tributaries to the Crooked River
Upper Deschutes River	1209151456389	116–222	pH	Fall/winter/spring/summer
			DO	Jan 1-May 15 – Spawning
			Temperature	Year round
			Turbidity	Spring/Summer
			Chlorophyll	Summer

Source: ODEQ 2012

Notes:

[a] Does not include all tributaries to LDR that are listed for temperature (e.g., Bakeoven Creek, Buckhollow Creek, Clear Creek, Gate Creek, Oak Canyon, Rock Creek, Sixteen Canyon, Tenmile Creek, Wapinitia Creek, White River, and Willow Creek).

[b] 0 = mouth of the LDR at RM 0.

[c] Waters of the State must be of sufficient quality to support aquatic species without detrimental changes in the resident biological communities (OAR 340-041-0011).

[d] LBC was not listed under aquatic weeds or algae in the 2012 Integrated Report, but DEQ expects that the updated report will list LBC based on the HABs listing criterion, which states s that any water body listed two or more times by the OHA is to be listed under a Category 5 (TMDL needed) listing (Becky Anthony, ODEQ, pers. comm., February 4, 2019).

2 Study Area

2.1 The Deschutes River Basin

The Deschutes River basin is often divided into upper, middle, and lower portions (Figure 2-1). The Upper Deschutes River basin (which also is the southernmost portion) originates in the Cascade Range and includes several natural lakes and impoundments. The U.S. Bureau of Reclamation (USBR) operates Wickiup Reservoir on the Upper Deschutes River, which stores water that can be diverted downstream to support irrigation districts located farther north. The Middle Deschutes River basin consists of the reach from the city of Bend to the inlet of LBC and includes the Crooked River on the east side of the basin. The Lower Deschutes River basin extends from LBC to the confluence with the Columbia River and includes all the Project area (LBC, Lake Simtustus, and the ReReg Reservoir). This study focuses on the Lower Deschutes River basin.

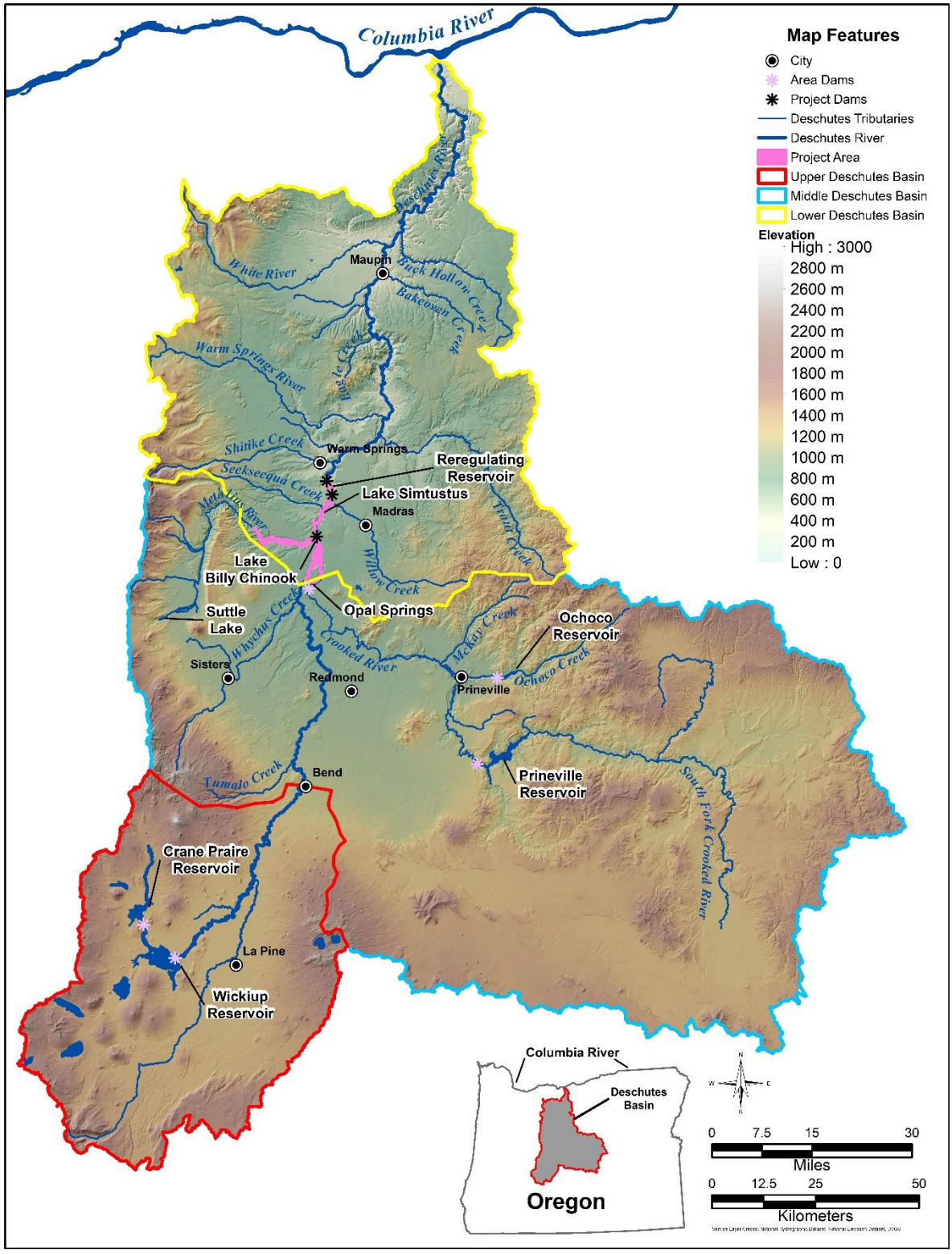

Figure 2-1. The division of the Deschutes River basin and its topographic relief.

2.1.1 Geology

The geology of the Deschutes River Basin is dominated by vulcanism, as evident by the volcanic rocks from the numerous volcanoes that span the length of the Oregon Cascade Range (Figure 2-2). The subduction zone created by the Pacific plate sliding under the continental plate results in tremendous friction, heating and creation of magma, some of which is released through the strato-volcanoes and some which has been released as large basalt flows extending over considerable portions of the basin. The study area included the Jefferson Creek formation to the north and west, the Metolius River formation to the west, the Deschutes River formation and the Trout Creek formation. To the east, the Deschutes formation transitions to the older and less permeable John Day formation (Caldwell and Truini 1997). The youthful formations on the west side of the basin are subject to weathering reactions, a process that is aided by the abundant fractures in the basalt and extensive vertical flow paths. This results in a relatively low-density stream network and abrupt discharge of groundwater in large springs. Some of these springs form the headwaters of rivers (e.g., Metolius River) and others are submerged under lakes (e.g., Lava Lake; Eilers et al. 2005). Gannett et al. (2001) estimate that about 50% of the groundwater flowing from the Cascades discharges as spring-fed rivers. The basalts are comparatively rich in phosphorus (c.f., Krauskopf 1979) and it is common to observe concentrations of ortho-phosphorus from 0.05 to 0.1 mg/L and greater. A brief compilation of phosphorus data from springs, rivers, lakes and wells in the area illustrates this widespread source of phosphorus to surface waters in the basin and throughout much of central Oregon adjacent to the Cascades (Table 2-1 and Figure 2-3). Springs that directly discharge in or near the Project area include the Metolius Springs, Opal Springs, Spring #12, and Oak Springs. Metolius Springs serves as the headwaters for the Metolius River and contains some of the highest concentrations of phosphorus. Spring #12 discharges into the Middle Deschutes River above the confluence with LBC and Opal Springs is one of a number of springs discharging into the lower six miles of the Crooked River. Further upstream in the Upper Deschutes River basin, there are multiple springs that impact the Deschutes River, including the area around Benham Falls (Gannett et al. 2001) and headwater lakes such as Lava Lake (Eilers et al. 2005). Thus, all three tributaries have major springs that contribute natural sources of phosphorus. Further downstream on the LDR, Oak

Springs and other unnamed springs continue to supply phosphorus to the river. Gannett et al. (2001) estimated that LBC receives about 420 cubic feet per second (cfs) as direct groundwater inflow. We have no chemical measurements of these inflows, but it is likely that the phosphorus concentrations in these inflows equal or exceed those values measured in the surface inflows. This adds to the natural loading of phosphorus to the system.

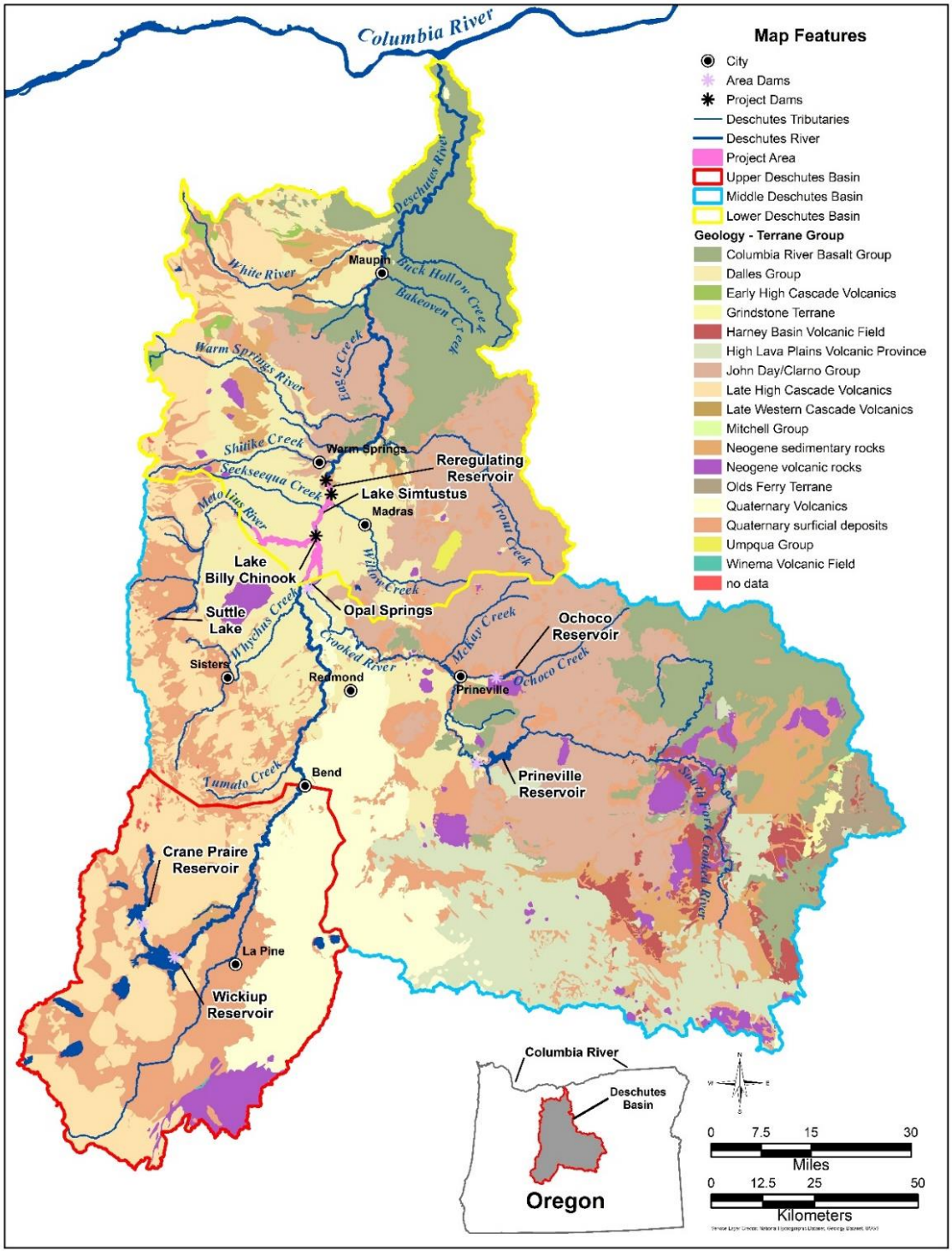

Figure 2-2. Geologic map units of the Deschutes River basin.

Table 2-1. Average phosphate (PO_4) and total phosphorous (TP) concentrations in springs, lakes, rivers, and wells in the Deschutes River basin. Locations are shown in Figure 2-3.

Site	Source	Sample Size	PO_4 (mg/L)	TP (mg/L)
Springs				
Metolius Spring *Headwater of the Metolius River*	ODEQ AWQMP Site #10515	15	0.249	--
Oak Springs *Along Deschutes River, RM 50.6*	Current study	6	0.062	--
BLM Spring #12 *Along Deschutes River, RM 129.2*	ODEQ AWQMP Site #35893	2	0.097	--
Opal Springs *Along Crooked River*	Caldwell & Truini 1997	1	0.08	--
Spring #1 *Big Lava Lake*	Eilers et al. 2005	4	0.083	--
Virgin River Springs *Along the Crooked River*	Caldwell & Truini 1997	1	0.08	--
Alder Springs *Along Squaw Creek*	Caldwell & Truini 1997	1	0.08	--
Paulina Springs *Along Indian Ford Creek*	Caldwell & Truini 1997	1	0.07	--
Source Springs *Along Bridge Creek*	Caldwell & Truini 1997	1	0.05	--
Spring River Springs *Along Deschutes River*	Caldwell & Truini 1997	1	0.12	--
Fall River Spring *Headwater of Fall River*	ODEQ AWQMP Site #35919	2	0.10	--
Rivers				
Short Creek *Tributary of Diamond Lake*	ODEQ AWQMP Site #35893	7	0.058	--
Silent Creek *Tributary of Diamond Lake*	ODEQ AWQMP Site #25248	7	0.056	--
Spring River *Tributary of Lemolo Lake*	Eilers et al. 2003	5	0.063	--
Lakes				
Devils Lake *Deschutes National Forest*	Johnson et al. 1985	1	--	0.072
Clear Lake *Willamette National Forest*	Johnson et al. 1985	1	--	0.039
Hosmer Lake *Deschutes National Forest*	Johnson et al. 1985	1	--	0.069
Todd Lake	Johnson et al. 1985	1	--	0.063

Site	Source	Sample Size	PO_4 (mg/L)	TP (mg/L)
Deschutes National Forest				
Suttle Lake *Deschutes Nation Forest*	Johnson et al. 1985	1	--	0.066
Wells				
Upper Deschutes River basin	Caldwell & Truini 1997	30	0.097	--

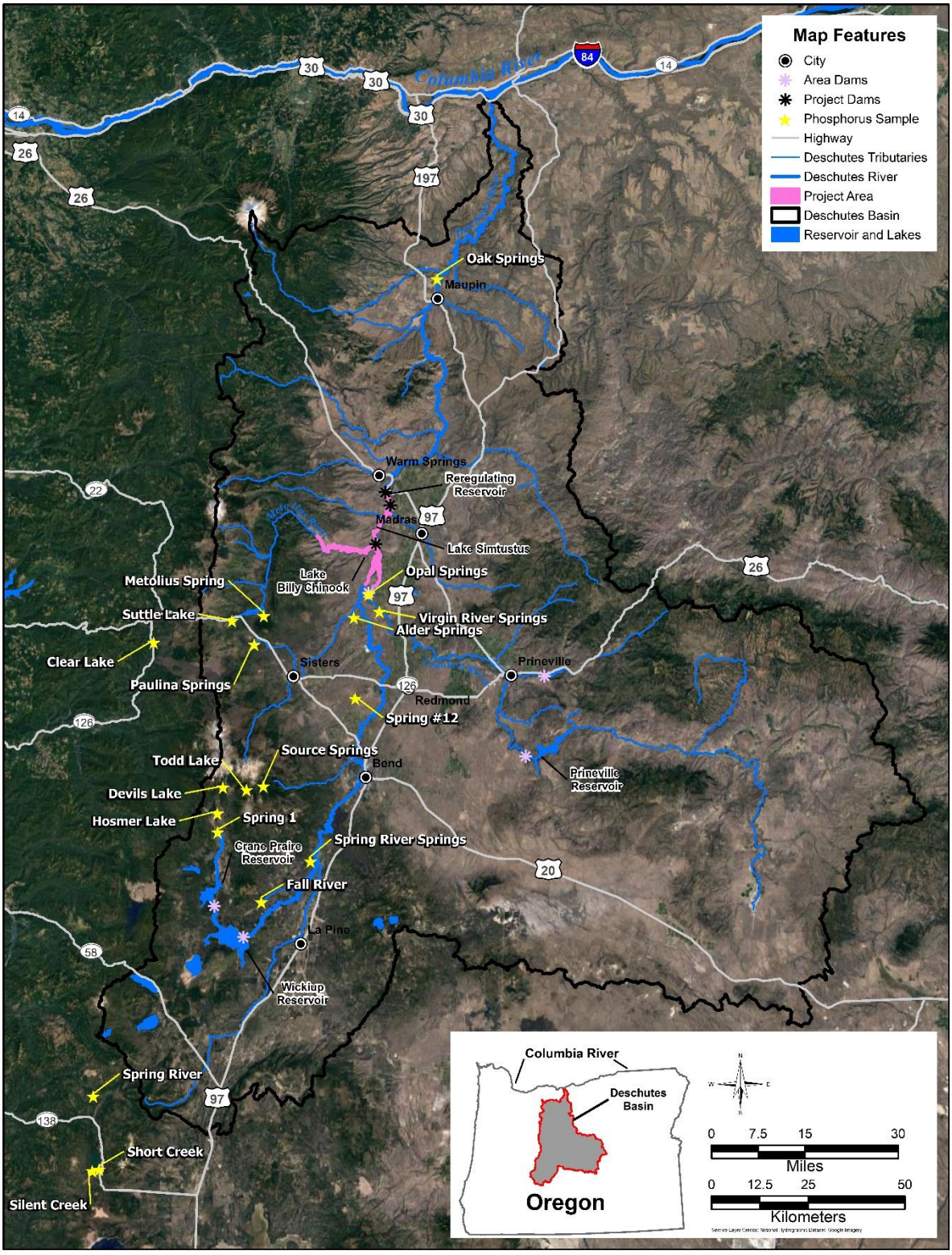

Figure 2-3. Locations of the phosphorus sampling sites summarized in Table 2-1.

2.1.2 Land Cover

The predominant land-cover types in the basin are coniferous forests in the uplands and desert shrub/scrub in the lower elevations (Figure 2-4). Developed and urban land areas are few (e.g., Bend, Redmond, and Prineville), but are located primarily along the Deschutes and Crooked rivers. The only significant area of developed land along the LDR is at Maupin (population 418), midway between the ReReg Dam and the mouth of the LDR.

Cultivated lands in the Middle and Lower Deschutes basins are generally located along the Crooked River, the Middle Deschutes reach, and tributary catchments to the LDR. The largest concentration of irrigated cropland is along the eastern shore of LBC and extends north to the Trout Creek drainage. Irrigated return flows along the Crooked River contain high concentrations of nitrogen and phosphorus (Crooked River Watershed Council, unpublished data). Other significant areas of cropland are located in Wapinitia and White River catchments. The role of cropland and water quality in the LDR is discussed in Section 8.4.2.

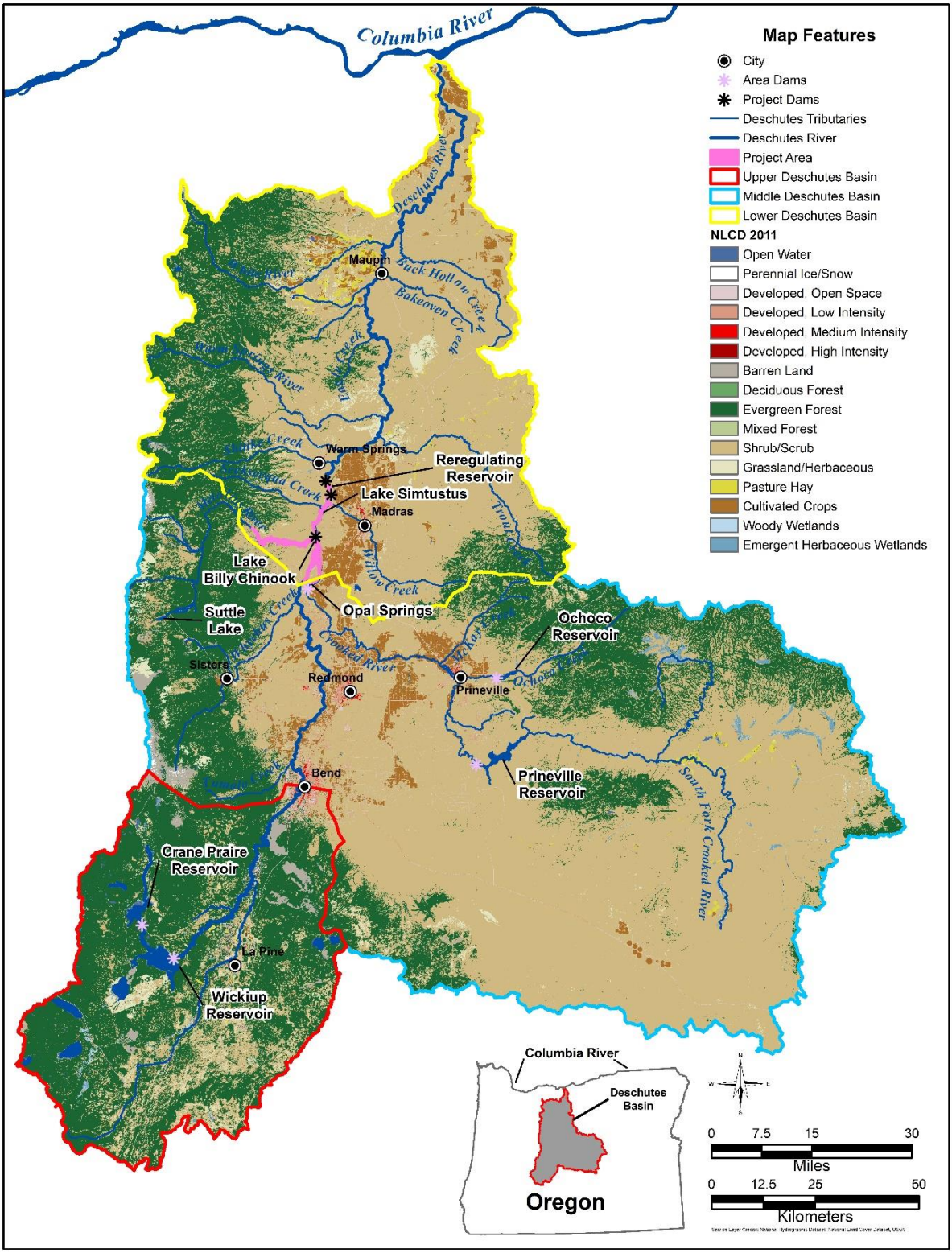

Figure 2-4. Land-cover types in the Deschutes River basin (*Source*: NLCD 2011).

2.2 Project Operations

The Project is comprised of three impoundments and dams: LBC and Round Butte Dam, Lake Simtustus and Pelton Dam, and ReReg Reservoir and ReReg Dam (Figure 2-5). LBC is a 4,000-acre (-ac) reservoir, comprising the Crooked, Deschutes, and Metolius river arms. Surface elevation in LBC fluctuates less than 10 ft seasonally and 1 ft daily. Spill is uncommon at Round Butte Dam. The last time spill was necessary for flow conditions at the dam was during the 1996 flood. In all other circumstances, water must flow through the SWW to move downstream.

Water enters the SWW through the surface water intake (0–40 ft) or deep-water intake (246 ft). It draws between 40% and 100% of discharge from the top 40 ft of LBC. Therefore, it is always drawing water from the surface of LBC; only the percentage of flow from the top and bottom gates varies. Regardless of where the water enters the SWW, it is combined in a vertical flow conduit and enters the turbines at the base of Round Butte Dam.

Fish passage and water quality requirements of the Project's FERC license and CWA Section 401 certification, designed to restore natural temperature regimes to the LDR and provide fish passage at Round Butte Dam, guide the blend of water between the two intakes. In general, maximum surface water is withdrawn from November to February to conserve cold water for the warmer months. From February to May, maximum surface water is provided to support fish collection at the SWW during the smolt outmigration. Starting in about May, when discharge temperatures at the ReReg Dam approach 13 degrees Celsius (°C), the percentage of bottom water is gradually increased to keep the discharge temperature below the calculated without-project temperature (by up to 0.5°C for 3 days). The without-project temperature is the temperature the river would have just below the ReReg Dam if the Project were not in place. It is expressed as a moving 7-day average of daily maximum temperatures. The percentage of bottom water continues to increase throughout the summer season, until full-bottom gate opening (60% bottom water) is reached, generally in July. The Project remains at full-bottom withdrawal until November 1, at which time withdrawal returns to 100% surface withdrawal.

From Round Butte Dam, water flows into the 540-ac Lake Simtustus. Similar to LBC, Lake Simtustus experiences minimal water elevation fluctuations, typically 3 ft seasonally and less

than 1 ft daily. Water discharged from Round Butte Dam takes approximately 30 hours (hr) to reach Pelton Dam, where it enters the dam through the bottom intakes at 145 ft. From Pelton Dam, water enters the ReReg Reservoir.

Unlike the other two reservoirs, the ReReg Reservoir is relatively small (190 ac), has large daily fluctuations (15 ft/day is typical), is closed to the public, and supports no public fisheries. Water moves through the ReReg Reservoir quickly, and remains in the reservoir less than 12 hr. Water is discharged from the ReReg Dam into the LDR through the bottom intakes or spills, depending on the time of year. The ReReg Reservoir is operated to attenuate high- and low-peak flows produced by Round Butte and Pelton dams. Flow release from the ReReg Dam is controlled to maintain an average daily flow in the LDR that approximates the average daily flow into the Project.

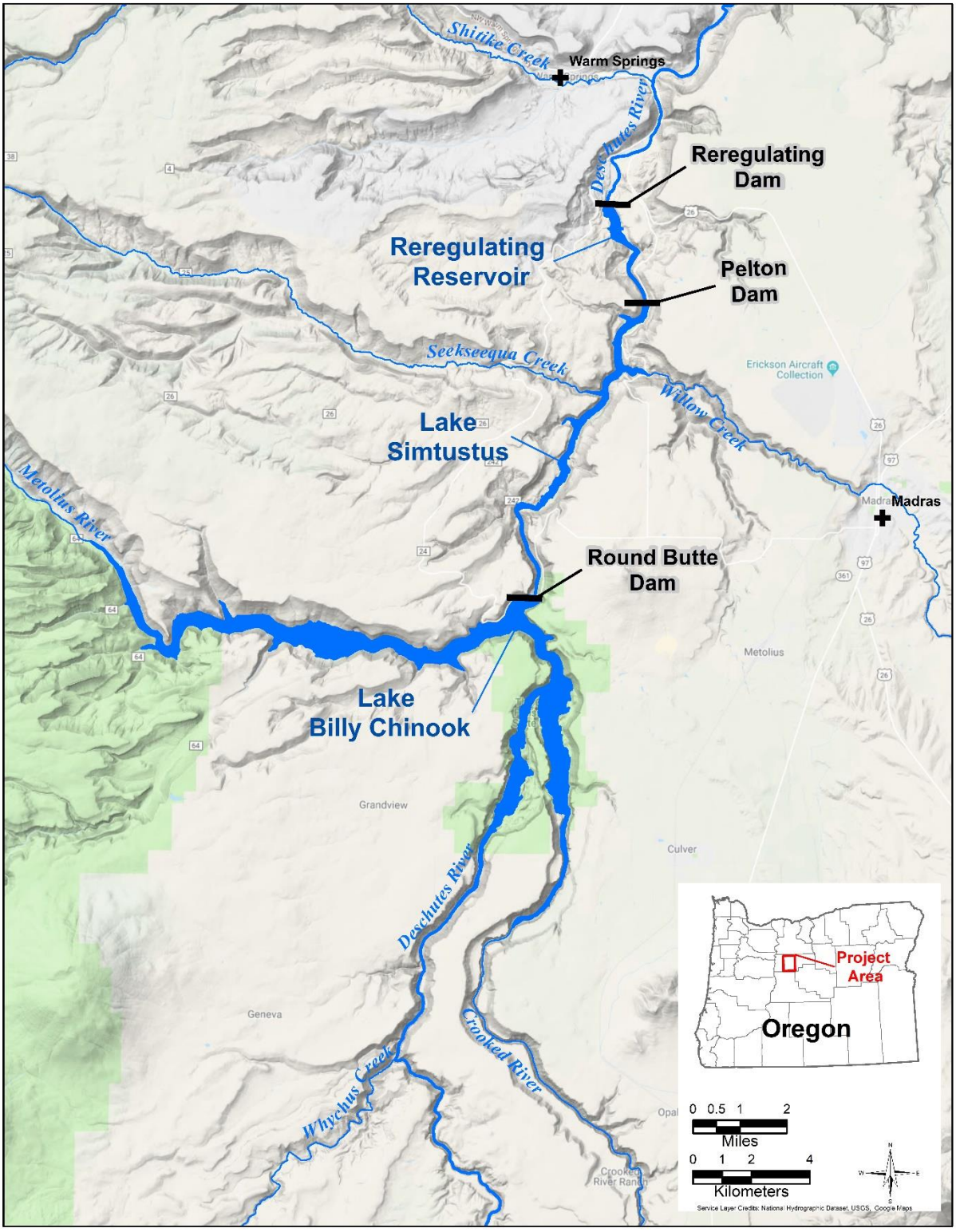

Figure 2-5. The Pelton Round Butte Project area.

2.3 Hydrology and Climate Overview

2.3.1 Meteorological Data

Meteorological data from one external site and six sites operated and maintained by PGE were compiled into a composite dataset for each of the three modeled reservoirs (Table 2-2). Decisions on which weather stations to use were based on proximity to the simulated reservoir and availability of certain data elements. For dates and weather variables PGE did not collect, data from the Madras AgriMet weather station (mrso) were used. AgriMet is the Cooperative Agricultural Weather Network sponsored by USBR with support from the U.S. Department of Agriculture, land grant universities, the Cooperative Extension System, electric utilities, power companies, and other public and private agencies and organizations. Cloud cover data, not available at the reservoir stations or through AgriMet, was taken from the weather station at Redmond Airport.

A prominent feature of the Deschutes River basin is the profound rain-shadow effect of the Cascade Range. Most of the precipitation driving the flows in the basin fall in the Cascade Range creating a semi-arid climatic regime in the eastern portion of the basin. Not only does the Cascade Range capture much of the precipitation, but the rain shadow it produces results in additional cloud-free days to the east. For example, the area near the ReReg Dam receives nearly 6 kilowatt-hours per square meter per day ($kWh/m^2/day$) of solar radiation compared to about 3 $kWh/m^2/day$ for the Portland area (NREL 2017). The combination of a high percentage of sunny days, exposed volcanic rocks, and lower elevation in the LDR canyon results in warm conditions throughout much of late spring to early fall.

Table 2-2. PGE weather stations and data available for model configuration. All weather data were collected at 15 minute intervals. Cloud cover data were derived from the Redmond Airport.

Site	Year	Dates	Temp	PAR	WS	GS	WD	RH
Buckhollow *LDR*	2015	3/5-10/22	x	x				
	2016	1/1-8/17	x	x				
	2017	1/1-9/14	x	x				
Chinook Island *Metolius River Arm, LBC*	2015	3/20-10/15	x	x	x	x	x	
	2016	1/1-8/9	x	x	x	x	x	
	2017	1/1-11/2	x	x	x	x	x	
Crooked River *Near Common Pool in LBC*	2015	NA						
	2016	1/1-8/9	x	x	x	x	x	
	2017	1/1-11/1	x	x	x	x	x	
LDR Mouth *LDR*	2015	3/5-10/21	x	x				
	2016	1/1-8/16	x	x				
	2017	1/1-11/10	x	x				
Pelton Dam	2015	5/27-8/10	x	x	x	x	x	
	2016	1/1-8/9	x	x	x	x	x	
	2017	2/20-11/10	x	x	x	x	x	x
Round Butte Dam	2015	2/18-7/29	x	x	x	x	x	
	2016	1/1-8/9	x	x	x	x	x	x
	2017	1/1-10/10	x	x	x	x	x	

Notes: DT = dew point temperature; GS = gust speed; NA = not available; PAR = photosynthetic active radiation; RH = relative humidity; Temp = temperature; WD = wind direction; WS = wind speed.

2.3.2 Water Flow Data

Flows in the LDR comprise the Upper Deschutes River, the Metolius River, the Crooked River, and several smaller tributaries, including Trout Creek, the Warm Springs River, Nena Creek, Wapinitia Creek and the White River. These are supplemented by groundwater inputs in the Project area (Yonkofski et al. 2016) and other named (e.g., Oak Springs) and unnamed springs occurring in the river canyon. Little accretion of flows is observed in the LDR canyon below Buckhollow Creek (RM 42.7), although there are no systematic flow measurements in the lower canyon to fully exclude the possibility of exchanges along the course of the lower 40 miles (mi) of the river.

The estimated percentage of groundwater contribution to LBC is 10.8%. This estimate is based on the average discharge measured from the three tributaries to LBC at the USGS stream gage sites during the three water years of the study (Oct 2015 – September 2017) compared to the estimated groundwater contribution of 420 cfs to LBC by USGS (Gannett et al. 2001). The percentage of groundwater contribution would differ slightly if the average long-term discharge from the three tributaries were used to compute the percentage instead of the data from the study years. Additionally, it's unclear if groundwater contributions to LBC have changed over the last two decades.

The cumulative flow in the LDR increases about 25% from the ReReg Dam to the mouth of the LDR based on the conditions observed June 1, 2015 (Figure 2-6). As overall discharge increases downstream, the amount of flow from tributaries along the LDR increases. As flow decreases through the summer, however, the amount and percentage of discharge from the tributaries declines. For example, flows from September 1, 2015, show that discharge at the ReReg Dam was 3,860 cfs and, at the mouth of the LDR, it was only 4,080 cfs (Figure 2-6). Thus, net tributary flow to the LDR was only about 220 cfs, or 5% of the discharge at U.S. Geological Survey (USGS) Stream Gage #14103000 at Moody, near the mouth of the LDR. Although 2015 was a drought year, the patterns among years generally repeat so the amount of discharge from the ReReg Dam becomes an increasingly greater proportion of discharge in the LDR through the summer until the rain returns in the fall.

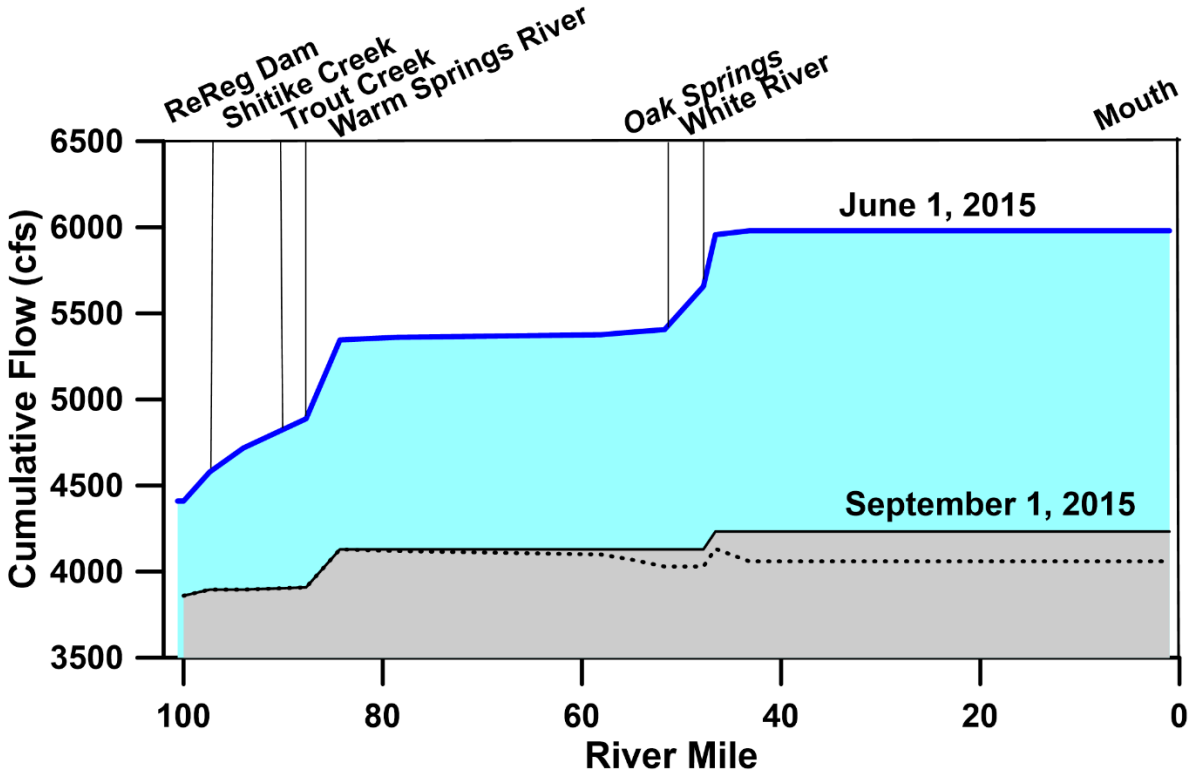

Figure 2-6. LDR cumulative flow for June 1 and September 1, 2015. For the September curve, the solid line represents the summation of measured flows and the dashed line is the summation of known flows adjusted to agree with measured flow at the mouth of the river.

Flows reflected in Figure 2-6 for the ReReg Dam, Shitike Creek, Warm Springs River, and mouth of the LDR are derived from USGS records. Flows for Trout Creek are from Oregon Water Resources Department (OWRD) and flows for Oak Springs and the White River are estimated from field observations and measurements by field personnel. All tributary inputs, except for Trout Creek, flow from the west.

Irrigation withdrawals from the LDR started in the 19th century. The relatively modest withdrawals in the basin increased through the first half of the 20th century as large impoundments were built or replaced by larger dams constructed by USBR. The large dams include Crane Prairie Dam (constructed in 1922, rebuilt in 1940) and Wickiup Dam (1949) on the Deschutes River, and Bowman Dam (1961) and Ochoco Dam (1920, 1949) on the Crooked River. Smaller diversions were constructed throughout the basin, many of which remain in

service. Consequently, the flows on the LDR have diminished over the last 150 years by some unknown amount. Additionally, the construction of dams upstream of the Project has likely altered the distribution of flows in the LDR by reducing flows associated with spring discharge.

The current cumulative flows along the LDR are punctuated by inputs from major and minor tributaries that extend between RM 97.6 (Shitike Creek) and RM 42.7 (Buckhollow Creek). There is little change in discharge in the lower 40 mi of the river because of the small contributing area along the lower reach.

Discharge in the LDR varied considerably during the study period, which includes water year (WY) 2015–17 (October 1, 2014–September 30, 2017). A comparison of flows at ReReg Dam and the mouth of the LDR illustrates the degree of synchronization of flows from the Project to the mouth for the 3 water years (Figure 2-7). In WY2015, the lowest discharge at Moody (near the mouth of the LDR) was only slightly greater than the discharge at Madras (just below the ReReg Dam), which reflects the diminished contributions of the tributaries to the LDR during that dry period. This is illustrated in an examination of the differences in discharge between the stream gauges at Madras and Moody (Figure 2-8). Summer flows in WY2015 at Moody were particularly low, whereas the minimum flows from the Project (at Madras) were nearly identical for all 3 years. This occurred despite the high flows recorded for Moody early in WY2015 and apparently reflects the greater proportion of surface flows relative to groundwater inputs in the LDR. The greater sustained flows in WY2017 reflect the abundant snowpack that year. The summer flows from the Project in WY2017 were similar to those of WY2016, despite the greater snowpack in 2017. Although WY2015 was perceived as the most intense year of drought in central Oregon in recent years, the LDR exhibited greater peak and average flows in WY2015 than those observed in WY2016. The flows during the summer of 2015 were extremely low, however, and helped to drive the declaration of a drought year in 2015. Detailed statistics for the 3 water years and the period of record (PoR) are summarized in Table 2-3.

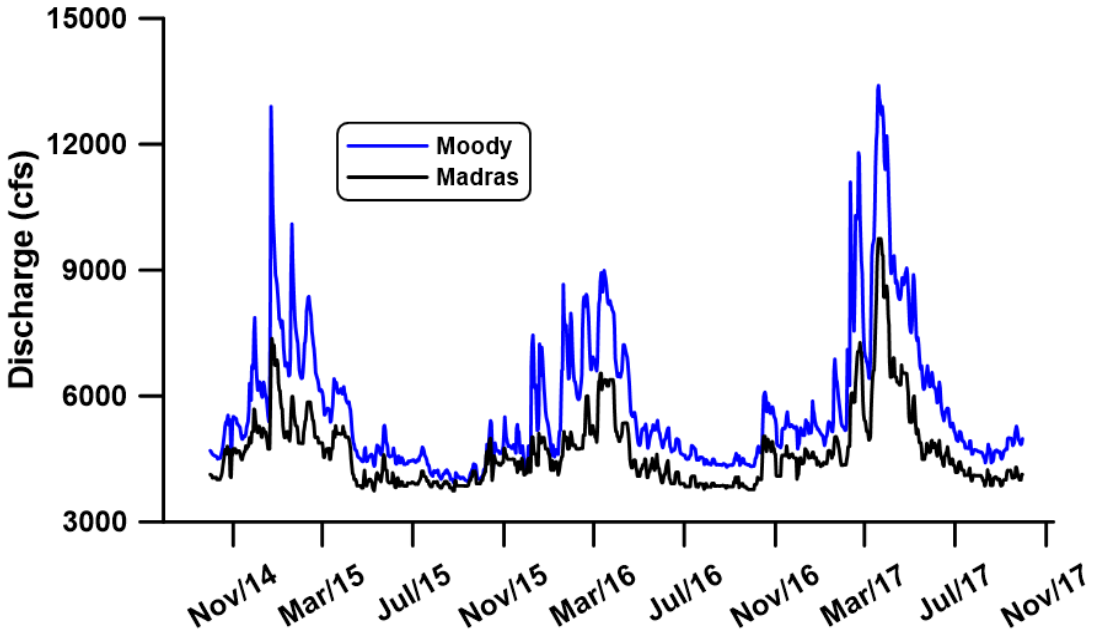

Figure 2-7. Daily discharge at the Moody (RM 1) and Madras (RM 100) USGS stream gages for water years 2015–2017.

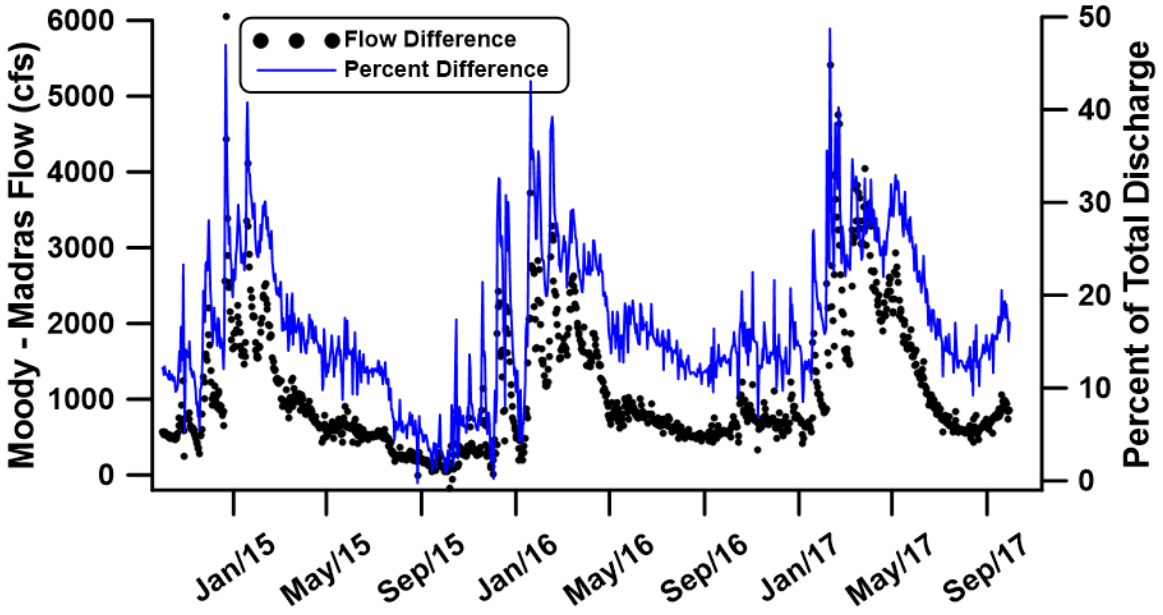

Figure 2-8. Differences in daily flows between the Moody (RM 1) and Madras (RM 100) USGS stream gages for WY 2015–2017.

Table 2-3. Discharge statistics for the Madras and Moody USGS stream gages on the LDR. Results are presented for water years and for the readily available PoR.

Daily Statistic	Madras Discharge (cfs) #14092500 (RM 100)				Moody Discharge (cfs) #14103000 (RM 1)			
	2015	2016	2017	PoR[a]	2015	2016	2017	PoR[b]
Mean	4,531	4,428	4,842	4,574	5,427	5,472	6,311	5,775
Standard Error Mean	38.1	34.4	63.8	6.0	74.0	66.0	109	10.4
Median	4,210	4,360	4,570	4,300	4,810	4,920	5,350	5,230
Minimum	3,740	3,770	3,770	2,440	3,920	4,020	4,320	2,880
Maximum	7,370	6,540	9,750	17,800	12,900	8,990	13,400	63,400
25th percentile	3,940	3,930	4,180	3,880	4,440	4,540	4,922	4,530
75th percentile	5,015	4,812	5,040	4,960	6,140	6,332	6,895	6,410

Notes:

a WY1924-2017. An incomplete water year was collected in 1923.

b WY1906-2017. Data extend to 1897 for a site listed as "near Moro" but are not included.

In the context of annual flows in the LDR over the last century, the data from 2015–2017 are typical of an average year. The flows in 2015 were low in late summer and fall, but overall were comparable to flows typically seen in the river. One feature that was significantly different in 2015 was the low flows observed in the tributaries to the LDR. One of the largest tributaries to the LDR, the Warm Springs River, exhibited a low total volume of snowmelt runoff during 2015 compared to runoff during a more typical snowpack year in 2016 (Figure 2-9). Consequently, much of the flow to the LDR during the spring of 2015 was composed of discharge from the Project, whereas in a year with a typical snowpack, a greater proportion of the flow in the river in the spring would be composed of discharge from the tributaries to the LDR downstream of the Project. Data from the Hogg Pass Snow Telemetry (SNOTEL) automated data collection site located west of the Middle Deschutes River basin near Santiam Pass on the border between Jefferson and Linn counties show the significant differences in snowpack for the 3 study years (Figure 2-10).

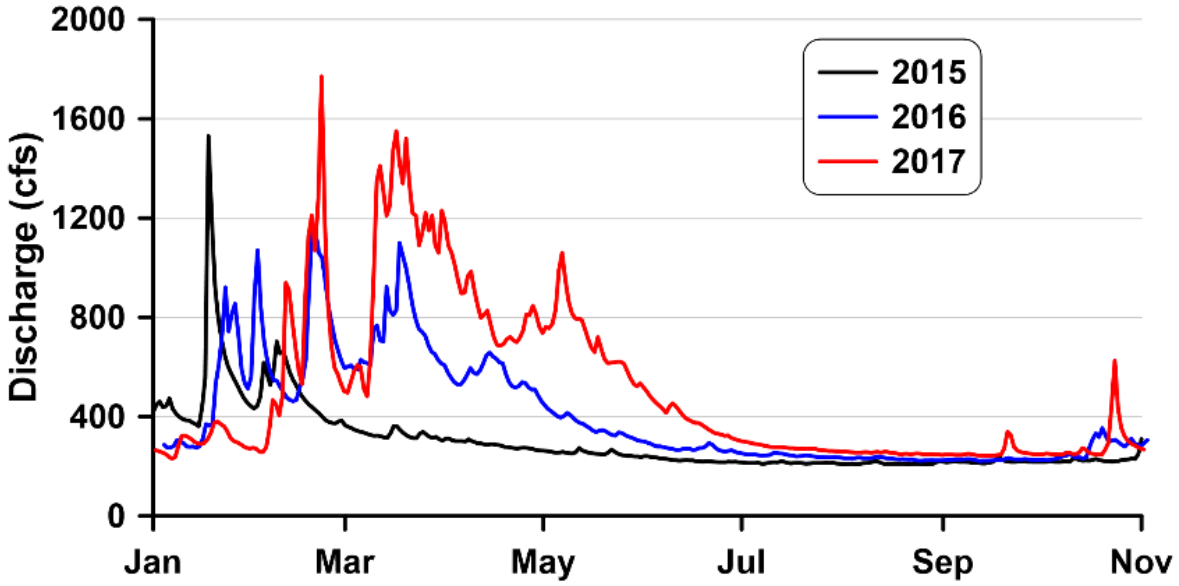

Figure 2-9. Warm Springs River flow from January to November for 2015–2017 (USGS Stream Gage #14097100).

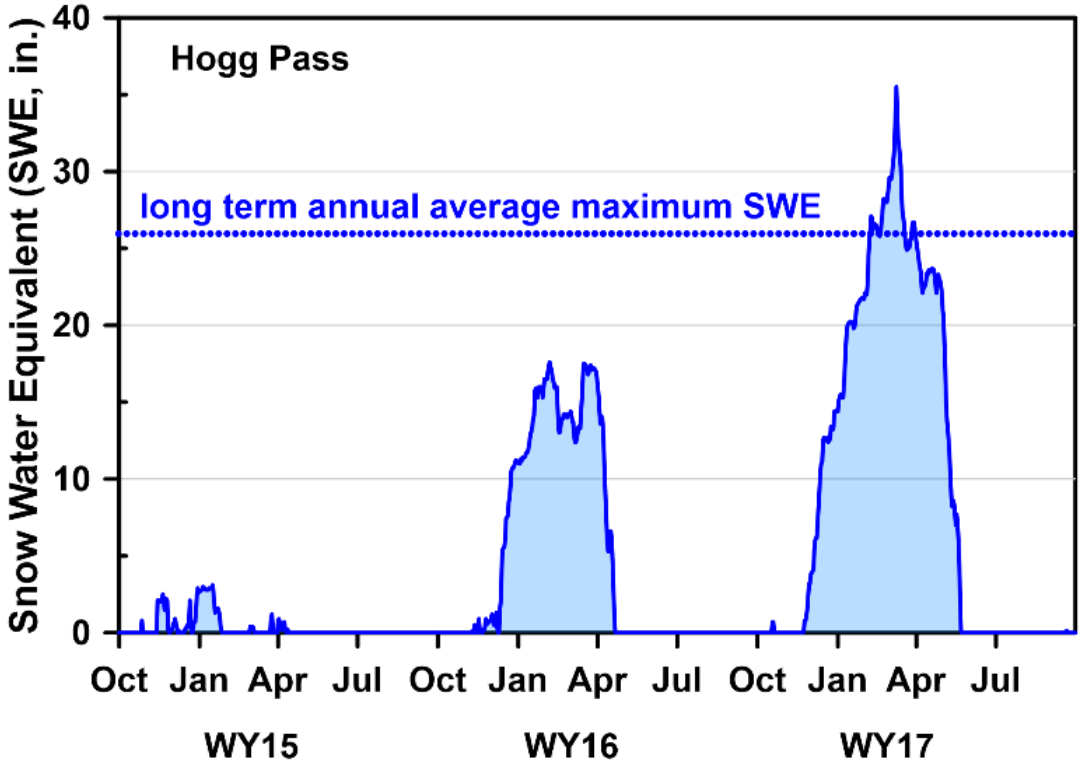

Figure 2-10. Daily snowpack at the Hogg Pass SNOTEL site (Site ID = 21E06S, elevation 4,790 ft; latitude 44.42, longitude -121.85 (NRCS, n.d).Although the LDR is characterized as having

relatively stable discharge (Gannett et al. 2003), in some years (e.g., 1964 and 1996), unusual precipitation events have resulted in high flows. An examination of annual peak discharge at the mouth of the LDR shows that 2015–2017 were characterized by low peak flows compared to most other periods during the last century (Figure 2-11). The last year when peak discharge exceeded 20,000 cfs was 2006 for a duration interval of 11 years. The only other period when peak flows did not exceed 20,000 cfs for more than 11 years was during the Dust Bowl years from 1928 to 1942. Therefore, while the mean annual flows during this study were typical of the long-term average, the study period is part of an extended period of low peak discharge.

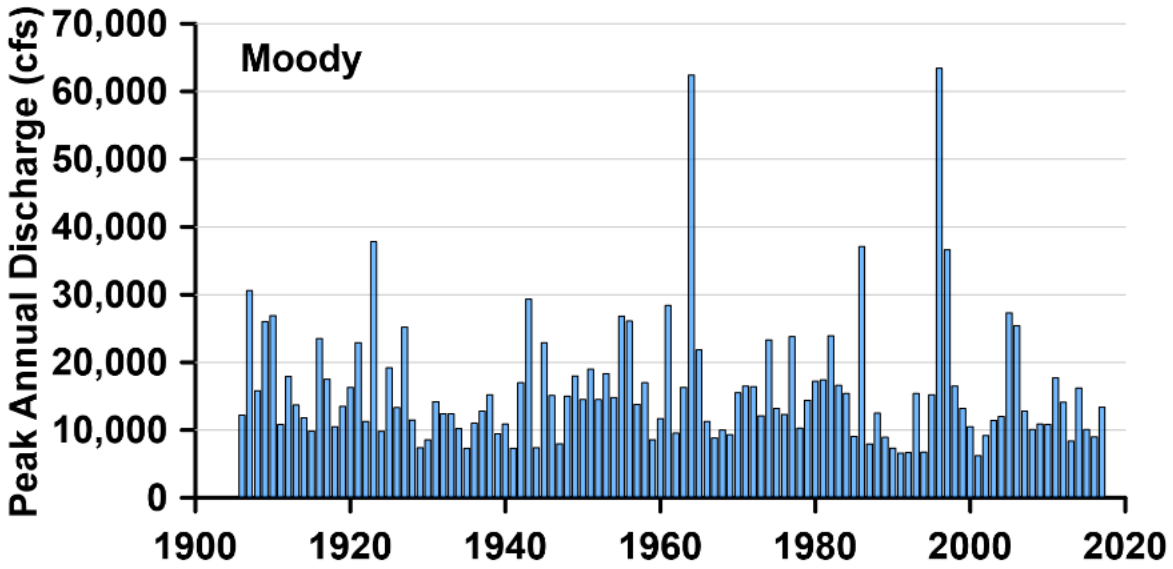

Figure 2-11. Peak annual flow for the LDR at Moody USGS Stream Gage #14103000 (RM 1).

3 Water Quality Monitoring Methods

The monitoring component of the Water Quality Study consisted of collecting grab samples for nutrient, periphyton, and phytoplankton, zooplankton, and *in situ* measurements of pH, DO, chlorophyll, phycocyanin, and turbidity. Water quality data were collected according to the procedures outlined in Appendix A. Sample sites were in the LDR and its tributaries, and LBC and Lake Simtustus and their tributaries.

Sample collection was supplemented by 72-hr continuous measurement events in the LDR and a river float in July 2016 that provided additional longitudinal data. Additionally, the field staff installed an experimental water quality instrument immediately downstream of the ReReg Dam to optically measure additional aspects of water quality. A dye study was completed in Lake Simtustus in August 2017. The components of the water quality monitoring program are described in this section.

3.1 Fixed Site Sampling

The field team selected 12 sites along the mainstem of the LDR and six tributary sites for sampling water quality conditions (Figure 3-1 and Table 3-1). Most of the mainstem sites were a subset of the 21 sites sampled in 1997 by Raymond et al. (1998). That study was conducted by floating the river and stopping at sites located at approximately 5-mi intervals. By contrast, the current study was designed to place a greater emphasis on temporal variability over the course of multiple years. Thus, it was not feasible to sample as many sites as were used in 1997. Sites were allocated along the river with sufficient density to characterize spatial variations in water quality as the river characteristics change.

Major tributaries to the LDR were also sampled monthly in the fall, irregularly in the winter, and twice a month in spring and summer. Those sites included Shitike Creek (co-located near USGS discharge site #14093000), Dry Creek, Trout Creek (co-located near OWRD discharge site #14095255), the Warm Springs River (co-located near USGS #14097100), Oak Springs at the Oregon Department of Fish and Wildlife (ODFW) fish hatchery, and the White River (at White River Falls State Park).

At each site, the field staff performed the following sampling activities:

- Deployed a water quality sonde.
- Collected rocks to be scraped for periphyton sampling.
- Measured light absorption.
- Measured *in situ* chlorophyll and phycocyanin.
- Collected water samples for analysis of nutrients and chlorophyll.

All samples were collected nearshore. The data collected, and the field methods employed are summarized in Table 3-2; additional details are provided in Appendix A.

The LDR sites were sampled once per month in February and April and twice a month in May–September in 2015 and 2016. Sites were sampled monthly in October and December 2015 and October 2016. In 2017, only seven sites were sampled monthly in June–September. The year with the most intensive river sampling was 2016, and during that year, the average depth of river sample collection ranged from the shore to a maximum depth of 69 cm (~ 2 ft). Average velocity at the collection sites was 0.22 m/s and average light transmittance was 56.6% on the bottom. These velocities were considerably lower than what would be experienced in the thalweg; based on average travel time for the LDR (discussed in Section 10.7.2.3), a typical mid-channel river velocity would be slightly less than 1 m/s (~ 3 ft/s).

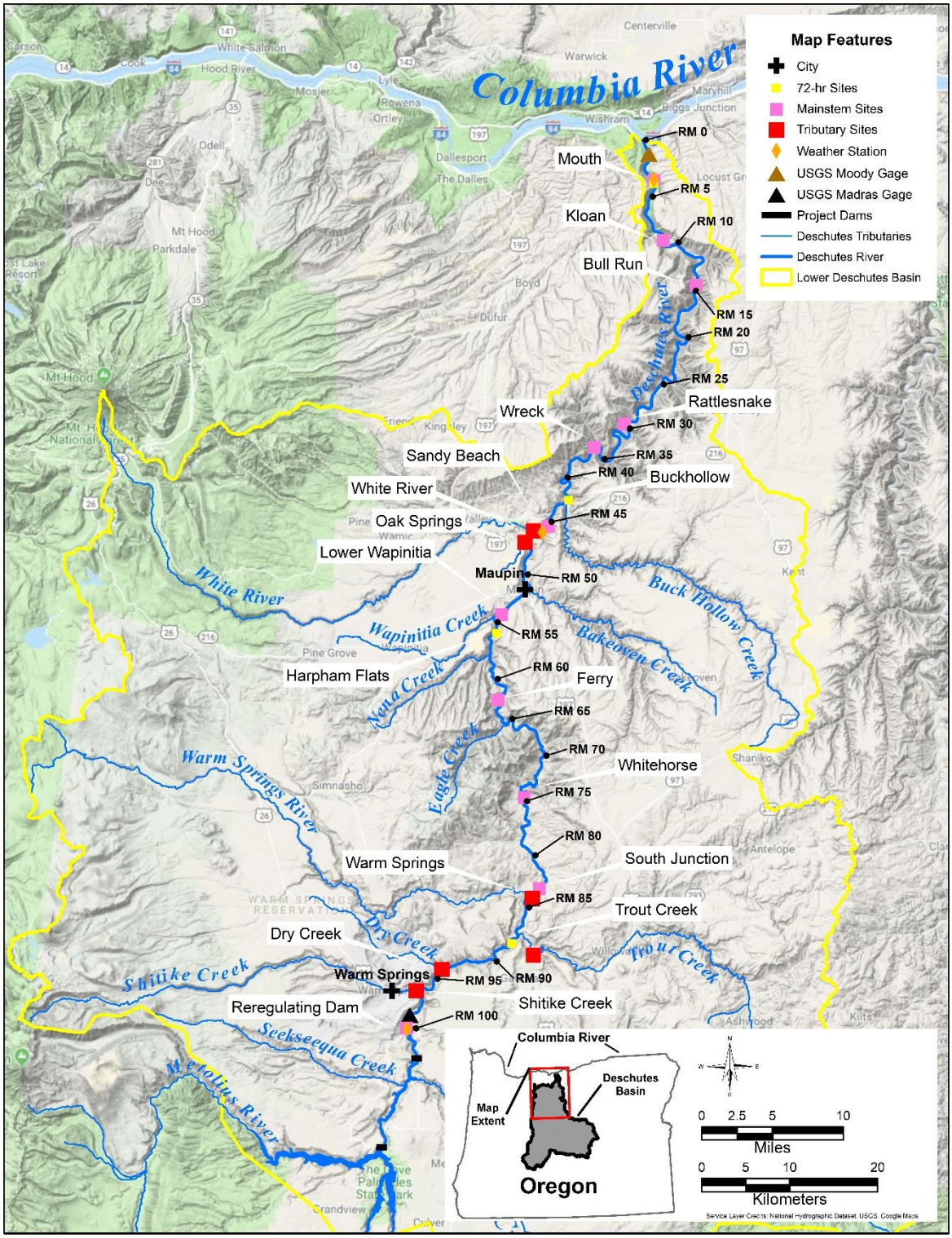

Figure 3-1. Sample sites along the LDR and its tributaries. Also shown are USGS stream gages, weather station locations, and 72-hr monitoring sites.

Table 3-1. Sample site locations on the LDR for the monitoring component of the Water Quality Study.

Site	Site ID	River Mile	Latitude	Longitude
Mainstem Sites				
ReReg Dam	LDR01	100.1	44.72565	-121.24754
Dry Creek	LDR03	94.3	44.78544	-121.19647
South Junction	LDR05	83.3	44.86941	-121.05814
Whitehorse	LDR07	75	44.96258	-121.08077
Ferry	LDR09	62.5	45.062264	-121.11978
Lower Wapinitia	LDR11	54.4	45.149631	-121.11586
Sandy Beach	LDR12	45.5	45.24045	-121.04897
Wreck	LDR14	36.2	45.32146	-120.98292
Rattlesnake	LDR16	29.6	45.34570	-120.93894
Bull Run	LDR18	14.2	45.48808	-120.83622
Kloan Rapids	LDR20	8.4	45.53384	-120.88410
River Mouth	LDR21	3.5	45.59534	-120.89751
72-Hr Sites				
Trout Creek Campground	TC	88.5	44.81255	-121.09661
Harpham Flats	HF	55.8	45.13021	-121.12205
Buckhollow Creek	BH	42.7	45.26719	-121.019
LDR Mouth	RM	3.5	45.61366	-120.90566
Tributary Sites				
Shitike Creek	SC	97.6	44.763861	-121.23405
Dry Creek	DC	94.7	44.7859	-121.1974
Warm Springs	WS	84.3	44.859189	-121.068
Trout Creek	TC	87.7	44.80135	-121.06629
Oak Springs	OS	50.6	45.224069	-121.08224
White River	WR	46.7	45.235839	-121.0705

Table 3-2. The data collected and analysis methods used at the LDR and tributary sampling sites.

Datasets	No. of sites (year)	Location	Sample Type	Instrument or Lab Method	Frequency	Measurements
LOWER DESCHUTES RIVER						
Sonde Measurements	3 (2015-2017)	ReReg, Dant, River Mouth	In-situ	YSI 6920	Continuous, 15 min	Temperature, DO (mg/L, % sat), pH, conductivity
Nutrient Chemistry	12 (2015)	Fixed LDR sites[a]	Grab	TP: SM18 4500PF PO_4: SM18 4500PF TN: SM204500NC NO_3: SM184500N03F NH_3: SM184500NH3H TDN: SM204500NC Cl^-: APHA (1998) 4110 B, EPA 9056A[c] TOC: SM205310B ALK: SM1810200H BOD: SM20 5120B	Monthly: Feb, Apr, Oct, Dec Bimonthly[b]: May-Sep	TP, PO_4, TN, NO_3,NH_3, TDN, Cl^- TOC, ALK, BOD (infrequent collection)
	12 (2016)				Monthly: Feb, Apr, Oct Bimonthly: May-Sep	TP, PO_4, TN, NO_3, NH_3, Cl^- TOC, ALK (infrequent collection)
	7 (2017)	ReReg Dam, South Junction, Ferry, Sandy Beach, Wreck, Rattlesnake, River Mouth			Monthly: Jun-Sep	TP, PO_4, TN, NO_3, NH_3, Cl^-
Water chemistry	12 (2015)	See Nutrient Chemistry sites for LDR	In-situ	YSI 6920	Monthly: Feb, Apr, Oct, Dec Bimonthly: May-Sep	Temperature, DO (mg/L, % sat), pH, conductivity
	12 (2016)				Monthly: Feb, Apr, Oct Bimonthly: May-Sep	
	7 (2017)				Monthly: Jun-Sep	
Periphyton[d]	12 (2015)	See Nutrient Chemistry sites for LDR	Grab	Periphyton: Academy of Natural Sciences Protocols CHL a: SM1810200H Pheo: SM1810200H AFDW: SM20 2540E PAR: LI-Cor LI-250A & LI-192	Monthly: Feb, Apr, Oct, Dec Bimonthly: May-Sep	Taxa ID, count, density, total biovolume; rocks scraped for chlorophyll a, pheophytin, and AFDW; solar radiation (PAR) measurement taken
	12 (2016)				Monthly: Feb, Apr, Oct Bimonthly: May-Sep	
	7 (2017)				Monthly: Jun-Sep	
Phytoplankton	4 (2015)	ReReg, Whitehorse, Sandy Beach, Bull Run	Grab	Academy of Natural Sciences Protocols for Phytoplankton	Monthly: Aug, Oct, Dec	Taxa ID, count, density, total biovolume
	6 (2016)	ReReg, Whitehorse, Lower Wapinitia, Sandy Beach, Bull Run, River Mouth			Monthly: Apr, Oct Bimonthly: May-Sep	
Zooplankton	4 (2015) 6 (2016)	See Phytoplankton sites for LDR	Grab	Methods developed by ZP's Taxonomic Services[e]	Monthly: Jul, Dec	Taxa ID, count, density
	6 (2016)				Monthly: Apr, Oct Bimonthly: May-Sep	
Algae Torch	12 (2015)	See Nutrient Chemistry sites for LDR	In-situ	bbe Moldaenke	Monthly: Feb, Apr, Oct, Dec Bimonthly: May-Sep	Cyanobacteria, total chlorophyll, turbidity
	12 (2016)				Monthly: Feb, Apr, Oct Bimonthly: May-Sep	
	7 (2017)				Monthly: Jun-Sep	
Water Column CHL	2 (2015)	Randomly selected	Grab	CHL a: SM1810200H Pheo: SM1810200H	Monthly: Apr, May, Aug-Oct, Dec Bimonthly: Jun, Jul	Chlorophyll a and pheophytin
	2 (2016)	ReReg, second site randomly selected			Monthly: Feb, Apr Bimonthly May-Sep	
	2 (2017)				Monthly: Jun-Sep	
Intensive surveys	4 (2015, 2016)	Mouth, Buck Hollow, Harpham Flats, Trout Creek	Grab & In-situ	See Nutrient Chemistry	Grabs every 6 hrs Continuous, 15 min	TP, PO4, TN, NO3, NH3, Cl^-, TOC
Synoptic Survey	2016 River Float	Entire LDR	Continuous	Weather: Hobo Sonde: In-Situ Aqua Troll 600 DO: Hobo Depth: Lowrance Chlorophyll: bbe	July 15-21, 2016	Wind speed, air temperature, relative humidity, solar radiation (PAR), temperature, pH, DO (mg/L, % sat), conductivity, depth, cyanobacteria, total chlorophyll, turbidity
TRIBUTARIES OF THE LOWER DESCHUTES RIVER						
Nutrient Chemistry	6 (2015)	Shitike Creek, Dry Creek, Warm Springs River, Trout Creek, Oak Springs, White River	Grab	See Lower Deschutes Nutrient Chemistry	Monthly: Feb, Apr, Oct, Dec Bimonthly: May-Sep	TP, PO_4, TN, NO_3, NH_3, TDN, Cl^-
	5 (2016)	Shitike Creek, Warm Springs River, Trout Creek, Oak Springs, White River			Monthly: Feb, Apr, Oct Bimonthly: May-Sep	TP, PO_4, TN, NO_3, NH3, Cl^-
	2 (2017)	Trout Creek, Warm Springs			Monthly: Jun-Sep	TP, PO_4, TN, NO_3, NH3
Water Chemistry	6 (2015)	See Nutrient Chemistry sites for tributaries of LDR	In-situ	YSI 6920	Monthly: Feb, Apr, Oct, Dec Bimonthly: May-Sep	Temperature, DO (mg/L, % sat), pH, conductivity
	5 (2016)				Monthly: Feb, Apr, Oct Bimonthly: May-Sep	
	2 (2017)				Monthly: Jun-Sep	
TRIBUTARIES TO LAKE BILLY CHINOOK & LAKE SIMTUSTUS						
Nutrient Chemistry	5 (2015)	Crooked River, Deschutes River, Metolius River, Willow Creek	Grab	See Lower Deschutes Nutrient Chemistry	Monthly: Apr, Oct, Dec Bimonthly: May-Sep	TP, PO_4, TN, NO_3,NH_3, TDN, Cl^- TOC, ALK, BOD (infrequent collection)
	4 (2016)	Crooked River, Deschutes River, Metolius, Willow Creek			Monthly: Feb, Apr, Oct Bimonthly: May-Sep	TP, PO_4, TN, NO_3, NH_3, Cl^- TOC, ALK (infrequent collection)
Water chemistry	5 (2015)	See Nutrient Chemistry sites for tributaries to reservoirs	In-situ	YSI 6920	Monthly: Apr, Oct, Dec Bimonthly: May-Sep	Temperature, DO (mg/L, % sat), pH, conductivity
	4 (2016)				Monthly: Feb, Apr, Oct Bimonthly: May-Sep	

Notes:

[a] The 12 main stem sites from ReReg Dam to River Mouth.

[b] bimonthly = twice a month

[c] This method was used by CCAL in 2016 and 2017. The 2015 chloride samples were analyzed by IEH using SM18 4500CL-C.

[d] Began using a new taxonomist in July 2015.

[e] These methods are derived from International Biological Programme (IBP) Handbook #17 and used in the US EPA National Lakes Assessment.

3.2 72-Hour Monitoring

Four sites were selected along the LDR for simultaneous deployment of water quality sondes and collection of water quality samples (Figure 3-1). The selected sites were at Trout Creek campground (RM 88.5), Harpham Flats (RM 55.8), and Buckhollow Creek (RM 42.7) and near the mouth of the LDR (RM 0.5). The 72-hr monitoring was conducted in July and August of 2016, when ambient air temperatures and primary production in the impoundments and river were expected to be high. At each site, the field team deployed the water quality sondes (generally YSI 6920 V2 logging instruments) in the river, where they remained for the duration of the monitoring period. Water quality samples were collected at 6-hr intervals starting at 1800 hr for 2 days during the deployment, yielding four samples per site per day. The field sampling methods used for the fixed-site monitoring also were used for the 72-hr water quality sample (Table 3-2).

3.3 ReReg Dam Tailrace Monitoring

A continuous water quality monitoring station is located immediately downstream of the Project near the tailrace of the ReReg Dam. This is a monitoring site stipulated by the terms of the relicensing agreement. The monitoring consists of continuous deployment of a water quality sonde to measure water temperature, pH, DO, turbidity, and conductivity. Co-located at the site is the USGS Stream Gage #14092500 (near Madras). For the analysis, we used the water temperature data from the gage.

Field personnel deployed an experimental instrument, the ZAPS LiquID™ Station, on October 1, 2015, at the ReReg site (LDR01). The instrument measured chlorophyll *a*, phycocyanin, turbidity, total organic carbon (TOC), fluorescent dissolved organic matter (FDOM), and nitrate (NO_3)+nitrite (NO_2) using a combination of fluorescence, absorption, and light-scattering measurements every 5 seconds. This developing technology produced reliable results for phycocyanin, turbidity, TOC, and FDOM, but yielded significant periods of unreliable data for chlorophyll and NO_3. These data were deemed unreliable based on large deviations of the light-related measurements from the values obtained from water samples analyzed using traditional analytical laboratory measurements. Data deemed unreliable was not used in the analyses (see

Appendix B). We relied largely on analytical laboratory measurements of chlorophyll and NO_3. Additionally, light-based measurements were taken of chlorophyll and phycocyanin at the ReReg site (LDR01) and other sites using an AlgaeTorch chlorophyll and cyanobacteria measurement instrument (bbe Moldaenke).

3.4 River Float

The field team conducted a longitudinal analysis of the LDR by rafting the river July 15–21, 2016 from the ReReg tailrace (RM 100) to the mouth of the river (RM 0.1). The raft was fitted with a HOBO weather station data logger (model #U30) equipped with sensors for wind speed, air temperature, relative humidity, and solar radiation (PAR); an In-Situ Aqua TROLL 600 water quality sonde; HOBO data loggers for DO and temperature (model #U26-001); multiple global positioning system units; and a Lowrance hydroacoustic device (model #HDS-7 Gen2) for recording depth. The water quality sonde recorded temperature, pH, DO, conductivity, and turbidity at 10-minute intervals, and the DO data loggers recorded at 1-minute intervals. The sonde and DO logger were submerged to a depth of approximately 0.6 m (~2 ft). The weather-related sensors recorded every 15 minutes. The hydroacoustic data were recorded continuously (except during stops) and an average depth was computed for each 1-minute interval. Raft position was recorded continuously. Periodic measurements of chlorophyll, phycocyanin, and turbidity were collected with an AlgaeTorch (*n = 65*). Periphyton communities were noted and photodocumented during more extensive stops (*n = 17*).

3.5 Impoundments and Tributaries to Impoundments

The field team sampled water quality monthly and twice a month at two sites each in LBC and Lake Simtustus (Figure 3-2 and Table 3-3). Each impoundment was sampled at the forebay. The second site sampled in LBC was near the confluence of the Deschutes River arm and the Crooked River arm in the Common Pool (RES08). The second sampling site in Lake Simtustus was a Mid-Lake site south of the inlet from Willow Creek. Sampling was not conducted in the ReReg Reservoir because of the large fluctuations in daily water level.

The data the team collected and the field methods we used are summarized in Table 3-4; additional details are provided in Appendix A. Water samples from the impoundments were

collected using a Van Dorn sampler lowered to the prescribed depth. Samples were collected in the epilimnion, metalimnion, and hypolimnion in 2015 by first collecting the vertical sonde data and then targeting appropriate depths. This approach was abandoned in mid-2015, and thereafter samples were collected at fixed depths. The conditional-depth sampling is often used by ODEQ in their lake investigations such as the sampling in LBC in 2006. Fixed depth sampling, however, allowed for greater reproducibility. Zooplankton samples were collected with a 64-micron-mesh plankton net, fixed in ethanol, and shipped to ZP's Taxonomic Services for identification and enumeration. Phytoplankton samples were split between Aquatic Analysts, Inc. and Rhithron Associates, Inc. in 2015 and, thereafter, most samples were sent only to Rhithron. Vertical profiles of algal pigments and turbidity were collected with an Algae Torch to a depth of 10 m (the maximum depth to which the Algae Torch can be lowered). Secchi disk measurements were recorded as the average of the depth of disappearance and reappearance.

A dye study was conducted in Lake Simtustus during August 2017. Fluorescent dye was added to the tailrace below Round Butte Dam and the fluorescence measured below the tailrace of Pelton Dam. The study was conducted to calculate the travel time through Lake Simtustus.

Nutrient and algae samples were also collected at the tailraces below Round Butte Dam and Pelton Dam. A Van Dorn sampler was lowered into the tailraces to no more than 1 m below the surface to collect water for the samples. Samples for nutrients and algae were processed following the procedures used at the LDR sites.

Water quality samples for nutrient analyses and sonde measurements were collected at the three tributaries to LBC (Crooked River, Deschutes River, and Metolius River) and Willow Creek, a tributary of Lake Simtustus monthly and twice a month. The samples were collected nearshore above the confluence with LBC in flowing water following the sampling procedures used in the LDR.

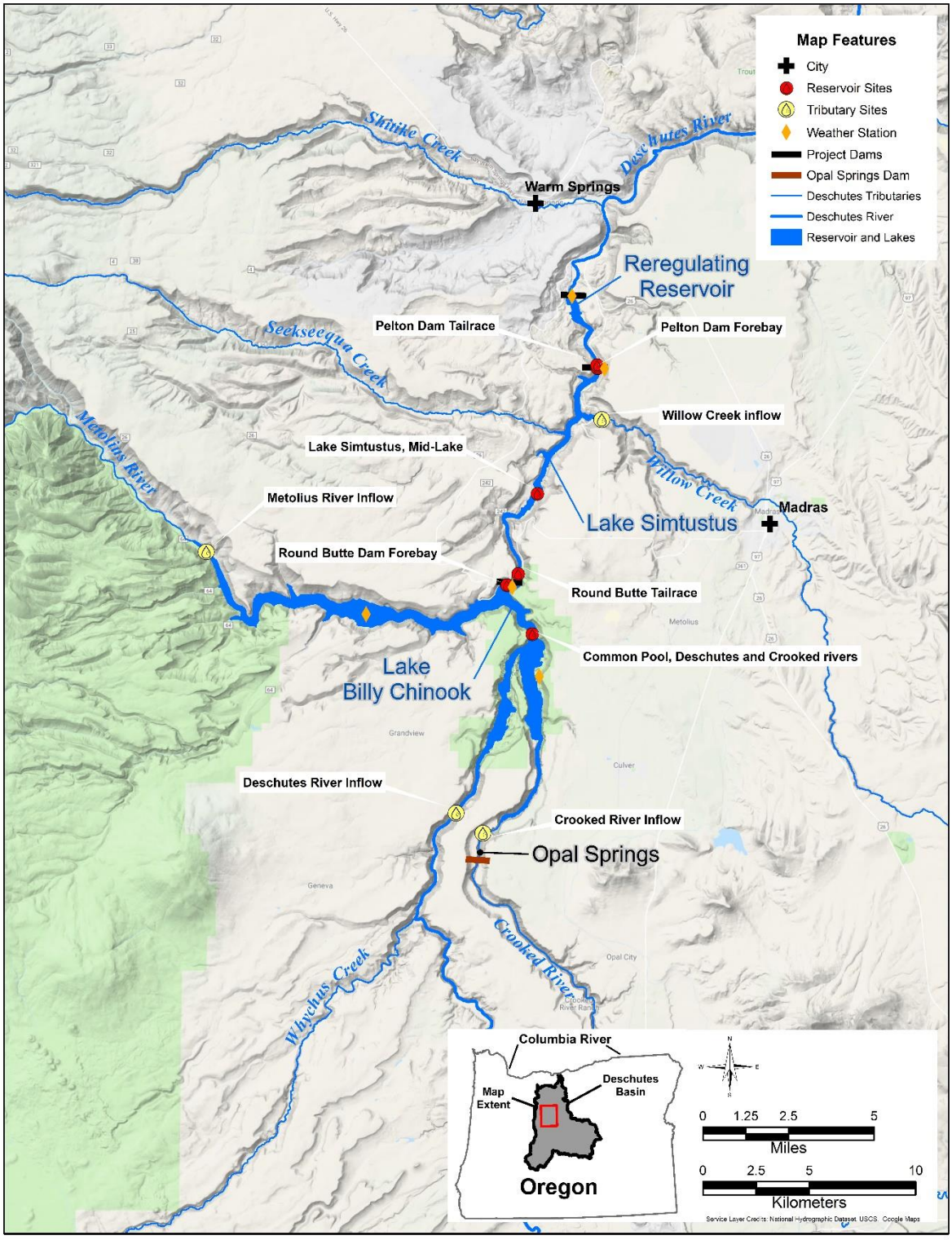

Figure 3-2. Monitoring sites in LBC, Lake Simtustus, and the tributaries of LBC. Weather station locations are also shown.

Table 3-3. Monitoring sites and locations in the impoundments and tributaries

Site	Site ID	Latitude	Longitude
Reservoirs			
Pelton Forebay	04	44.69330	-121.23085
Round Butte Forebay	07	44.60131	-121.28119
Common Pool, Deschutes and Crooked rivers	08	44.58089	-121.26818
Round Butte Tailrace	09	44.60586	-121.27694
Pelton Tailrace	10	44.69438	-121.23158
Mid-Lake, near Indian Campground, Lake Simtustus	25	44.63958	-121.265708
Tributaries			
Willow Creek Inflow	05	44.67191	-121.22785
Deschutes River Inflow	14	44.49869	-121.32075
Metolius River Inflow	17	44.62113	-121.47536
Crooked River Inflow	11	44.49697	-121.29401

Table 3-4. The data collected and analysis methods used at LBC and Lake Simtustus sampling sites.

Dataset	No. of sites (year)	Profile Depths	Sample Type	Instrument or Lab Method	Frequency	Measurements
RESERVOIR SITES (Lake Billy Chinook: Common Pool & Round Butte forebay; Lake Simtustus: Mid-Lake & Pelton forebay)[a]						
Nutrient Chemistry	4 (2015)	1 sample at 1m, mid-epilimnion, mid-metalimnion, and mid-hypolimnion[b]	Grab	TP: SM18 4500PF PO_4: SM18 4500PF TN: SM204500NC NO_3: SM184500N03F NH_3: SM184500NH3H TDN: SM204500NC Cl-b: APHA 4110 B, EPA 9056A TOC: SM205310B ALK: SM1810200H BOD: SM20 5120B	Monthly: Apr, Oct, Dec Bimonthly[c]: May-Sep	TP, PO_4, TN, NO_3,NH_3, TDN, Cl^- TOC, ALK, BOD (infrequent collection)
	4 (2016)	1 sample at 1 m, 10 m, 25 m, 45 m, and 75 m			Monthly: Feb, Apr, Oct Bimonthly: May-Sep	TP, PO_4, TN, NO_3, NH_3, Cl^- TOC, ALK (infrequent collection)
	2 (2017)				Monthly: Jun-Sep	TP, PO_4, TN, NO_3, NH_3, Cl^-
Water Chemistry	4 (2015)	2 m interval to 20 m, then every 10m	In-situ	YSI 6920	Monthly: Apr, Oct, Dec Bimonthly: May-Sep	Temperature, DO (mg/L, % sat), pH, conductivity
	4 (2016)	Measurement at 0.5 m and every 2-m from 2 to 20 m 5-m from 20 to 40 m 10-m from 40 to 60 m 20-m from 60 to bottom			Monthly: Feb, Apr, Oct Bimonthly: May-Sep	
	2 (2017)				Monthly: Jun-Sep	
Phytoplankton	4 (2015)	1 sample at 1 m and mid-epilimnion	Grab	Academy of Natural Sciences Protocols for Phytoplankton	Monthly[d]: Apr, Oct, Dec Bimonthly: May-Sep	Taxa ID, count, density, total biovolume
	4 (2016)	1 sample at 0.5 m and 10 m			Monthly: Feb, Apr, Oct Bimonthly: May-Sep	
	2 (2017)				Monthly: Jun-Sep	
Zooplankton	4 (2015)	One 10 m to surface tow	Tow	Methods developed by ZP's Taxonomic Services[e]	Monthly: Oct, Dec Bimonthly: May-Sept	Taxa ID, count, density
	4 (2016)	One 20 m to surface tow			Monthly: Feb, Apr, Oct Bimonthly: May-Sept	
	2 (2017)				Monthly: Jun-Sep	
AlgaeTorch	4 (2015)	0.5 m and 1 m interval from 1-10 m	In-situ	bbe Moldaenke	Monthly: Apr, Oct, Dec Bimonthly: May-Sep	Cyanobacteria, total chlorophyll, turbidity
	4 (2016)	0.5 m, 2 m, 4 m, 6 m, 8 m, 10 m			Monthly: Feb, Apr, Oct Bimonthly: May-Sep	
	2 (2017)				Monthly: Jun-Sep	
Water Column Chlorophyll[f]	4 (2015)	Composite sample from depths between 1-10 m	Grab	CHL a: SM1810200H Pheo: SM1810200H	Monthly: Apr, Oct, Dec Bimonthly: May-Sep	Chlorophyll a and pheophytin
	4 (2016)	0.5 m			Monthly: Feb, Apr, Oct Bimonthly: May-Sept	
	2 (2017)	0.5 m, 2 m, 10 m			Monthly: Jun-Sep	
Solar Radiation	4 (2015-2017)	1 air measurement; 1 subsurface measurement every 1 m until PAR is 1% of first subsurface readings	In-situ	LI-Cor LI-250A & LI-192	Monthly: Apr, Oct, Dec Bimonthly: May-Sep	Photosynthetically Active Radiation
					Monthly: Feb, Apr, Oct Bimonthly: May-Sep	
					Monthly: Jun-Sep	
Transparency	4 (2015-2017)	1 measurement	In-situ	Secchi Disk	Monthly: Apr, Oct, Dec Bimonthly: May-Sep	Transparency
					Monthly: Feb, Apr, Oct Bimonthly: May-Sep	
					Monthly: Jun-Sep	
TAILRACES: ROUND BUTTE TAILRACE & PELTON TAILRACE						
Nutrient chemistry	2 (2015)	n/a	Grab	See methods listed for Reservoir Nutrient Chemistry	Monthly: Jun, Oct, Dec, Bimonthly: Jul-Sep	TP, PO_4, TN, NO_3,NH_3, TDN, Cl^- TOC, ALK, BOD (infrequent collection)
	2 (2016)				Monthly: Feb, Apr, Oct Bimonthly: May-Sept	TP, PO_4, TN, NO_3, NH_3, Cl^- TOC, ALK (infrequent collection)
Water Chemistry	2 (2015)	n/a	In-situ	YSI 6920	Monthly: Jun, Oct, Dec, Bimonthly: Jul-Sep	Temperature, DO (mg/L, % sat), pH, conductivity
	2 (2016)				Monthly: Feb, Apr, Oct Bimonthly: May-Sept	
AlgaeTorch	2 (2015)	n/a	In-situ	bbe Moldaenke	Monthly: Jun, Oct, Dec, Bimonthly: Jul-Sep	Cyanobacteria, total chlorophyll, turbidity
	2 (2016)				Monthly: Feb, Apr, Oct Bimonthly: May-Sept	
Phytoplankton	2 (2015)	n/a	Grab	Academy of Natural Sciences Protocols for Phytoplankton	Monthly: Jul, Aug, Oct, Dec	Taxa ID, count, density, total biovolume
	2 (2016)				Monthly: Feb, Apr, Oct Bimonthly: May-Sept	

Notes:

[a] Common Pool in Lake Billy Chinook and Mid-Lake in Lake Simtustus were not sampled in 2017.

[b] Composite samples ranging in depth from surface to 10 m were taken in April, May, and June. Starting with the second sampling event in June, samples were taken at the middle of the epilimnion, metalimnion, and hypolimnion. These sample depths varied throughout 2015.

[c] bimonthly = twice a month

[d] Samples taken in April, May, and one sampling event in June were determined to be unreliable. Samples were sent to a new lab starting with the second June sampling event.

[e] These methods are derived from International Biological Programme (IBP) Handbook #17 and used in the US EPA National Lakes Assessment.

[f] Sample taken at one randomly selected reservoir site in 2015 and 2016. In 2017, a sample was taken at each depth listed in Round Butte forebay and Pelton forebay.

3.6 Data Review

This multi-year study produced a large amount of data. Data were reviewed for completeness, accuracy, precision, and representativeness. The field data were measured with a water quality sonde that was calibrated each sampling day according to manufacturer recommendations. Few discrepancies were noted in the field data; discrepancies were judged based on analysis of times series data, comparison with data from other sources (e.g., ODEQ) or were considered highly unlikely given the acid-base chemistry of the site. In cases where the field staff noticed anomalous data in profiles measurements, the measurements were repeated. Field sheets were reviewed a second time prior to being entered into the database. The measurements of light transmittance were made with a LiCOR light meter. The field staff noted that the meter began to yield erratic measurements and returned it to the manufacturer for repair. Measurements made prior to the repair were not used in the analysis. The AlgaeTorch would occasionally produce erratic values. These were attributed to transient movement of algal colonies in front of the sensor. Consequently, the field staff would repeat the measurements. The Algae Torch instrument produced results that were not considered as accurate or precise as data from the analytical laboratory, but were judged to be useful because it allowed for measurements of phytoplankton pigments in a water column that could not be obtained without considerable additional analytical expense.

The analytical laboratory selected for the study was IEH/Aquatic Research in Seattle. This decision was based on the senior investigator's highly favorable prior experience with the laboratory. The laboratory data were reviewed upon receipt. When anomalies were found, and the laboratory still had sufficient volume of material available, analyses were rerun. This only occurred on a couple samples. Most other suspicious sample results were removed from the results database, which occurred in a small percentage of the data (Table 3-5). In those cases, the samples results appeared to be highly inconsistent with previous data collected at the site or data from adjacent sites. One pair of sample results was removed from the database because it appeared that the sample labels had been switched either in the field or the laboratory. The accuracy of the chloride data from IEH was reviewed in 2015 and judged to be insufficient for evaluating sources of water, especially following chloride inputs from the tributaries.

Consequently, analysis of subsequent chloride samples was switched the Cooperative Chemical Analytical Laboratory (CCAL) at Oregon State University, operated jointly by the Department of Forestry and the US Department of Agriculture

Table 3-5. Summary of the quality assurance analysis.

Parameter	Number of Duplicates/ Replicates	Percent of Samples Removed	Comparative Analysis	Used in Models	Notes
Field Measurements					
Temperature	0	0	Second sonde	Yes	Measured with sonde
pH	0	1	Second sonde	Yes	Measured with sonde
DO	0	3	Second sonde	Yes	Measured with sonde
Conductivity	0	2	Second sonde	Yes	Measured with sonde
PAR	0	2	n/a	No	Measured with meter
Total Chlorophyll	22	0.8	IEH	No	Measured with AlgaeTorch
Phycocyanin	22	0.8	ZAPS	No	Measured with AlgaeTorch
Analytical Measurements					
TP	66	0.3	IEH/CCAL[a]	Yes	
PO_4	64	0.8	IEH/CCAL	No	
TN	66	0.1	IEH/CCAL	Yes	
NO_3	64	0	IEH/CCAL	Yes	
NH_3	64	0	IEH/CCLA	Yes	
Cl^-	40	0.4	IEH/CCAL	Yes	
TOC	18	0	IEH/CCAL	Yes	
Alkalinity	18	0	IEH/CCAL	Yes	
BOD	6	0	IEH/CCAL	Yes	
Silica	0	0	n/a	No	
Water Column Chlorophyll	4	0	IEH	Yes	
Periphyton CHL	20	0	IEH	Yes	

Parameter	Number of Duplicates/ Replicates	Percent of Samples Removed	Comparative Analysis	Used in Models	Notes
AFDW	20	0.01	IEH	Yes	
72-Hour Monitoring					
TP	0	0	n/a	No	Used for contextual analysis in the modeling
PO_4	0	0	n/a	No	Used for contextual analysis in the modeling
TN	0	0	n/a	No	Used for contextual analysis in the modeling
NO_3	0	0	n/a	No	Used for contextual analysis in the modeling
NH_3	0	0	n/a	No	Used for contextual analysis in the modeling
Cl^-	0	0	River float	No	Used for contextual analysis in the modeling
Temperature	0	2	River float	Yes	
pH	0	2	River float	Yes	
DO	0	2	River float	Yes	
Conductivity	0	16	River float	Yes	
Turbidity	0	3	River float	Yes	
ZAPS					
NO_3	n/a	100	IEH	No	Unusable because of significant drift
Chlorophyll	n/a	All data after 12/31/16 removed	IHE	No	Retained data from 10/30/15 to 12/31/16
Phycocyanin	n/a	0	AlgaeTorch	No	Strong agreement with cyanobacteria biovolume
FDOM	n/a	0	n/a	No	Some abrupt increases suspect
TOC	n/a	0	IEH	No	Values within range of analytical lab
Turbidity	n/a	0	n/a	No	Short-term spikes averaged to produce reliable daily patterns
Biologicals					

Parameter	Number of Duplicates/ Replicates	Percent of Samples Removed	Comparative Analysis	Used in Models	Notes
Phytoplankton	22[b]	0	Aquatic Analysts	Yes	
Periphyton	19[b]	0	Aquatic Analysts	Yes	Additional splits with PhycoTech and Georgia College.
Zooplankton	12	0	Rhithron	No	
Meteorological					
Air Temperature	n/a	Small percent of missing data (identified as -999) removed from files	Adjacent stations and AgriMet data	Yes	Measured with Onset Computer
Wind Direction	n/a			Yes	Measured with Onset Computer
Wind Velocity	n/a			Yes	Measured with Onset Computer
Relative Humidity	n/a			Yes	Measured with Onset Computer
PAR	n/a			Yes	Measured with Onset Computer

Notes:

[a] began using CCAL in 2016 for replicate analysis. Used IEH in 2015.

[b] Numbers represent Rhithron data only

Several analytical results were initially flagged for further review. In some cases, re-analysis of suspect samples was possible and helped to reduce data uncertainty. Values flagged as likely errors were documented, removed from the active data set, and placed in a reserve folder. No data substitutions were employed. Some of the results for groups of data were removed from consideration entirely or marked for cautions interpretation. This included the chloride (Cl^-) results from IEH-Analytical for 2015, in which the precision and accuracy of the data was considered less than optimal, but still usable.

Results of field replicates show that the mean absolute differences among replicates were generally low and indicative of low variability (Table 3-6). Although most of the sample results showed statistically significant differences between replicates, the values of the differences were low relative to the concentrations reported for the sites. Total nitrogen replicates displayed a moderate degree of variability as did chloride and biological oxygen demand (BOD_5). Total nitrogen (which includes particulate nitrogen) may reflect the random inclusion of algal cells in aliquots which can alter the results. The chloride data from IEH was acceptable for most application; however, it was preferable to increase the level of precision and subsequent samples were sent to an alternate laboratory that routinely analyzed samples with lower concentrations of chloride. Only six replicates were collected for analysis of BOD_5 and these displayed considerable differences between replicates. Concentrations of BOD_5 are generally low in the Project and the LDR and these results are consistent with low concentrations of BOD_5 and a small sample size.

Table 3-6. Analysis of replicate samples from 2015–2017. All samples presented were analyzed by IEH Aquatic Research. Units are in mg/L.

Parameter	Sample Size	Method Reporting Limit	Absolute Mean Difference	T-test[a]	*p*-value[b]
Total Phosphorus	63	0.002	0.008	5.65	0.0000
Ortho-Phosphorus	64	0.001	0.003	6.17	0.0000
Total Nitrogen	63	0.050	0.126	5.02	0.0000
Total Dissolved Nitrogen	30	0.050	0.078	2.59	0.0150
Nitrate/nitrite	63	0.010	0.014	2.59	0.0118
Ammonia	64	0.010	0.007	4.50	0.0000
Total Organic Carbon	17	0.250	0.318	6.18	0.0000
Chloride[c]	30	0.50	0.260	4.83	0.0000
Alkalinity	17	1.0	2.8	4.67	0.0003
Biochemical Oxygen Demand (5-day)	6	1.0	1.71	1.43	0.2119

Notes:

[a] One-sample T-test

[b] Null hypothesis $\mu = 0$

[c] Results for IEH in 2015. Chloride analyses in 2016 and 2017 analyzed by CCAL Laboratory at Oregon State University

The ZAPS LiquID unit instrument was installed below the ReReg Dam. The instrument pumped river water from a stilling well installed at the shore. The instrument measured analytes continuously and afforded an opportunity to examine water quality of the LDR at a high temporal resolution. This experimental instrument yielded what appeared to be excellent quality data for FDOM, phycocyanin, TOC, and turbidity. The review of the data unfortunately showed that much of the NO_3 and chlorophyll data were erratic and showed poor comparisons with the analytical laboratory data to be used for modeling the LDR system (Appendix B). ZAPS chlorophyll data from March to October 2017 were rejected as unreliable based largely on comparison with chlorophyll data measured from the analytical laboratory. There were no analytical measurements of FDOM available for comparison, so confirmation of the accuracy of these measurements cannot be affirmed. The phycocyanin measurements recorded with the ZAPS instrument were consistent with the onset of high densities of cyanobacteria in LBC and were consistent with AlgaeTorch measurements of cyanobacteria in LBC. Values of turbidity

and TOC were reasonably comparable to sonde measurements of turbidity and the analytical measurements of TOC. A more complete assessment of the ZAPS data is presented in Appendix B.

Quality assurance of biological data presents a challenge because the data are derived from small samples (relative to the number of individual organisms) and because there is considerable professional judgement involved in identifying microscopic organisms. We were aware of these challenges beginning the project and elected to use two taxonomic laboratories: Aquatic Analysts (AA) and Rhithron Associates, Inc. (Rhithron). AA was selected because it had conducted the phytoplankton analysis for the Raymond et al. (1997) study of the reservoirs and had conducted the periphyton analyses for the samples collected in the LDR (Raymond et al. 1998). Using AA for analysis would allow for a direct comparison of phytoplankton and periphyton results with the results from the earlier studies. However, the review of the phytoplankton samples from AA showed considerable differences between samples for the non-cyanobacteria species, although there was reasonable agreement at the level of genus. Both laboratories showed reasonable agreement identifying the onset of cyanobacteria, their relative abundance and identification of genera. However, the results from AA showed a consistent difference from Rhithron in biovolume; Rhithron typically reported biovolumes that were an order of magnitude greater than what was reported by AA. To allow the use of AA phytoplankton in a manner consistent with the Rhithron results, the phytoplankton biovolumes from AA were multiplied by 10. The comparison of AA and Rhithron results for periphyton were radically different. Both laboratories reported numerous species of diatoms; however, AA seldom reported more than one genus of cyanobacteria in the periphyton and the abundance of the cyanobacteria reported by AA was small compared to the biovolume measurements of cyanobacteria reported by Rhithron. In processing the periphyton samples, it appeared that AA did not adequately include a representative amount of filamentous material on the slides. AA did not report many filamentous green algae, such as *Cladophora*. However, field samples examined by the senior investigator in the field indicated that filamentous algae and cyanobacteria were common and that the results reported by AA were not representative of the periphyton communities. Consequently, all periphyton results reported by AA were excluded from the study.

Another component of the quality assurance review of the periphyton results involved sending split periphyton results from five samples to three laboratories, Rhithron, PhycoTech, Inc., and Georgia College. The objective of this comparison was to evaluate the reproducibility of identification of filamentous cyanobacteria that were reported to be abundant by Rhithron. Specifically, Rhithron had reported high abundance and widespread occurrence of the genus *Rivularia*. It was determined that the importance of this finding be confirmed by others with expertise in this area. The results of the comparison with the laboratories confirmed *Rivularia* as a dominant cyanobacteria, although the findings highlighted the variability in the taxonomic processing of complex periphyton communities. The results of these comparisons are shown in Appendix C.

Twelve zooplankton samples analyzed by ZP Taxonomic Services were split with Rhithron for a comparative analysis. The results showed general agreement with major zooplankton groups; however, results from ZP Taxonomic showed greater detail with taxonomic classifications and results from Rhithron tended to undercount the number of individuals compared to that reported by ZP Taxonomic. No changes were made to the results provided by ZP Taxonomic as a result of the comparative analysis with Rhithron.

The weather stations (Onset Computer) appeared to operate accurately and reliably. One problem was encountered at the Chinook Island weather station on LBC, the station orientation with regard to due north was not correctly installed. This problem was identified, and the station orientation was corrected; however, the early wind direction and velocity data from 2015 were discarded. Adjacent station results were compared with one another and found to be consistent, although wind-related data from the stations were not comparable among sites because of local variation in wind patterns.

A wide range of physical, chemical, and biological parameters were measured for this study. The standard sonde measurements (temperature, pH, DO, conductivity) were generally acceptable, although data review identified some observations that did not meet typical performance standards. The loggers from Onset Computer (temperature, DO, weather station) generally performed well and met nearly all criteria for acceptance. Analytical measurements from IEH

were nearly universally accepted. IEH's reporting limit for chloride was too high for the needs of this study and from 2016–2017, chloride samples were analyzed by CCAL. The ZAPS instrument required considerable adjustment during the installation period, but data collected from WY2016 into 2017 generally produced high-quality data. The exception was chlorophyll, where extensive instrument drift resulted in discarding data for this parameter. The most challenging data relative to meeting QA goals were those associated with the taxonomic analyses, especially the periphyton samples. Periphyton data from Aquatic Analysts from this study and the historical data from 1997 were rejected as unusable. The remaining periphyton data were still subject to a moderately high degree of variability.

3.7 Data Analysis

Statistical analysis of data was conducted using *Statistix* (Version 10), a software program produced by Analytical Software, Tallahassee, FL. The program has been used by researchers since 1985. Additional statistical and graphical analyses were performed with *Grapher* (Versions 13 & 14), produced by Golden Software, Golden, CO. This program has been available since 1992. Contour plots of temperature, pH, DO, conductivity, turbidity, light transmission, and chlorophyll were created for the sample sites in the impoundments. To create these plots, the algorithm interpolates values between observations; the farther apart that these values are located, either vertically in the water column or temporally, results in greater potential distortion of the value space. In some cases, the plots contain "islands" of values slightly different than the adjoining space. These constitute artifacts, which were judged acceptable for this application because of the benefit achieved in effectively displaying large amounts of data in a single figure and allowing the reader to quickly identify major patterns in the data. The reader should refer to Appendix D for line profiles of the data.

4 Reservoir Water Quality Data Results

4.1 Tributaries to Lake Billy Chinook

Flows into LBC are dominated by discharge from the three primary tributaries: the Metolius, Deschutes and Crooked rivers, each of which has distinct hydrology, temperature, and chemistry characteristics. Those characteristics result in heterogeneous water quality in LBC and profoundly impact the nature of the discharge to the LDR.

4.1.1 Hydrology

The largest tributary inflows are associated with the Metolius River. During the study years of WY2015–17, flows from the Metolius represented 39.5% of the inflow from the three tributaries, with an average discharge of 1,575 cfs (Table 4-1). The Metolius River is renowned for its large proportion of groundwater discharge emanating from the Cascades. This explains the relatively stable flows observed in the system, although some rain-on-snow events resulted in major episodic flows during the PoR. The Metolius River is also noteworthy because of the absence of impoundments in the drainage. By contrast, the Deschutes River above LBC also has influence from substantial groundwater inputs, but its discharge is highly regulated by impoundments (the Wickiup and Crane Prairie reservoirs) and by irrigation withdrawals located between Wickiup Dam and the city of Bend. The Deschutes River constituted 22.2% of the inflow into LBC during the period of study. The Crooked River contributed 38.3% of inflow into LBC during the study, although those flows are significantly affected by impoundments in the river's upper reaches (the Ochoco and Prineville reservoirs). There are substantial withdrawals for irrigation demands downstream of those two impoundments, but there is also a pronounced impact from groundwater inputs. For most of the year, discharge from Opal Springs, located immediately above the confluence with LBC, contributes about 80% of the discharge of the Crooked River to LBC, based on the difference in measured flows between the discharge downstream of Opal Springs and the discharge of the Crooked River upstream of the springs at Osborne Canyon.

Table 4-1. Daily average discharge statistics for the three primary tributaries to LBC for the water years of the study (2015–17) and for the PoR.

Discharge Statistic	Metolius River USGS #14091500 (cfs)		Deschutes River USGS #14076500 (cfs)		Crooked River USGS #14087400 (cfs)	
	2015–17	PoR	2015–17	PoR	2015–17	PoR
Years	3	97	3	64	3	56
Mean	1,575	1,507	887	907	1,528	1,543
Median	1,510	1,450	856	783	1,330	1,340
Minimum	1,310	1,080	461	425	1,220	1,090
Maximum	3,300	7,100	2,580	4,790	4,840	6,130
1st Quartile	1,400	1,330	552	537	1,280	1,270
3rd Quartile	1,698	1,630	1,142	1,140	1,460	1,510

The daily discharge for the three tributaries during the study illustrates the seasonal variations and patterns in flow (Figure 4-1). The Metolius River exhibited the least daily variation in discharge with modest high flows during winter and spring and a long gradual recession curve extending into fall. The Crooked River exhibited the largest peak flows during the study with increasing peak flows from 2015 to 2017. The Upper Deschutes River showed the most striking effects of irrigation withdrawals with abrupt changes during the onset and cessation of irrigation season. The dry years of 2015 and 2016 resulted in depletion of flows to the minimum allowable flows for the Upper Deschutes River under current USBR operating rules governing releases of water from Wickiup Reservoir and irrigation withdrawals managed through the Deschutes Basin Board of Control.

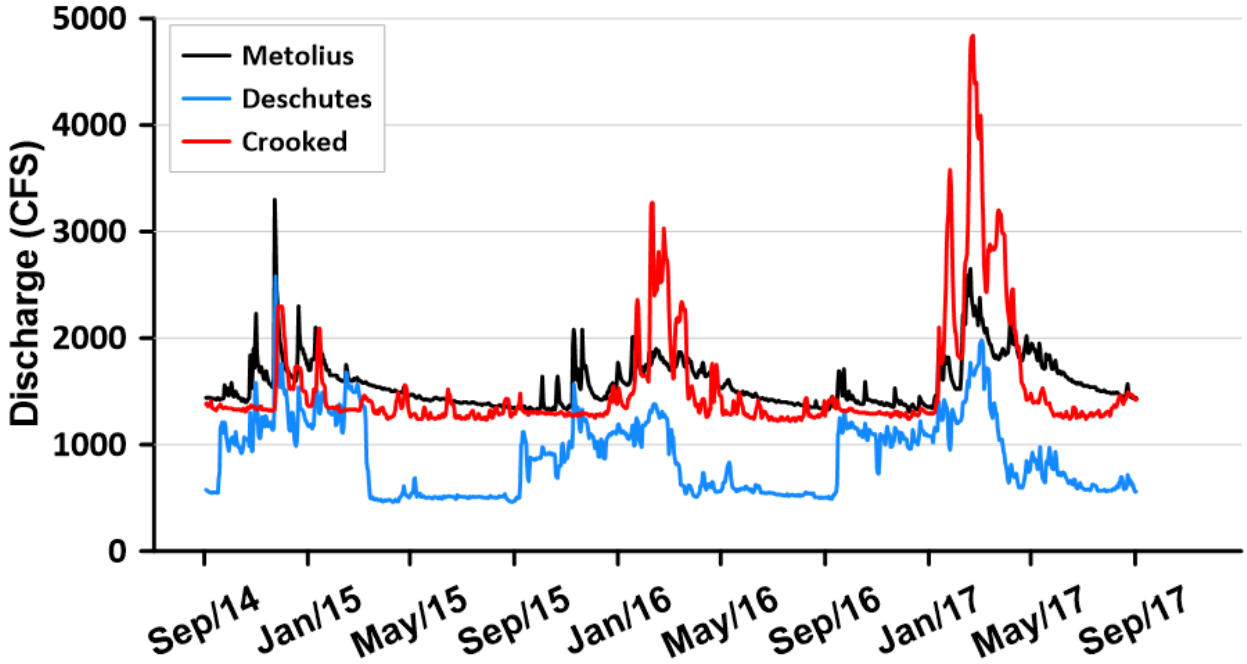

Figure 4-1. Daily average flow for the three major tributaries to LBC for WY2015–2017 (*Source*: USGS, n.d.).

The distinction in flows among tributaries becomes more apparent during the warm months of May–September when discharge from the Metolius and Crooked rivers changes only slightly, and discharge from the Middle Deschutes River, which has been reduced substantially due to irrigation diversions, represents only 16.9% of total summer inflow (Table 4-2). Historical patterns in irrigation withdrawals from the Deschutes River, however, are in flux as irrigation districts, agencies, and other interested parties have entered into a cooperative agreement to alter flows in the Upper Deschutes River basin to benefit the spotted frog and other aquatic species (Deschutes Basin Board of Control, 2016). These surface inflows do not include an estimated 420 cfs that enters LBC directly as groundwater inflow (Gannett et al. 2001). Yonkofski et al. (2016) surmised that the sources of groundwater to the Project area served as a net source of heat to these waters.

Table 4-2. Daily average discharge statistics for the three primary tributaries to LBC (WR2015–2017) from May through September (*Source*: USGS).

Discharge Statistic	Metolius River USGS #14091500 (cfs)	Deschutes River USGS #14076500 (cfs)	Crooked River USGS #14087400 (cfs)
Mean	1,515	585	1,354
Median	1,470	554	1,290
Minimum	1,340	461	1,220
Maximum	2,220	978	2,460
1st Quartile	1,400	511	1,260
3rd Quartile	1,570	620	1,390

4.1.2 Temperature

Temperatures of the major inflows to LBC greatly affect the mixing in the reservoir and, therefore, they also affect the nature of the water discharged downstream. The Metolius River is the coldest of the three inlets with an annual mean temperature of 7.2˚C and a maximum of 10.5˚C recorded during the study (Table 4-3). The warmest inlet based on maximum temperature recorded during the study was the Middle Deschutes River (16.2˚C), but on an annual basis, the Crooked River is the warmest with a mean temperature of 12.2˚C. During the warmer months of May–September, the mean temperature of the Upper Deschutes River increases to 13.7˚C, slightly warmer than the Crooked River at 13.3˚C during the same period. The Upper Deschutes River exhibits the most extreme temperature values, partly because of its lower degree of groundwater influence and partly because its low summer flow allows more solar warming. The data shows that water temperatures in the Upper Deschutes River exceed those in the Crooked River during summer months, although the reverse is true in the winter (Figure 4-2). Although the Crooked River is the warmest of the three rivers on average, it is also the least variable in water temperature. Whereas the Metolius River is recharged by cold groundwater inflow derived from snowmelt, the Crooked River spring influx is warmed by geothermal activity on the east side of the basin (Yonkofski et al. 2016).

Table 4-3. Daily average water temperature statistics (in ˚C) for the three primary tributaries to LBC (WY2015–2017) from May through September and for the entire period.

Temperature Statistic	Metolius River		Deschutes River		Crooked River	
	May - September	WY 2015–17	May - September	WY 2015–17	May - September	WY 2015–17
Mean	8.9	7.2	13.7	10.2	13.3	12.2
Median	9.0	7.3	14.0	11.0	13.4	12.4
Minimum	6.9	2.2	11.1	1.6	11.8	7.3
Maximum	10.5	10.5	16.2	16.2	14.2	14.2
1st Quartile	8.3	5.9	12.6	7.1	13.1	11.3
3rd Quartile	9.5	8.8	14.6	13.6	13.6	13.3

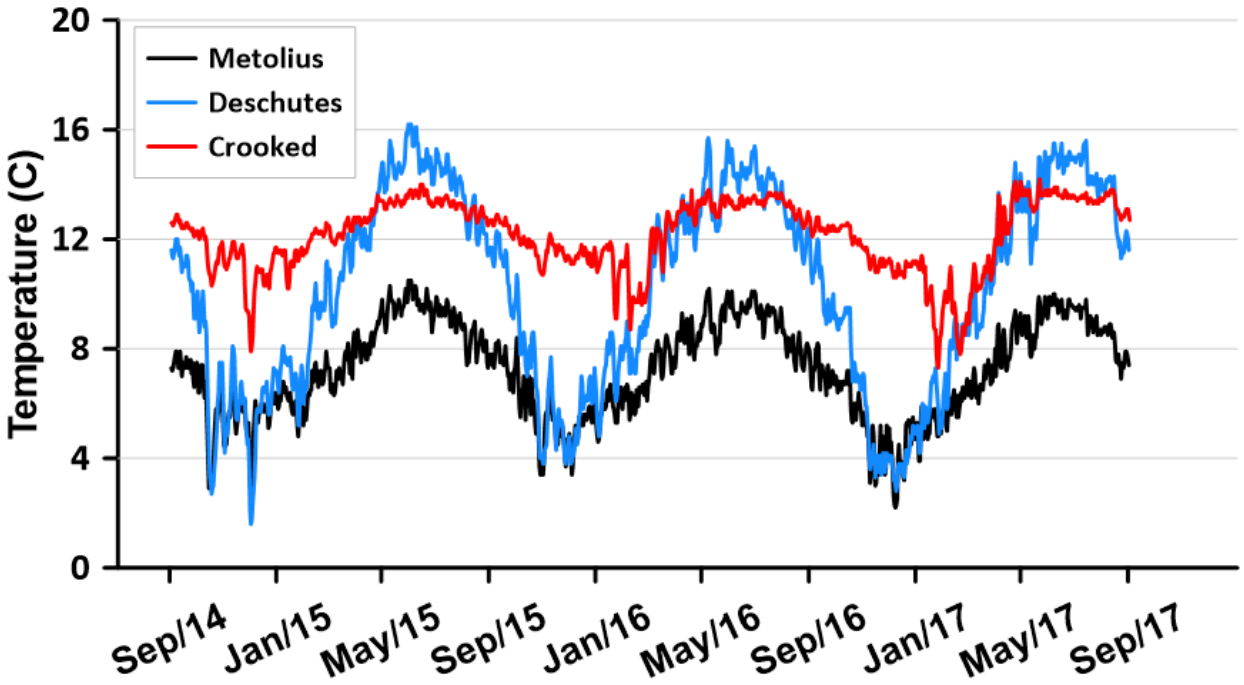

Figure 4-2. Daily average river temperature for the three major tributaries to LBC for WY2015–2017 (*Source*: USGS, n.d.).

4.1.3 Ambient Water Quality Monitoring Data

Water quality data for the three tributaries are available from the ODEQ AWQMP database. The ODEQ sites for the Metolius and Deschutes rivers are considered close enough to LBC to be representative. The ODEQ monitoring sites for the Crooked River, however, are located above Opal Springs. Because Opal Springs provides most of the flow for the Crooked River into LBC, the ODEQ sites are disproportionately impacted by point and nonpoint discharges in the watershed. A comparison of discharge above and below Opal Springs shows that input from the spring is nearly constant (Figure 4-3). Nevertheless, we present the long-term results from the ODEQ site in the Crooked River above Opal Springs (Crooked River at Lone Pine Road, Terrebonne) because it provides some indication of the nutrients that flow into LBC from the Crooked River.

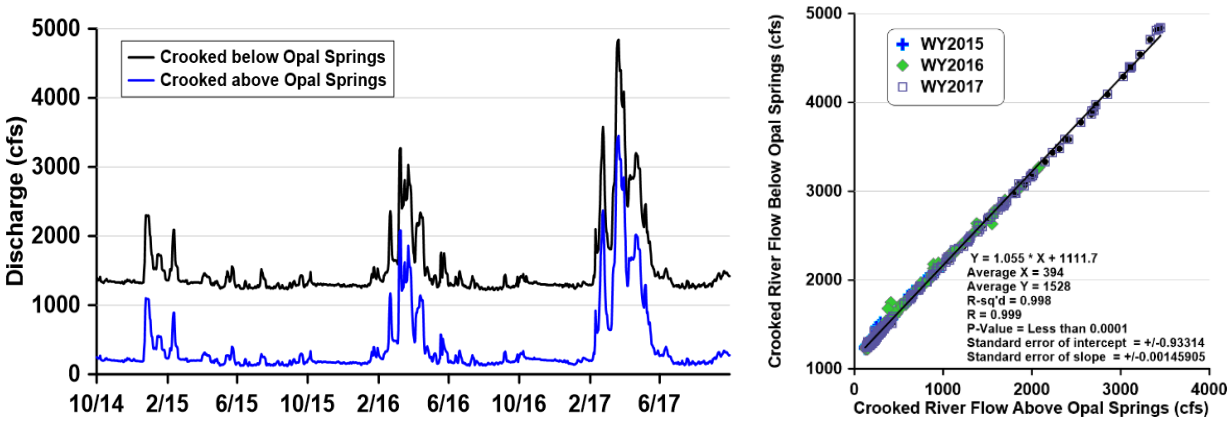

Figure 4-3. Discharge in the Crooked River above and below Opal Springs for WY2015–2017. Data from USGS Stream Gage #14087380 above Opal Springs and USGS Stream Gage #14087400 below Opal Springs.

The ODEQ AWQMP data include parameters not addressed in this study and observations that extend back several decades. We focused on the parameters with the greatest potential for nutrient-related issues—total phosphorus (TP), PO_4, NO_3, pH, and turbidity—and used the more than 50 years of observations in time-series plots (see Figure 4-4). Boxplots of the ODEQ monitoring results by tributary illustrate important differences among the sites (Figure 4-5).

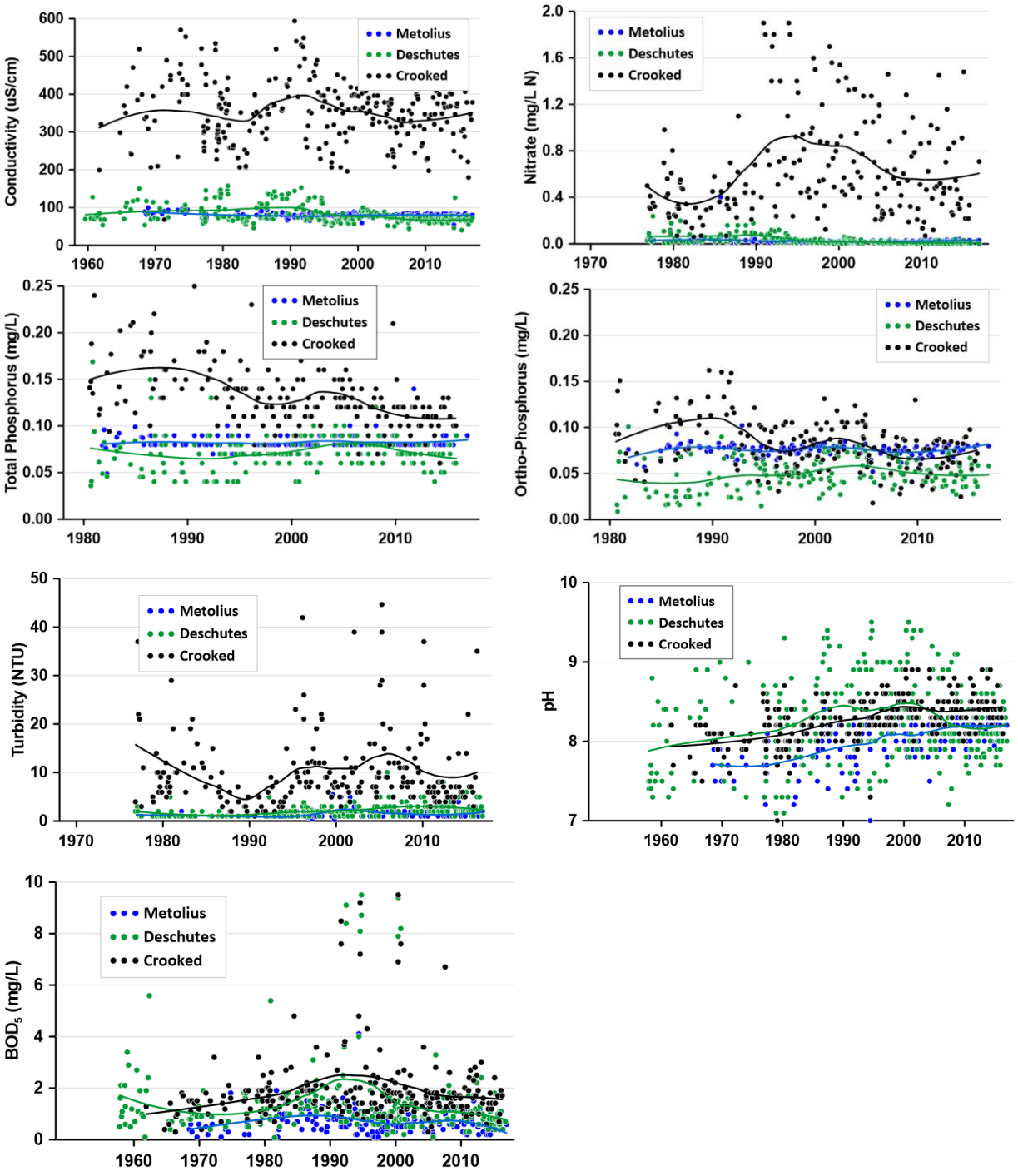

Figure 4-4. Time-series plots of water quality data for the three major tributaries to LBC. The curves are LOESS fits of the observed data (*Source*: ODEQ AWQMP, n.d.). Note that the Crooked River data were collected above Opal Springs. The pH plot has the y-axis truncated to provide better data resolution.

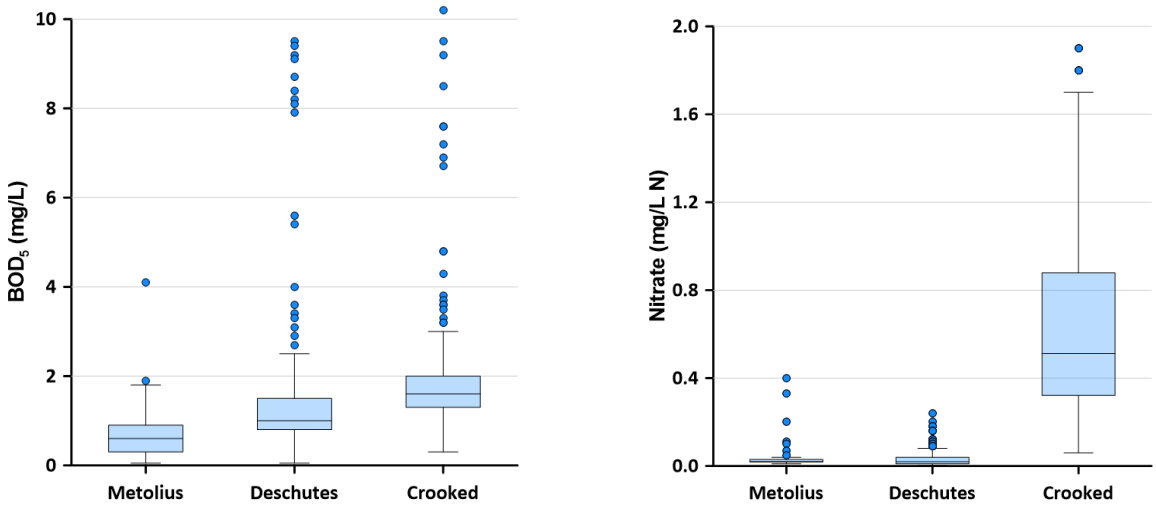

Figure 4-5. Distributions of turbidity, PO_4, biochemical oxygen demand (BOD_5), and NO_3 for the three tributaries monitored by the ODEQ AWQMP. The Metolius River site is near Camp Sherman, the Deschutes River site is at the lower bridge over the Deschutes inlet, and the Crooked River site is near the town of Terrebonne. Note that the Crooked River site is located upstream from Opal Springs and nearby unnamed springs in the lower canyon downstream of Osbourne Canyon, which comprise about 80% of the discharge from the Crooked River into LBC.

Median values from the Crooked River site were higher than from the other two sites for BOD_5, PO_4, turbidity, and NO_3/NO_2 (see Figure 4-5). The disparity is particularly striking for turbidity and NO_3. The Crooked River was far more turbid than the other two inlets, with values up to 70 Nephelometric Turbidity Units (NTUs) compared to a maximum turbidity of 5 NTUs at the Metolius site and 10 NTUs at the Deschutes site. The most significant disparity was with NO_3: the median NO_3 concentration in the Crooked River exceeded the outliers from the other two sites.

Time-series data for the three ODEQ tributary sites illustrate important distinctions and trends among the sites. The conductivity values showed close agreement and no trend for the Metolius and Deschutes sites (Figure 4-4). The conductivity values for the Crooked site, upstream of Opal Springs, were about four times higher than for the other two sites and peaked around 1990. The Crooked site also showed considerably more variability than the Metolius and Deschutes sites. The Metolius and Deschutes sites had little or no measurable NO_3 present, whereas the Crooked site showed NO_3 concentrations over 2 milligrams per liter (mg/L) (several outliers not displayed

but are assumed to be accurate) as well as highly variable values. The apparent peak in NO_3 in the Crooked River occurred in the early 1990s, although the median concentration stabilized near 0.6 mg/L in the last decade. Concentrations of TP for the Metolius and Deschutes rivers were stable for the PoR, whereas concentrations for the Crooked River were considerably higher and appear to have declined since the 1990s. Throughout the PoR, the Deschutes River had the lowest concentration of PO_4. More recent data showed that PO_4 concentrations were nearly equal in the Metolius and Crooked rivers at about 0.07 mg/L. PO_4 values for the Crooked River apparently have declined since the 1980s and early 1990s. Turbidity values for the Metolius and Deschutes rivers were low and stable, often below 1 NTU, whereas typical values for the Crooked site were nearly 10 NTUs and sometimes much higher (several outliers were also truncated in this plot). pH measurements showed consistent increases at all three sites for the PoR.

The pH values at the Metolius site were consistently about 0.25 units lower than at the Crooked and Deschutes sites. Nearly all increases in pH occurred prior to 2000. Concentrations of BOD_5 were lowest for the Metolius (usually less than 1 mg/L) and highest for the Crooked River. Both the Deschutes and Crooked river sites exhibited increases around 1990 but have since declined.

4.1.4 2015–2017 Water Quality Data

Field staff collected field measurements at each of the three inlets to LBC as part of this study. The sites were similar to those monitored by ODEQ with the exception of ODEQ's site in the Crooked River upstream of Opal Springs; the field staff sampled at a site downstream of Opal Springs just above the confluence with LBC. This is an important distinction because Opal Springs combined with other springs in the lower Crooked River canyon downstream of Osbourne Canyon provide 80% of the flow to the Crooked River. Comparing discharge in the Crooked River both above and below Opal Springs shows that the springs contributed 1,100 cfs to the flow of the river at baseflow during the study and 1,134 cfs on average. Flow from Opal Springs was stable, and all large increases in flow from the Crooked River were associated with storm and snowmelt contributions from the watershed as modified by discharges from the Ochoco and Prineville reservoirs.

During the staff's field collection, conductivity was noticeably different among the three tributaries (Figure 4-6). Conductivity represents the equivalent sum of individual ions, so it is relatively conservative and serves as an excellent tracer for the inlets in LBC (see Section 4.2.2). pH values for all tributaries generally peaked in July and declined slightly into winter. Values for the tributaries showed minor differences in 2015, but the Metolius River was considerably lower than the other sites in 2016 (Figure 4-7). The pH values in June were low in 2015 for all three sites and even lower in 2016 for the Metolius River. The validity of the data is suspect, given that ODEQ never measured such low pH values over decades, and they were removed from the dataset.

DO concentrations peaked in late April/early May during spring runoff when flows were elevated (Figure 4-8). One DO value of nearly 16 mg/L reported for the Metolius River in 2015 was suspect and was discarded. Single outliers of DO, however, have little effect on either the modeling or water quality in LBC.

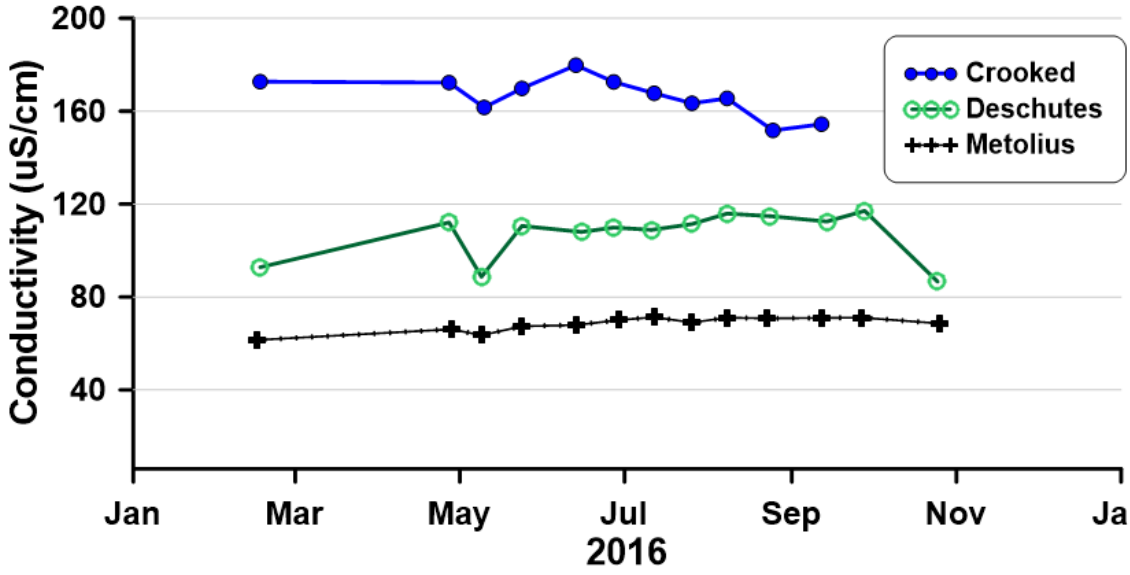

Figure 4-6. Conductivity values collected by field staff for the three tributaries in 2016. Only sporadic measurements of conductivity were recorded in 2015 and no measurements were made in 2017. Note that the Crooked River data were collected downstream from Opal Springs.

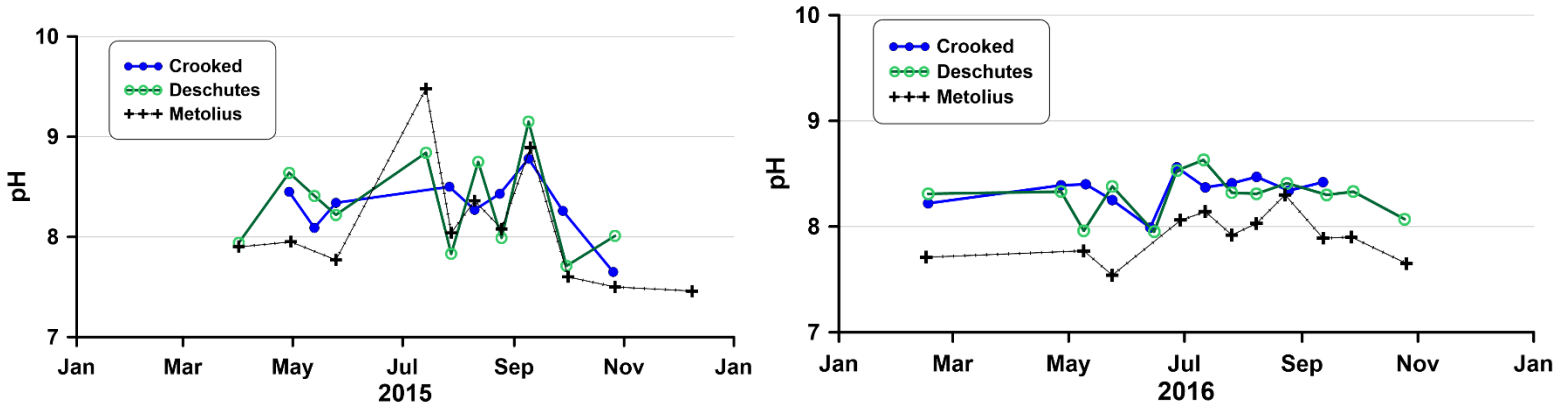

Figure 4-7. pH measured at the three tributaries to LBC in 2015 and 2016. No measurements were made in 2017. Note that the Crooked River data were collected downstream from Opal Springs.

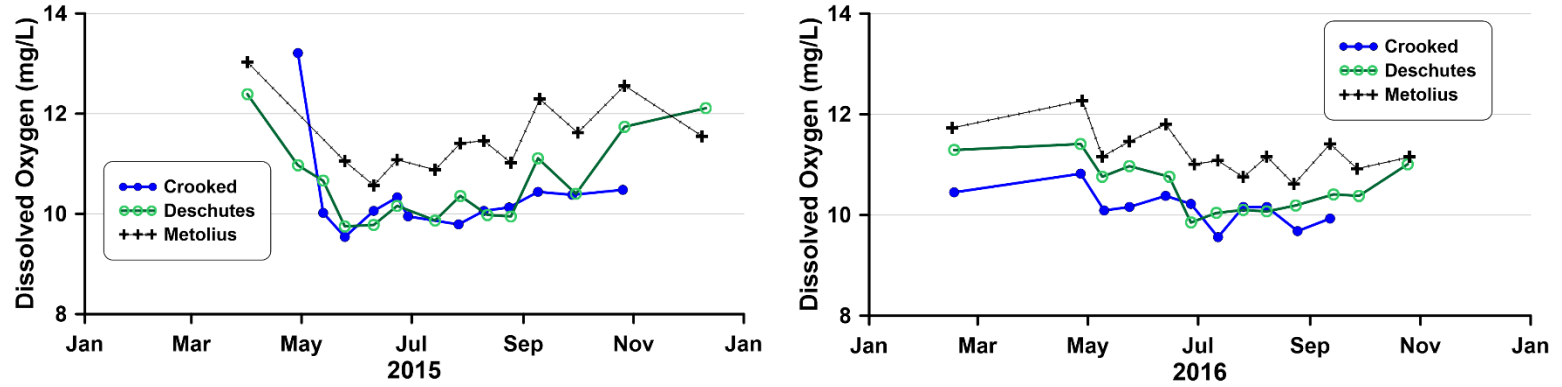

Figure 4-8. DO concentrations measured at the three tributaries to LBC in 2015 and 2016. No measurements were made in 2017. Note that the Crooked River data were collected downstream from Opal Springs.

Concentrations of total nitrogen (TN) were always highest at the Crooked River site and lowest at the Metolius River site (Figure 4-9). During 2015, the TN measurements of several samples from the Metolius River were below the detection limit (DL) of <0.050 mg/L, as were the NO_3 measurements (DL < 0.010 mg/L), which highlights the profound N-limited nature of this river. The concentrations of TN in the Deschutes River fell between those in the Metolius and Crooked rivers, which was the case for most of the nutrients from the site. NO_3 concentrations for each tributary site were similar between the 2 years of monitoring (Figure 4-10). Concentrations of NO_3 for the Metolius River were at or near the DL (0.010 mg/L) on all sample dates, whereas those for the Deschutes and Crooked rivers were about 0.2 mg/L and 0.4 mg/L, respectively. These high concentrations likely reflect strong influence from irrigation return flow or enrichment of the aquifers from fertilizer applications. Inflow from Opal Springs dilutes NO_3 concentrations by nearly 50% from those measured at the Terrebonne site upstream of Opal Springs. Most of the analyses of ammonia (NH_3) were at or below the DL (0.010 mg/L) and are not displayed.

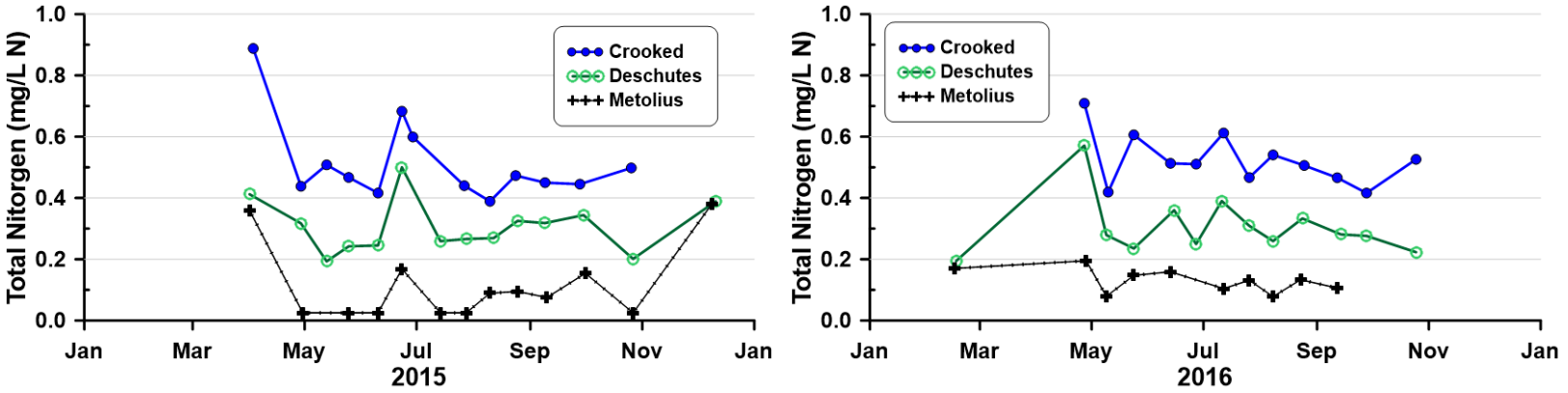

Figure 4-9. Concentrations of TN in the tributaries to LBC for 2015 (*left*) and 2016 (*right*).

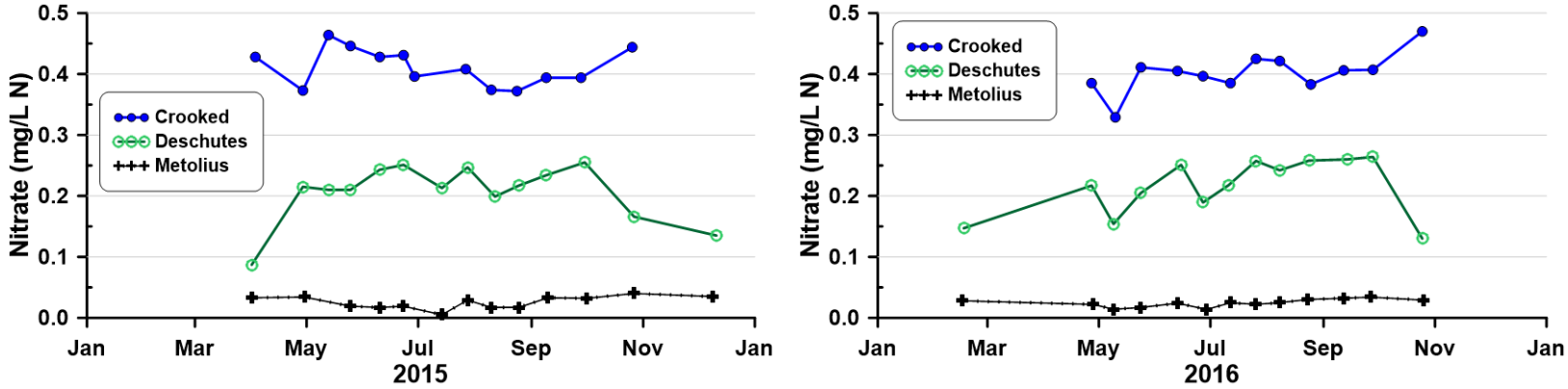

Figure 4-10. Concentrations of NO_3 at the three tributaries to LBC measured during the study.

Concentrations of TP in all three tributaries were relatively high and stable (Figure 4-11). Again, the values for the Crooked River were highest and those for the Metolius River were lowest, but the differences were comparatively small. Concentrations of PO_4 were moderately variable across sites and years (Figure 4-12), with concentrations generally highest at the Crooked River, while the lowest values alternated between the Metolius and Deschutes rivers. PO_4 concentrations were generally similar between all sites and were relatively high entering the impoundment regardless of date.

The summary of nutrient concentrations collected in this study shows that the Crooked River had the greatest concentrations of TP and TN among the three inlets (Table 4-4), with significantly greater concentrations of PO_4, TN and NO_3. The Metolius River had high concentrations of TP and PO_4, but low concentrations of TN and NO_3.

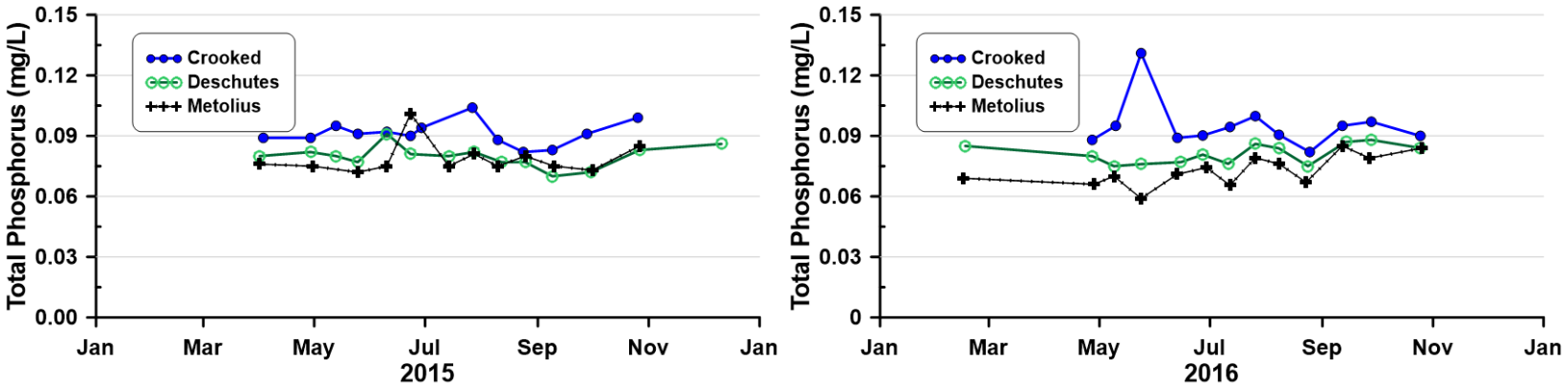

Figure 4-11. TP concentrations for the tributaries to LBC for 2015 (*left*) and 2016 (*right*).

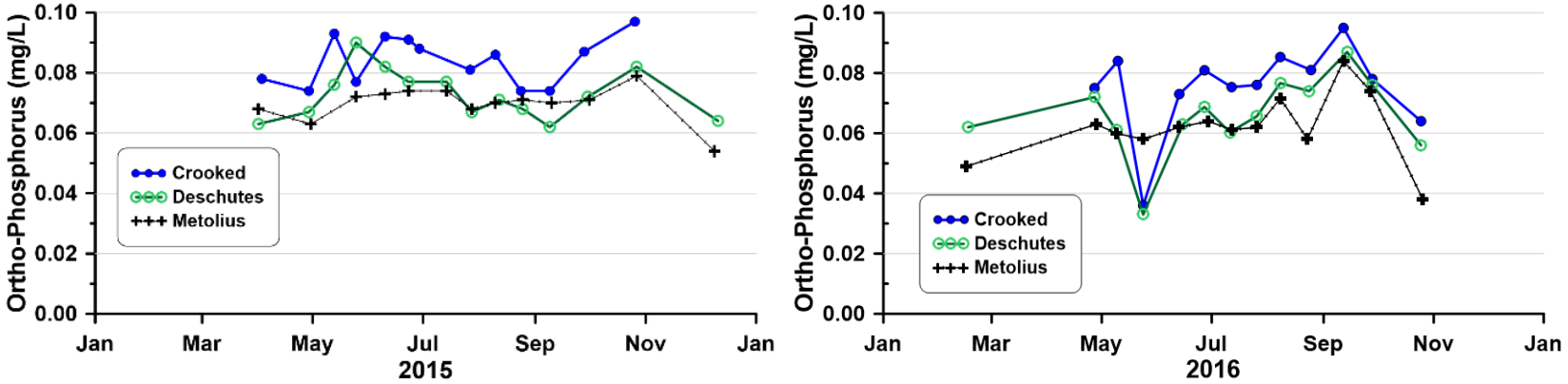

Figure 4-12. PO_4 concentrations for the tributaries to LBC for 2015 (*left*) and 2016 (*right*). Tributary data were not collected in 2017.

Table 4-4. Nutrient concentrations measured in the three principal tributaries to LBC for 2015–2016. Sample sizes ranged from 24 (Crooked) to 27 (Deschutes). Ammonia is not shown because most observations were reported at the DL (0.010 mg/L).

		Crooked (mg/L)	**Deschutes (mg/L)**	**Metolius (mg/L)**
TP	mean	0.093	0.081	0.083
	sd	0.010	0.005	0.040
PO_4[a]	mean	0.080 **	0.069	0.066
	sd	0.012	0.011	0.009
TN[b]	mean	0.495 **	0.314 **	0.110 **
	sd	0.100	0.094	0.095
NO_3[b]	mean	0.396 **	0.219 **	0.025 **
	sd	0.050	0.065	0.009

Notes:

[a] Crooked is significantly greater than the Deschutes and Metolius

[b] All sites are significantly different from one another

** where p is < 0.01

The ratio of nitrogen to phosphorus provides an indication of the relative availability of these critical nutrients in aquatic systems. The most common expression of this relationship is the ratio of total nitrogen to total phosphorus (TN:TP), shown in Figure 4-13 as a mass ratio. Values greater than 7.2 generally indicate some degree of phosphorus limitation, although some researchers express it as a range of values to indicate the uncertainty in the relationship (Allan 1995). Regardless of the specific value selected, the study's monitoring results showed that the Metolius River was consistently low in nitrogen in relation to phosphorus, a pattern that was consistent in both years. The ratio in the Deschutes River was between those of the Metolius and Crooked rivers but was still low relative to TN. The Crooked River exhibited some periods, notably in the spring, when the ratio indicated low phosphorus relative to nitrogen. Note that those samples were associated with high runoff events and often coincided with elevated inputs of total suspended solids (ODEQ AWQMP data).

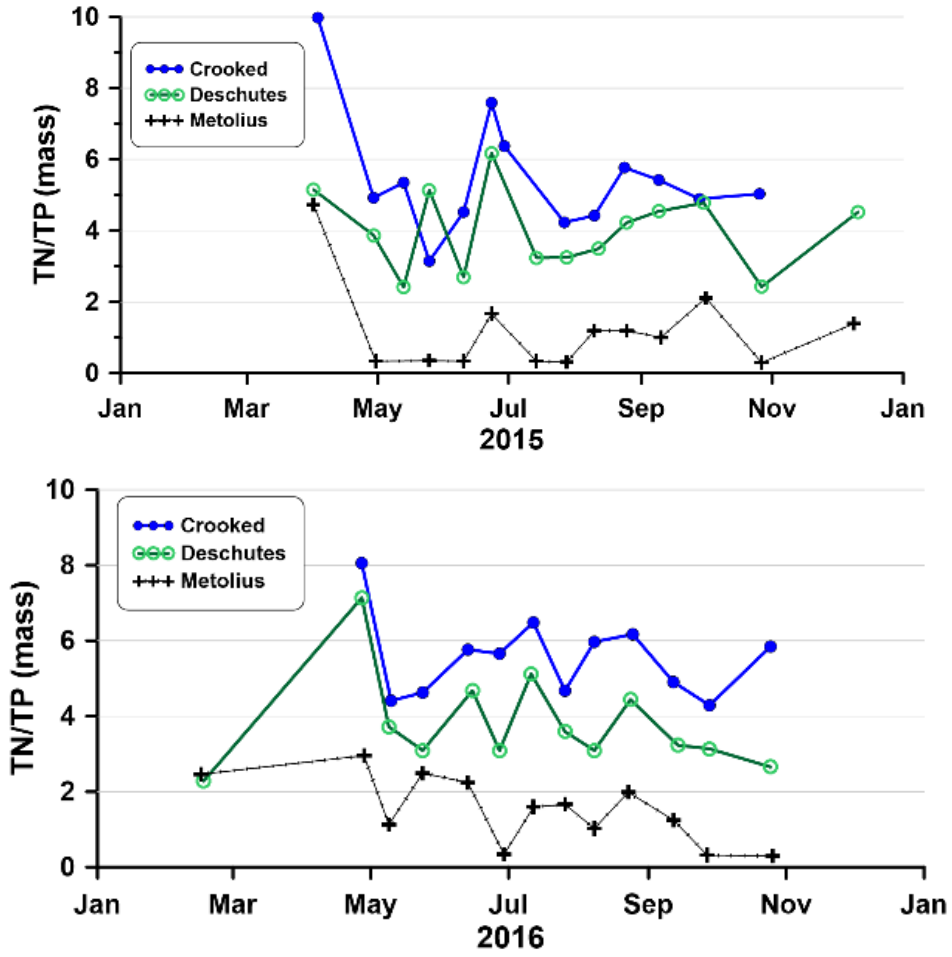

Figure 4-13. Mass ratios of TN:TP for the three inlets for 2015 (*top*) and 2016 (*bottom*).

Concentrations of TN and TP can sometimes obscure what may be available to algae as nutrients, because particulate forms of nitrogen can be associated with plant matter and particulate forms of phosphorus can be associated with entrained soil. An alternate method of examining the nitrogen and phosphorus relationship is to compare the inorganic forms, in this case, NO_3 and PO_4. Note that NH_3 was not considered in this comparison because almost all the NH_3 measurements were less than the DL (0.010 mg/L). The study results highlighted the impressive lack of nitrogen available in the Metolius River (Figure 4-14). Except for values in late May, the ratios were relatively stable.

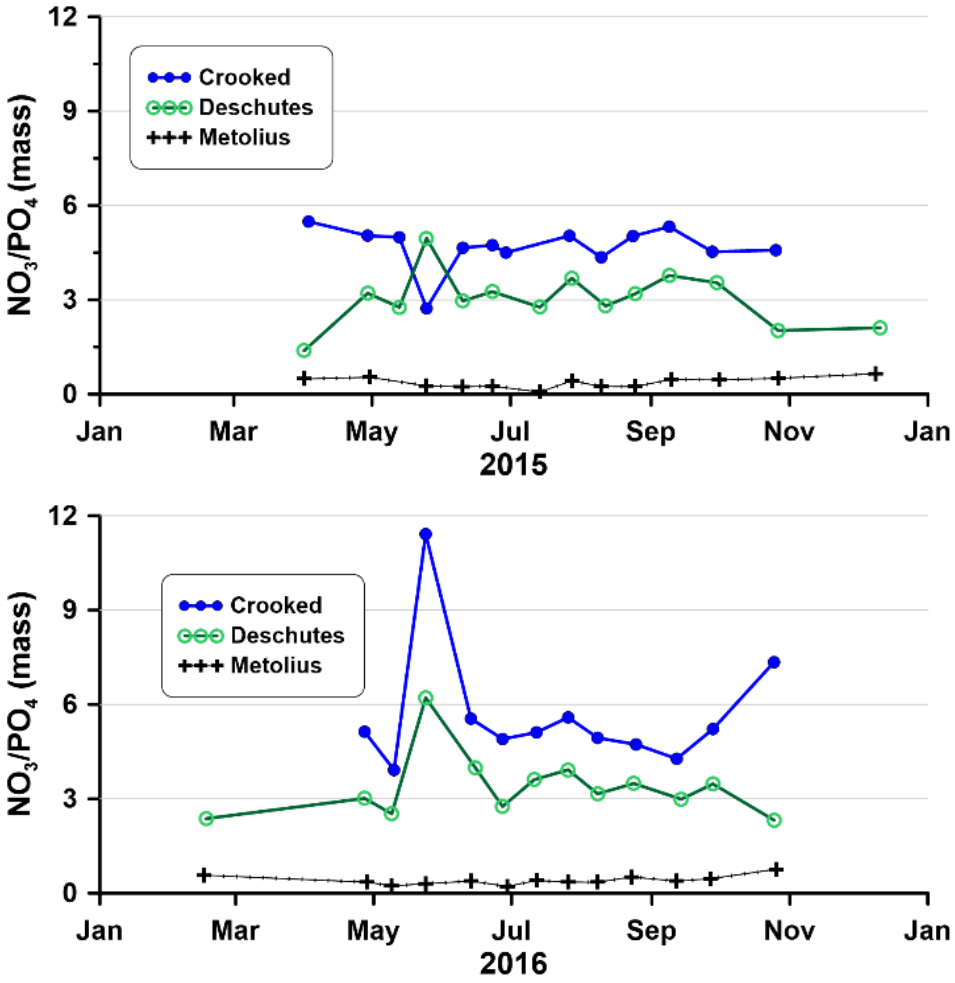

Figure 4-14. Mass ratio of NO_3 to PO_4 in the three tributaries to LBC in 2015 (*top*) and 2016 (*bottom*).

Both the ODEQ AWQMP data and the two years of nutrient chemistry collected as part of the Water Quality Study showed that all three tributaries contribute moderate to high concentrations of phosphorus and that most of the phosphorus is present as highly available PO_4. Other parameters in the ODEQ AWQMP data indicated that the Crooked River had the highest values of NO_3, TN, BOD, and turbidity among the three tributaries. The contrast between the two largest tributaries by inflow volume—the Metolius and Crooked rivers—is considerable, with the nitrogen concentration particularly elevated in Crooked River inflows, much of it highly available as NO_3. The inflow from the Crooked River is also distinctive because it was considerably more turbid than the inflow from the other tributaries, with enough turbidity to

reduce light transmission (and be viewed as such with the naked eye), but not enough to materially add to the density of the inflows. Consequently, the Crooked River inflows remained less dense than the colder waters from the Metolius River during much of the year. During the summer, however, the Deschutes River was considerably warmer and represented a disproportionately higher percentage of epilimnetic waters in LBC. The effect of the tributaries on LBC is described in Section 4.2.1.

4.1.5 Periphyton

Measurements of benthic chlorophyll concentration collected at the tributary sites provide a reasonable measure of the relative productivity of the three sites. The data showed sporadic high levels of chlorophyll on the substrate for the Crooked and Deschutes river sites but consistently low levels of benthic chlorophyll for the Metolius River site (Figure 4-15). All three sites showed low levels of benthic chlorophyll in September, consistent with expected decline of the periphyton in the fall. Values indicative of high stream productivity (eutrophy) range from 50 to 200 milligrams per square meter (mg/m^2) (Dodds et al. 1998), which includes both the Crooked and Deschutes river sites.

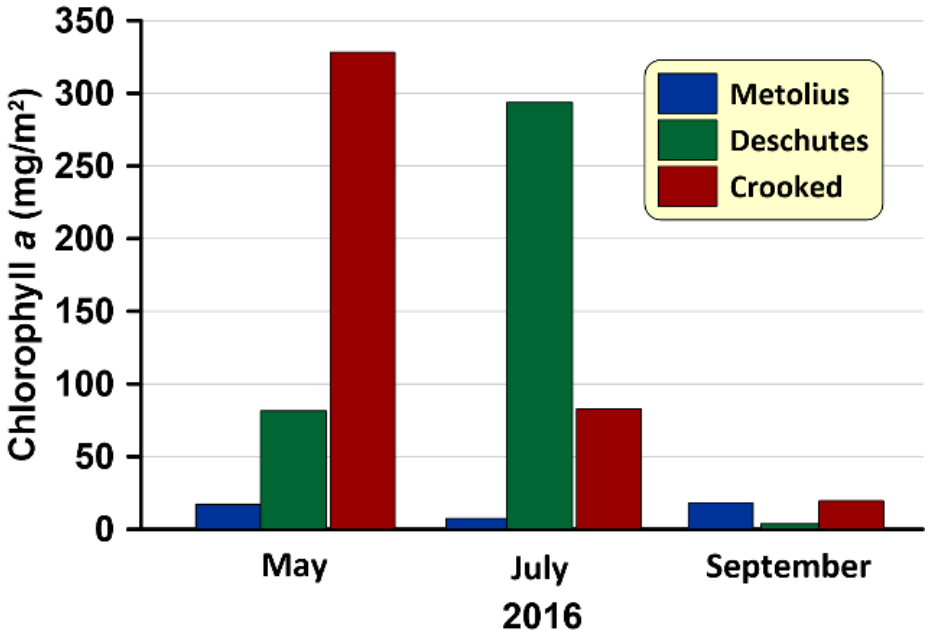

Figure 4-15. Benthic chlorophyll values at the three inlets to LBC.

The periphyton communities, sampled on several occasions in 2015 and 2016, varied widely among the tributaries and among dates for a given site (Figure 4-16). At the Metolius River site, total periphyton biovolume was relatively low (< 10^8 µm^3/cm^2) in August 2015 and May 2016; however, the October 2015 sample had high chlorophyte and cyanophyte biovolumes (> 10^9 µm^3/cm^2), which exceeded the combined biovolumes at the Deschutes and Crooked river sites. Chlorophytes at the Crooked River site were high in the August 2015 and May 2016 samples, although chlorophyte biovolume from the October sample was low.

Like periphyton biovolume, the taxonomic composition of the periphyton community varied widely among the tributaries to LBC and among dates for a given site. The two samples from the Crooked River site with high chlorophyte biovolumes were dominated by *Cladophora*. This taxon was abundant throughout much of the LDR, but was only abundant at the Crooked River tributary site. The abundant chlorophyte from the October Metolius sample was *Zygnema*, a taxon not common in the LDR. *Zygnema*, like *Cladophora*, is a filamentous green alga that can develop into large mats. However, some species of *Zygnema* are notable for being indicators of pristine water quality, as reported for streams sampled in California (Stancheva & Sheath, unpublished poster). The most abundant chlorophyte identified at the Deschutes River site was *Stigeoclonium*, which was also present in the May Crooked River sample.

The two dominant cyanophyte genera among the sites were the non-heterocystous taxa (non-N fixing) *Hydrococcus* and *Homoeothrix*. *Hydrococcus* was the dominant cyanophyte taxon for the Metolius samples in 2015; however, *Homoeothrix* was the dominant cyanophyte for all three sites in May 2016. Diatoms represented a minor portion of the periphyton biovolume among the tributary periphyton samples. The more abundant diatom taxa included *Gomphoneis mammilla* (Crooked River, August), *Diatoma vulgaris* (Crooked River, May), *Melosira varians* (Crooked River, October) and *Cymbella mexicana* (Deschutes River, May).

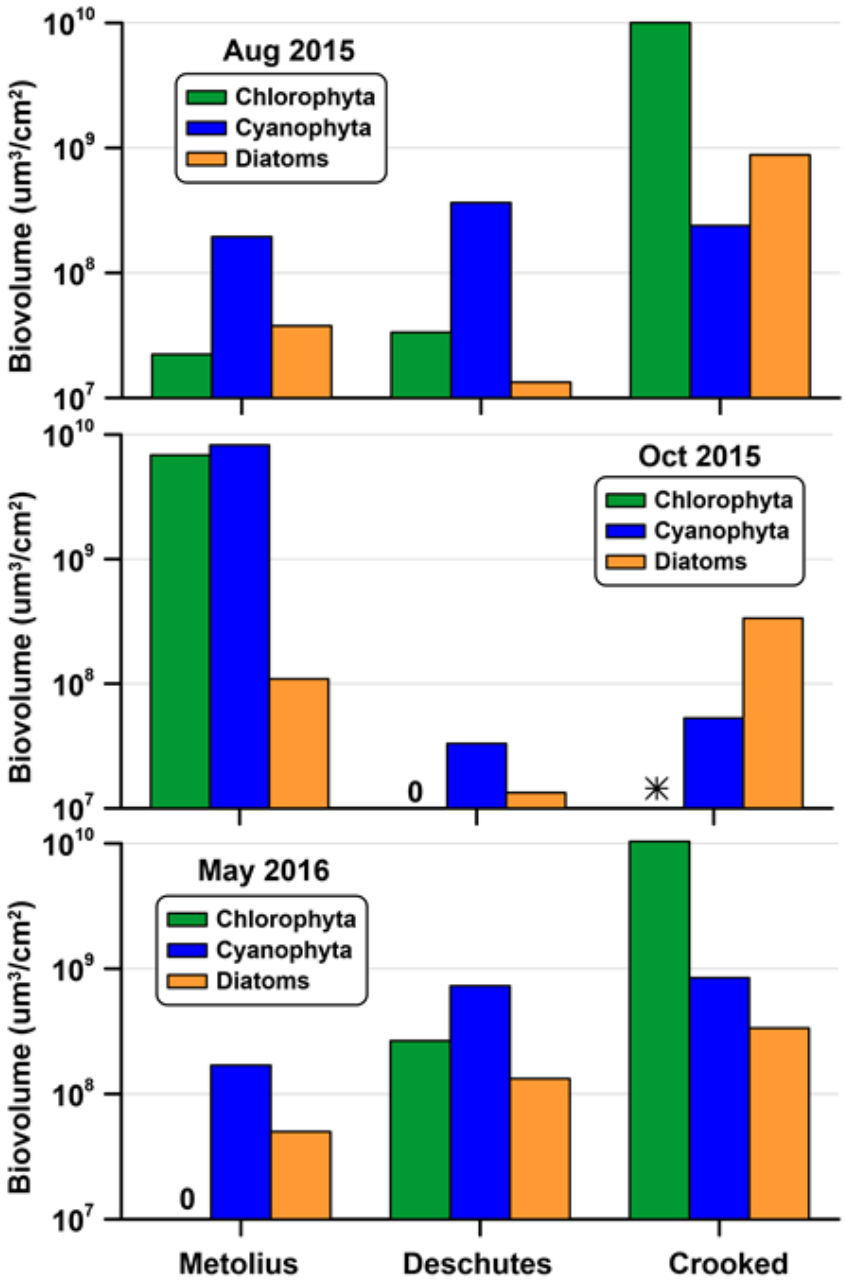

Figure 4-16. Periphyton biovolume for the major taxonomic groups from the three sites tributary to LBC in August and October 2015 and May 2016. The "*" designates that chlorophytes were present but the biovolume was < 10^7 µm^3/cm^2.

4.2 Project Impoundments

4.2.1 Lake Billy Chinook

LBC is a large, complex reservoir impounding three rivers, each with a well-defined arm. Two sites were studied in LBC: the Common Pool (RES08) is located near the confluence of the Crooked and Deschutes river arms, and Round Butte forebay (RES07) is located downstream of the confluence of the combined Crooked and Deschutes river arm and the Metolius River arm. The mixing of the three inflows is enormously important in affecting the vertical distribution of nutrients and other constituents. Before the SWW was installed, all outflow from LBC exited the forebay from the hypolimnetic withdrawal. Consequently, flows from the generally warmer Crooked River flowed over the surface of LBC and extended up most of the length of the Metolius arm. Flow from the Metolius River encountered the warm epilimnetic water from the Crooked River and plunged deep and flowed to the hypolimnetic intake in Round Butte forebay. With the installation of the SWW, Crooked River waters are preferentially drawn to the surface collector and discharge from LBC now comprises a mixture of epilimnetic and hypolimnetic waters. Because of the complexity of the lake morphometry and the configuration of the withdrawal structure, additional monitoring sites would be required to fully characterize the water quality throughout. This section provides information on the water quality in the reservoir as it approaches the dam. The results are arranged showing the profile data first, followed by water chemistry (e.g., nutrients), and concluding with planktonic biological communities. Much of the water quality data collected during the study are represented as depth contours. Profiles for selected individual dates are provided in Appendix D as an alternative method for displaying the same data.

4.2.1.1 Temperature

The field team collected temperature profiles in LBC at two locations in 2015 and 2016: Round Butte forebay (RES07) and the Common Pool (RES08) near the confluence of the Deschutes and Crooked river arms. Profiles were collected only at Round Butte forebay (RES07) during the summer of 2017. The results showed that surface water temperatures peaked at about 20-22˚C at Round Butte forebay (RES07) in all three years and at the Common Pool (RES08) in 2015 and

2016 (Figure 4-17). Peak surface temperatures were generally observed in July or August. The temperature profiles seldom exhibited distinct demarcations. Instead, recognizable epilimnetic features typically developed in spring, but temperature exhibited a gradual decline from the surface to the hypolimnion. A plot of temperature profiles for Round Butte forebay (RES07) illustrates differences in temperature stratification across months (Figure 4-18). April, May, and June 2016 had distinct epilimnia with abrupt transitions from near-uniform values in the surface waters and a sharp decline in temperature below the epilimnion. In contrast, temperature profiles for July and August had less distinct epilimnia despite the warmer conditions. The absence of a distinct boundary between the surface waters and deeper in the water column allowed for increased mixing of waters generally above 35 m during much of the year. Factors that contribute to thermal profiles such as those observed in LBC include a high degree of mixing from wind, a high degree of primary production resulting in reduced light penetration, and release of water from multiple depths. Output from the numerical modeling of LBC and the data from the thermistor arrays deployed in Round Butte forebay (RES07) by field staff indicated the likely presence of internal waves, or "seiches." The seiche is identified as a temperature pattern out of synchronization with normal heating and cooling (Figure 4-19). In particular, the temperature pattern at 2 m and 6 m peak in concert with the surface temperatures on July 12, 2016, but the following day, the temperatures at these two depths are depressed when the surface temperatures are peaking.

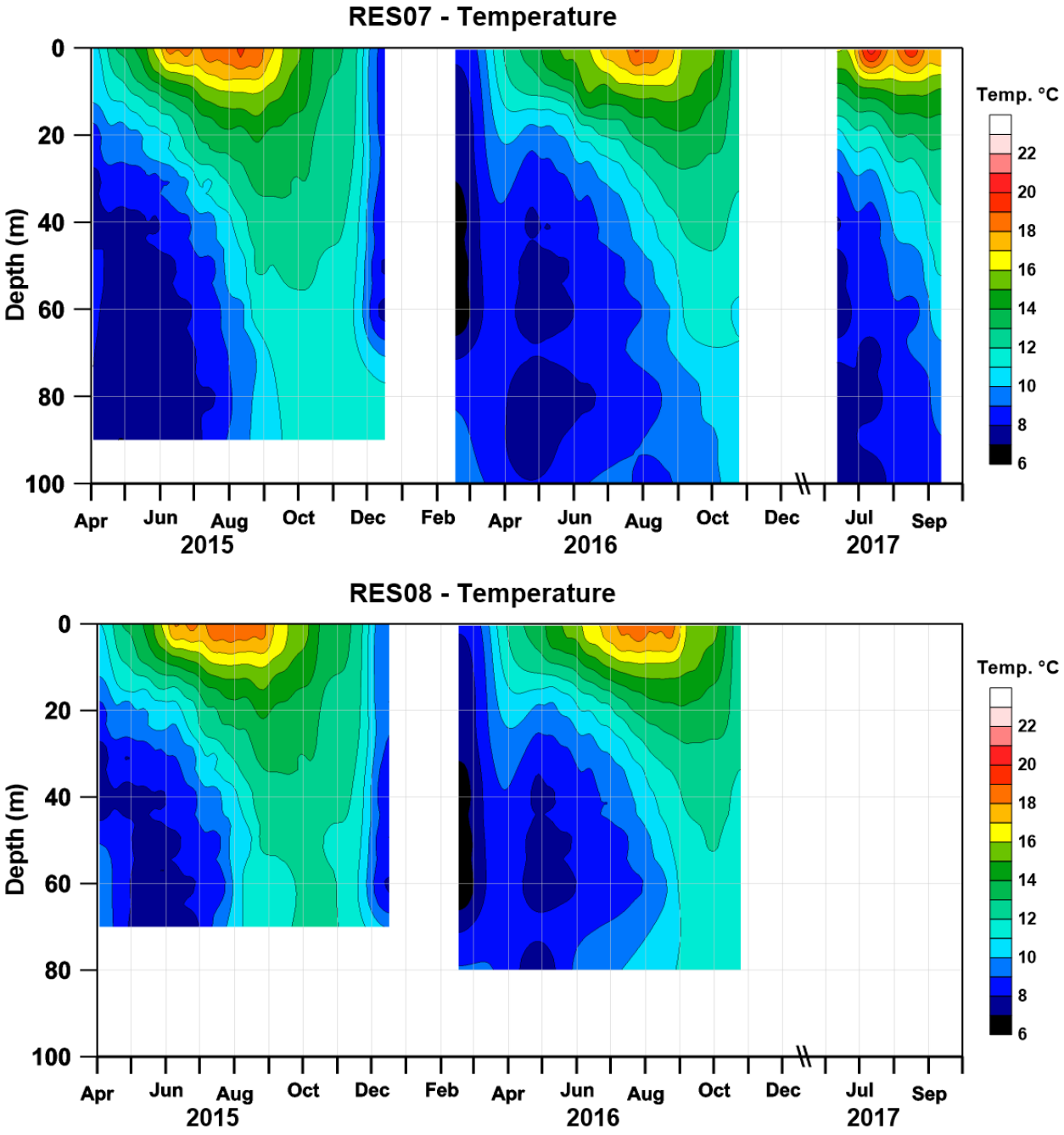

Figure 4-17. Temperature contours for Round Butte forebay (RES07) (*top*) and the Common Pool (RES08) (*bottom*). Field measurements were not collected at the Common Pool (RES08) in 2017.

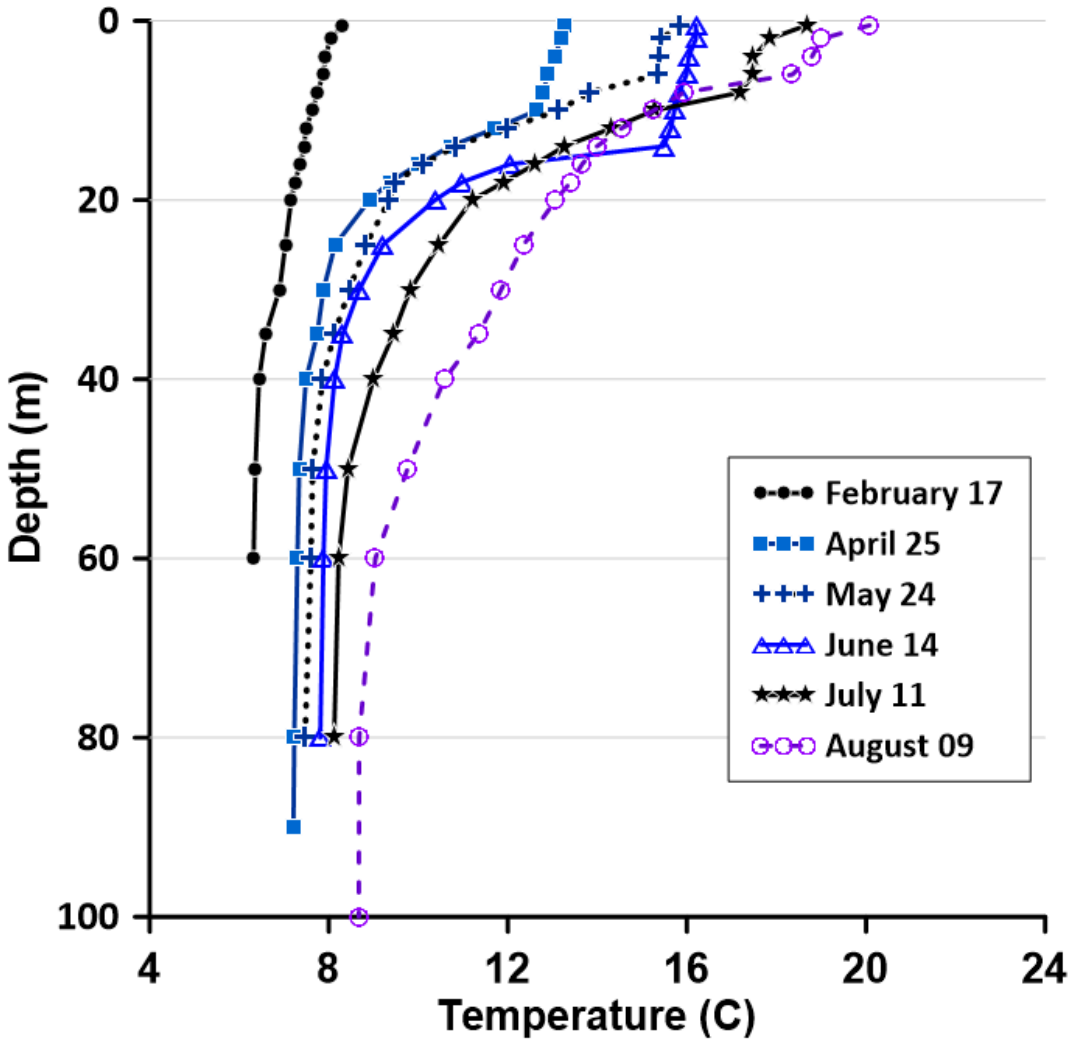

Figure 4-18. Selected temperature profiles in LBC for Round Butte forebay (RES07) in 2016.

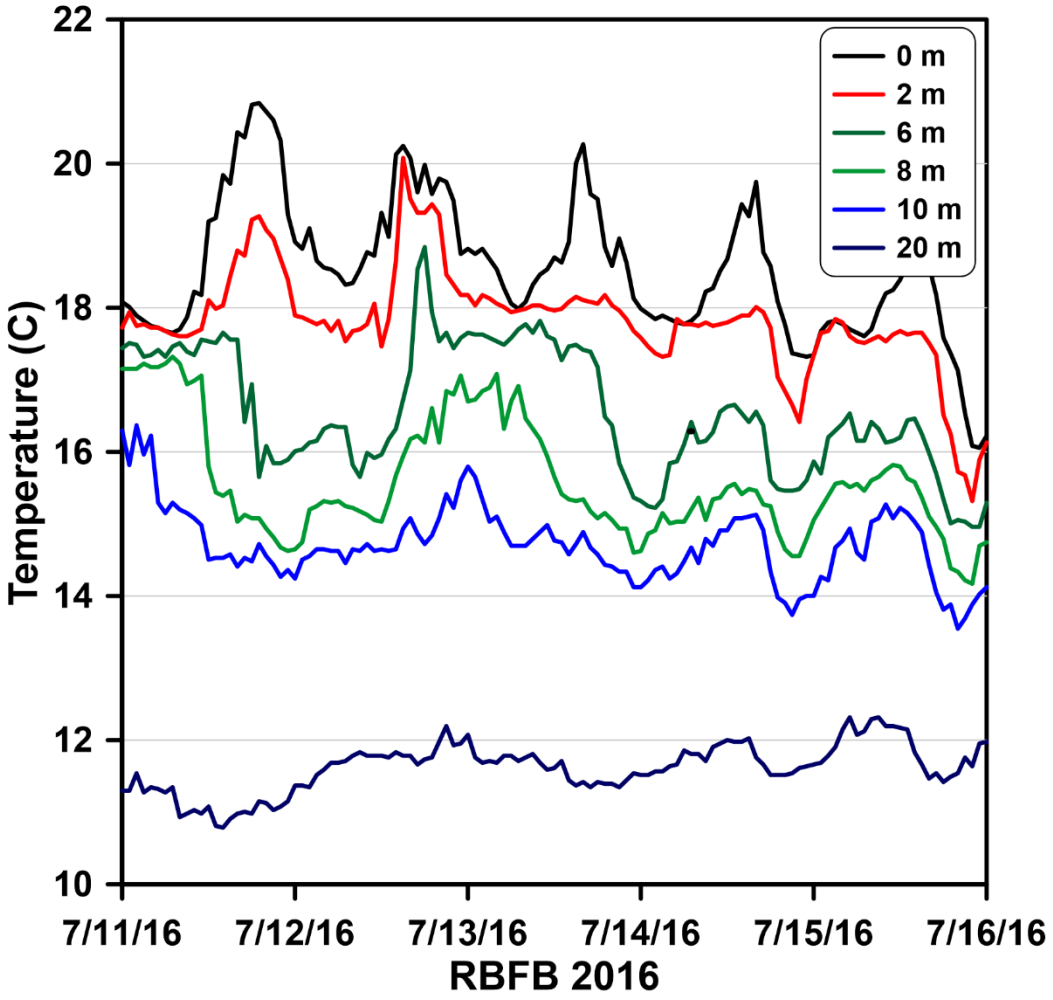

Figure 4-19. Temperature data for thermistors deployed in Round Butte forebay (RES07) July 16, 2016. The ellipse identifies a zone of temperature changes likely caused by an internal wave, or seiche.

Water temperature is important to water quality for several reasons. Temperature affects the growth of phytoplankton and the suitability of the habitat for various species of fish. In the case of LBC, lake temperature also determines the temperature of the water released downstream. Water temperature and its distribution also affects the stability of the water column, which, in turn, affects mixing. A typical lake in temperate latitudes during the summer will display the greatest degree of stability in the metalimnion. Stability can be calculated as relative thermal resistance (RTR) and displayed to show where in the water column the stability is greatest. In addition, RTR can be summed to compute the entire stability of the water column. RTR is a

dimensionless number computed as the density difference of an upper and lower layer of water divided by the difference in density of water at 5˚C and 4˚C (Wetzel 2001). Sites with low RTR values (e.g., 20) require little energy to mix the water column, whereas sites with high RTR values (e.g., 200) require considerable energy to mix. Under natural conditions, the energy for mixing is supplied by wind. LBC often displayed an atypical pattern of RTR in which the greatest resistance was present in the upper several meters of the water column rather than the metalimnion, as is the case in typical mid-latitude lakes (Figure 4-20). As summer progressed and less water was drawn from the epilimnion into the SWW, a more typical distribution of thermal resistance became evident.

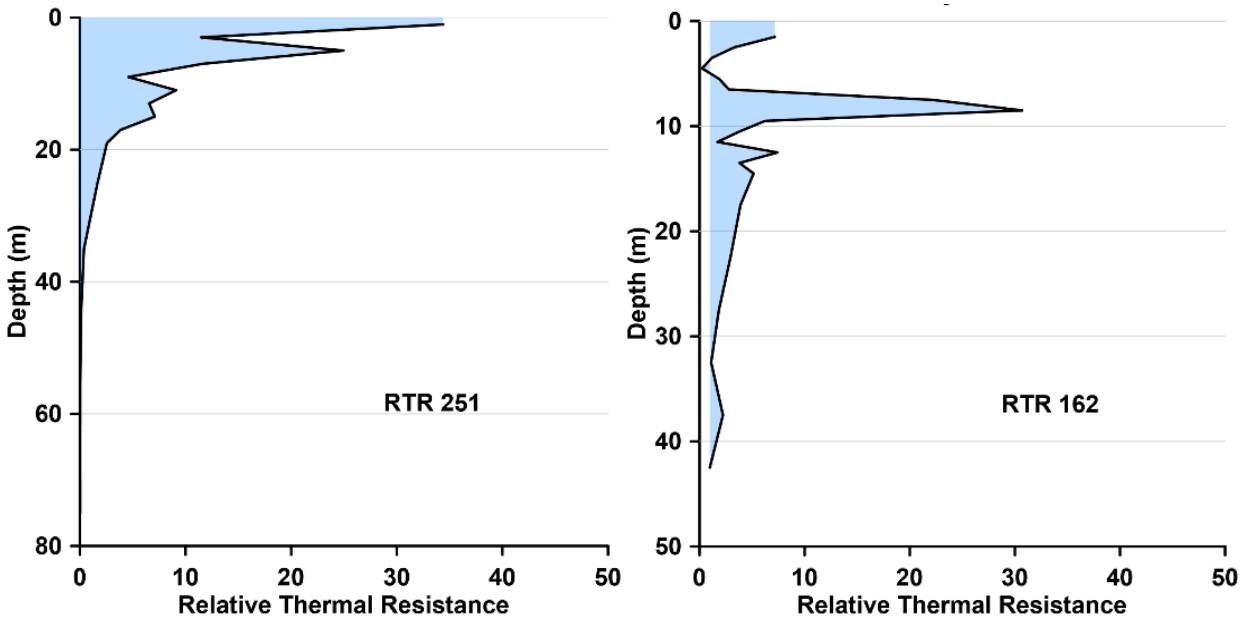

Figure 4-20. RTR at Round Butte forebay (RES07) on June 9, 2015 (*left*) and July 29, 2015 (*right*). Total RTR for the water column is listed in the plot. The greater the RTR value, the greater is the resistance of the total water column to mixing.

Total RTR reflected the general heat gain of the lake (Figure 4-21). The differences among years reflected variations in annual weather and the amount and timing of tributary inflow and water drawn into the SWW compared to the amount drawn from the deep-water intake. The RTR for the Common Pool (RES08) was less than the RTR for Round Butte forebay (RES07)

primarily because Round Butte forebay (RES07) is deeper than the Common Pool (RES08) and a deeper water column is more resistant to mixing than a shallower water column.

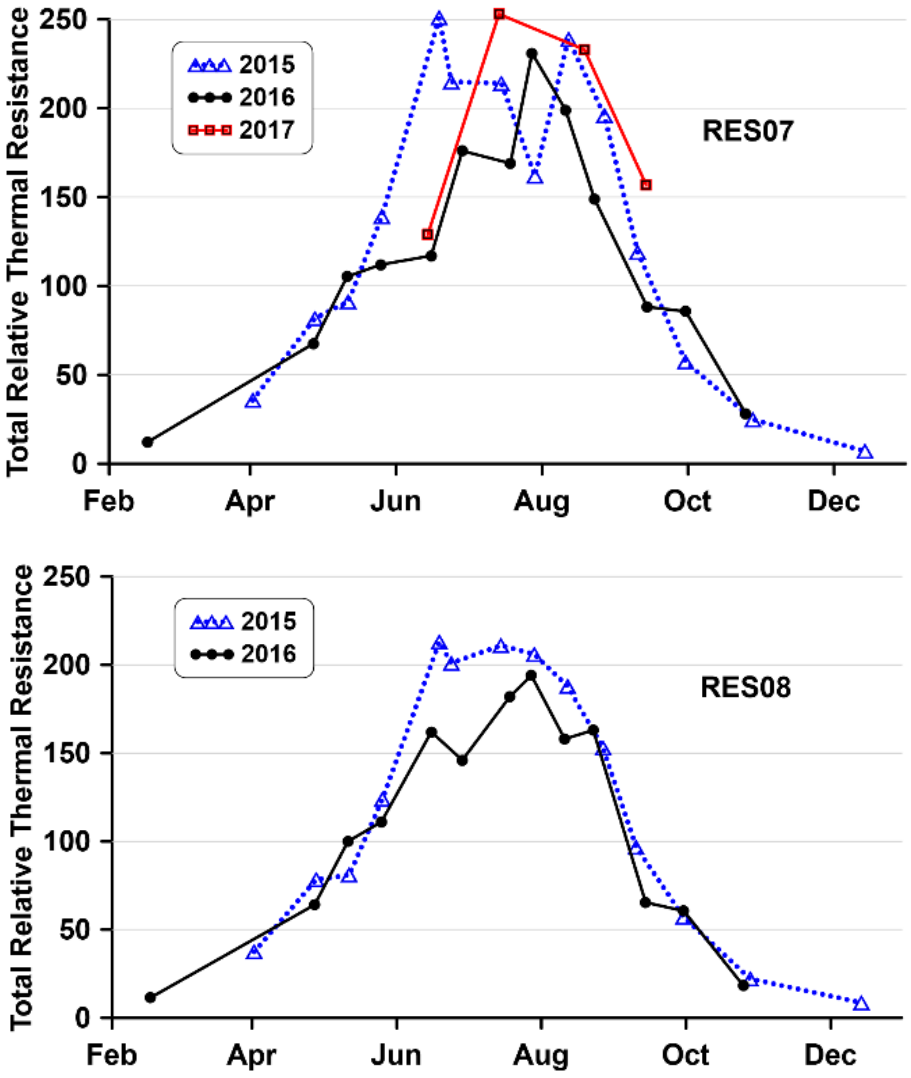

Figure 4-21. Total RTR for Round Butte forebay (RES07) (*top*) and the Common Pool (RES08) (*bottom*) during the study.

4.2.1.2 Conductivity

Conductivity is a conservative tracer of inlet water through which the team associated high values with waters from the Crooked River and low values with waters from both the Metolius and the Deschutes rivers. Conductivity values for the Crooked River were typically about 160 microsiemens per centimeter (µS/cm), compared to only about 70 µS/cm for the Metolius River and 110 µS/cm for the Deschutes River. The strong influence of Crooked River water was evident in the higher conductivity values at both monitoring sites in LBC during the study (Figure 4-22). A recognizable body of low conductivity water was present at a depth of 20–45 m during the summer in Round Butte forebay (RES07). This identifiable dilute water mass was initially visible as a small isolated mass in May 2016 at a depth of 15–20 m that moved deeper in the water column and became more extensive throughout the summer. A major thrust of dilute water in 2017 extended underneath the epilimnion at about 10 m and down to about 30–40 m, depending on the month. The significance of this pattern in conductivity is that the influx of Metolius River water occurred much higher in the water column than it did before the SWW was put into operation (Raymond et al. 1997).

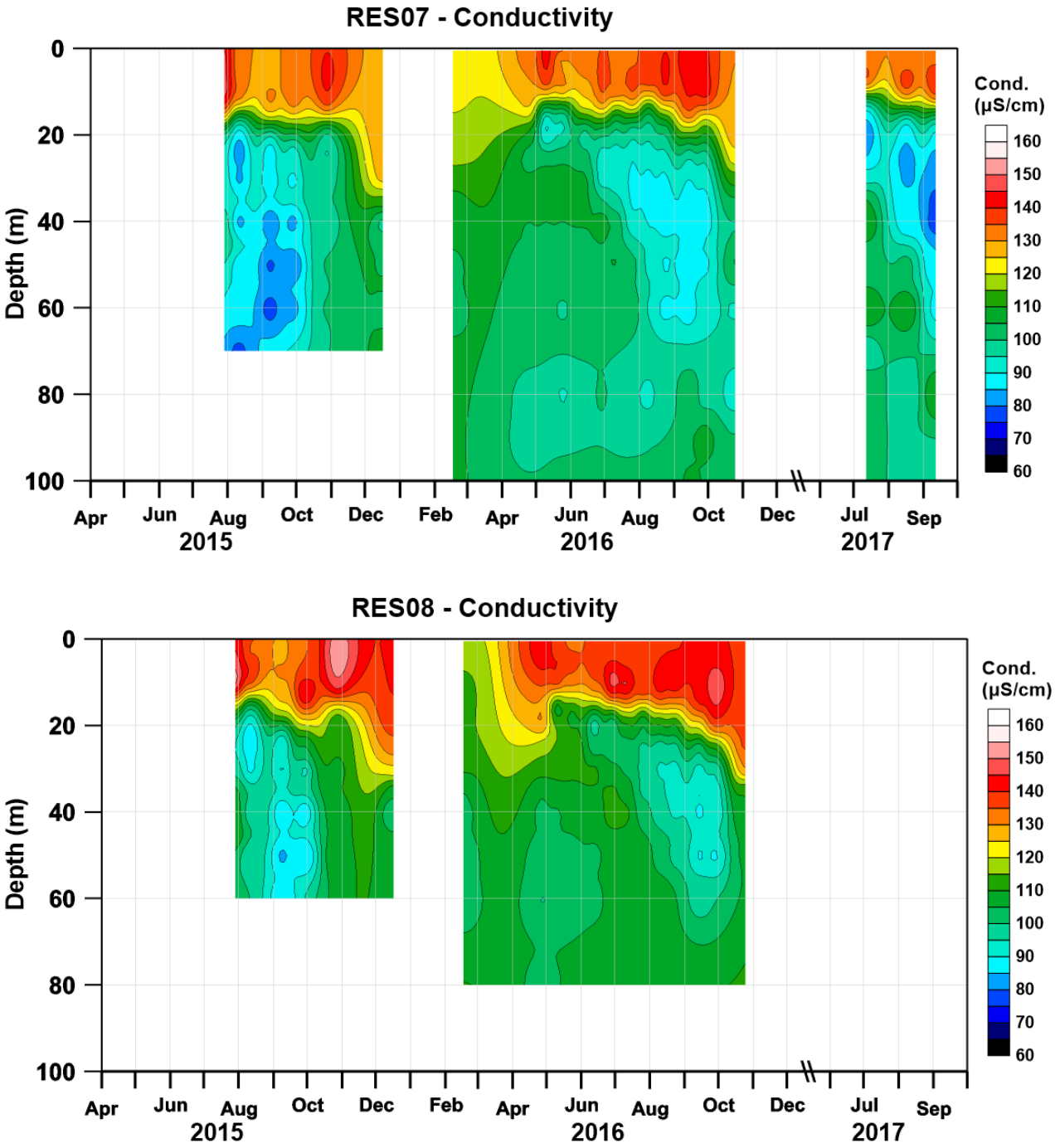

Figure 4-22. Conductivity contours for Round Butte forebay (RES07) (*top*) and the Common Pool (RES08) (*bottom*).

4.2.1.3 Dissolved Oxygen

DO (presented as percent saturation) was elevated in the epilimnion but was often undersaturated deeper in the water column (Figure 4-23). Peak periods of DO in the surface waters often started in late April and extended through July, which was a pattern most evident in 2015. The only month in which the DO profile approached near-uniform conditions was in February 2016. Even into December 2015, a distinct stratification of DO saturation existed. Maximum DO measurements occurred in April–July and were limited to the upper few meters of the water column. Below a depth of about 15 m, DO generally declined steadily.

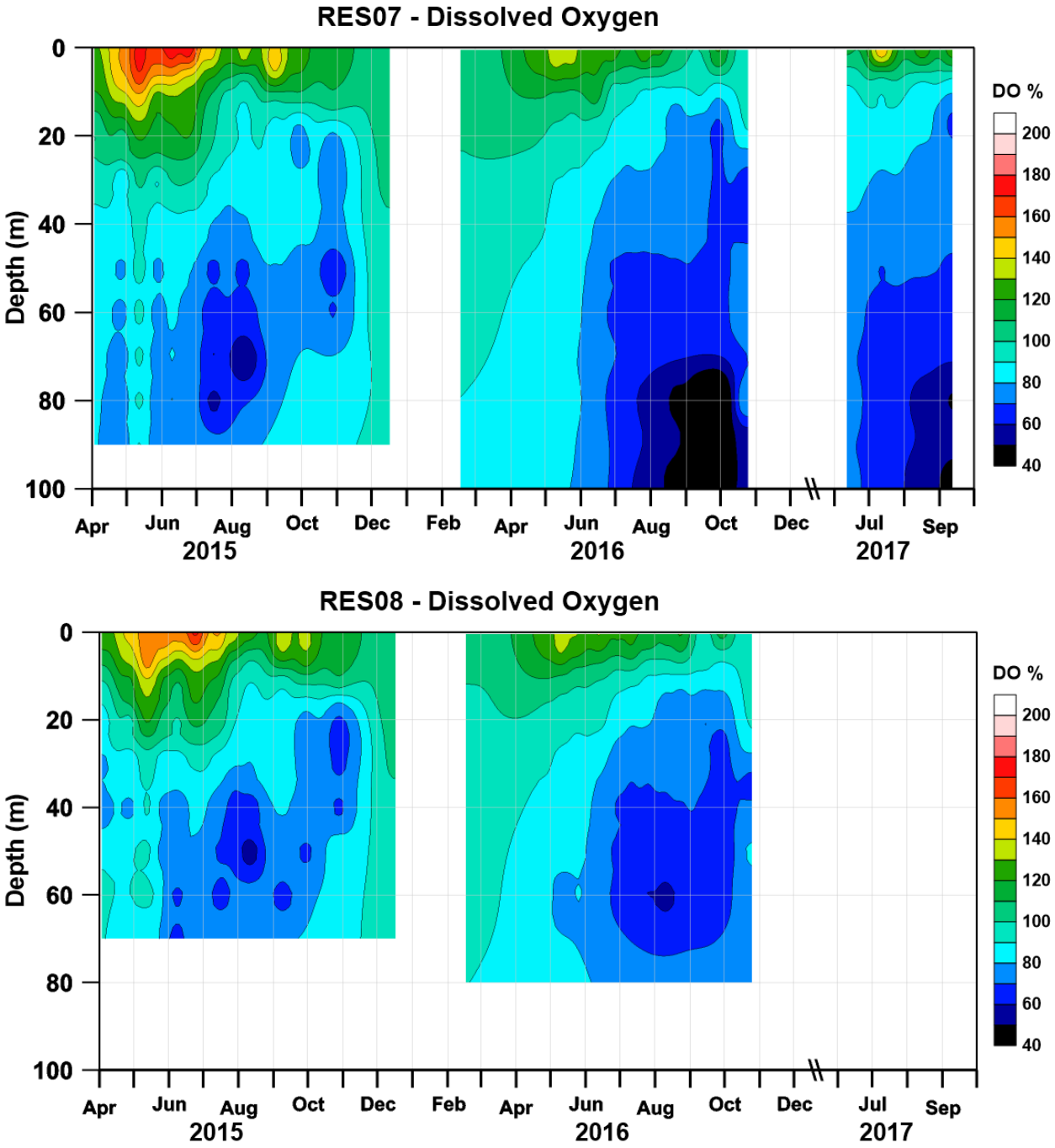

Figure 4-23. DO saturation contours for Round Butte forebay (RES07) (*top*) and the Common Pool (RES08) (*bottom*) in 2015.

4.2.1.4 pH

pH values were elevated in the epilimnetic waters of LBC for 2015–2017. Values were highest in 2016, but elevated levels extended deeper into the epilimnion in 2015 (Figure 4-24). In 2015, values in the epilimnion approached pH 10 and declined in the hypolimnion to almost pH 6. The pattern of pH values was similar to the DO saturation pattern: high values in the epilimnion, which indicate high rates of primary production, and low values in the hypolimnion, which indicate respiration.

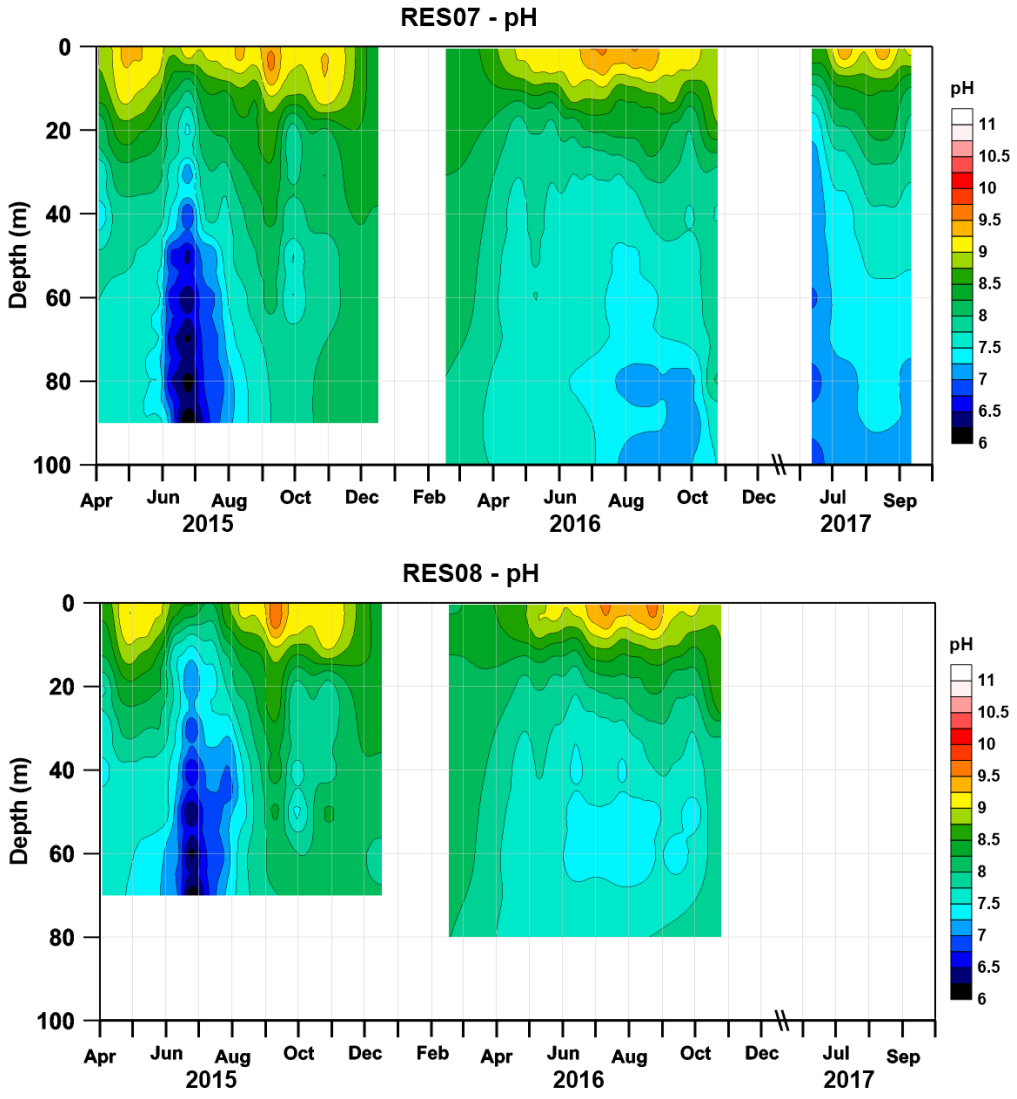

Figure 4-24. Contours of pH in Round Butte forebay (RES07) (*top*) and the Common Pool (RES08) (*bottom*).

4.2.1.5 Transparency and Light Attenuation

Secchi disk transparency is a long-standing method of measuring lake transparency and provides another approach for evaluating water clarity. Water clarity was low in LBC from April to early October in both 2015 and 2016 (Figure 4-25). In late October of each year, the lake began to clear and, from December through February, it was quite clear. Note that Figure 4-25 does not include data from 2017 as only three measurements were collected that year. All 2017 measurements were in the summer (July–September) and ranged from 1.5 to 1.8 m, similar to data from the previous years.

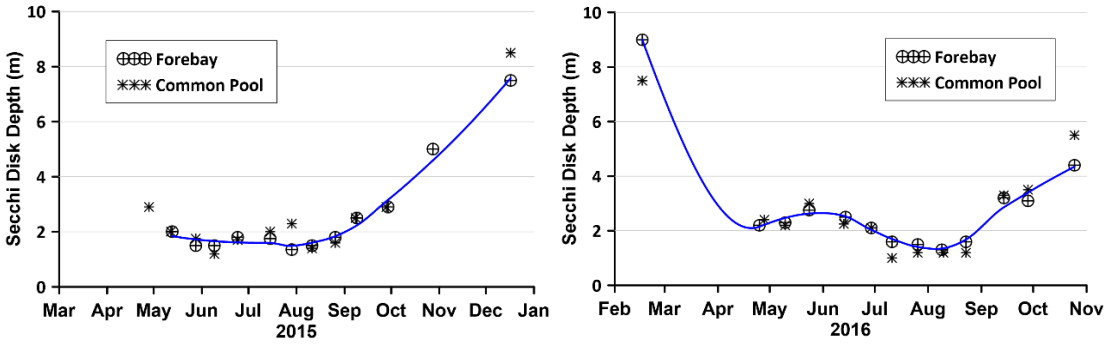

Figure 4-25. Secchi disk transparency for Round Butte forebay (RES07) and the Common Pool (RES08) in 2015 (*left*) and 2016 (*right*). The LOESS fits are to the data at the forebay.

The amount of light penetrating a lake is influenced by scattering of inorganic particulates and phytoplankton and by attenuation associated with dissolved organic compounds. These naturally occurring compounds are characterized by complex organic compounds representing partially decomposed plant material and impart a yellow-brown stain to the water. Judging by the generally clear water entering the lake (from visual observations), dissolved humic compounds are low in the tributaries entering LBC and are not a major factor affecting light transmission. Only phytoplankton and suspended inorganic particles are associated with the reduction of light in the water column. Monitoring data showed that light attenuation was highest in 2015 and lowest in 2017 (Figure 4-26). Light penetration reached the 1% level, a threshold often used as the demarcation at which light becomes limiting to most algae, at a depth of about 4 m in all 3

years. In all 3 years, the highest light attenuation occurred near the early part of August, when inflow from the tributaries approached minimum discharge, and the highest transparency levels were observed from the onset of winter into April, when inflow was highest and primary production was lowest.

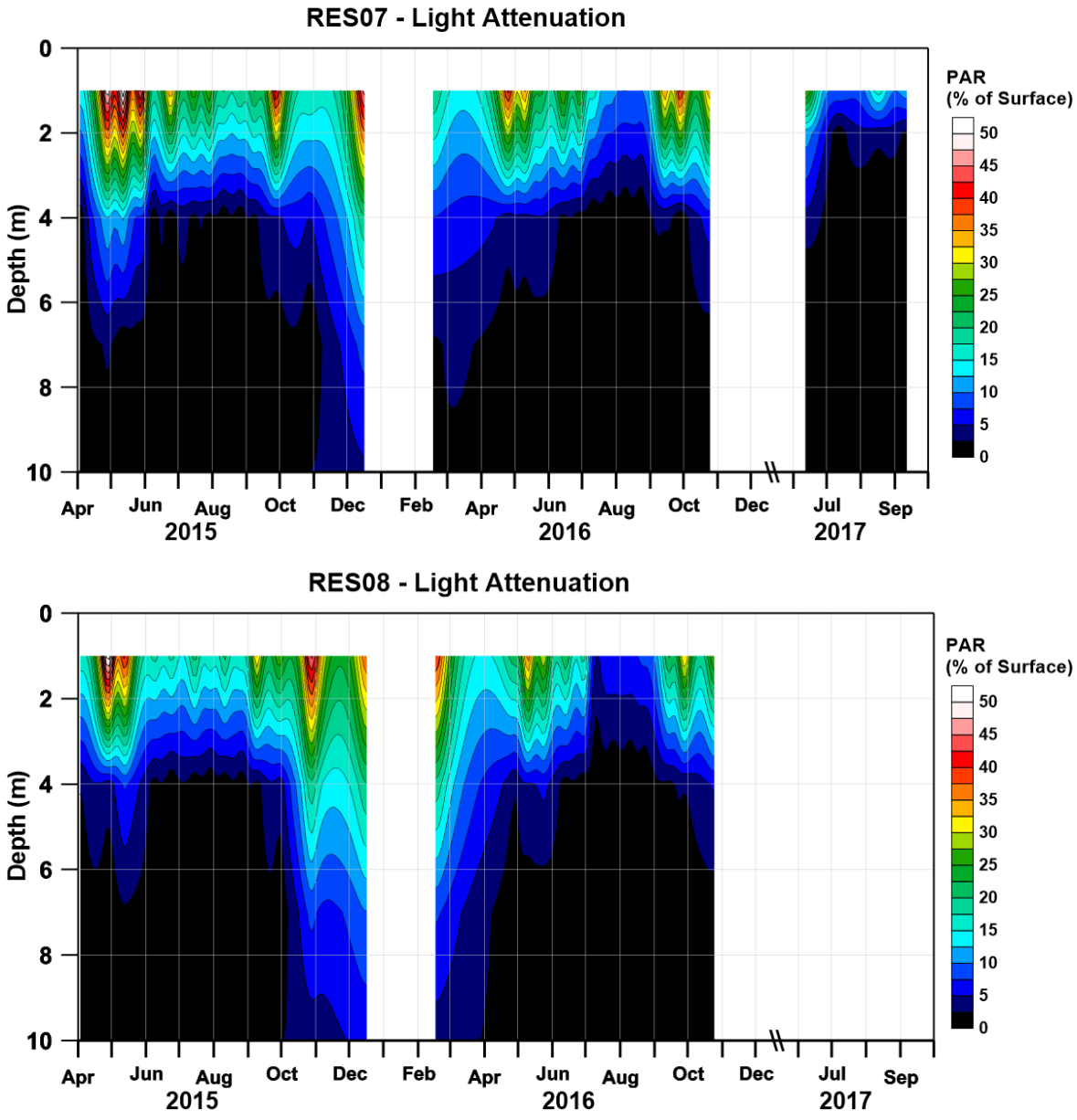

Figure 4-26. Contours of light attenuation in Round Butte forebay (RES07) (*top*) and the Common Pool (RES08) (*bottom*).

4.2.1.6 Turbidity

Turbidity is a measure of light scattering caused by particles suspended in the water, which can be either inorganic suspended sediment or biological organisms such as algae. Turbidity profiles were collected in the impoundments during the three years. Turbidity levels increased in June and remained elevated into October (Figure 4-27). The clear-water period extended from fall into early spring of each year. Peak turbidity was observed in July and August. The patterns in turbidity generally extended vertically in near-uniform levels, except for the highest turbidity values, which were restricted to the upper portion of the water column in the summer. The turbidity data were generally consistent with the data for light transmission and Secchi disk transparency. Together, the data indicates that the water in LBC was highly turbid, with low transparency from spring into early fall, and then cleared up in late fall and through the winter. The turbidity data from the AlgaeTorch, if accurate, showed considerable turbidity down to at least 10 m (33 ft), which suggests that algae derived from the epilimnion was falling through the water column. The reported turbidity, however, is highest in the summer months when cyanobacteria become dominant. The *Dolichospermum/Anabaena* colonies possess gas vacuoles to assist the organisms in maintaining their presence high in the water column. An alternate explanation for the relatively high turbidity down to 10 m is that the instrument might not have had sufficient time to equilibrate to lower values as it was lowered through the water column. We lack the data to resolve these turbidity values.

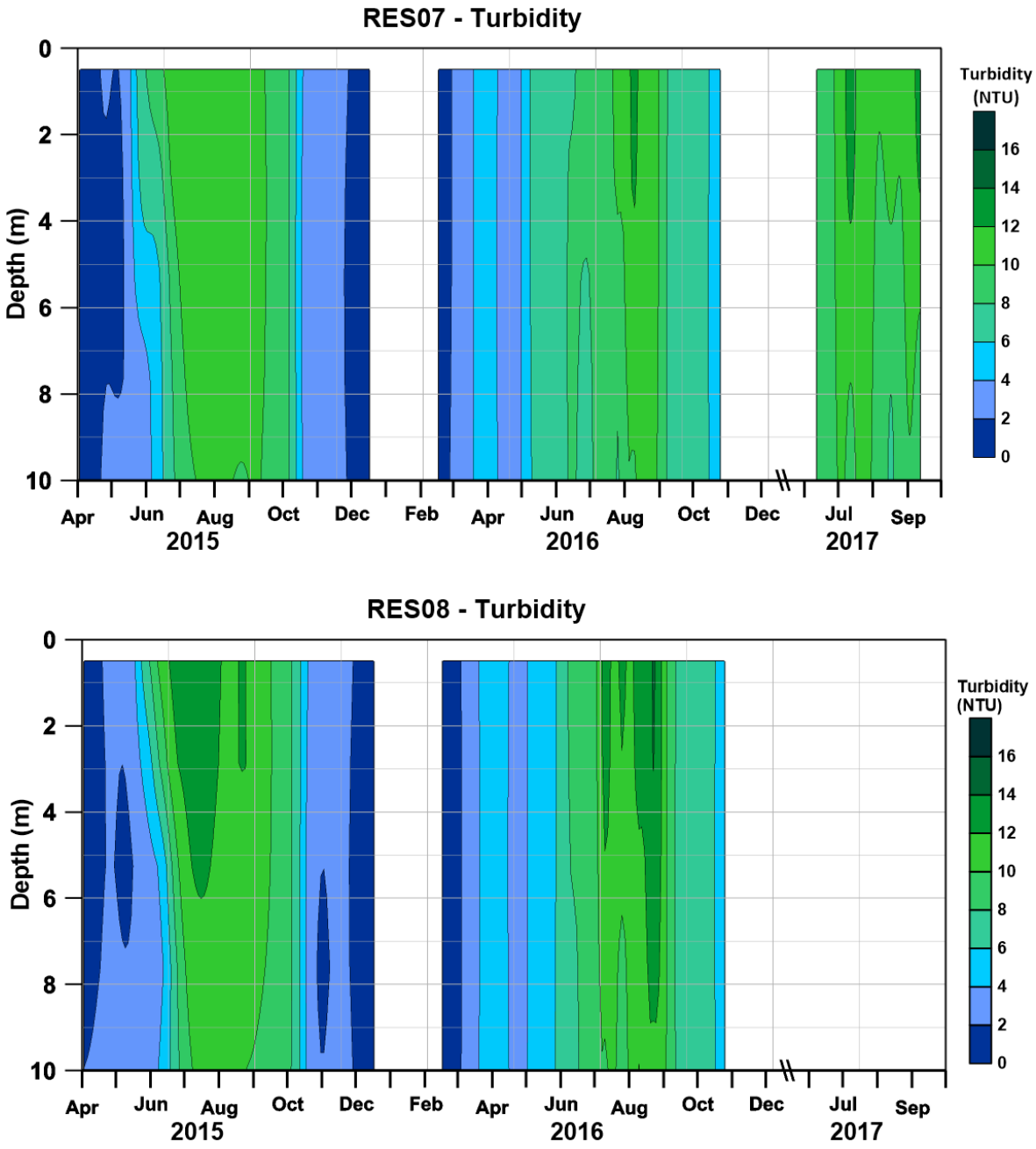

Figure 4-27. Turbidity contours in Round Butte forebay (RES07) (*top*) and the Common Pool (RES08) (*bottom*).

4.2.1.7 Total Phosphorus

Concentrations of TP in the three major tributaries typically ranged from about 0.08 mg/L for the Metolius and Deschutes rivers to close to 0.10 mg/L for the Crooked River. Thus, it was somewhat surprising that the highest concentrations of TP in LBC were usually observed in the hypolimnion (Figure 4-28). The water column in February 2016 was fully mixed with a TP concentration of about 0.085 mg/L. However, by late May/early June of each year, TP concentrations in the hypolimnion increased to about 0.108 mg/L. Phosphorus is not conservative, so it is likely that the TP in the hypolimnion during late spring to early summer could represent mineralization of phosphorus from particulate matter (dead phytoplankton) sinking through the water column. The phosphorus concentrations in the epilimnion declined through this period, which would be consistent with loss of the TP associated with phytoplankton uptake, death, and sinking. Concentrations of DO in the hypolimnion demonstrate that there was no anoxia (at least to the depths measured) and, therefore, solubilization of phosphorus from the sediments appear to be an unlikely source of the increased phosphorus, at least in the upper portions of the hypolimnion. These and other issues regarding details of the impoundments are better addressed through a specific monitoring program that focuses on the impoundments.

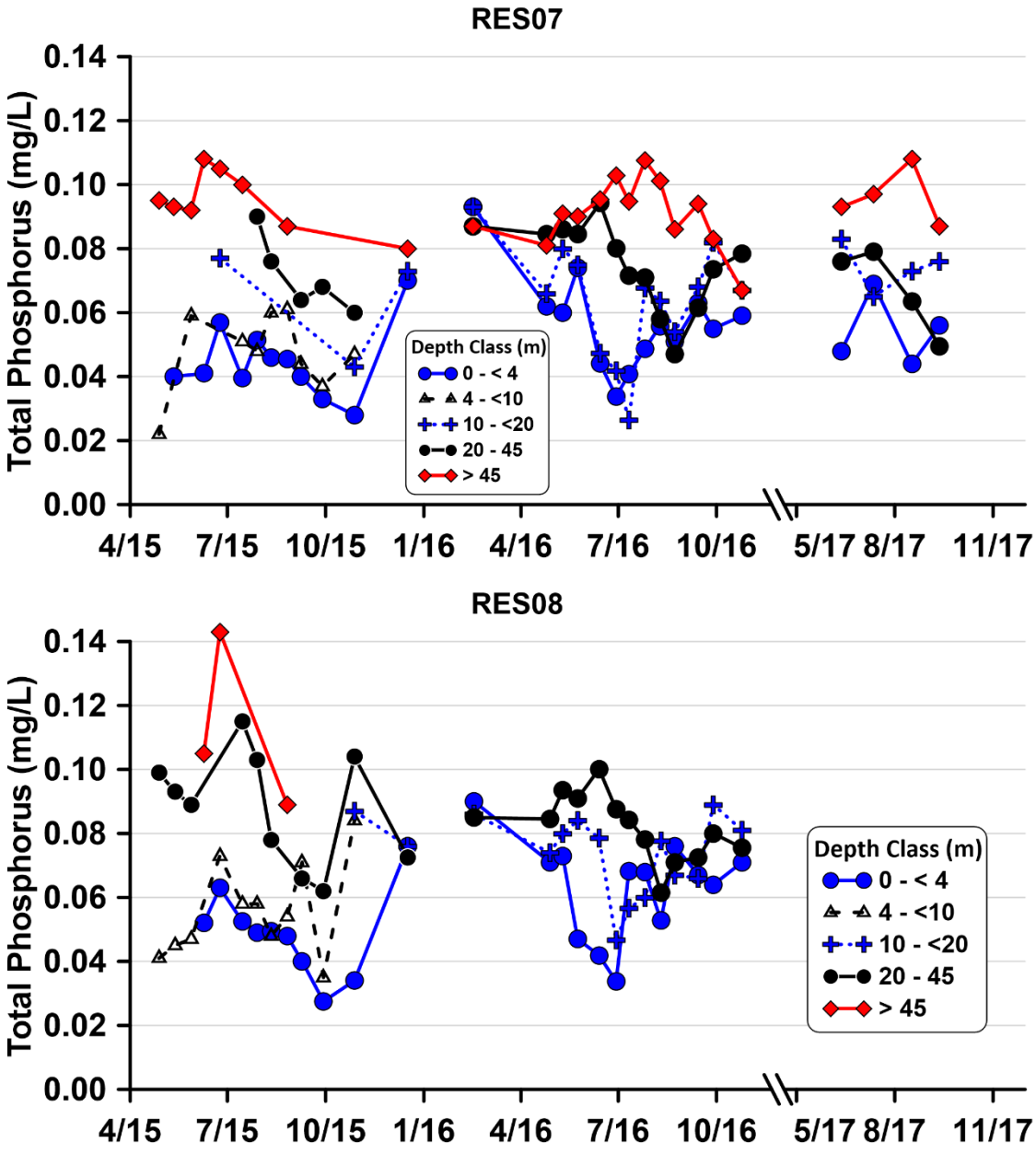

Figure 4-28. TP concentrations for Round Butte forebay (RES07) (*top*) and the Common Pool (RES08) (*bottom*).

4.2.1.8 Phosphate

Concentrations of PO_4 showed a pattern similar to that observed for TP, but PO_4 values were lower than those for TP and declined more in the epilimnion than TP values (Figure 4-29). Again, the values of PO_4 were similar throughout the water column in February 2016, with values of about 0.06–0.07 mg/L. The epilimnetic waters had low concentrations of PO_4 generally from May to October until fully mixing in late November to early December. The low concentrations in the warmer months reflect high rates of primary production and uptake by phytoplankton.

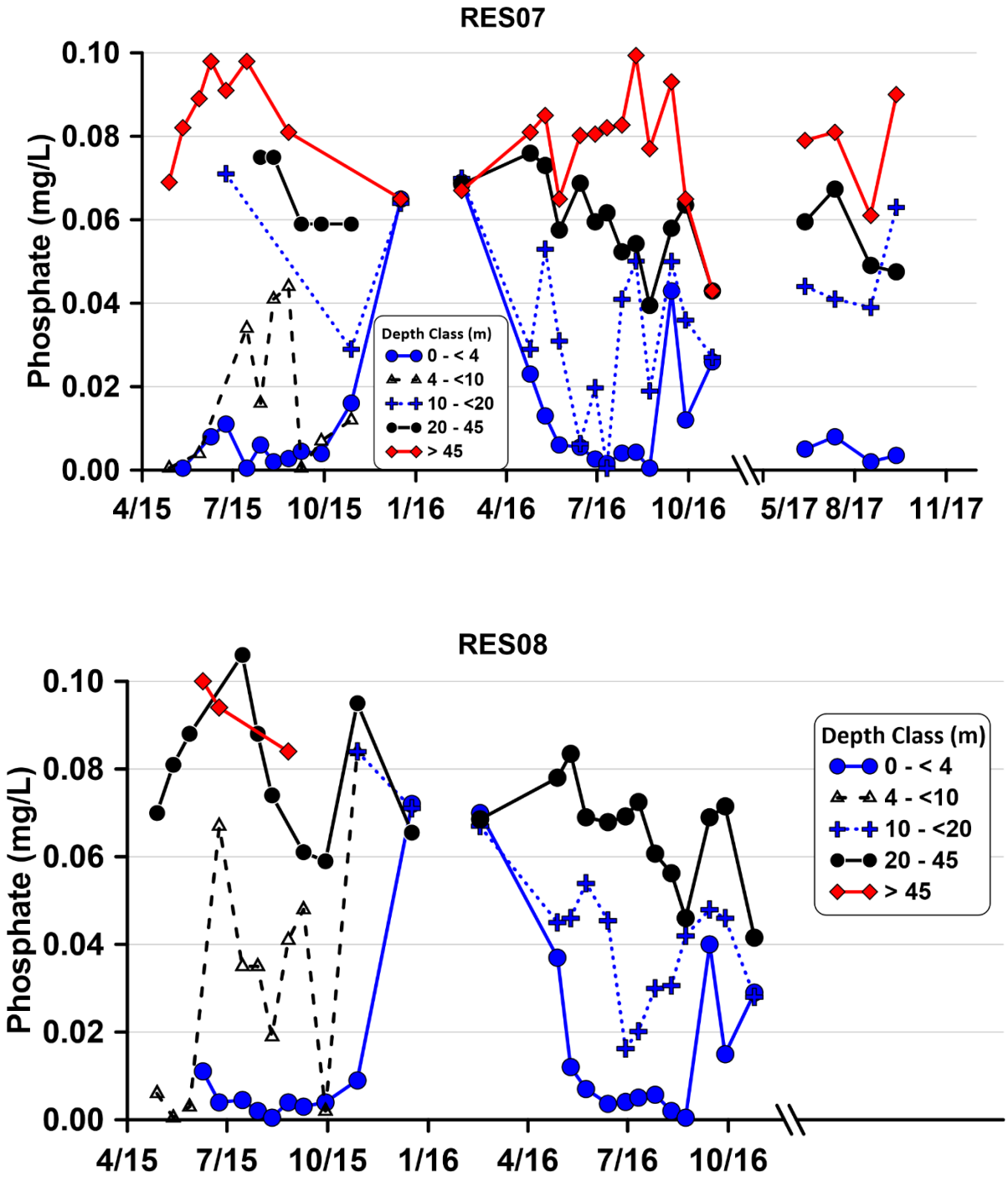

Figure 4-29. PO_4 concentrations at Round Butte forebay (RES07) (*top*) and the Common Pool (RES08) (*bottom*).

4.2.1.9 Total Nitrogen

TN concentrations were generally less than 0.40 mg/L in LBC much of the time (Figure 4-30). However, during summer, elevated TN concentrations were present in the epilimnion. The peak values started in June 2015 (1.58 mg/L) and later in July during 2016 (0.916 mg/L) and 2017 (1.016 mg/L). The inlets to LBC had concentrations that typically were less than 0.60 mg/L (Figure 4-9), so it appears that higher TN concentrations were generated within the lake through photosynthetic activity. Since there is insufficient inorganic nitrogen to account for all the increases, it appears that some of the elevated TN was associated, in part, with nitrogen fixation by cyanobacteria. The most obvious anomaly in TN distribution occurred in 2015 at the Common Pool (RES08), which had high values in the hypolimnion. That pattern was not repeated so it is difficult to determine the source of the values.

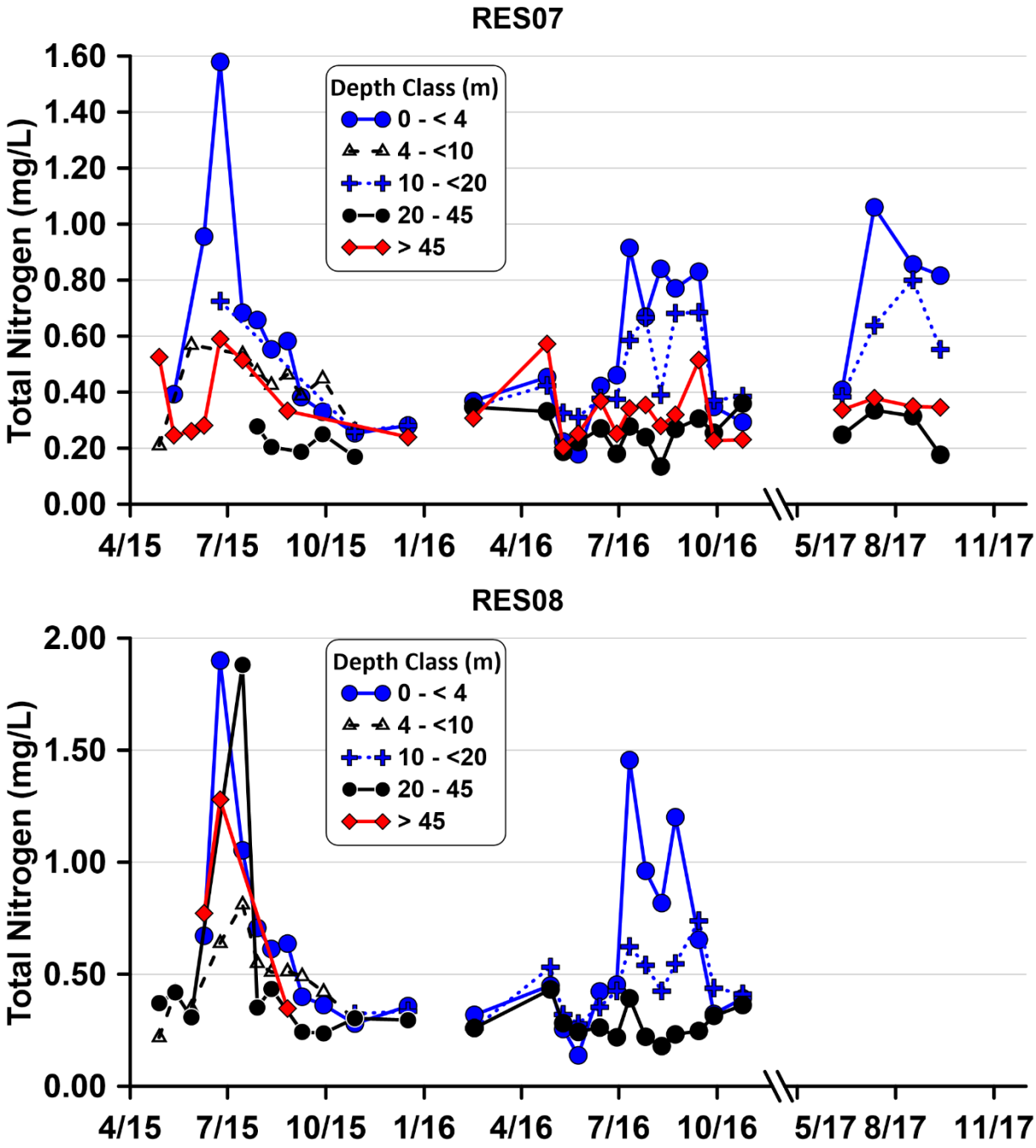

Figure 4-30. TN concentrations at Round Butte forebay (RES07) (*top*) and the Common Pool (RES08) (*bottom*).

4.2.1.10 Nitrate

Patterns in NO_3 distributions were complex in LBC. Unlike other analytes that were largely uniform throughout the water column in winter, NO_3 still exhibited vertical heterogeneity, except in October 2016 at the Common Pool (RES08) (Figure 4-31). This heterogeneity in vertical concentrations of NO_3 reflects the (1) large difference in NO_3 concentrations among the tributaries, (2) the likely rapid assimilation of NO_3 in this productive reservoir, and (3) the mineralization of nitrogen in the water column. In most cases, NO_3 was measurable at depth, which reflects mineralization of nitrogen from higher in the water column rather than influx from the Metolius River, which typically had no measurable NO_3. NO_3 concentrations increased noticeably at the Common Pool (RES08) in the fall. The source of this NO_3 is unclear although the time period coincides with increased flows from the Deschutes River into LBC as withdrawals from irrigation were shut down.

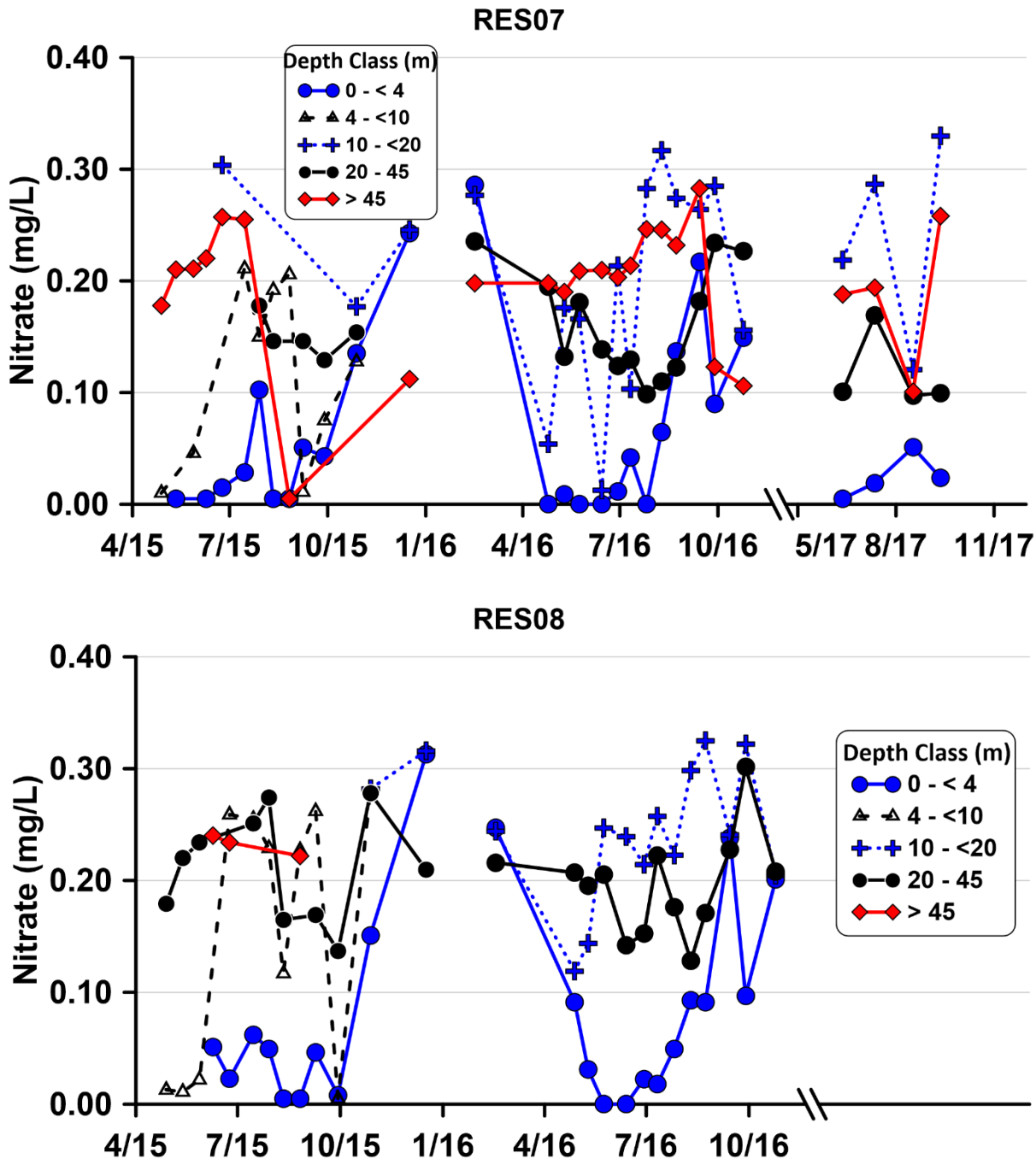

Figure 4-31. NO_3 concentrations in Round Butte forebay (RES07) (*top*) and the Common Pool (RES08) (*bottom*).

4.2.1.11 Ammonia

Concentrations of NH_3 were at or near the DL (<0.010 mg/L) in many of the samples (Figure 4-32). There were several isolated cases of measurable NH_3 in LBC when primary production was high, and some localized instances where NH_3 might have been available through mineralization. The first instance occurred in June 2015, with the second instance in August 2016. They were relatively short-lived and limited in spatial extent, but they were observed at both sites and at similar depths, so they appear to represent real events rather than analytical artifacts. Elevated NH_3 levels in well-oxygenated waters can be associated with rapid lysing of phytoplankton cells following the termination of a bloom.

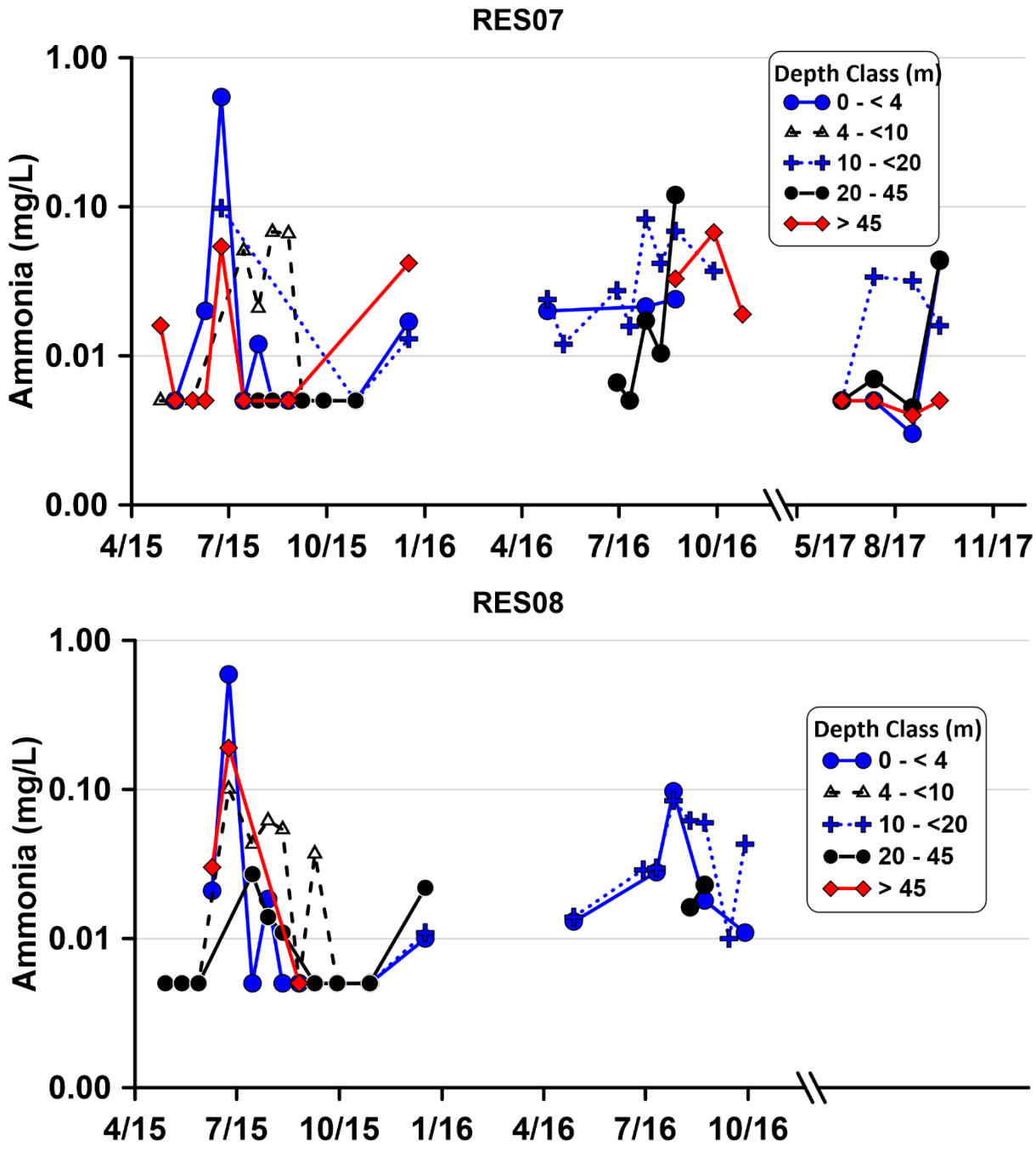

Figure 4-32. NH_3 concentrations in Round Butte forebay (RES07) (*left*) and the Common Pool (RES08) (*right*) from 2015 to 2017.

4.2.1.12 Total Nitrogen:Total Phosphorus Ratio

The ratio of TN:TP showed that LBC, at least for these two sites, was depleted in nitrogen relative to phosphorus when the system was well mixed in the winter (Figure 4-33). When phytoplankton production ramped up in the spring, the ratio changed to reflect a deficiency of phosphorus relative to nitrogen. There was a major difference regarding the extent of the high TN:TP water between 2015 (high) and 2016 (low), illustrating the importance of different hydrological years in affecting conditions in LBC. These annual variations can result in differences in the timing and degree of cyanobacteria blooms in the impoundment. The snowpack in 2015 was extremely low, and temperatures were slightly warmer than 2016. The RTR for LBC showed an earlier onset of more stable conditions in 2015 (Figure 4-21), which likely promoted earlier onset of high rates of primary production.

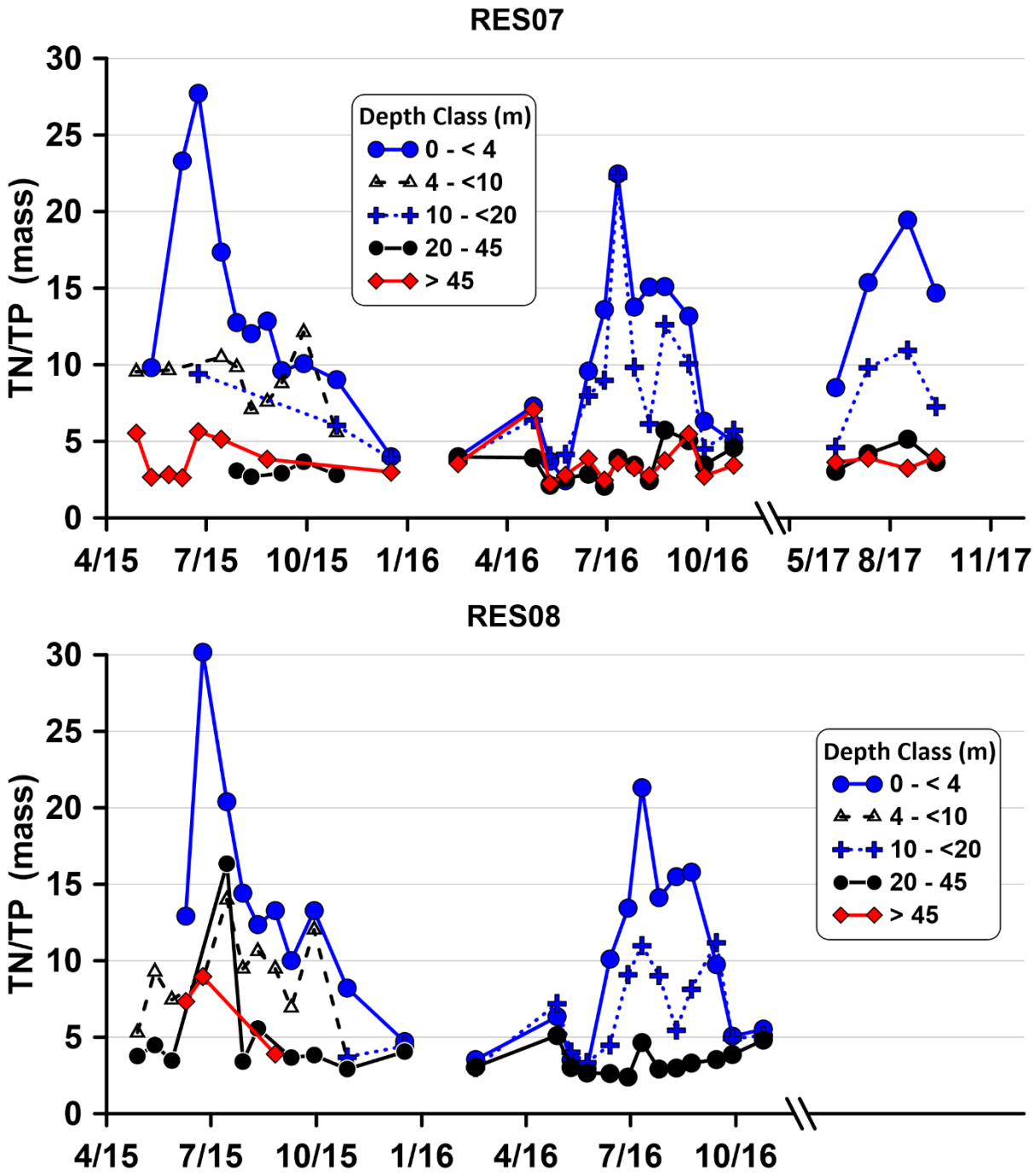

Figure 4-33. Mass ratio of TN:TP in Round Butte forebay (RES07) (*top*) and the Common Pool (RES08) (*bottom*).

4.2.1.13 Nitrate:Phosphate Ratio

The ratio of NO_3:PO_4 showed most of the same features observed in the distributions of TN:TP presented in Section 4.2.1.12 (Figure 4-33 and Figure 4-34). In 2015, the NO_3:PO_4 distributions showed high values in May until mixing in the fall. In 2016, the NO_3:PO_4 ratio showed low values until July, when there was a rapid and intense shift to high values in the epilimnion. An even more attenuated signal was present in the limited data from 2017. The high values of the ratio (e.g., greater than 15) indicate that the phytoplankton community probably was more limited by phosphorus than by nitrogen during those periods. When the ratio is low (e.g., less than 5) the phytoplankton probably are limited by nitrogen. However, it is equally important to examine the actual concentrations of NO_3 and phosphorus because when concentrations of both nutrients are low, they can be co-limiting. Figure 4-35 shows concentrations of dissolved inorganic nitrogen (DIN) and PO_4 in the surface waters of LBC. In June, we observed that concentrations of both DIN and PO_4 approached DLs (<0.010 mg/L and <0.001 mg/L, respectively). When we express these concentrations as a ratio, it appears the surface waters were briefly N-limited (Figure 4-36). However, concentrations of both nutrients were extremely low and were likely co-limiting for a short period. Similarly, in winter and again in fall concentrations of both DIN and PO_4 were relatively high with neither nutrient appearing to limit primary production.

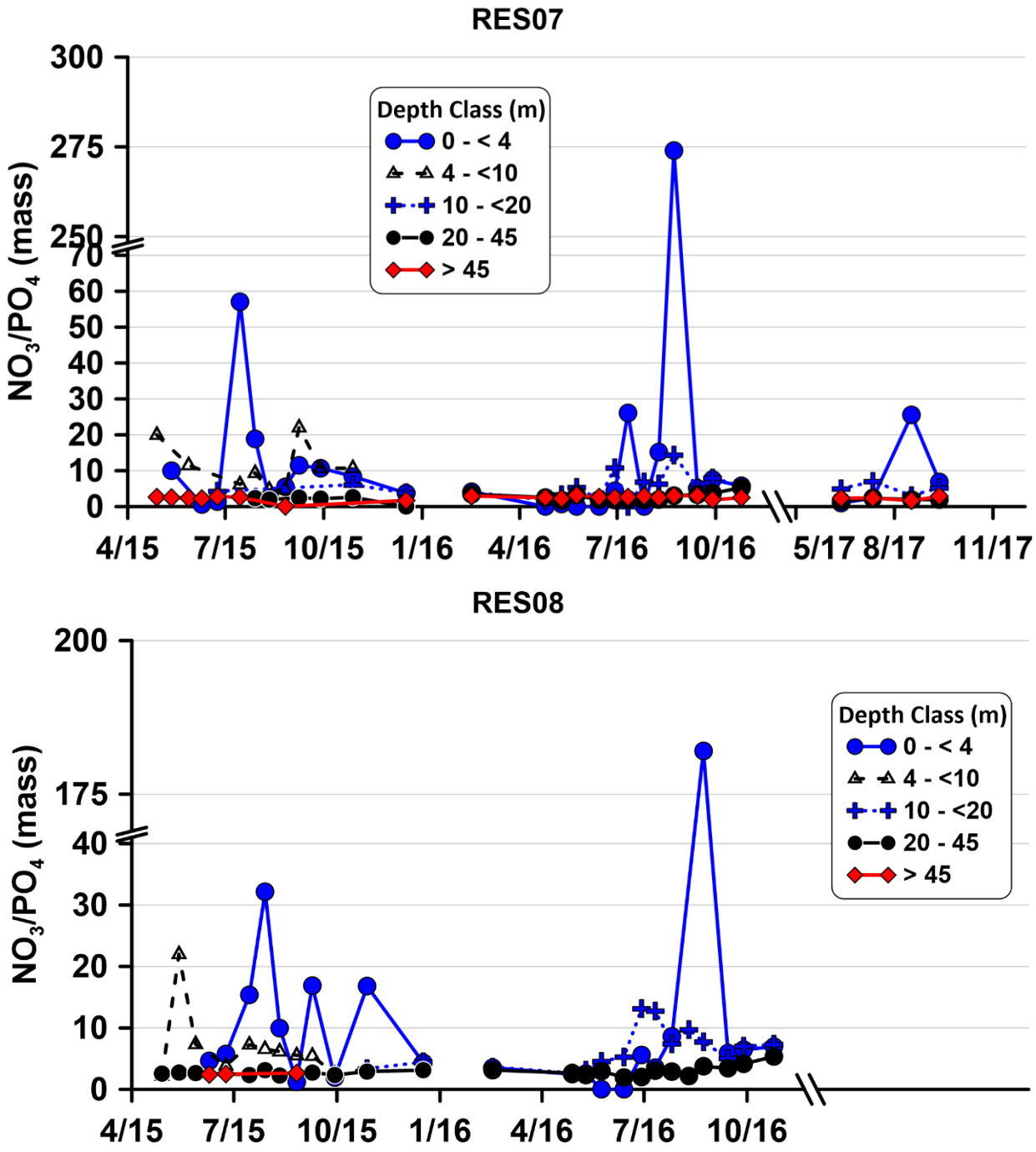

Figure 4-34. Mass ratio of NO3:PO4 in Round Butte forebay (RES07) (*top*) and the Common Pool (RES08) (*bottom*).

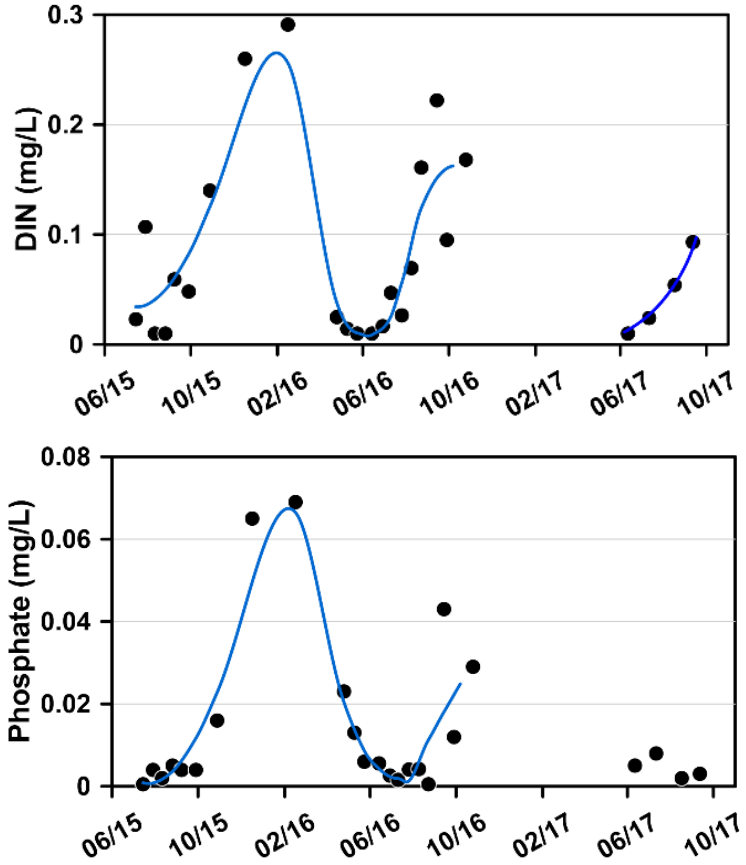

Figure 4-35. Concentrations of DIN (*top*) and PO_4 (*bottom*) in the surface waters of LBC at Round Butte forebay (RES07). The lines are LOESS fits of the observed data.

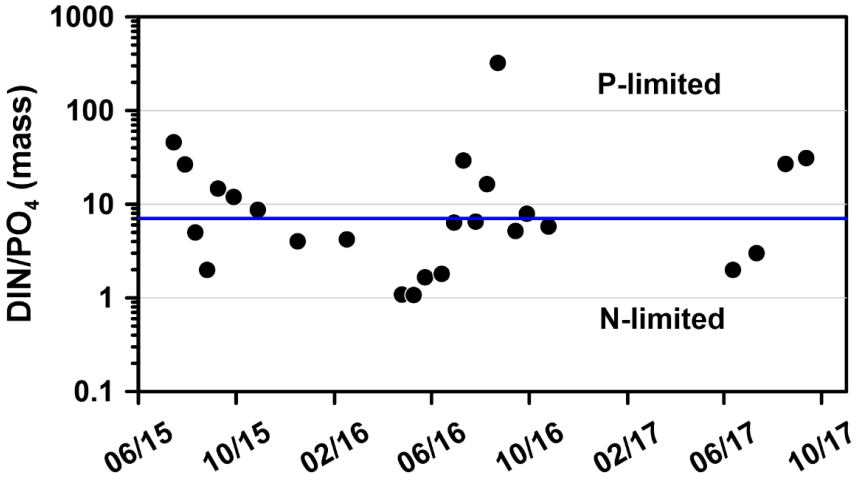

Figure 4-36. Mass ratio of DIN to PO4 in the surface waters of LBC at Round Butte forebay (RES07). The blue line at 7.2 is a guideline for possible relationships in nutrient limitation.

4.2.1.14 Chloride

Cl^- is a relatively conservative ion in lakes (Sullivan et al. 1988) and provides another indication of mixing in the impoundments. The Cl^- data for 2016 were analyzed by a laboratory with better quality assurance results for Cl^- than the laboratory that conducted the Cl^-analyses for 2015; therefore, the 2016 results should receive greater weight. No Cl^- measurements were gathered in 2017. The results showed high Cl^- values in the epilimnion in 2016 and some of the lowest values immediately below the epilimnion for both sites in 2016 (Figure 4-37). Cl^- concentrations (mean and standard deviation [sd]) for the three tributaries were 1.17 (0.04) mg/L, 1.76 (0.14) mg/L, and 2.78 (0.25) mg/L for the Metolius, Deschutes, and Crooked rivers, respectively. The highest concentrations of Cl^- in the surface waters of LBC corresponded with those from the Crooked River, and the lowest concentrations were similar to those from the Metolius River.

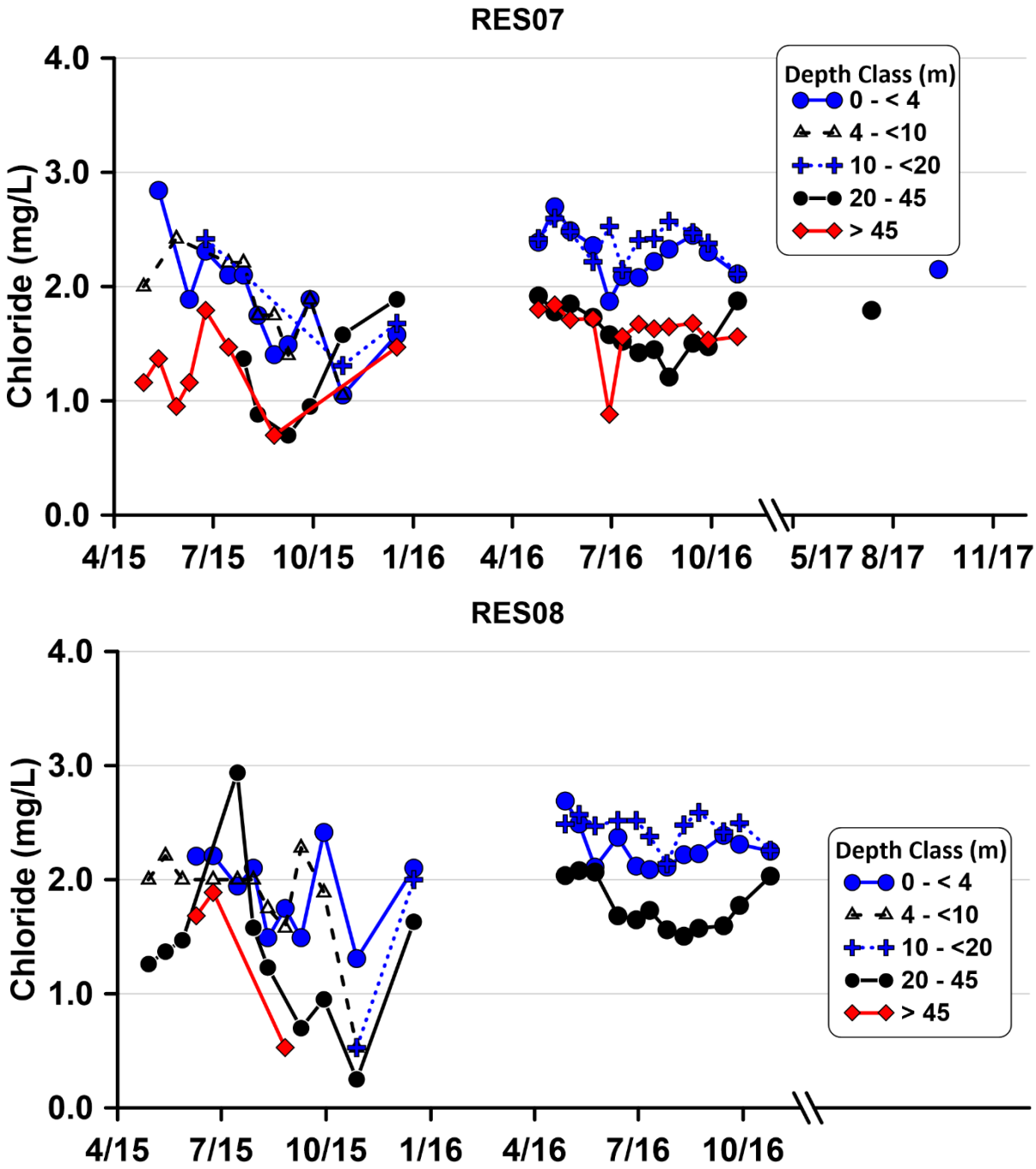

Figure 4-37. Cl^- concentrations in Round Butte forebay (RES07) (*top*) and the Common Pool (RES08) (*bottom*).

4.2.1.15 Total Chlorophyll

Fluorometric measurements were collected using the AlgaeTorch to a depth of 10 m in addition to the standard profile measurements. The measurements included total chlorophyll and cyanobacterial pigment fluorescence. The patterns in chlorophyll measurements (based on AlgaeTorch measurements) showed peak values in April 2015 and July/August 2016 (Figure 4-38). Pigment values were relatively uniform in the upper water column, with the notable exception of the low values measured below 6 m in the summer of 2015. Another noteworthy aspect of the results was the considerable range in chlorophyll observed throughout the year with values less than 5 µg/L during the winter and up to 50 µg/L in spring (2015) and summer (2016). Peak chlorophyll concentrations occurred in July during the abbreviated monitoring of 2017 with a strong vertical variation observed in August. The range of chlorophyll values observed in the monitoring program highlights the different factors that affect primary production in LBC. As was observed in the turbidity results, the chlorophyll results from the AlgaeTorch tended to report a small range of values throughout the water column to 10 m for any observation.

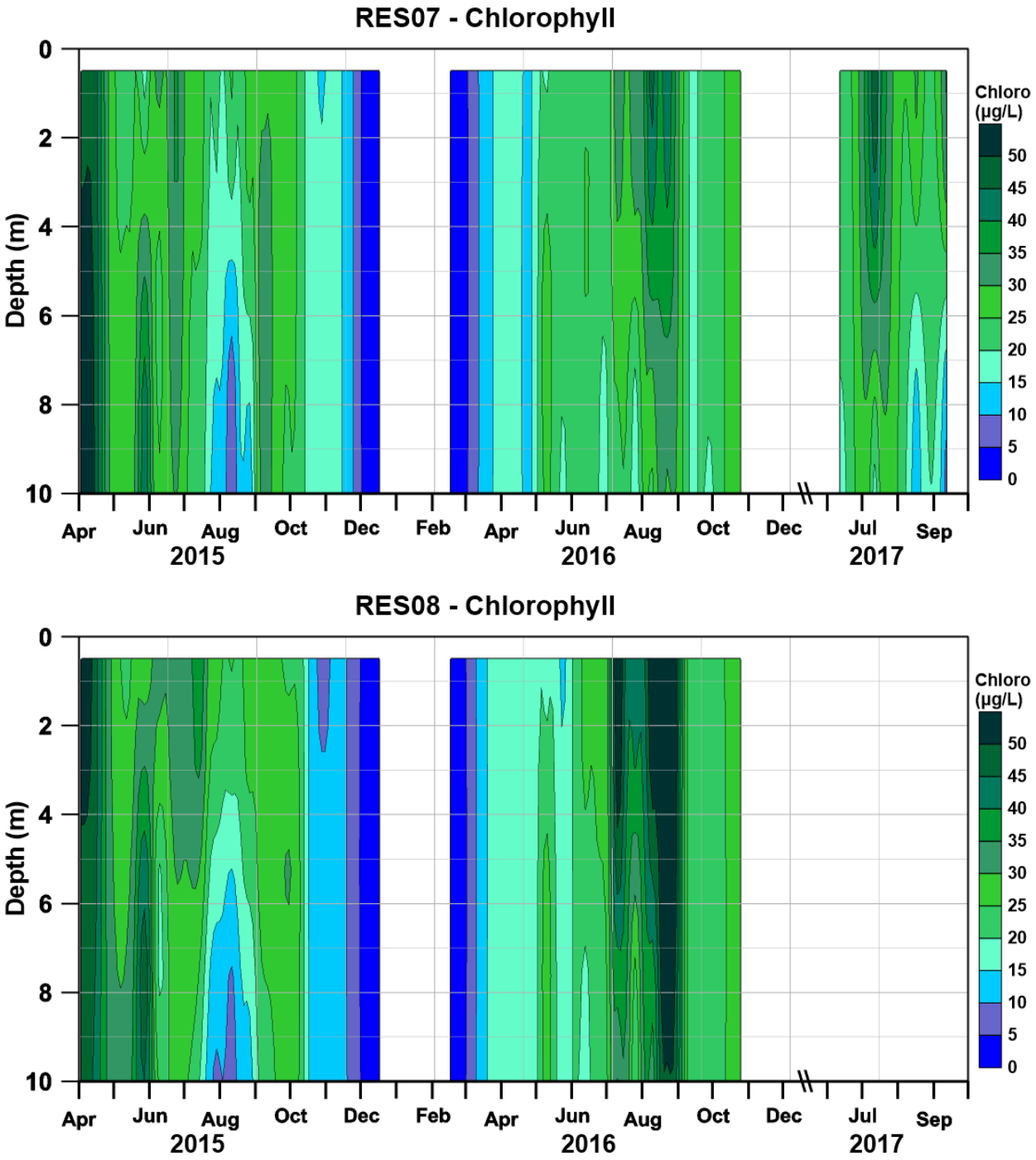

Figure 4-38. Chlorophyll concentration contours in Round Butte forebay (RES07) (*top*) and the Common Pool (RES08) (*bottom*).

4.2.1.16 Cyanobacterial Pigment

Cyanobacteria density, as indicated by the fluorescent pigment data from the AlgaeTorch measurements, peaked in late June/early July in 2015 and 2017, and in August 2016 (Figure 4-39). That result mirrors some of the phytoplankton responses observed for chlorophyll pigments shown previously. The most intense cyanobacteria signal was measured at the Common Pool (RES08) in August 2016. The weakest cyanobacteria signal was observed at Round Butte forebay (RES07) in 2015. Unlike chlorophyll, which was sometimes elevated from spring to fall, the cyanobacterial pigments were elevated only from June to September. That result corresponds well with the dominance of cyanobacteria during this period, which is presented in the following section.

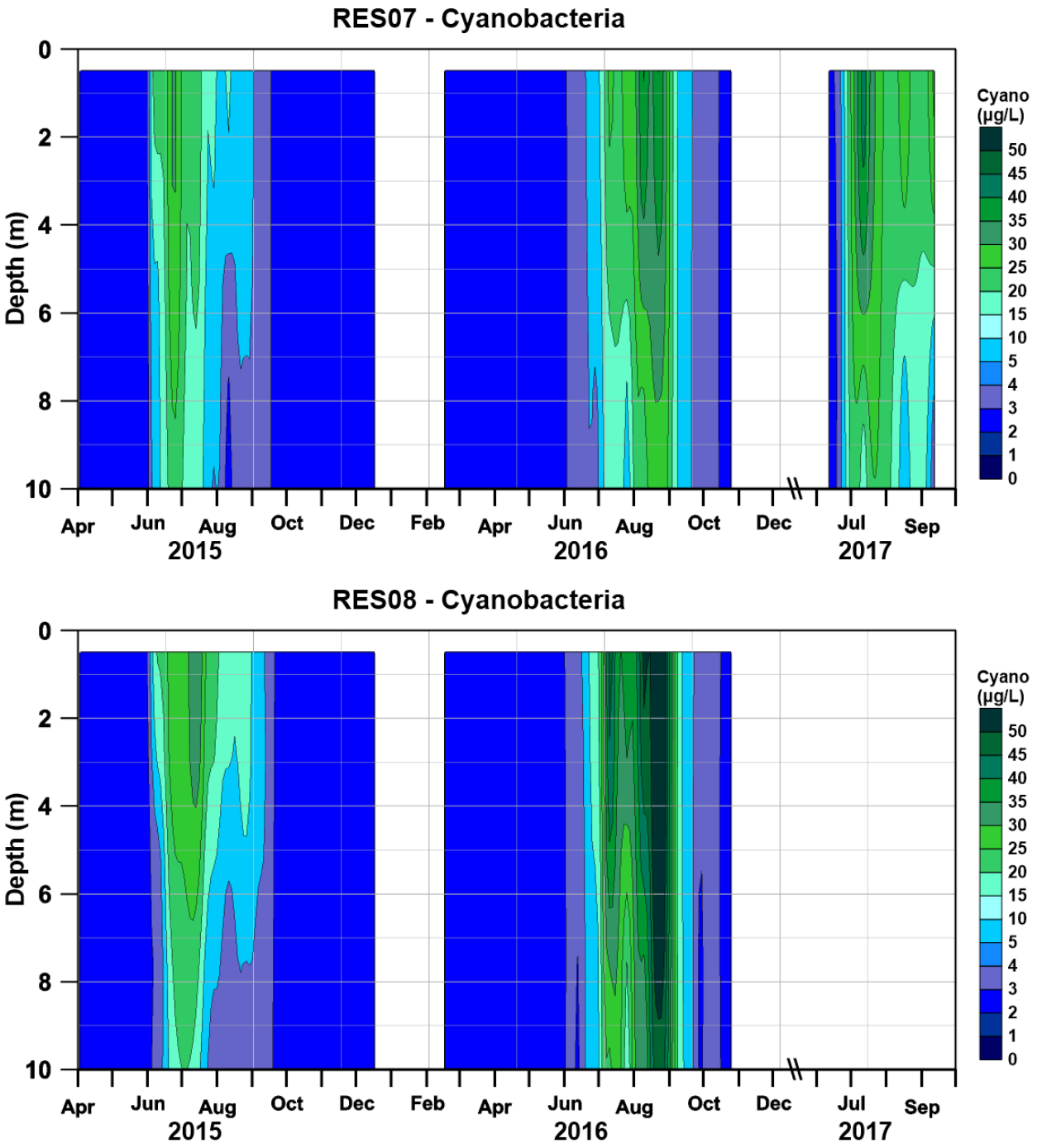

Figure 4-39. Cyanobacteria pigment density contours in the Round Butte forebay (RES07) (*top*) and the Common Pool (RES08) (*bottom*).

4.2.1.17 Phytoplankton Community Composition

Total algal abundance (biovolume) for the epilimnion showed moderate abundance at the beginning of 2015, high abundance later in 2015 and throughout most of 2016, and more moderate abundance in 2017 (Figure 4-40). Phytoplankton abundance is characterized in this study by biovolume instead of cell counts to avoid the characterization of the mass of the phytoplankton community being skewed by many small cells. Although there might have been as many as 50 individual taxa counted in a sample of 300 natural units, the mass of the phytoplankton was typically dominated by just a couple of taxa. The boxplot of the cumulative percent biovolume shows that over 88% of the biovolume in most samples was represented by a single taxon (Figure 4-41). Once a third taxon was included in the cumulative biovolume, nearly 98% of the biovolume was represented. Thus, from the viewpoint of community composition, most of the samples were sufficiently represented by examining one-to-three taxa in any given sample. For a more detailed description of the phytoplankton community composition in LBC, see Appendix E.

The dominant phytoplankton taxa were centric diatoms (primarily *Stephanodiscus niagarae*) in the spring and fall and *Dolichospermum* (*Anabaena*) in the summer (Figure 4-42, Figure 4-43, Figure 4-44, and Figure 4-45). *S. niagarae* is a large centric diatom that can become heavily encased in silica and thus acquire a rapid settling rate. *Dolichospermum* is an N-fixing filamentous cyanobacterium. Both taxa thrive in high-phosphorus waters; however, *Dolichospermum* has a distinct advantage in being able to fix atmospheric nitrogen, whereas *S. niagarae* must rely on DIN to sustain growth. Prior to the appearance of *S. niagarae* in large numbers, the other centric diatoms that dominated earlier in spring included other species of *Stephanodiscus* such as *S. minutulus* and *S. medius*. Pennate diatoms were often abundant, but seldom dominant in the phytoplankton assemblage. The most notable pennate diatom was *Fragilaria crotonensis*, another taxon often associated with eutrophic conditions such as high-phosphorus waters (Reynolds 2006). Thus, the seasonal transition was from diatoms in the spring to cyanobacteria in the summer, transitioning back to diatoms in the fall and winter.

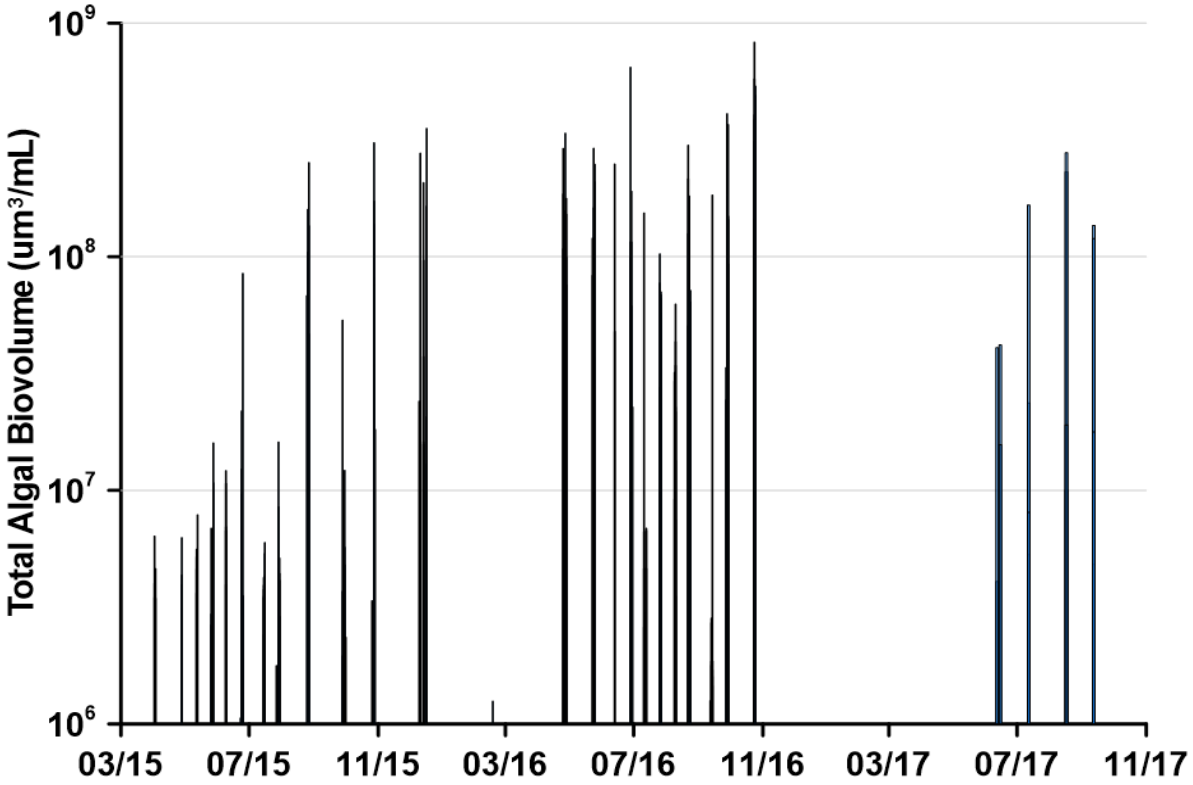

Figure 4-40. Total algal biovolume in Round Butte forebay (RES07) at 1 m during the study. All sample results are displayed.

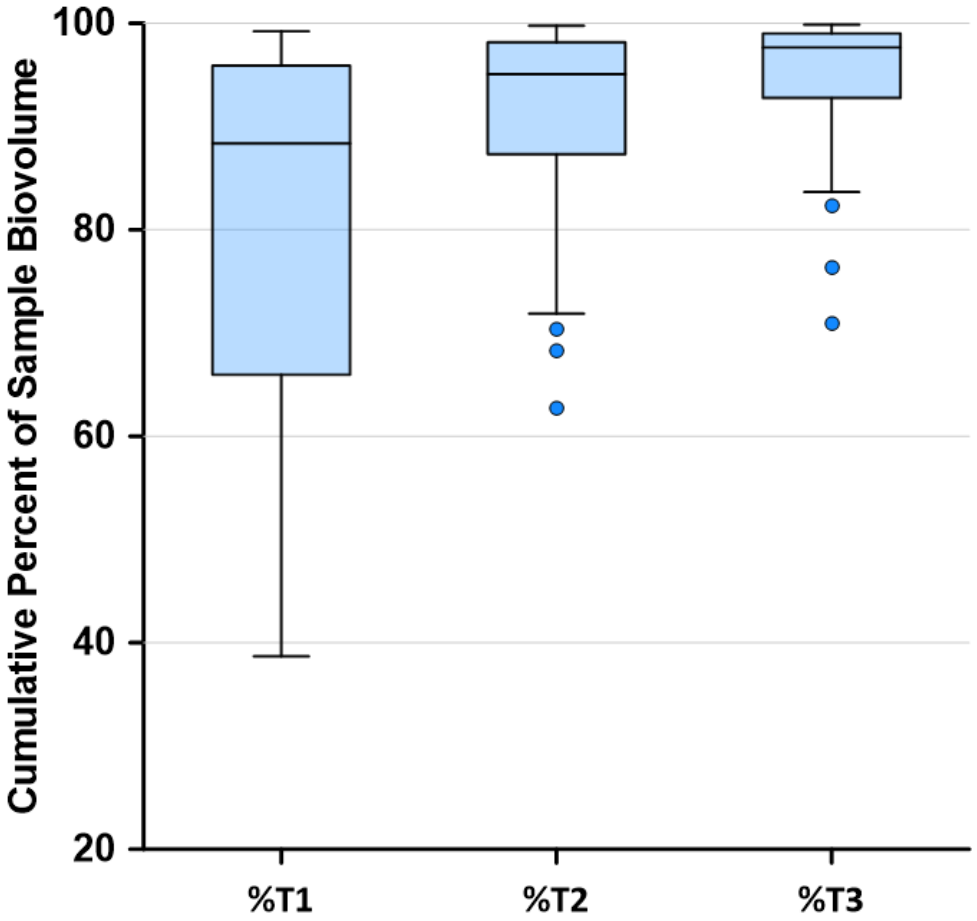

Figure 4-41. Boxplot of the cumulative algal biovolume of dominant phytoplankton taxa for all phytoplankton samples from 2016. %T1 = biovolume of the most dominant taxon for a specific sample, %T2 = cumulative biovolume of the two most dominant taxa for a specific sample, and %T3 = cumulative biovolume of the three most dominant taxa in any given sample.

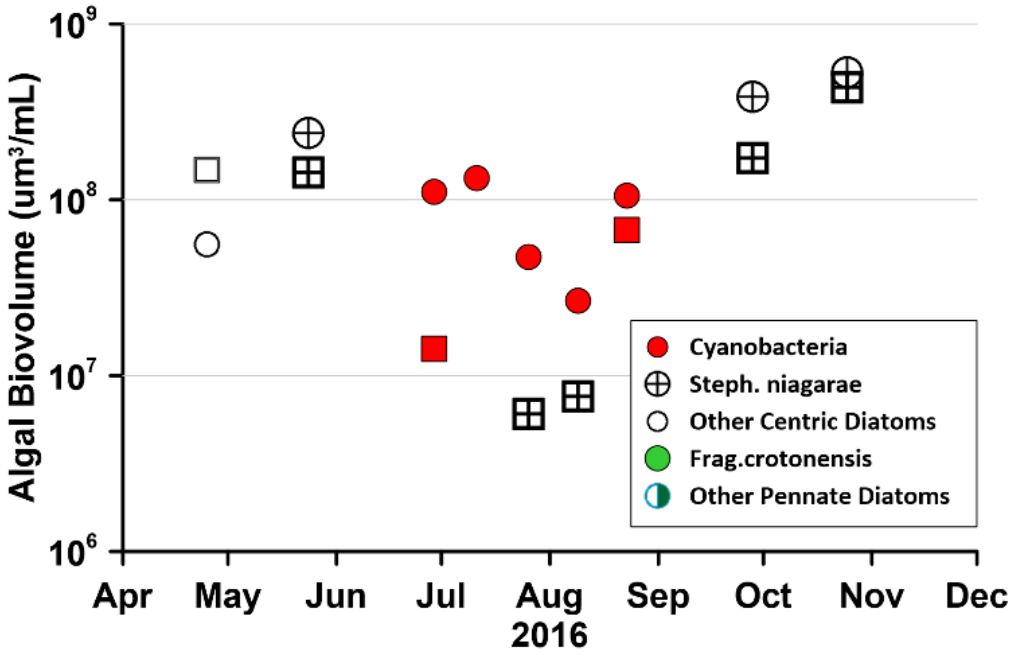

Figure 4-42. Dominant phytoplankton taxa in Round Butte forebay (RES07) in 2016. Round symbols represent upper 1 m, and square symbols represent 10 m depth.

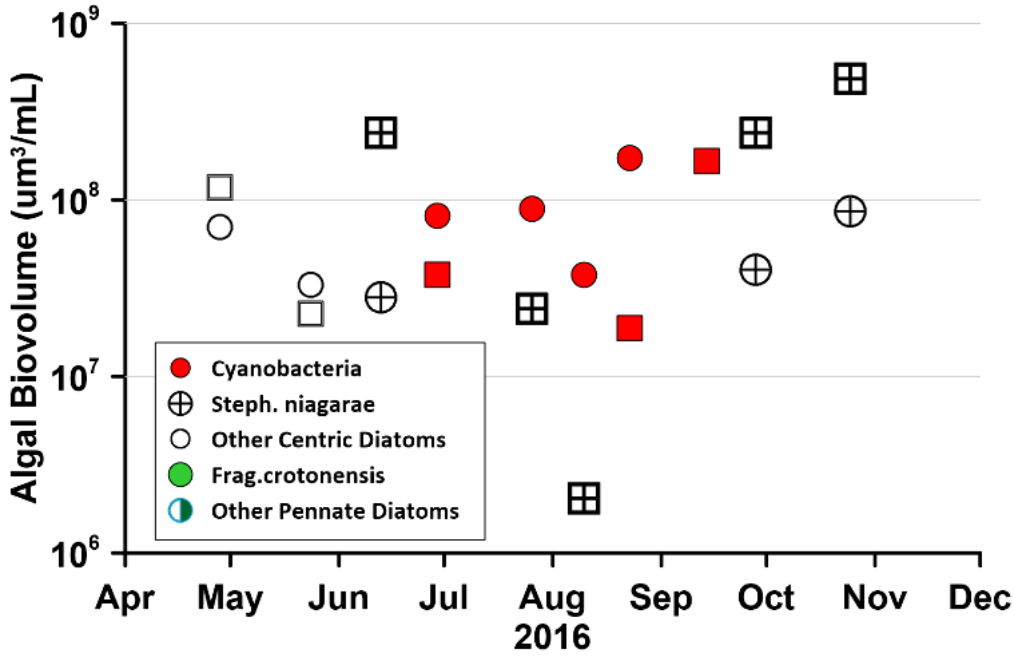

Figure 4-43. Dominant phytoplankton taxa in the Common Pool (RES08) in 2016. Round symbols represent upper 1 m, and square symbols represent 10 m depth.

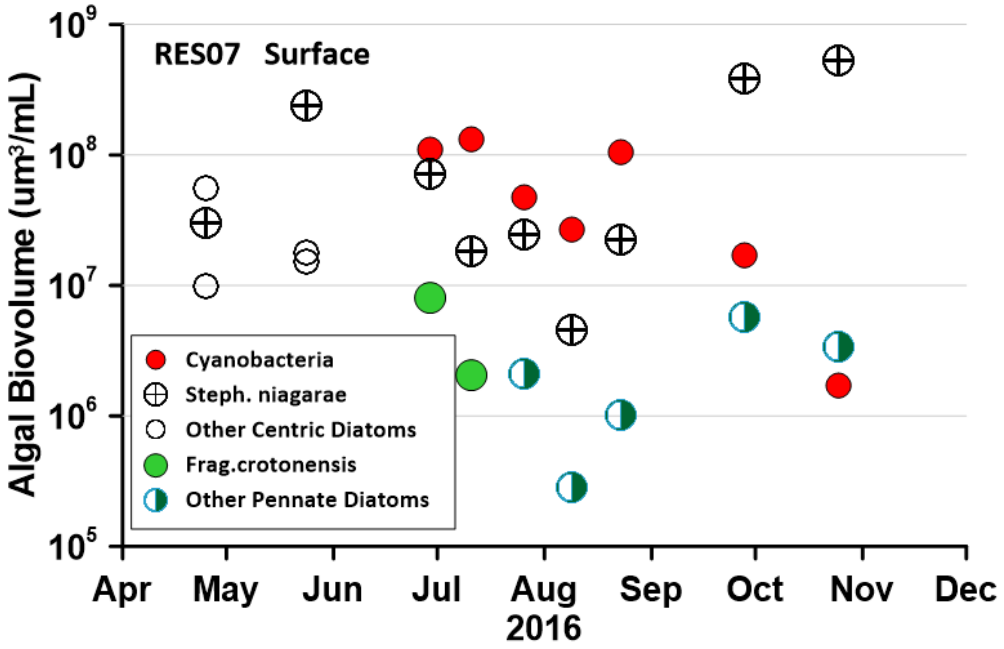

Figure 4-44. The three dominant phytoplankton taxa for each sampling date in 2016 in the upper 1 m of Round Butte forebay (RES07).

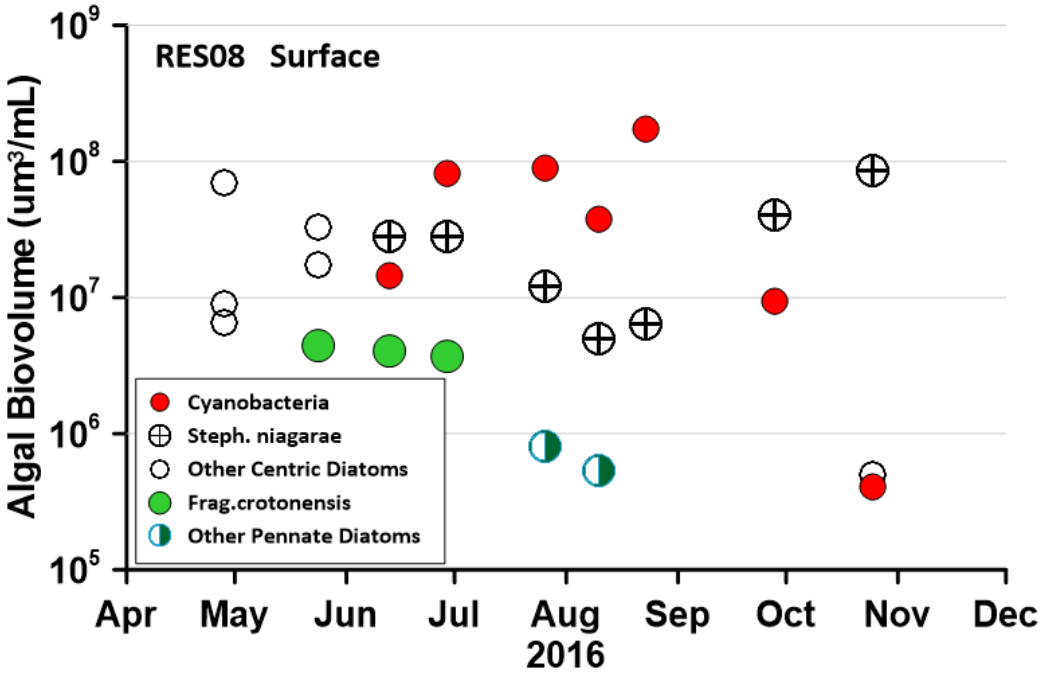

Figure 4-45. The three dominant phytoplankton taxa for each sampling date in 2016 in the upper 1 m of the Common Pool (RES08).

As a large impoundment with complex morphometry, LBC would be expected to have spatial differences in distribution of algal populations. Of the two sampling sites, Round Butte forebay (RES07) generally had a more abundant phytoplankton community than the Common Pool (RES08), but the principal taxa and temporal distributions were similar (Figure 4-46). Cyanobacteria (*Dolichospermum* [*Anabaena*]) were dominant at both sites throughout much of the summer with the centric diatoms, *S. niagarae* and *S. minutulus,* dominant in the spring and fall.

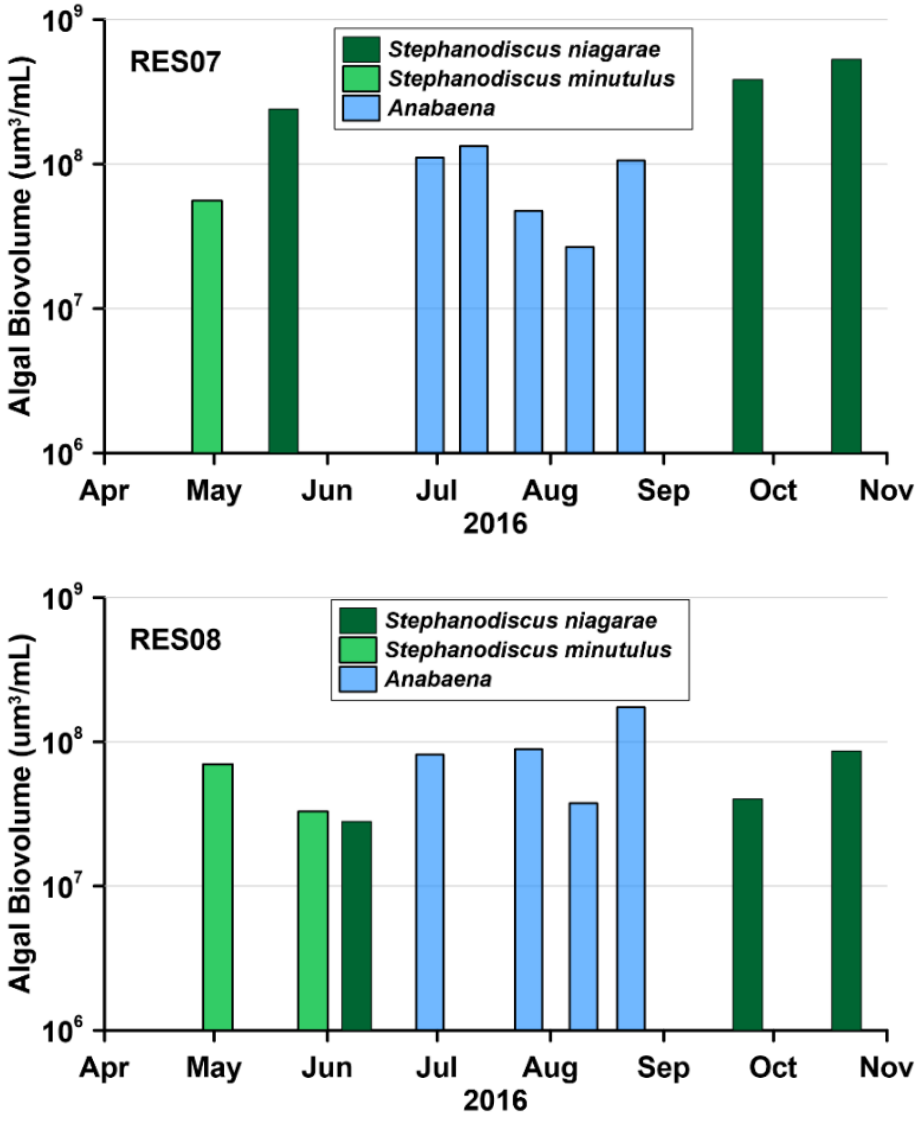

Figure 4-46. Comparison of dominant phytoplankton taxa from surface samples collected at Round Butte forebay (RES07) and the Common Pool (RES08) in LBC in 2016.

4.2.1.18 Zooplankton

The dominant zooplankton group present in LBC samples was the rotifers, the smallest of the major groups of zooplankton (Figure 4-47.). Generally, the most effective grazers of phytoplankton are large cladocerans such as *Daphnia pulicaria* and *Daphnia rosea.* Both species were present in LBC, but in relatively low densities (Figure 4-48.). The relative paucity of large cladocerans can be caused by a high degree of predation by fish because they are an important food source for planktivores. Also, abundant populations of large cladocerans help reduce primary production through consumption of phytoplankton. However, the phytoplankton community in LBC comprised primarily large taxa such as *S. niagarae* and the relatively unpalatable *Dolichospermum* (Fulton 1988), thus providing relatively poor-quality food for zooplankton. Copepods were abundant in LBC, with calanoids more abundant than the cyclopoids in the spring of 2016; their densities were similar for the remainder of the year. Copepods feed on a wide variety of foods, including algae, pollen, detritus, bacteria, rotifers, and other organisms (Williamson 2001). Both the calanoids and cyclopoids are largely omnivorous, with the early life stages generally more herbivorous than adults.

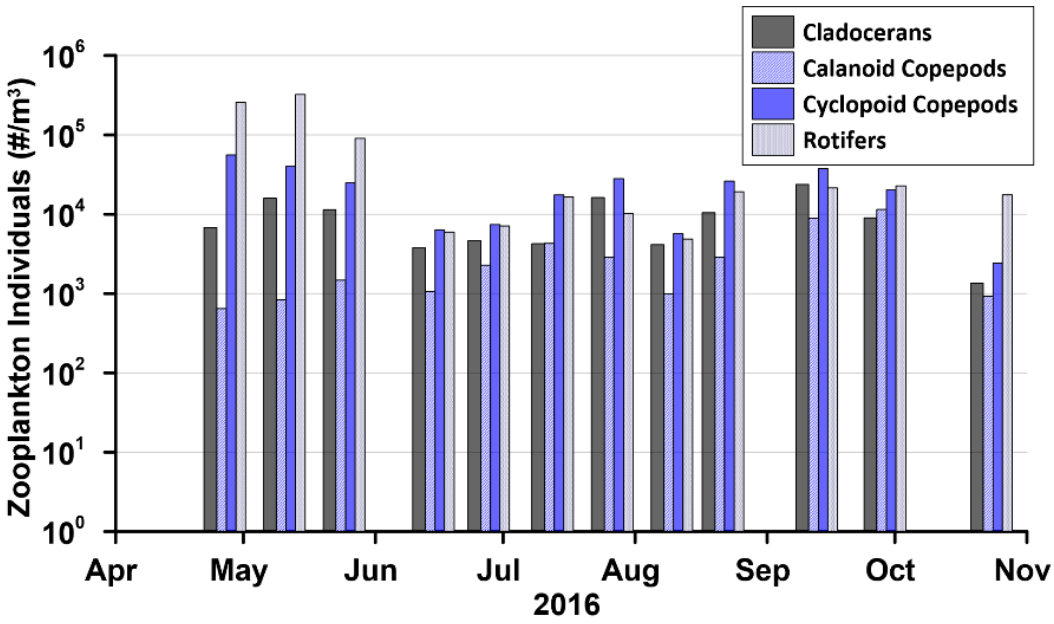

Figure 4-47. Abundance of the major zooplankton divisions collected in the upper 10 m at Round Butte forebay (RES07) in 2016.

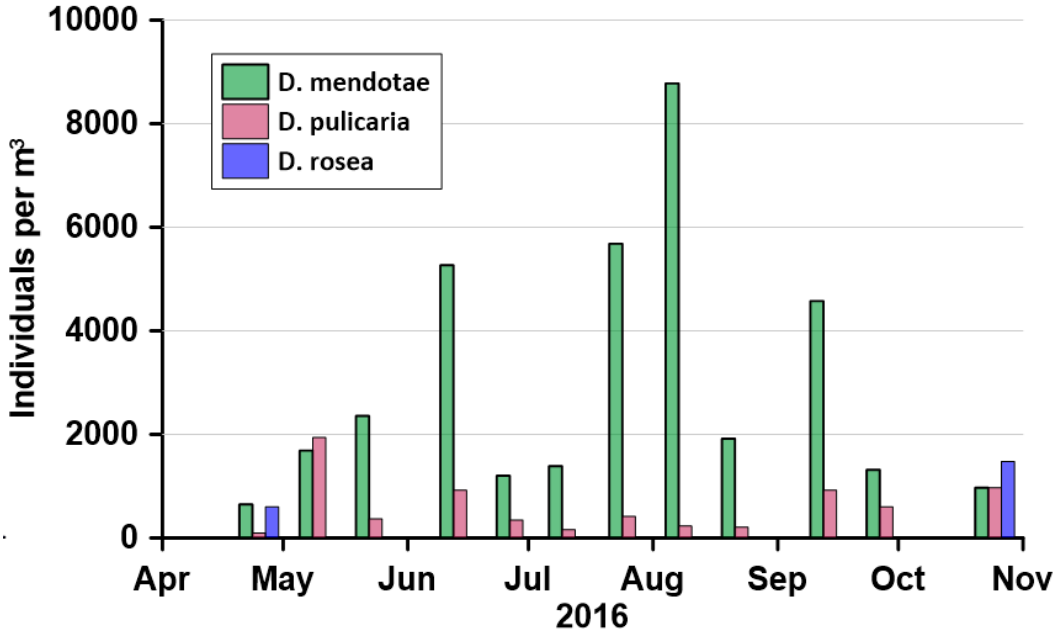

Figure 4-48. Density of the three species of *Daphnia* present in the upper 10 m tows from Round Butte forebay (RES07) in 2016.

It should be noted that zooplankton populations are notoriously variable in space and time and the limited spatial sampling conducted in this study might not accurately represent the impoundment-wide community. Additionally, only daytime sampling was conducted during this project and zooplankton communities tend to move up in the water column at night. However, these results showed a consistent pattern and were strongly suggestive of a community with a low density of cladocerans and a comparatively high density of rotifers.

4.2.2 Lake Simtustus

Lake Simtustus is a long, narrow impoundment with most of the inflow derived from discharge from Round Butte Dam. Two sites were sampled in Lake Simtustus. The Mid-Lake site (RES25) is located downstream of the Round Butte tailrace and before the Seekseequa Creek and Willow Creek inflows. The Pelton forebay (RES04) is near the Pelton Dam.

During the winter, the flows from LBC were of temperature and density similar to those in Lake Simtustus and readily mixed with waters in the lake. However, in the warmer months when Lake Simtustus stratifies, the cooler (and denser) releases from LBC passed into the lake's

hypolimnion and moved toward Pelton Dam without much interaction with the surface waters of the reservoir. The surface waters of Lake Simtustus remained relatively isolated until the fall turnover. Note that there is one other sizeable surface inlet to Lake Simtustus: Willow Creek, which enters the impoundment about 1.7 mi south of Pelton Dam. That stream had comparatively little discharge, with average flows of about 20 cfs (0.6 cubic meters per second [m^3/s]), but its influence on nutrient loading was disproportionately significant because it had high concentrations of NO_3 (Table 4-5). The Willow Creek discharge varied little across measurements taken from 2015 to 2016. The creek's warm waters (*mean = 19.9˚C, sd = 2.3˚C, n = 22*) entered the epilimnion of Lake Simtustus and appeared to move laterally to the north and south. The high conductivity waters in Willow Creek contribute to the relatively high conductivity values observed in the epilimnion of Lake Simtustus.

Table 4-5. Water chemistry of Willow Creek measured in 2015 and 2016.

Statistic (*n* = 18)	**Total P (mg/L)**	**PO_4 (mg/L)**	**Total N (mg/L)**	**NO_3 (mg/L)**	**Chloride (mg/L)**	**Conductivity (µS/cm)[a]**
Mean	0.0295	0.0203	4.92	3.76	10.6	384
Median	0.0196	0.0183	4.82	4.06	11.1	390
Minimum	0.013	0.0048	3.82	0.78	2.3	349
Maximum	0.092	0.0530	6.35	4.65	12.3	404
1st Quartile	0.0179	0.0090	4.43	3.56	10.6	370
3rd Quartile	0.040	0.0225	5.47	4.37	12.3	399

Note:
[a] n = 14

4.2.2.1 Temperature

Lake Simtustus was slightly cooler on the surface than LBC, but below the surface it was considerably warmer than the hypolimnetic waters in LBC (Figure 4-49). The impoundment developed a shallow lens of warm water during the summer (sometimes exceeding 22˚C), but much of the deeper water maintained a temperature near 13˚C for May–October. When the temperature at the ReReg Dam approaches 13˚C, PGE increases the percentage of bottom withdrawal so the river temperature at the ReReg Dam does not exceed the without-Project temperature by more than 0.3˚C (or by more than 0.5˚C for up to 3 days). The "without-Project

temperature" refers to estimated water temperature in the LDR that would have been experienced without the dams present.

Lake Simtustus had a shallow epilimnion of only 3 to 4 m depth, a transition to cooler waters in the thermocline down to about 10 m, and the hypolimnion extended downward from there. The relatively uniform expanse of 13˚C waters provides a strong indication of how water passes from LBC through Lake Simtustus during spring through fall. The field team conducted a dye study in Lake Simtustus during August 2017. Fluorescent dye was added to the tailrace below Round Butte Dam on August 2 and again on August 3, and the fluorescence was measured below the tailrace of Pelton Dam (Figure 4-50). The results indicated a travel time of about 26–30 hr through Lake Simtustus at flows of about 3,565 cfs at the Madras gauge below the ReReg Dam. The rapid demarcation of dye on the descending portion of the dye signal suggests that the water from LBC moved through Lake Simtustus as a continuous mass with little additional mixing. If there had been considerable mixing of Round Butte tailrace waters in the hypolimnion of Lake Simtustus, the measurement of dye in the Pelton Dam tailrace would have been of longer duration.

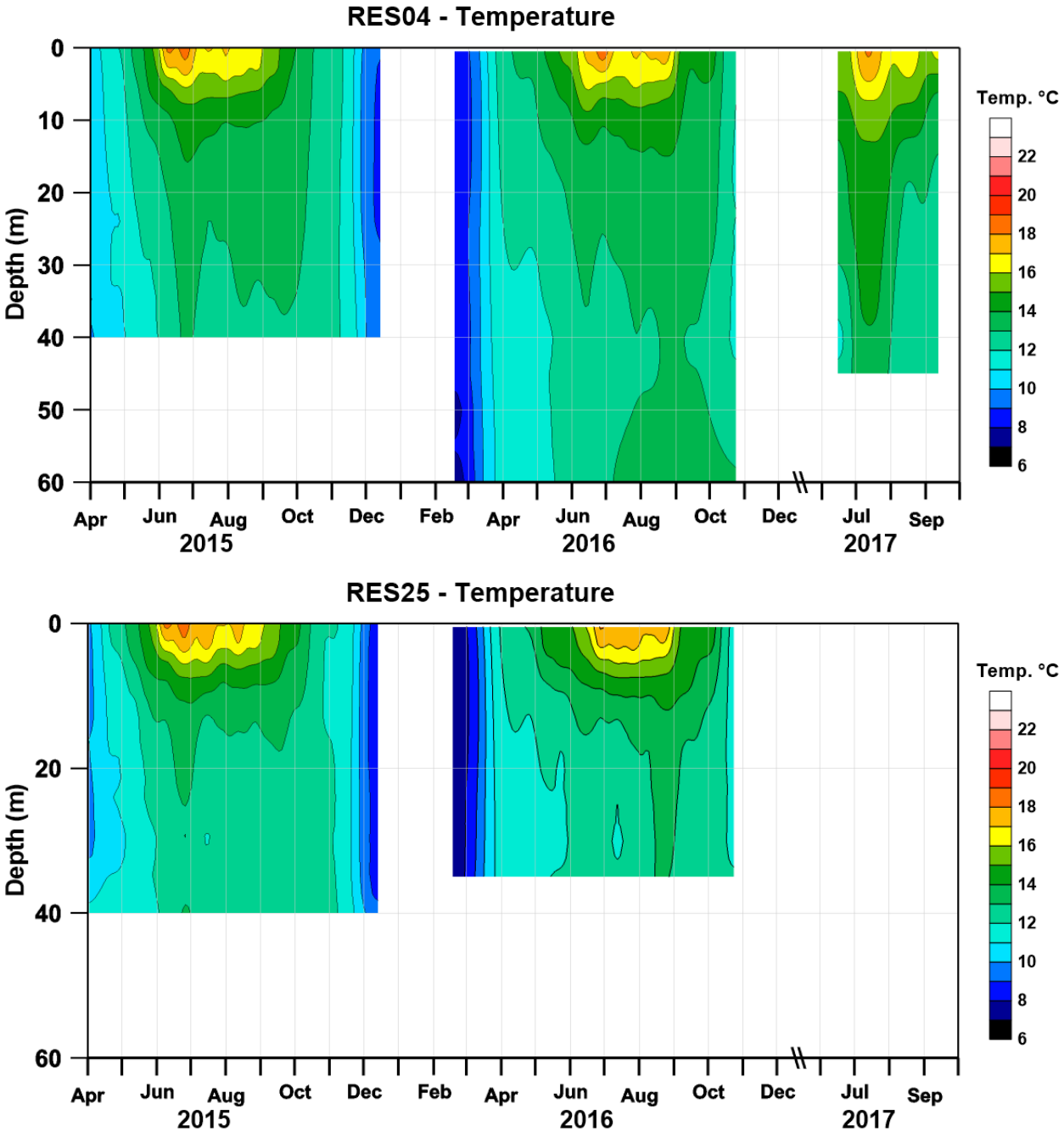

Figure 4-49. Temperature contours at Pelton forebay (RES04) (*top*) and Mid-Lake site (RES25) (*bottom*).

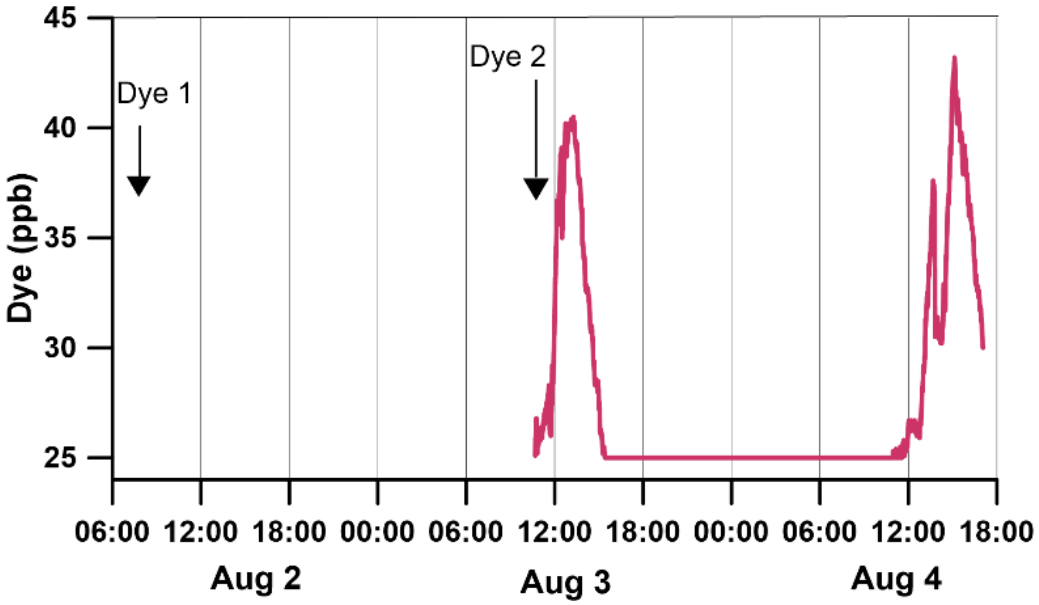

Figure 4-50. Dye signal strength measured at Pelton Dam tailrace following the addition of dye at Round Butte Dam tailrace in August 2016. Average discharge from Round Butte Dam during the first dye study was 3,308 cfs (se = 51.3) and 3,565 cfs (se = 52.2) during the second dye event.

The RTR in Lake Simtustus showed results similar to LBC, with high stability at the surface and no metalimnetic maximum, which is experienced in most lakes in temperate climates (Figure 4-51). Again, this reflects the relatively weak metalimnion. The patterns in total RTR showed intense peaking in the Pelton forebay (RES04) in 2015 and 2016, but a much reduced total RTR in summer 2017 (Figure 4-52). That result likely reflected a reduction in solar warming and increased wind in 2017.

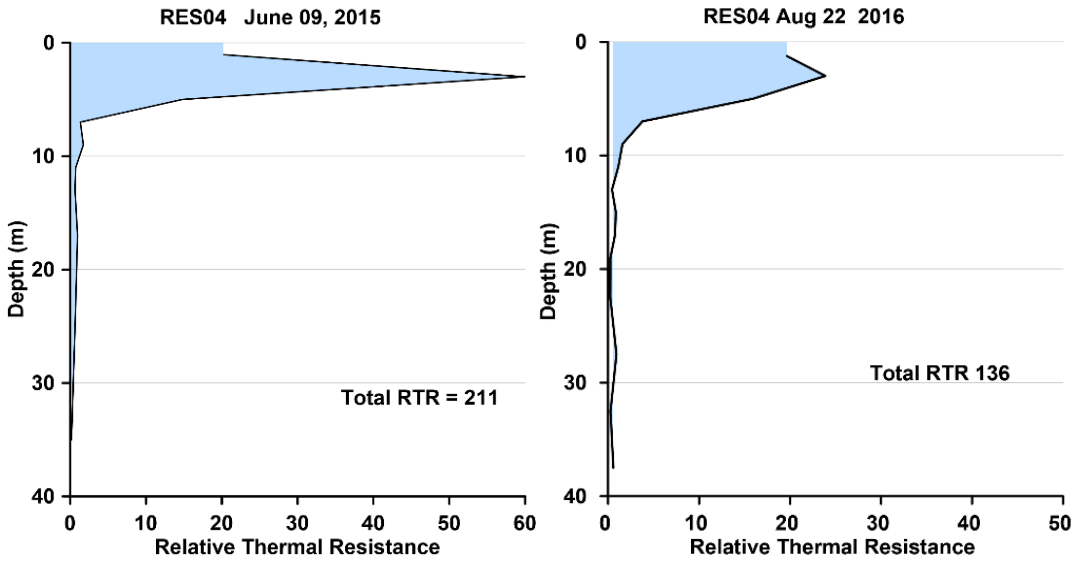

Figure 4-51. RTR in the Pelton forebay (RES04) on two summer dates.

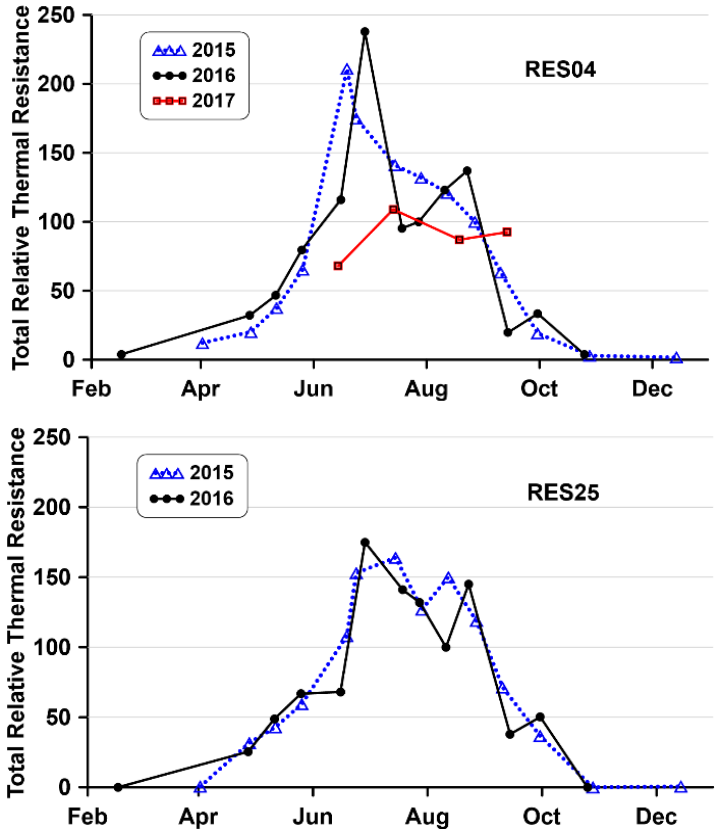

Figure 4-52. Total RTR at Pelton forebay (RES04) and Mid-Lake site (RES25) during the study.

4.2.2.2 Conductivity

Conductivity in Lake Simtustus was relatively low within the body of the lake at or about 120 µS/cm (Figure 4-53). The epilimnion had a higher conductivity of about 140–150 µS/cm. Conductivity values were uniform during winter and spring but partitioned into distinct vertical bands in summer and fall. The epilimnetic conductivity values in Lake Simtustus were similar to those observed in LBC, but the sources of the additional solutes are different between impoundments. In LBC, the higher conductivity values are associated directly with the inflow from the Crooked River. In Lake Simtustus, the higher epilimnetic conductivity values appear to be associated with inflow from Willow Creek. Although the discharge from Willow Creek is small, the conductivity values averaged 384 µS/cm and the warm inflow remains in the epilimnion of Lake Simtustus throughout the stratification period.

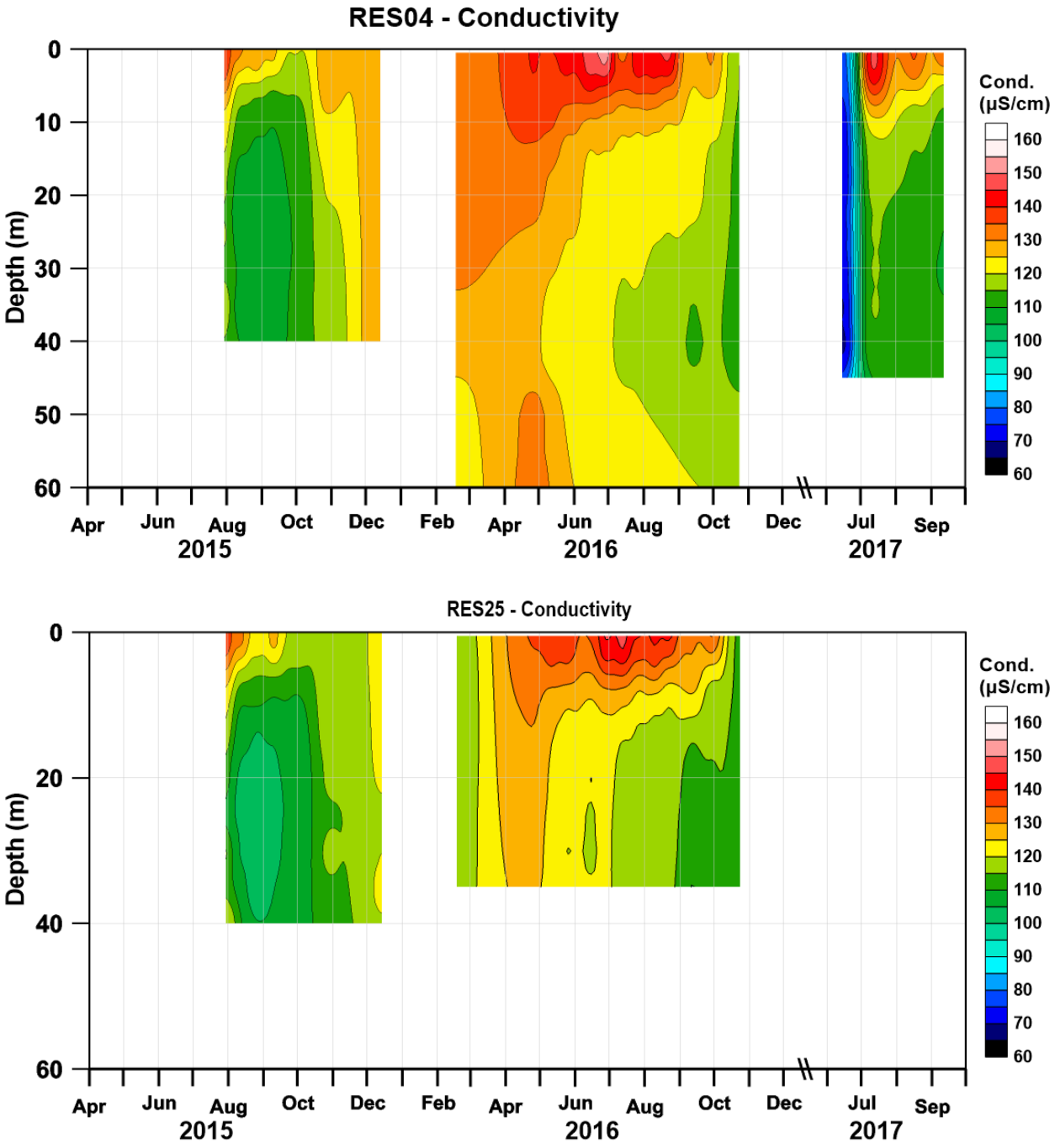

Figure 4-53. Conductivity contours for Pelton forebay (RES04) (*top*) and Mid-Lake site (RES25) (*bottom*). Conductivity measurements were not recorded until August 2015.

4.2.2.3 Dissolved Oxygen

DO saturation ranged from highly supersaturated in the surface waters to undersaturated in the hypolimnion (Figure 4-54). Peak saturation values exceeded 200% for a short period in June 2015 but were closer to 150% saturation in 2016 and 2017. Minimum saturation tended to occur near the lower thermocline/upper hypolimnion at the Pelton forebay (RES04), but generally occurred deeper in the hypolimnion at the Mid-Lake site (RES25). The period of undersaturation in the hypolimnion typically began in June and extended into the fall for 2015–2017.

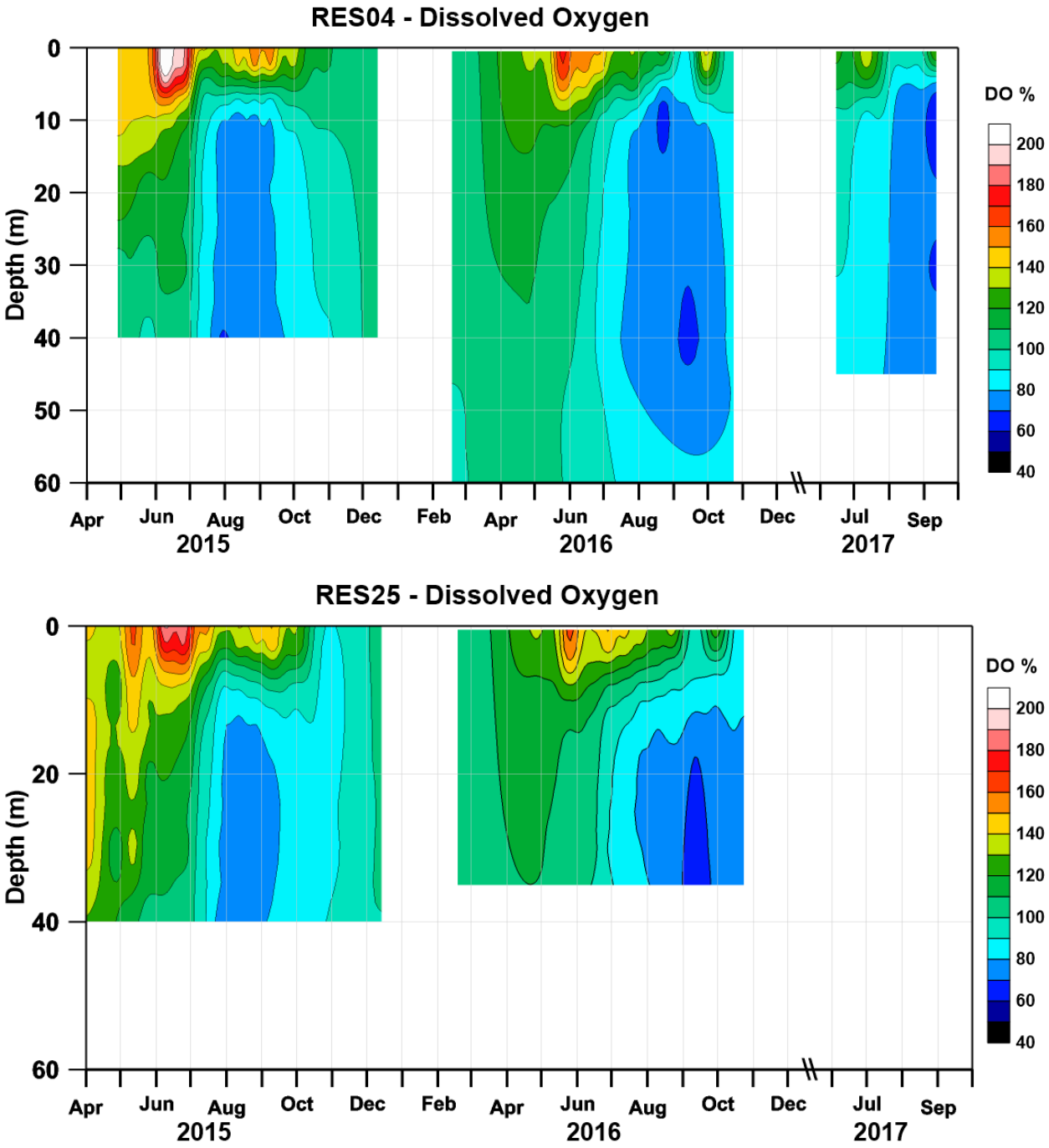

Figure 4-54. DO saturation contours for Pelton forebay (RES04) (*top*) and Mid-Lake site (RES25) (*bottom*).

4.2.2.4 pH

pH values generally ranged from 7.5 to 9.5 in Lake Simtustus. The highest values occurred in the epilimnion in summer (Figure 4-55). The hypolimnion typically maintained pH values from 8.0 to 8.5.

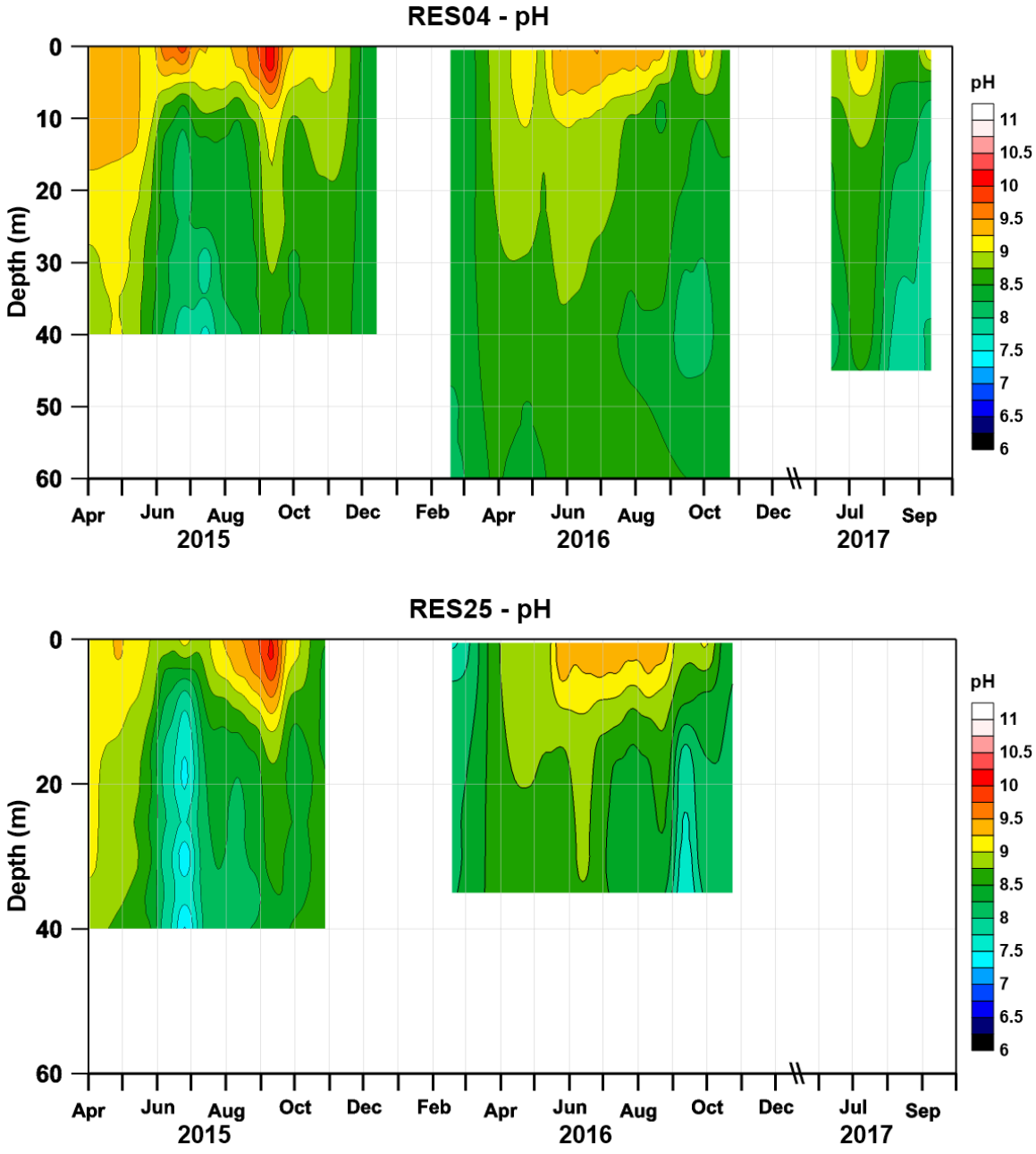

Figure 4-55. pH contours for Pelton forebay (RES04) (*top*) and Mid-Lake site (RES25) (*bottom*).

4.2.2.5 Transparency and Light Attenuation

Secchi disk transparency was high in winter, declined in spring and summer, and increased again in fall (Figure 4-56). There was a brief increase in transparency in May of both 2015 and 2016 but returned to about 2 m throughout the summer. Transparency oscillated in an irregular manner between years, although much of the transparency fluctuated between 2–3 m in the summer.

Transmission of light into Lake Simtustus was rather limited, particularly in the summer, when measurable transmission of surface light seldom exceeded 5 m (Figure 4-57). The highest degree of light transmission was observed in the winter from November through February, and typically the lowest was observed in July and August. Light transmission was consistently limited to less than 5 m in summer of 2017, when light profiles were virtually identical across the four months measured.

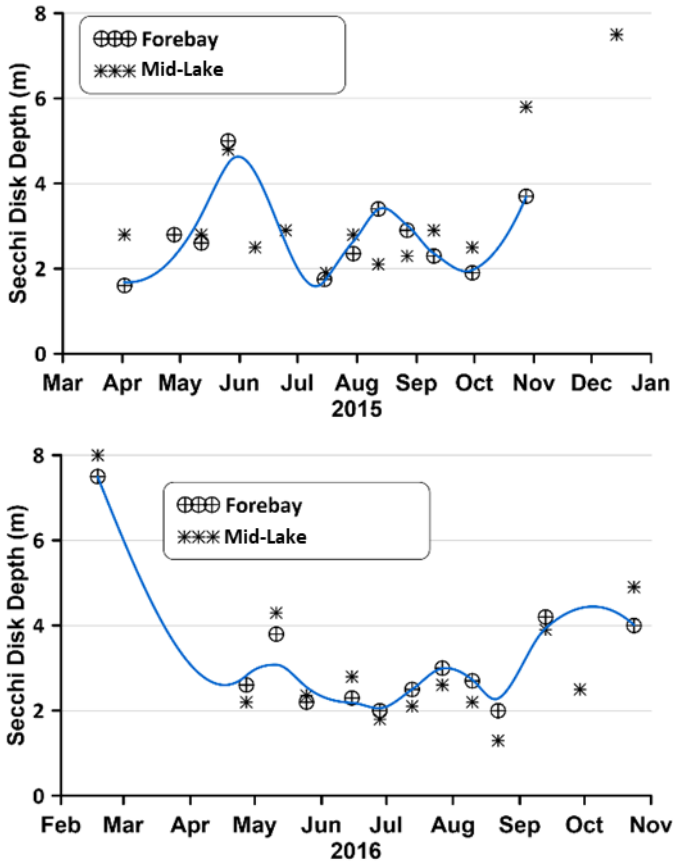

Figure 4-56. Secchi disk transparency in Lake Simtustus in 2015 (*top*) and 2016 (*bottom*).

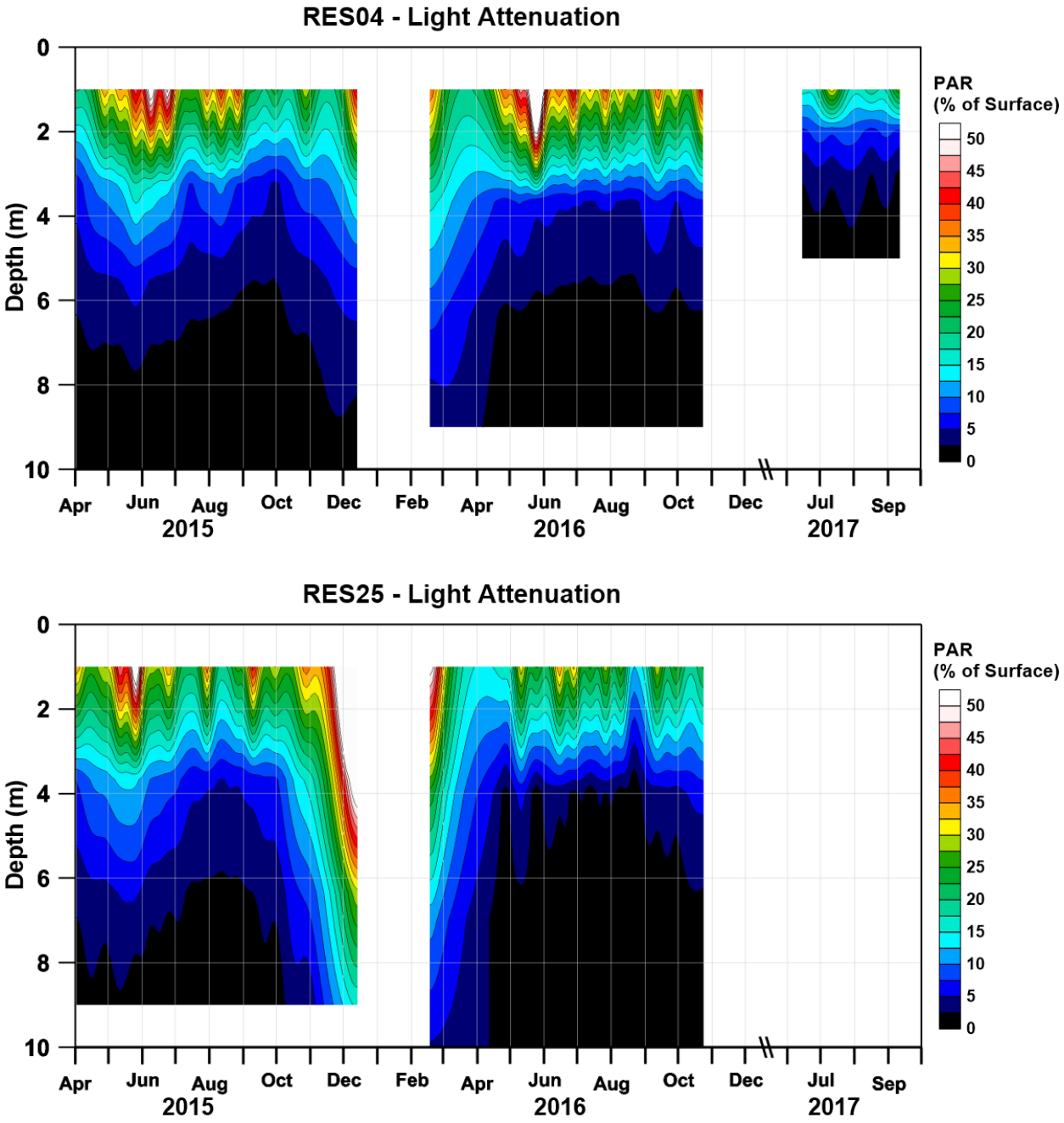

Figure 4-57. Light attenuation contours for Pelton forebay (RES04) (*top*) and Mid-Lake site (RES25) (*bottom*).

4.2.2.6 Turbidity

Turbidity in Lake Simtustus was similar among the 3 years and similar between the two samples sites within years (Figure 4-58). Turbidity was low in the winter and reached values of about 8–10 NTUs in the summer. There was little vertical variation in turbidity within the 10-m range of measurements.

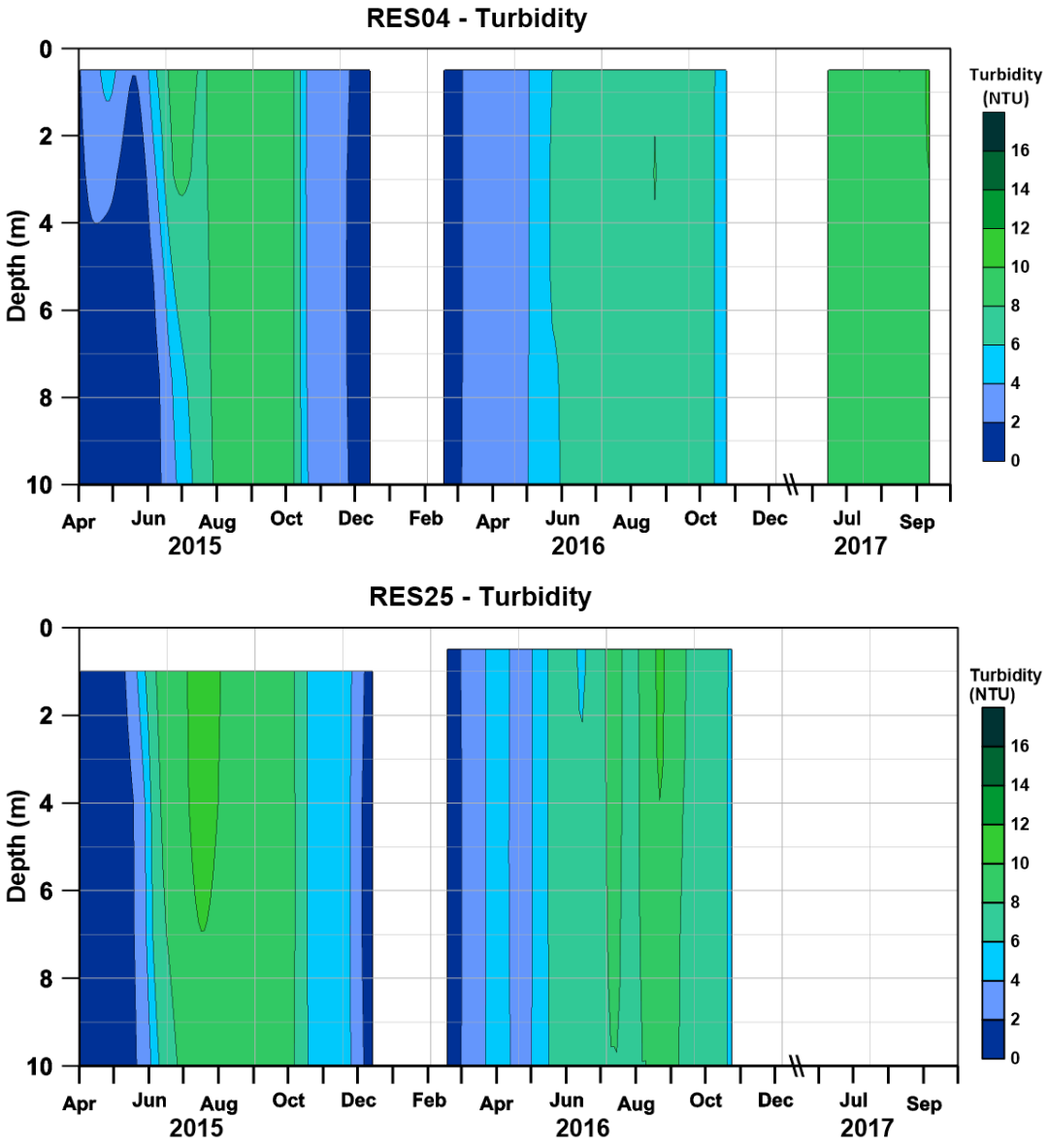

Figure 4-58. Turbidity contours for Pelton forebay (RES04) (*top*) and Mid-Lake site (RES25)(*bottom*).

4.2.2.7 Total Phosphorus

Concentrations of TP varied substantially between the epilimnion and the hypolimnion (Figure 4-59). In 2015, a distinct mass of high TP waters (over 0.10 mg/L) deeper in the lake was prominent in July, whereas the surface waters had concentrations approaching 0.025 mg/L. That apparent depletion of TP in the surface waters was also observed in 2016 and 2017, but the TP concentrations in the bottom waters remained relatively high throughout 2016.

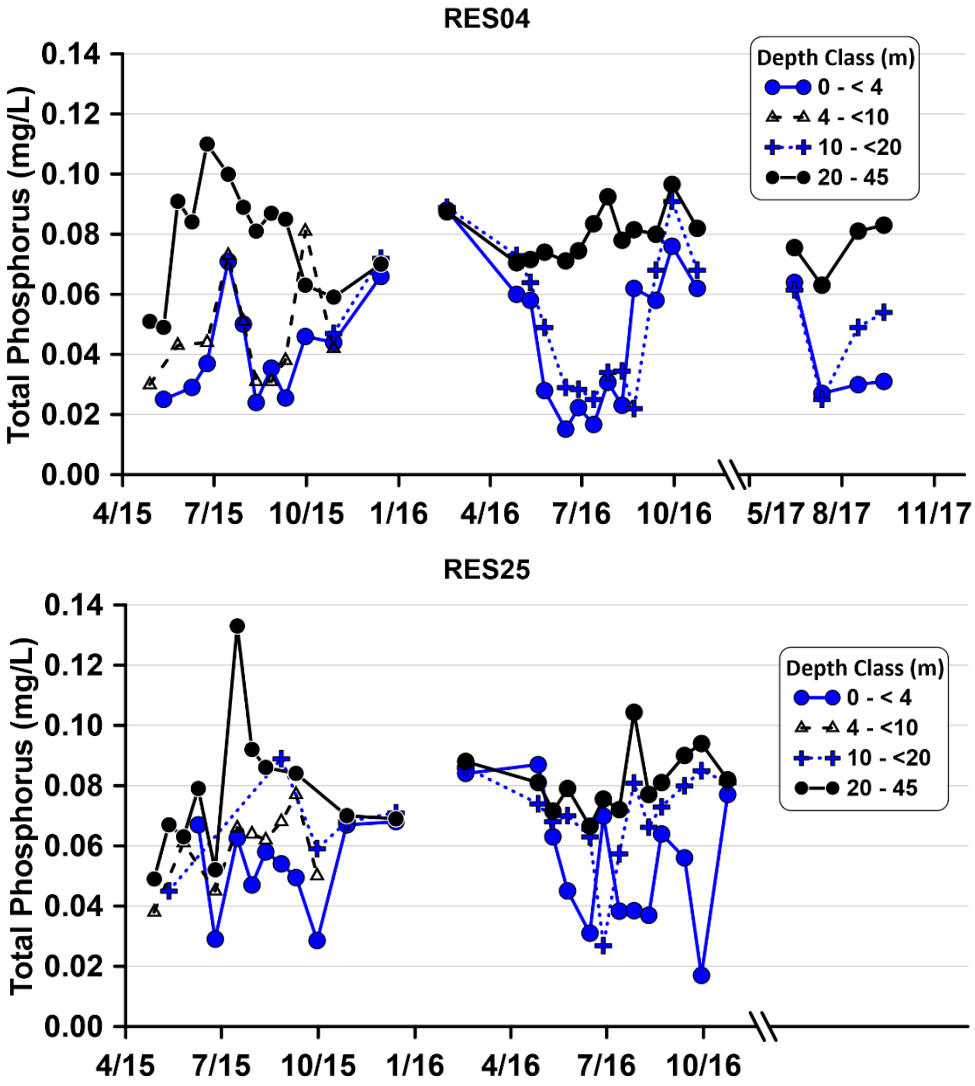

Figure 4-59. TP concentrations at Pelton forebay (RES04) (*top*) and Mid-Lake site (RES25) (*bottom*).

4.2.2.8 Phosphate

Concentrations of PO_4 reached the detection limit (0.001 mg/L) in the surface waters of Lake Simtustus during the summers of 2015–2017 (Figure 4-60). In 2015, concentrations in the hypolimnion were low throughout the spring but increased by June. In contrast, in 2016, PO_4 concentrations were high and uniform from November to March, but gradually declined towards summer.

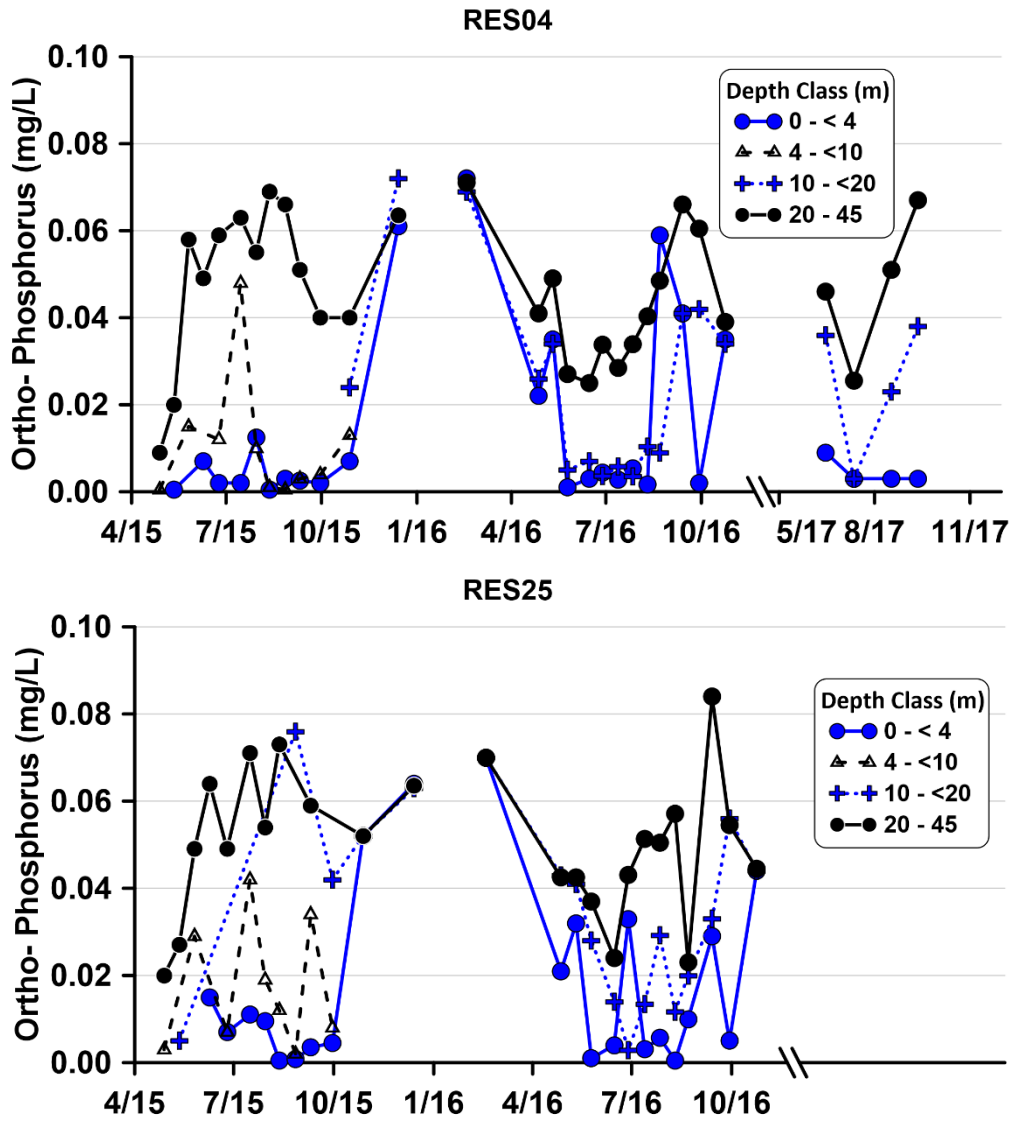

Figure 4-60. PO_4 concentrations at Pelton forebay (RES04) (*top*) and Mid-Lake site (RES25) (*bottom*).

4.2.2.9 Total Nitrogen

TN concentrations showed unusual patterns in Lake Simtustus. In late June/early July 2015, concentrations of TN were relatively high from top to bottom with the highest values observed near a depth of 30 m (Figure 4-61). It is more typical to observe concentrations of TN peaking near the surface or generally no deeper than the metalimnion. This pattern was not repeated in 2016 or 2017, and it is unclear what mechanism was responsible for the observed values. However, concentrations of TN were generally low throughout the impoundment during much of the year, with minimum values observed in fall 2015, May 2016, and June 2017.

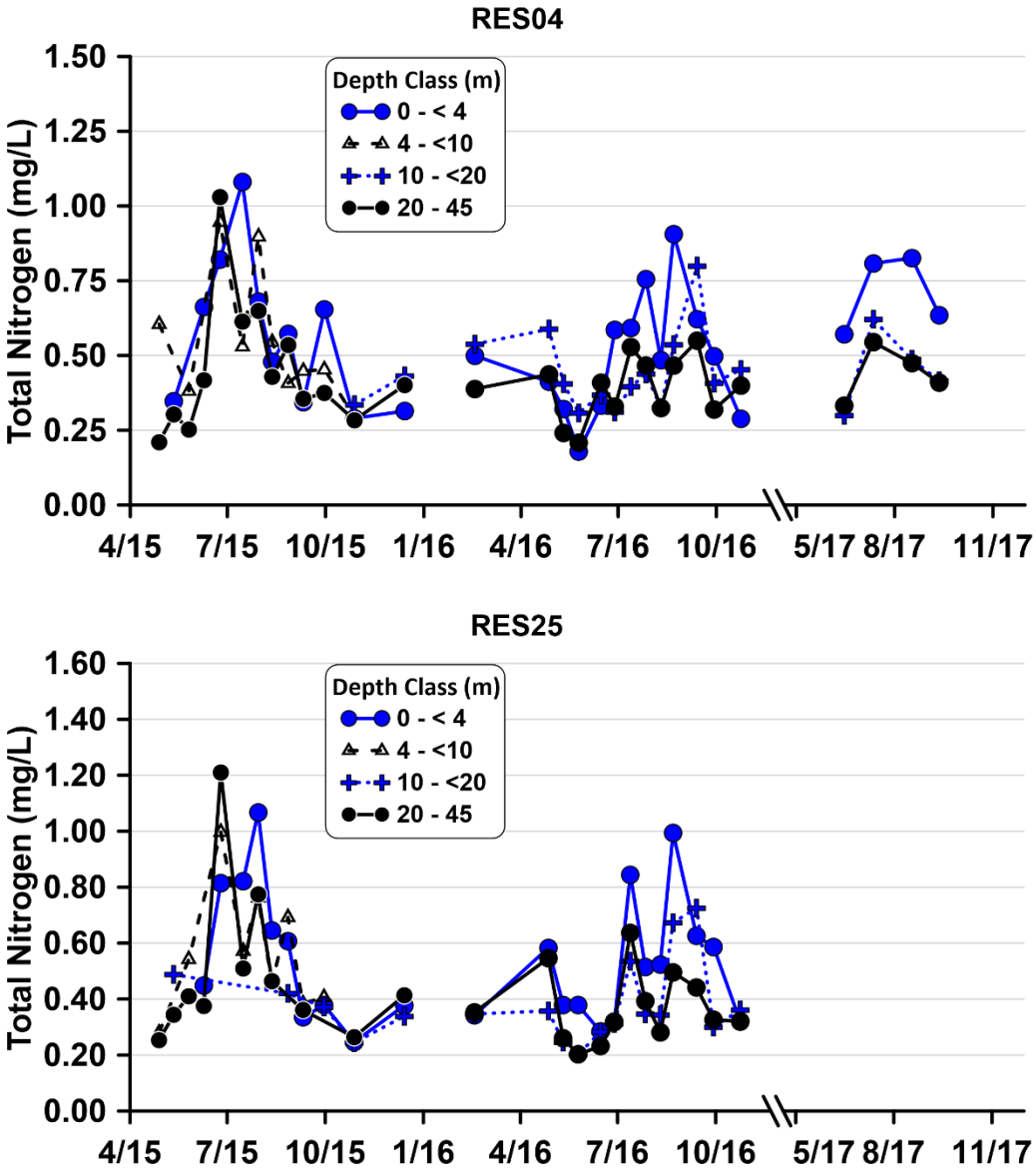

Figure 4-61. TN concentrations at Pelton forebay (RES04) (*top*) and Mid-Lake site (RES25) (*bottom*).

4.2.2.10 Nitrate

Concentrations of NO_3 varied throughout the water column and appeared different in 2015 than in the following 2 years. In May 2015, NO_3 was uniform and near the DL (<0.010 mg/L), but by July, concentrations of NO_3 reached 0.25 mg/L from about 15 m to the bottom and were still above 0.15 mg/L at the surface (Figure 4-62). By December, concentrations returned to 0.25

mg/L from top to bottom. In 2016, concentrations of NO_3 started high in February but declined in spring. Values again increased in mid-summer, although not to the level observed in 2015. NO_3 concentrations were less than the DL in September 2016 at Mid-Lake site (RES25), while at the Pelton forebay (RES04), concentrations remained comparatively high. In 2017, the abbreviated sampling revealed a pattern similar to the one the previous year at Pelton forebay (RES04).

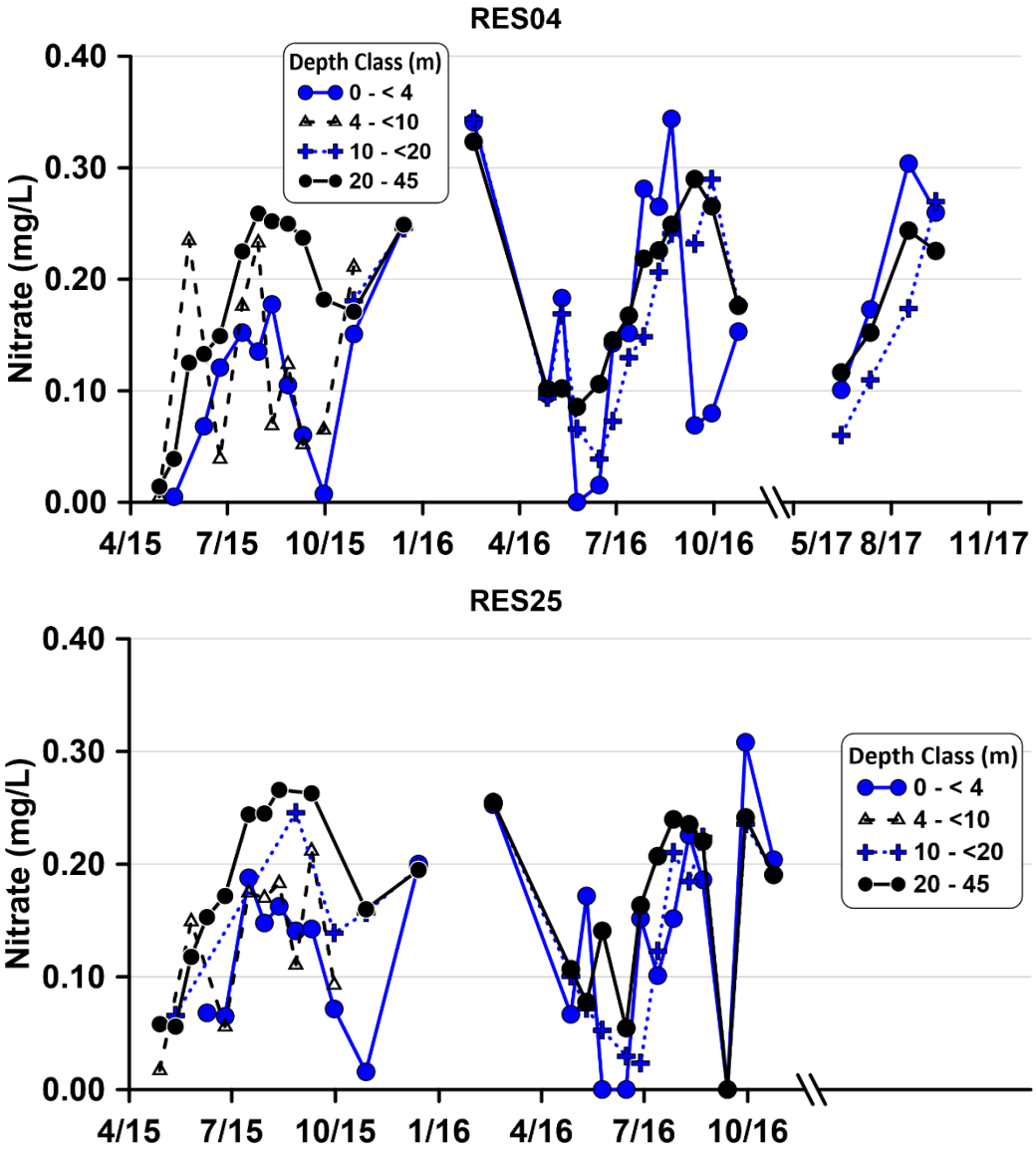

Figure 4-62. NO_3 concentrations at Pelton forebay (RES04) (*top*) and Mid-Lake site (RES25) (*bottom*).

4.2.2.11 Ammonia

Concentrations of NH_3 were generally at or near the DL (<0.010 mg/L). However, some isolated pockets of elevated values existed, particularly in the thermocline (Figure 4-63). The isolated zones of elevated NH_3 concentrations were present all 3 years of monitoring but rapidly formed and dissipated. These likely represented zones of intense mineralization associated with rapid phytoplankton population declines.

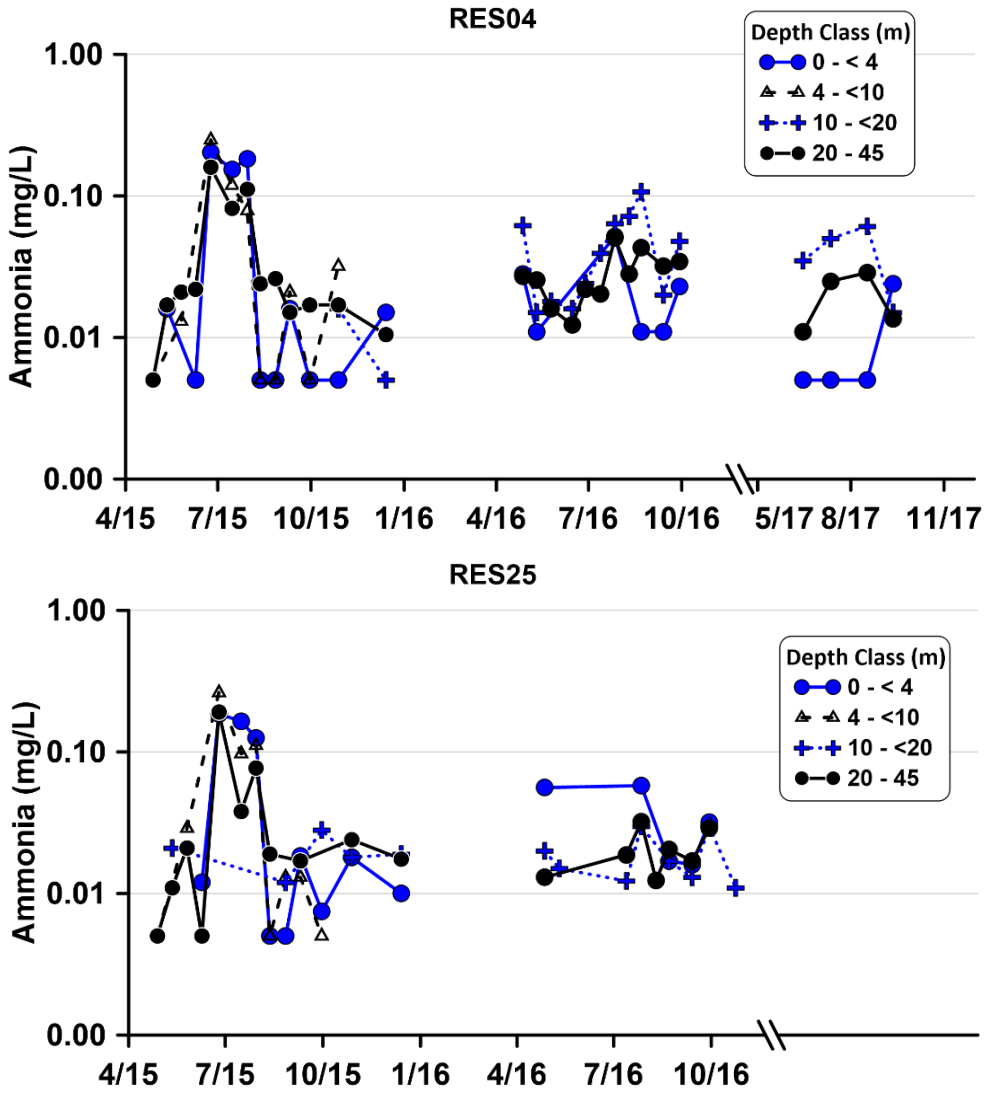

Figure 4-63. NH_3 concentrations at Pelton forebay (RES04) (*top*) and Mid-Lake site (RES25) (*bottom*).

4.2.2.12 Total Nitrogen:Total Phosphorus Ratio

The ratio of TN:TP in Lake Simtustus showed a deficit of phosphorus in the epilimnetic waters and an excess of nitrogen in the bottom waters in the Pelton forebay (RES04) (Figure 4-64). However, the depth and duration of relative phosphorus depletion (or excess nitrogen) was evident further upstream in the lake, particularly in 2016. The high TN/TP ratios in the epilimnetic waters reflect the uptake of phosphorus by phytoplankton and the accumulation of total nitrogen in the form of algal biovolume. Both of these factors appear to be more prominent at the forebay compared to the common pool site.

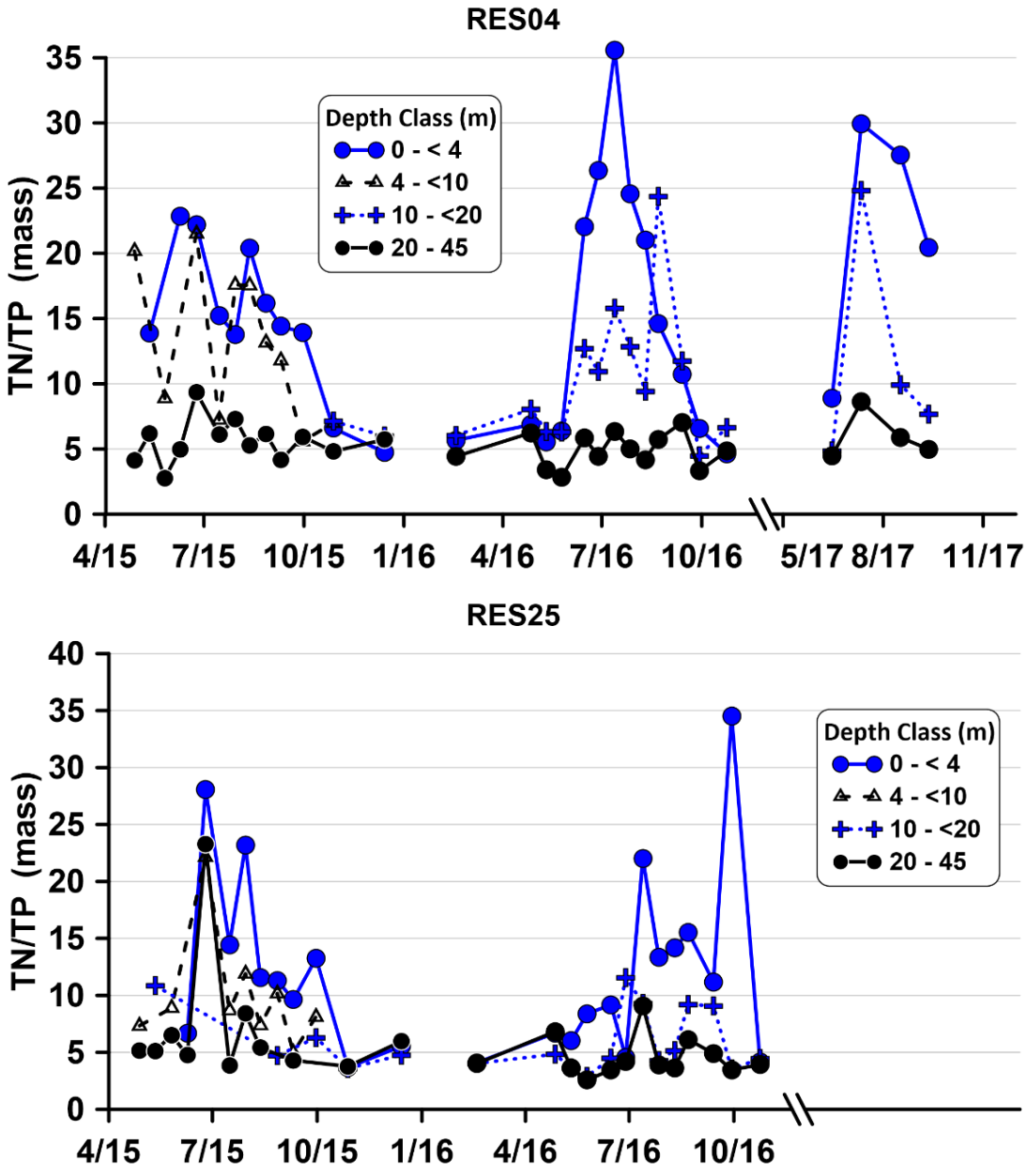

Figure 4-64. Mass ratio of TN:TP at Pelton forebay (RES04) (*top*) and Mid-Lake site (RES25) (*bottom*).

4.2.2.13 Nitrate:Phosphate Ratio

The NO_3:PO_4 ratio showed low values (< 7.2), particularly deeper in the water column (Figure 4-65). Under many circumstances, this would indicate nitrogen deficiency, but examination of the nitrate concentrations shown earlier indicate that NO_3 concentrations are high in the deeper

waters (Figure 4-61). Comparison with the previous figures for NO_3 and PO_4 concentrations indicates that the relatively high values of NO_3:PO_4 in the upper waters of Lake Simtustus are driven largely by low concentrations of PO_4, and not high values of NO_3.

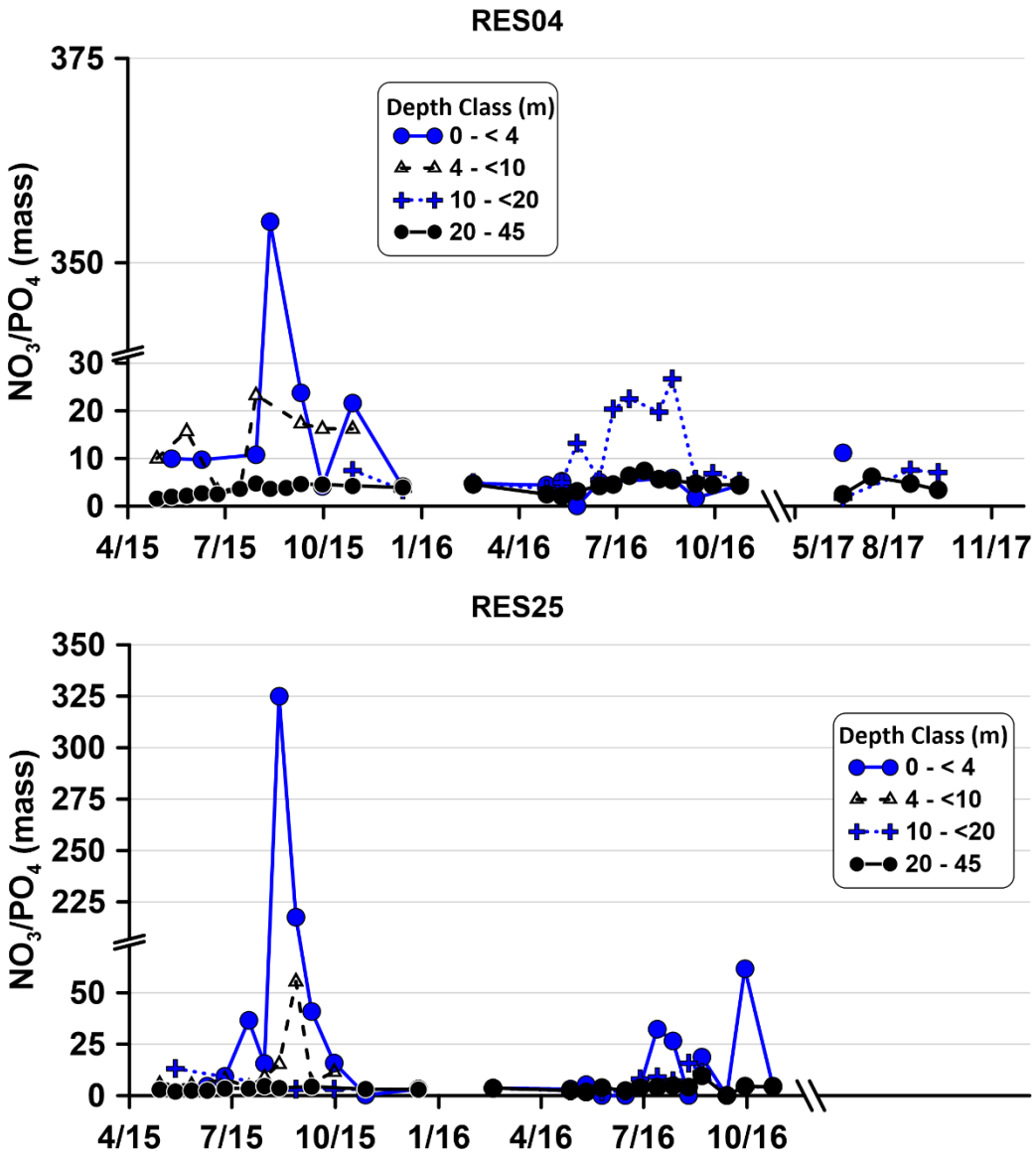

Figure 4-65. Mass ratio of NO_3:PO_4 at Pelton forebay (RES04) (*top*) and Mid-Lake site (RES25) (*bottom*).

4.2.2.14 Chloride

Concentrations of Cl^- in Lake Simtustus were highly variable but were generally highest in the epilimnion (Figure 4-66). Concentrations were lowest in winter, generally less than 1 mg/L, but increased substantially in the epilimnion during the summer.

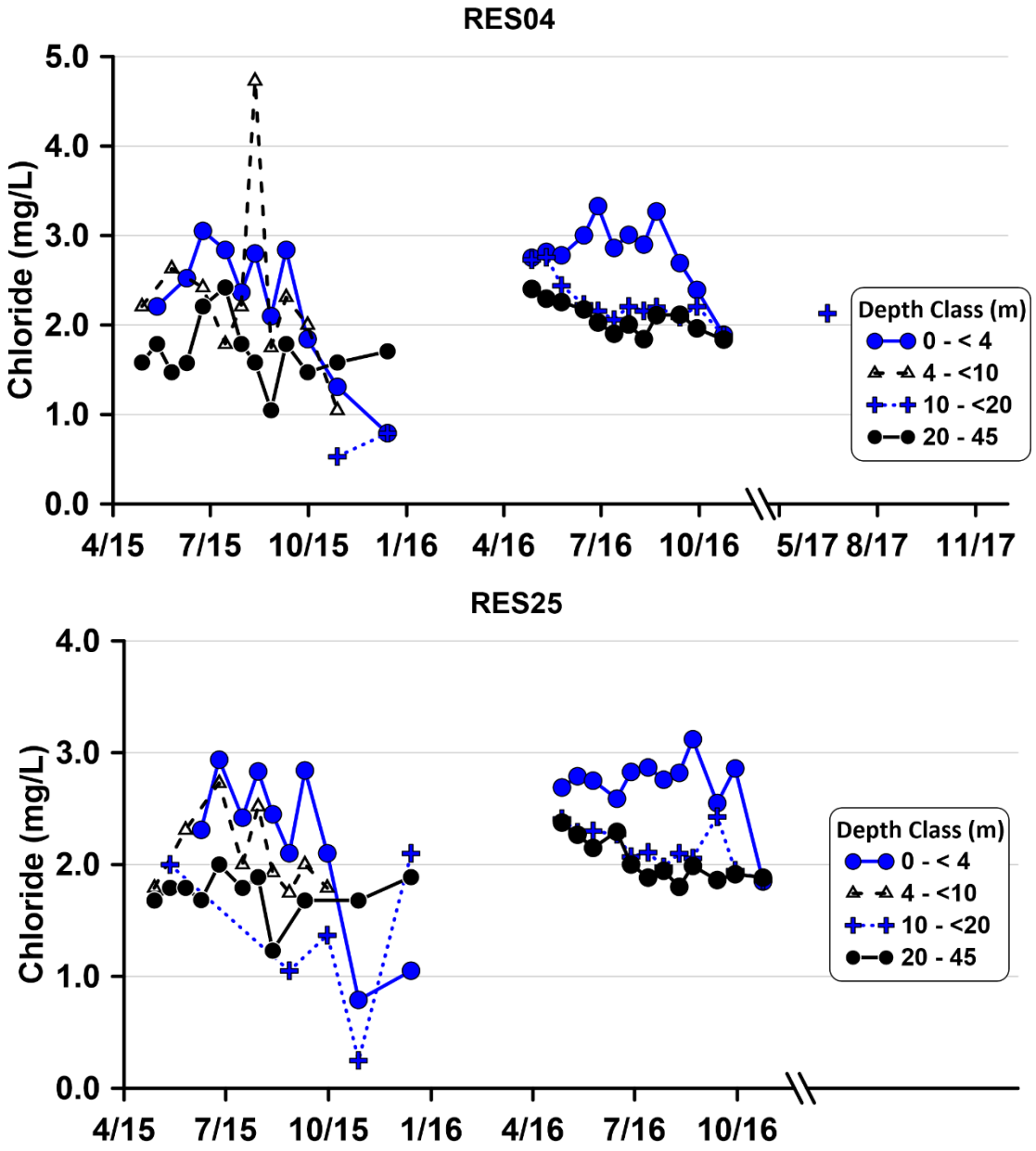

Figure 4-66. Cl^- concentrations at Pelton forebay (RES04) (*top*) and Mid-Lake site (RES25) (*bottom*). Cl^- was not analyzed in 2017.

4.2.2.15 Total Chlorophyll

Chlorophyll concentrations measured with the AlgaeTorch in Lake Simtustus ranged from the resolution of the instrument (near zero) to almost 50 µg/L (Figure 4-67). Concentrations reached maximum levels in April and again in the early fall of 2015. Maximum values peaked in late May 2016, and no extremely high values were observed in the abbreviated sampling in 2017. Concentrations of chlorophyll in the winter (December–February) were at the resolution of the instrument (zero). Concentrations were often uniform within the sampling zone (10 m), although the higher values were observed closer to the surface. If we compare the June–September period for all 3 monitoring years, it is evident that the chlorophyll was highest in 2015 and lowest in 2017. Once Lake Simtustus stratifies, the chlorophyll concentrations in the epilimnion are derived entirely from production within the lake. During the warmer months, all discharge from Round Butte Dam enters the hypolimnion of Lake Simtustus and passes through the lake without further mixing.

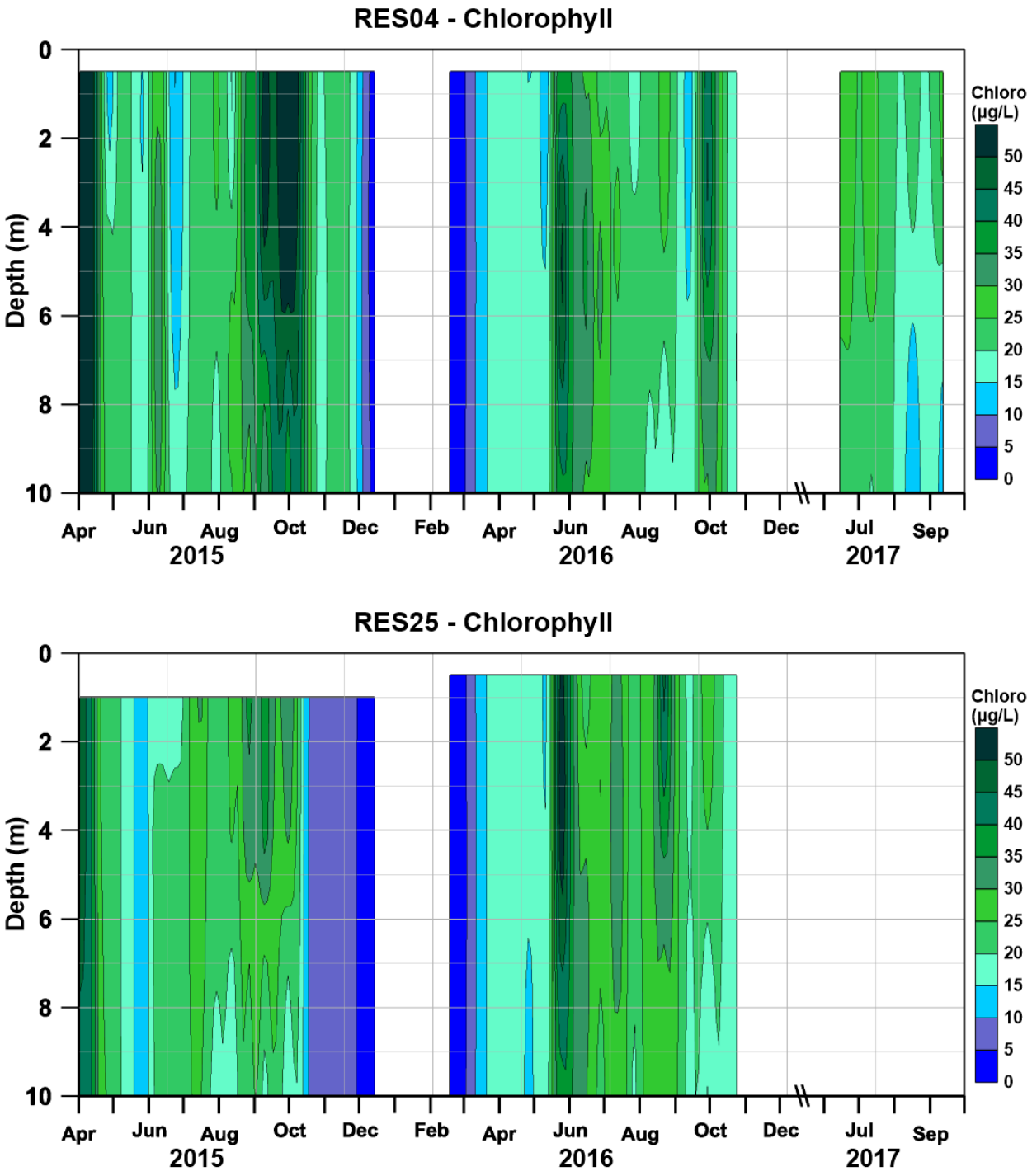

Figure 4-67. Chlorophyll pigment concentrations (µg/L) at Pelton forebay (RES04) (*top*) and Mid-Lake site (RES25) (*bottom*). Measurements were made with the AlgaeTorch.

4.2.2.16 Cyanobacteria

The field staff used the AlgaeTorch probe to measure cyanobacteria levels in Lake Simtustus for the study period (Figure 4-68). The highest concentrations of cyanobacteria were observed at Mid-Lake site (RES25), where values over 20 µg/L were observed down to a depth of 7 m in August 2016; values over 10 µg/L were observed at this site in 2015. The density and duration of cyanobacteria in the forebay of Lake Simtustus were far less than the team observed in LBC, where cyanobacteria were dominant for much of the summer. Our hypothesis for the relatively low cyanobacteria densities in Lake Simtustus is that inflow from Willow Creek contains high concentrations of NO_3 (*median = 4.06 mg/L, n = 18*) (Table 4-5). which increase the competitive advantage of diatoms and green algae to the detriment of cyanobacteria. At the Mid-Lake site (RES25) in Lake Simtustus, cyanobacteria are more abundant than at Pelton forebay (RES04), because the Mid-Lake site likely receives less high-nitrate inflow from Willow Creek. The Coriolis effect would act to direct much of the inflow from Willow Creek towards Pelton forebay.

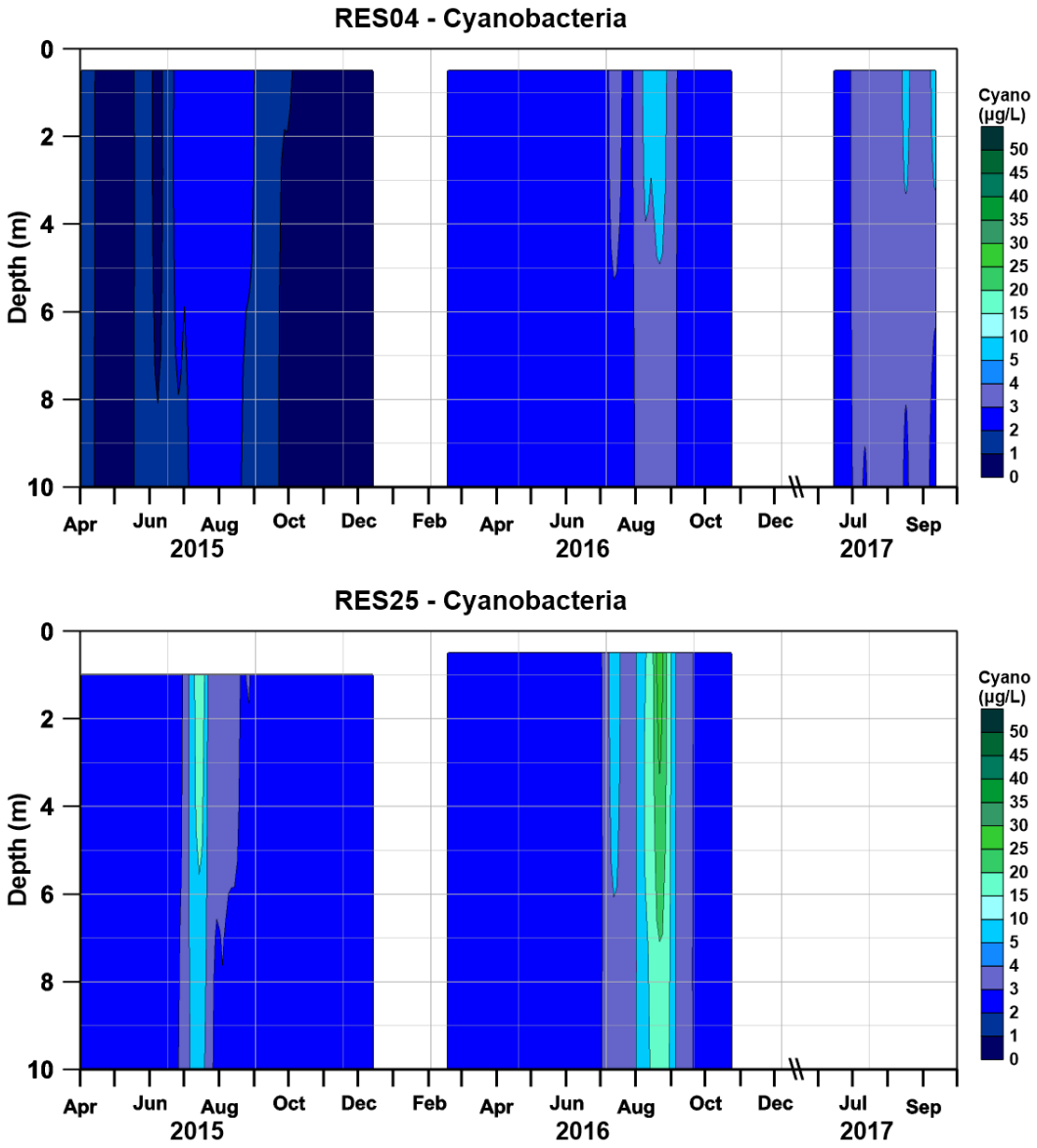

Figure 4-68. Cyanobacteria pigment levels (µg/L) at Pelton forebay (RES04) (*top*) and Mid-Lake site (RES25) (*bottom*).

4.2.2.17 Phytoplankton Community Composition

Total abundance of phytoplankton in Lake Simtustus generally increased from spring to fall (Figure 4-69). The results of dominant taxa from 2015 and 2016 showed the strong dominance of centric and pennate diatoms and a much-reduced role of cyanobacteria in the impoundment (Figure 4-70).

Another noteworthy feature in the dominant taxon for Lake Simtustus was the repeated dominance of the diatom *Fragilaria crotonensis*. This taxon is often associated with eutrophic conditions, particularly at these high levels of abundance. The associations of *S. niagarae*, *Dolichospermum*, and *F. crotonensis* along with other centric and pennate diatoms in Lake Simtustus appears repetitive (Figure 4-69). Those three taxa were dominant or subdominant phytoplankton in Lake Simtustus despite the wide range of hydrologic conditions in the 3 years of the study. See Appendix E for addition discussion on the phytoplankton community composition in Lake Simtustus.

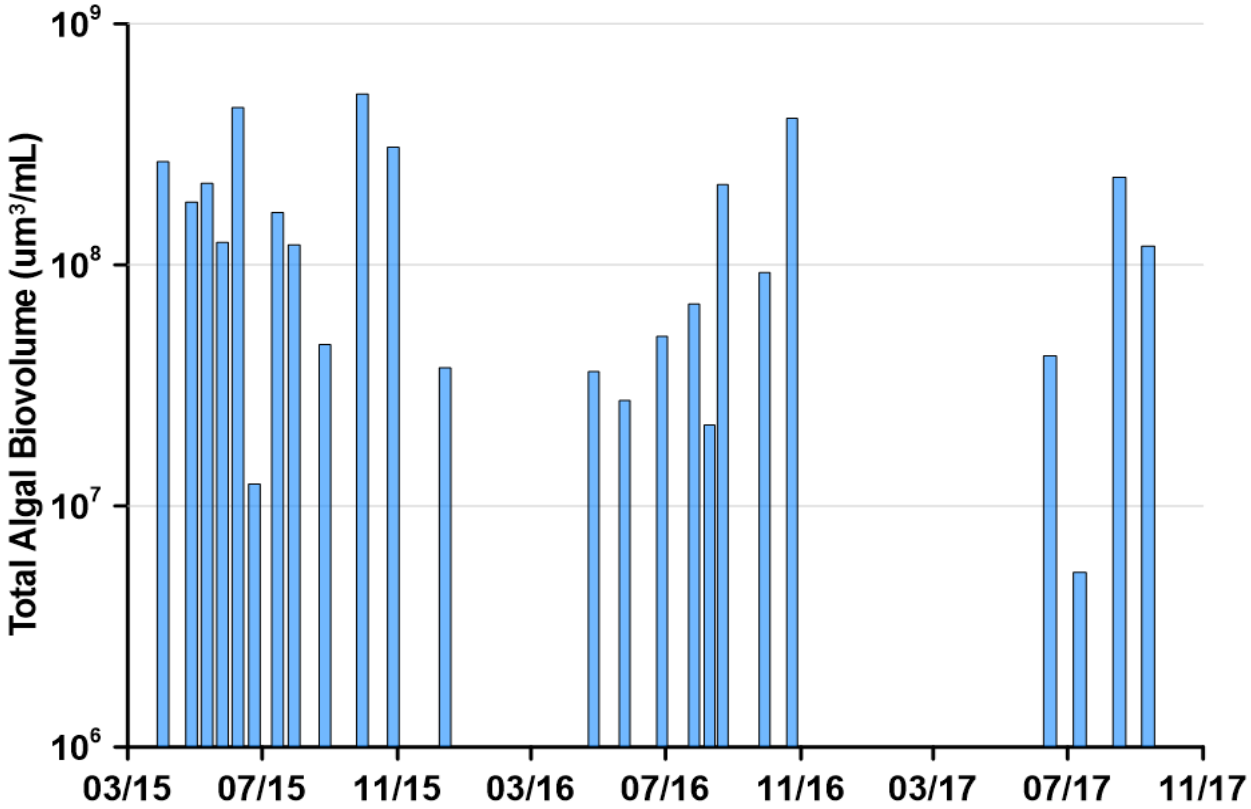

Figure 4-69. Total algal biovolume at Pelton forebay (RES04) at 1 m.

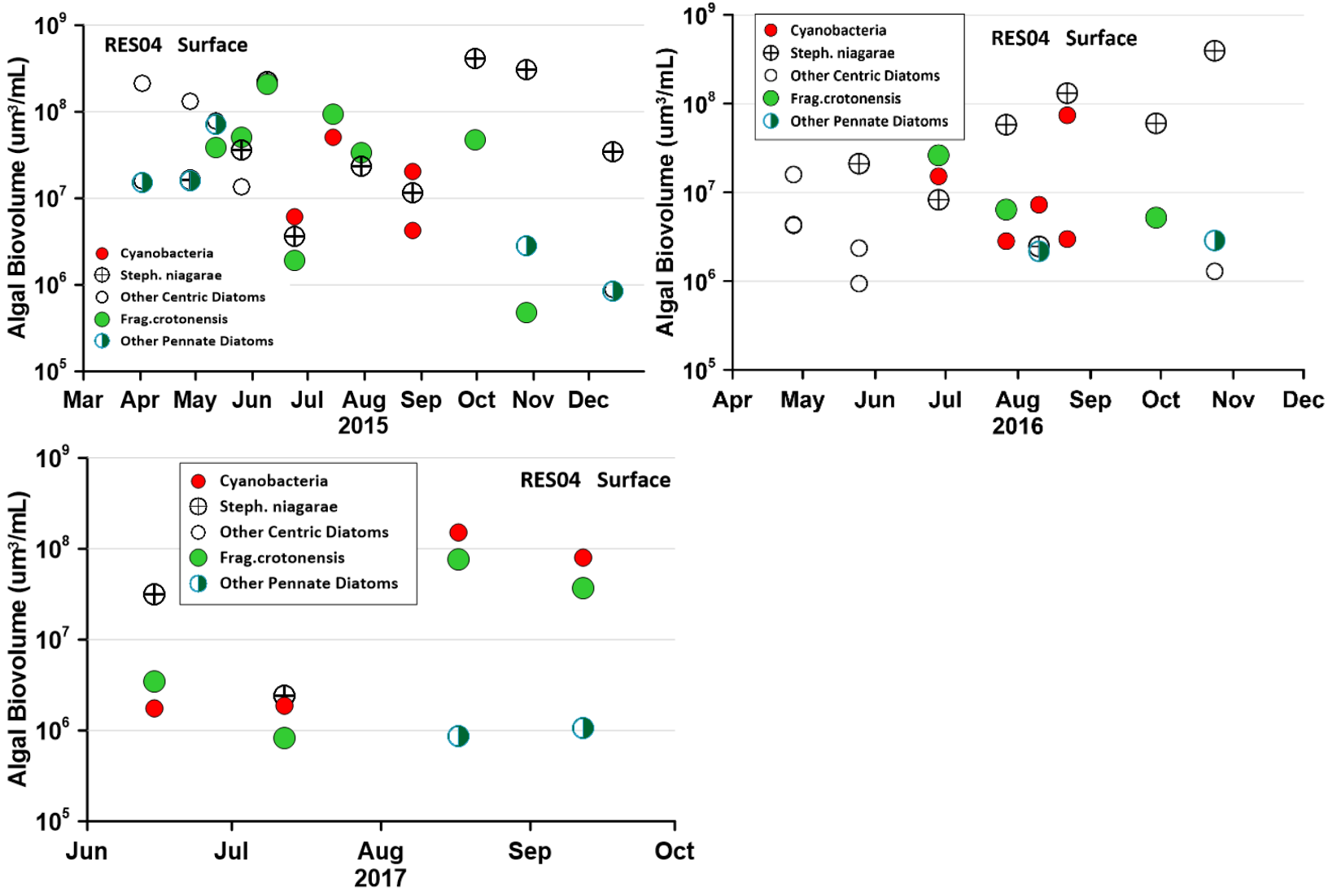

Figure 4-70. The three dominant algal taxa groups at Pelton forebay (RES04) at 1 m 2015–2017.

As noted previously, only two sites in Lake Simtustus were sampled for phytoplankton community composition: the Pelton forebay (RES04) and Mid-Lake site (RES25). In contrast to the high degree of similarity in phytoplankton results between the two sites in LBC, the two sites in Lake Simtustus showed more substantial differences (Figure 4-71). Only one sample from the Pelton forebay (RES04) was dominated by cyanobacteria as compared to three successive samples at the Mid-Lake site (RES25). Both sites showed dominant *F. crotonensis* at the end of May and both sites were dominated by *S. niagarae* in the spring and fall. In addition, the abundance of the dominant phytoplankton gradually increased in biovolume at the forebay, peaking in October, whereas the Mid-Lake site (RES25) showed a bimodal abundance with peaks in spring and late summer. The prevalence of non-cyanobacteria taxa in at the Mid-Lake site in Lake Simtustus is likely associated with the influx of NO_3 entering from Willow Creek. Willow Creek enters Lake Simtustus between the two sampling sites; the closer proximity of the Pelton forebay (RES04) to Willow Creek and suppression of N-fixing cyanobacteria by the available nitrate could explain the higher proportion of cyanobacteria at Mid-Lake site (RES25).

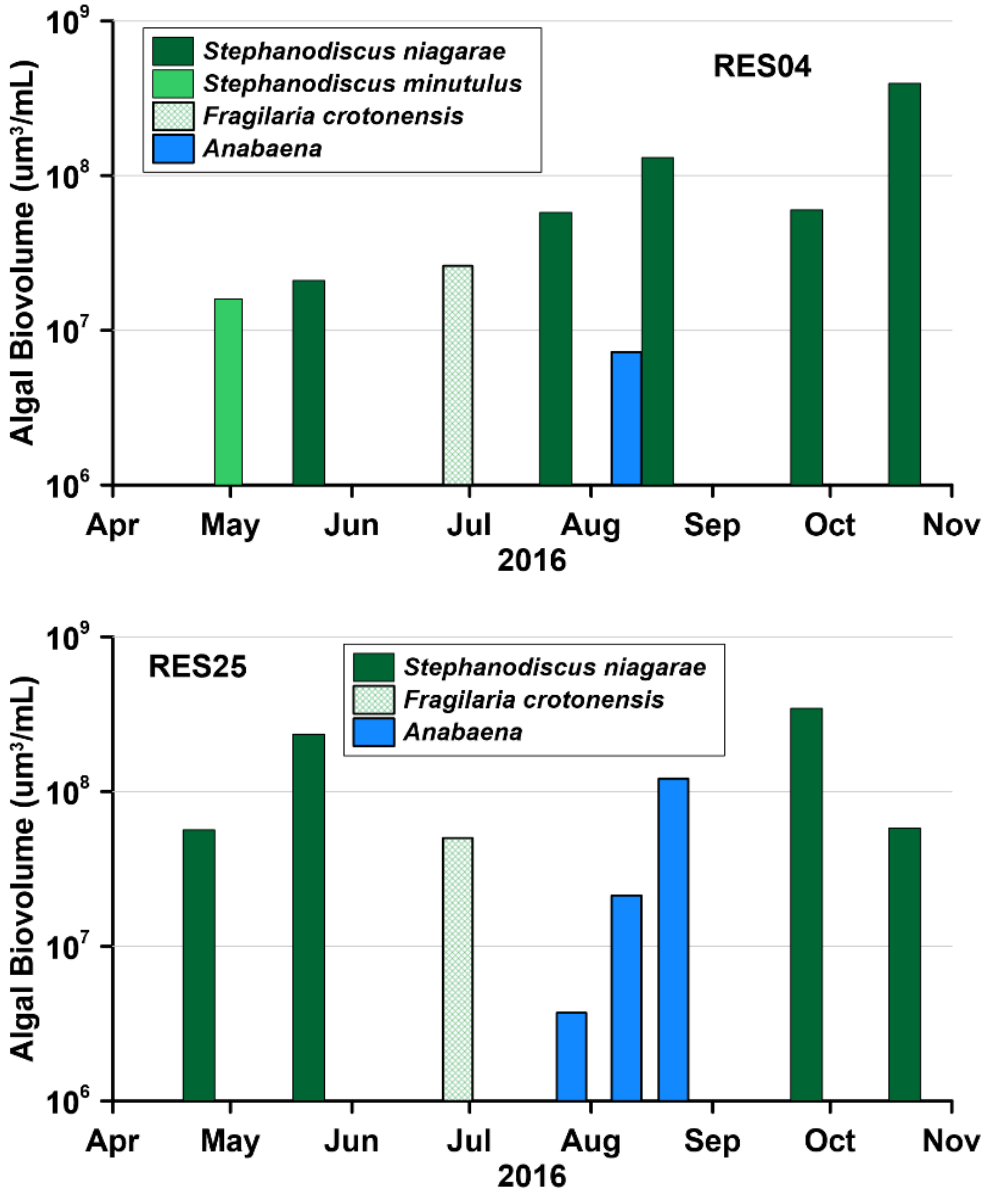

Figure 4-71. Comparison of dominant phytoplankton taxa at Pelton forebay (RES04) and Mid-Lake site (RES25) for 2016.

4.2.2.18 Zooplankton

Like LBC, the zooplankton community composition in Lake Simtustus was dominated by rotifers and secondarily by cyclopoid copepods (Figure 4-72). Densities of the cladocerans were modest, possibly reflecting considerable predation pressure from fish. Among the cladocerans, *Daphnia* species were dominated by *D. mendotae* with low densities of *D. pulicaria* and *D. rosea*, two of the larger taxa (Figure 4-73). *D. rosea* was present only in the cooler months, whereas the other two species were present throughout the sampling period.

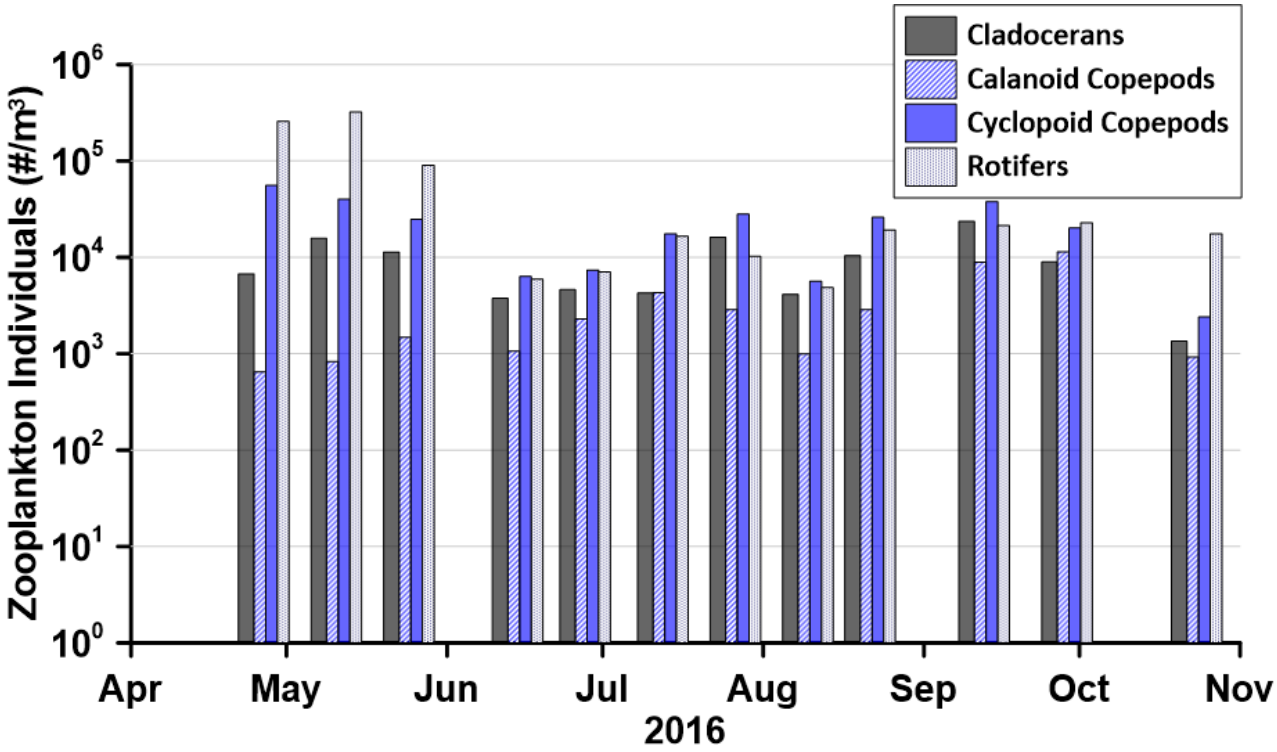

Figure 4-72. Density of zooplankton groups at Pelton forebay (RES04) (10 m tow) in 2016.

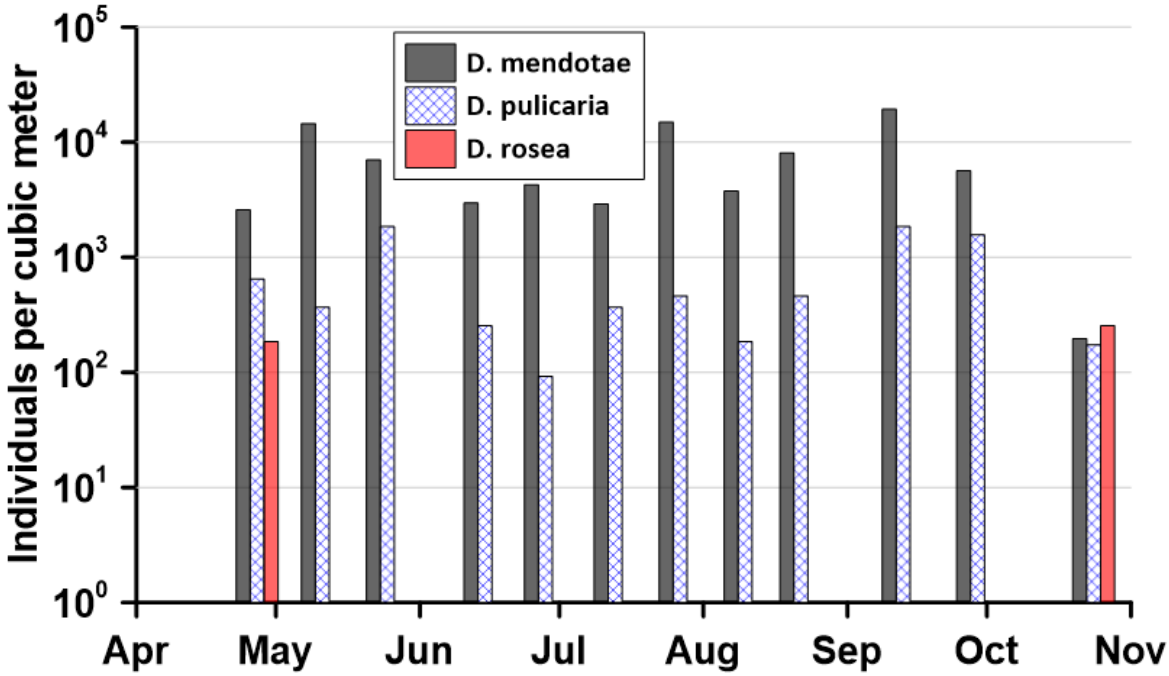

Figure 4-73. Density of *Daphnia* species at Pelton forebay (RES04) (10 m tow) in 2016.

4.2.3 Transitions and Transformations between Impoundments

Data were collected at the three tailraces from June 2015 through October 2016 and analyzed for nutrient chemistry. Nutrient concentrations at the three sites track reasonably closely through the reservoirs (Figure 4-74) and generally peaked in winter and again in fall. Only TN exhibited significant differences among sites, which likely reflects variation in incorporation of organic particulate matter, phytoplankton cells, in the sample (Table 4-6).

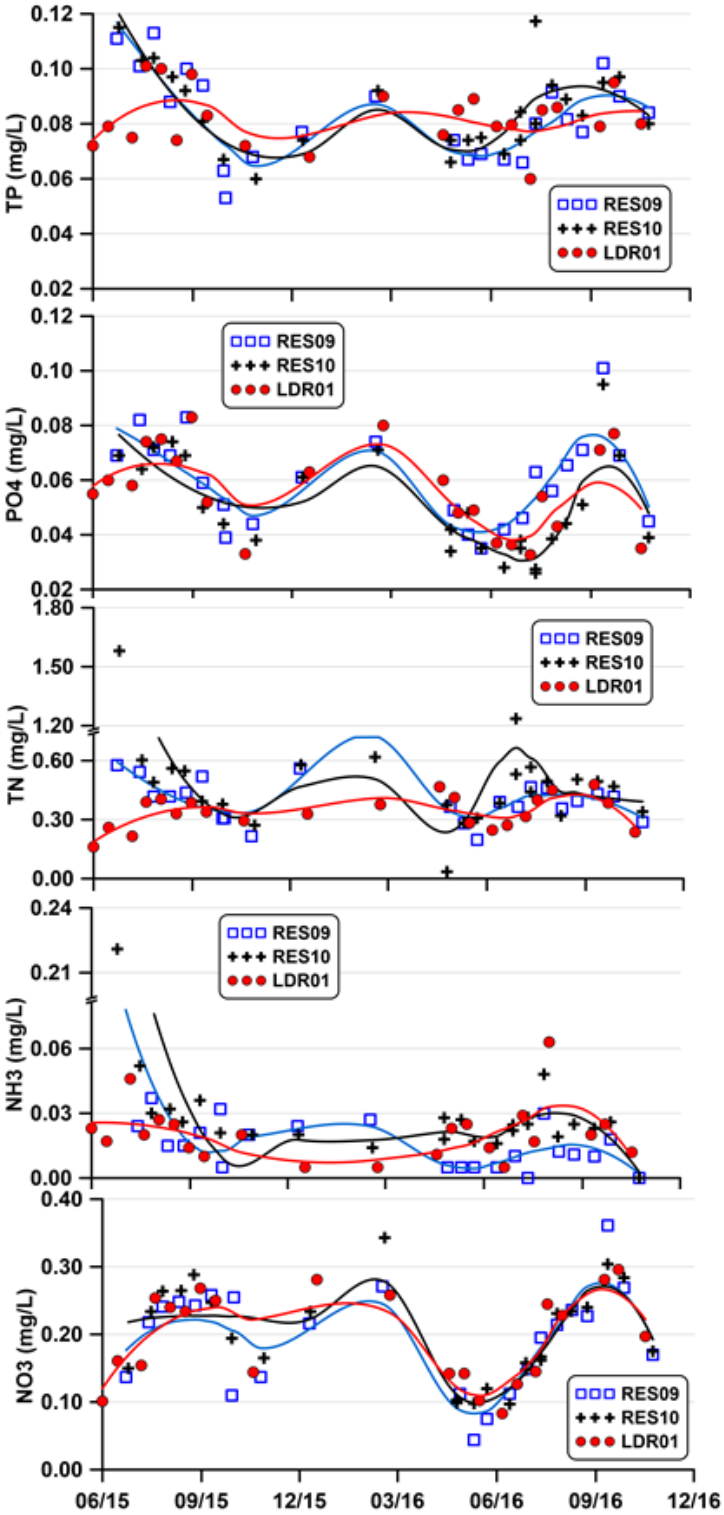

Figure 4-74. Nutrient chemistry measured at Round Butte tailrace (RES09), Pelton tailrace (RES10), and ReReg site (LDR01) in 2015–2016. LDR01 is immediately downstream of Reregulating Dam.

Table 4-6. Summary statistics for concentrations of nutrients from the three tailraces for 2015–2016.

Nutrient	Statistic	Round Butte (RES09)	Pelton (RES10)	ReReg (LDR01)
TP	mean	0.083	0.085	0.079
	sd[a]	0.016	0.015	0.014
PO_4	mean	0.060	0.050	0.055
	sd	0.017	0.018	0.017
TN[b]	mean	0.413**	0.512**	0.320**
	sd	0.131	0.304	0.095
NO_3	mean	0.196	0.200	0.183
	sd	0.076	0.071	0.083
NH_3	mean	0.020	0.033	0.018
	sd	0.026	0.040	0.013

Notes:

[a] standard deviation

[b] All sites are significantly different from one another

** where p is < 0.01

One of the significant issues related to the tailrace chemistry is the relationship between dissolved inorganic nitrogen (NO_3 + NH_3) and export of DIN from the Project to the LDR. DIN represents forms of nitrogen that are highly available to algae. Nitrogen that is in particulate form, some of which is measured as TN, requires further decomposition to become available and is relatively unavailable to support algae growth, at least on a short-term basis. DIN is important to algae growth in the LDR; therefore, knowledge of DIN export from the Project is critical if DIN concentrations are to be reduced in an effort to limit algae growth. There is reasonable concordance in DIN concentrations among the three tailraces (Figure 4-75). Similarly, concentrations of DIN are similar at the surface of LBC forebay and the ReReg tailrace from fall 2015 to February 2016. However, that agreement is poor in April and May 2016 despite continuation of 100% surface withdrawal. During April and May, despite LBC forebay concentrations of DIN near detection limits, the export of DIN to the LDR increased substantially. By mid-June, the proportion of SWW surface releases began to decline and the DIN present at the lower depths is reflected in increases in DIN downstream. The increases in

DIN observed in April and May likely reflect mixing dynamics in Lake Simtustus and greater availability of DIN for export in the spring.

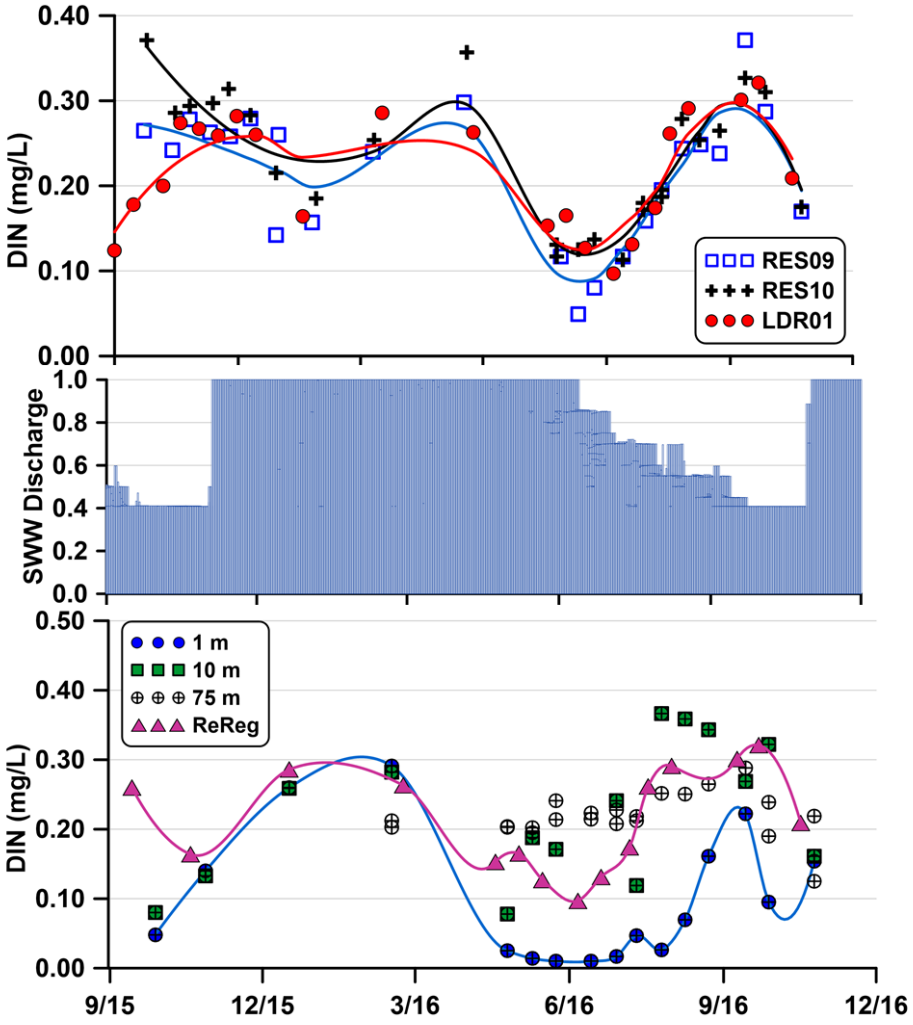

Figure 4-75. Concentrations of dissolved inorganic nitrogen (DIN) at Round Butte tailrace (RES09), Pelton tailrace (RES10), and ReReg site (LDR01) *(top)* compared with DIN at several depths at Round Butte forebay (RES07). The proportion of surface water released from the SWW is shown in the middle.

Conductivity, a largely conservative parameter, was measured at the three tailraces in 2016 (Figure 4-76). The results show minimal change in conductivity as water passes through the impoundments. Conductivity values are higher in winter and early spring when 100% of the

SWW withdrawal is derived from the surface. As bottom water withdrawals increase through the summer, conductivity values leaving the Project decrease, indicating a greater proportion of water from sources other than the Crooked River.

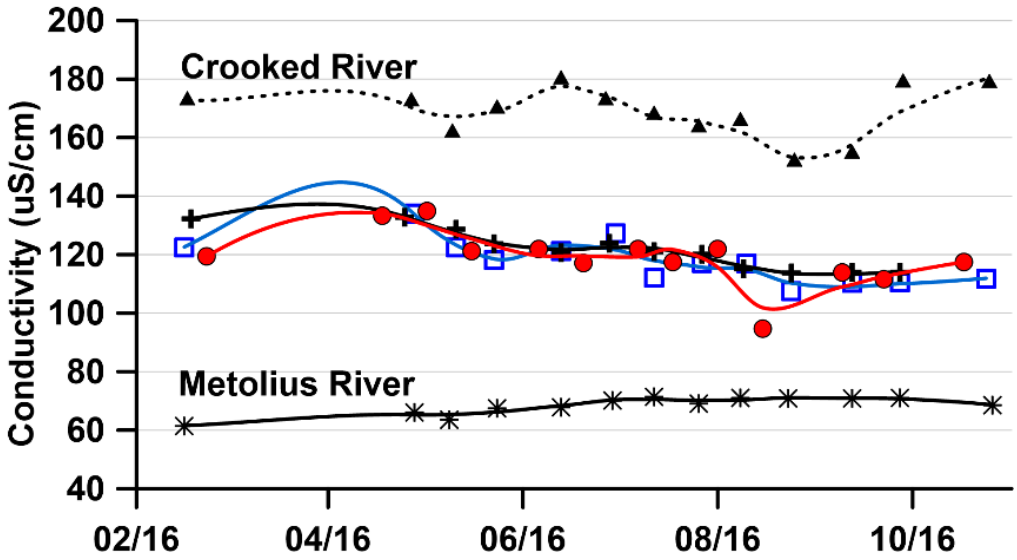

Figure 4-76. Conductivity measured in 2016 at the Crooked River and Metolius River sample sites and measurements at the three tailraces shown in the middle. Conductivity values in the Middle Deschutes River inflow were intermediate between those of the other two tributary sample sites.

Seston, the algae suspended in the river, are comprised of benthic algae dislodged from the substrate and planktonic taxa from upstream reservoirs. Because there are three reservoirs upstream of the LDR, it is reasonable to expect that there would be considerable planktonic seston present in the tailraces. This is especially the case following the installation of the SWW, which captures at least some surface flow (40–100%) from LBC throughout the year.

The phytoplankton results show considerable differences in the amount of phytoplankton present in each tailrace (Figure 4-77). Although the amounts of chlorophytes and chrysophytes passing through the Project are similar, other phyla exhibit moderate to large differences from one tailrace to another. The cyanophytes appear to decline between Round Butte tailrace and Pelton tailrace, but then rebound below the ReReg Dam. The diatoms show a slight decline from

upstream to downstream, as might be expected for any given group. The Pyrrophyta show the least abundance exiting LBC, exhibit an apparent increase of two orders of magnitude downstream of Pelton Dam and then diminish at the ReReg Dam. The increase of Pyrrophyta downstream of Lake Simtustus is somewhat understandable because this phylum was moderately abundant in Lake Simtustus. However, it is not clear why Pyrrophyta decreased so abruptly in the ReReg Pool.

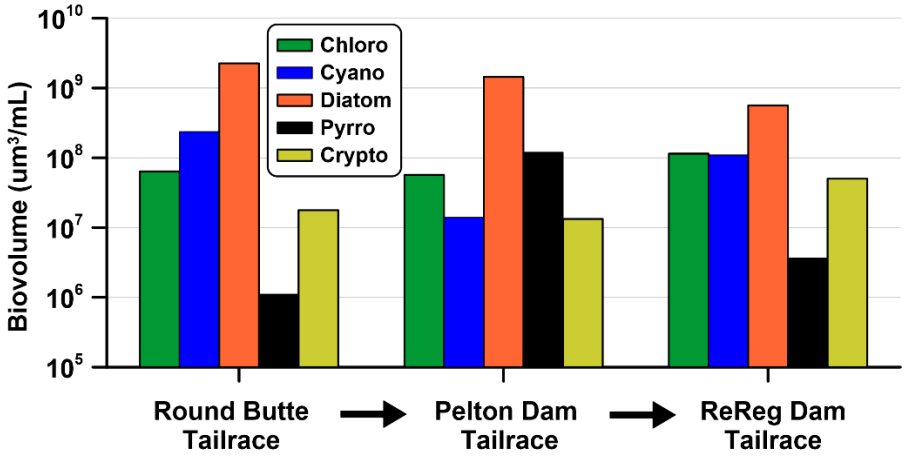

Figure 4-77. Average biovolume of the major phyla in the three tailraces of the Project from 2015–2016.

Phytoplankton biovolume and composition leaving the Project are highly variable and are extremely difficult to characterize with low-frequency sampling. The lack of correspondence between phytoplankton abundance at the three sites is not easily explained by changes over time. We would expect to observe equal or lower biovolume of phytoplankton as it passes downstream through the project (i.e., lower biovolume at the ReReg tailrace compared to LBC). However, the results do not reflect this (Figure 4-78). There are two factors likely contributing to the variability: 1) sampling dates for the sties and 2) turbine flow at the time of sampling.

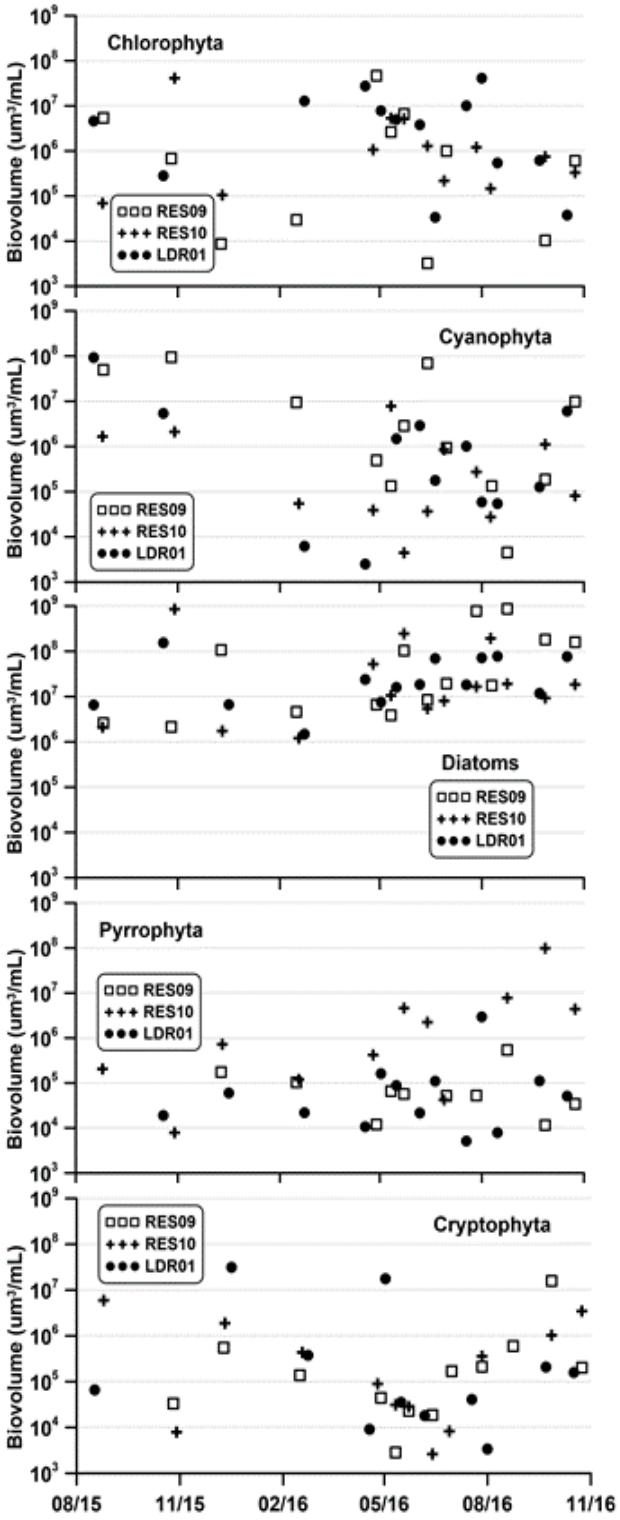

Figure 4-78. Phytoplankton biovolume by phyla for Round Butte tailrace (RES09, upstream), Pelton tailrace (RES10), and ReReg site (LDR01, downstream) from 2015–2016.

4.3 Comparison with Other Impoundments

The water quality status of lakes throughout the region are poorly characterized. Unlike the streams in Oregon, which ODEQ monitors through the AWQMP, no comparable efforts exist to systematically monitor lakes and reservoirs in the state. Most of the large reservoirs were built and are operated by the US Army Corps of Engineers and the USBR. Federal agencies have no requirement to monitor their reservoirs for water quality and are not subject to relicensing requirements imposed on private entities. A modest number of samples are available for reservoirs operated by the USBR in eastern Oregon that provide a limited basis for comparison with LBC and Lake Simtustus. Concentrations of TP are generally similar and high for the sample set (Figure 4-79). Ochoco Reservoir has a particularly high TP concentration, probably because of a relatively high influx of suspended material into the reservoir. No results for PO_4 are available for these impoundments, which might reveal a different pattern. LBC had the highest concentrations of chlorophyll among the lakes shown here. Crane Prairie Reservoir had some high concentrations of chlorophyll, but all other comparative results were less than 20 µg/L. Median values of transparency were low for Crane Prairie, Ochoco, and Phillips reservoirs and values for LBC and Lake Simtustus were midway for the sample set.

It is difficult to assess the similarity of water quality in the Project impoundments against the water quality in other lakes in central and eastern Oregon because of the paucity of data. For example, most of the lakes in the state have no reported concentrations of PO_4 or inorganic nitrogen. Any available nitrogen measures are for total Kjeldahl nitrogen (TKN), a measure of all reduced forms of nitrogen, which is not accurate at the concentrations typically encountered in these systems. When data were collected, sample sizes were small and much of the data are relatively old. Additionally, USBR does not input biological data on the Water Portal (*https://www.waterqualitydata.us/*).

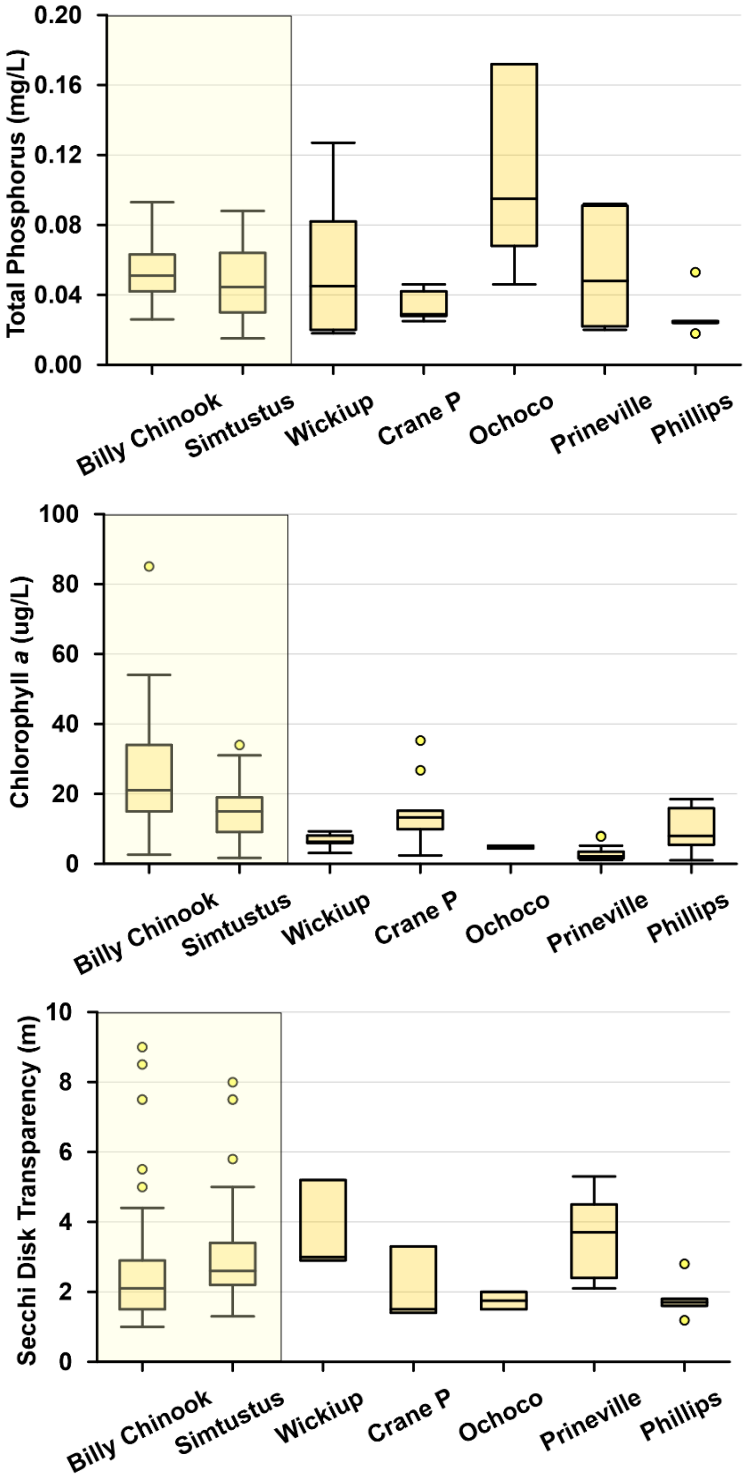

Figure 4-79. Boxplots of water quality results for surface water samples from the Project and other impoundments in central and eastern Oregon. Data for the non-Project lakes were obtained from the Water Portal (*https://www.waterqualitydata.us/*). The analytical methods for TP and chlorophyll are believed to be comparable to those from this study.

5 Water Quality Changes in the Reservoirs

A variety of changes in the Deschutes River basin, some of which have been associated with the Project itself, have occurred in the years between the Project relicensing and when this study was conducted. Water quality in the Project area is variable and subject to a variety of external factors, including land-use changes in the basin, climate modification, and reservoir operations. The changes associated with land use, including urban and agricultural development, occur in small increments that can take years to be reflected in the Project impoundments. Some of those changes increase export of nutrients and decrease flows to the impoundments; other changes, primarily those associated with conservation practices, decrease export of nutrients and increase flow downstream. Thus, we cannot assume that increased development in the basin has resulted in a unidirectional increase in nutrient export. The effects of climate change are not detectable on a yearly basis and will be measurable only on decadal scales. Some changes in reservoir management are abrupt such as those associated with the installation and operation of the SWW structure. Other operational conditions have been modified over the years, gradually altering the hydropower generation schedule. For example, the initial use of hydropower generation at the Project was for peaking power. With the introduction of wind turbines, power generation now also serves to helps stabilize grid performance.

Furthermore, studies conducted prior to construction of the SWW and this study all were of comparatively short duration. A more ideal comparison would have been possible if any of these studies had involved continuous monitoring of water quality before, during, and after the period of interest.

Most of the relevant water quality data were collected in studies in 1994–1996, 1997, 2006, and 2015–2017. The studies included a prelicensing study of impoundments (Raymond et al. 1997), a prelicensing survey of water quality in the LDR (Raymond et al. 1998), ODEQ's 2006 study of the impoundments done in anticipation of a total maximum daily load for the Deschutes River basin (which has not been completed to date), and this monitoring and modeling water quality study of the impoundments and the LDR.

Most of the comparisons presented in this report for LBC and Lake Simtustus are based on data from 2016 because it was the most complete year of sampling with data collected from February through November. Similarly, the 1994–96 study by Raymond et al. encompassed parts of 1994 and 1996, but only 1995 involved sampling throughout the year.

5.1 Lake Billy Chinook

5.1.1 Temperature Regime

Both an apparent long-term increase in air temperature (Dalton et al. 2013) and a possible relationship between the water temperature in the three main tributaries appear to have interacted to change the temperature dynamics in LBC. Water temperatures have increased in all three tributaries since 2007, with the largest increase in the Deschutes River and the smallest increase in the Crooked River (Figure 5-1). Continuous river temperatures are available starting in 2005 and are shown for complete water years. Although the increases in temperature for the Metolius and Crooked rivers over this period were minor, the Deschutes River inflow increased substantially. The more muted response observed for the Metolius and Crooked rivers is consistent with the primary source water for these rivers, which consists of groundwater and a comparatively short path from source to the inlet. In contrast, the upper and middle portions of the Deschutes River have been subject to considerable atmospheric influence from the sources of the river's inflow to its confluence with LBC. Both the Crooked and Upper Deschutes rivers have multiple reservoirs upstream of LBC. Those upstream impoundments likely experience a net heat gain independent of long-term climate trends. In addition, the available water temperature data for the three major inlets to LBC represent a relatively short time frame (11 years) and the apparent temperature increase could be related to factors other than increased air temperature. A much longer time frame of water temperature data will be required to establish a definitive relationship between the observed changes in the three tributaries and climate change.

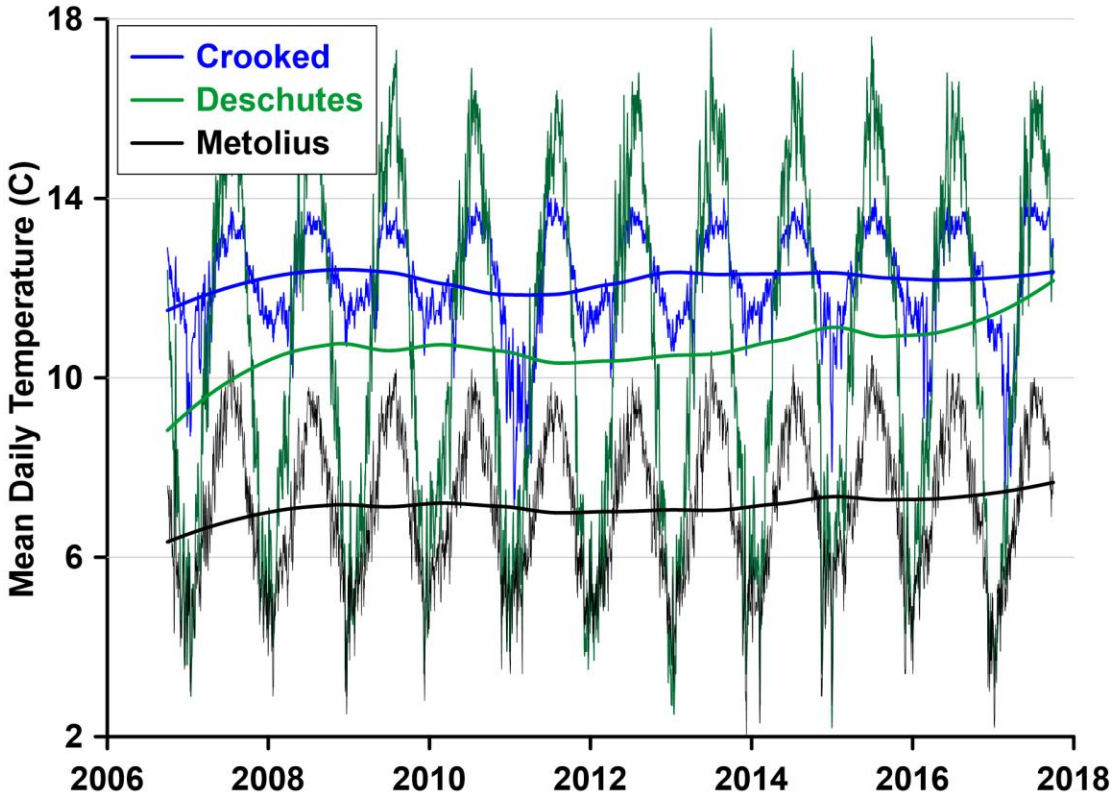

Figure 5-1. Mean daily temperature in the three tributaries to LBC. The lines represent LOESS fits of the observed data. (*Source*: USGS).

Two important factors demonstrating the response of LBC to additional warming are expressed in two significant outcomes. The first, the additional warming of the epilimnion, would likely contribute to increased rates of primary production and create a more favorable habitat for cyanobacteria (Paerl and Huisman 2008; Paerl and Paul 2012). The second, the overall warming of LBC, would decrease the pool of cold hypolimnetic water available for discharge to the LDR.

The installation and operation of the SWW has also affected the temperature regime in the impoundments. The SWW draws between 40% and 100% of the discharge from the top 40 ft of LBC, depending on operating directives. Thus, the SWW is always drawing water from the surface; only the percentage of flow from the top and bottom gates varies. Full flow through the surface entrance occurs from approximately November 1 to when the without-Project temperature reaches 13˚C at the ReReg Dam, typically in May. Reduced surface flow to the SWW (as low as 40% of total flow) is more typical during the summer and fall. Nevertheless,

some surface flow from LBC is always occurring. CWA Section 401 certification conditions from both ODEQ and the CTWS Water Control Board require increased release of water from the bottom gates to reduce Project warming of the LDR when temperatures at the ReReg Dam approach 13°C.

The patterns in the temperature of the release water from Round Butte Dam varied considerably between 2015 and 2016/17 (Figure 5-2). In 2015, the temperatures reflected a narrower range within any given period, whereas in 2016 and 2017 there were much wider ranges in the temperature of water released daily (Figure 5-3). This increase in the daily temperature range during 2016 and 2017 was particularly significant between May and August. During 2015, the average temperature of the release water was warmer from May through July compared to the releases during the same time period in 2016 and 2017. The temperature of the release water has direct influence on the temperature of the LDR, but it also impacts the thermal properties in LBC. Release of water with a steady temperature will result in water temperatures in LDR with small daily variations at a given location. The SWW draws water from the upper 40 ft (12.2 m), which corresponds to the entire epilimnion and a portion of the upper metalimnion. As the proportion of water drawn from the epilimnion changes, it alters the rate of replacement flow to the forebay, which in turn changes the rate that additional nutrients are supplied to this portion of the reservoir.

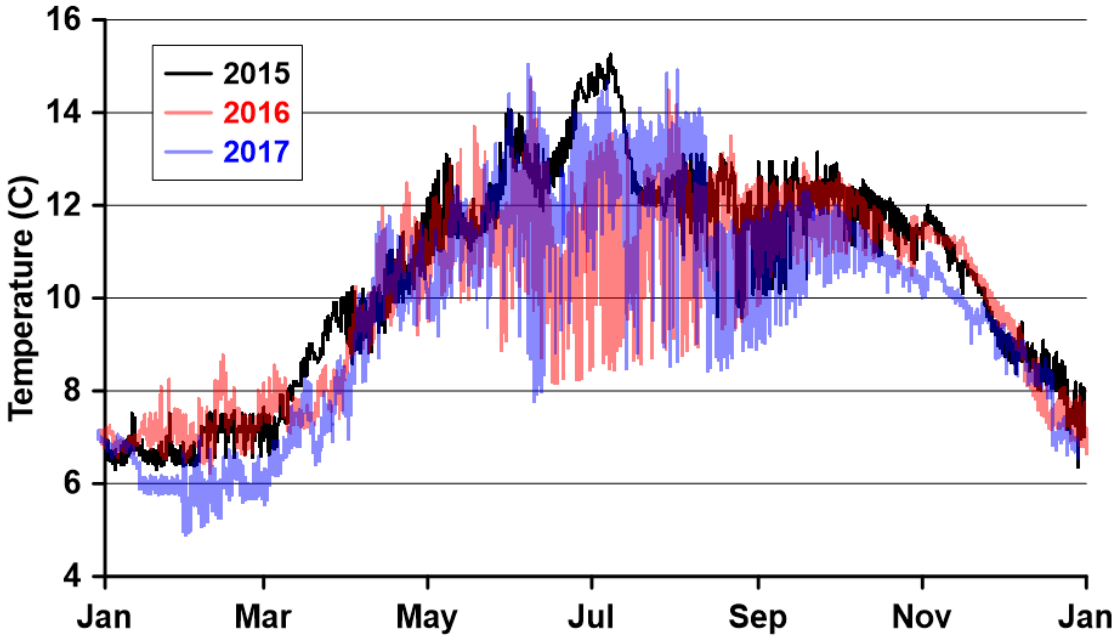

Figure 5-2. Temperature of tailrace water from Round Butte Dam for 2015–2017.

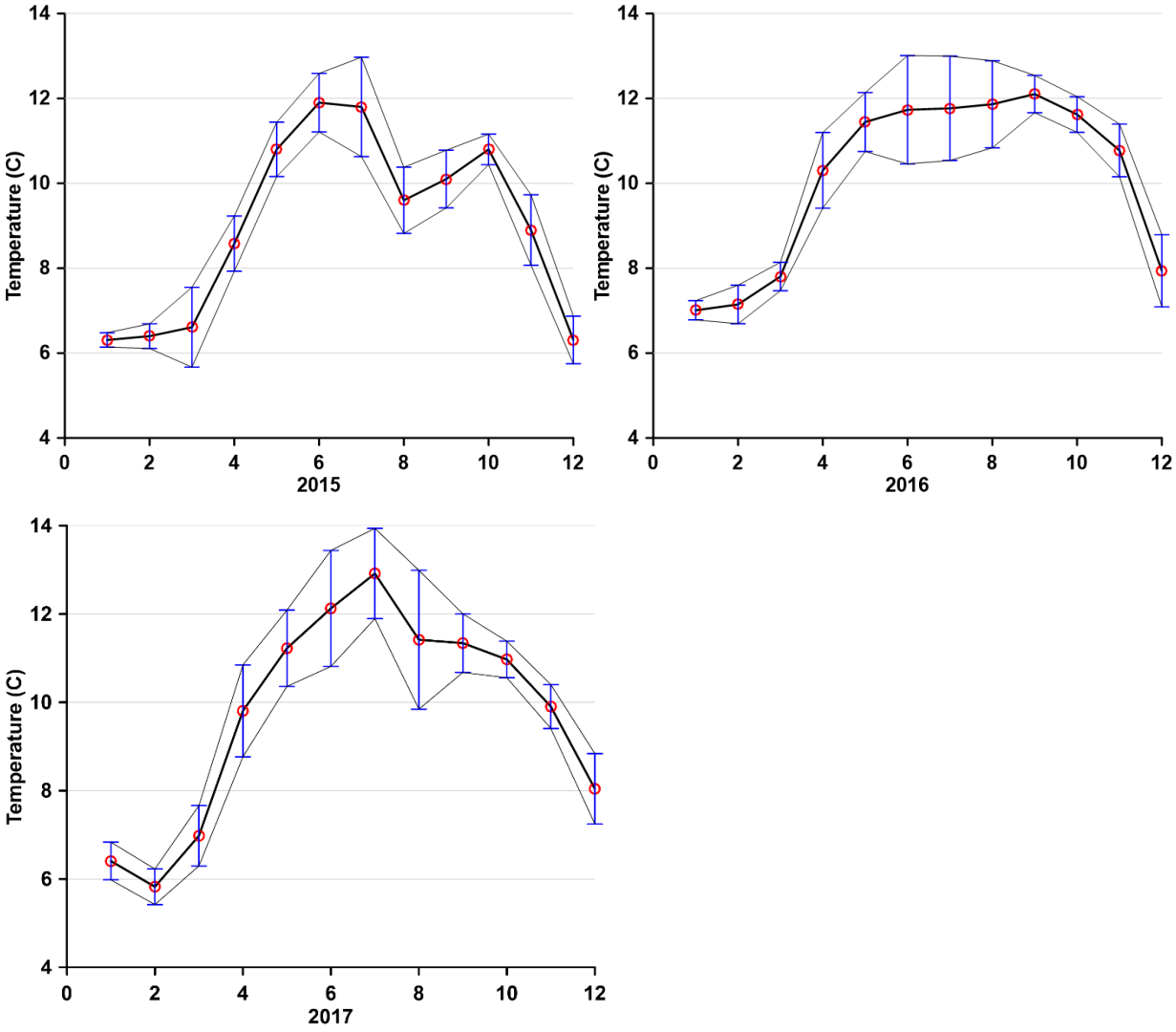

Figure 5-3. Mean monthly temperature of tailrace water from Round Butte Dam for 2015–2017. The vertical bars represent the standard deviation.

Examination of the temperature profiles in LBC from the 1990s (Raymond et al. 1997) found that the epilimnion was slightly more distinct and bounded by a relatively distinct metalimnion, whereas, during the current study, the epilimnion and metalimnion were poorly defined and the water temperatures declined gradually with depth (Figure 5-4 and Figure 5-5). Using 16˚C as a point of comparison, the warmer waters extended to a depth of more than 20 m in 1995 and to less than 10 m in 2016. By the end of summer 1995, the hypolimnetic waters did not drop below 11˚C, whereas, in 2016, hypolimnetic waters were considerably cooler (8.4˚C at 100 m on July

26, 2016). In 2016 the water from the Metolius River remained in the lake longer, some at a relatively shallow depth, whereas, in 1996, much of the cold water that remained in the impoundment was below 75 m (246 ft), the depth of the hypolimnetic intake. The hypolimnetic intake remained unchanged pre- and post-SWW. Based on the reported maximum depth of 126.5 m (415 ft) (Johnson et al. 1985), the "deadpool" of water below the hypolimnetic intake represented 51.5 m (169 ft) of the water column that is inaccessible through the bottom intake.

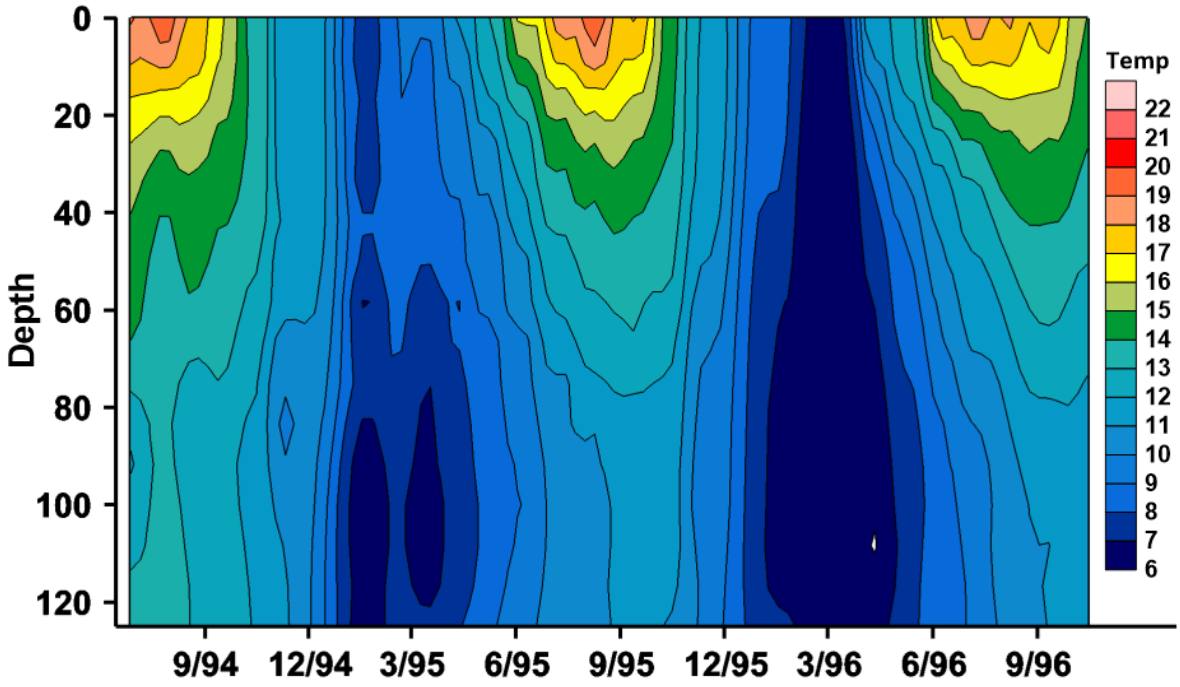

Figure 5-4. Temperature contours for Round Butte forebay (RES07) from 1994–1996 (Raymond et al. 1997). Depth is in meters; temperature is in ˚C.

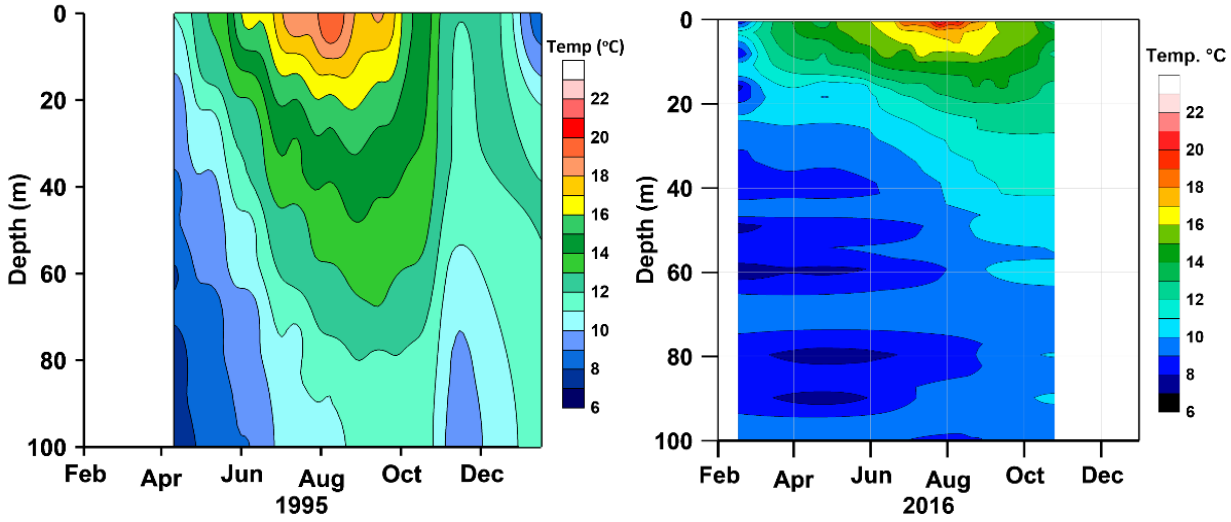

Figure 5-5. Temperature patterns in Round Butte forebay (RES07) for 1995 (*left*) and 2016 (*right*).

The consequences of a change of this magnitude in thermal regime include the likelihood of greater mixing under the current regime and decreased residence time in the surface waters in LBC. Greater mixing of LBC can lead to increased primary production, although if the epilimnetic waters are exported at a rate greater than the phytoplankton reproduce, then total primary production could likely decrease. However, the age of water at the surface of Round Butte forebay (RES07) is almost always more than 20–30 days, allowing ample time for phytoplankton to reproduce as it moves into the forebay (see sections 9.6 and 10.7).

The most comprehensive temperature data for LBC were collected by field staff deploying thermistors at up to 12 depths from 2005 to 2017. Those data documented the change in the thermal structure of Round Butte forebay (RES07) that occurred with the installation of the SWW. The results illustrate the cooling of LBC, particularly from May through October (Figure 5-6). The cooling of the surface waters post-SWW reflects the export of warm waters from the epilimnion (Figure 5-7). The cooling of the deeper waters reflects a greater retention of water from the Metolius River (Figure 5-8), which was one of the intended outcomes of the SWW.

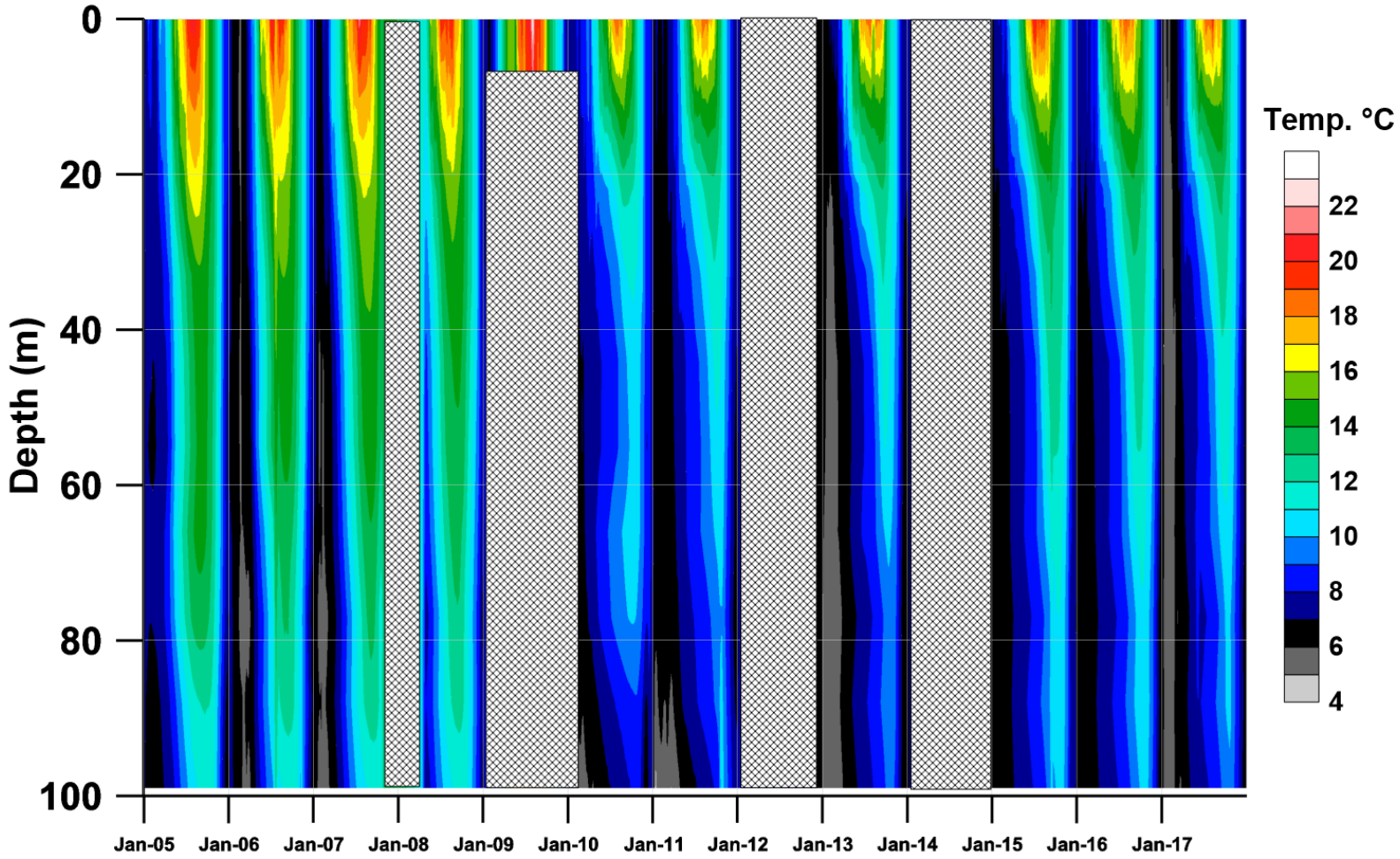

Figure 5-6. Water temperature at Round Butte forebay (RES07) collected by PGE from January 2005 through 2017. Gaps in 2007, 2008, 2009 (at depth), 2012 and 2014 represent periods when data were not collected.

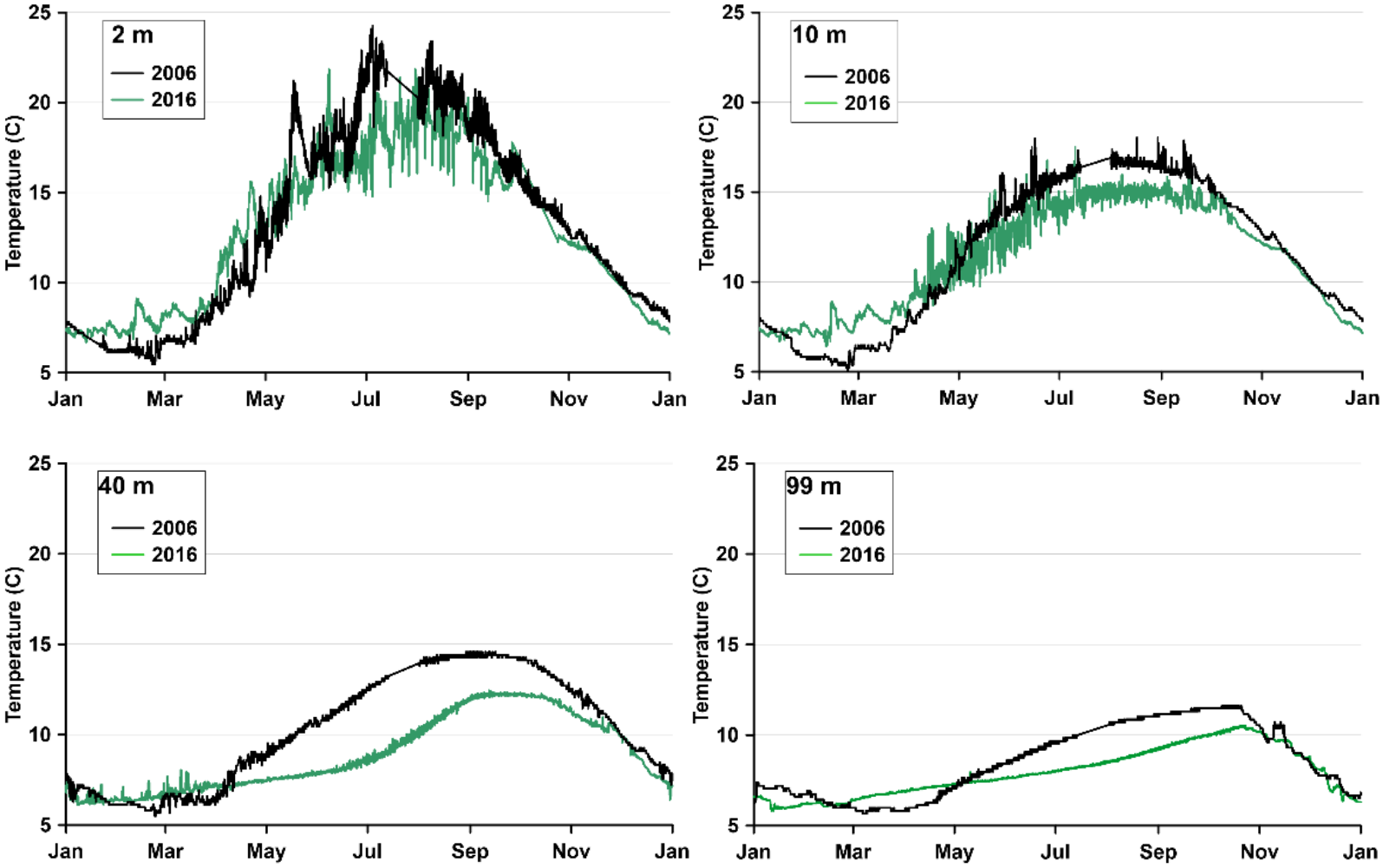

Figure 5-7. Temperature at Round Butte forebay (RES07) in 2006 and 2016 at selected depths.

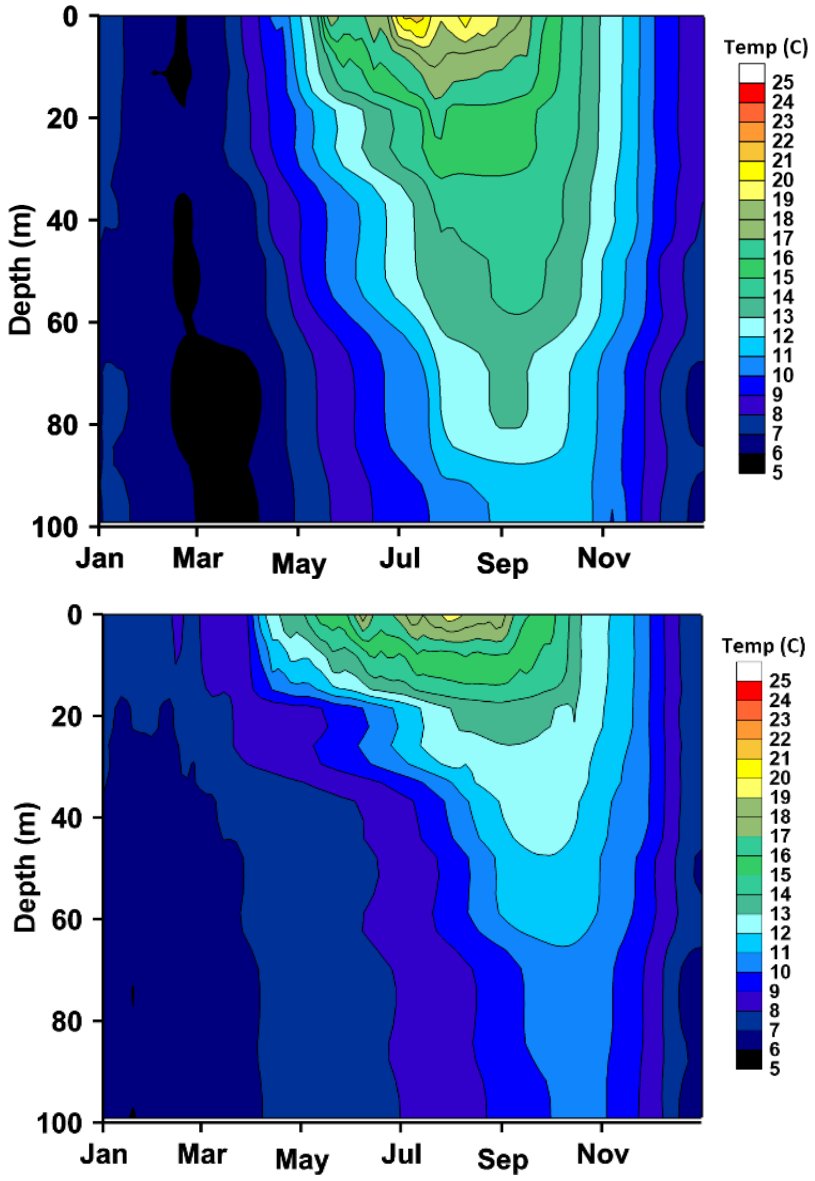

Figure 5-8. Temperature patterns at Round Butte forebay (RES07) measured in 2006 (*top*) and 2016 (*bottom*).

Although much of the attention to lake temperature in LBC is rightly devoted to temperatures of tributary inputs and changes in discharge from the impoundment associated with the SWW, other temperature/circulation issues also warrant consideration. The distribution of waters from the tributaries prior to SWW installation showed that, during the warmer months, water from the Crooked River flowed to the forebay and continued moving over the surface up the Metolius River arm (Raymond et al. 1997). Crooked River water essentially comprised much of the

epilimnetic water and the extent of that water could be traced to the distal end of the Metolius arm where a null point was formed. This represented a line across the Metolius arm where cold Metolius waters plunged under the warmer epilimnetic waters derived largely from the Crooked River. The cold Metolius waters moved towards the forebay, always remaining deep and staying cold. The epilimnetic waters formed an insulating barrier and absorbed the solar heating. That pattern continued until the fall, when surface waters cooled and all water mixed throughout.

Since installation of the SWW, waters from the Crooked River move toward the forebay, as before, but instead of moving up the Metolius arm unimpeded, much of the Crooked River water is now "captured" by the surface intake of the SWW and discharged downstream. That means there is relatively little Crooked River water available to move up the Metolius arm. A brief field investigation of conductivity and temperature profiles conducted in July 2018 documented the presence of high conductivity water from the Crooked River only part way up the Metolius arm instead of occupying the entire Metolius arm as it had done before the SWW (Figure 5-9). This means that there is a substantial reduction in the former insulation barrier for the Metolius arm, thus exposing the Metolius arm to solar heating. Also note the movement of Metolius-derived water extending into a zone of a 20–30m depth at the forebay. The Crooked arm exhibits little change in conductivity from the inlet to the forebay which indicates little mixing of Crooked River water with the other two tributaries.

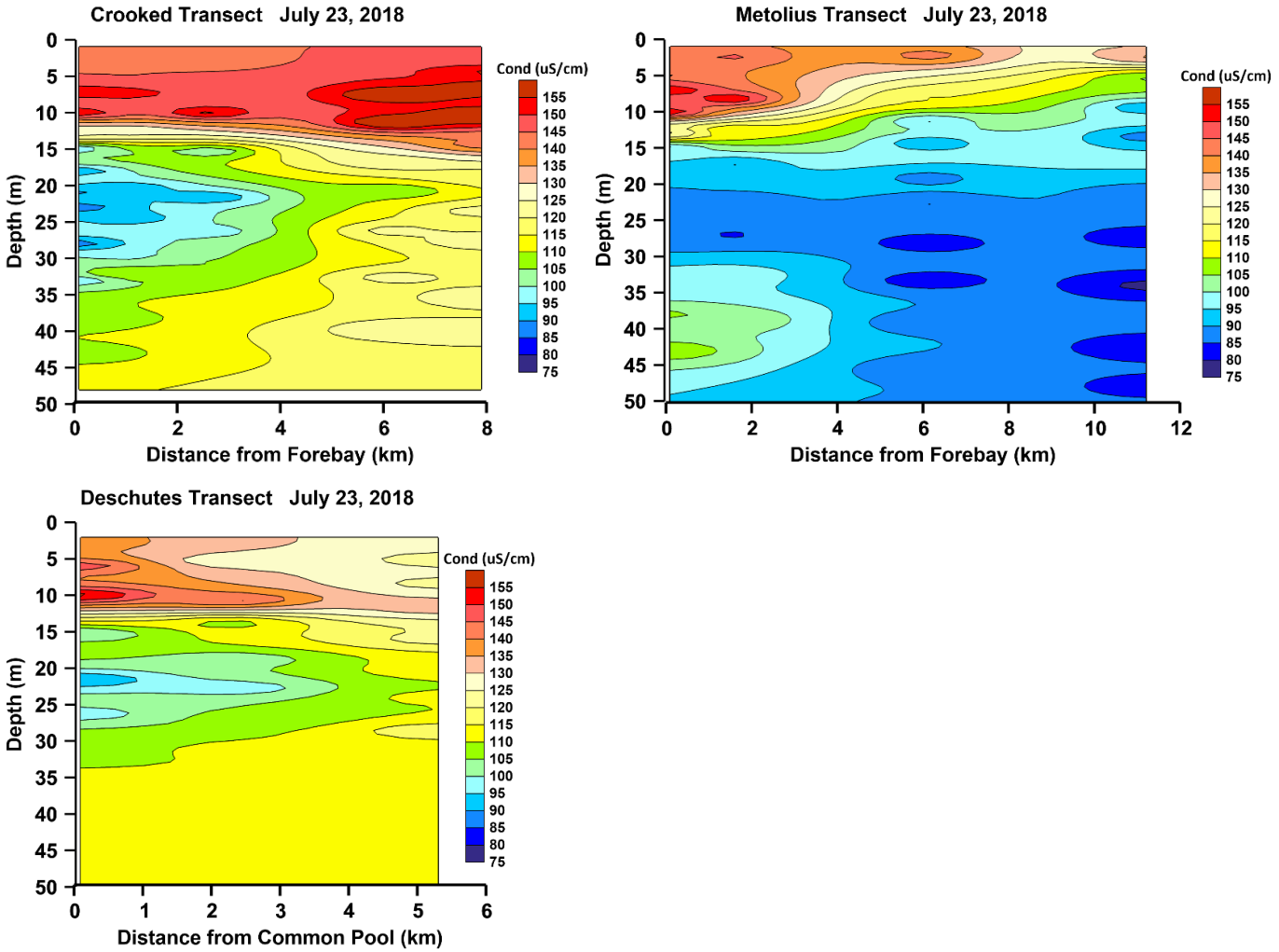

Figure 5-9. Cross sections of the three arms of LBC showing conductivity (µS/cm) contours on July 23, 2018. Red shading identifies waters derived from the Crooked River, blue shading identifies waters from the Metolius River, and yellow identifies water from Deschutes River or mixing of waters from the Crooked and Metolius rivers. The x axis represents the length of the arms and varies among plots. The Metolius arm is viewed looking south and the Deschutes and Crooked arms are viewed looking east.

The water derived from the Metolius River is now subject to greater solar warming, resulting in a slightly warmer hypolimnion than would have been the case prior to the SWW. However, it is unclear if this has resulted in a net change in water temperature for LBC.

5.1.2 Conductivity

Conductivity is a conservative tracer and an excellent indicator of tributary inputs to LBC, with high values found to be coming from the Crooked River (typically around 160 µS/cm), values of about 70 µS/cm from the Metolius River, and 110 µS/cm from the Deschutes River inlet. During the earlier study by Raymond et al. (1997), conductivity values varied widely with depth and time (Figure 5-10). The surface waters generally had higher values of conductivity than the hypolimnetic waters. That pattern, however, was inverted in March 1996 following a major storm that generated high flows in the Crooked River, resulting in elevated turbidity inputs that passed through Round Butte Dam and into the LDR as a distinct turbid flow.

A comparison between conductivity in 1995 and 2016 illustrates a dramatic change in conductivity with depth (Figure 5-11). In spring 1995, conductivity in the epilimnion was already higher than deeper in the lake, whereas there was only a modest difference from top to bottom in spring 2016. Concentrations at depths above 30 m remained above 125 µS/cm until October 1995. In 2016, conductivity was only above 125 µS/cm in the upper 12 m and showed a mass of low conductivity water immediately below the epilimnion that began in May and extended into the fall. Input from the Deschutes River inlet had already mixed with the Crooked River inlet input further upstream in the impoundment. Therefore, the low-conductivity water present at depths of 15–70 m in the Round Butte forebay (RES07) was derived from the Metolius River inlet. The water from the Metolius River arm appears to have warmed sufficiently to effectively mix with the water from the Crooked and Deschutes river arms a relatively short distance from the Round Butte forebay in the Metolius arm. The change in conductivity patterns in LBC does not appear to be related to any external factors such as conductivity values in the tributaries, which have remained relatively stable (Figure 4-4). It is more likely that the changes in conductivity patterns are a response to installation and operation of the SWW. The high

conductivity Crooked River waters are drawn to the SWW, causing widespread changes in mixing throughout the impoundment.

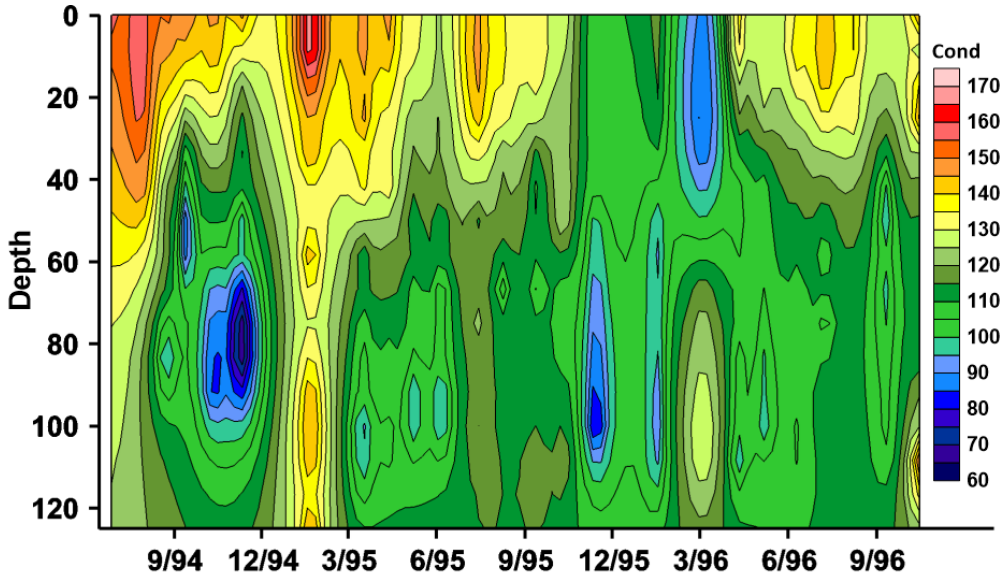

Figure 5-10. Conductivity patterns at Round Butte forebay (RES07) from 1994–1996. Depth is in meters; conductivity is in µS/cm. (*Source*: Raymond et al. 1997)

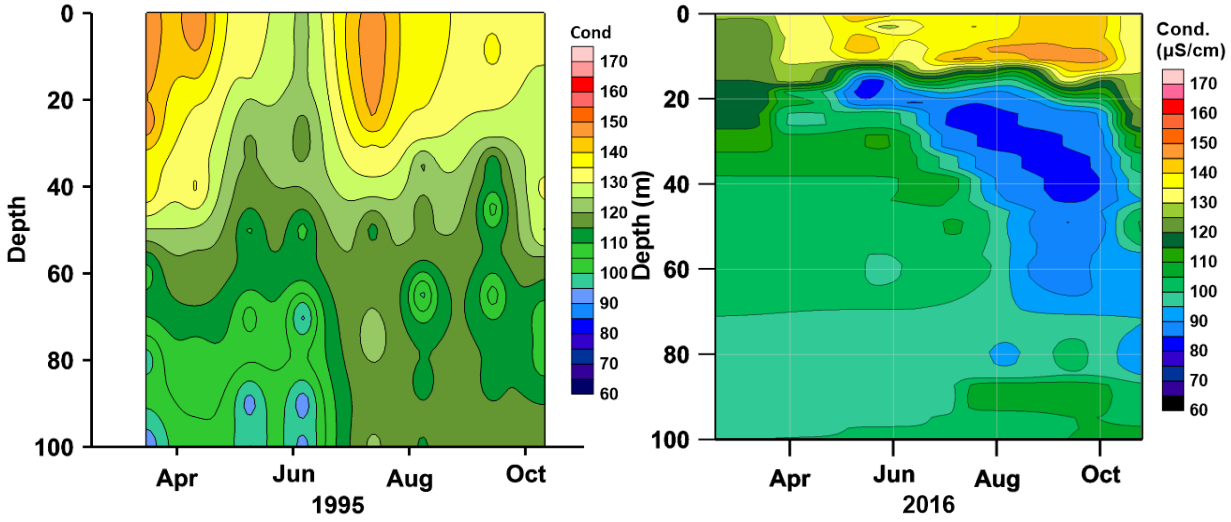

Figure 5-11. Conductivity at Round Butte forebay (RES07) for 1995 (*left*) and 2016 (*right*).

5.1.3 pH

pH values in LBC seldom exceeded 9.0 in 1994 and 1996, and only for short periods in the upper few meters (Figure 5-12). A comparison between pH values in 1995 and 2016 showed that epilimnetic pH values increased by a full pH unit by 2016 (Figure 5-13). The higher pH values in the epilimnion of 2016 reflect increased intensity of primary production in the surface waters (see Section 5.1.7). High pH values are generated when algae consume carbon dioxide (CO_2) from the water, which is acidic, and drive the equilibrium towards alkaline conditions. Low pH values such as those observed in the bottom waters reflect an increase in dissolved CO_2, which in this case was likely associated with decomposition reactions. Although pH in the tributaries to LBC has also increased in recent decades, pH of the incoming water has little direct impact on the pH in LBC because pH is not conservative and will rapidly equilibrate to alkalinity and the partial pressure of CO_2 conditions in the impoundment. pH in the deeper waters has also increased between the two studies.

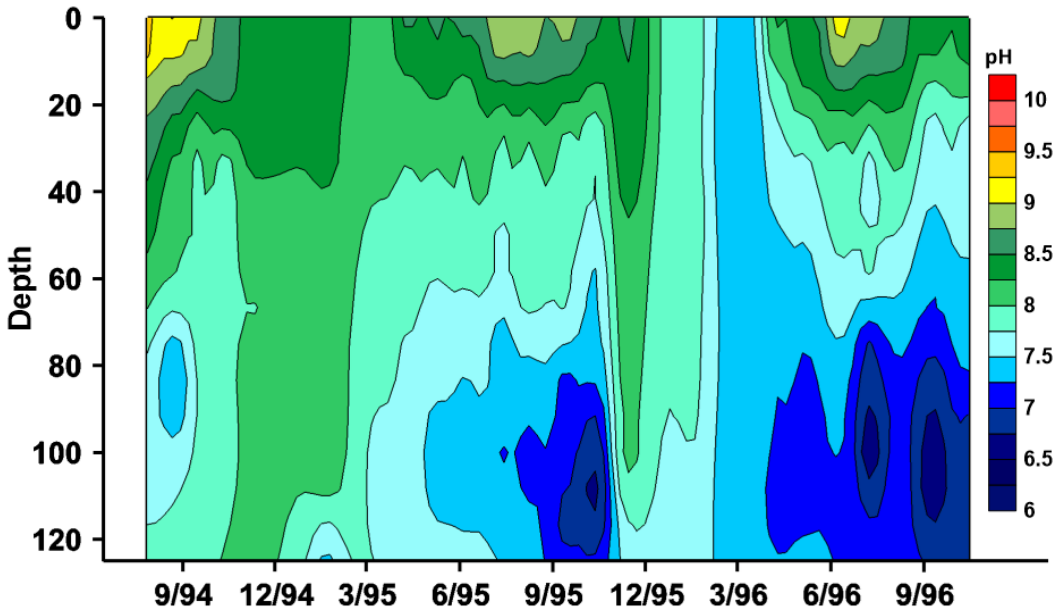

Figure 5-12. pH patterns at Round Butte forebay (RES07) from 1994–1996.

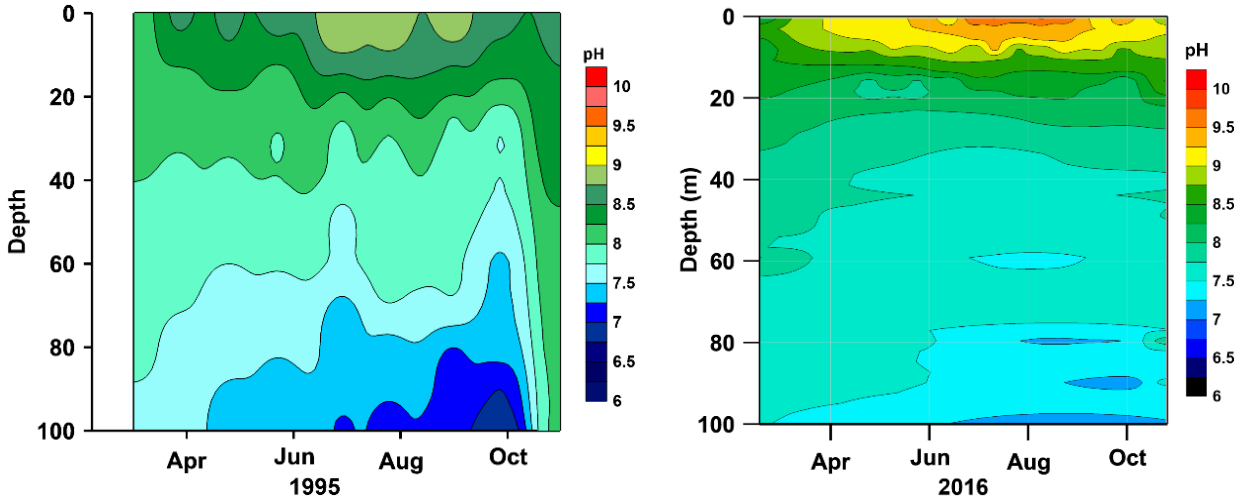

Figure 5-13. pH patterns at Round Butte forebay (RES 07) from 1995 (*left*) and 2016 (*right*).

5.1.4 Dissolved Oxygen

DO concentrations were considerably different across the years during the historical study (Figure 5-14). DO was the lowest in the epilimnion in summer 1994 and the highest in spring 1995 and 1996. The duration and vertical extent of the decline in hypolimnetic DO increased substantially from 1995 to 1996. DO in LBC was uniform (< 7.5 mg/L) throughout the water column in winter 1995/96, a feature that is unusual in two respects. The first is that DO concentrations declined from fall 1995 to winter 1996, which was counter to expected trends; as water cools, solubility of oxygen increases. In addition, the low values observed in spring 1996 continued to decline in the hypolimnion throughout 1996. It is likely that these anomalous patterns in 1996 reflect the inputs associated with the flood of February 1996. The flood generated large flows from the Crooked River that transported elevated solids, which likely included organic material that added to the oxygen demand in the hypolimnion.

A comparison of DO in 1995 and 2016 showed that hypolimnetic DO was more depleted in 2016 than in 1995, with DO less than 7.5 mg/L observed immediately below the epilimnion in 2016 (Figure 5-15). Additionally, the surface DO in 1995 (0–3 m) reached only about 12 mg/L, whereas values approaching 14 mg/L were observed in 2016. The changes observed with DO

are consistent with those for pH, reinforcing the supposition that LBC has experienced increased primary productivity, at least in the forebay.

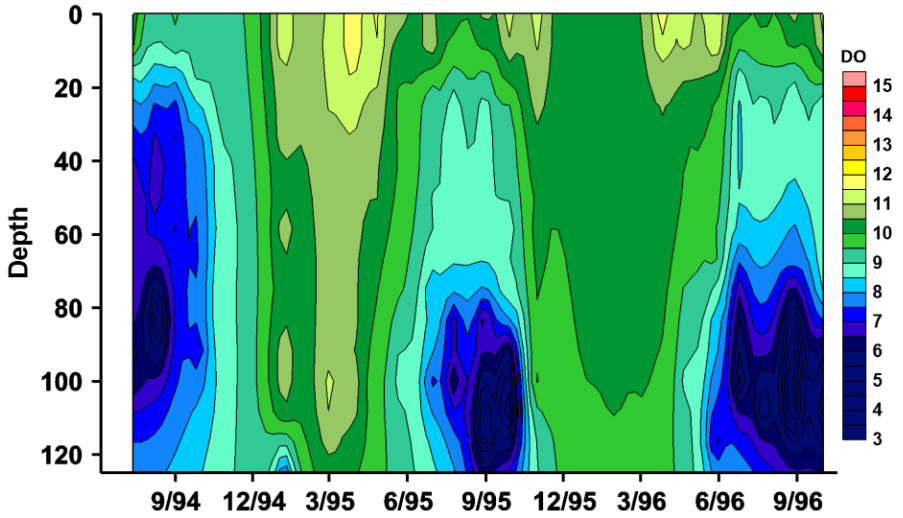

Figure 5-14. DO patterns at Round Butte forebay (RES07) in 1994–1996.

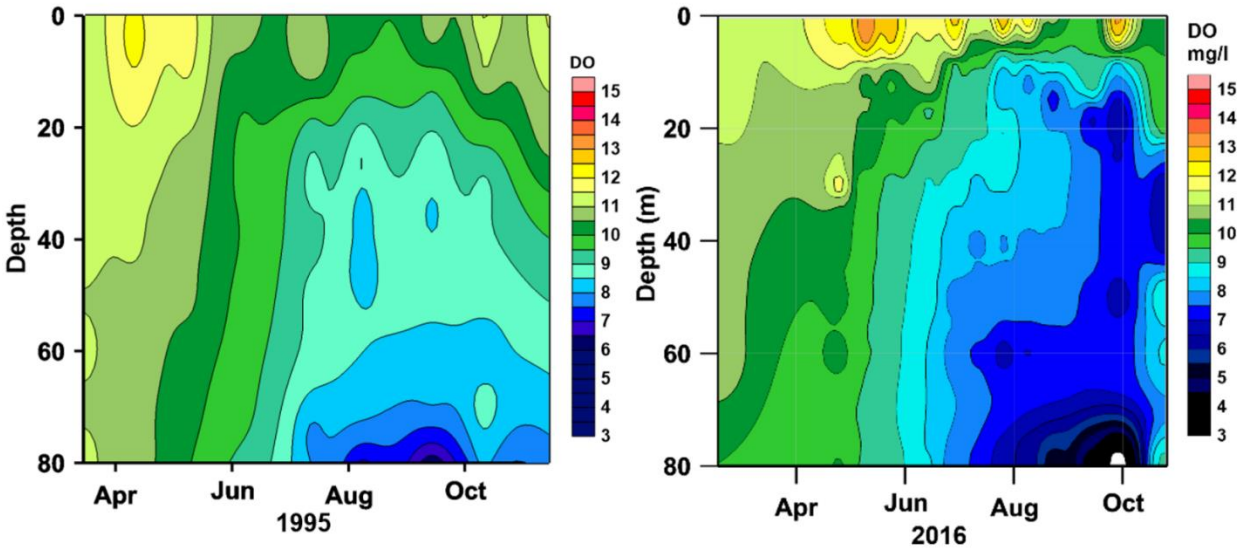

Figure 5-15. DO patterns at Round Butte forebay (RES07) in 1995 (*left*) and in 2016 (*right*). Depth is in meters.

5.1.5 Transparency

Transparency is another indicator of possible change in primary production in LBC. Both inorganic and organic particles can diminish transparency, the latter of which are usually caused by phytoplankton in these impoundments. Concentrations of dissolved organic carbon are low in LBC and can be discounted as a factor affecting transparency because concentrations of TOC measured at the ReReg Dam with the ZAPS LiquID unit were low (< 2.0 mg/L) In Section 4.2.2.5, it was shown that inorganic particles represented a minor portion of the total particulate load because when flows were high in the Deschutes and Crooked rivers during winter and spring high flow events (i.e., when the capacity to transport inorganic particles was high), transparency in LBC was highest. Thus, a measure of transparency using Secchi disk transparency is a reasonable surrogate for phytoplankton density in these impoundments. Secchi disk transparency recorded from 1994 to 1996 showed that the average transparency in LBC was 4.0 m (Figure 5-16).

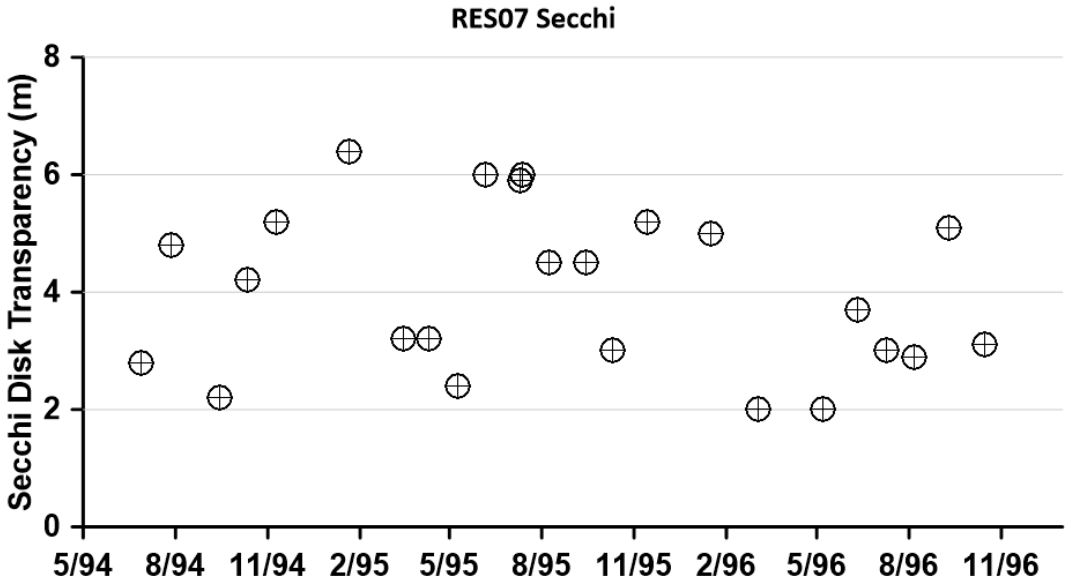

Figure 5-16. Secchi disk transparency at Round Butte forebay (RES07) from 1994 to 1996.

The average Secchi disk transparency measured in 2015/16 was 2.5 m (no measurements were made in 2017). The one-way analysis of variance indicates that this is a highly significant reduction in transparency compared to the data collected in 1994–1996 by Raymond et al (*df* = 47, *F* = 12.62, *p = 0.0009, n* for both periods = 24).

5.1.6 Nutrients

Comparing various analytes can be challenging over the span of decades because of improvements in analytical chemistry. This is the case for nitrogen where in the 1990s there was no direct measure of TN commonly available. Instead, TKN was measured, and TN was derived from the sum of TKN and NO_3. Measurement of TKN was not highly precise. Historical measures of TKN, especially at concentrations less than 1 mg/L (as N), are considered imprecise and are not included in this analysis. Also, since concentrations of NH_3 in the impoundments are usually low, there is little opportunity to gauge potential changes in NH_3. However, other major nutrients, TP, PO_4, and NO_3, were measured accurately and are compared across the two study periods (Table 5-1).

Although changes in nutrient concentrations in LBC between data collected in 1994–1996 and the current study (2015–2017) were generally relatively modest, they are potentially important, because changes in LBC can lead to changes in the LDR. For TP, the only significant change was measured in the lower hypolimnion, where the mean TP concentration was greater in 1994–1996 compared to the current study (0.116 mg/L to 0.093 mg/L) (Table 5-1). For PO_4, the pattern was different, with the mean concentration in the epilimnion significantly less in the current study than it had been in 1994–1996 (0.042 mg/L to 0.012 mg/L). PO_4 concentrations in the other three depth zones were less in the current study than they had been in 1994–1996, although not significantly; the concentration changes ranged from 0.010–0.014 mg/L.

NO_3 concentrations in three of the four depth zones were less in the current study than they had been in 1994–1996. However, the changes were statistically significant only in the two hypolimnetic zones. In 2015–2017, the NO_3 concentration was 0.040 mg/L less in the epilimnion than they had been in 1994–1996, but the *p* value was only 0.115, reflecting the high standard error in the NO_3 data.

Table 5-1. Comparison of nutrient concentrations at Round Butte forebay (RES07) in 1994–1996 to 2015–2017 for four depth classes.

Statistic	Epilimnion[a]		Metalimnion[b]		Upper Hypolimnion[c]		Lower Hypolimnion[d]	
	1994–1996	2015–2017	1994–1996	2015–2017	1994–1996	2015–2017	1994–1996	2015–2017
TP (mg/L)								
n	23	33	22	21	23	19	23	25
mean	0.054	0.051	0.062	0.066	0.071	0.065	0.116	0.093
se[e]	0.0041	0.0034	0.0041	0.0042	0.0037	0.0040	0.0065	0.0063
F[f]	0.39		0.30		1.48		6.63	
p[g]	0.535		0.589		0.231		0.013*	
PO_4 (mg/L)								
n	13	33	12	21	13	19	13	25
mean	0.042	0.012	0.048	0.038	0.057	0.050	0.093	0.079
se[e]	0.0063	0.0040	0.0064	0.0048	0.0040	0.0037	0.0073	0.0053
F[f]	16.33		1.59		1.53		2.13	
p[g]	0.0002**		0.216		0.226		0.153	
NO_3 (mg/L)								
n	24	33	23	21	24	19	24	25
mean	0.101	0.061	0.184	0.212	0.226	0.121	0.252	0.194
se[e]	0.0190	0.0162	0.0191	0.0200	0.0151	0.0169	0.0204	0.0200
F[f]	2.57		0.98		21.56		4.10	
p[g]	0.1146		0.3275		0.0000**		0.0486*	

Notes:

[a] Includes samples from a depth range of 0–3 m, although most of samples were from 1 m.

[b] Includes samples from a depth range of 7–15 m, although most of samples were from 10 m.

[c] Includes samples from a depth range of 20–30 m, although most of samples were from 25 m.

[d] Includes samples from a depth range of 50–105 m, although most of samples were from 75 and 100 m.

[e] standard error of the mean.

[f] *F* statistic is the ratio of the paired variances (technically two mean squares).

[g] *p* value; probability that the observed differences are significant; "*" where *p* is 0.05 and "**" where *p* is 0.001.

5.1.7 Chlorophyll *a*

Concentrations of chlorophyll *a* (pheophytin corrected) were highly variable during both the historical study (1994–1996) and this study (2015–2017). During the historical study, the highest epilimnetic chlorophyll values were observed in fall, although moderately high values were measured in spring and summer (Figure 5-17). The most consistent pattern during 1994–1996 was the low chlorophyll values measured in mid-to-late winter. In both years in which the chlorophyll was measured, the spring values spiked to over 30 µg/L and declined through summer. The October values for all 3 years (1994–1996) were elevated, indicating a phytoplankton bloom that occurred during mixing.

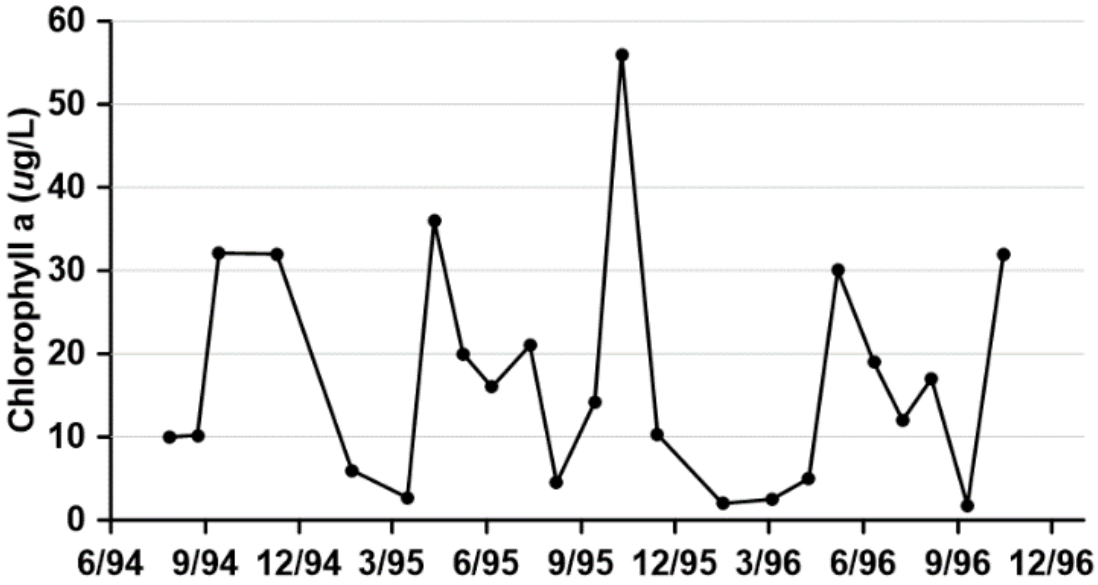

Figure 5-17. Concentrations of chlorophyll *a* (pheophytin corrected) at Round Butte forebay (RES07) for 1994–1996.

Fewer samples were collected for chlorophyll *a* during the current study because of the decision to use fluorometric measurements as the principal measure of chlorophyll. Nevertheless, 17 samples were collected for chlorophyll in the current study from the epilimnion of LBC. The results of the comparison showed that the historical mean chlorophyll was 17.1 µg/L (*n* = 23*; se*

2.97) compared to the current mean of 25.3 µg/L (*n* = 17*; se* 3.43), which is a 48% increase in chlorophyll between the two studies (*P* = 0.0764, *F* = 3.32). A plot of the monthly mean chlorophyll values from 1994–1996 compared to 2015–2017 shows that the largest increase in chlorophyll occurred in the months of June through August (Figure 5-18). The only months in this historical data set in which chlorophyll was higher than the values measured in the more recent study were in May and October, months typically dominated by diatoms. In contrast, the large increases in summer chlorophyll was associated with increases in cyanobacteria.

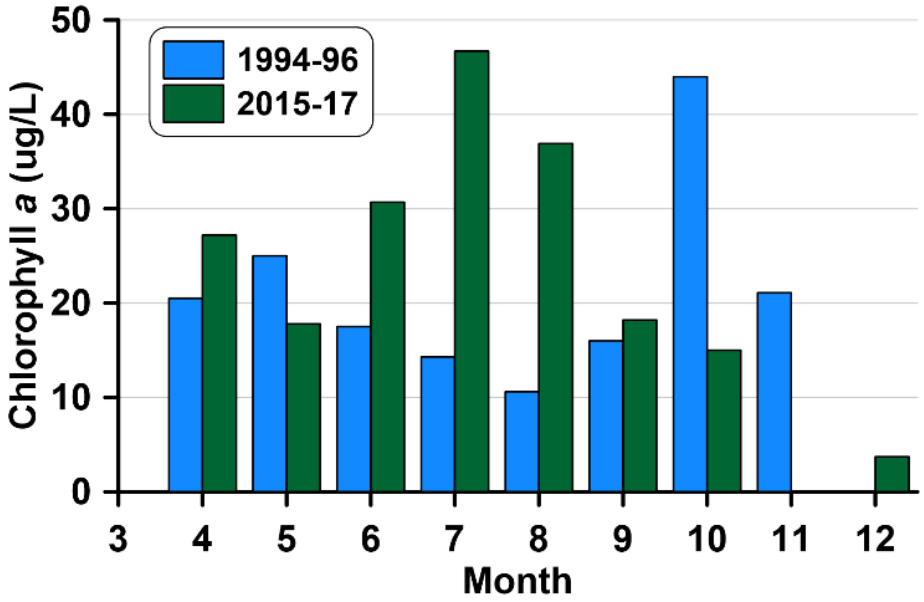

Figure 5-18. Monthly average chlorophyll *a* concentrations measured at Round Butte forebay in 1994–96 and 2015–17.

Unless stated otherwise, chlorophyll results presented in the report refer to chlorophyll *a*. Chlorophyll is a gross measure of phytoplankton abundance and does not allow for directly separating cyanobacteria chlorophyll from non-cyanobacteria chlorophyll. Those distinctions are derived from phytoplankton community composition and measurements of pheophytin, a pigment present in cyanobacteria.

5.1.8 Phytoplankton Community Composition

During 1994–1996, the dominant taxa in LBC (based on mean biovolume) appeared to be *Stephanodiscus astraea* (582,000 cubic micrometers per milliliter [μm^3/mL]), blue-green algae, or cyanophytes (306,000 μm^3/mL), and *Fragilaria crotonensis* (175,000 μm^3/mL). *S. astraea* was present in all 16 surface samples from LBC during the 1994–1996 period, whereas the other two groups were present on only 10 of the 16 sampling dates. *S. niagarae* in LBC is not reported in the historical data. Cryptophytes were numerous but, because of their small size, they were not as important to algal biovolume compared to the diatoms and cyanophytes. The dominant cyanobacteria reported was *Anabaena circinalis* with several reportings of *A. flos-aquae* and *Aphanizomenon.* Cyanobacteria became dominant during July–September, but otherwise the phytoplankton community was dominated by centric diatoms.

The dominant phytoplankton in Lake Simtustus in the Raymond et al. (1997) dataset was largely the same taxa dominant in LBC, although *S. astraea* was even more dominant in Lake Simtustus and the occurrence and biovolume of cyanobacteria was substantially less. The mean biovolume of *S. astraea* in Lake Simtustus was greater than was observed in LBC (1.89×10^6 μm^3/mL), with cyanobacteria far less (73,000 μm^3/mL) and *F. crotonensis* about the same (165,000 μm^3/mL) as in LBC.

The dominant phytoplankton taxa in LBC based on the current study shows that some taxa remain important (e.g., *Anabaena/Dolichospermum, F. crotonensis*). The issue of *Stephanodiscus* is curious because its identification is usually considered relatively unambiguous (unless the *S. niagarae* were small) and yet no mention is made of this taxon in the historical data, whereas other species of this genera were numerous in the historical data. If we aggregate all species of *Stephanodiscus* in both the historical and current studies, this genus is one of the major phytoplankton genera in both periods. Both the historical and current phytoplankton communities were representative of eutrophic lakes, although given the suspected larger role of *Dolichospermum* (*Anabaena*) in 2015–17, LBC would appear to have become even more eutrophic in recent years. That conclusion is also supported by the 48% increase in epilimnetic chlorophyll between the two periods.

Another comparison of changes in phytoplankton community composition in the Project reservoirs can be made between the ODEQ data collected in 2006 and the data collected in 2015. Both datasets were analyzed by the same taxonomist (Aquatic Analysts) using the same methods. The results showed that the 2016 epilimnetic phytoplankton were more abundant than they were in 2006 and that a shift in dominant taxa appears to have occurred. Phytoplankton in the 2015 samples were considerably more abundant in May and June than the 2006 results and indicated that cyanobacteria were present and abundant earlier in the season in 2015 (Figure 5-19). The dominant cyanobacterium present in 2006 was *Aphanizomenon*, whereas in 2015 the dominant cyanobacterium was *Anabaena* (*Dolichospermum*).

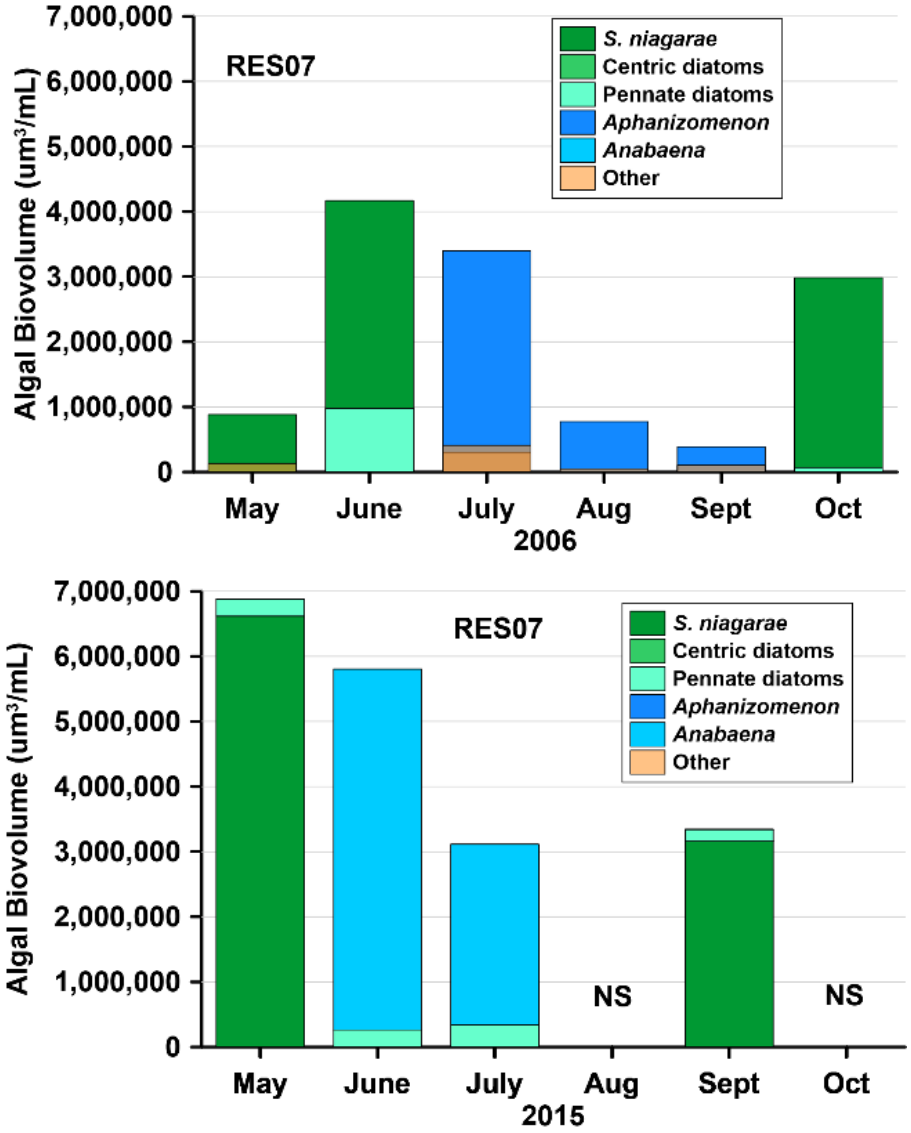

Figure 5-19. Dominant phytoplankton at Round Butte forebay (RES07) from 2006 and 2015. Both sets of samples are from the epilimnion and were analyzed by the same taxonomist (Aquatic Analysts) using the same methods.

5.1.9 Zooplankton

Whereas phytoplankton abundance was based on cell biovolume, zooplankton abundance is based on counts of individual organisms. In a table combining the results from Lake Simtustus and LBC sites for the entire study, *Daphnia* sp. was listed as the most abundant taxon, representing 35.9% of all individuals in the impoundments (Raymond et al. 1997). The

remaining top four taxa listed were nauplius larvae (20.5%), *Cyclops* sp. (18.3%), and *Diaptomus* sp. (15.5%). All rotifers combined represented less than 9% of zooplankton individuals in the Raymond et al. (1997) study. There appears to have been significant changes in the zooplankton communities in the two impoundments between the 1994–96 study and the 2015–17study (Figure 5-20). The cladoceran and copepod communities at Round Butte forebay appear similar between the two study periods. However, the rotifer community appears to have increased dramatically in LBC. At Pelton forebay, all three groups appear to have increased dramatically, again with the largest increases associated with the rotifers.

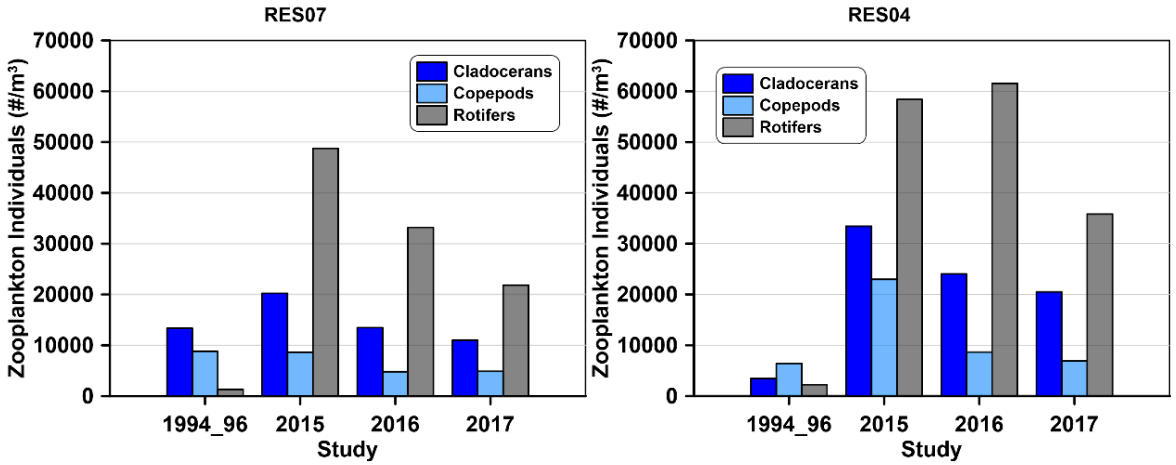

Figure 5-20. Density of zooplankton groups at Round Butte forebay (RES07) and Pelton forebay (RES04) comparing data collected by Raymond et al. (1997) and this study.

The two studies do not provide an ideal comparison for several reasons. First, Raymond et al. (1997) used a net with a mesh size of 80µ, whereas this study used a mesh size of 64µ. Second, the earlier study collected vertical tows down to 30 m, whereas this study had a vertical tow length of 10 m. Finally, the taxonomists were different; Raymond et al. used Dr. Meg Falter, Aqua ID Laboratory, whereas this study used Dr. Allan Vogel, ZP Taxonomic. If the results from the two studies are representative of the communities, then dramatic changes have occurred. However, without better controls, it is impossible to definitively attribute the differences in zooplankton communities to changes in the reservoirs.

The best available pre-SWW data on zooplankton populations in the reservoirs are derived from data collected by ODEQ in 2006. Those data showed a zooplankton population in 2006 with a relatively low proportion of rotifers and a higher proportion of cladocerans than in 2016 (Figure 5-20). Additionally, abundance of other planktonic organisms such as protozoa was lower in 2006 than in 2016. Not only were there significant differences in zooplankton groups, but there were also important changes in species abundance. A keystone zooplankton species for Oregon lakes is the large cladoceran, *Daphnia pulicaria*. *D. pulicaria* exhibited a reduction in density of 90% at the Round Butte forebay (RES07) from 2006 to 2016 based on a comparison of samples for May to October of both years (Figure 5-21). The four species of *Daphnia* identified in 2006 and 2016 illustrated not only the large decrease in *D. pulicaria* from 2006 to 2016, but also the absence of *D. schodleri*, another large daphnid, in 2016 (Figure 5-22). Instead, in 2016, we observed the presence of a small number of a different large daphnid, *D. rosea*. Zooplankton distributions are notoriously variable, and it is possible that the differences observed between the two studies are an artifact of sample variation. However, because there were differences in both abundance and species composition, the variations might reflect actual changes in zooplankton populations. Changes of this nature are often associated with changes in abundance of planktivorous fish such as kokanee, which will exert considerable pressure on the larger zooplankton taxa.

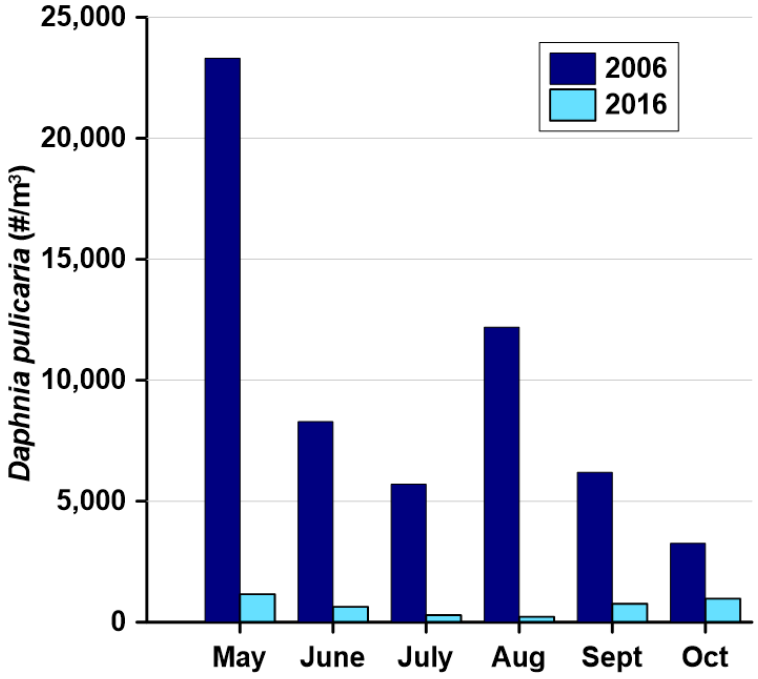

Figure 5-21. Density of *Daphnia pulicaria* at Round Butte forebay (RES07) in 2006 and 2016.

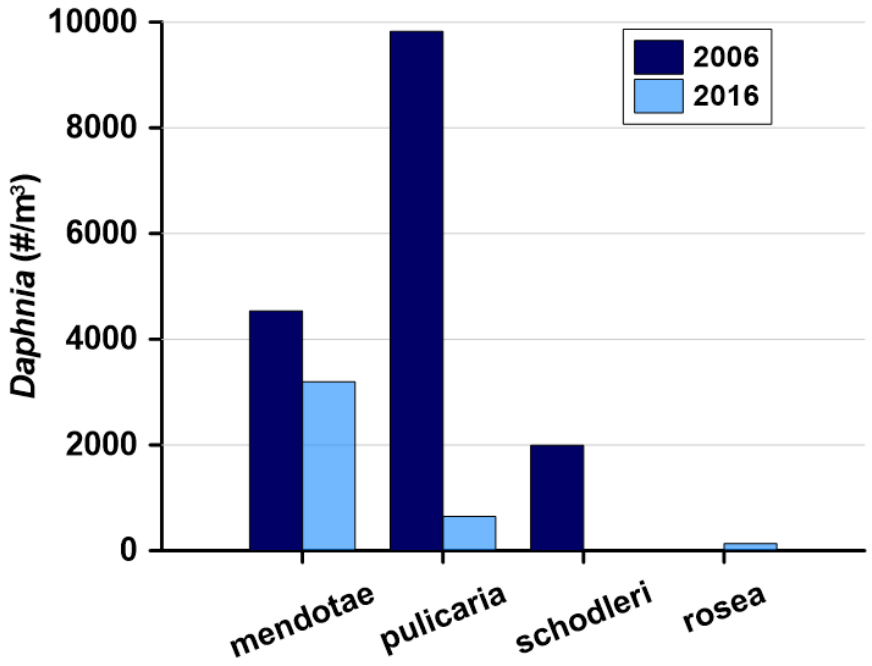

Figure 5-22. Species of *Daphnia* present in 2006 and 2016 at Round Butte forebay (RES07).

The differences in zooplankton populations between 2006 and 2016 might reflect differences in abundance of fish in LBC between the two years. Hydroacoustic analysis of limnetic fish over repeatable transects showed that the abundance of fish in 2006 was the lowest recorded in the 50 surveys conducted through 2017 (Figure 5-23). The fish population estimate for November 2006 was only 178,090 compared to 2,657,603 in November 2016. Although the greatest numbers of fish were estimated to have been present in 1999 (3,864,364), significantly more fish were present in the lake following installation of the SWW (data calculated from Mueller and Degan (2017): *AOV, P = 0.033, F = 4.80, pre-SWW mean = 1.29 E6 [+/- 135,918], post-SWW mean = 1.86 E6 [+/- 217,954]).*

A comprehensive analysis of the salmon and kokanee fisheries and zooplankton communities of LBC was conducted by ODFW from 1996 to 1998 as part of the relicensing effort (Thiesfeld et al. 1999). They found that rotifers and copepods were the most abundant groups of zooplankton, but that *Daphnia* and *Bosmina* (Cladocera) were the most common prey items consumed by the kokanee.

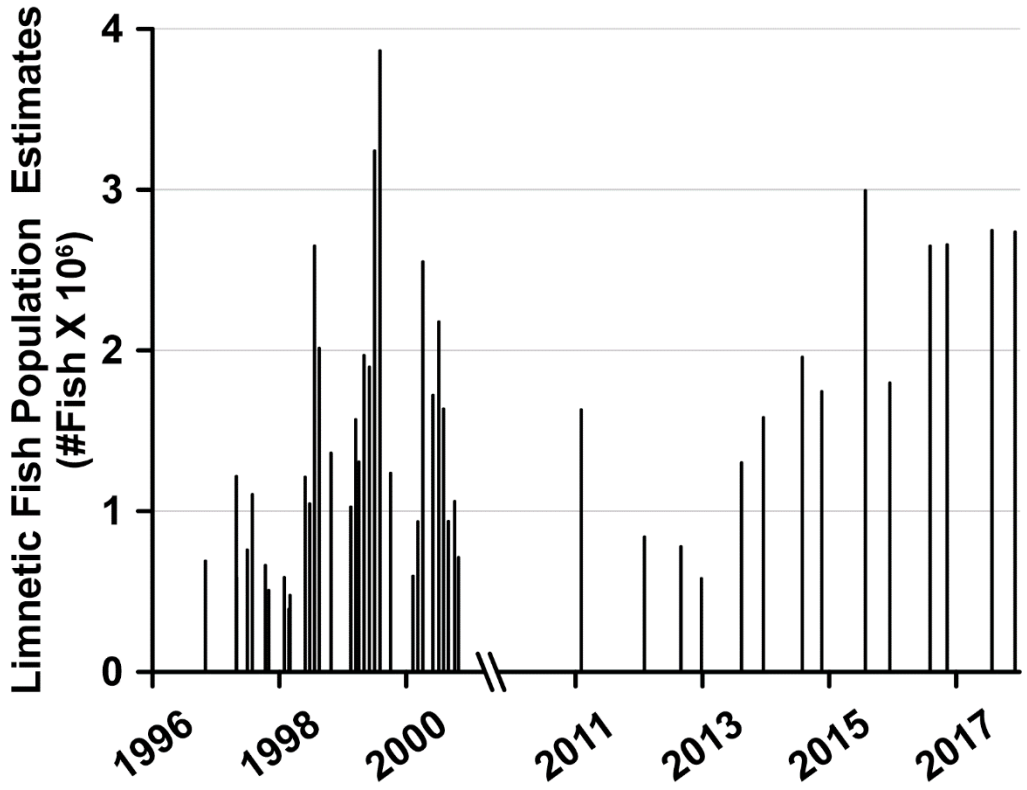

Figure 5-23. Fish population estimates for LBC conducted using hydroacoustic methodology (Mueller and Degan 2017).

5.2 Lake Simtustus

5.2.1 Temperature Regime

The historical temperature data for Lake Simtustus are limited to the study conducted in 1994–1996 (Raymond et al. 1997), which are compared with the results from this study. The temperature patterns in Lake Simtustus were comparatively simple and predictable. The lake fully mixed in the winter and slowly warmed as solar radiation and increasing temperatures from LBC discharge increased temperatures in the lake (Figure 5-24). Lake Simtustus developed a shallow epilimnion that was slightly cooler than LBC. The lake temperatures were 2–3˚C cooler in March 1995 than in 2016 and remained cool until June, when a thermocline started to develop (Figure 5-25). In contrast, the formation of the epilimnion was much more advanced in 2016. In 1995, the hypolimnion warmed to about 14˚C in September, whereas the hypolimnion remained

slightly cooler in September 2016, reflecting the higher retention of cool discharge waters in LBC with the operation of the SWW.

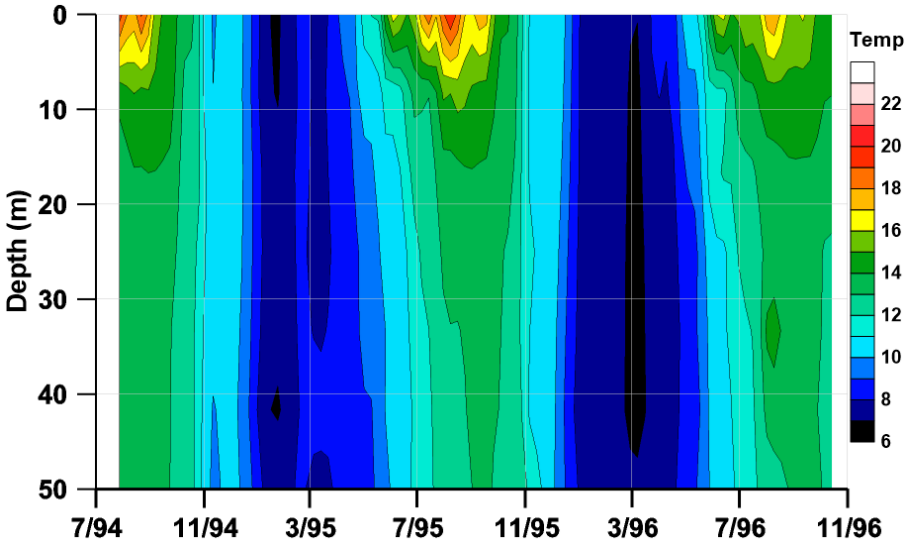

Figure 5-24. Temperature patterns at Pelton forebay (RES04) 1994–1996.

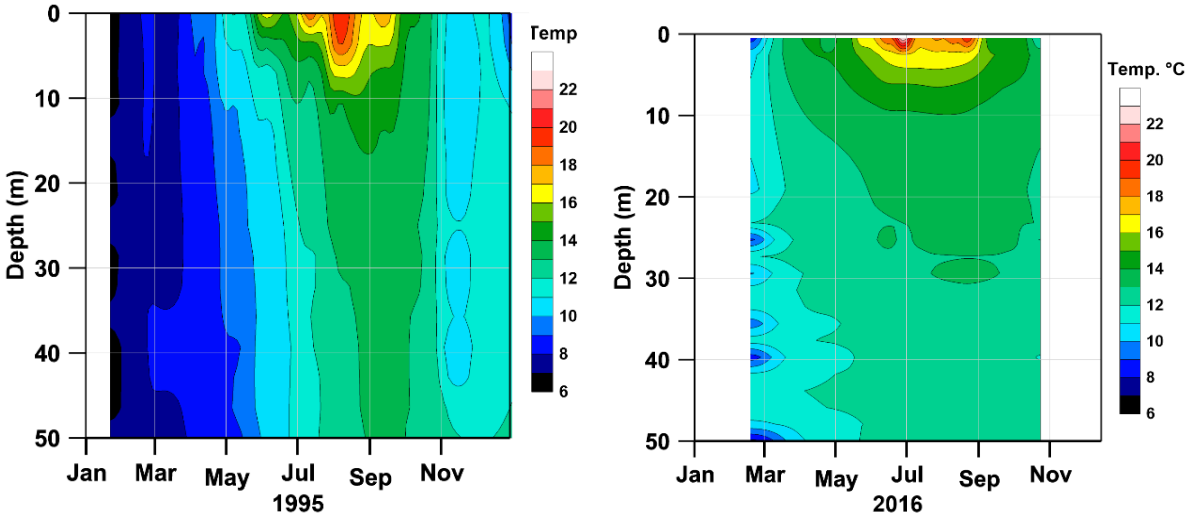

Figure 5-25. Temperature patterns at Pelton forebay (RES04) for 1995 (*left*) and 2016 (*right*).

5.2.2 Conductivity

Historical data on Lake Simtustus are limited to those collected by Raymond et al. (1997). Conductivity varied greatly in Lake Simtustus from 1994 to 1996 (Figure 5-26). The 1994/95 fall-to-winter transition showed a major change from low values in the hypolimnion to high values throughout the water column when the lake fully mixed. In winter 1995/96, the fully mixed lake had a low conductivity that gradually increased into summer. These patterns differed significantly in 2016, showing higher conductivity in the epilimnion and a lower degree of variation throughout the impoundment than in 1995 (Figure 5-27). Data from 2016 indicated that the epilimnion in Lake Simtustus had high conductivity waters in the late winter/early spring because of the surface discharge from LBC, which is primarily derived from the Crooked River. As in 1994–1996, the surface waters in Lake Simtustus then become isolated from the deeper waters in the lake and experience evapo-concentration. Also, during late spring to fall, the only significant surface inflow to the epilimnion of Lake Simtustus is from Willow Creek, which has high conductivity [mean of 386 µS/cm in 2016 (n= 10, se = 4.9 µS/cm)].

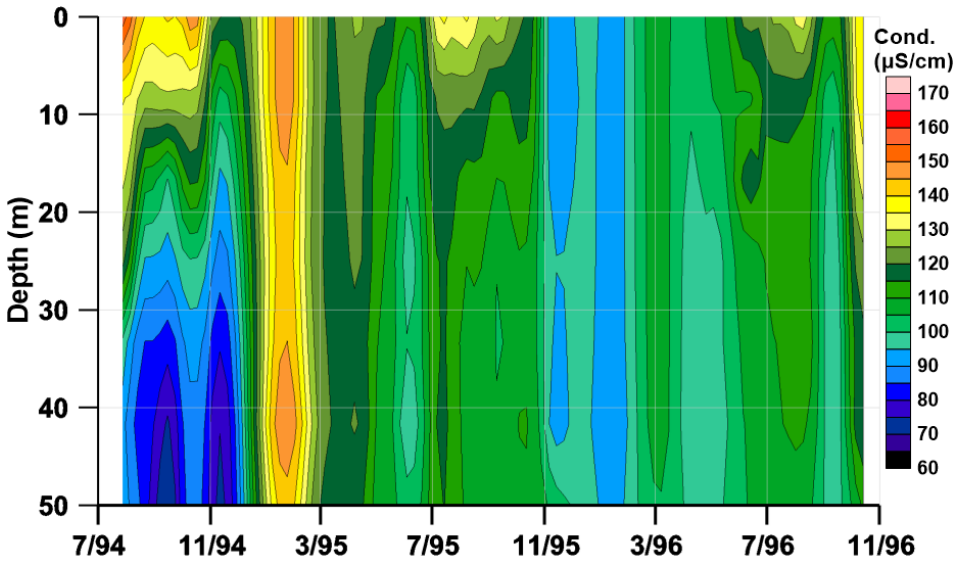

Figure 5-26. Conductivity patterns at Pelton forebay (RES04) from 1994–1996.

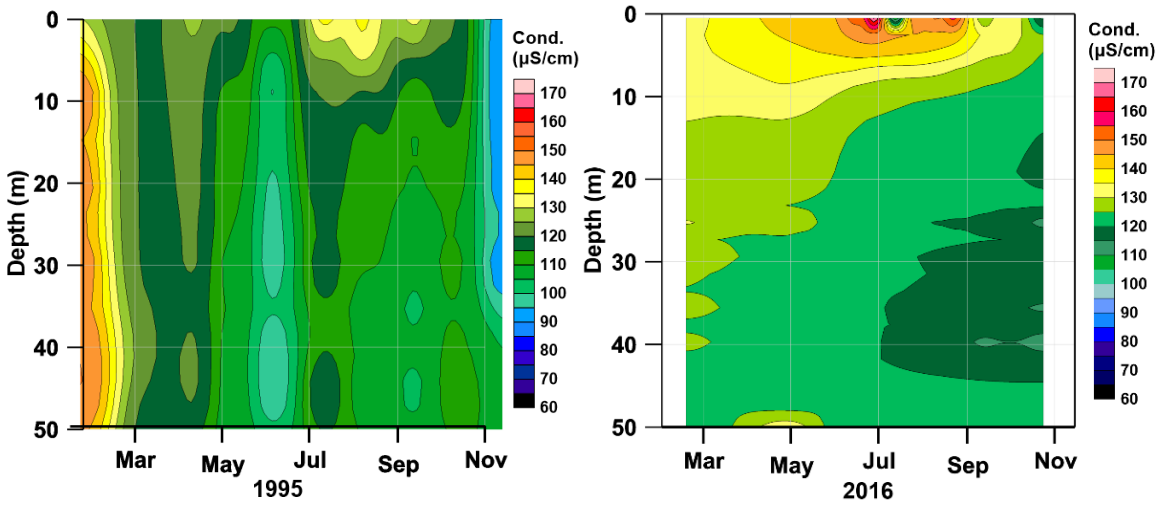

Figure 5-27. Conductivity patterns at Pelton forebay (RES04) in 1995 (*left*) and 2016 (*right*).

5.2.3 pH

The only historical pH data available for Lake Simtustus are derived from the study by Raymond et al. (1997). Lake Simtustus developed a shallow lens of high-pH water that was relatively elongated in 1995 and more intense but abbreviated in 1996 (Figure 5-28). pH values typically ranged from 7.5 to 8.0 in 1995 and slightly lower in 1996. In 2016, the extent of high-pH values in the epilimnion expanded in depth and duration (Figure 5-29). The entire metalimnion and hypolimnion in the lake increased by up to 0.5 pH units as more productive epilimnetic waters from LBC filled the impoundment.

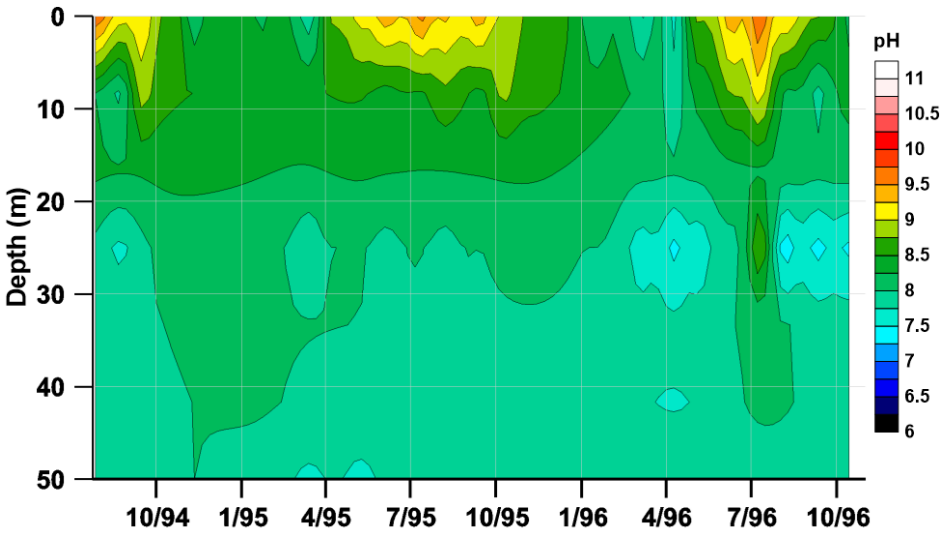

Figure 5-28. pH patterns at Pelton forebay (RES04) from 1994–1996.

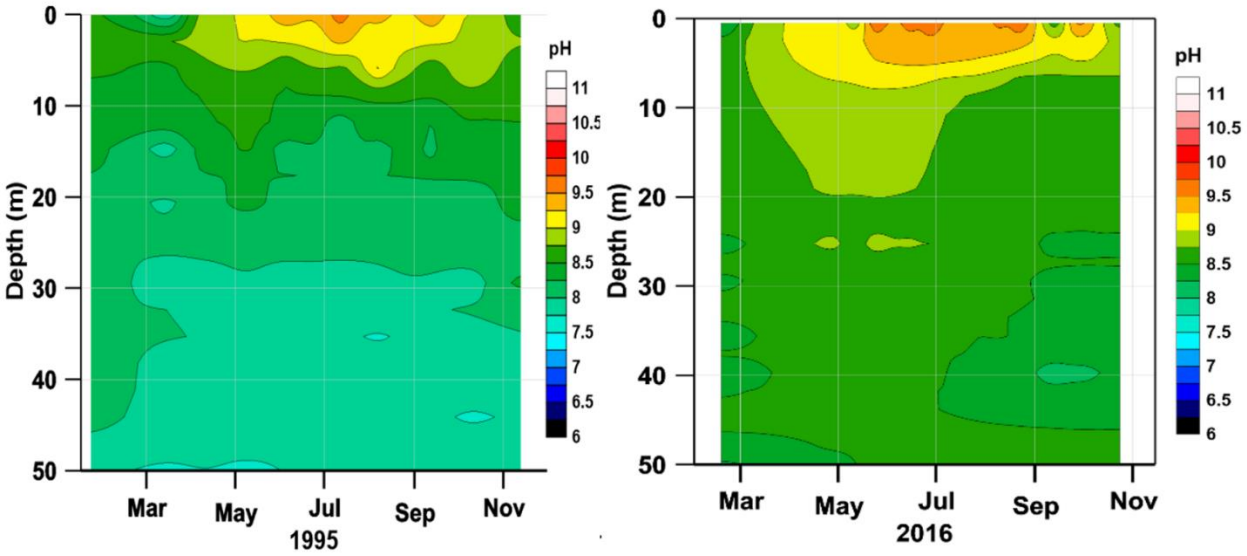

Figure 5-29. pH patterns at Pelton forebay (RES04) in 1995 (*left*) and 2016 (*right*).

5.2.4 Dissolved Oxygen

Concentrations of DO exhibited significant oxygen depletion (from 5 to 50 m) in late summer of 1994, but that pattern was not repeated in subsequent years (Figure 5-30). A distinctive feature of the DO profiles in Lake Simtustus was the onset of supersaturated conditions in the epilimnion starting in May. The 2016 profile also showed the rapid onset of elevated DO in the epilimnion of Lake Simtustus, with only brief excursions of high DO thereafter (Figure 5-31). The metalimnetic and hypolimnetic DO concentrations declined substantially in 2016, with a minimum in the metalimnion. The most distinct differences in DO concentrations between 1995 and 2016 are the apparent reduction in supersaturation of the surface waters in the recent data and an increase in DO undersaturation in the hypolimnetic waters.

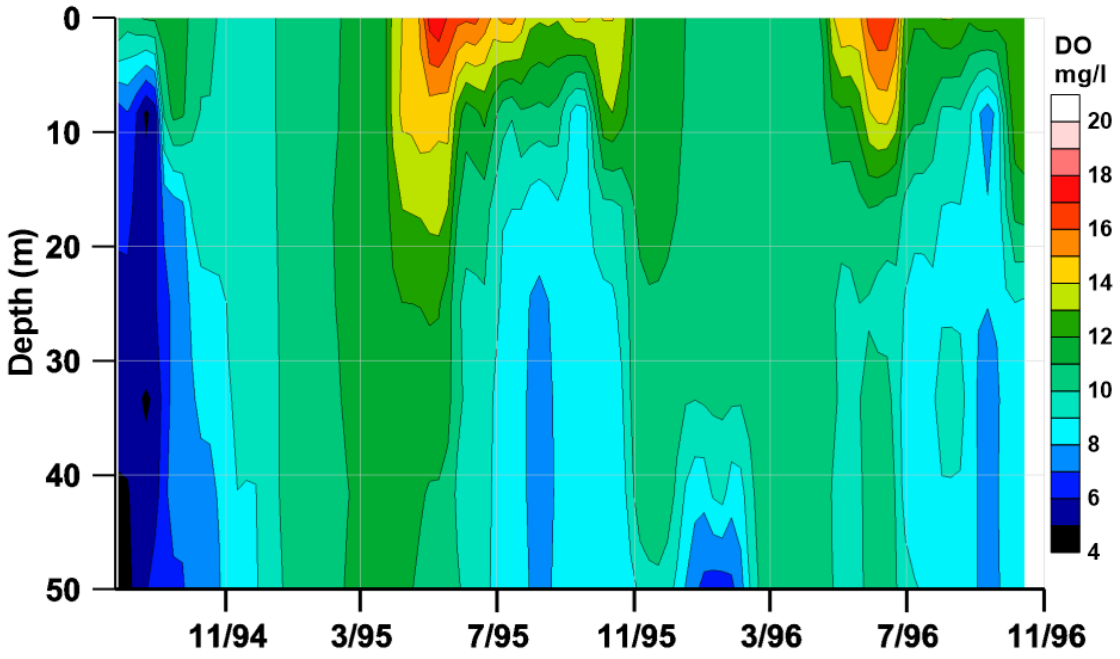

Figure 5-30. DO patterns at Pelton forebay (RES04) from 1994–1996.

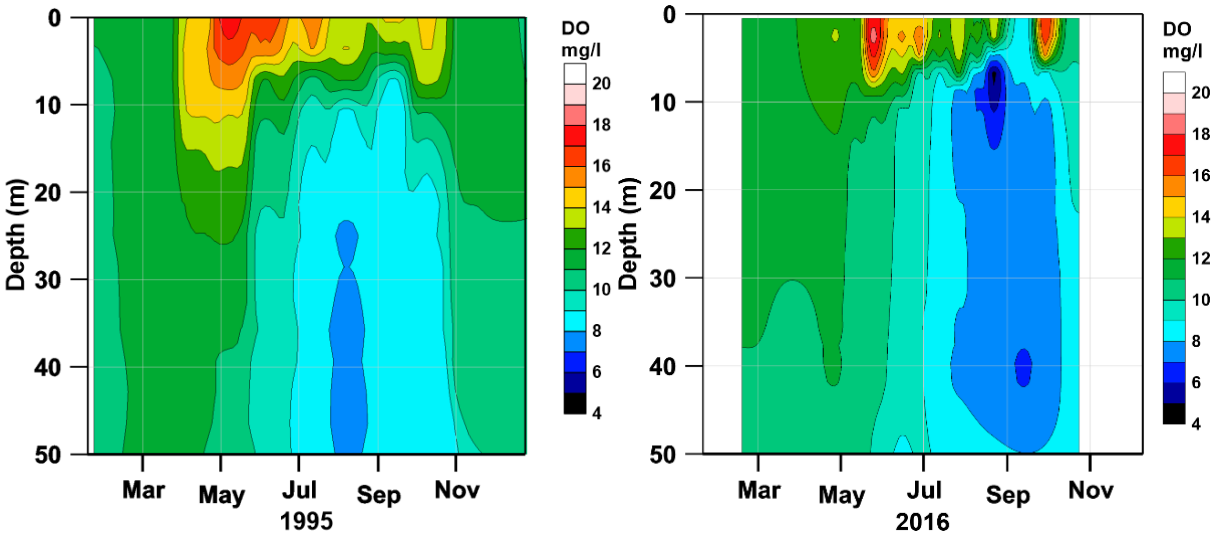

Figure 5-31. DO patterns at Pelton forebay (RES04) in 1995 (*left*) and 2016 (*right*).

5.2.5 Transparency

The only data available for historical comparison of transparency are from Raymond et al. (1997). Secchi disk transparency in Lake Simtustus during 1994–1996 showed an annual repeating pattern. Transparency increased linearly through the course of each year, with low values early in the year that increased steadily throughout the sampling season (Figure 5-32). Transparency at the Pelton forebay (RES04) had a mean value of 3.0 m (*se 0.29; n = 24*) for the 1994–1996 period, virtually identical to the mean value for the current study from 2015–2017 (mean = 2.97, *se 0.29 n = 23*). Although transparency between any two months between the two studies might have changed somewhat, the overall assessment is that there was no change in Secchi disk transparency between the studies.

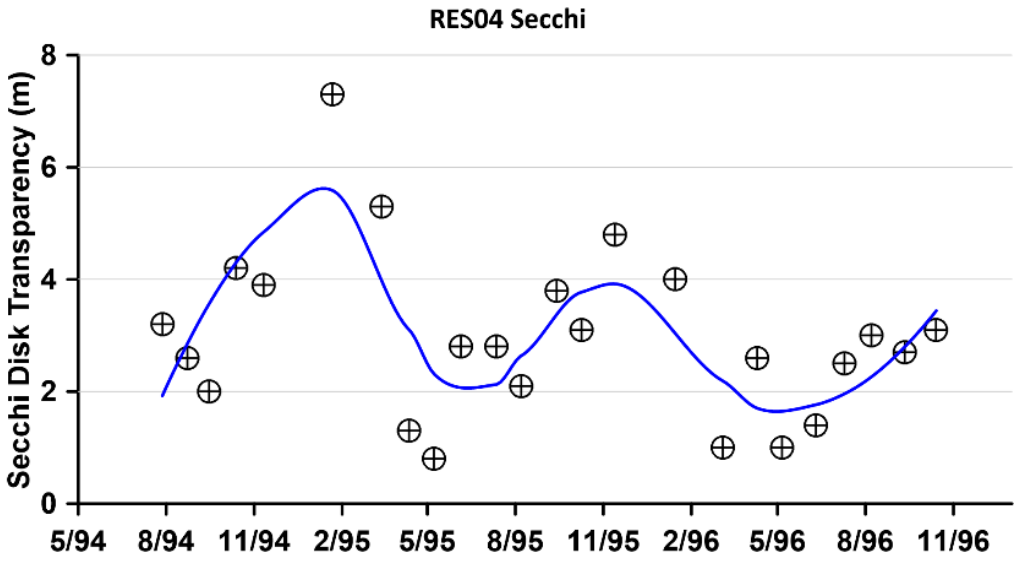

Figure 5-32. Secchi disk transparency at Pelton forebay (RES04) for 1994–1996. The blue line is the LOESS fit of the observed data.

5.2.6 Nutrients

TP did not exhibit a statistically significant change in Lake Simtustus between the data collected in 1994–1996 and that collected in the current study (2015–2017), although the mean epilimnetic concentration was 46% less in 2015–2017 (0.043 mg/L) than it had been in 1994–1996 (0.079 mg/L) (Table 5-2). However, PO_4 was significantly less in the epilimnion and metalimnion of Lake Simtustus in the current study compared to 1994–1996. PO_4 concentrations in both the epilimnion and the metalimnion were 0.022 mg/L less in the current study compared to 1994–1996, whereas the concentration in the hypolimnion was only 0.010 mg/L less (not significant [ns]). NO_3 concentrations were significantly greater in the epilimnion and metalimnion in 2015–2017 (0.148 mg/L and 0.170 mg/L, respectively) compared to 1994–1996 (0.080 mg/L and 0.109 mg/L, respectively). NO_3 was greater in the hypolimnion in 2015–2017, but it was not statistically significant.

The relatively large and statistically significant changes in PO_4 and NO_3 concentrations in the epilimnion and metalimnion of Lake Simtustus and the absence of significant changes in the hypolimnion are surprising because we anticipated that changes in release waters from LBC would affect the hypolimnion. Furthermore, the decreases in PO_4 and increases in NO_3 are

atypical. Decreases in PO_4 for the same water body often reflect greater utilization of phosphorus by phytoplankton. That decrease in PO_4 is typically accompanied by corresponding decreases in NO_3 as both N and P are assimilated by the phytoplankton.

Table 5-2. Comparison of nutrient concentration at Pelton forebay (RES04) in 1994–1996 to 2015–2017 for three depth classes.

Statistic	Epilimnion[a]		Metalimnion[b]		Hypolimnion[c]	
	1994–1996	2015–2017	1994–1996	2015–2017	1994–1996	2015–2017
TP (mg/L)						
n	31	31	19	23	20	27
mean	0.079	0.043	0.060	0.054	0.084	0.082
se[d]	0.0133	0.0133	0.0049	0.0044	0.0042	0.0036
F[e]	3.67		0.79		027	
p[f]	0.060		0.379		0.605	
PO_4 (mg/L)						
n	16	31	11	22	11	27
mean	0.035	0.013	0.048	0.026	0.059	0.049
se[d]	0.0062	0.0045	0.0073	0.0052	0.0055	0.0035
F[e]	7.75		5.99		2.25	
p[f]	0.0078**		0.020*		0.142	
NO_3 (mg/L)						
n	30	31	19	22	20	27
mean	0.080	0.148	0.109	0.170	0.164	0.180
se[d]	0.0155	0.0153	0.0187	0.0174	0.0150	0.0129
F[e]	10.05		5.72		0.64	
p[f]	0.0024**		0.0217*		0.427	

Notes:

[a] Includes samples from a depth range of 0–3 m, although most of samples were from 1 m.

[b] Includes samples from a depth range of 7.5–10 m, although most of samples were from 10 m.

[c] Includes samples from a depth range of 30–45 m, although most of samples were from 40-45 m.

[d] standard error of the mean.

[e] *F* statistic is the ratio of the paired variances (technically two mean squares)

[f] *p* value; probability that the observed differences are significant; "*" where *p* is 0.05 and "**" where *p* is 0.001.

5.2.7 Chlorophyll *a*

In this section, we compare concentrations of laboratory-measured chlorophyll *a* from the study by Raymond et al. (1997) and similar analytical measurements in this study. Chlorophyll concentrations at the Pelton forebay (RES04) were higher than those in LBC by a considerable margin (Figure 5-33.). The highest historical concentrations of chlorophyll were observed in spring and fall, with substantial declines in the summer. Chlorophyll concentrations in the epilimnion of the Pelton forebay (RES04) declined significantly between the 1990s and 2015–2017. The average chlorophyll value in 1994–1996 was 33.4 µg/L (*se = 4.58, n = 23*) compared to only 15.4 µg/L in 2015–2017 (*se = 5.35, n = 17*). This 54% decline in chlorophyll is statistically (*p = 0.015, F = 6.49*) and ecologically significant because of the major change it reflects in algal biomass. It can be argued that the most important chlorophyll data to present are for the warmer months. Limiting the historical and current data to only May–October makes the differences between the two periods even more distinct. Historical chlorophyll during those months averaged 45.2 ug/L (*se = 6.6, n =15*) compared to the current study average of 13.6 ug/L (*se = 1.7, n = 14*).

Although chlorophyll concentrations in Lake Simtustus showed a large decrease between the two study periods, there was no comparable change in transparency. This condition can sometimes occur when there is a change to larger celled phytoplankton or colonial taxa, which can cause a wide variation in the chlorophyll-Secchi disk relationship (Canfield et al. 1985). Some of the phytoplankton changes in Lake Simtustus also might reflect changes in fish biomass or fish species composition; however, few quantitative data are available with which to address this question.

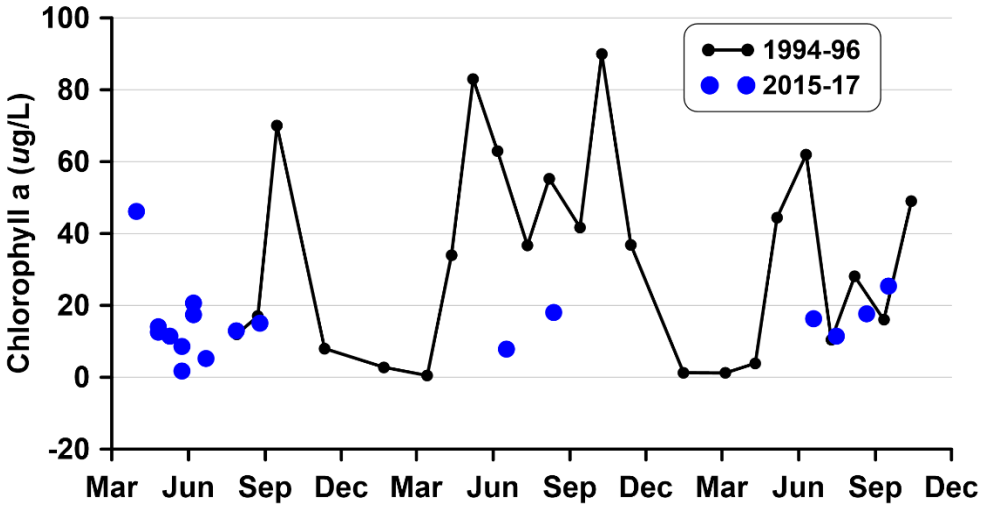

Figure 5-33. Concentrations of chlorophyll *a* (pheophytin corrected) at Pelton forebay (RES04) at 1-m depth from 1994–1996.

5.2.8 Phytoplankton Community Composition

As noted earlier for LBC, the detailed historical phytoplankton results from Raymond et al. (1997) are not available on a per-sample basis. Nevertheless, summary figures indicate that Lake Simtustus historically had low densities of *Dolichospermum* (*Anabaena*) and other cyanobacterial taxa. Bloom conditions were caused by high densities of diatoms, especially *Stephanodiscus* spp., with some notable contributions from *Ulnaria* (*Synedra) ulna*, *F. crotonensis, Melosira* (now *Aulacoseira*), and *Asterionella formosa*. Other taxa of note in Lake Simtustus were *Ceratium hirudinella, Chlamydomonas*, and the cryptophytes *Rhodomonas* and *Cryptomonas*.

Present-day phytoplankton taxa were similar to those identified in the 2006 historical data collected by ODEQ in that cyanobacteria were seldom dominant in Lake Simtustus (Figure 5-34). *Stephanodiscus* taxa were a significant component of the phytoplankton community, especially in the cooler months. *F. crotonensis* was an important taxon during the summer. Although other diatom taxa were present in Lake Simtustus during the present study, in few instances did they approach the high biovolume in the data from 1994–1996. Similarly,

Ceratium and *Chlamydomonas* were not abundant in the current dataset, whereas they achieved significant densities in the historical data.

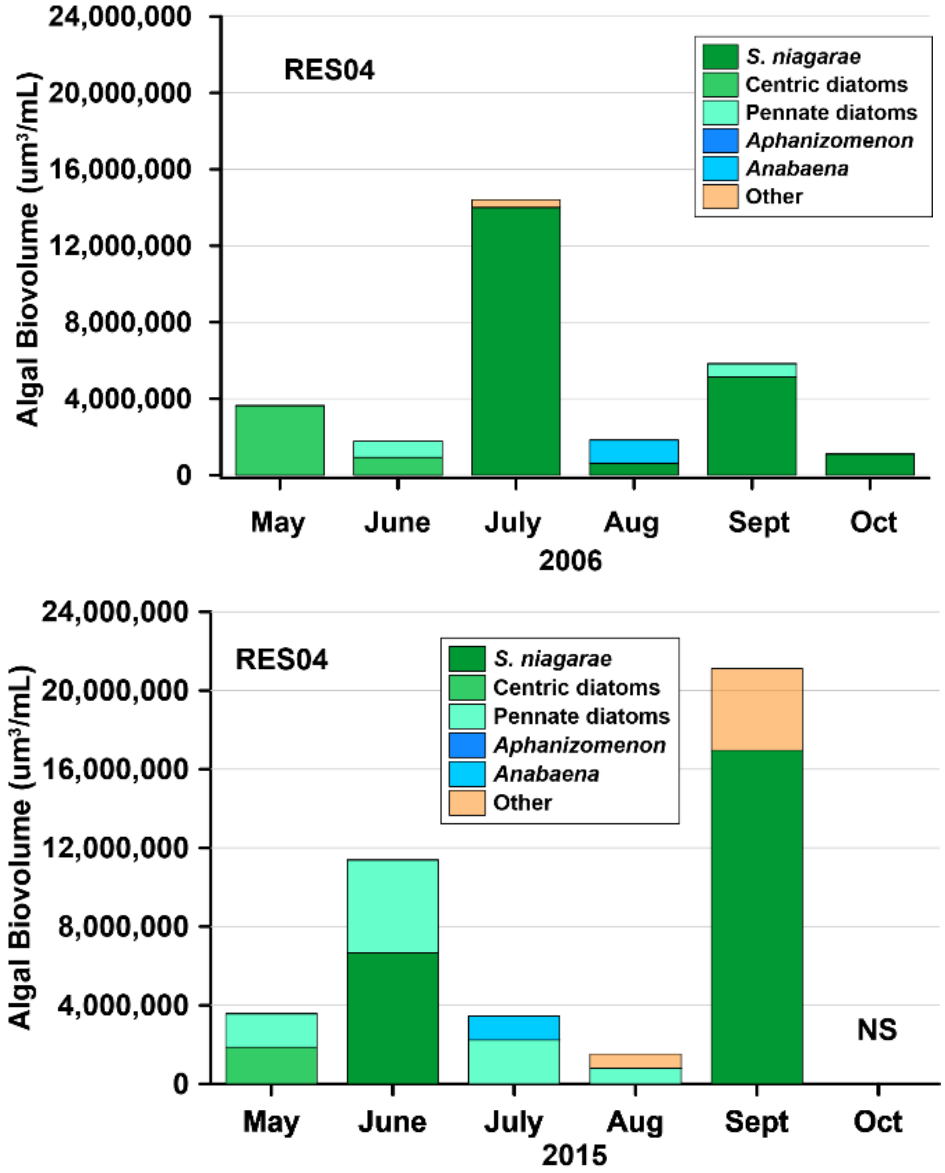

Figure 5-34. Epilimnetic algal biovolume at Pelton forebay (RES04) in 2006 and 2015.

5.2.9 Zooplankton

As noted previously, historical zooplankton results were not available on a per-sample basis from the 1994–1996 dataset. Therefore, only general assessments of possible changes in zooplankton populations can be made based on the 1994–1996 data. The more recent study data indicated that the zooplankton population in Lake Simtustus was dominated by rotifers, although not quite to the extent observed in LBC. If the historical zooplankton group summaries are representative of zooplankton present in Lake Simtustus two decades ago, a major shift has occurred in the community from copepods and cladocerans to the much smaller rotifers (Figure 5-35). Of course, in Lake Simtustus, the bottom outlet structure has not been altered and, therefore, any possible change in the zooplankton community cannot be attributed to increased export of zooplankton from the impoundment. We are unaware of any historical or current fisheries abundance data to assess if there is a possible relationship between changes in zooplankton community composition and changing fisheries. Prior to installation of the SWW, a proportion of kokanee and bull trout that entered the turbines would survive passage into Lake Simtustus, supporting a popular fishery. With construction of the SWW, all intakes were screened and fish no longer can enter Lake Simtustus from LBC, leading to a large reduction of kokanee and bull trout in the lake. The current Lake Simtustus fishery is maintained by annual stocking of hatchery rainbow trout (Megan Hill, PGE, pers. comm., September 2018).

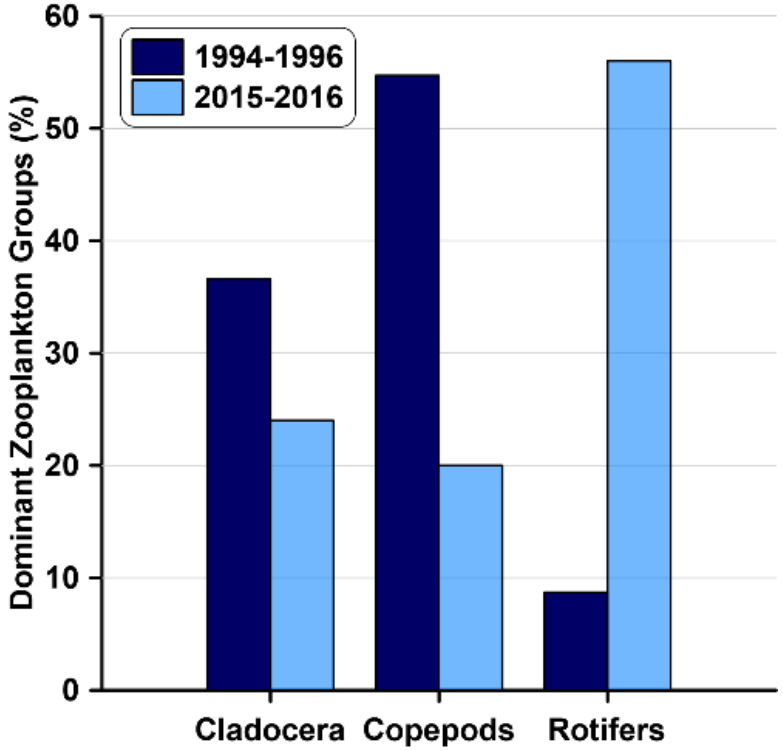

Figure 5-35. Major zooplankton groups at Pelton forebay (RES04) in 1994–1996 compared to 2015 and 2016.

6 Water Quality in the Lower Deschutes River

6.1 River Morphometry

The channel slope, depth, and width of a river help to determine the available habitat for periphyton and directly affect parameters such as pH and DO through aeration. Information about river morphometry is also essential for more accurately characterizing river reaches for numerical modeling of water quality. From the ReReg Dam (RM 100.1) to the mouth of the LDR (RM 0), the slope of the channel, measured using the LiDAR data, is relatively constant at 0.23% (12.2 ft/mi) (Figure 6-1) (DOGAMI, n.d.).

During the river float in 2016, hydroacoustic data were recorded for most of the river. Clearly those data are not meant to fully characterize river depth, but they do provide information about surprisingly deep reaches and depth variability. The maximum depth recorded was 9.4 m (30.9

ft) in a trough downstream of Buckhollow Creek. The mean and median depths recorded (*n = 1305 for 1-minute averages*) were 2.4 m (7.8 ft) and 2.1 (7.0 ft), respectively. The averaged SONAR depth shows a slight increase approaching RM 50 followed by a pronounced decrease in average depth in the lower 40 river miles. Although the recorded depths are likely biased towards deeper values, they are still instructive in illustrating that the LDR cannot be fully characterized exclusively by sampling biota in knee-deep waters.

River channel width was also derived from the LiDAR data. There is a substantial decrease in channel width mid-river as the river passes through narrow basalt passages, best represented by the reach immediately below Sherars Falls. The decrease in channel width results in an increase in stream velocity peaking near mid-river. Downstream of this zone, velocity declines and remains rather stable to the mouth.

Another important feature affecting river productivity is the amount of sunlight reaching the channel. Using the LiDAR data, it was possible to combine canyon topography with nearshore vegetation to compute sunlight reaching the channel (Figure 6-1 and Figure 6-2). Higher canyon walls closer to the river channel contribute to shading on the river as do trees ling the riverbank, whereas wide canyons and shorter nearshore vegetation result in increased duration of sunlight. The result shows increasing sunlight from RM 100 to RM 80, stable sunlight duration from RM 80 to RM 40, and another increase in sunlight duration in the lower reach of the river (Figure 6-1). The detailed example in Figure 6-2 shows a plan view of the river canyon at Maupin for bare ground to provide the canyon morphometry and with vegetation to show tree canopy height in the canyon.

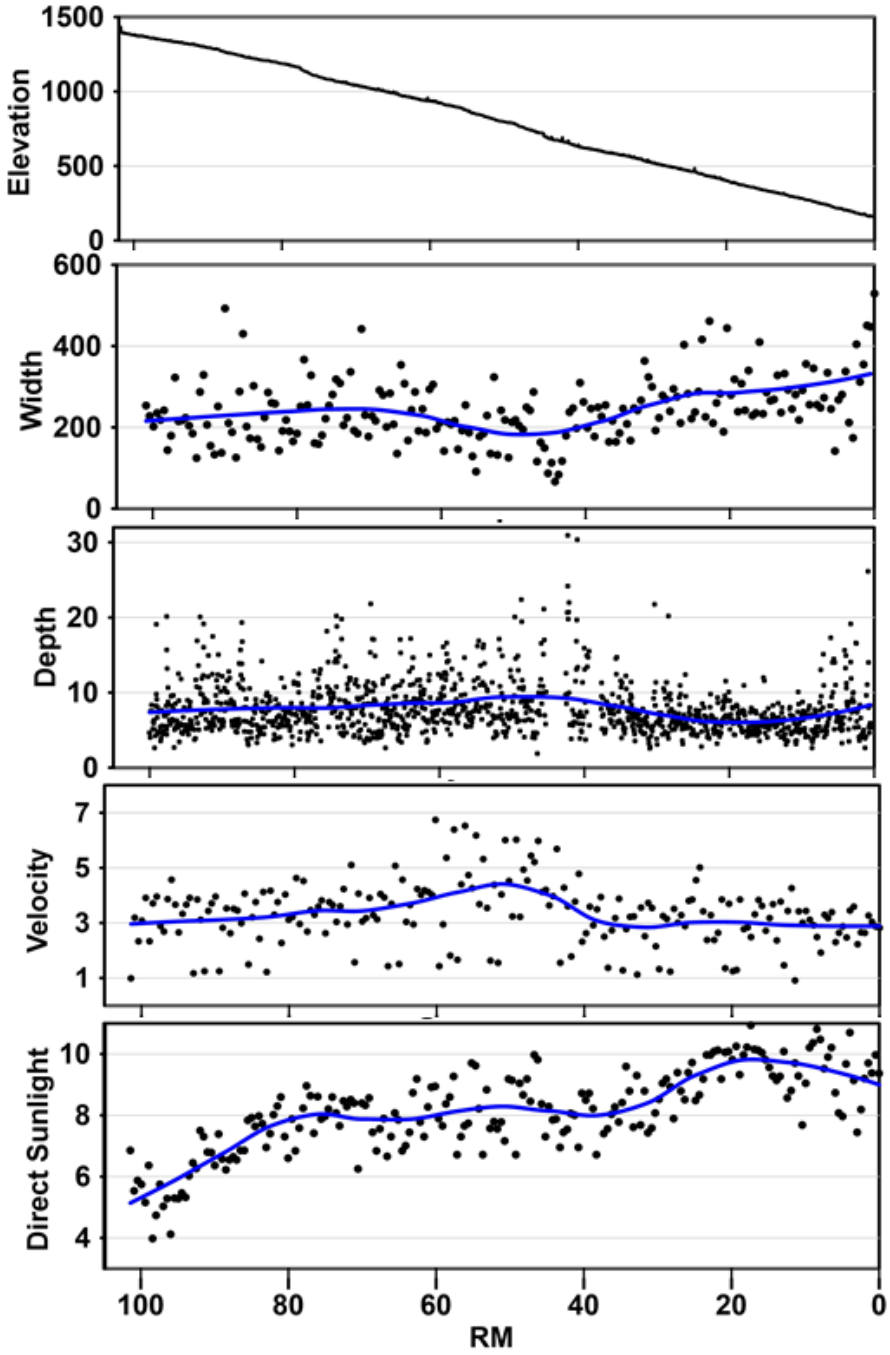

Figure 6-1. Summary of physical attributes for the LDR. Elevation, depth and width units are in feet. River velocity is in mph based on flows from July 15, 2015. Direct sunlight is calculated sunlight reaching the mid-line of the river on July 15, 2015 using the LiDAR data on canyon topography and nearshore vegetation height. The blue lines are LOESS fits of the observed data.

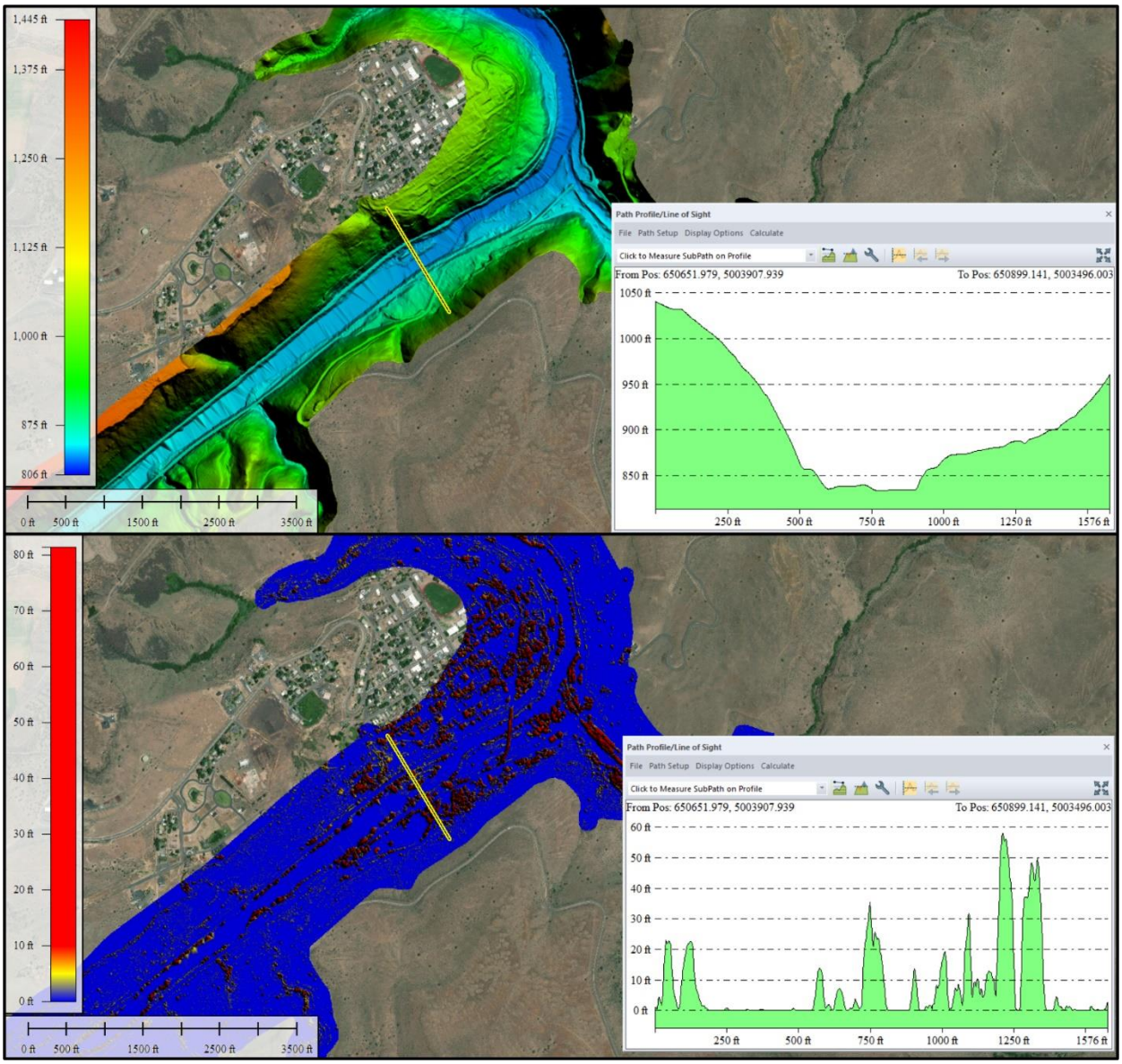

Figure 6-2. LiDAR images of the LDR at Maupin. The top figure shows LiDAR return signal for bare ground compared to the bottom figure which shows the vegetation signal for the same area. The same cross-sections are shown for each image illustrated as a yellow line across the channel.

6.2 Water Temperature and Quality

6.2.1 Temperature

Water temperature is a critical component of water quality because it affects chemical transformation rates and directly affects the survivability of aquatic organisms. LDR water temperatures can be characterized as cold in winter, regardless of location. At the ReReg Dam, the water is cool throughout the remainder of the year, and temperatures at the mouth of the LDR are typically warm as ambient air temperatures increase during the summer. Figure 6-3 shows continuous temperature data immediately downstream of the ReReg Dam for 2015 through 2017. The coldest initial temperatures at the site occurred in 2017, when values approached 5˚C and remained lower than those measured in 2015 and 2016 until April. Temperature values increased rapidly from winter to June, when there was a brief decline before reaching a peak in early July. From July through much of August, temperatures differed considerably among the 3 years before stabilizing in September and then declining throughout the remainder of the year.

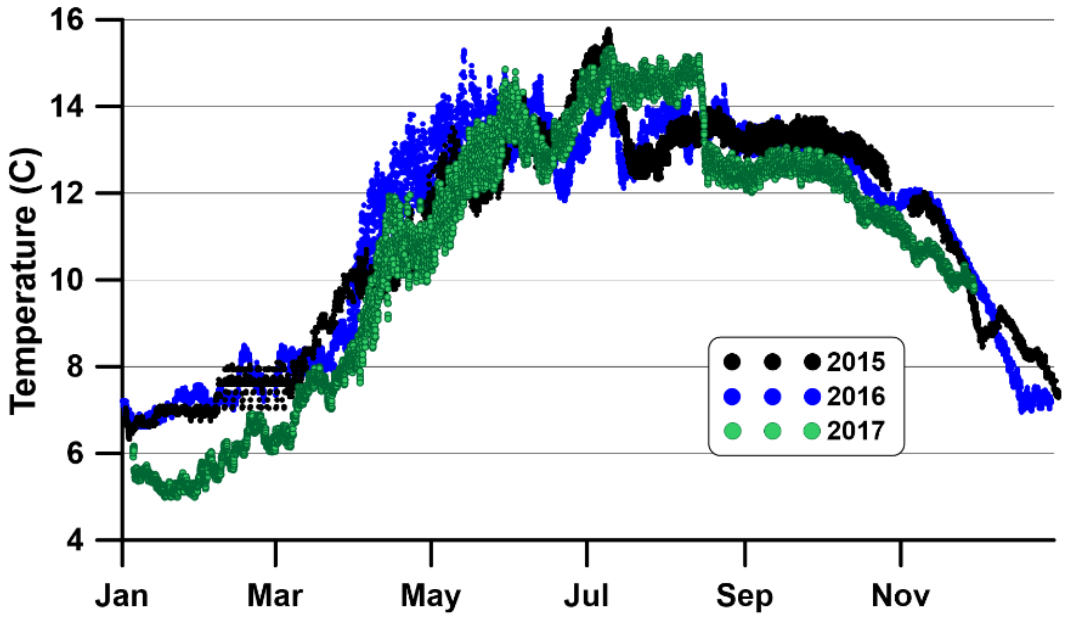

Figure 6-3. Water temperature measured below the ReReg Dam (RM 100.1) from 2015 through 2017.

As ambient air temperatures increased during the summer, water temperatures at the mouth of the LDR approached 24°C (Figure 6-4). The figure illustrates the warming that occurs downriver, where the river can gain about 0.1°C per mile during midsummer. The pattern in temperature increase is not constant, but varies daily with solar radiation, changes in discharge from the Project, and influx of water from tributaries and groundwater.

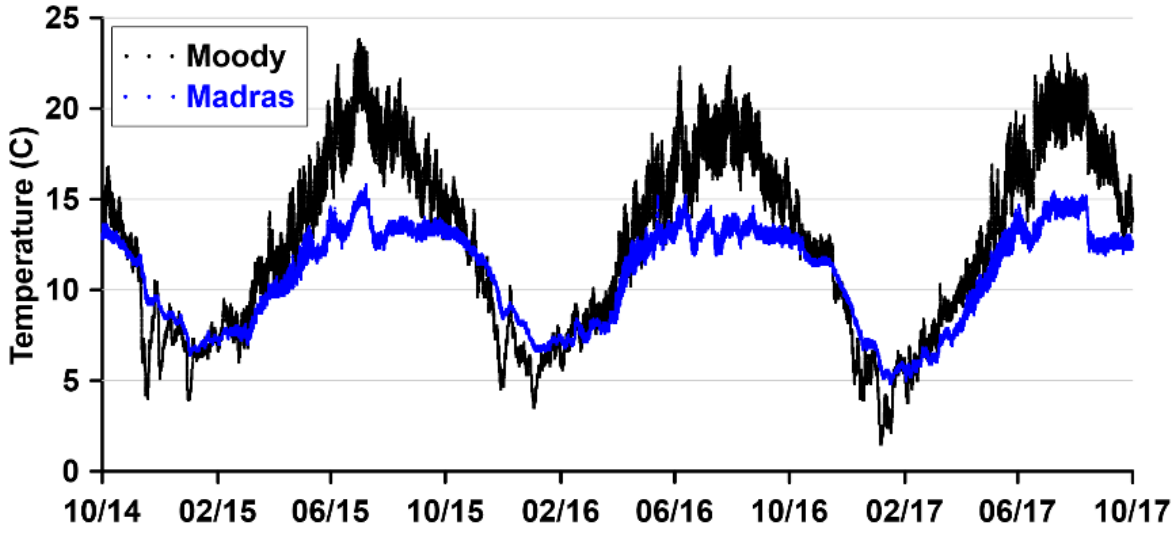

Figure 6-4. River temperatures below the ReReg Dam (RM 100.1) and at Moody (RM 1) of the LDR for WY2015–2017 using 15-min data from USGS (n.d).

The series of 72-hr surveys conducted in July and August of 2015 and 2016 illustrate the small diel variations in temperature at the ReReg Dam, which increased substantially by the time flows reached the mouth of the river (Figure 6-5). However, in the vicinity of Harpham Flats (RM 55.8), the expected sinusoidal diel variations in temperature were replaced by more complex patterns that appear to moderate to both higher and lower river temperatures and to alter the regular pattern of response to thermal loading from solar radiation. A minor effect is caused by damping associated with cool tributary inputs above selected sites. These temperature patterns along the river are addressed in greater detail in the modeling results (Section 10.7).

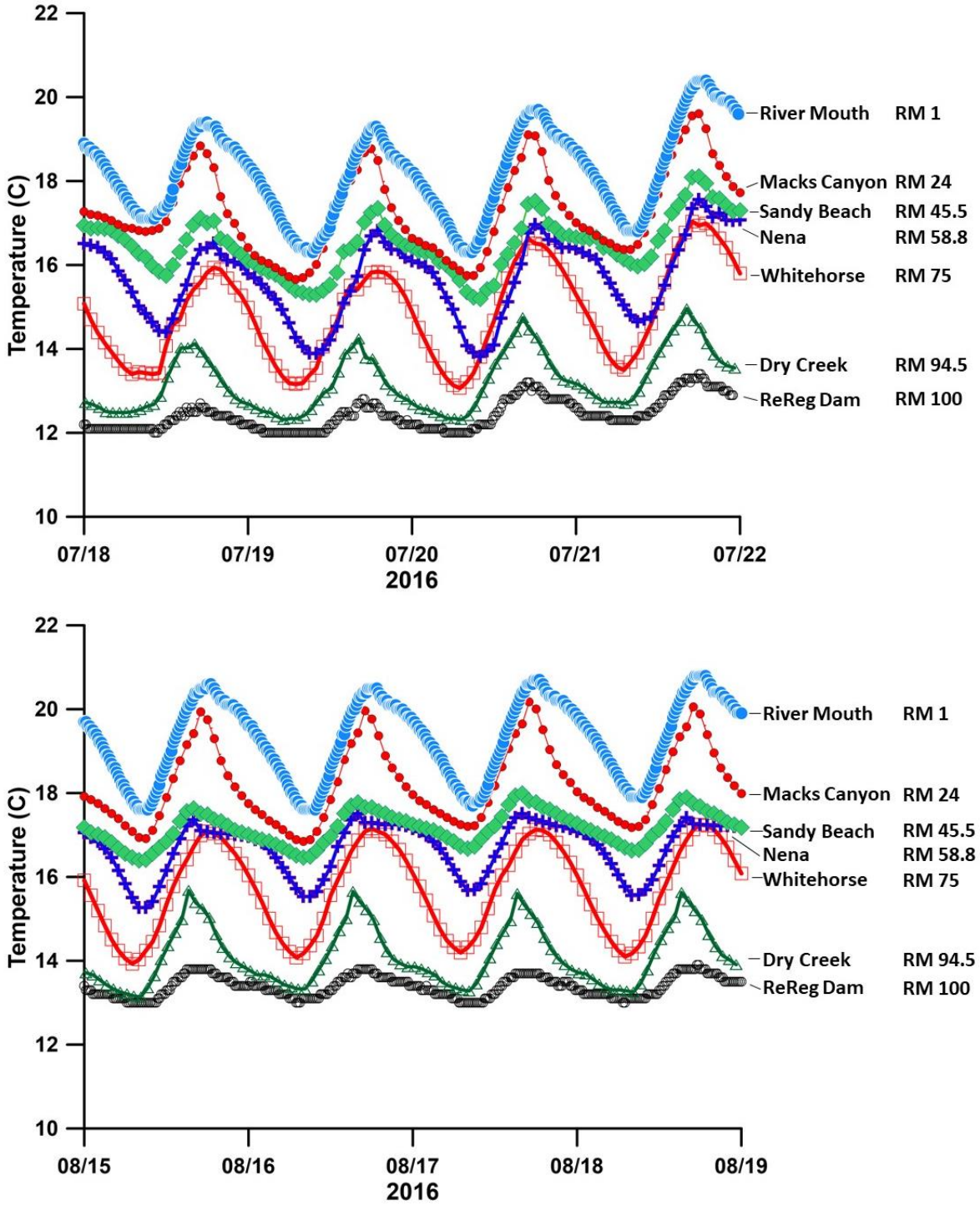

Figure 6-5. River temperature measured at six sites on the LDR during July 2016 (*top*) and August 2016 (*bottom*). Measurement locations are listed top to bottom in order of the data lines (*insets*). The sites labeled River Mouth and ReReg are USGS stream gage sites; other data are from PGE.

The progression in water temperature from the ReReg Dam to the mouth of the river is further illustrated with continuous measurements during a float of the river in July 2016 (Figure 6-6). The diel pattern is clearly illustrated, although data for the zone of likely the most significant distortion in the pattern are not available because of equipment issues and the portage over Sherars Falls from Sandy Beach to Buckhollow Creek.

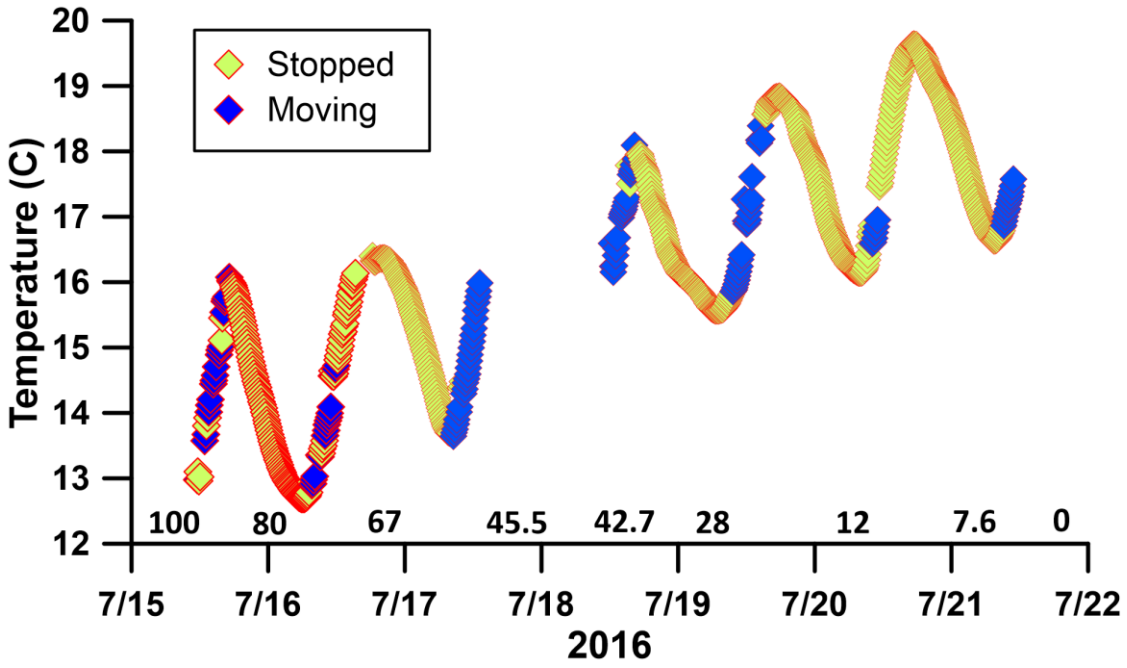

Figure 6-6. River temperature recorded during a float of the river in July 2016. River miles for selected locations are shown above the dates for reference. River mile 100 is immediately below ReReg Dam, RM 45.5 is Sandy Beach, and RM 0 is the mouth of the LDR.

6.2.2 pH

pH is an important parameter that reflects photosynthetic activity; as aquatic plants assimilate CO_2 dissolved in water, the acidity of water decreases, which increases pH. pH is regulated by ODEQ because of its potential effects on aquatic organisms. The upper pH water quality standard for much of Oregon, including the LDR, is 8.5. The pH data at the ReReg Dam for the 3 study years illustrate some of the challenges in measuring pH during extended deployments (Figure 6-7). The data included values below pH 7.0 in January 2015 that are unlikely to have

occurred because the moderate alkalinity in the river normally (typically > 50 mg/L as calcium carbonate [$CaCO_3$]) buffers the water against such low excursions. Two other issues with the 2015 pH data were the extended periods of similar values that occurred from March to July and the abrupt decrease in pH at the beginning of October 2015. The patterns in pH measured in 2016 are likely more representative of typical pH values in the river at the ReReg Dam. However, pH values plummeted significantly in September 2016, much more so than was expected given the acid-base chemistry of the river. pH values from April through August 2016 were above 8.5. The average pH in 2017 was slightly lower than that observed in 2016, with a significant decline in early August, and then relatively stable throughout the remainder of the sampling period. These data were not used in the water quality modeling because, as noted earlier, the models calculated pH from other chemical constituents.

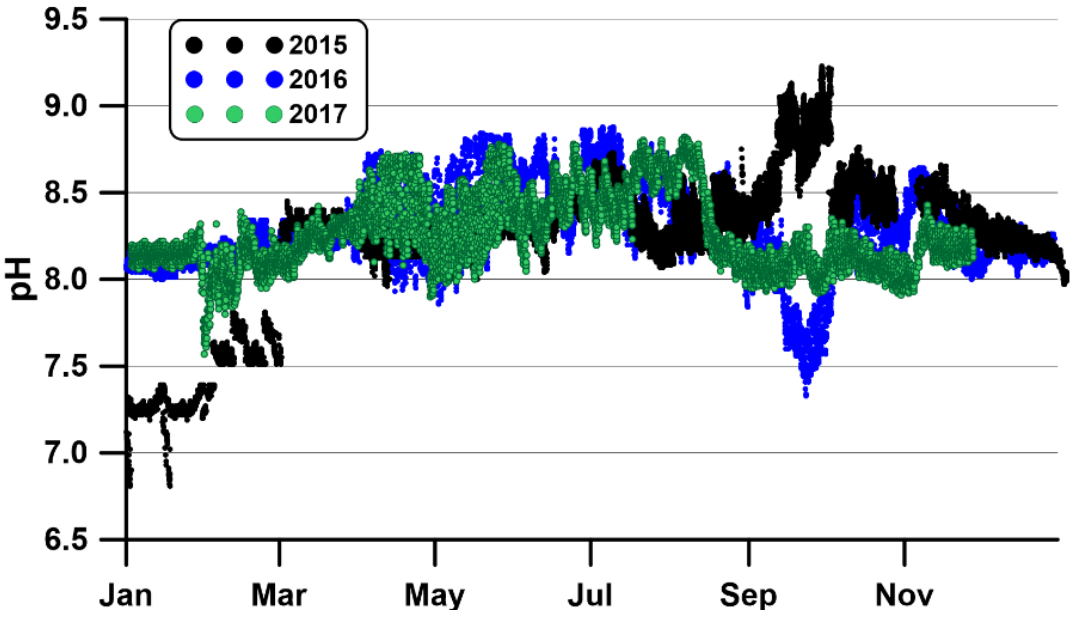

Figure 6-7. pH measured at the ReReg site (LDR01) from 2015 through 2017.

During the 72-hr surveys, the pH values showed an increasing diel amplitude at sites in locations further downstream (Figure 6-8). The diel peak-to-peak amplitude of pH below the ReReg Dam is only about 0.2 pH units, whereas at the mouth, the same metric is about 1.5 pH units. It is unclear if the lower pH values observed in August 2016 for the Trout Creek Campground site

(RM 88.5) were measurement artifacts or represented actual conditions (Figure 6-9). The pH measurements recorded during the river float mimicked the same general patterns as those recorded in the 72-hr surveys (Figure 6-10). The dampening of pH values mid-river was similar to values observed for temperature patterns as well. pH reflects photosynthetic activity and so, if temperature is suppressed, as in the case of the mid-river data, photosynthetic rates would be expected to respond in a similar manner.

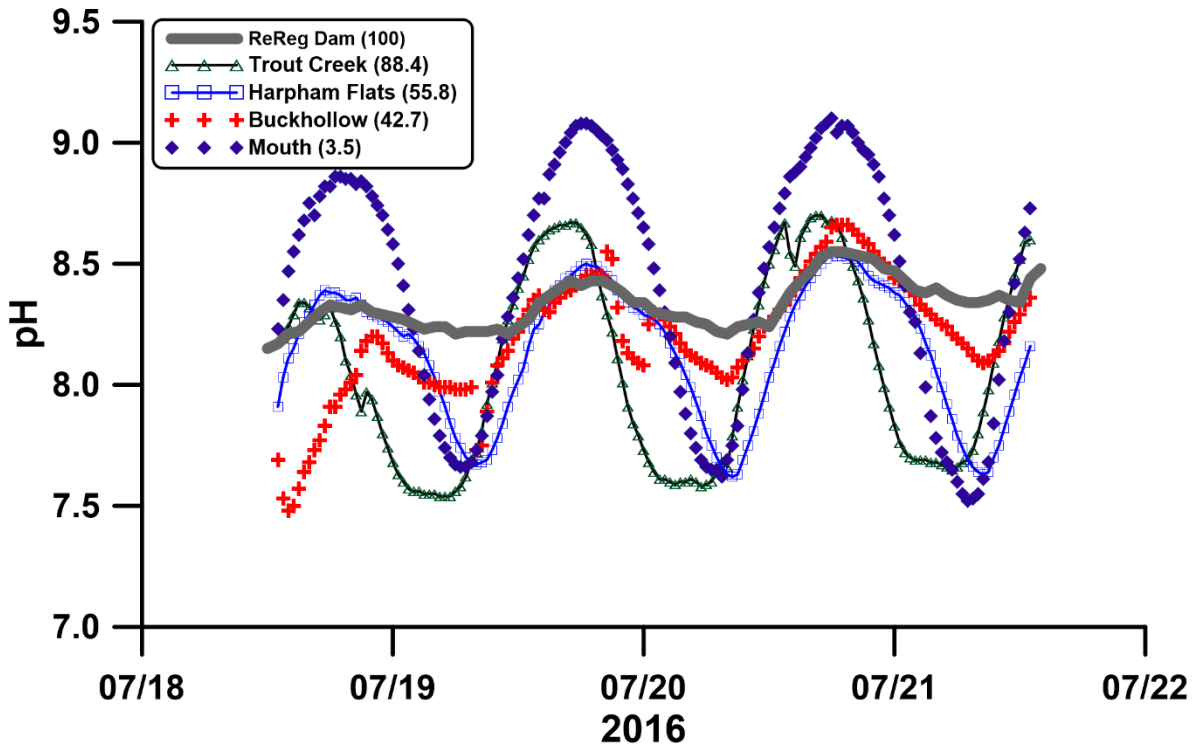

Figure 6-8. pH measured at the 72-hr monitoring sites in July 2016.

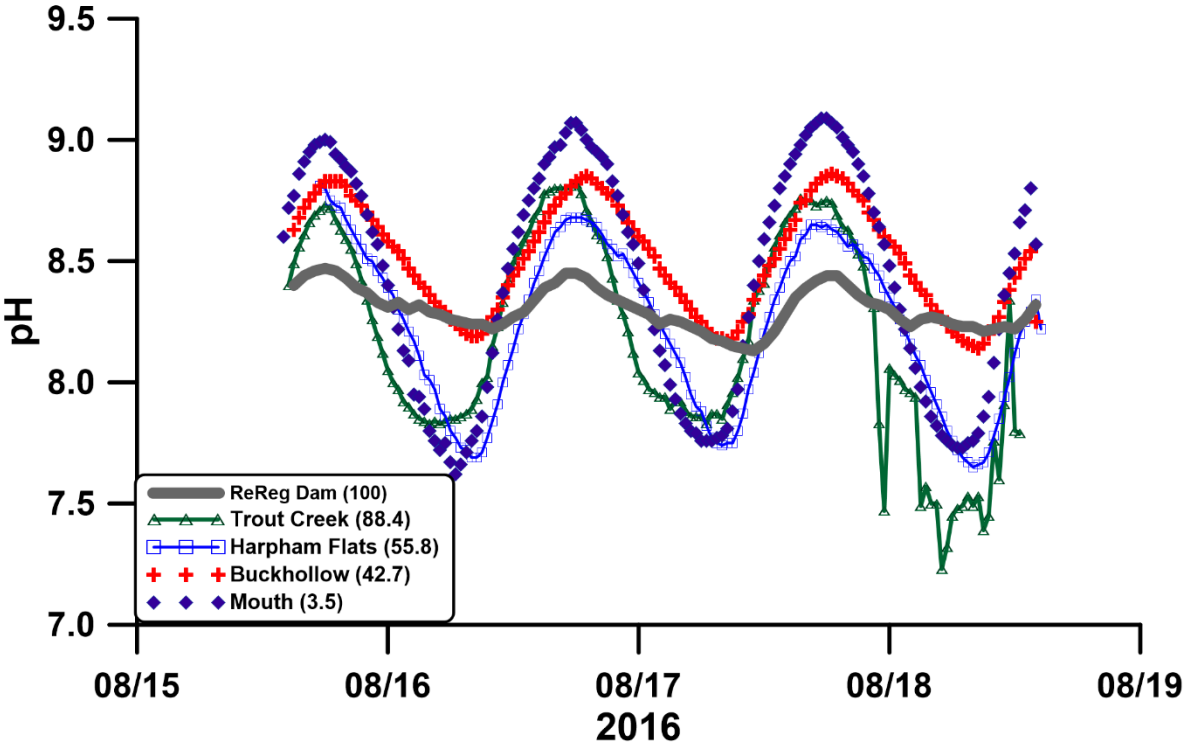

Figure 6-9. pH measured at the 72-hr monitoring sites in August 2016.

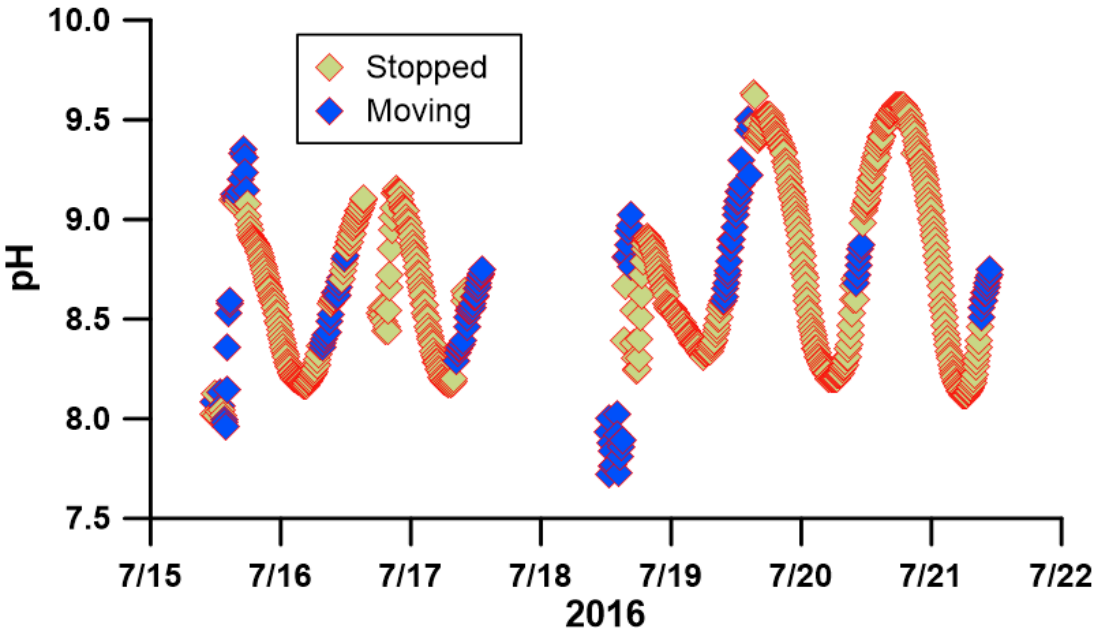

Figure 6-10. pH measured during the river float of July 2016. The gap in data collection represents the portage around Sherars Falls (RM 44). See Figure 6-7 for approximate river miles.

6.2.3 Dissolved Oxygen

Concentrations of DO at the ReReg site (LDR01) indicate that DO remained high through March and then began to decline as water temperatures increased more rapidly in April (Figure 6-11). The decline in DO concentrations from spring through summer represented, in part, the decreasing solubility of oxygen (and gases in general) in warmer water. Exceptions to this condition occur on a short-term basis as high rates of oxygen released from photosynthetic activity exceed equilibration with the atmosphere.

Other factors contributing to declining oxygen concentrations during summer could be associated with increases in oxygen consumption from degrading organic matter present in the water, night-time respiration of algae suspended in the water and attached to the substrate, a greater release of hypolimnetic water from the SWW during the summer. DO concentrations reached a minimum in late July 2015, but that minimum was not repeated until early in September 2016. Both DO concentrations and percent saturation began to recover after water temperatures began to decrease in the fall. Percent saturation during 2015 and 2016 declined well below the saturation values expected for the site (elevation 1,390.25 ft) through much of the summer. For example, the solubility of oxygen at this elevation would yield a concentration of DO of 10.5 mg/L at 12°C, considerably higher than the minimum observed values of near 7 mg/L. Some of the abrupt changes in values shown in Figure 6-11 might be attributed to monthly maintenance activities associated with downloading data and recalibrating the instrument. Other changes such as those that occurred in summer can be attributed, in part, to actions by PGE operators to increase DO at the site by spilling water through the ReReg Dam to increase aeration. Additionally, a change in instruments was made in September 2017 from a Hydrolab DSX-5 to a Sea-Bird Scientific sonde. These data would typically be edited to remove artifacts; however, they have been reported to ODEQ.

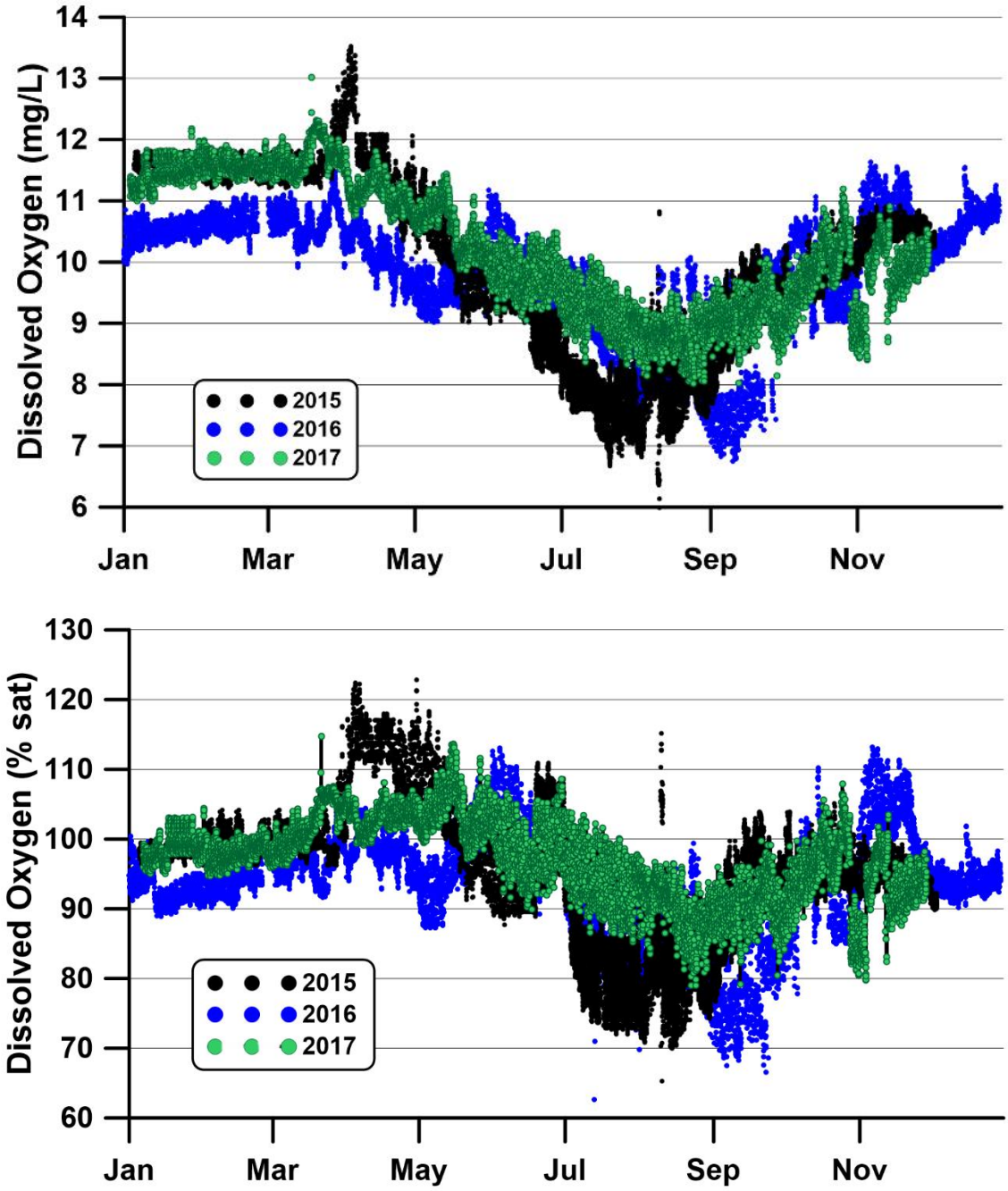

Figure 6-11. DO concentration (*top*) and DO percent saturation (*bottom*) measured at the ReReg site (LDR01) from 2015 through 2017.

The results from the 72-hr surveys provide data that illustrated the non-linear behavior along the course of the river. DO concentrations and saturation had low amplitudes at the ReReg Dam and high diel amplitudes at several locations in the river (Figure 6-12). Daily concentrations of DO at the ReReg Dam varied by about 0.6 mg/L in July 2016 and by over 2 mg/L further downstream. However, at the Buckhollow Creek site, the diel variation was only about 0.3 mg/L. The Buckhollow Creek site is located downstream of Sherars Falls and apparently aeration associated with the turbulence at the falls stabilized both DO concentrations and degree of supersaturation. The river float revealed a pattern in DO concentrations and saturation similar to the pattern observed in the 72-hr surveys (Figure 6-13). Again, there was a pronounced increase in the diel amplitude of DO in the lower reaches of the river.

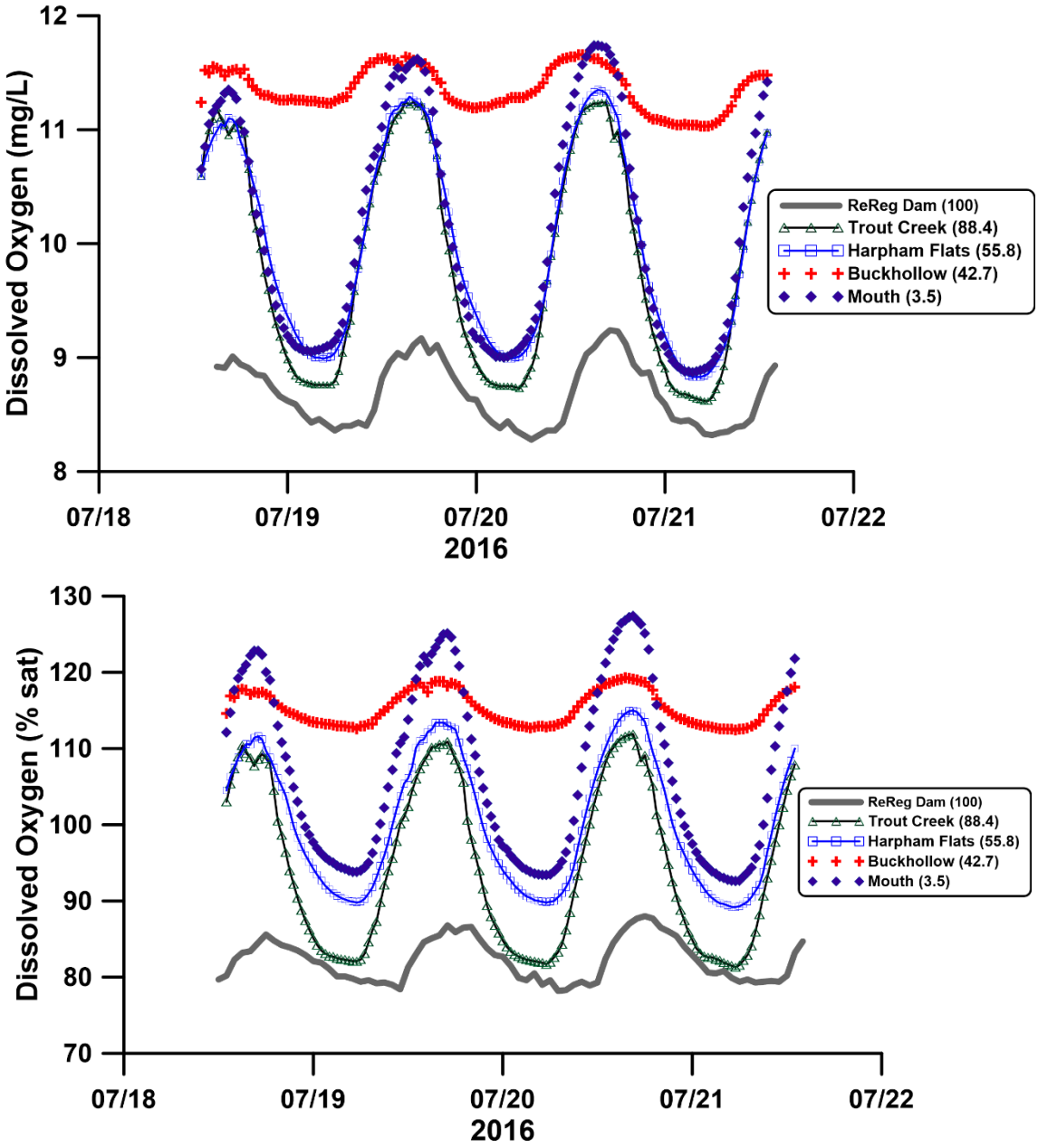

Figure 6-12. DO concentration (*top*) and DO percent saturation (*bottom*) of at the four diurnal monitoring sites on the LDR for July 2016.

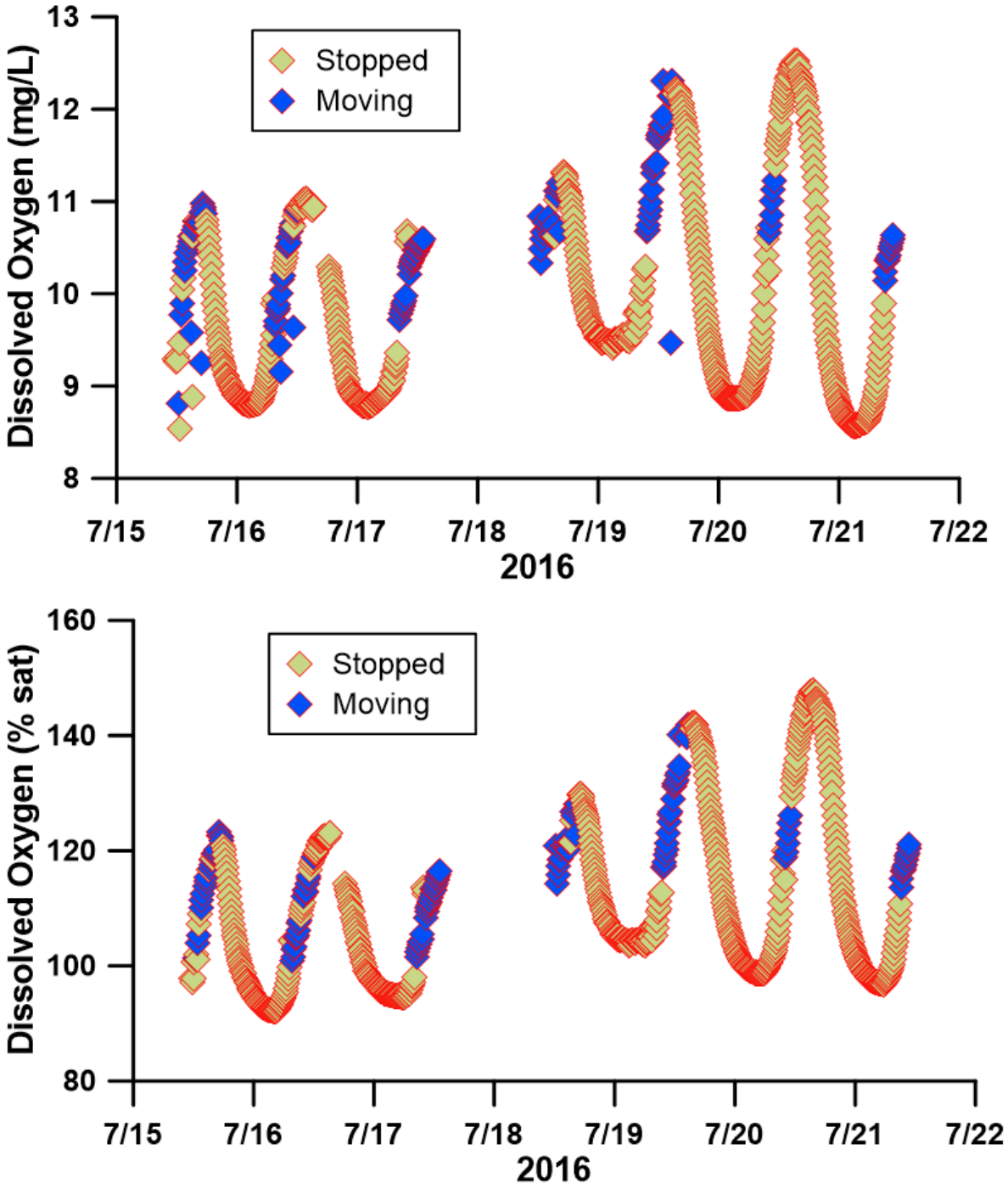

Figure 6-13. DO concentration (*top*) and DO percent saturation (*bottom*) in the LDR measured during a river float in July 2016. The gap in data collection represents the portage around Sherars Falls (RM 44). See Figure 6-7 for approximate river miles.

As part of the river float, high-density temporal resolution (1 min) measurements of DO were collected on the lower portion of the river starting on July 19, 2016 and ending on July 21, 2016. The measurements showed a highly symmetrical pattern with minimum concentrations of DO occurring from about 0300 hr to 0500 hr and a peak near 1500 hr (Figure 6-14). A total diel variation of 4 mg/L is substantial for a river of this magnitude. Water temperature at this location (near Harris Canyon) and date lagged behind the peak in DO by 3 hr, whereas the minimum temperatures lagged behind the minimum values of DO by up to 6 hr. This was the only site where there was an extended stay to examine this effect, although we expect this condition would be observed throughout much of the river.

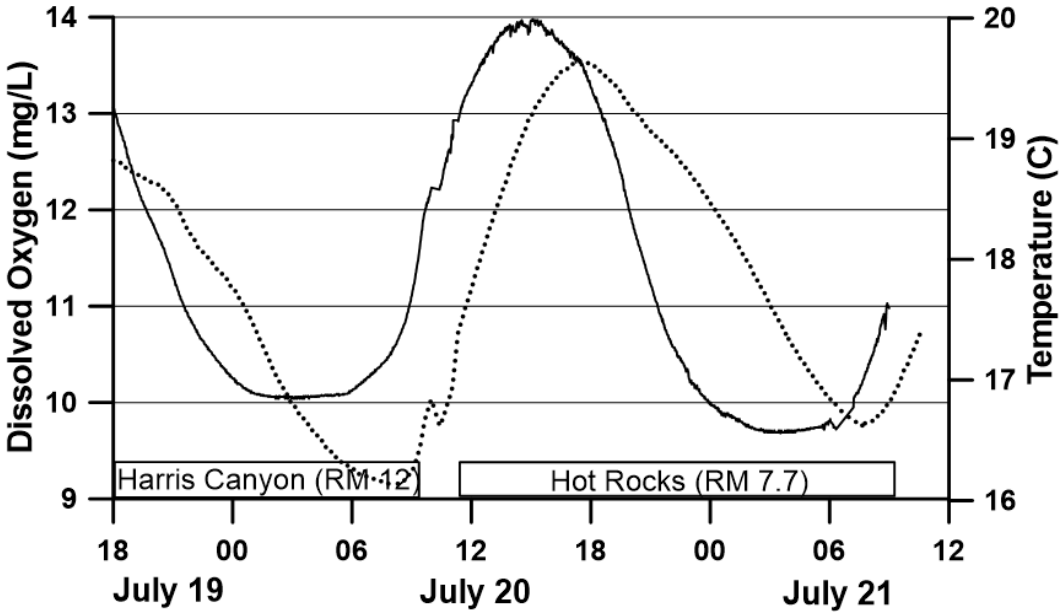

Figure 6-14. DO measurements (*solid line*) and water temperature (*dashed line*) during stationary conditions in the LDR in 2016. The period in late morning of July 20 represents moving sites downstream from Harris Canyon to Hot Rocks.

6.2.4 Turbidity

In the LDR at the ReReg Dam, typically there is little input of suspended inorganic solids from erosional processes because the dams capture much of the entrained sediment from tributary inputs. Some pumice enters LBC from tributary and shoreline erosion but tends to be larger

material rather than the small, micron-level particles measured by turbidity sensors. Additionally, major runoff events can promote turbid flows from tributaries. In that situation, larger suspended solids will settle rapidly in the impoundment, but clay particles will remain suspended for considerably longer. These runoff events can be highly transient and might not be well represented with the sampling frequency used in this study, although the ZAPS LiquID unit might have captured one such event. In mid-March 2017, a moderately large runoff event occurred in the Crooked River watershed. Peak discharge in the Crooked River above Opal Springs reached 3,270 cfs, considerably more flow than was experienced during the previous two years. That flow likely transported turbid water to LBC. A notable spike in turbidity was measured at the ReReg Dam in early April, which gradually dissipated over several weeks (Figure 6-15). However, throughout most of the year, we believe turbidity at the ReReg site (LDR01) is likely caused by entrained algae. Support for this conclusion is discussed in the section of the report showing chlorophyll and turbidity measurements in Round Butte forebay (RES07) (see Section 6.2.1.16).

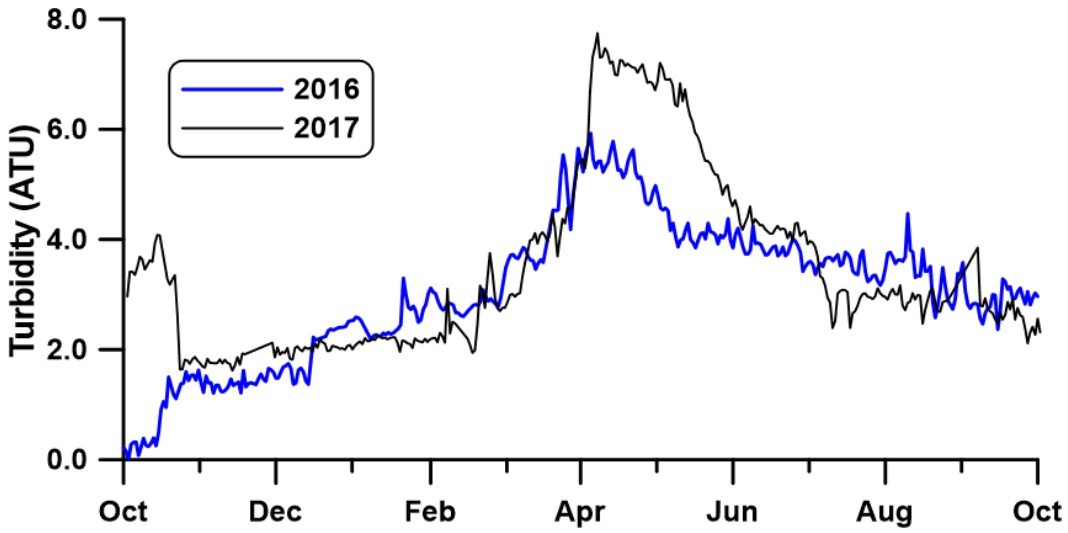

Figure 6-15. Daily average turbidity measured at the ReReg site (LDR01) for WY2016–2017 measured by the ZAPS LiquID unit. Two outliers (117 and 84 ATU) were removed from the file for August 26–27, 2017.

The most comprehensive time series of turbidity data available for the Project is the continuous measurements below the ReReg Dam with the ZAPS LiquID unit. It measured scattering using a zero-angle path, which results in a slightly different measurement process than most turbidity sensors employing a 90-degree path angle. Turbidity remained low throughout the winter and gradually increased in early spring until a pronounced increase was observed towards the end of March. The peak in April was followed by a relatively rapid decline in May and a more gradual decline through the remainder of the water year.

The spatial data available for turbidity showed a slight increase in turbidity from the Project to the mouth of the LDR. The turbidity values at the mouth during the July 2016 72-hr survey were about 1–3 NTU values higher than those observed at the upstream sites (Figure 6-16). The higher values might be associated with the influx of turbid waters from the White River, a glacially fed tributary just upstream of Sherars Falls, although differences in sonde performance at these low levels also is possible. The turbidity values at Buckhollow Creek were elevated by discharge from the White River, which is less than 4 RM upstream from Buckhollow Creek, and by entrained air bubbles from Sherars Falls, which is only 1 RM upstream. The data from the river float using a sonde showed a slight, but nonsignificant increase in turbidity from the Project to the mouth of the LDR (Figure 6-17).

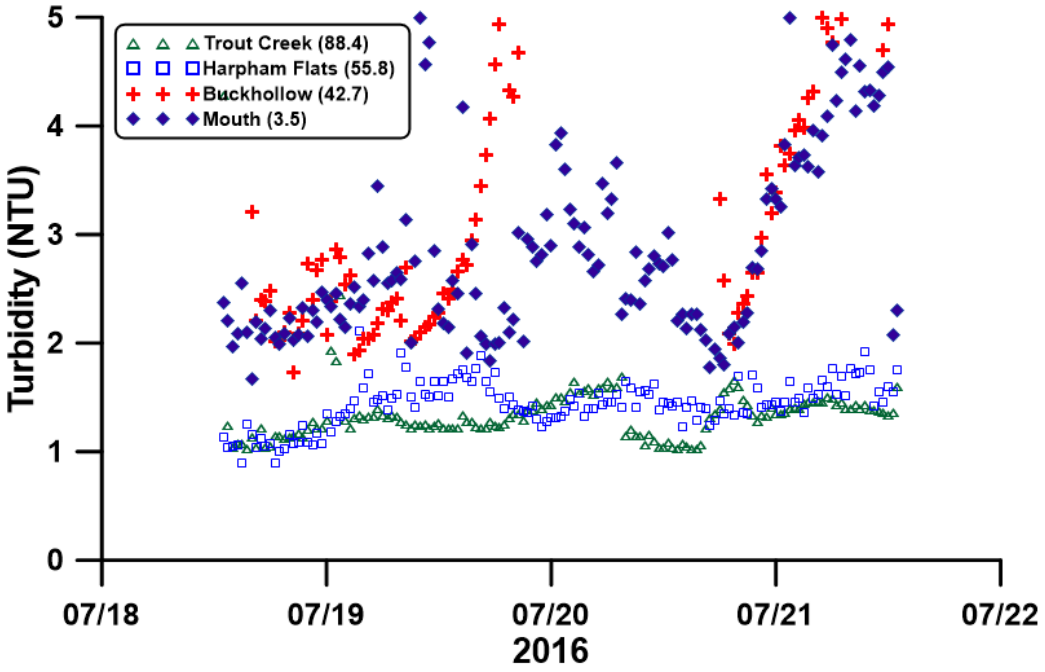

Figure 6-16. Turbidity measured at the 72-hr study sites in July 2016. Several outliers higher than 5 NTUs (primarily from Buckhollow Creek) are not shown.

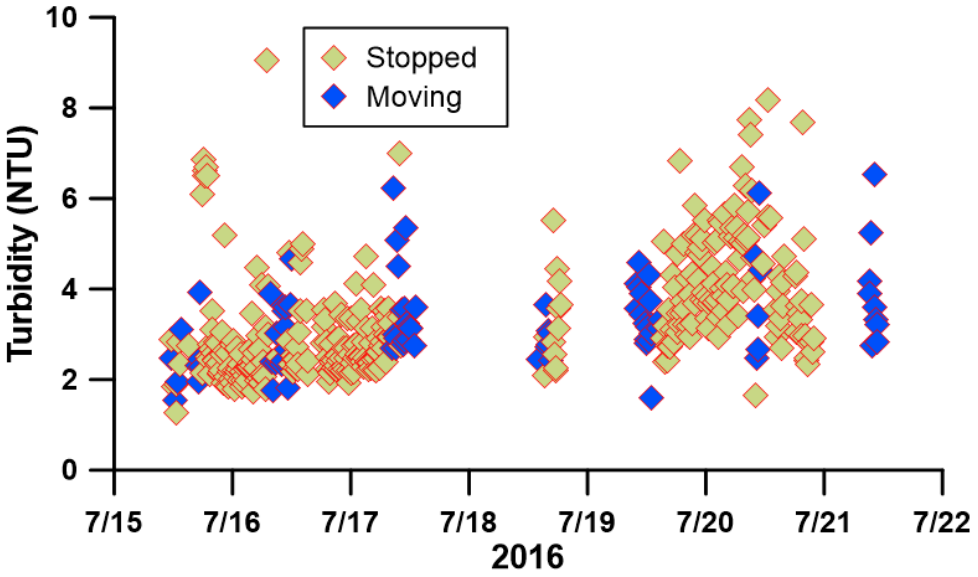

Figure 6-17. Turbidity measured during the river float in July 2016. The gap in data collection represents the portage around Sherars Falls (RM 44). See Figure 6-7 for approximate river miles.

6.2.5 Nutrient Chemistry

In addition to light, temperature, substrate composition, bedload movement, macroinvertebrate grazing, and current velocity, river periphyton communities can be strongly influenced by availability of nutrients. The nutrients most commonly associated with limiting algal growth are phosphorus and nitrogen, although silicon can be limiting for diatoms. Trace elements can sometimes be limiting, but that is uncommon and difficult to confirm. Trace elements that have been found to limit some algal growth include barium, cobalt, copper, iron, manganese, molybdenum, selenium and zinc (Sigee 2005).

Silicon is abundant in the LDR because of the weathering of highly siliceous basalts and other volcanic rocks in the basin. Concentrations of silica (as SiO_2) measured in the three inlets in April 2018 ranged from 30.0 mg/L (Metolius River) to 37.8 mg/L (Crooked River) and, in the Round Butte forebay (RES07), they ranged from 30.2 mg/L at the surface to 31.6 mg/L at 80 m. Only when silica concentrations are less than 0.5 mg/L do they become a limiting factor for a number of diatom species (Wetzel 2001); consequently, silica is never limiting for diatoms either in the Project reservoirs or the LDR.

Phosphorus concentrations exhibited only slight changes along the length of the LDR (Figure 6-18). PO_4 concentrations declined about 0.015 mg/L from the ReReg dam to the mouth (ns) and TP showed no measurable change. Both TN and NO_3 exhibited significant declines from RM 100 to RM 0, whereas concentrations of NH_3 remained low but above detection limits for the length of the river. The ratio of DIN:PO_4 shows a substantial decline along the length of the river but particularly downstream of RM 20, signaling the likelihood of N-limitation at times throughout the river. Cl^- concentrations are relatively unchanged in the river, which provides some evidence that other major anthropogenic or agricultural factors are not dramatically altering conservative components in the river. Nutrient concentrations by RM are summarized in Table 6-1.

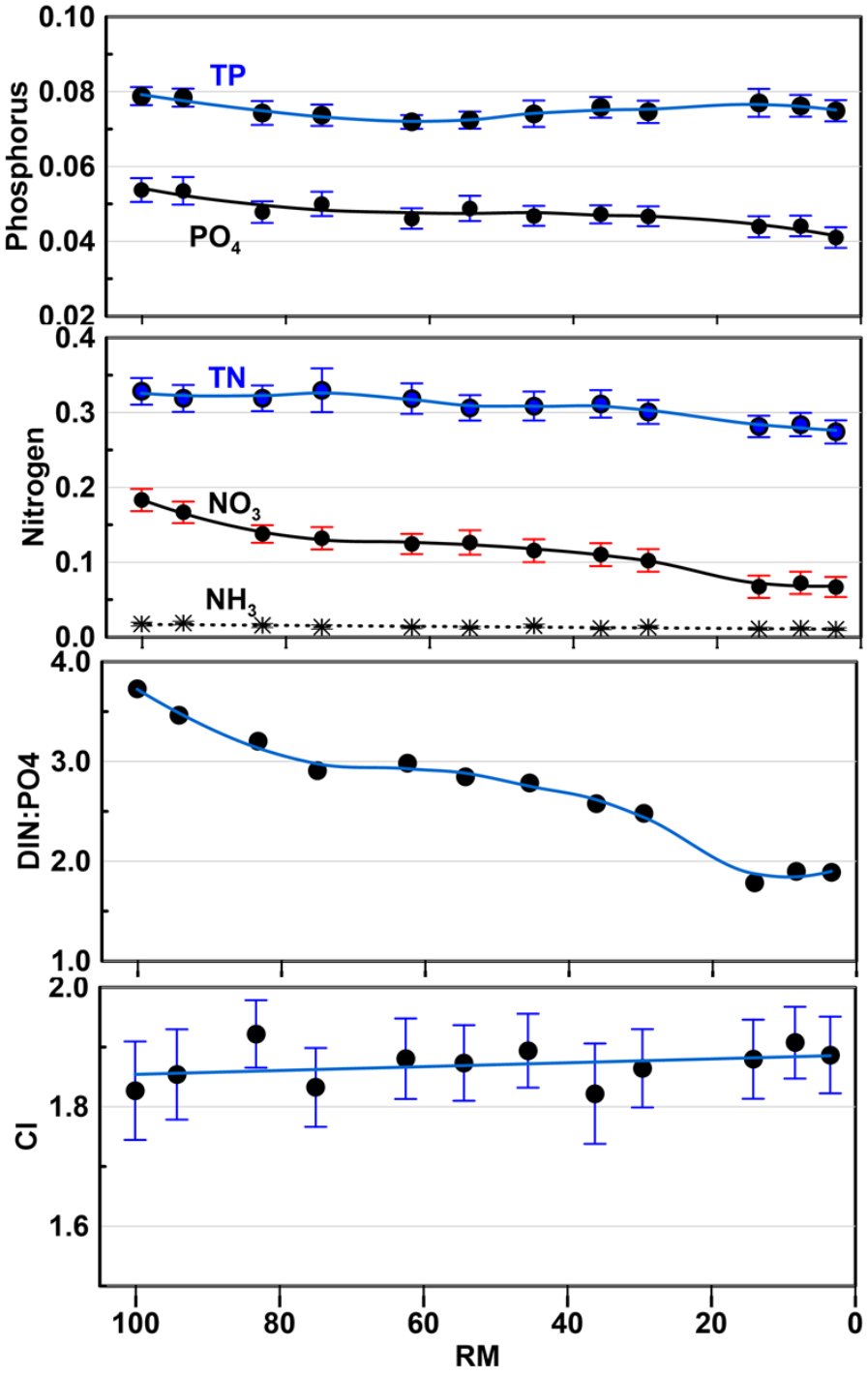

Figure 6-18. Mean and standard error of nutrient concentrations, DIN:PO4 ratio, and Cl^- in the LDR from 2015–2017. Concentrations are reported in mg/L.

Table 6-1. Mean and standard error of nutrients concentrations measured in the LDR. Results for Runs tests illustrate which parameters show significant changes along the length of the river.

RM	Sample Size	TP		PO4		TN		NO3		NH3		DIN:SRP	
		Mean	se[a]	Mean	se	Mean	se	Mean	se	Mean	se	Mean	se
3	24	0.076	0.0032	0.041	0.0031	0.272	0.0171	0.064	0.0148	0.012	0.0017	1.91	0.352
8	26	0.076	0.0029	0.044	0.0027	0.284	0.0156	0.073	0.0148	0.012	0.0017	1.94	0.293
14	26	0.077	0.0037	0.044	0.0027	0.281	0.0143	0.070	0.0153	0.012	0.0016	2.00	0.283
29	26	0.076	0.0034	0.047	0.0029	0.292	0.0166	0.099	0.0169	0.015	0.0018	2.38	0.273
36	25	0.076	0.0031	0.047	0.0026	0.298	0.0193	0.107	0.0171	0.013	0.0017	2.48	0.280
45	25	0.075	0.0041	0.046	0.0029	0.299	0.0193	0.111	0.0171	0.017	0.0023	2.70	0.290
54	27	0.072	0.0023	0.048	0.0033	0.306	0.017	0.126	0.0163	0.013	0.0015	2.96	0.304
62	25	0.072	0.0021	0.046	0.0030	0.302	0.0204	0.119	0.015	0.015	0.0020	3.04	0.352
75	25	0.074	0.0028	0.049	0.0032	0.330	0.0292	0.133	0.0149	0.014	0.0027	3.04	0.285
83	27	0.075	0.0036	0.048	0.0031	0.311	0.0179	0.136	0.013	0.016	0.0028	3.16	0.258
94	27	0.078	0.0024	0.053	0.0035	0.319	0.018	0.167	0.0144	0.019	0.0024	3.54	0.317
100	26	0.079	0.0028	0.054	0.0034	0.320	0.0187	0.183	0.0163	0.019	0.0026	3.85	0.226
Runs Test		ns		ns		**		**		ns		**	

Notes:

a standard error

ns = not significant

** = Significant at $p < 0.05$

An examination of TP illustrates two important features about the LDR (Figure 6-19). First, TP values change little longitudinally from the ReReg Dam to the mouth of the river. Second, TP values are relatively high, commonly exceeding 0.05 mg/L. TP includes both particulate and dissolved forms of phosphorus, and it is possible that high concentrations of particulate phosphorus can obscure an actual phosphorus limitation; particulate forms are difficult for organisms to access. An examination of PO_4 provides a better indication of potential phosphorus limitation to algal growth. Concentrations of PO_4 changed little from the ReReg Dam to the LDR's mouth (Figure 6-20), and concentrations of both TP and PO_4 were moderately high throughout the LDR. There appeared to be little or no net uptake of phosphorus in the river, indicating that phosphorus was not limiting to the algae.

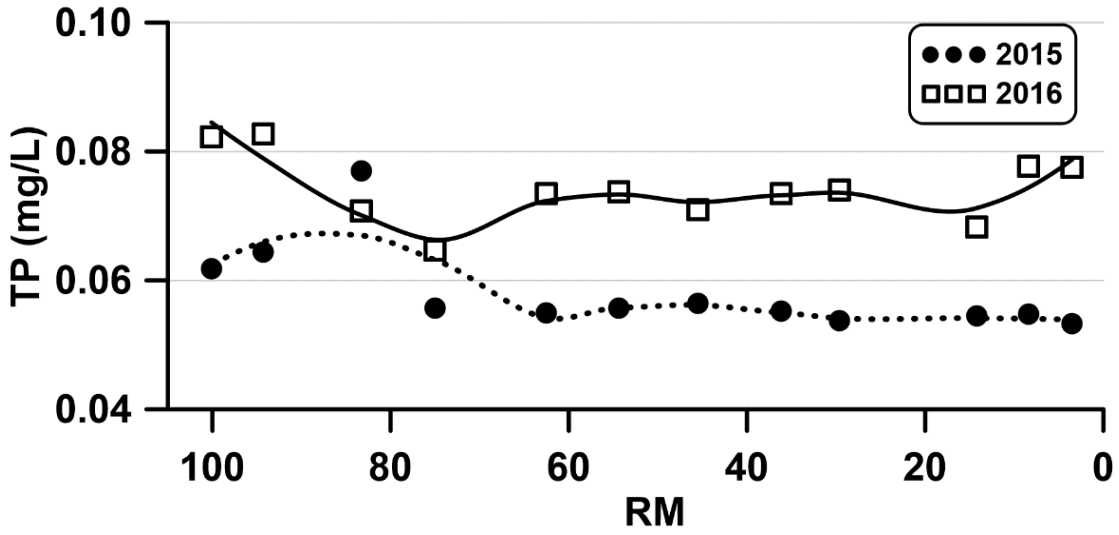

Figure 6-19. Mean TP concentrations by river mile for 2015 and 2016.

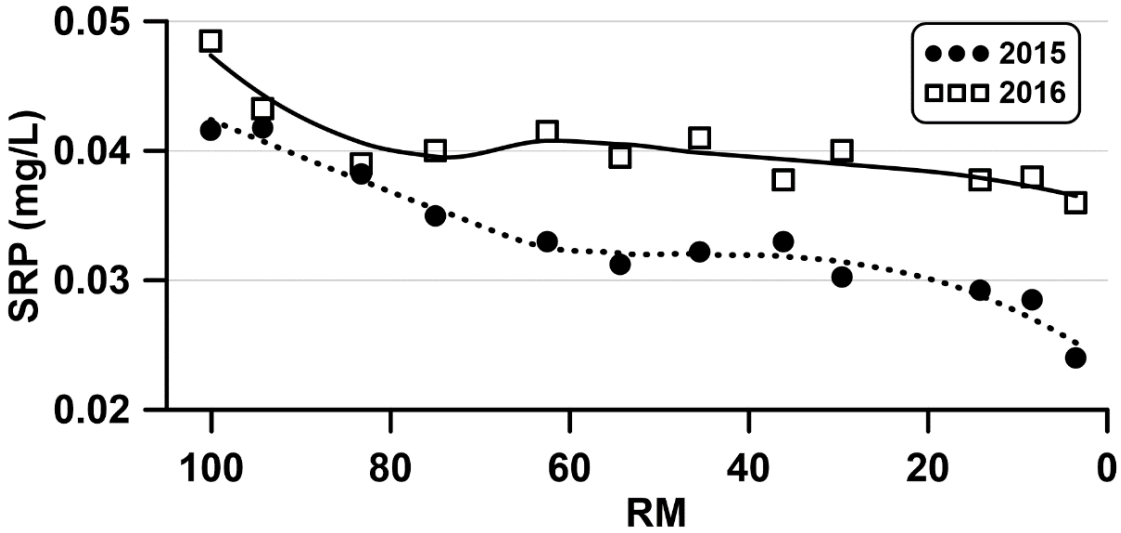

Figure 6-20. Mean concentrations of PO_4 by river mile for 2015 and 2016.

The rather high concentrations of TP and PO_4 are typical of other streams in central and eastern Oregon. However, they are higher than those in many streams and rivers in predominantly forested and rangeland watersheds with relatively little agricultural or urban inputs in North America, where concentrations of TP are often less than 0.025 mg/L (Omernik 1977, cited in Allan 1995). At first glance, it might be reasonable to attribute the high phosphorus concentrations in the LDR to the large agricultural area in the Crooked River drainage. However, the results from monitoring the reservoir tributaries conducted in this study and by ODEQ as part of the AWQMP showed that all tributaries in the basin have high phosphorus concentrations. The highest concentrations were associated with the Metolius River, which has no agricultural land use in its drainage. The high phosphorus concentrations in the LDR are derived largely from weathering of basalt and other igneous rocks in the basin and are not subject to control. Additionally, the proportion of inorganic phosphorus in the LDR is greater than typically is found in many streams. The inorganic fraction of TP across the United States was generally between 40% and 50% (Omernik 1977) compared to an average of 59% in the LDR in 2016 (*n = 232, se of mean = 1.28*).

Nitrogen was measured as TN, NH_3, and NO_3-NO_2. NO_2 will oxidize rapidly to NO_3 in oxygenated environments and the NO_2 fraction will become very small, which is why we refer to

NO_3 as the oxidized form of inorganic nitrogen. Additionally, total dissolved nitrogen (TDN) was measured in 2015 but then was discontinued because TDN values were only slightly less than TN concentrations and offered little additional insight into nitrogen metabolism in the river. The general pattern in TN is a slight (ns) longitudinal decline in values from the ReReg Dam to the mouth of the river (Figure 6-21). Concentrations of TN typically ranged from about 0.10 mg/L to 0.5 mg/L with some of the lower values observed in early June. Maximum concentrations of TN were more variable across seasons. Concentrations of TDN were slightly less than TN but exhibited a similar pattern (Figure 6-22).

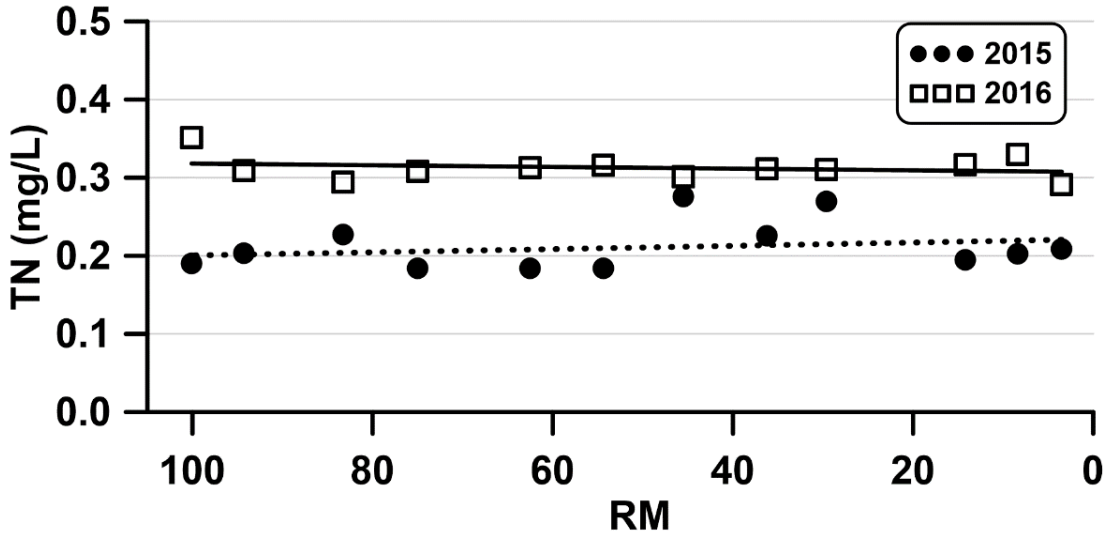

Figure 6-21. Mean concentrations of TN in the LDR for 2015 and 2016.

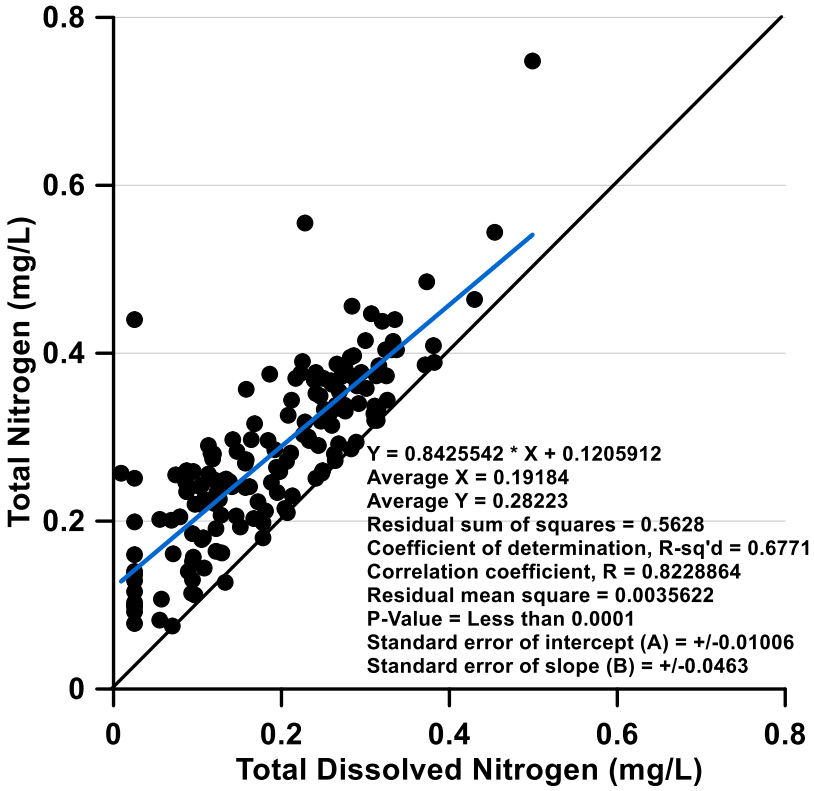

Figure 6-22. TDN versus TN for samples collected from the LDR in 2015.

Concentrations of NH_3, although low in comparison with TN, were surprisingly high given the abundance of DO in the river (Figure 6-23). This was especially true during the cooler months of 2015, but those levels were not observed in 2016. The most abundant form of inorganic nitrogen in the LDR was NO_3 (Figure 6-24). The export of NO_3 from the Project ranged from near the DL (<0.010 mg/L) in April 2015 to nearly 0.30 mg/L in February 2015, although the range of values was narrower in 2016. It is likely that the difference in NO_3 in the LDR between 2015 and 2016 was associated with low flows in 2015. Concentrations of NO_3 showed a decline from the Project to the LDR's mouth, particularly during warmer months of 2015 when as much as 0.25 mg/L was assimilated. Most rivers in the western United States are nitrogen-limited, meaning that the concentrations of available nitrogen (either NH_3 or NO_3) in them are low and often approach DLs (Allan 1995). Thus, it is unusual to have a moderately large river with concentrations of NO_3 periodically approaching 0.25 mg/L.

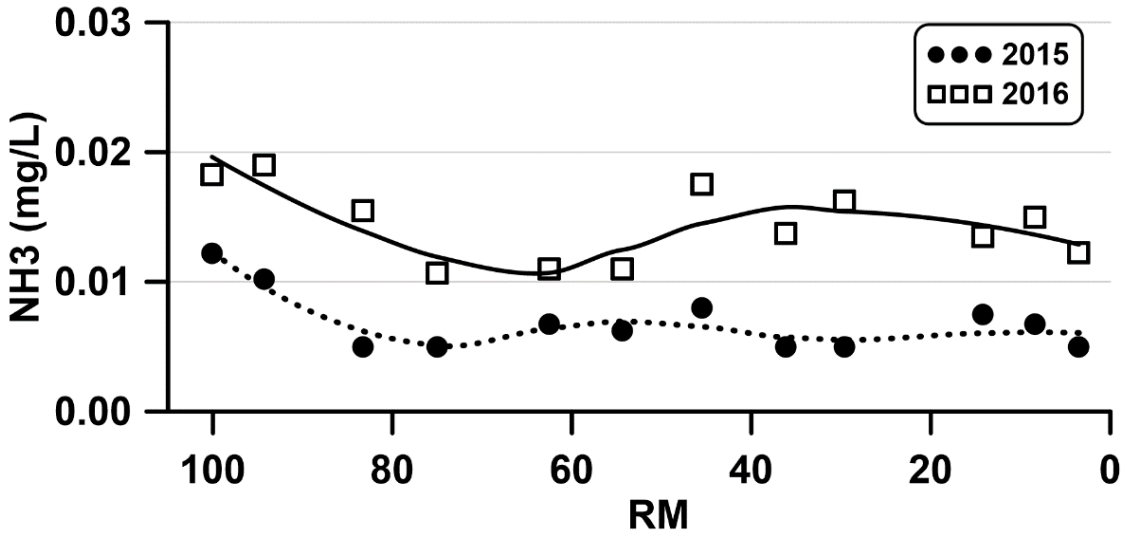

Figure 6-23. Concentrations of NH_3 in the LDR for 2015 and 2016.

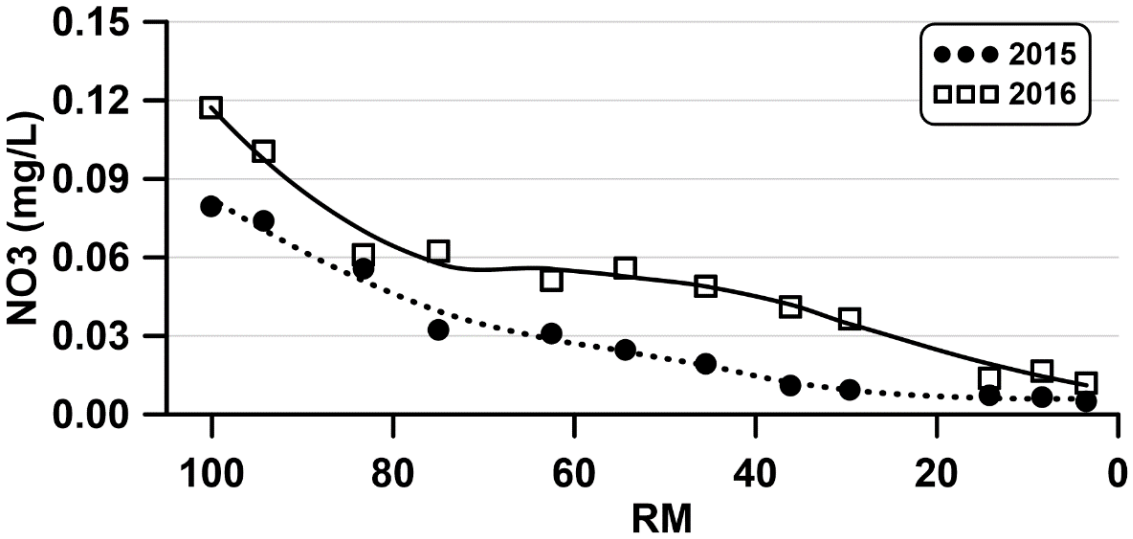

Figure 6-24. Concentrations of NO_3 in the LDR for 2015 and 2016 .

6.2.6 Other Chemical Constituents

In this study, several other analytes were measured to help calibrate the numerical model of the LDR. They include TOC and relatively conservative constituents such as Cl^-. In addition, the ZAPS LiquID unit also monitored FDOM. Concentrations of TOC typically ranged from below the DL (< 0.25 mg/L, with values set at 0.125 mg/L) to 1.2 mg/L and showed little spatial variability. We observed a pronounced seasonality, with the lowest TOC values measured in September and the highest concentrations measured in April (Figure 6-25). FDOM showed a similar pattern in which the highest values were observed in April and the lowest were observed in the fall (Figure 6-26). FDOM is a particularly sensitive measure of anthropogenic sources of organic carbon because of the strong propensity of manufactured cyclic compounds of carbon to fluoresce. Examples of chemical groups that highly fluoresce include fungicides, herbicides, and pesticides. The FDOM values reported in this study are very low compared to stream sites reported for New Hampshire (Snyder et al. 2018).

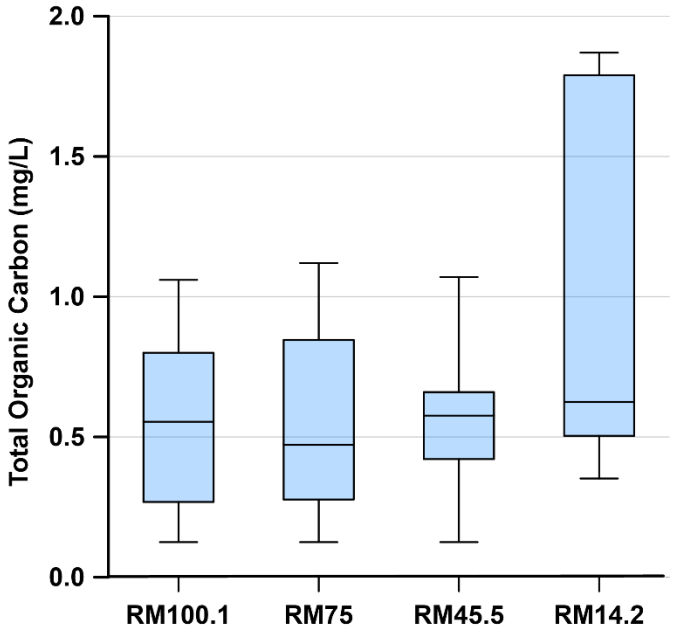

Figure 6-25. Concentrations of TOC measured in the LDR during 2016.

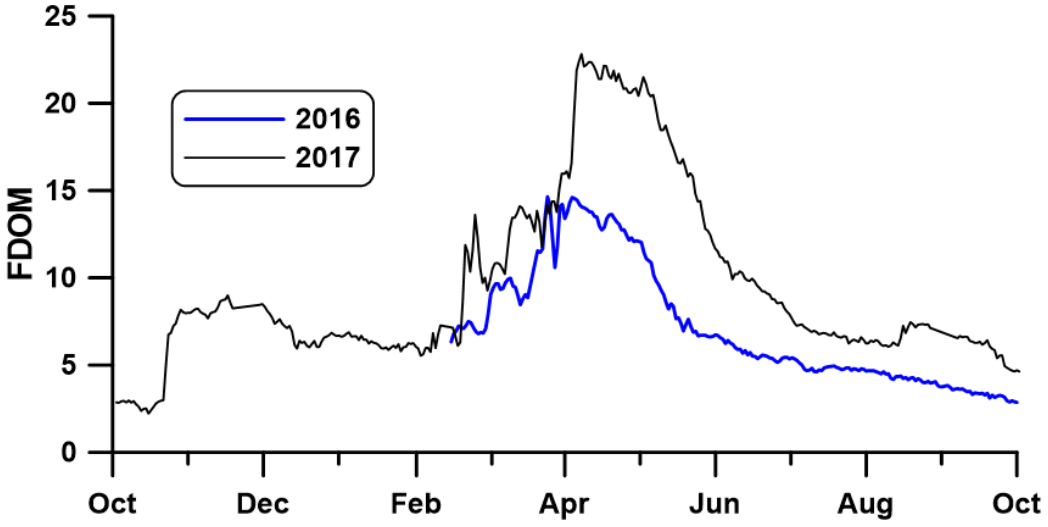

Figure 6-26. Relative measurements of FDOM measured using the ZAPS LiquID unit at ReReg site (LDR01) in WY2016–2017.

There was virtually no change in concentration of Cl^- from the ReReg site (LDR01) to the River Mouth (LDR21) (Figure 6-27). The concentrations of Cl^- were near 2.5 mg/L in the winter and early spring but declined to values ranging from about 2 mg/L to 2.25 mg/L for the summer through the fall. The values at the River Mouth (LDR21) typically were within 0.1 mg/L of those at ReReg site (LDR01) for the same sampling interval. These data illustrate the utility of Cl^- as a conservative tracer in the LDR and demonstrate that inputs from tributaries do not significantly alter the Cl^- balance of the system.

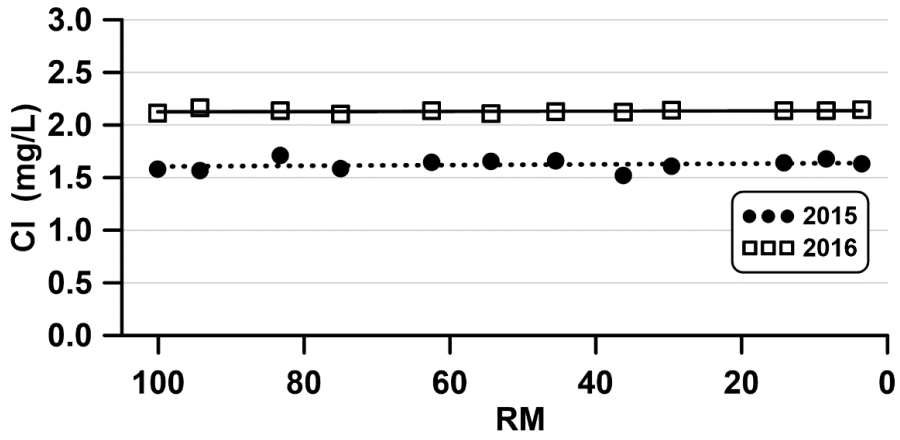

Figure 6-27. Concentrations of chloride in the LDR during 2015 and 2016. Different analytical laboratories were used in the two years.

During the study, alkalinity was measured occasionally to provide input data on the carbonate system for the LDR water quality modeling effort. For 2016, the mean alkalinity was 60.3 mg/L (as $CaCO_3$) with a 95% confidence interval of 59.1–61.4 mg/L (n = 30) and a range of 49.7–67.8 mg/L. These values are indicative of a well-buffered stream that provides ample bicarbonate to support photosynthesis.

6.2.7 Chlorophyll and Phycocyanin

Chlorophyll was measured using a combination of *in-situ* light fluorescence measurements with the AlgaeTorch, the ZAPS LiquID unit, and traditional laboratory analytical methodology. Phycocyanin was measured with fluorescence technology at the ReReg Dam with the ZAPS LiquID unit and the AlgaeTorch. Chlorophyll is a photosynthetic pigment in both eukaryotes and prokaryotes, but phycocyanin is a photosynthetic pigment present only in the cyanobacteria. Consequently, phycocyanin is an unambiguous sign of cyanobacteria in the water. The ZAPS unit exhibited significant drift in measuring chlorophyll, but a substantial portion of the data is still useful to evaluate seasonal trends.

The dominant algal pigment measured in the LDR was chlorophyll (Figure 6-28). Only during July and August were significant quantities of phycocyanin measured, and they were still substantially less than the chlorophyll measurements. Analysis of the results by specific river site showed that the general pattern of chlorophyll present in larger quantities than phycocyanin was consistent across sites, although concentrations of phycocyanin generally declined downstream (Figure 6-29). The measurement process for the AlgaeTorch is different than for most fluorescent instruments and the manufacturer classifies the signals as Total Chlorophyll and Phycocyanin or Blue-Green Algae.

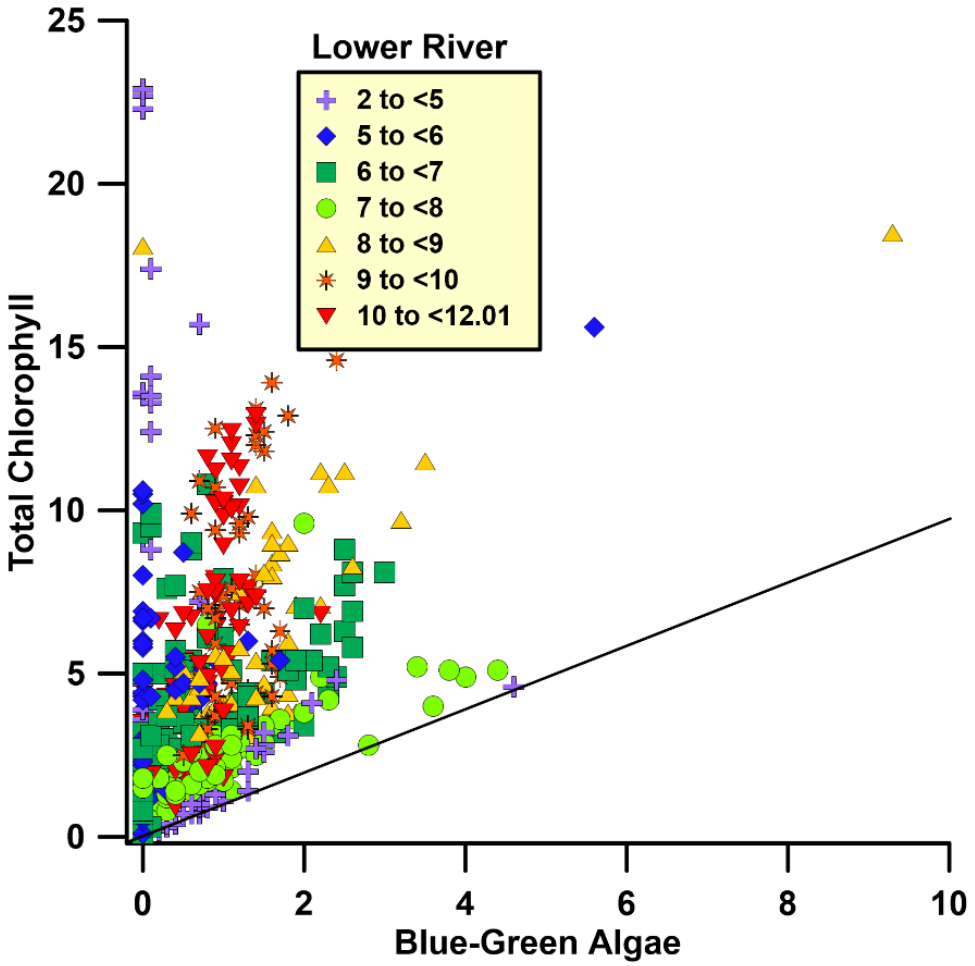

Figure 6-28. Measurements of algal pigments using the AlgaeTorch in the LDR for 2015, coded by month. Units are reported in µg/L of chlorophyll. The line indicates equal values of blue-green algae and total chlorophyll.

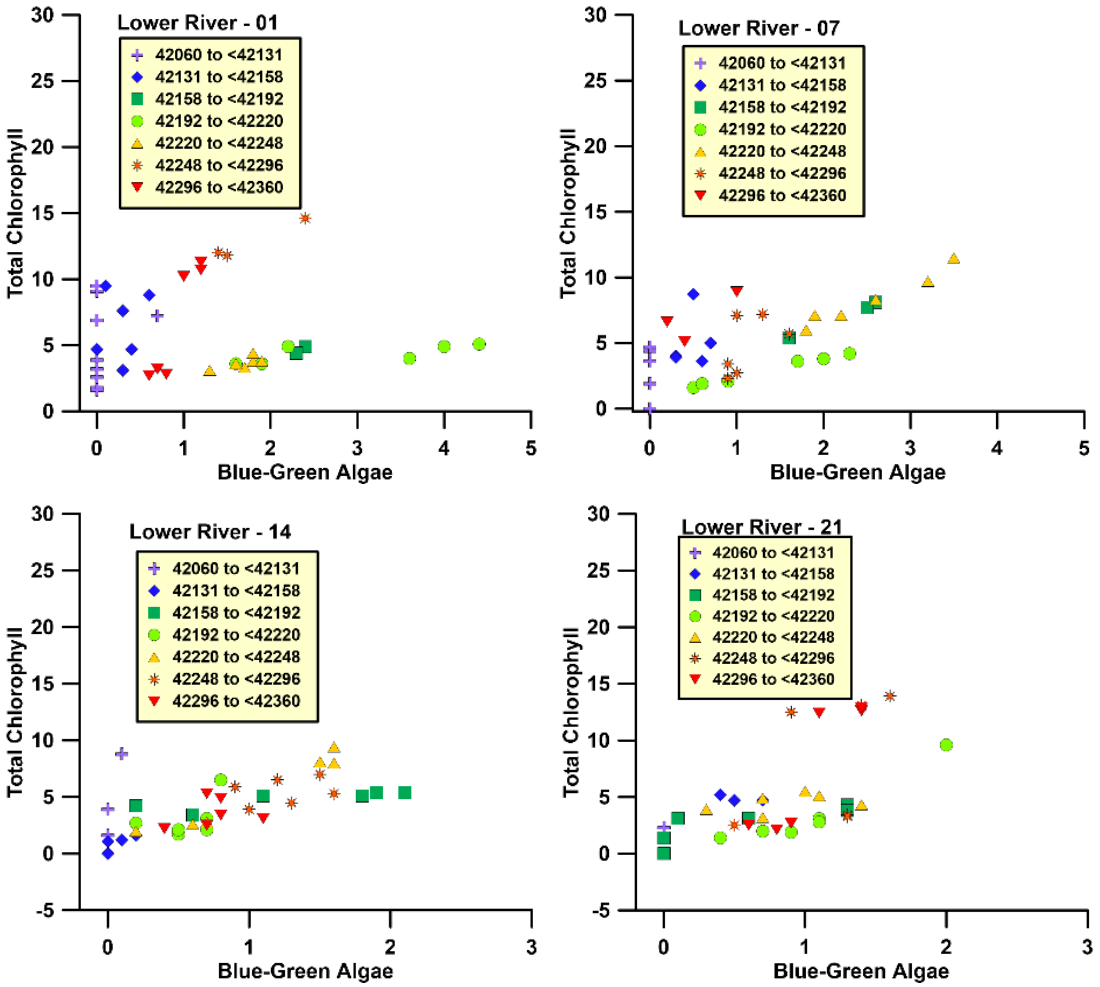

Figure 6-29. AlgaeTorch pigment measurements from 2015 at ReReg site (LDR01), Whitehorse (LDR07), Wreck (LDR14), and River Mouth (LDR21), coded by month. Units are in µg/L of chlorophyll. Note variability in scale of the x-axis.

The AlgaeTorch data at the ReReg site (LDR01) showed a bimodal distribution for total chlorophyll with peaks in June and October, but a unimodal distribution for blue-green algae with a peak in early August (Figure 6-30.). The AlgaeTorch data (shown for selected fixed-station monitoring sites) indicated an increase in total chlorophyll peaking in June, declining again through summer, and peaking in fall (Figure 6-31). Those patterns for total chlorophyll were generally well synchronized across the sites. In contrast, there was a distinctly different pattern for blue-green algae, with a single peak in August and a pronounced decrease from the ReReg site (LDR01) to the River Mouth (LDR21).

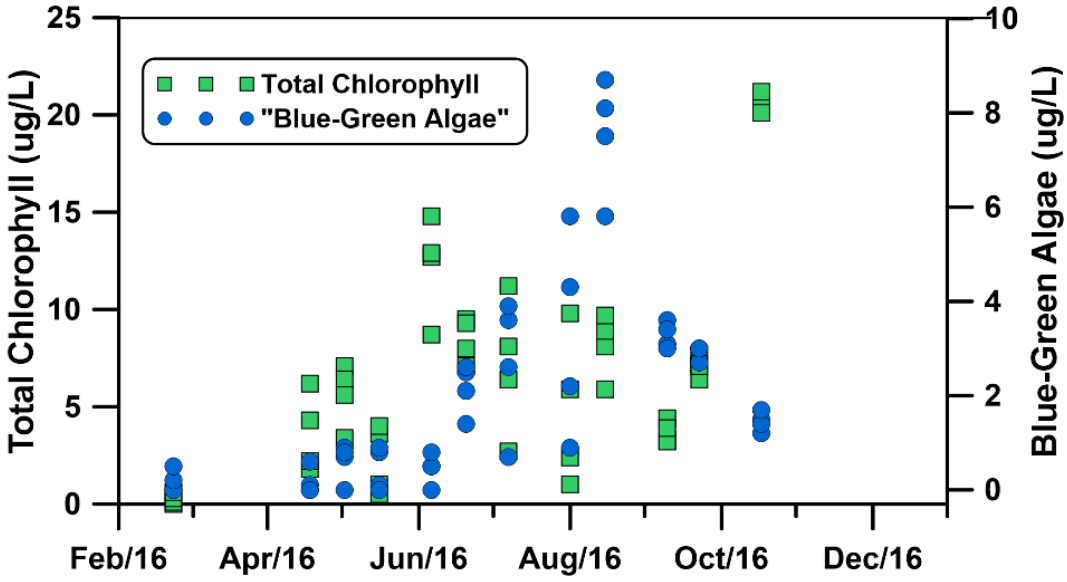

Figure 6-30. Chlorophyll measured at the ReReg site (LDR01) for green algae and blue-green algae using the Algae Torch in 2016.

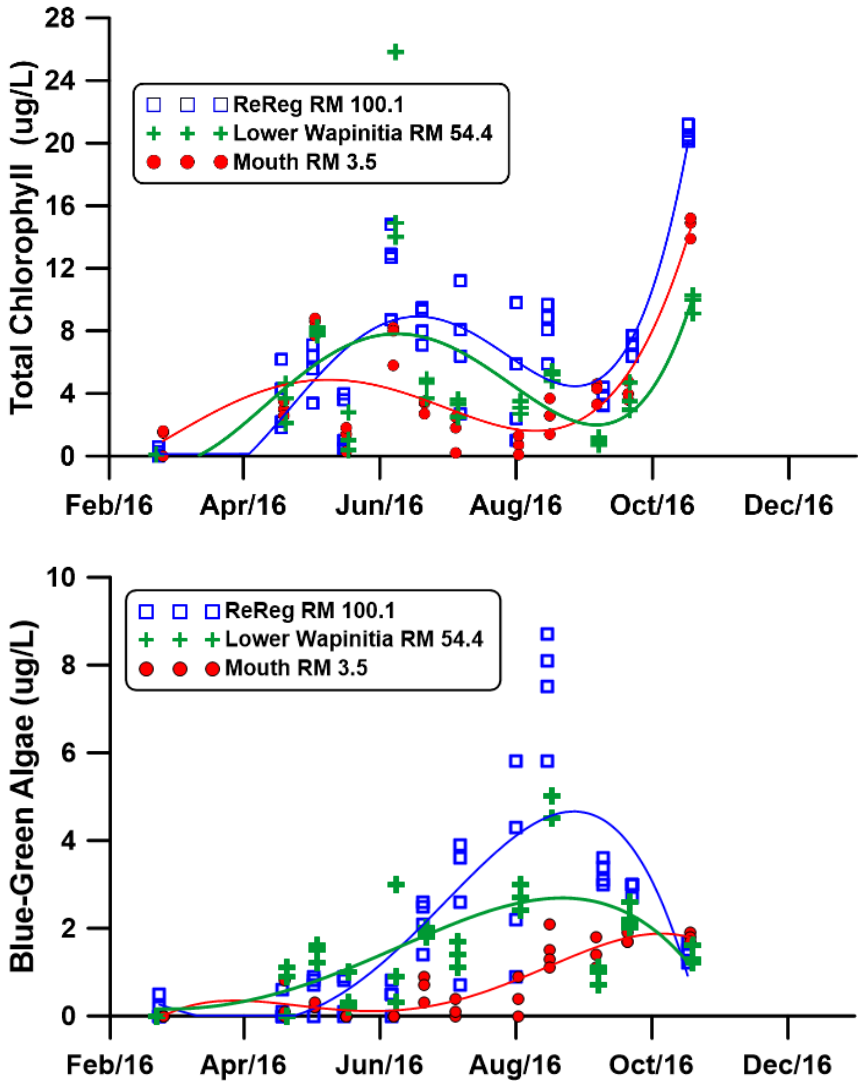

Figure 6-31. Chlorophyll from green algae measured with the Algae Torch at the ReReg site (LDR01), Lower Wapinitia (LDR11), and River Mouth (LDR21) for 2016. Results for chlorophyll for green algae and polynomial fits of the observed data (*left*); the same results for blue-green algae (*right*). Note the differences in scale between the two figures.

The continuous monitoring of chlorophyll and phycocyanin at the ReReg site (LDR01) using the ZAPS LiquID unit showed that the fall and winter data for chlorophyll were similar from 2016 to 2017 (Figure 6-32). Note that the ZAPS instrumentation measures algal pigments at specific excitation frequencies and thus the results were not directly comparable with those from the AlgaeTorch. Although the ZAPS chlorophyll data from the remainder of 2017 were suspect (Appendix B), the chlorophyll data from 2016 had two pronounced peaks—one in April and one

in May, with only modest values during the summer. In contrast, the values show that phycocyanin was present in significant amounts only during the summer and early fall.

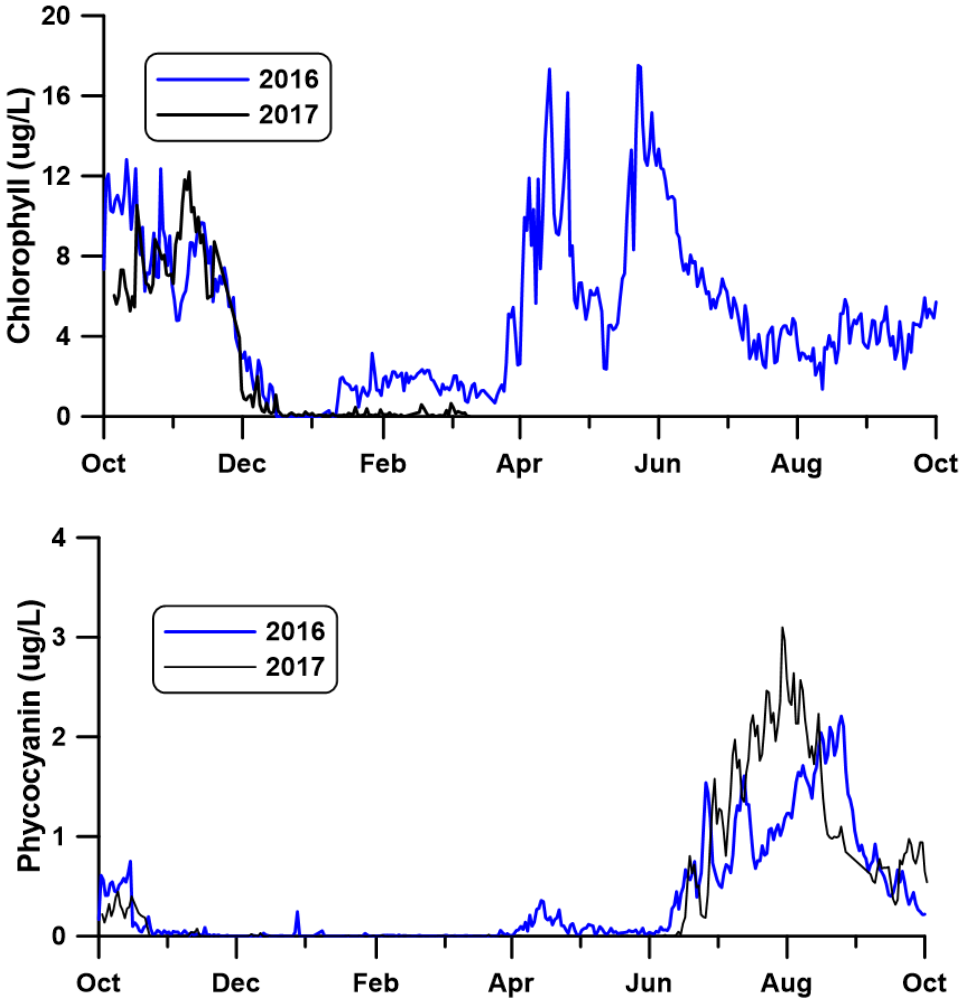

Figure 6-32. Chlorophyll (*upper*) and phycocyanin (*lower*) measured with the ZAPS LiquID unit at the ReReg site (LDR01) for WY2016–2017.

The analytical measurements of chlorophyll collected at the ReReg site (LDR01) in 2016 were sparse, but a peak appears to have occurred in late spring and a decline through the summer and into fall (Figure 6-33).

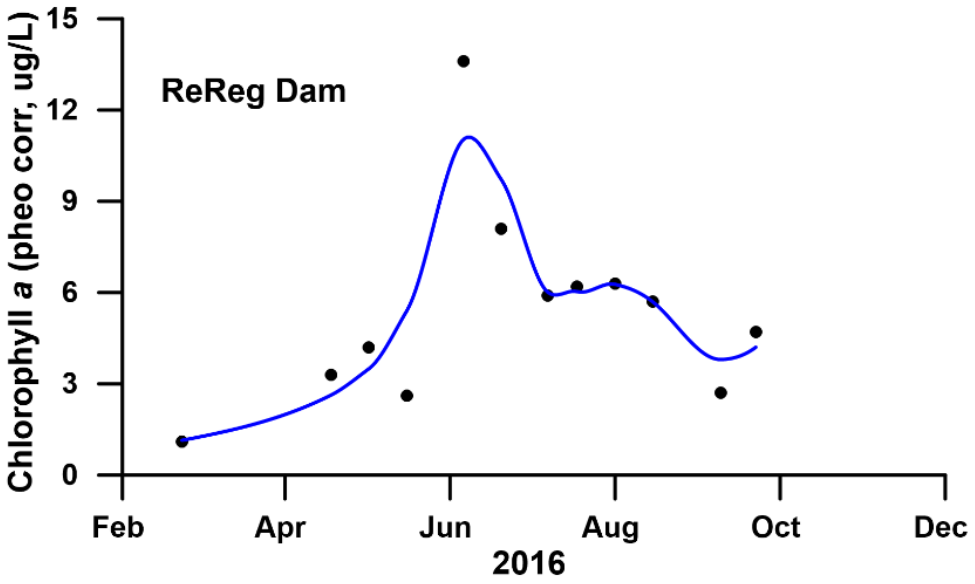

Figure 6-33. Analytical laboratory measurements of chlorophyll *a* for samples collected at the ReReg site (LDR01). The curve is LOESS fit of the observed data.

6.2.8 Periphyton

Periphyton abundance and community composition in streams can be highly variable and are affected by a variety of factors including water temperature (Goldman and Carpenter 1974; Robarts and Zohary 1987; Raven and Geider 1988), light penetration (Singh and Singh 2015), current velocity (Biggs and Gerbeaux 1993; Biggs 2000; Smolar-Žvanut and Mikoš 2014), substrate type (Cao et al. 2019), nutrient availability (Chételat et al. 1999) and grazing pressure (Feminella and Hawkins 1995; Steinman 1996; Anderson et al. 2001). This section assesses the status of periphyton in the LDR, the spatial and temporal variability of periphyton biovolume and community composition, and plankton that becomes enmeshed in the periphyton.

The abundance of periphyton can be expressed in several ways, including cell density, biovolume, chlorophyll *a*, ash-free-dry-weight and substrate coverage. In this study, we have elected to use periphyton biovolume to express periphyton abundance. Periphyton biovolume is the most common metric for representing periphyton abundance and is not subject to distortion, as is the case with cell density, in which many small cells can skew an analysis involving less abundant but much larger cells. To accommodate for the large disparity in cell size and

numerical abundance of periphyton cells, the biovolume of individual taxa were computed for each sample event at each site and then summed. The sum of each sampling event at each site was then used as a basis for computing average biovolume

Periphyton biovolume exhibited greater differences among years compared to intra-annual variations (Figure 6-34). This is particularly evident in the substantial decline in abundance between 2015–16 to 2017. In 2016, the only study year with sampling through all seasons, periphyton biovolume was lowest at the ReReg site (RM 100.1), the River Mouth site (RM 3.5), and at four sample sites between RM 45.5–83.3 (Figure 6-35). The sites with the greatest biovolume were between RM 40 and RM 5.

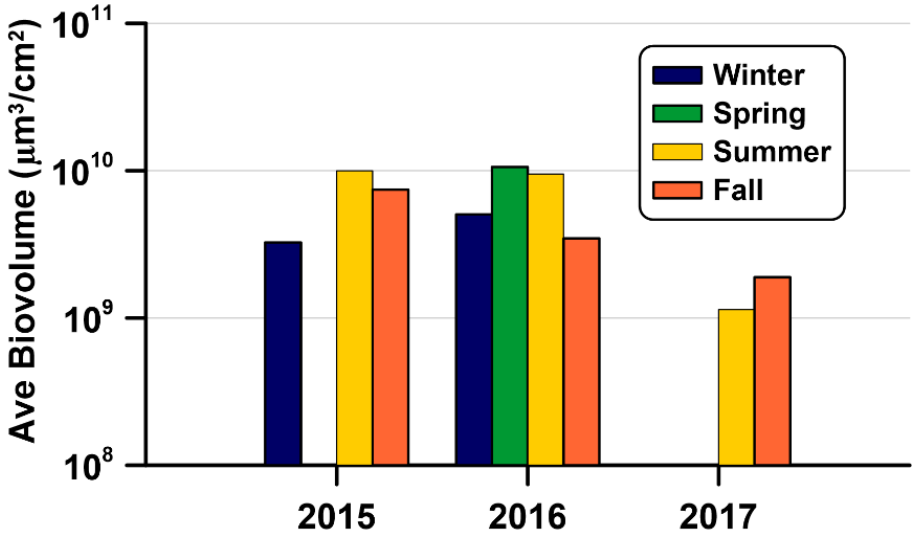

Figure 6-34. Periphyton biovolume by season for 2015–2017 for the study sites. There were no complete river samples of periphyton analyzed by Rhithron in spring 2015. Sampling in 2017 consisted of three monthly samples at seven sites during summer and one set of samples in fall.

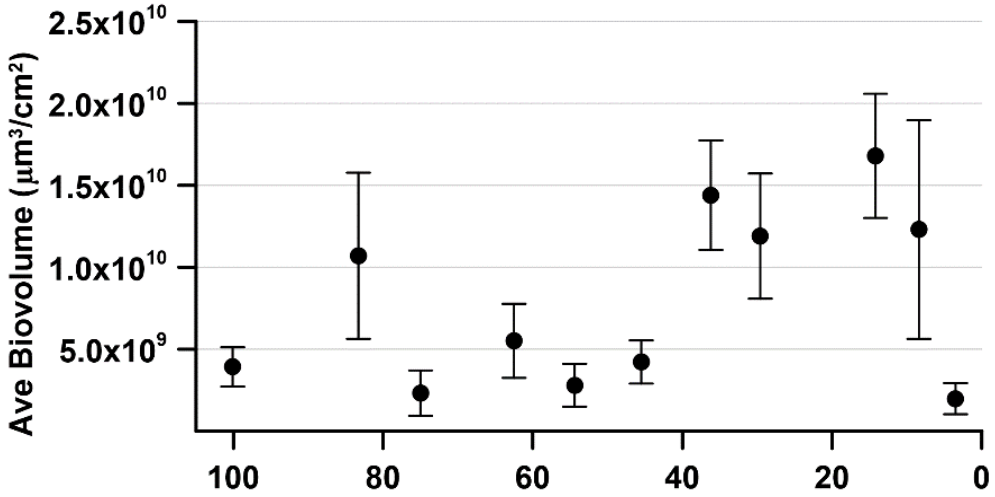

Figure 6-35. Average periphyton biovolume by river mile in 2016. The standard errors of the mean are represented as vertical bars.

In 2016, average periphyton biovolume in the LDR was generally highest from April to June, except for the Wreck site (RM 36.2), which peaked in August, and the ReReg site (RM 100.1), which peaked in October (Figure 6-36). April to June also corresponded with the growth of *Cladophora*, which commonly develops in the spring and then diminishes in late summer as filaments slough off from the substrate (Dodds and Gudder 1992). Average monthly chlorophyll concentrations and average biovolume demonstrated a similar seasonal pattern – a peak in April and general decline through the fall. The two exceptions were 1) in June when average biovolume exhibited a secondary peak, whereas chlorophyll concentrations decreased and 2) in July when average biovolume was at its lowest, but average chlorophyll concentrations were higher than in the previous month (Figure 6-36).

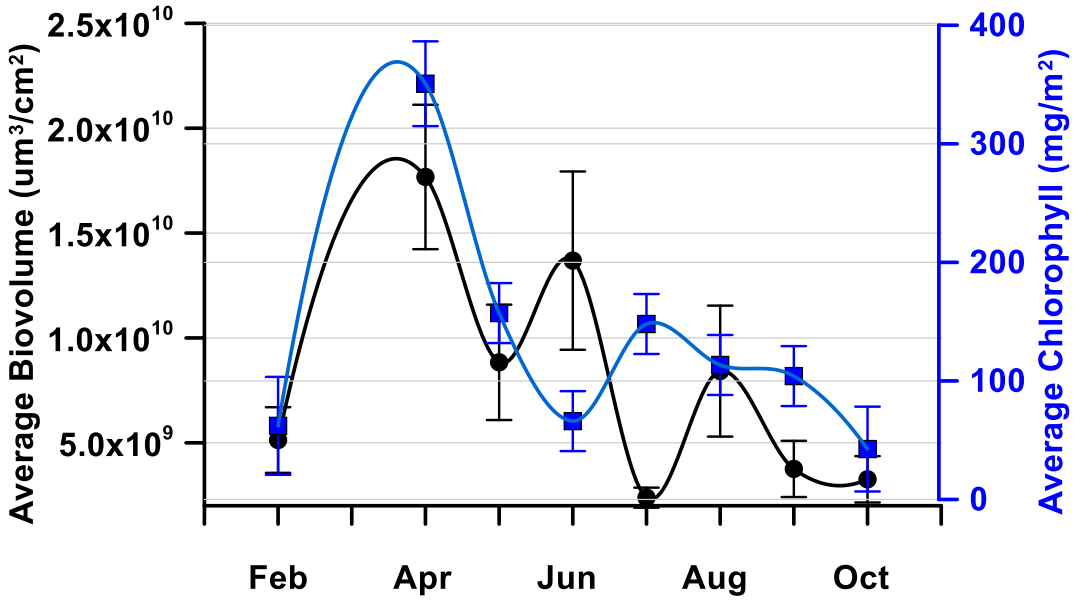

Figure 6-36. Average periphyton biovolume and chlorophyll *a* in the LDR for 2016 by month. The vertical bars are standard errors of the mean.

Seven periphyton phyla were present in the LDR, but only three were present in significant numbers. The four rare phyla, Cryptophyta, Euglenophyta, Pyrrophyta, and Rhodophyta, had only one to several individuals present in the entire sample. Consequently, these four phyla were excluded from the analyses and the focus of the periphyton investigation was devoted to the major phyla: Chlorophyta (green algae), Cyanophyta (blue-green algae) and Heterokontophyta. The heterokontophytes are a recently designated phyla comprising a diverse collection of algae. These were represented in the LDR almost entirely by the Bacillariophyceae, commonly called diatoms.

Periphyton in the LDR was generally dominated by chlorophytes, secondarily by cyanophytes and lastly by diatoms (Figure 6-37, Figure 6-38). Chlorophytes comprised almost 65% of the biovolume in 2015 and over 84% of the biovolume in 2016. However, in summer 2017, the three major periphyton groups had similar biovolumes as the chlorophyte biovolume decreased 95% from summer 2016 levels. With the decline in chlorophytes from 2016 to 2017, the relative abundance of the three major groups in summer 2017 ranged from 28.4% for the chlorophytes up to 40.3% for the cyanophytes. Cyanophyte biovolume declined by 63% from

2015 to 2016 and represented only 7.8% of the total biovolume in 2016, which was similar to the diatom biovolume percentage of 7.9%.

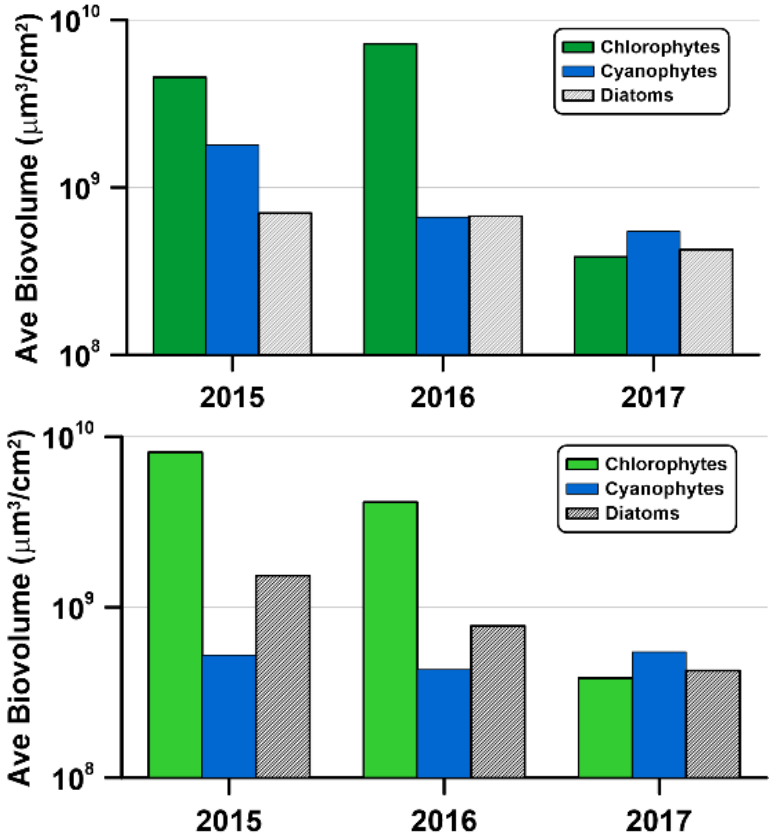

Figure 6-37. Average periphyton biovolume in the LDR for 2015–2017 for each of the three major groups. All sites and seasons are shown in the top figure. The bottom figure shows the results for samples collected in the summer at the 7 sites in common with 2017. Biovolume for summer 2015 is based only on the one complete summer sample in August.

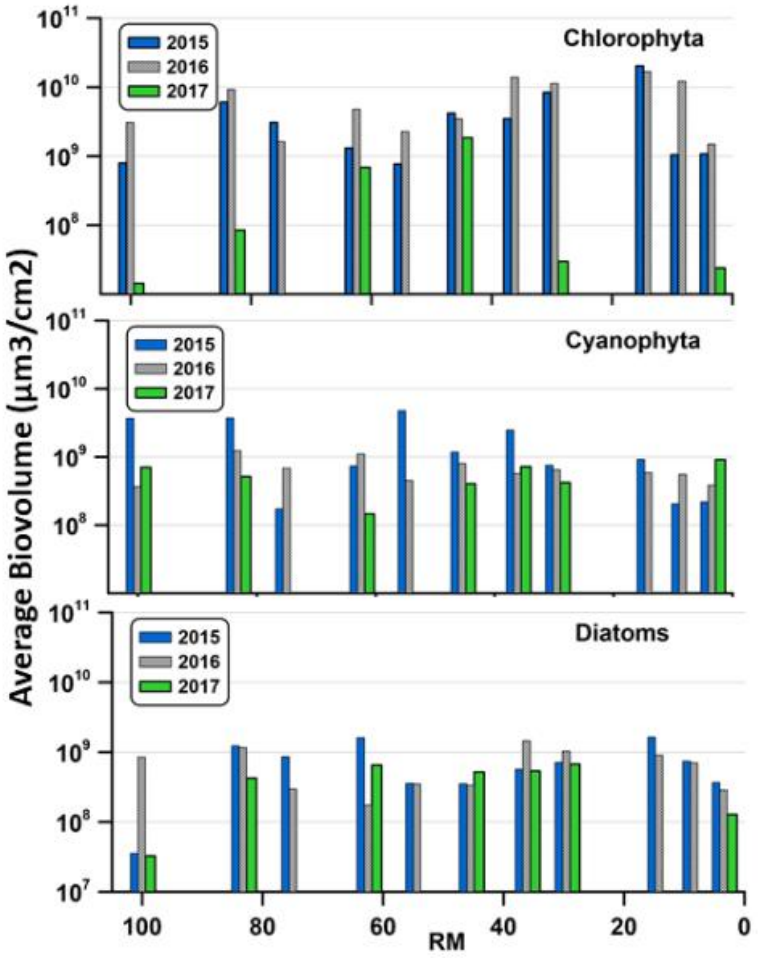

Figure 6-38. Average biovolume of major groups of periphyton by river mile for 2015–2017. Note that only seven of the sites were sampled in 2017.

The 2016 results show how average biovolume varied seasonally (Figure 6-39). Chlorophytes and cyanophytes biovolume was greatest in spring, whereas the diatoms peaked in summer. The largest percentage change occurred between summer and fall when the cyanophytes declined by an order of magnitude.

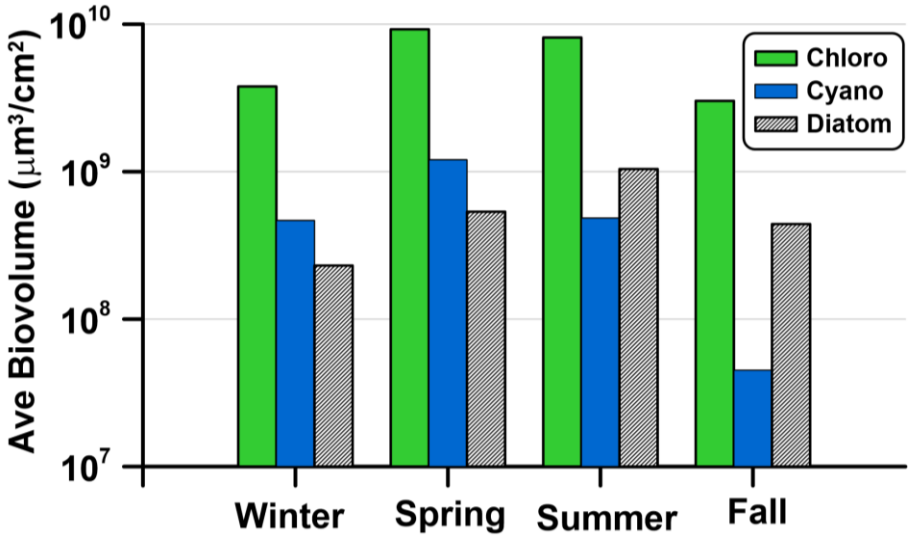

Figure 6-39 Average seasonal biovolume for the three major periphyton groups in the LDR for 2016.

The dominant taxa in each of the three major groups were *Cladophora* and *Stigeoclonium* for the chlorophytes, *Homoeothrix* and *Calothrix* for the cyanophytes, and *Gomphoneis* spp. and *Cymbella* spp. for the diatoms (Figure 6-40). Both *Cladophora* and *Stigeoclonium* are filamentous. The filaments of *Cladophora* can extend for several feet from the point of attachment, whereas those of *Stigeoclonium* more commonly occurs as tufts or mats on hard surfaces. Both taxa have widespread distributions and can be found in polluted and clean water environments (Whitton 1970; Dodds and Gudder 1992). *Homoeothrix* and *Calothrix* are filamentous on a microscopic scale, although they are generally visible as short tufts on rocks and other hard surfaces. *Homoeothrix* is non-heterocystous (unable to fix nitrogen)and typically found in swift, unpolluted rivers whereas *Calothrix* is heterocystous (fixes nitrogen) and is present in a variety of conditions (Wehr et al. 2015). *Gomphoneis* and *Cymbella* are both benthic diatoms that attach to substrates at their base. *Gomphoneis* and *Cymbella* are common benthic diatoms distributed worldwide and were represented in the LDR by 7 and 11 species, respectively. The most noteworthy change in abundance of these dominant taxa was the dramatic reduction in abundance of *Cladophora* in 2017, whereas other dominant taxa remained relatively unchanged.

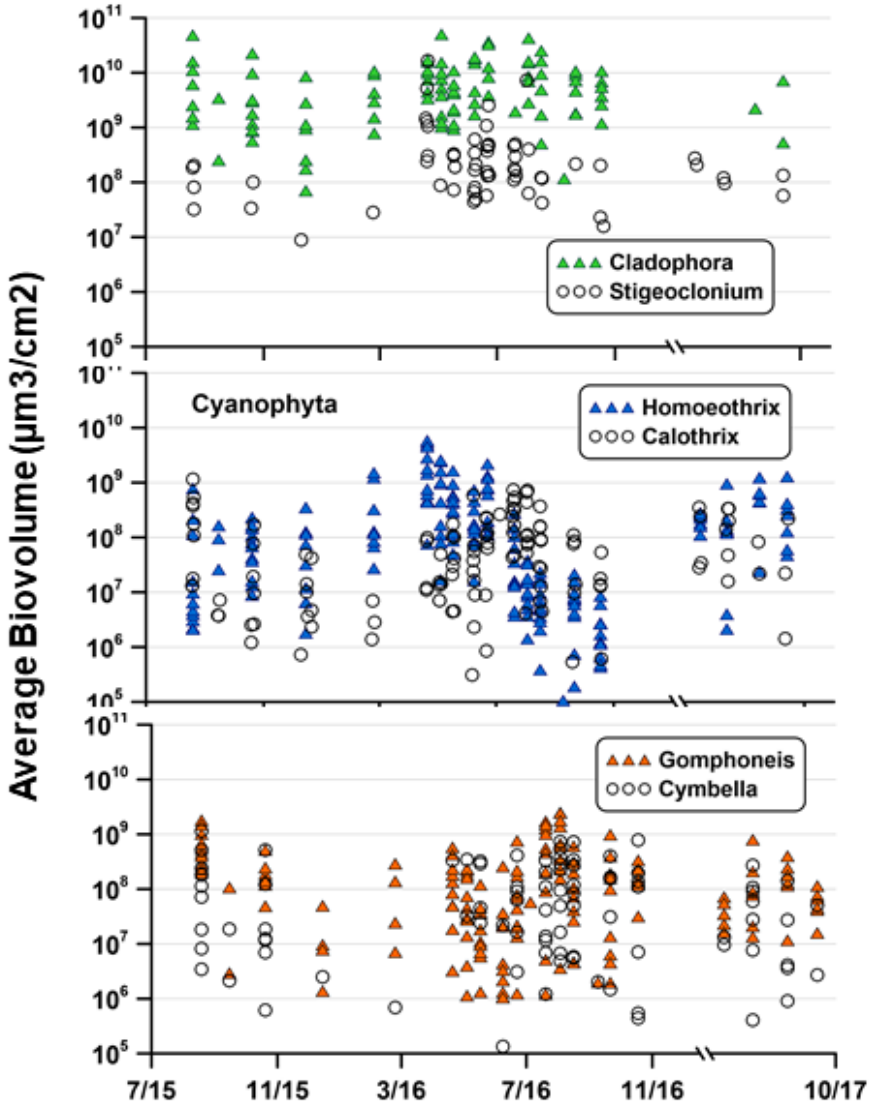

Figure 6-40. Dominant genera in each of the three major periphyton groups from 2015–2017. Note the break in the x axis. Each symbol represents the sum of genera by site.

The most abundant taxon present in 2015 and 2016 was *Cladophora* and it was abundant throughout much of the river, although it was greatest between RM 40 and RM 10, peaking in 2015 and 2016 at RM 14.2 (Figure 6-41). Only two sites contained *Cladophora* in the samples from 2017, whereas *Cladophora* was present at all sites during 2015 and 2016. *Cladophora* was abundant throughout the sample period except in July when only one site contained *Cladophora*

(Figure 6-42). The apparent absence of *Cladophora* in July is difficult to explain considering the widespread abundance of the alga in June and August.

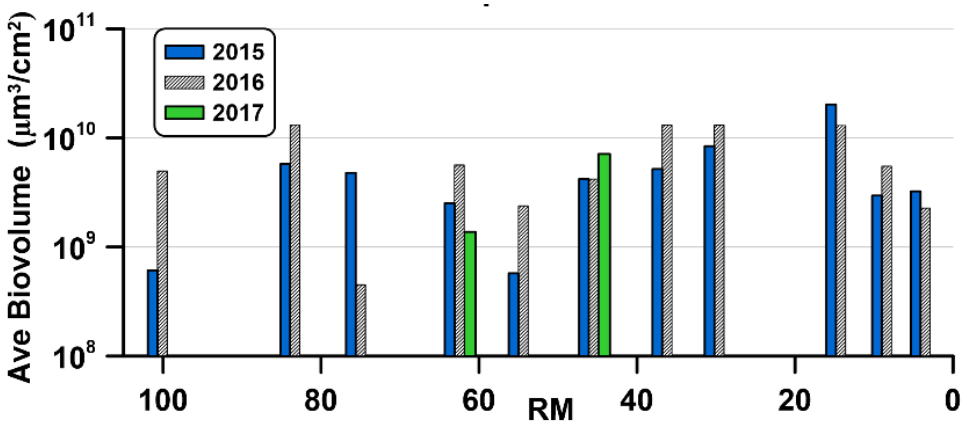

Figure 6-41. Average biovolume of *Cladophora* in the LDR for 2015-2017.

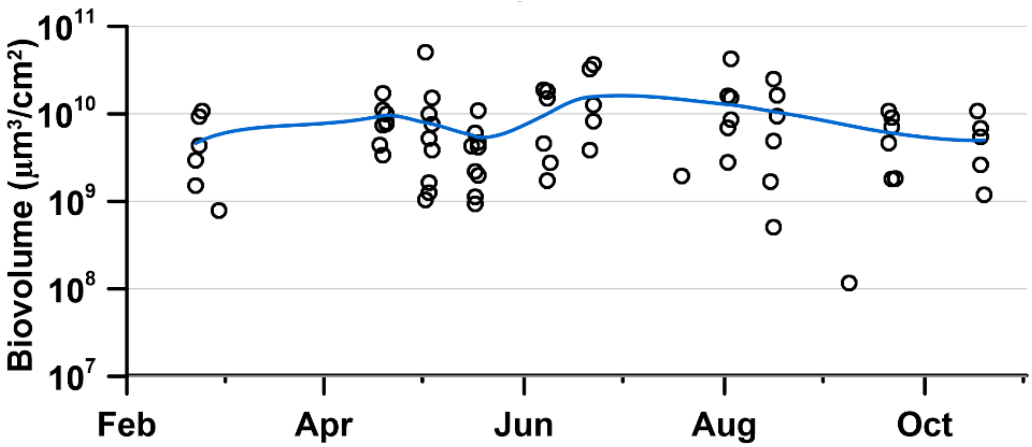

Figure 6-42. Biovolume of *Cladophora* by sample date in 2016. Each circle represents the biovolume of *Cladophora* for an individual site. The line is a LOESS fit of the observed data.

Another genus of filamentous chlorophytes, *Ulothrix*, was abundant in 2016 but not reported in either 2015 or 2017. It was abundant throughout the river with the notable absences at RM 100.1 and RM 62.5 in 2016 (Figure 6-43). It appeared to exhibit a decline mid-river and showed a

peak at RM 8.3, which also corresponds to the site of peak abundance for *Cladophora*. However, unlike *Cladophora*, *Ulothrix* was present only from April to June.

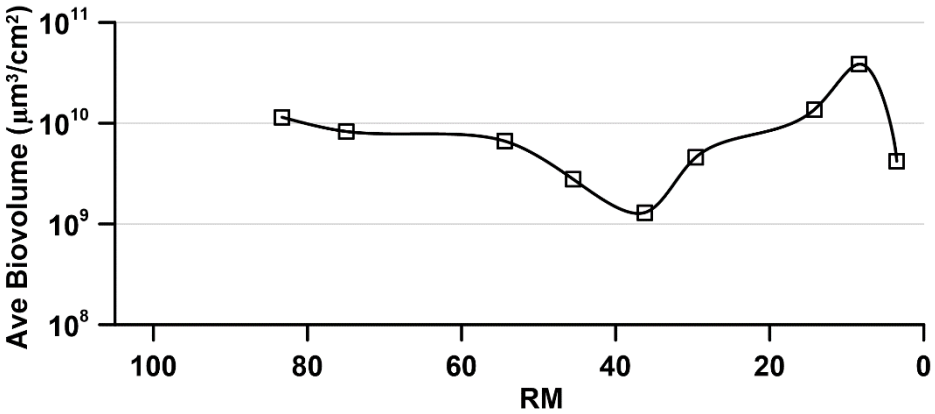

Figure 6-43. Average biovolume of Ulothrix spp. by RM for April to June 2016.

6.2.8.1 *N-Fixing Periphyton*

Some species of periphyton can fix nitrogen, meaning they can acquire atmospheric nitrogen instead of relying exclusively on nitrogen dissolved in water for a primary source of nitrogen. This capability is made possible by the presence of specialized structures called heterocysts. Heterocystous periphyton are almost exclusively limited to certain families of cyanobacteria. An exception to this N-fixing capability in cyanophytes is found in two genera of diatoms (*Epithemia* and *Rhopalodia*) that contain endosymbiotic cyanobacteria-like cells. Only *Epithemia* occurred in significant numbers in the LDR. Comparison of heterocystous and non-heterocystous periphyton biovolume shows a clear dominance of non-heterocystous taxa regardless of year based on the common seven sites sampled in the summers of 2015–2017 (Figure 6-44). The biovolume of heterocystous taxa is greatest in 2015 and declined in 2016 and 2017.

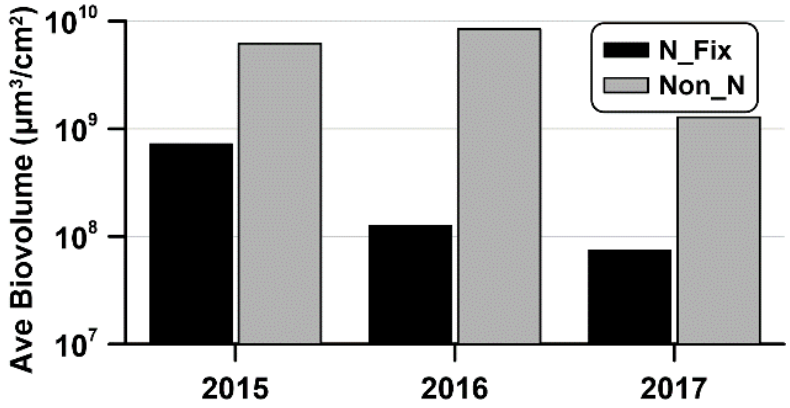

Figure 6-44. Average biovolume of heterocystous (N-fixing) and non-heterocystous (non N-fixing) periphyton by year in the LDR for the 7 sites sampled in the summers of 2015–2017.

An examination of N-fixing capability by season in 2016 shows that average biovolume of non-heterocystous taxa was similar among seasons, whereas average biovolume of heterocystous taxa increased by an order of magnitude from winter to summer and declined in fall (Figure 6-45). However, even at maximum biovolume in summer, the N-fixing periphyton represented only 2.8% of the average periphyton biovolume. Non-heterocystous periphyton were more abundant than heterocystous periphyton by nearly two orders of magnitude at the upper end of the LDR but by only about one order of magnitude towards the mouth (Figure 6-46).

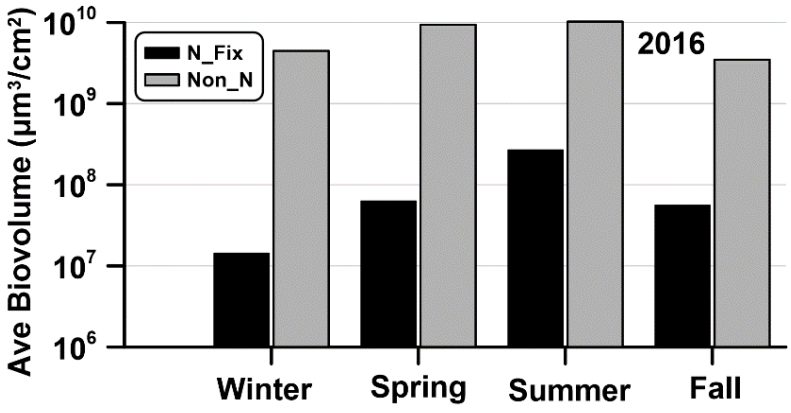

Figure 6-45. Biovolume of heterocystous (N-fixing) and non-heterocystous (non N-fixing) periphyton in the LDR by season in 2016.

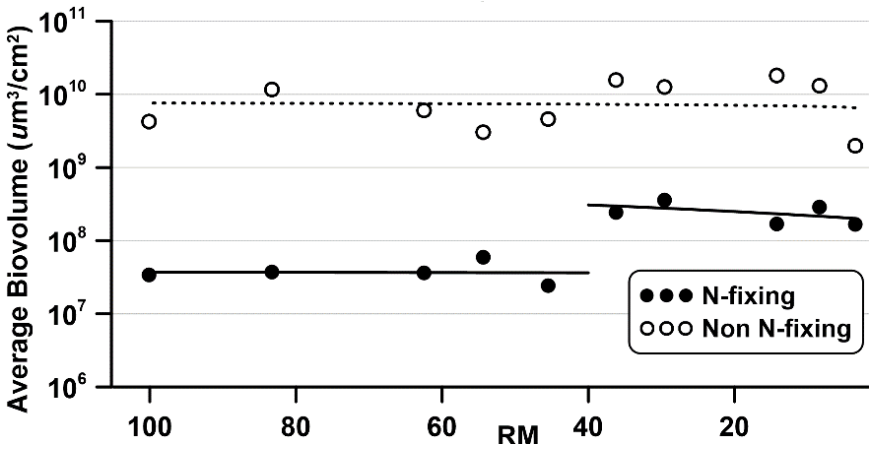

Figure 6-46. Average periphyton biovolume of N-fixing (heterocystous) and non N-fixing (non-heterocystous) periphyton in the LDR by river mile for 2016.

The heterocystous Cyanophyta benthic taxa present in the LDR included *Calothrix*, *Stigonema*, *Rivularia*, *Nostoc*, *Capsosira* and *Tolypothrix.* The planktonic *Dolichospermum* (*Anabaena*) was also present and originated from LBC. The biovolume of *Calothrix*, the dominant N-fixing taxon, was lowest in February, gradually increased during the spring, and peaked in late July (Figure 6-47). *Calothrix*'s biovolume increased from the ReReg Dam (RM 100.1) to RM 8.4.

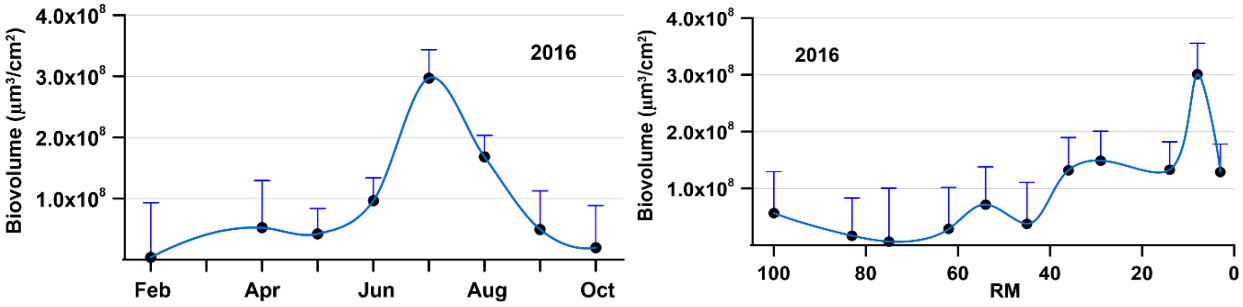

Figure 6-47. Average biovolume of *Calothrix* by month for 2016 *(left)* and by river mile *(right)*. The vertical bars are standard errors of the mean (positive direction shown for clarity).

Of the two heterocystous diatoms present in the LDR, *Epithemia* was common in the river, whereas *Rhopalodia* was identified in only one sample. *Epithemia* abundance increased significantly (p = 0.0159) downstream, particularly below RM 40, in both 2015 and 2016 but was nearly absent in 2017 (Figure 6-48). The temporal distribution of *Epithemia* in 2016 is

notable because no *Epithemia* was sampled in April and May, yet biovolume peaked in June and declined in the fall (Figure 6-49).

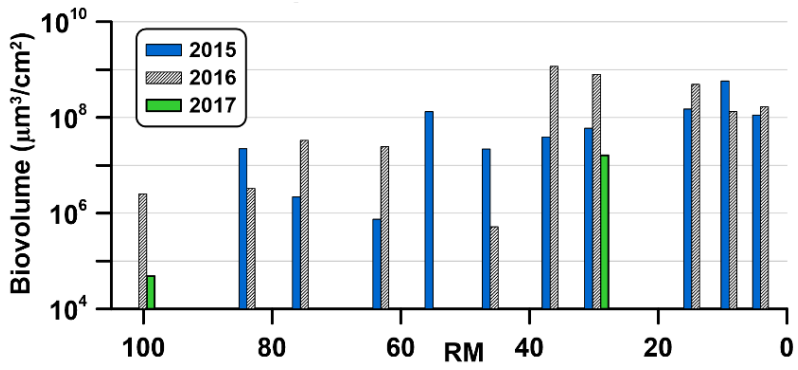

Figure 6-48. Average biovolume of *Epithemia* spp. by river mile for 2015–2017.

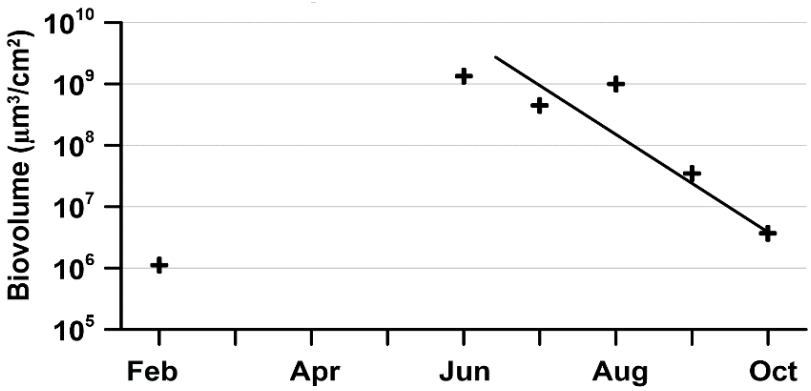

Figure 6-49. Average biovolume of *Epithemia* spp. by month for 2016.

6.2.8.2 Planktonic Algae Attached to Periphyton

Periphyton consists of a matrix of obligate benthic taxa that grow on rocks or are epiphytes that grow on other attached periphyton or macrophytes. An example of the latter is *Cladophora*, which serves as an important substrate for diatoms such as *Epithemia sorex* (Dodds and Gudder 1992). Additionally, plankton released from the reservoirs can become enmeshed in the periphyton and remain viable while entrained in the matrix. The planktonic algae attached to the periphyton are important because they can be a significant component of the total periphyton biovolume and seston (floating algae in the river) biovolume.

When comparing the biovolume of periphyton taxa of different origins, the biovolume of benthic taxa is greater by about an order of magnitude compared to the planktonic taxa (Figure 6-50). Nevertheless, the planktonic taxa comprise a surprisingly large proportion of the total periphyton likely due to high rates of plankton released from the reservoirs and the abundance of benthic filamentous periphyton to entrain the seston. Average biovolume for the 7 sites in common from summer 2015–2017 shows that the percentage of planktonic-derived biovolume was 31% in 2015 but declined to 16.3% in 2016 and 12.2% in 2017.

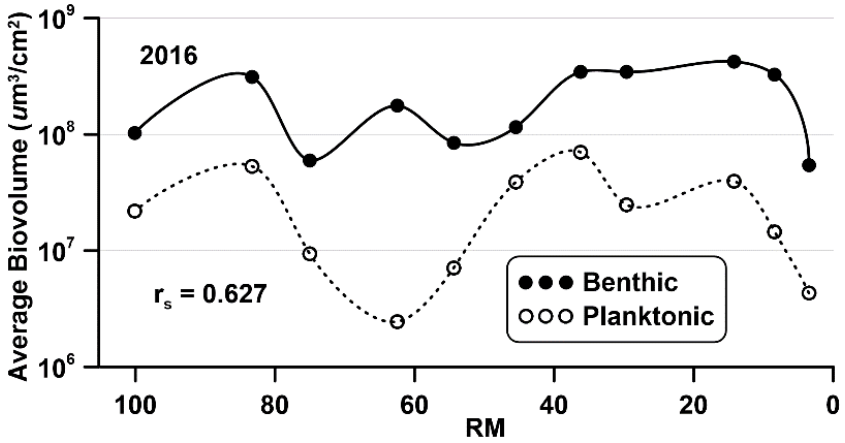

Figure 6-50. Average biovolume of benthic periphyton taxa compared with planktonic taxa present in the periphyton in the LDR for 2016. The r_s represents the Spearman rank correlation coefficient between average benthic and planktonic biovolume. A paired T-test is significant at $p = 0.0006$.

The most noteworthy genus of planktonic taxa found in the periphyton was the centric diatom, *Stephanodiscus*; it was the most abundant taxon (based on biovolume) in several periphyton samples (Figure 6-51). Also, it was one of the most common genera in LBC, and the high degree of entrainment in the periphyton in summer corresponds to when it was abundant in the reservoir and periphyton was abundant in the river. *Stephanodiscus biovolume* was greatest in the upper reach of the LDR (> 80 RM), declined between RM 80 and RM 50, and increased in in the lower reach. This pattern is similar ($r_s = 0.653$) to that observed for *Cladophora* and suggests that *Cladophora* is an important taxon in "capturing" *Stephanodiscus* from the seston. However, other taxa are also effective in entraining *Stephanodiscus* as seen in 2017 when

Cladophora was largely absent but *Stephanodiscus* was still present in the periphyton assemblage.

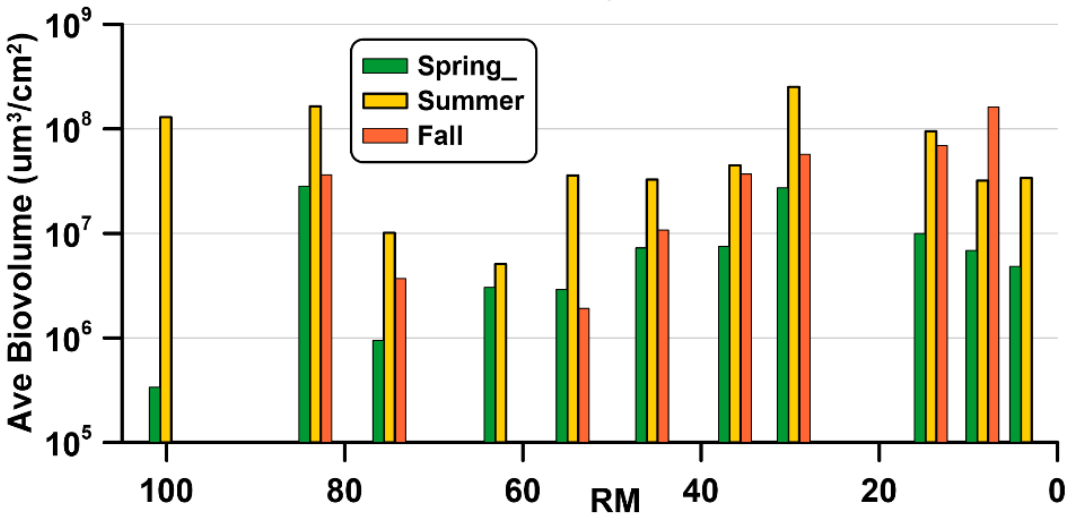

Figure 6-51. Average biovolume of *Stephanodiscus* spp. by RM for spring, summer, fall 2016. Results for winter are not shown because several of the sites showed no *Stephanodiscus* present and where it was present, its biovolume was low.

In addition to *Stephanodiscus*, other plankton released from the impoundments can become enmeshed in the periphyton and remain viable while entrained in the matrix. The sporadic presence of *Dolichospermum* in the periphyton samples throughout the LDR corresponded well with its abundance in LBC (cf. Figure 4-45). The average biovolume of the nine periphyton samples with *Dolichospermum* present in 2016 was 3.19 x 10^6 $\mu m^3/cm^2$ and all were found from June to September with the majority (n = 5) found in August.

6.2.9 Volatile Solids

Another measure of periphyton abundance is ash free dry weight (AFDW). The laboratory measured a slightly different parameter: volatile solids, which differs from AFDW in that the former is ignited at a higher temperature (550˚C versus 500˚C) and AFDW is rewetted after ignition at 500˚C to rehydrate clays, carbonates, and other minerals that might have lost moisture on ignition. Since the LDR is low in carbonates and clays, the results should be similar. The volatile solids were quite different between 2015 and 2016 (Figure 6-52). The data showed little

pattern in 2016, whereas the data from 2015 showed a peak density at Ferry (RM 62.5) and a temporal peak in July (all sites combined). The plots by month indicate how little periphyton mass was present during the winter and early spring; but that changed rapidly in April and May when periphyton mass increased fivefold to tenfold (Figure 6-53).

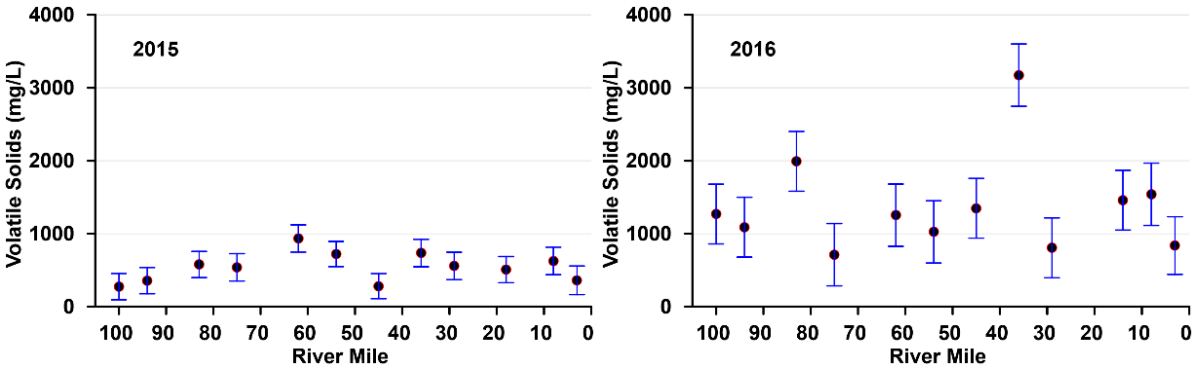

Figure 6-52. Volatile solids in periphyton by river mile for 2015 (*left*) and 2016 (*right*). The vertical bars are standard errors of the mean.

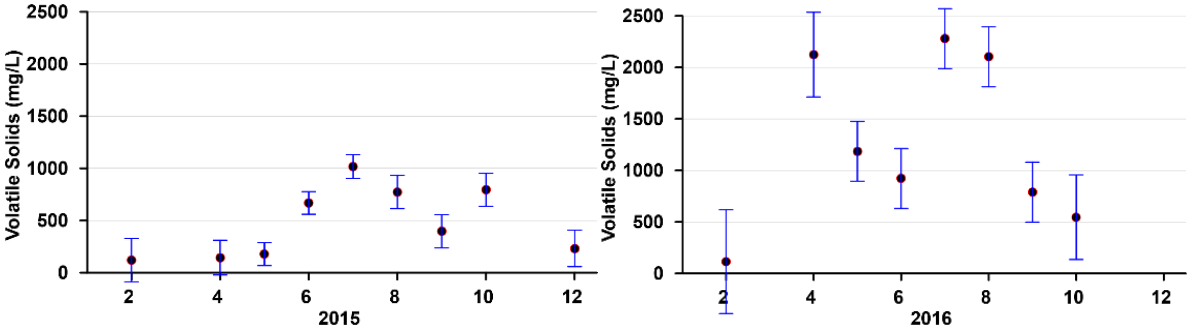

Figure 6-53. Volatile solids in periphyton for 2015 (*left*) and 2016 (*right*) by month.

6.2.10 Periphyton Chlorophyll

The chlorophyll content present in periphyton was highly variable between sample years and spatially along the LDR (Figure 6-54). The annual mean values by river mile in 2015 were low in the upper reach of the river but, from Whitehorse (RM 75) downstream to the mouth, periphyton chlorophyll increased by more than 100 micrograms per square meter ($\mu g/m^2$) and generally remained moderately high for much of the LDR. Sandy Beach (RM 45.5) was a major exception, with results similar to those at the ReReg (LDR01).

Values for 2016 were higher at the three sites above RM 80 and remained stable until Wreck Rapids (RM 36.2), where they showed a dramatic increase followed by a gradual decline to the mouth. The same data are shown by month (Figure 6-55). The results for 2015 showed low biomass for samples through May and values that increased in June and remained stable for the remainder of the year. The results for 2016 showed a different pattern in which the results for April increased dramatically before declining to more typical values for the remainder of the year. In 2016 there were a considerably greater number of observations with elevated periphyton biomass, illustrating that these high values were largely associated with samples collected in April 2016. Results for 2017 (not shown) were intermediate between samples collected in 2015 and 2016.

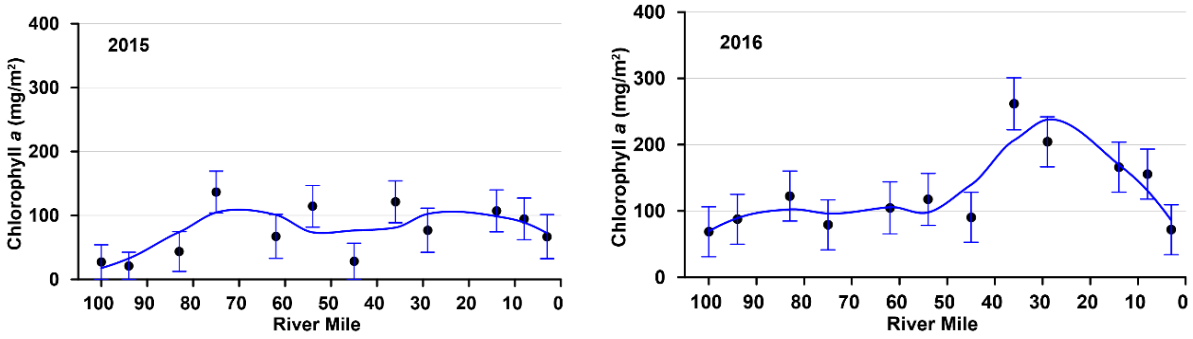

Figure 6-54. Periphyton chlorophyll content by river mile in 2015 (*left)* and 2016 (*right*).The vertical bars are the standard errors of the mean. The line is the LOESS fit of the observed data.

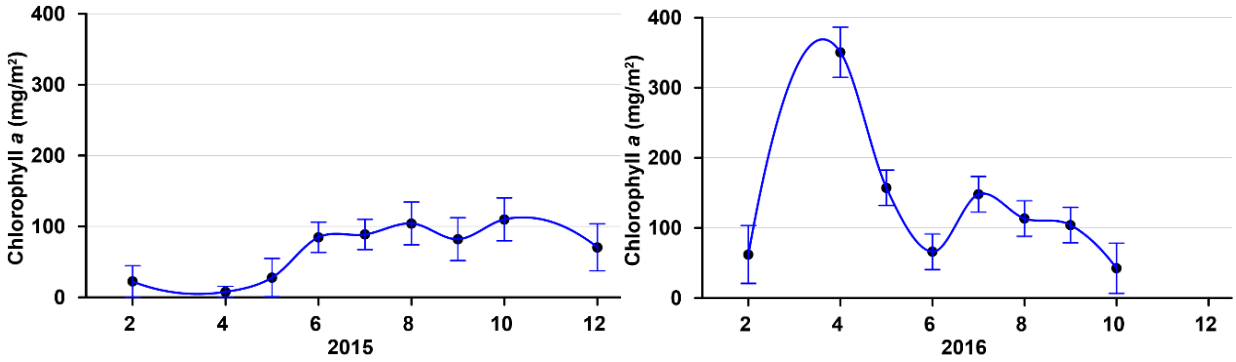

Figure 6-55. Periphyton chlorophyll content by month in 2015 (*left)* and 2016 (*right*). The vertical bars are the standard errors of the mean. The line is the LOESS fit of the observed data.

6.2.11 Seston (Floating Algae)

Seston are algae suspended in the river and is comprised of planktonic taxa from upstream reservoirs and benthic algae dislodged from the substrate. Because there are three reservoirs upstream of the LDR, it is reasonable to expect that there would be considerable planktonic seston present in the LDR. This is especially the case following the installation of the SWW, which captures at least some surface flow (40–100%) from LBC throughout the year. The distinction between algae derived from plankton and that derived from benthic sources is not always precise because some taxa can function in both habitats. Nevertheless, most planktonic taxa are readily distinguishable from benthic taxa, which allows us to approximate the degree to which plankton from the Project impoundments are present in the LDR.

The total biovolume of algae and cyanobacteria seston present in the river water column was comparable to the biovolume of phytoplankton present in the epilimnion of the LBC and Lake Simtustus (Table 6-2). Although high degrees of natural variability and small reservoir sample sizes make comparisons among samples challenging to interpret, the results show that in 2016 nearly 95% of the seston at the ReReg site (RM 100.1) was comprised of seston released from the Project, and the proportion of planktonic:benthic sources of seston approaches unity towards the mouth of the river (Figure 6-56). Although the measures of central tendency show that the proportion seston in the periphyton samples was greatest at sites RM 100.1 and RM 75, the high degree of variability resulted in no significant difference between plankton and benthic biovolume at these two sites. The two exceptions are sites RM 45.5 and RM 54.4, which exhibited statistically greater benthic taxa compared to phytoplankton taxa (p = 0.0357 and 0.0253, respectively using a paired T-test).

Table 6-2. Phytoplankton total biovolume (10^8 µm3/mL) in the epilimnion of the two impoundments and the LDR in 2016

Statistic	Lake Billy Chinook	Lake Simtustus	Lower Deschutes River
n	9	8	49
Mean	2.14	1.15	2.38
sd	1.67	1.33	6.24
Median	1.54	0.59	0.77
1st Quartile	0.92	0.29	0.39
3rd	3.50	1.85	1.76
Maximum	5.37	4.05	33.3

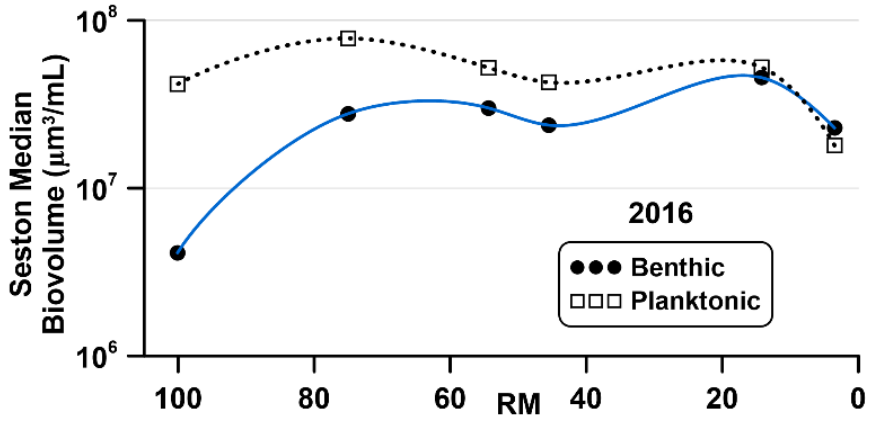

Figure 6-56. Partitioning of seston from LDR samples in 2016. Benthic taxa represent organisms typically occupying the substrate in rivers, whereas planktonic taxa are generally found as free-floating algae in lakes and reservoirs.

Of the 49 LDR seston samples collected in 2016, 41 (84%) of them were dominated by planktonic forms (Table 6-2). The remaining eight samples included five that were fully benthic taxa and three comprised other groups that can be found in benthic or planktonic habitats. The proportions changed in the subdominant groups in which truly benthic taxa comprised the majority of organisms and planktonic forms comprised only 39% of the taxa.

Two of the more dominant taxa in the seston released from the Project were *Stephanodiscus* spp.

and *Dolichospermum*. *Stephanodiscus* spp. was common at the reservoir sites and became proportionately even more dominant in the LDR, where 71% of the seston samples were dominated by this taxon. Also, it represented nearly a quarter of the biovolume in the plankton measured in the seston at site RM 100.1. The abundance of *Stephanodiscus* declined mid-river but increased again towards the mouth (Figure 6-57). The most abundant species of *Stephanodiscus* encountered in the river was *S. niagarae*, a large centric diatom that was also common in LBC. The cyanobacterium *Dolichospermum* (*Anabaena*) was dominant in only two of the river plankton samples and was subdominant in seven other samples. The abundance of *S. niagarae* and *Dolichospermum* in LBC shows a similar temporal pattern with the same dominant taxa as seston in the LDR (Figure 6-58). However, whereas *Dolichospermum* becomes dominant in LBC in the summer, it never exceeds the abundance of *S. niagarae* in the river.

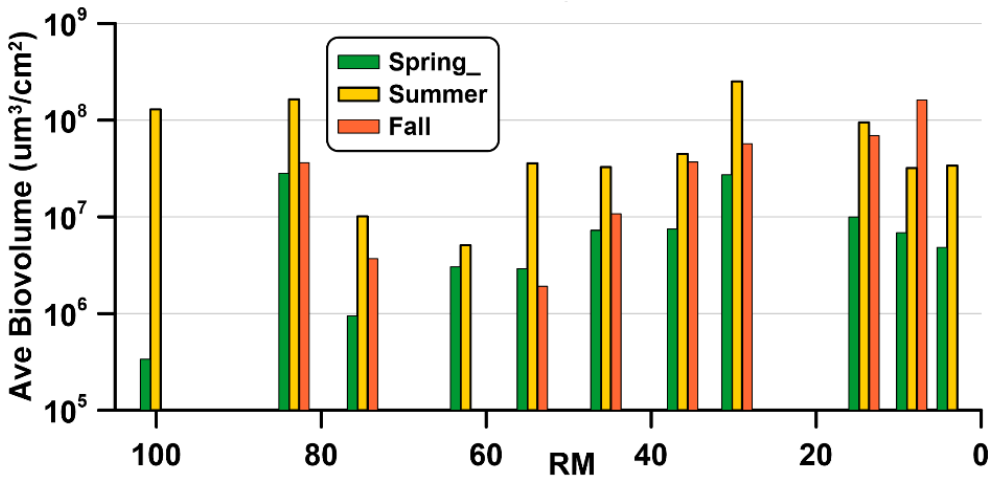

Figure 6-57. Average biovolume of *Stephanodiscus* spp. by RM for spring, summer, and fall 2016. Results for winter are not shown because several of the sites showed no *Stephanodiscus* present and where it was present, its biovolume was low.

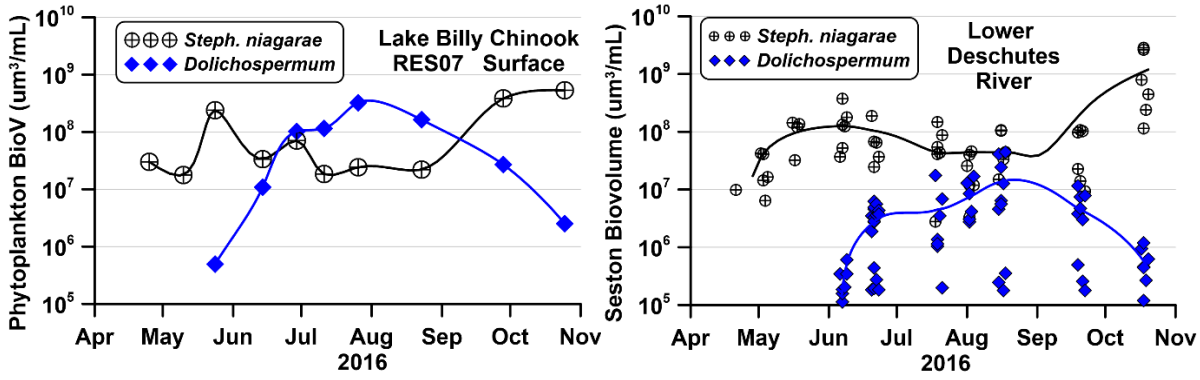

Figure 6-58. Algal biovolume of *Stephanodiscus niagarae* and *Dolichospermum* in Round Butte forebay (RES07) from surface samples (*left*) compared to biovolume of same taxa from seston samples in the LDR *(right)* in 2016.

Dolichospermum entrained from the reservoirs remain a significant portion of the seston to the mouth of the river (Figure 6-59). This is surprising considering the LDR is turbulent with an average gradient of 12.3 ft/mi. Williamson et al. (2018) found that cyanobacteria abundance dissipated rapidly in the Hunter and Cudgegong rivers (Australia), which are below large reservoirs and have an average gradient between 6.1–10 ft/mi. Most of the cyanobacteria had dissipated within 15 mi. They observed that cyanobacteria die-off was particularly rapid for filamentous taxa such as *Dolichospermum* and attributed the die-off to turbulence in the rivers and the length of riffle reaches. However, a study of the Klamath River found that intact *Microcystis* cells originating from Copco and Irongate reservoirs in California passed the length of the river to the estuary, a distance of more than 186 mi (Otten et al. 2015). A similar observation was made by Yu et al. (2015) for the Tanglang River downstream of Dianchi Lake (China), where *Microcystis* cells still constituted the majority of the seston 71 mi downriver. Grabowska and Mazur-Marzec (2016) also observed that *Planktothrix agardhii* traversed 81 mi of the Narew River in Poland, downstream of the Siemianówka Reservoir.

Other benthic taxa that were moderately abundant in the seston some sites include the diatoms *Cocconeis placentula sensu lato, G. eriense, G. herculeana,* and *C. mexicana. Cocconeis* was dominant in two samples and subdominant in another 15 samples. Neither *G. herculeana* or *C. mexicana* were dominant in any samples, although *G. herculeana* was subdominant in 11 samples and *C. mexicana* was subdominant in three samples. These organisms obviously are

cells dislodged from the benthos, however, there did not appear to be an association between position on the river and the dominant benthic taxa in the plankton (as determined by Runs tests of dominant benthic taxa and river mile [Sokal and Rohlf 1981]).

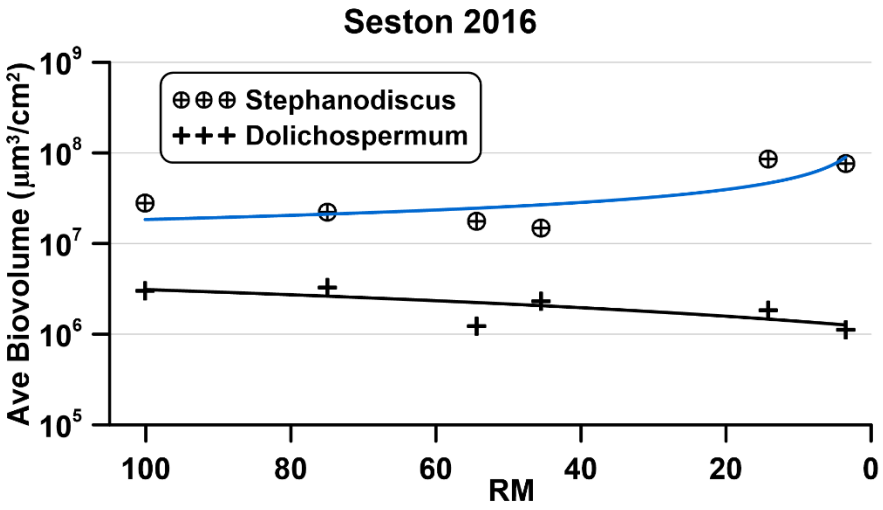

Figure 6-59. Average biovolume of Dolichospermum present in the seston of the LDR in 2016 compared to that of Stephanodiscus niagarae.

6.3 Comparison with Other Oregon Rivers

Every river is the unique product of its climate, hydrology, geology, vegetation, topography, and watershed activities. Nevertheless, it can be instructive to compare the water quality of different river systems. The ODEQ does this as part of its mandate to monitor and assess the quality of rivers and lakes throughout the state. For this study, we selected six rivers and compared available water quality parameters to results from ReReg Dam (LDR01) and the River Mouth (LDR21) (Figure 6-60). All data are from the AWQMP database, including those for the LDR. All data are from 2010 to 2017 to allow for comparison with current operating conditions in the Project.

None of the six rivers selected for comparison with the LDR are a perfect match (Table 6-3). As noted by others, the geology, geomorphology, and hydrology of the LDR are unique (O'Connor and Grant 2003). However, the Oregon rivers chosen for comparison are the following:

Figure 6-60. Location of the six rivers used in the LDR water quality comparison.

- The John Day River, which is located in the basin immediately to the east of the Deschutes River basin and discharges into the Columbia River. The John Day River basin is similar in area to the Deschutes River basin, but its geology is significantly different, resulting in much reduced groundwater inputs to the river. No major dams are located in the John Day River basin.
- The Grand Ronde River, which is in the northeast corner of the state, drains the Wallowa Mountains and is also free of major impoundments.
- The Powder River, which originates in the Blue Mountains of eastern Oregon, flows easterly through Baker City. Phillips Lake is a major reservoir located upstream of the sampling site near Baker City.
- The Silvies River, which is a free-flowing river that originates in the Strawberry Mountains of eastern Oregon, discharges to Malheur Lake.
- The Rogue River, which is in southern Oregon, originates in the Cascades but flows to the west. It is impounded by Lost Creek Lake and receives agricultural and municipal influence farther downstream.
- The Williamson River, which is in southern Oregon and discharges into Upper Klamath Lake. It receives considerable groundwater discharge and is not impounded.

Table 6-3. River sites in Oregon used for comparison with the two ODEQ sites on the Deschutes River below the Project.

River	DEQ Site #	Description	Upstream Impoundment?
Deschutes	10506	At Hwy 26	Yes – PRB
Deschutes	10411	Above LDR mouth	Yes – PRB
John Day	11386	At Hwy 206	No
Grande Ronde	10720	Hilgard Junction Park	No
Powder	11490	At Hwy 7 (Baker City)	Yes – Phillips Reservoir
Silvies	33929	West Loop Road	No
Rogue	10418	At Robertson Bridge (Merlin)	Yes – Lost Creek Lake
Williamson	10770	At Williamson River Store	No

The boxplots in Figure 6-61 show the distributions of pH values for the two sites on the LDR and the six selected rivers. The John Day River had the highest pH values among the selected sites (slightly exceeding the results for the LDR). The median pH for all the rivers, except the Rogue River, exceeded 8.0 and the upper limit of the range observed at all sites, except the Silvies River, had exceeded 8.5.

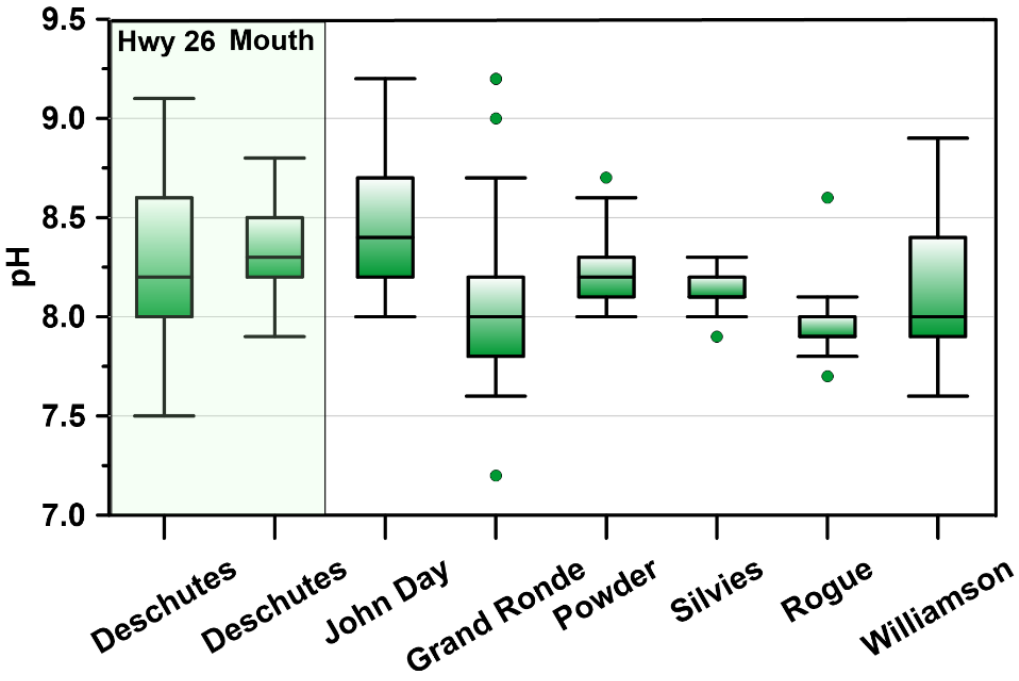

Figure 6-61. Boxplots of pH distributions for the two ODEQ sites on the LDR and several other rivers in the ODEQ AWQMP database.

DO saturation was highest in the John Day and Grand Ronde rivers, although the LDR at its mouth and the Powder River had the highest median values (Figure 6-62). The median DO saturation value for the LDR at U.S. Highway (Hwy) 26 was comparatively low because of the depressed values associated with the summer release of undersaturated water. Conductivity values indicate the cumulative concentrations of dissolved ions present in the water. The measured levels were not high enough to cause any water quality impact to aquatic life at any of the sites. The conductivity differences among sites reflect the geology and weathering of minerals in the basins (Figure 6-63).

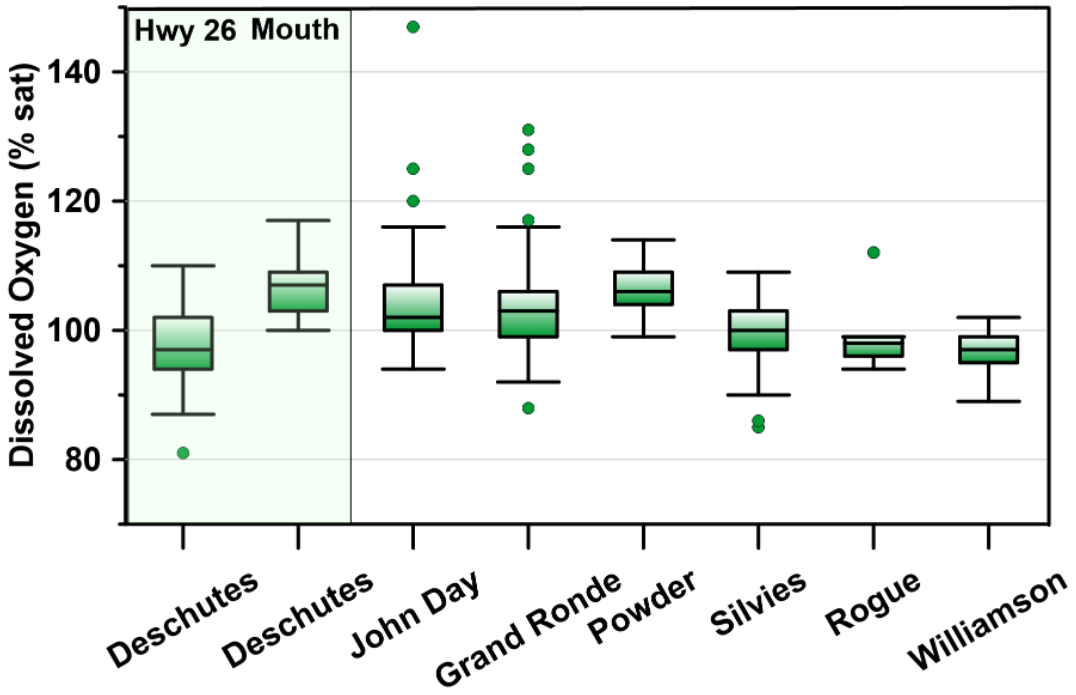

Figure 6-62. Boxplots of DO saturation for the two ODEQ sites on the LDR and other selected Oregon rivers.

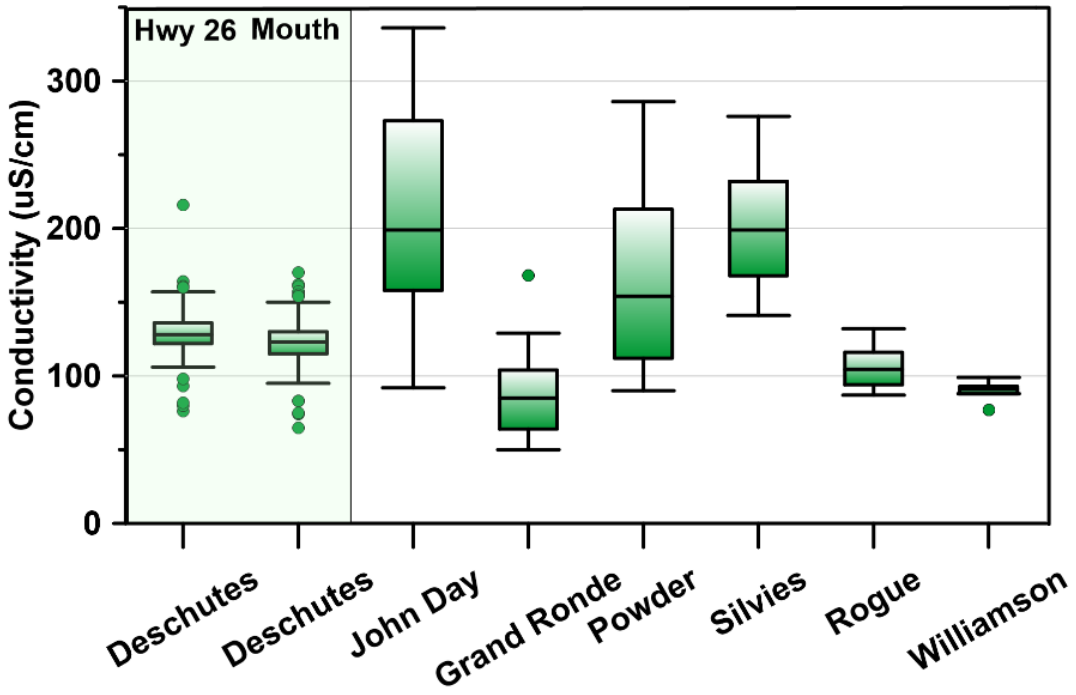

Figure 6-63. Boxplots of conductivity for the two ODEQ sites on the LDR and other selected Oregon rivers.

The highest median concentrations of PO_4 were observed at the upstream site in the LDR and in the Williamson and Rogue rivers (Figure 6-64). Although the Rogue River drains the west side of the Cascade Range, it offers a reasonable water quality comparison with the LDR because it drains volcanic terrain like the Deschutes River, and both the LDR and the Rogue River sites are downstream of large impoundments. In contrast, the Williamson River has no upstream impoundment, but it has a high proportion of groundwater inflow and is also located in volcanic terrain. The Rogue River has moderate urbanization above the Merwin site, whereas the Williamson River has little development in the watershed. In some respects, the Williamson River is similar to the Metolius River in that both are derived from substantial groundwater inputs that are comprised of high-phosphorus waters from weathering of volcanic bedrock.

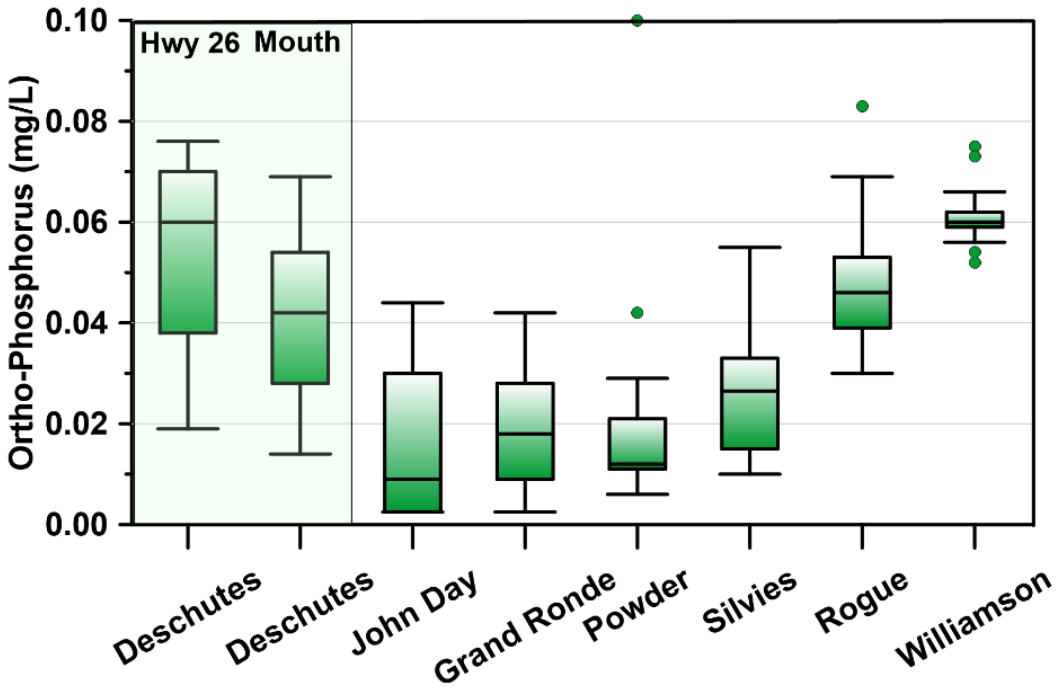

Figure 6-64. Boxplots of PO_4 concentrations for the two ODEQ sites on the LDR and other selected Oregon rivers.

Unlike phosphorus, which can have a major geologic source, concentrations of NO_3 are largely attributed to anthropogenic sources from discharge of urban waste, unused fertilizer applications, or mineralization of decaying phytoplankton in upstream impoundments. All the free-flowing rivers shown in Figure 6-65 had low concentrations of NO_3, whereas the LDR and Rogue River had elevated NO_3 levels. Both the LDR and Rogue River sites are downstream of very productive reservoirs and both sites also have substantial anthropogenic sources upstream (agricultural in the case of the LDR and mixed agricultural/development in the Rogue drainage). On the Powder River, Mason Dam (which impounds Phillips Lake) withdraws water from the hypolimnion, so the bottom waters might be depleted of NO_3.

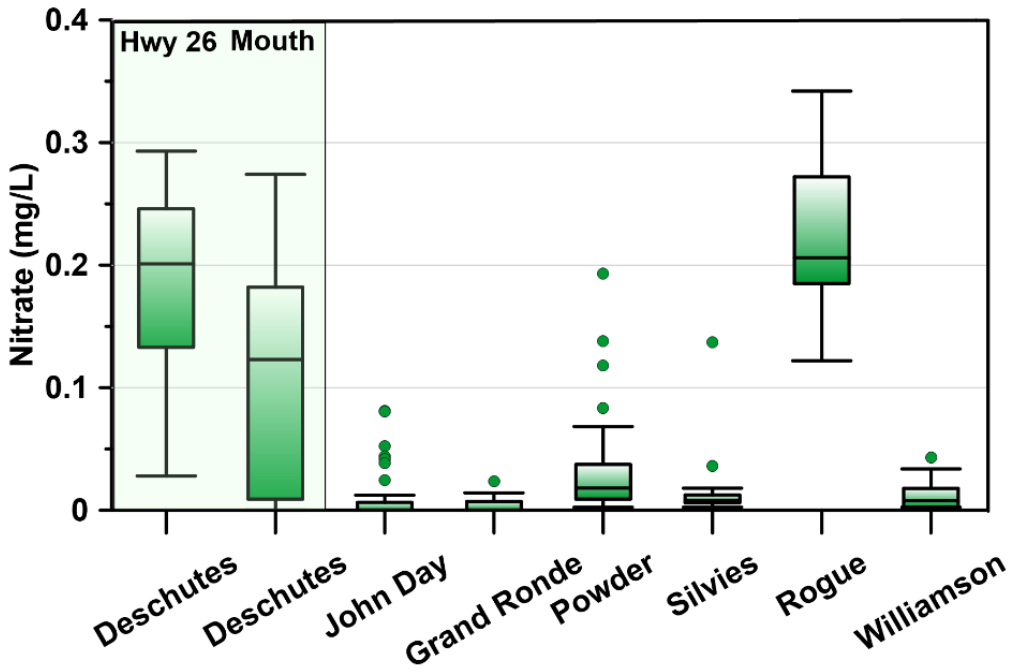

Figure 6-65. Boxplots of NO_3 for the two ODEQ sites on the LDR and other selected Oregon rivers.

Concentrations of chlorophyll at the sites showed the LDR sites to be major outliers. Median values for the other sites were around 6 µg/L, while outliers for the LDR exceeded 30 µg/L (Figure 6-66). All chlorophyll values reported in this section are derived from analytical

measurements of chlorophyll *a*. Lost Creek Lake (on the Rogue River) has a multiport intake tower for blending the temperature of release water and generally takes little water from the surface, unlike the SWW at the Round Butte Dam, which can discharge up to 100% surface water from LBC. Concentrations of BOD were generally low across the group of selected river sites (Figure 6-67). The highest median concentration of BOD was observed at the LDR (mouth) and the lowest was on the Williamson River. The amount of organic matter as live and dying phytoplankton/ zooplankton discharged from Round Butte Dam might explain the slightly greater BOD_5 values observed at the mouth of the Deschutes River.

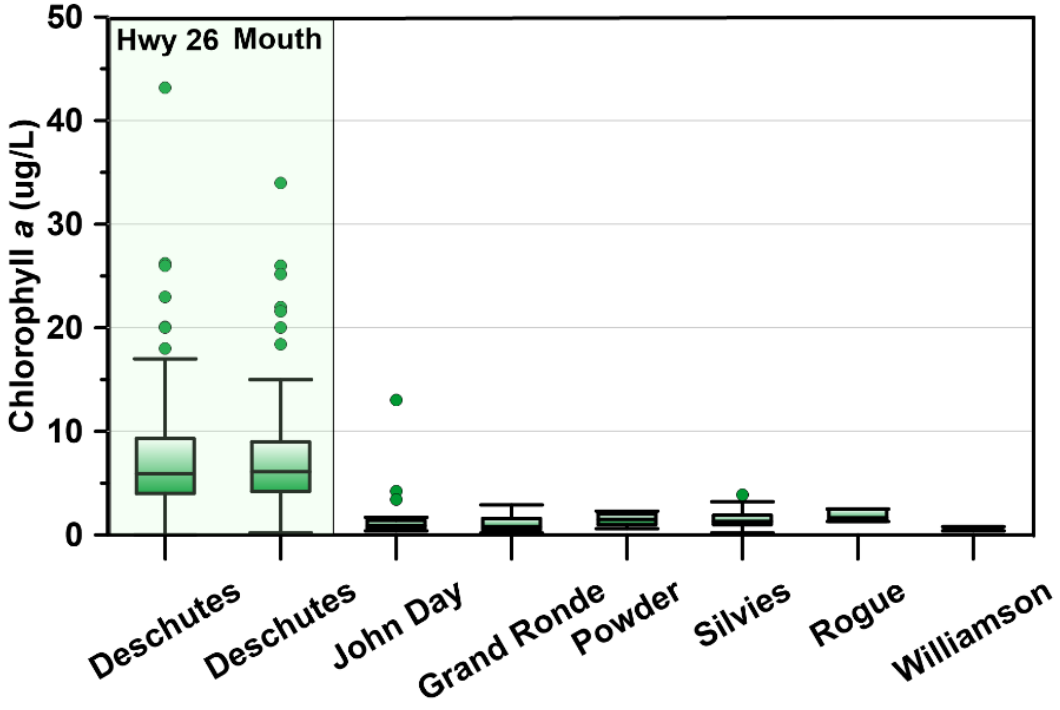

Figure 6-66. Boxplots of chlorophyll *a* for the two ODEQ sites on the LDR and other selected Oregon rivers.

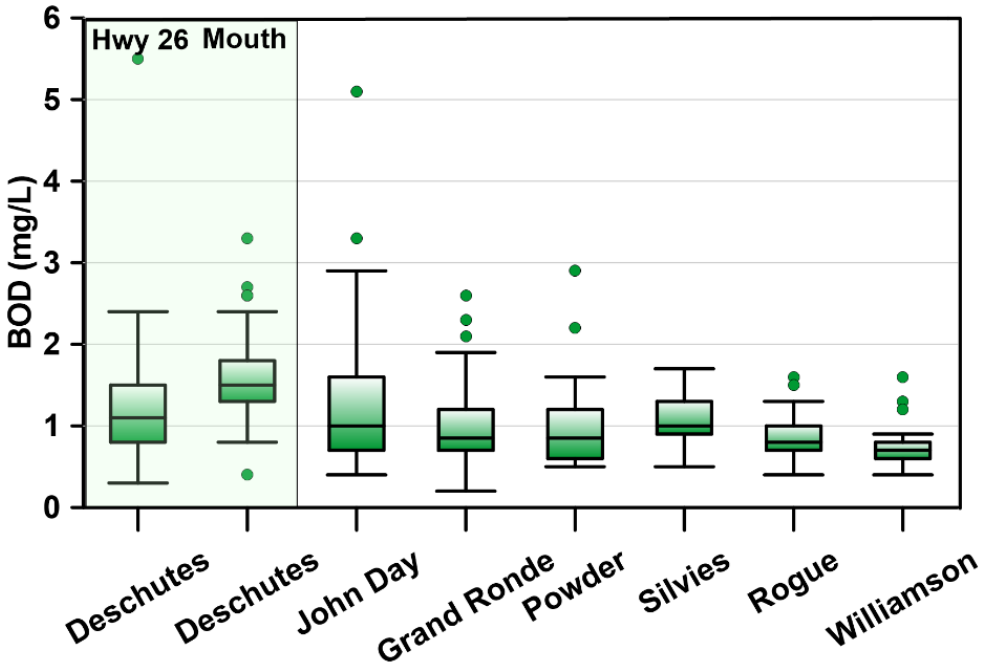

Figure 6-67. Boxplots of BOD_5 for the two ODEQ sites on the LDR and other selected Oregon rivers.

Viewed collectively, chlorophyll and NO_3 levels were substantially elevated on the LDR. Among the sites examined, only the Rogue River had higher concentrations of NO_3 than the LDR. Median pH values in the LDR and the John Day River were higher than in the other rivers. DO levels in the LDR were similar to those observed in the other rivers and phosphorus concentrations in the LDR were naturally elevated largely because of geologic sources. The Metolius River, which supplied 43.9% of the surface inflow to LBC during the study, had PO_4 concentrations measured in this study of 0.066 mg/L *(se = 0.002, n = 26)*. The Middle Deschutes River tributary to LBC had nearly identical concentrations of PO_4 *(mean = 0.069, se = 0.002, n = 27)* and flows that represented 16.9% of the surface inflow. The Crooked River supplied 39.2% of the surface inflow during the study and had mean PO_4 concentrations of 0.080 mg/L *(se = 0.002, n =25)*. The mean concentration of PO_4 in the Crooked River, which is about 18% higher than the concentrations in the Metolius and Middle Deschutes rivers, is significantly affected by agriculture and development, which contribute to the higher concentrations of PO_4 in LBC. Some of this anthropogenic contribution of phosphorus is subject to treatment and reduction in load.

7 Changes in Water Quality in the Lower Deschutes River

The project team used data from several sources from the era before the SWW was installed to assess how the water quality in the LDR has changed. The study by Raymond et al. (1998) summarized the water quality at 21 sites visited on three float trips in May, July, and September 1997. ODEQ collected long-term ambient monitoring data at the Hwy 26 bridge (Site #10506 at RM 97.6) and near the mouth of the LDR at the Deschutes River SRA (Site #10411 at RM 0.1). Those data cover several decades, but the duration of the data varies by site and parameter. A third dataset includes water quality sonde measurements collected below the ReReg Dam by PGE starting in 2005. There is also temperature data collected on the LDR by USGS and, more recently, by PGE.

The 1997 survey included an abbreviated list of water quality analytes, periphyton/ macroinvertebrate sampling, and several fixed-station sonde deployments to characterize diel changes in water quality. The ODEQ data included a much more comprehensive list of analytes for water chemistry but no biological sampling. ODEQ's ambient monitoring data consisted of irregular sampling of the sites, but typically included 6–10 visits per year extending back several decades. The PGE data consisted of near-continuous pH and DO measurements along with conductivity and temperature, and the USGS data included water temperatures at the Madras and Moody gauges over irregular periods, with the most extensive data available for the Madras gauge. Where PGE and USGS both collected temperature data at the same site (such as at the ReReg Dam), the USGS data were used.

7.1 River Temperature

River temperature data were available at the Madras gauge immediately below the ReReg Dam for periods before and after SWW installation. The river temperature prior to the installation peaked in September and was remarkably consistent from 2006 to 2008 (Figure 7-1). That consistency is likely associated with the source water being derived from the hypolimnion of LBC. More recent data showed peak temperatures in June 2016 and in July 2015 and 2017. The temperatures from 2015 to 2017 were considerably more variable, in part, because water was

being blended to achieve a desired outcome. Once LBC mixes in October, the reservoir becomes nearly isothermal and the differences in temperature between years are minimal.

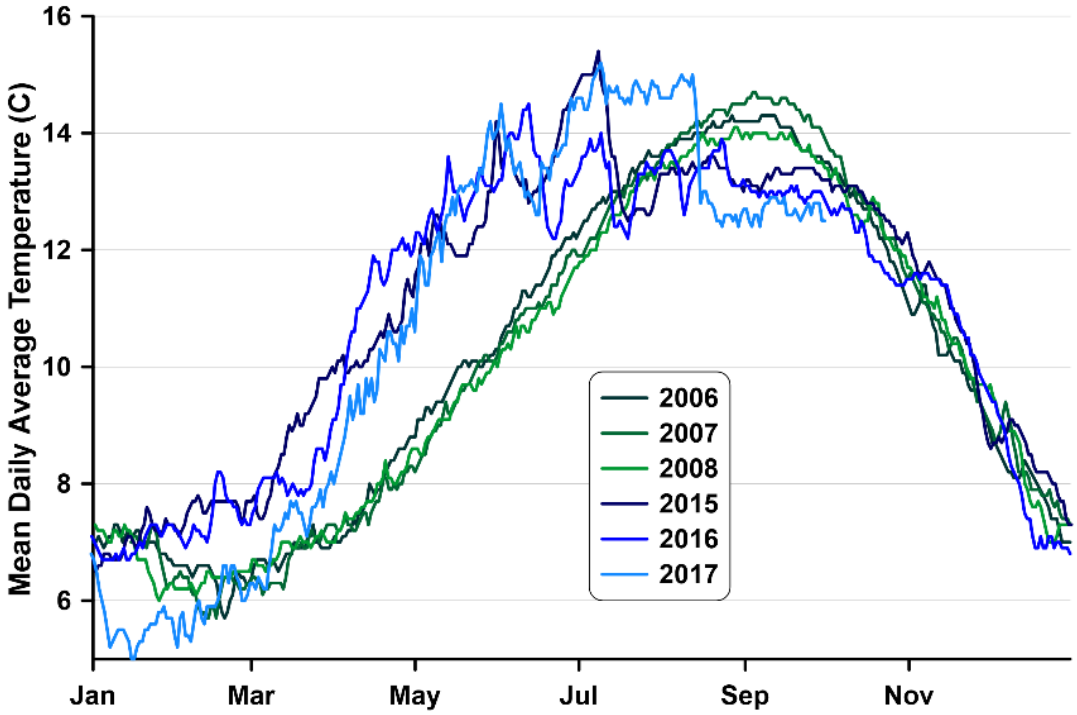

Figure 7-1. Daily average temperature of the LDR at the USGS Madras gage (RM 100.1) for the periods 2006–2008 and 2015–2017.

7.2 1997 Survey

TP and NO_3 were the primary analytes from the Raymond et al. study (1998) relevant to assessing changes in nutrient chemistry. Concentrations of TP were similar in 1997 and 2015–2017, except for the data collected in July (Figure 7-2). The concentrations of TP in July 2015 and 2016 were twice as high as the 1997 results. This was a substantial increase in TP during July; alternatively, the 1997 data could have been an aberration. Another difference in results for

TP was the elevated TP at Sandy Beach (RM 45.5) in 2016. It is unclear whether that difference was caused by a localized disturbance associated with a heavily used rafting takeout or reflected

turbid flows from the White River confluence a short distance upstream. Regardless of the explanation, TP concentrations declined to pre-Sandy Beach values immediately downstream.

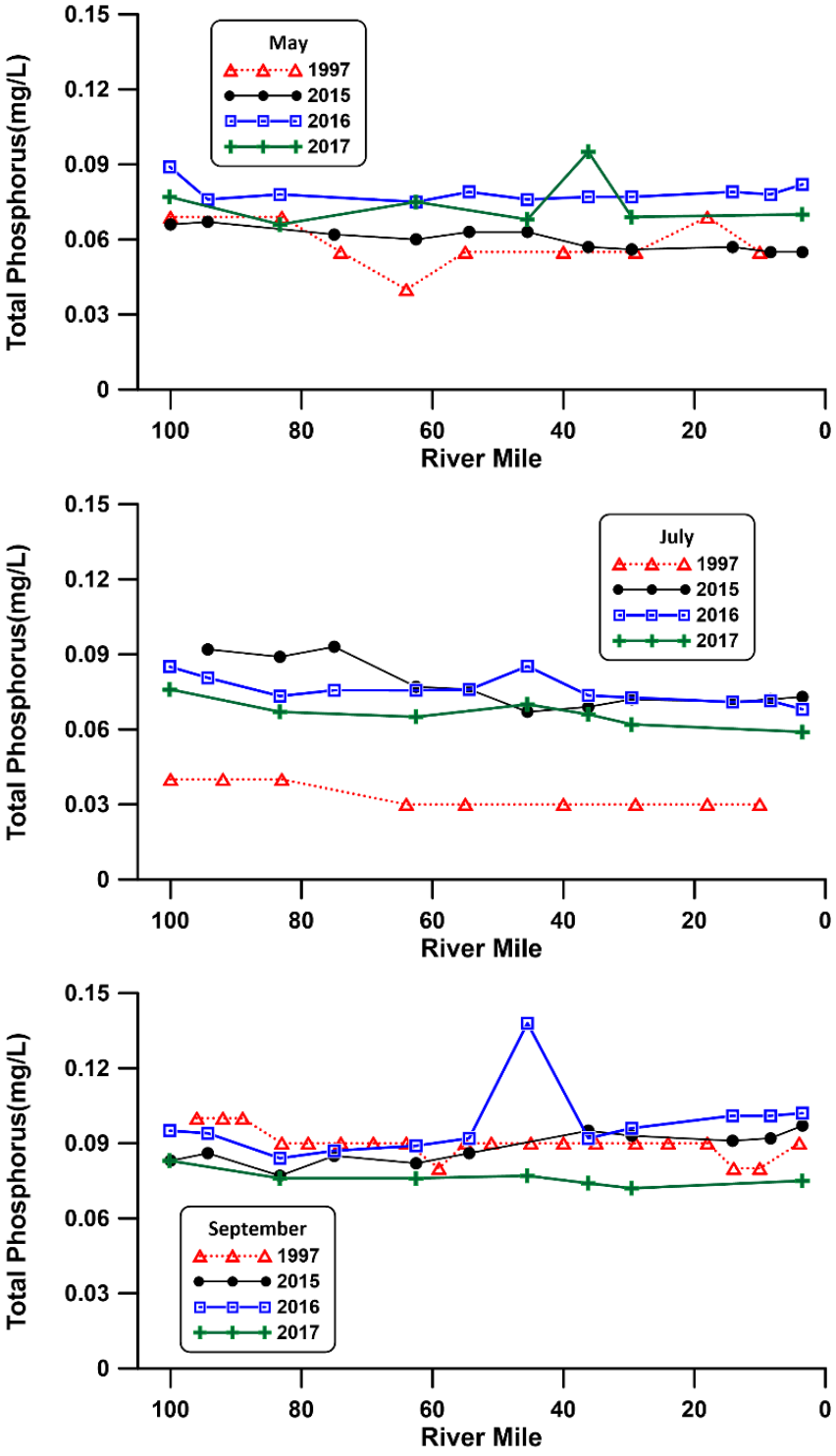

Figure 7-2. Concentrations of TP by river mile and year (1997, 2015, 2016, and 2017) for May (*top*), July (*middle*), and September (*bottom*). Note that the river was not sampled in May 2017, thus the spring comparison is for May 1997 and June 2017.

The results for NO_3 were more variable between years and months, which likely reflected larger variations in supply to the LDR and differences in assimilation by periphyton (Figure 7-3). In May 1997 and 2015, initial NO_3 concentrations from the Project were relatively low and approached DLs (0.010 mg/L) near the mouth of the river. A similar pattern was observed for samples collected in early May 2016. However, sample results from 2 weeks later, which overlaps with the calendar dates from 1997, showed a major increase in NO_3 for the 2016 data and a moderate increase for the 2017 data. In July 1997 and 2015, concentrations of NO_3 reached DLs downstream of RM 30, whereas, in July 2016, concentrations of NO_3 remained high throughout the river. In September 1997, 2015, and 2016, the NO_3 export from the Project was high and the load decreased by nearly one-half through the course of the river. The high NO_3 values from the Project in September might reflect decreased utilization of NO_3 by algae as ambient temperatures decline and sunlight diminishes. The elevated concentrations of NO_3 observed in the LDR in 2015 were likely related to the low precipitation/runoff and subsequent response in LBC and the LDR, although the precise cause of the increase is unclear.

It should be noted that 1997 might represent an outlier regarding conditions in the LDR. In 1996, the flows were the highest recorded and the stream velocities achieved during the flood likely moved portions of the substrate. Rocks dislodged during the flood would likely have lost all or a portion of any accumulated periphyton and consequently water chemistry measured in the river during 1997 might have demonstrated reduced effects from periphytic algae.

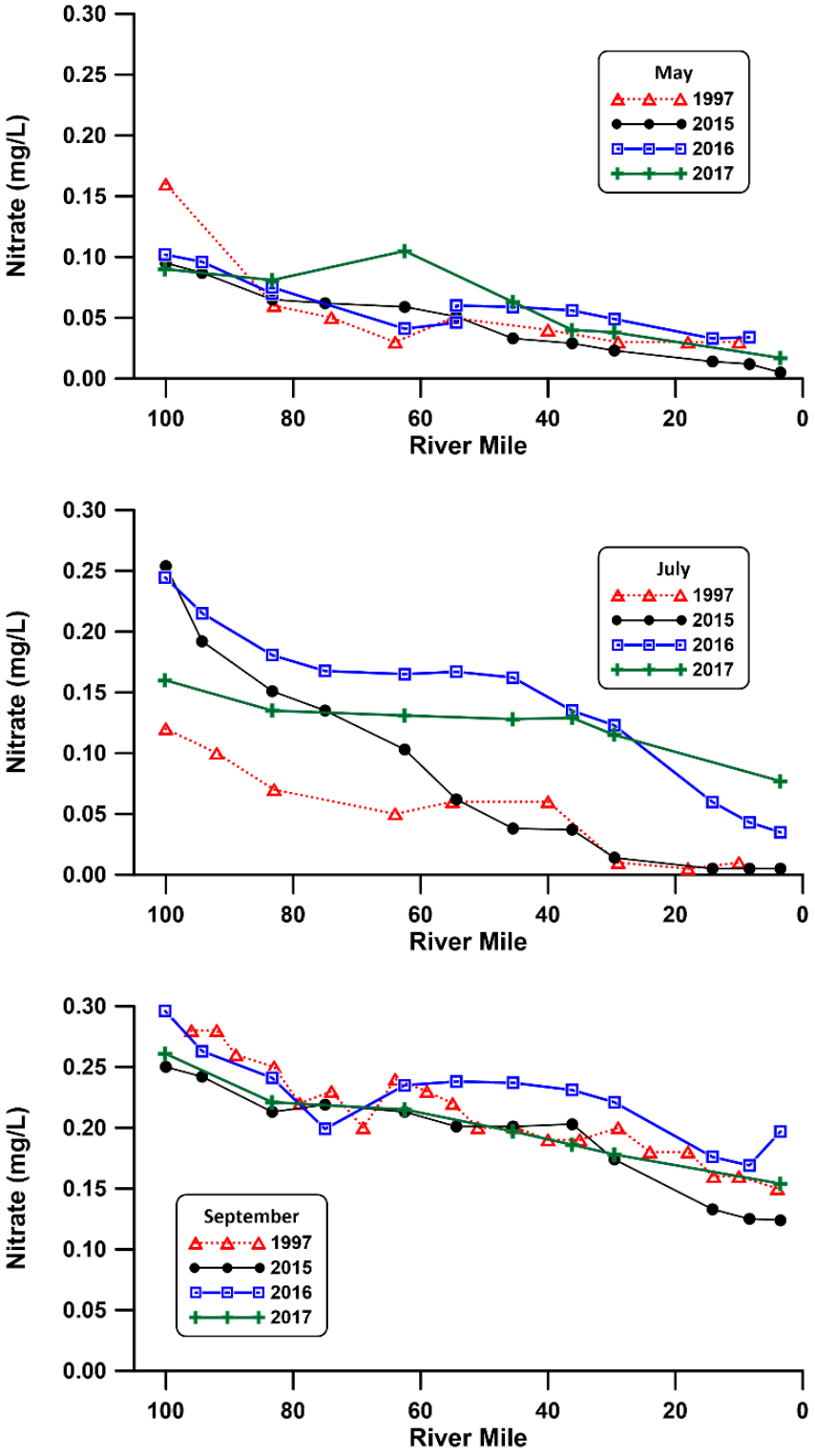

Figure 7-3. Concentrations of NO_3 by river mile and year (1997, 2015, 2016, and 2017). Values at the DL (<0.010 mg/L) were set at 0.005 mg/L for these plots.

Table 7-1. Significant actions and events upstream of the ODEQ monitoring sites.

Year	Activity	Note
1929 -1945	Dust Bowl Era Drought	13 of 17 years had summer mean flows of less than 4,000 cfs; considered the longest drought in over 500 years.[a]
1949	Wickiup Dam Completed	Located on the Upper Deschutes River; this was a substantial enlargement of an earlier dam.
1949	Ochoco Dam	Located on the Ochoco River; this was a substantial enlargement of an earlier dam.
1958	Pelton and ReReg Dams	Located on the Deschutes River.
1961	Bowman Dam	Located on the Crooked River.
1964	Round Butte Dam	Located on the Deschutes River.
1964	Christmas Flood	Flood resulted in rapid filling of LBC; peak discharge of 62,400 cfs at Moody on Dec 23.
1968	Drought[b]	Mean Jul-Sep flow of 3,970 cfs.
1985	Opal Springs Dam	Dam enlargement on the Crooked River planned for 2019.
1994	Drought	Mean Jul-Sep flow of 3,720 cfs.
1996	Flood	Peak discharge of 63,400 cfs at Moody on Feb 8.
2010	Operation of SWW	Allows for surface and hypolimnetic withdrawals.

Notes:

[a] Pohl et al. 2002.

[b] Drought defined as mean monthly discharge for July–September of less than 4,000 cfs (7.5 percentile of daily discharge at Moody from 1906-2017).

Periphyton samples were collected as part of the 1997 survey, but a detailed analysis of the data showed they are not usable for assessing change in periphyton community composition. The 1997 data appear to have a major bias as to how filamentous periphyton were subsampled. As part of the current study, a series of split samples using the same analyst and methods from the 1997 work compared with analyses by two independent taxonomists showed that filamentous algae (both cyanophytes and chlorophytes) were grossly underrepresented in the Raymond et al. study (1998), giving them little value for assessing historical changes in periphyton (see Appendix C).

7.3 ODEQ AWQMP Data

As part of the AWQMP, ODEQ collects water quality data at the Hwy 26 bridge (RM 97.6) and near the mouth of the LDR (RM 0.1). Data collection for the dataset from the Hwy 26 bridge site began in 1958 and for the river mouth, it began in 1964. ODEQ initially sampled only on a quarterly basis, although over time the agency has increased its sampling frequency to almost monthly. Over the years, several changes to the river system have affected flow through the Deschutes River basin, including major dam construction activity and natural hydrologic events

The pH data for the Hwy 26 bridge site showed a steady increase from 1958 to 1990, a stable period from 1990 to about 2005, and small changes thereafter (Figure 7-4). The pH data for the LDR mouth showed a decline from 1962 to 1980, a sharp increase by 1990, and a stable period from 1990 to about 2010, when it increased slightly.

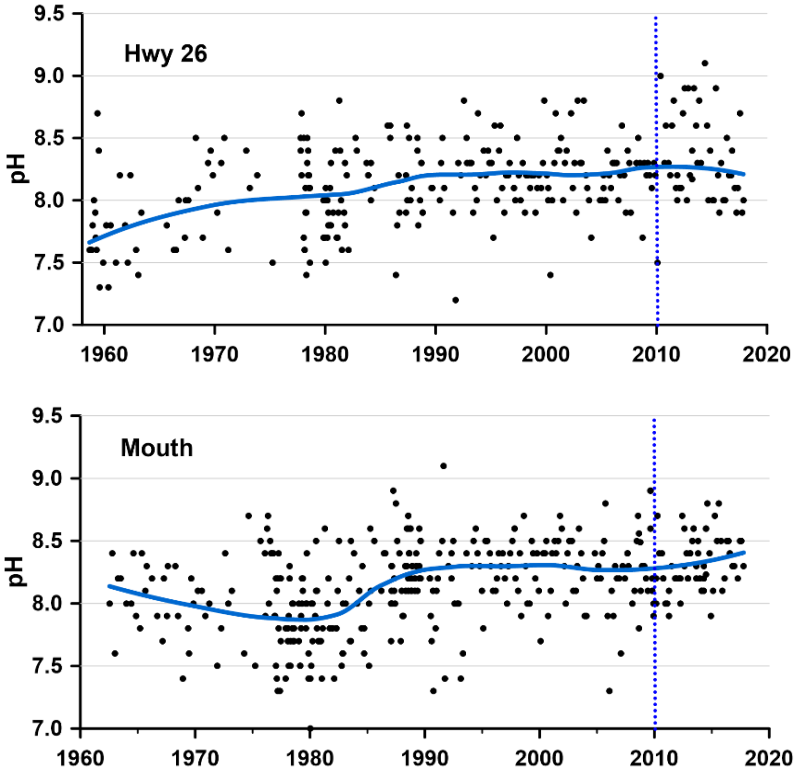

Figure 7-4. ODEQ AWQMP pH results at the Hwy 26 bridge site (RM 97.6) (*top*) and the LDR Mouth (RM 0.1) (*bottom*). The solid blue line is the LOESS fit of the observed data. The dashed vertical line denotes the start of operation of the SWW.

DO saturation at the Hwy 26 bridge site increased from 1958 to 1970, followed by a decline of 10% by 1990 (Figure 7-5). DO remained stable for another decade, but declined shortly after 2000, then increased again in 2010. The pattern at the LDR mouth showed a slight increase in DO from 1962 until the late 1980s. DO then declined until about 2005 and increased around 2010. However, the change in DO saturation at the mouth seldom exceeded 3%–4%.

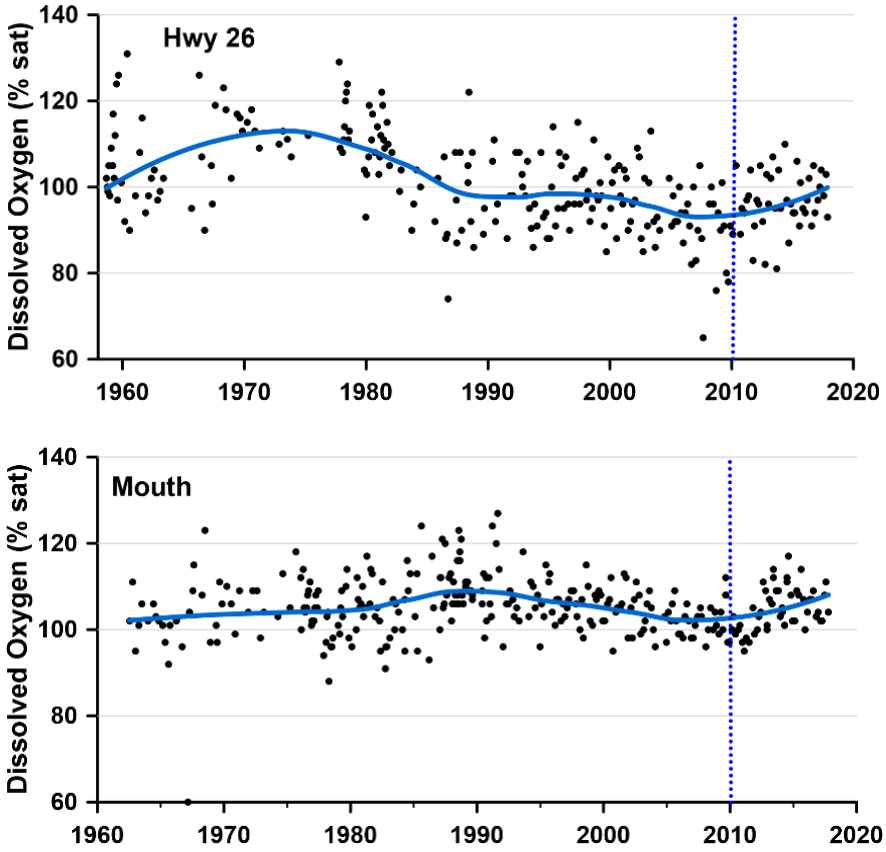

Figure 7-5. ODEQ AWQMP DO results at the Hwy 26 bridge site (RM 97.6) (*top*) and the LDR Mouth (RM 0.1) (*bottom*). The solid blue line is the LOESS fit of the observed data. The dashed vertical line denotes the start of operation of the SWW.

Concentrations of NO_3 at the Hwy 26 bridge site increased from near 0.10 mg/L in 1961 to a median near 0.225 mg/L in 2017 (Figure 7-6). Several small increases and declines occurred during this period, but the overall increase is noteworthy. Although the overall increase in NO_3 at the Hwy 26 bridge site appears substantial, there was significant short-term variability that is

not readily explained by seasonality. The concentrations of NO_3 at the LDR mouth had a different pattern, with an apparent increase from the 1960s to the late 1970s, a decline over the next decades, and then stable values to the present. The NO_3 values at the mouth showed a slight increase over the last three decades, with nearly one-half of the observations below 0.10 mg/L and many values at the DL (<0.010 mg/L) for NO_3. That result is in stark contrast to the observations at the Hwy 26 bridge site, which showed few values below 0.1 mg/L. Most of the low concentrations of NO_3 measured at the LDR mouth occurred during the months from April through September (Figure 7-7). During the cooler months, little NO_3 assimilation took place and concentrations at the mouth were accordingly higher.

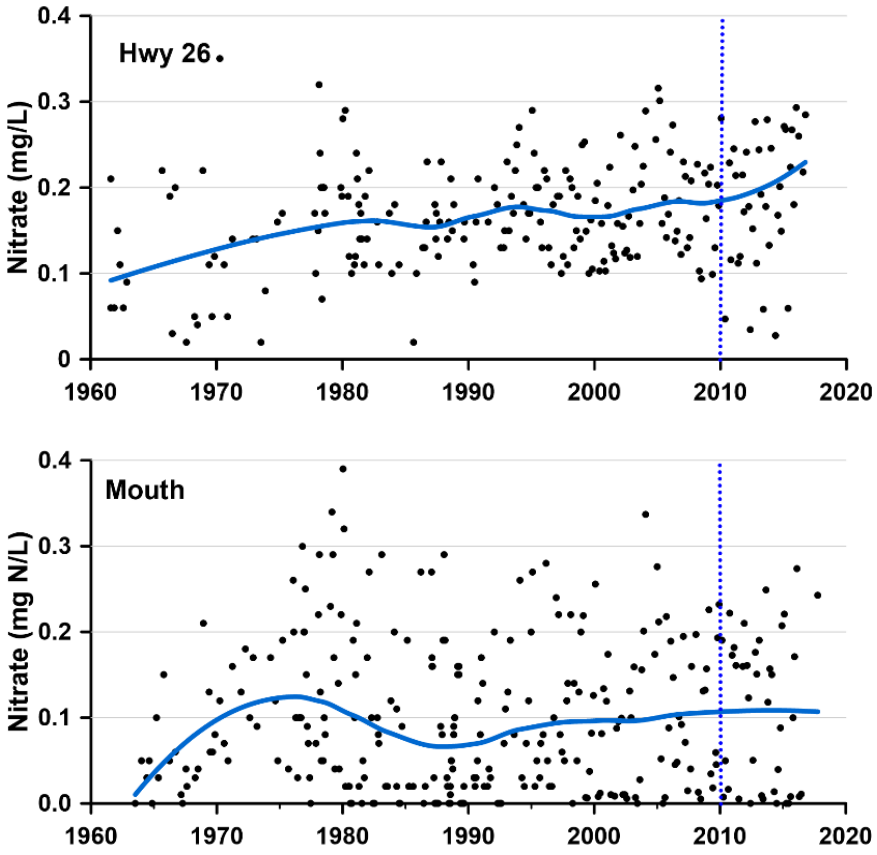

Figure 7-6. ODEQ AWQMP NO_3 results at the Hwy 26 bridge site (RM 97.6) (*top*) and the LDR Mouth (RM 0.1) (*bottom*). The solid blue line is the LOESS fit of the observed data. The dashed vertical line denotes the start of operation of the SWW. Several outliers have been removed from the plots.

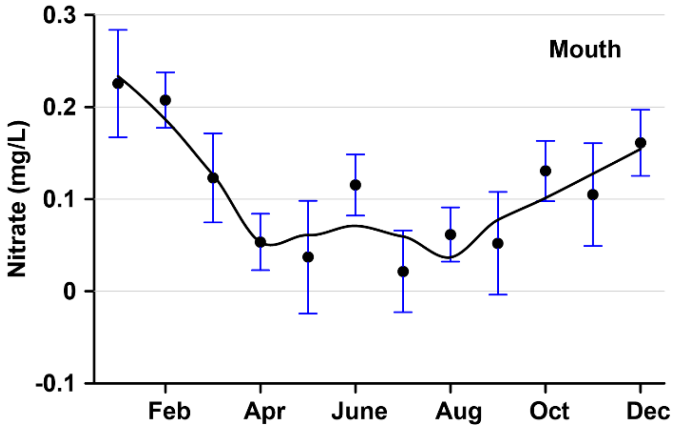

Figure 7-7. NO_3 concentrations at the LDR Mouth (RM 0.1) shown by month based on ODEQ AWQMP data. The vertical bars are the standard errors of the mean. The line is the LOESS fit of the observed data (1960 – 2017).

There were issues with the phosphorus methodology in the historical data that could not be rectified in time to be included in this study; consequently, observations for total phosphorus and phosphate were limited to after 1980. Concentrations of TP showed a slight decline at both sites for the PoR (Figure 7-8), but neither of the declines are significant. TP concentrations were similar at both sites and indicate that there are no permanent sinks of TP in the LDR.

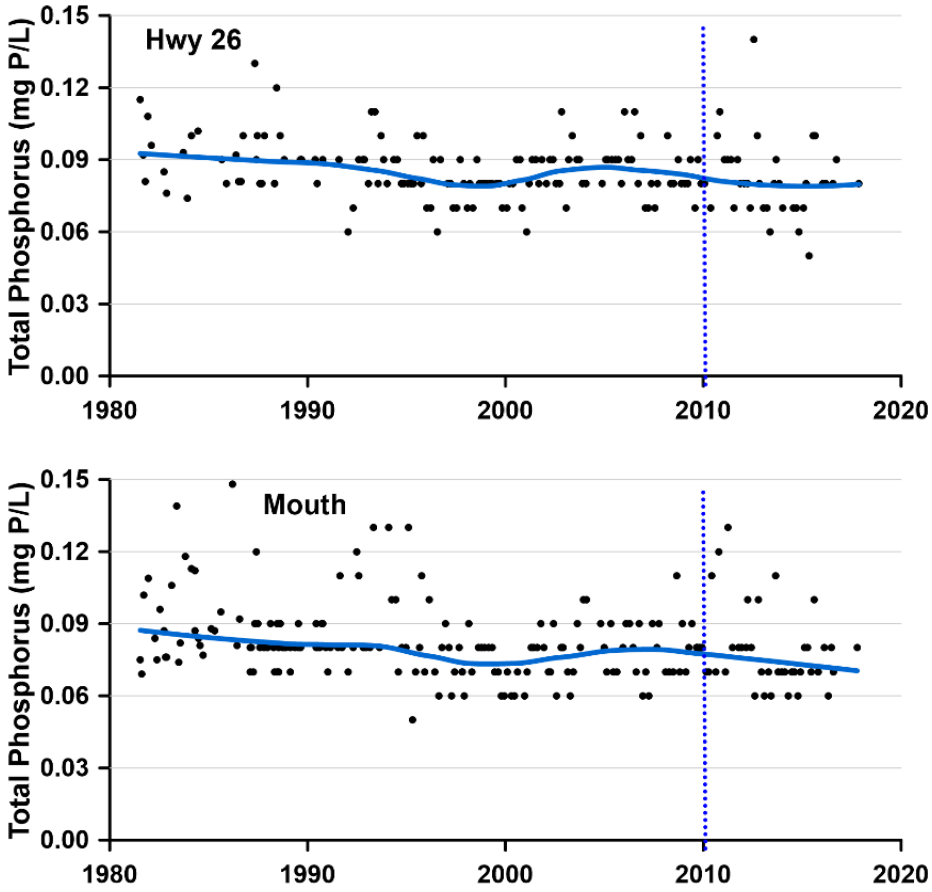

Figure 7-8. ODEQ AWQMP TP results at the Hwy 26 bridge site (RM 97.6) (*top*) and the LDR Mouth (RM 0.1) (*bottom*). The solid blue line is the LOESS fit of the observed data. The dashed vertical line denotes the start of operation of the SWW.

Concentrations of PO_4 at the Hwy 26 bridge site showed modest oscillations over the last several decades, with local peaks in 1990, 2005, and 2017 (Figure 7-9). Whereas PO_4 at the Hwy 26 bridge site had a slight upwards trend since 2014, PO_4 concentrations at the mouth showed a substantial downward trend over the same period. The 40% decline in PO_4 at the mouth seems to occur despite increased PO_4 concentrations at the Hwy 26 bridge site. The results suggest that PO_4 was being assimilated by periphyton at a higher rate in the LDR beginning in 2010. TP concentrations showed no trend at either site. Thus, the total mass of phosphorus appears unchanged in the LDR; only the form of phosphorus has been altered. PO_4 is soluble and is, therefore, more biologically available.

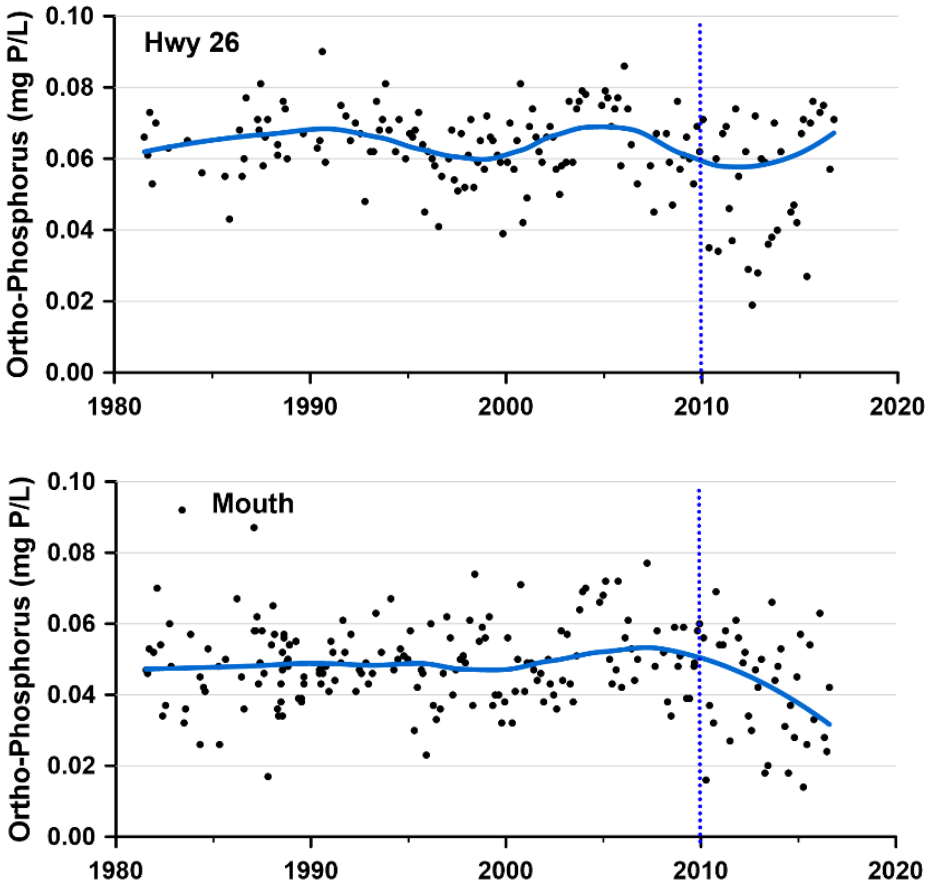

Figure 7-9. ODEQ AWQMP PO_4 results at the Hwy 26 bridge site (RM 97.6) (*top*) and the LDR Mouth (RM 0.1) (*bottom*). The solid blue line is the LOESS fit of the observed data. The dashed vertical line denotes the start of operation of the SWW.

BOD_5 is not a nutrient, but high concentrations of BOD can be a sign of organic pollution that will also affect pH and DO. BOD at the Hwy 26 bridge site showed a slight increase in the late 1980s, declined to a minimum in 2005, and has increased since then (Figure 7-10). The pattern at the mouth showed an even larger increase, peaking in the late 1980s, followed by a decline until about 2005, and an upward trend since that time. The magnitude of the changes in BOD were relatively modest, but they appear to be consistent at both sites.

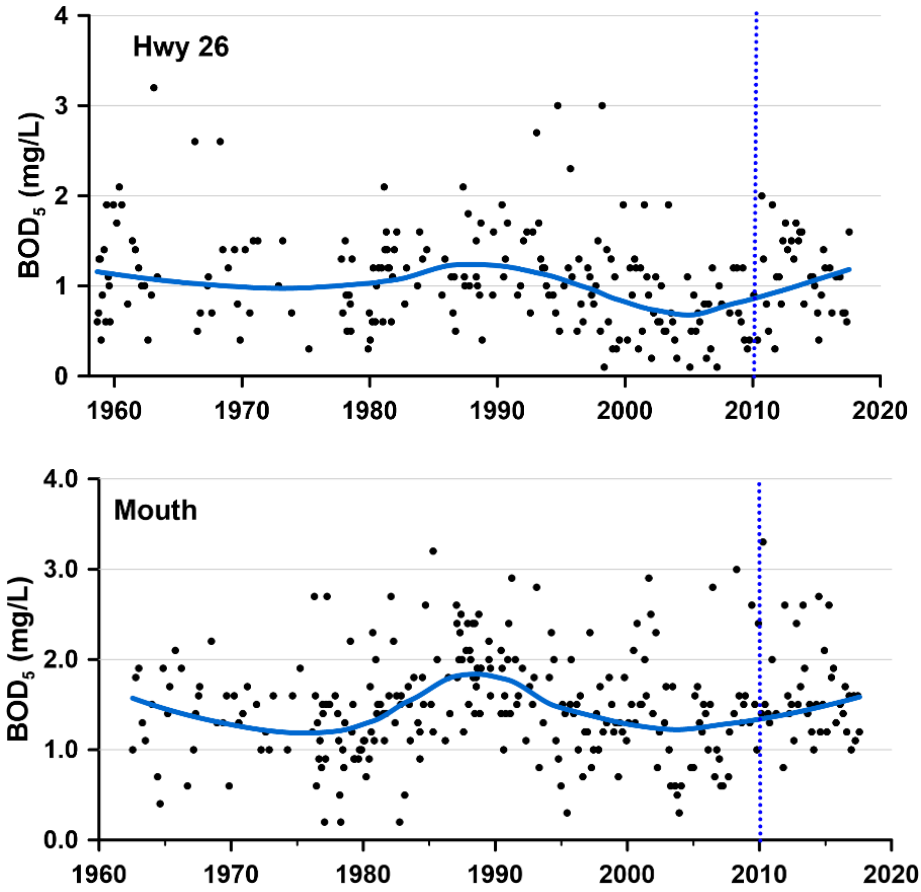

Figure 7-10. ODEQ AWQMP BOD results at the Hwy 26 bridge site (RM 97.6) (*top*) and the LDR Mouth (RM 0.1) (*bottom*). The solid blue line is the LOESS fit of the observed data. The dashed vertical line denotes the start of operation of the SWW.

Concentrations of chlorophyll at the Hwy 26 bridge site increased substantially in the 1990s, declined to a minimum in 2000, and has increased gradually since then (Figure 7-11). The pattern for chlorophyll at the mouth was quite different. Values were stable from 1985 to about 2005, but they have increased since. Several high concentrations of chlorophyll were recorded at the mouth in the 1990s, but they were not consistent enough to alter the relatively stable conditions represented by the locally estimated scatterplot smoothing (LOESS) fit. The apparent increase in chlorophyll *a* at the mouth might offer some insight into the decrease in PO_4 observed at the mouth in recent years. A decrease in PO_4 at the mouth could have been caused by an increase in periphyton upstream or by an increase in algae entrained in the water column or both.

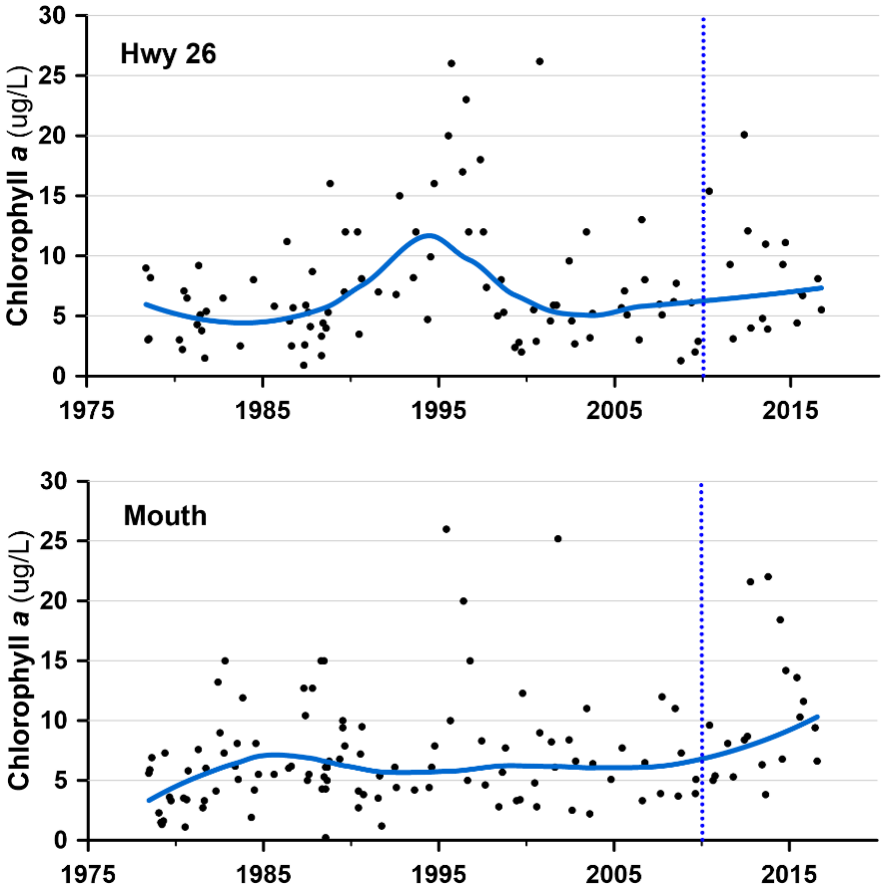

Figure 7-11. ODEQ AWQMP chlorophyll *a* results at the Hwy 26 bridge site (RM 97.6) (*top*) and the LDR Mouth (RM 0.1) (*bottom*). The solid blue line is the LOESS fit of the observed data. The dashed vertical line denotes the start of operation of the SWW.

The figures shown above present all data collected by ODEQ throughout the year. Several variables were filtered to show only values collected from April through September of each year. Combining results from the cool period with those from the spring and summer might mask effects on the LDR associated with operation of the SWW. Primary production in the LDR is relatively low in the late fall through early spring and, if there is a demonstrable effect of increased chlorophyll in the LDR associated with the installation of the SWW, it would likely be more evident when primary production is at its highest. The SWW operates at full surface flow from November 1 to mid-May; then 100% discharge from the surface is more intermittent and, while it declines in proportion, the SWW still releases at least 40% surface flows for the remainder of the summer. The truncated dataset shows pronounced increases in DO and NO_3 at

the Hwy 26 bridge site (Figure 7-12). These changes could be ecologically significant, although the reduction in sample size reduces confidence in the observed changes.

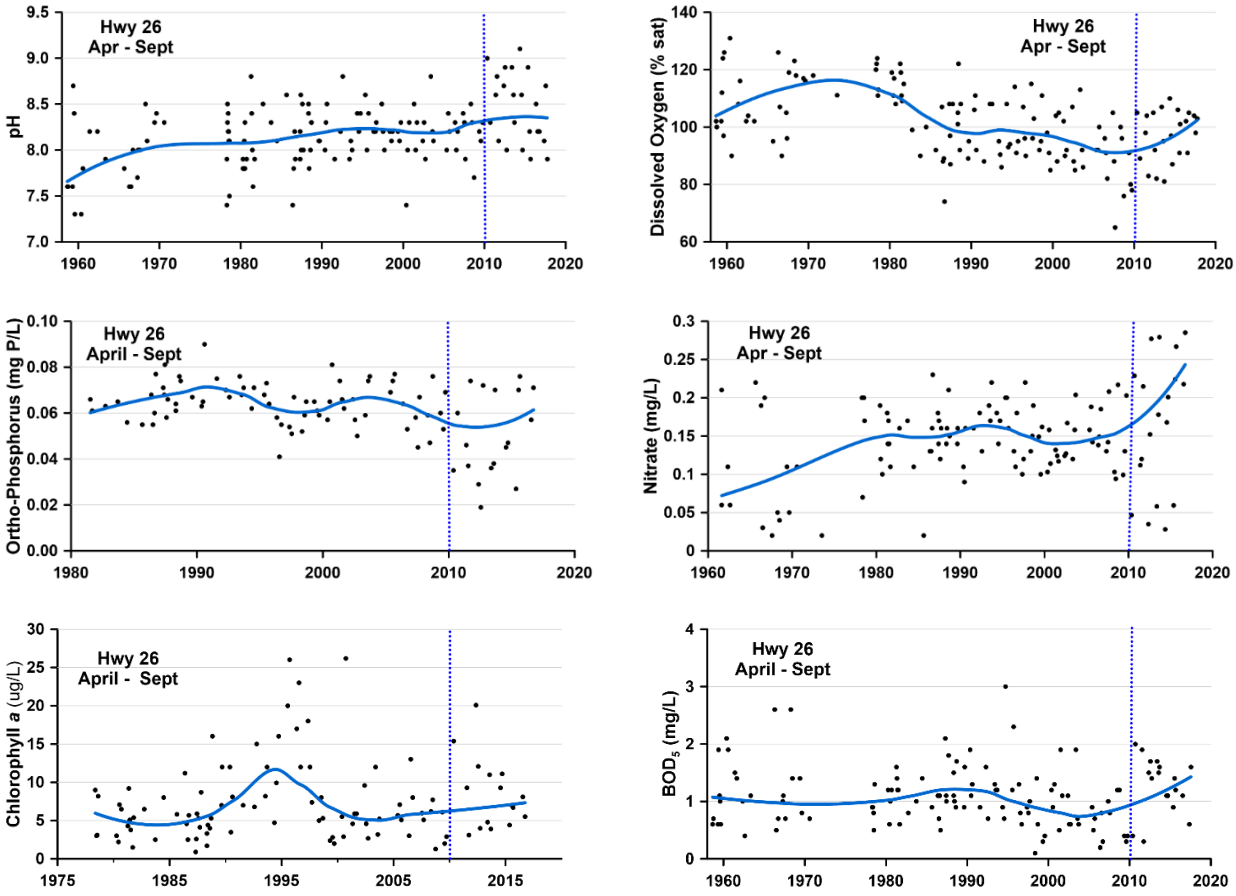

Figure 7-12. Data from the ODEQ AWQMP for pH (*upper left*), DO (*upper right*), PO_4 (*middle left*), NO_3 (*middle right*), chlorophyll (*lower left*), and BOD (*lower right*) at the Hwy 26 bridge site (RM 97.6). Observations from October through March have been excluded.

8 Discussion

8.1 Tributaries

The three major tributaries to LBC differ greatly from one another in many respects. During this study (WY2015–2017), the Metolius River discharge represented 43.9% of the measured flow entering LBC. The Crooked River was close with 39.2% of the measured flow and the Middle Deschutes River represented 16.9% of the flow. An important attribute of the three rivers is water temperature. The Metolius River is the coldest and the Crooked River is the warmest on average, but temperatures in the Deschutes River peak during summer. Because the Crooked River is the warmest on average, it is the dominant signature water over the Crooked arm of LBC, as well as in the lower portions of the Metolius arm. The Crooked River signature extended up most of the Metolius arm pre-SWW but now extends only a few kilometers from Round Butte forebay. The Metolius River's water now extends at or near the surface for much of the length of the Metolius arm and even extends up to a depth of 20 m below the surface in the forebay. The attractant flow on the surface created by the SWW results in Crooked River water flowing towards the forebay and forming a pronounced tributary signature discharged from LBC.

Conductivity is the sum of the equivalent conductivity values of the individual ions and, therefore, is reasonably conservative. It provides an excellent signature for the three tributaries and independently verifies the spatial patterns described earlier. The Metolius River has the lowest conductivity at about 75 µS/cm. Conductivity in the Deschutes River is about 110 µS/cm and, in the Crooked River, it is typically above 160 µS/cm.

The tributaries all have high concentrations of phosphorus, much of it available as PO_4 (0.066 to 0.080 mg/L PO_4). The Crooked River has substantial irrigation return flow as well as urban inputs from the City of Prineville, OR, both of which add to the phosphorus load in LBC. However, water flowing through the Crooked River valley accounts for only 20% of the Crooked River flow into LBC; the remaining 80% enters the Crooked River just upstream of the confluence from LBC via a major groundwater influx from Opal Springs. The most significant difference between the nutrient input of the tributaries is nitrogen, specifically NO_3. The Metolius River is largely devoid of measurable NO_3, whereas the Crooked River enters the

impoundment with an average of 0.40 mg/L of NO_3 and the Deschutes River enters the impoundment with an average of 0.22 mg/L of NO_3. The influx of high concentrations of both phosphorus and nitrogen provides fertile conditions for abundant growth of phytoplankton.

It is important to understand whether the nutrient loading to LBC is natural versus anthropogenic. While this study was not designed to specifically address that concern, the data can be used to provide some insight into the general magnitude of these sources. Starting with the average flows from each of the three tributaries measured during the study (Table 4-1) and multiplying by the average concentrations of nutrients measured in the inflow (Table 4-4), we can estimate a rate of nutrient input to LBC. Assuming that the chemistry of the Metolius River, which is largely unimpacted by development, approximates natural river chemistry, then any additional rate of input beyond that baseline is presumably from anthropogenic sources. Using this crude approximation, 92% of the input of PO_4 to LBC is natural. Using these same approximations, only 12% of the NO_3 input is naturally derived. Note that these are crude approximations relying on assumptions that need to be examined in detail, but they provide some indication that the vast majority of the phosphorus loading to LBC is natural and the vast majority of the nitrate loading is anthropogenic.

8.2 Lake Billy Chinook

LBC is a large, complex impoundment that was sampled at only two locations during this study. Consequently, we are unable to fully describe the lake's water quality. Assessments of change based on monitoring data apply only to Round Butte forebay (RES07) and the portion of the impoundment extending up to the Common Pool (RES08) (i.e., the confluence of the Deschutes and Crooked arms of LBC). Nevertheless, the water quality model has enabled us to make estimates that can help fill in some of the spatial gaps in LBC.

LBC retains many of the characteristics observed prior to installation of the SWW. Historically, it was highly productive, and it appears to have become even more productive, at least in the areas sampled: transparency declined, chlorophyll increased, epilimnetic pH increased, and the extent of DO supersaturation increased. As noted earlier, at least some of these increases can be

attributed to a continuous supply of nutrients to the forebay associated with the slow-moving river of Crooked arm water moving towards the SWW.

Composition of the phytoplankton community continues to be dominated by *Stephanodiscus niagarae*, but in greater abundance than pre-SWW. The principal cyanobacterium in earlier years was *Aphanizomenon flos-aquae*, but it is now *Dolichospermum/Anabaena*. These qualitative changes in the phytoplankton community are probably not as important as the apparent increase in phytoplankton biomass as reflected in the measurements of chlorophyll *a*. Chlorophyll values at Round Butte forebay (RES07) showed an increase of 48% between 1994–96 and this study. The zooplankton community exhibited a large shift in community composition. The pre-SWW zooplankton community was well represented by large cladocerans such as *Daphnia pulicaria.* The current zooplankton is dominated by rotifers, small filter-feeders that are less efficient grazers on phytoplankton and serve as a less desirable food source for planktivorous fish. Fish biomass has increased in LBC and the impoundment contains a substantial population of kokanee, so it appears that the current zooplankton population is adequate to support the fisheries in its present state according to PGE fish biologists (Terry Shrader, PGE, pers. comm., February 2019).

All three tributaries deliver relatively high concentrations of phosphorus to LBC, most of it derived from natural sources. In contrast, concentrations of nitrogen, especially NO_3, vary widely among the tributaries with little measurable NO_3 entering from the Metolius River (0.025 mg/L) and moderately high concentrations of NO_3 entering from the Crooked River (0.396 mg/L).

It is common knowledge that algal populations are affected by the availability of nutrients. The nutrients most often cited as limiting are phosphorus and nitrogen, although minor elements can sometimes be limiting or co-limiting. The prevailing opinion among limnologists is that, in lakes and reservoirs, phosphorus is the primary nutrient for controlling eutrophication (Schindler et al. 2008; Schindler et al. 2016). Schindler and others (e.g., Carpenter 2008) argue that controlling eutrophication can be addressed only by reducing phosphorus and that attempts to control eutrophication by reducing nitrogen can lead to cyanobacteria blooms. However, there is a

growing number of researchers who argue that the most effective method for controlling eutrophication is reducing both N and P (Conley et al. 2009; Xu et al. 2010; Paerl et al. 2011; Lewis et al. 2011; Cotner 2016). One of the arguments for reducing phosphorus is that nitrogen-fixing cyanobacteria will achieve a competitive advantage because they can acquire nitrogen from the atmosphere. However, Scott and McCarthy (2010) in a reexamination of the long-term fertilization experiment on Lake 227 in the Experimental Lakes Area (Canada) show that, when nitrogen additions to the lake were halted, phytoplankton biomass and chlorophyll declined and nitrogen fixation by cyanobacteria was insufficient to offset the reduction in nitrogen loading. In another long-term (37 yrs) study, Shatwell and Köhler (2019) found that recovery of a shallow lake was achieved by reducing nitrogen by 79% and phosphorus by 69%. They observed that the biovolume of cyanobacteria and phytoplankton decreased by 89% and 76%, respectively. Furthermore, the concentration of heterocysts and estimated nitrogen fixation did not change and cyanobacteria did not compensate for the nitrogen deficit. They argued that a P-only control strategy would not have been successful.

One of the limitations of research into nutrient limitation in lakes and the consequences to lake eutrophication is that most of the research has been conducted on systems that were likely P-limited, at least prior to the influence of anthropogenic contributions. Reservoirs in the Deschutes River basin are supplied with ample amounts of phosphorus from natural weathering processes. Consequently, some of the reservoirs are N-limited at least during some portion of the year, including LBC, which receives PO_4 inputs from its primary tributaries (typically ranging from 0.05–0.10 mg/L) several times the concentration of phosphorus required to support a eutrophic lake. There have been reported cases of P-enriched lakes that have become eutrophic as the result of nitrogen being added. Bunting et al. (2005) documented the "degradation" of a lake in Northern Ireland located in a P-saturated watershed. Finlay et al. (2010) also reported N-additions in the form of urea made to a phosphorus-rich lake in the Northern Great Plains that caused the lake to become "polluted." These reports seem to support that where phosphorus is locally abundant, the addition of nitrogen appears to be the critical factor in promoting eutrophication.

However, this study was not designed to provide a complete characterization of the impoundment. The monitoring conducted in LBC was done specifically to provide data for characterizing the LDR. Water quality monitoring was limited to two sites in LBC, one in the Round Butte forebay and one in the Common Pool (RES08). A much more spatially extensive monitoring network with multiple sites in all three arms would be required to characterize conditions in LBC. Consequently, we offer no recommendations for changes to LBC.

8.3 Lake Simtustus

The assessment of Lake Simtustus is more definitive than the LBC assessment because Lake Simtustus is smaller, morphometrically simpler, receives almost all its input from Round Butte Dam, and discharges from a single depth. The hypolimnion of Lake Simtustus has been replaced with warmer discharge from LBC, increasing water temperatures from about 10˚C to 13˚C. Despite the increase in hypolimnetic temperature, the impoundment remains stratified in the warmer months, allowing discharge from Round Butte Dam to pass through the hypolimnion of Lake Simtustus in about 26–30 hr with relatively little mixing with water higher in the water column. The pH of the hypolimnion has also increased since the SWW was installed and put into operation, and a considerable amount of entrained phytoplankton is passed through Lake Simtustus rapidly enough that the cells remain viable as they pass to the ReReg Reservoir.

Chlorophyll concentrations in the surface waters of Lake Simtustus have declined, although the transparency of the impoundment has remained unchanged. Lake Simtustus has significantly lower densities of cyanobacteria than LBC, which may be associated with NO_3-enriched waters entering the lake from Willow Creek. Willow Creek is relatively warm and delivers a high concentration of nitrogen to Lake Simtustus. The long, narrow geometry of Lake Simtustus promotes surface mixing up and down the impoundment depending on wind conditions. During the warmer months, the stratification of Lake Simtustus isolates the epilimnion from the hypolimnion. The hypolimnion is continually turned over by discharge from Round Butte Dam; however, during the summer, the epilimnion receives discharge only from Willow Creek. The high concentrations of NO_3 flowing into the epilimnion of Lake Simtustus suppress cyanobacteria growth by providing a competitive advantage to noncyanobacteria. Cyanobacteria

can develop in waters where NO_3 is fully assimilated, but not usually to the extent observed in LBC. If flows from Willow Creek were reduced or if concentrations of NO_3 in that stream were reduced, we would expect Lake Simtustus to experience a proliferation of cyanobacteria.

While the input of nitrogen to Lake Simtustus has the benefit of suppressing cyanobacteria, it has relatively little impact on periphyton growth in the LDR. This is because the NO_3 loading to Lake Simtustus in the warmer months is retained in the epilimnion. When the impoundment cools and mixes, it allows for increased transport of NO_3 to the LDR, but that occurs when light is decreasing, air temperature is declining, and periphyton growth is waning. Consequently, the additional NO_3 loading from Lake Simtustus released after the lake has mixed in the fall has little opportunity to stimulate periphyton growth in the LDR.

As noted earlier, this study focused sampling work on documenting major inputs and the discharge downstream. A more comprehensive sampling program would be required to fully understand processes and factors affecting water quality in Lake Simtustus.

No sampling was conducted in the ReReg Reservoir, primarily because of safety concerns associated with rapidly changing lake levels. However, we did sample at the inlet to the ReReg Reservoir, Pelton forebay (RES04), as well as at the base of the ReReg site (LDR01).

8.4 Lower Deschutes River

8.4.1 Water Chemistry

During the warmer months, LDR water temperatures increase significantly from the ReReg Dam (RM 100.1) to the mouth (RM 0). It is common to observe an increase of 10°C over that distance in July and August, or an average of +0.1°C per river mile. The many factors that affect temperatures in the LDR include (in no particular order of importance) (1) SWW operation, which varies the proportion of water released from the surface compared to the hypolimnion; (2) the time of day of discharge from the Round Butte Dam; (3) the variation in the volume of water released; (4) contributions from tributaries to the LDR; and (5) the ambient conditions in the canyon during the passage from the Project to the mouth of the river. Consequently, the water temperature over the diel cycle varies widely depending on the position in the river and the

degree of synchronization with discharge and air temperature. The diel variations in river temperature generally increase as the water moves downriver; however, some degree of muting of the diel range occurs mid-river because of these factors.

Although *in-situ* measurements of pH and DO are not as continuous as temperature measurements, enough of them were taken during the 2015–2017 study to identify robust patterns in the data. pH values increased slightly from the Project to the mouth of the river. The diel extremes in pH increased as the water moved downstream, displaying a daily range of 1.5 pH units at the mouth of the river during the summer. In contrast, the diel range at the ReReg Dam was typically only 0.2–0.3 pH units. The diel ranges decreased in the cooler months as photosynthesis and the linked decrease in carbonic acid in the river declined. The diel effect of pH is facilitated by the relatively slow rate of equilibrium between atmospheric CO_2 and CO_2 dissolved in the water. Consequently, pH measured at a particular site is not necessarily reflective of the intensity of photosynthetic activity in the river at that point in time.

DO concentrations followed a pattern similar to the one observed for pH. The range of diel variation increased as the water flowed downstream and generally increased in the summer. There were two noteworthy exceptions to the pattern in DO by river mile. The first exception was the decline in oxygen saturation at the ReReg site (LDR01) during the summer, most noticeably during July and August, when DO saturation fell to 80%. In contrast, DO was much more likely to display supersaturation, sometimes as high as 130%, especially below RM 30. Values of DO supersaturation recorded during the river float even exceeded 140% on the last 2 days, although values measured near the shore during the 72-hr monitoring deployment on the same date exhibited somewhat lower values. It is unclear whether the difference is a function of measurement location (the middle of the channel versus nearshore) or simply reflects use of different equipment (*in-situ* versus YSI sondes). Regardless of the reason, the LDR exhibits a considerable diel range in DO, again reflecting the lag in equilibrium between atmospheric DO and DO dissolved in water and the high rates of photosynthesis. The second exception in DO saturation in the river occurred below Sherars Falls, where DO became entrained in the water and remained supersaturated for a considerable distance downstream.

The relatively high pH and DO values and the high diel patterns measured in the LDR are reflective of high rates of primary production in the river. The lower concentrations of DO occur in the immediate vicinity of the ReReg tailrace, but the waters rapidly equilibrate downstream. The small amount of BOD present in the discharge from the Project appears to show little lasting impact downstream.

8.4.2 Nutrient Contributions

The nutrients that receive the most attention in most rivers are phosphorus and nitrogen. There are some uncommon cases in which other elements become a factor, but they were not considered in this study. For most rivers in North America, phosphorus is strongly associated with limiting growth of periphyton (Allan 1995). When examining the issue of nutrient limitation, many investigators use the Redfield ratio, which is the elemental ratio of C:N:P present in algae (Redfield 1958). Carbon is abundant in most rivers and can usually be ignored as a possible limiting element; the critical ratio becomes N:P (16:1). Although the atomic ratio is precise, in practice, investigators have observed a moderate amount of variation around it so waters with ratios less than 10 are clearly N-limited. Molar ratios from 10 to 20 tend to be somewhat ambiguous and values higher than 20 are generally P-limited (Schanz & Juon 1983). The LDR had a moderately high level of both TP and PO_4; concentrations of nitrogen were of similar magnitude. However, the availability of N and P is more important than their total abundance. Examining the available, inorganic fractions of N (NO_3 + NH_3) and PO_4 results in a more accurate understanding of the limiting nutrients. An examination of the ratio of DIN to PO_4 shows that the atomic ratio of much of the LDR is N-limited most of the time (Figure 8-1). Whereas phosphorus in many rivers in North America is derived from anthropogenic-related sources such as elevated erosion and pollutant discharges, phosphorus in the Deschutes River basin is the product of natural weathering of basalt and other volcanic rocks. With that high natural loading of phosphorus, nitrogen becomes the limiting nutrient by default. Nitrogen is often limiting in the LDR, particularly from May through July. In Figure 8-2, the data grouped by site shows that nitrogen limitation increases towards the mouth as periphyton assimilate NO_3.

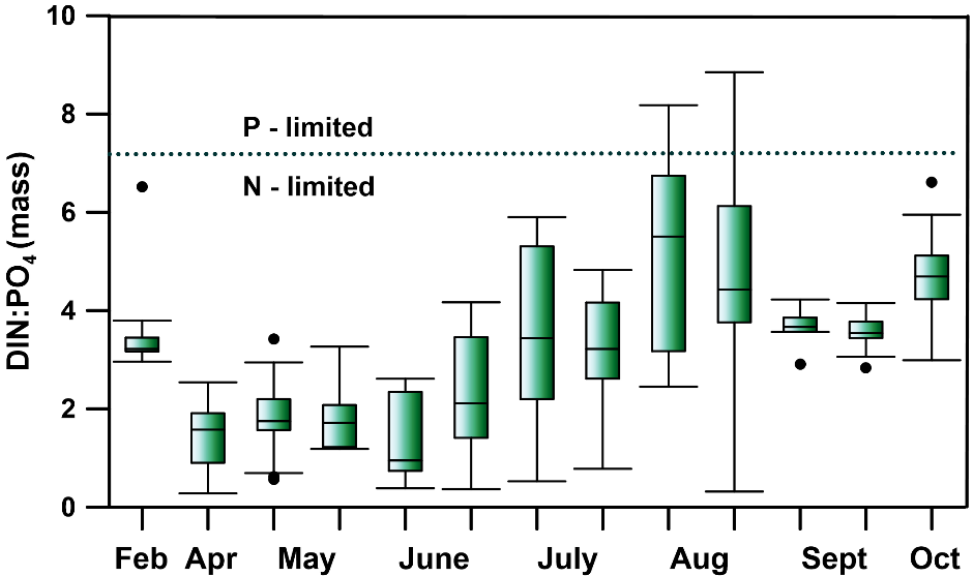

Figure 8-1. Boxplot of the ratio of DIN to PO_4 (mass) for all sites in the LDR grouped by sampling date (2016). Filled circles indicate outliers in the distributions; the dashed line represents the Redfield ratio (7.2:1).

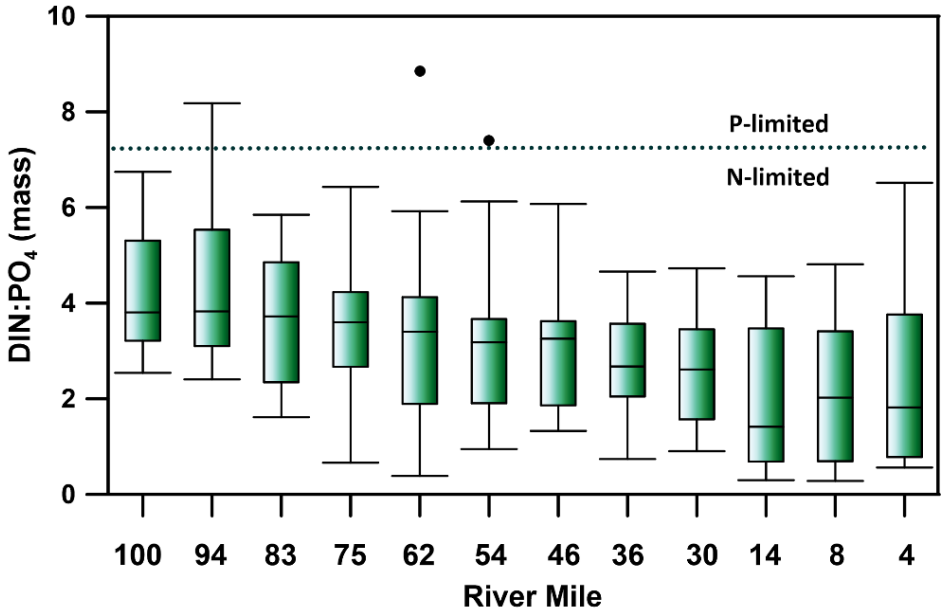

Figure 8-2. Boxplot of the ratio of DIN to PO_4 (mass) for all samples collected in 2016 in the LDR grouped by sample site. Filled circles indicate outliers in the distributions; the dashed line represents the Redfield ratio (7.2:1).

Nitrogen uptake occurs throughout the year as shown with the net assimilation of NO_3 between the ReReg site (LDR01) and the River Mouth (LDR21) in Figure 8-3. Regardless of the time of year, biota in the river are removing NO_3 from the water at a fairly steady pace. As external loads of NO_3 from the Project decline from winter to spring, available NO_3 at the mouth approaches the DL. Once the export of NO_3 increases in mid-to-late June, nitrogen is no longer limiting at the mouth. This pattern indicates that substantial primary production occurs much of the year in the LDR.

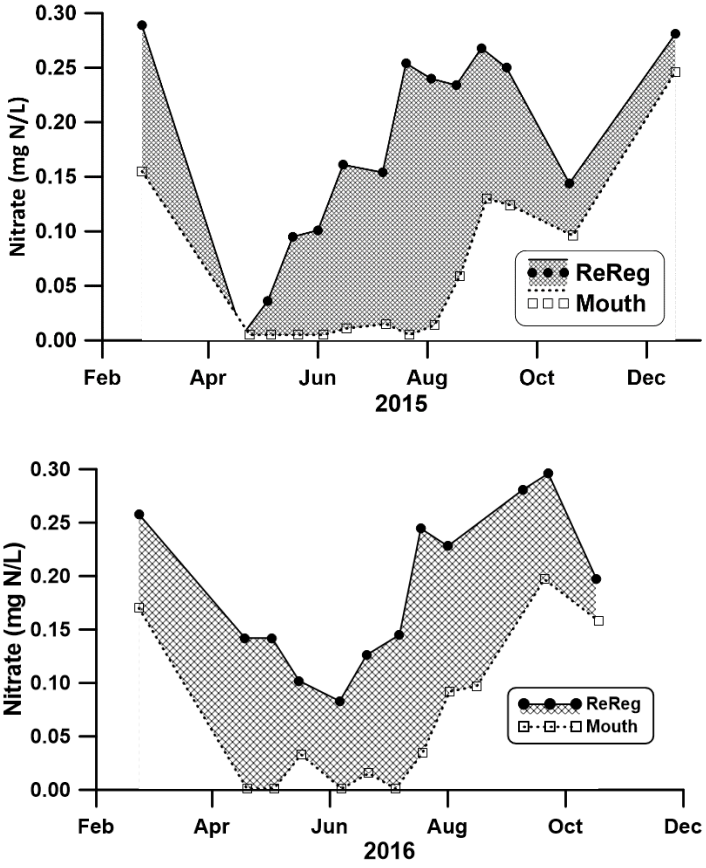

Figure 8-3. NO_3 concentrations at the ReReg site (LDR01) and the River Mouth (LDR21) for 2015 *(top)* and 2016 *(bottom)*. The shaded area in between the lines represents the net assimilation of NO_3. The analytical DL of NO_3 is 0.01 mg/L; values reported at the DL were set at zero.

An examination of the ODEQ AWQMP NO_3 data for the PoR shows a similar pattern of NO_3 uptake, although not to the degree to which NO_3 is completely assimilated, as shown in this

study (Figure 8-4). Note that assimilation by periphyton is only one mechanism of nitrogen uptake: others include uptake by bacteria and other heterotrophs (cf. Mulholland 1996). This examination of the N:P ratio in the LDR suggests that there are some observations from August in which phosphorus could be limiting (Figure 8-1). However, this is somewhat misleading because concentrations of phosphorus are seldom less than 0.03 mg/L indicating that ample phosphorus is always available for the algae.

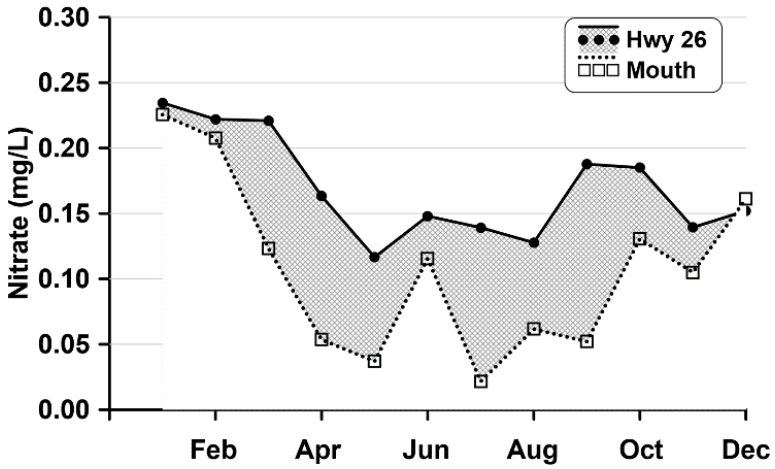

Figure 8-4. Average NO3 concentrations by month for all ODEQ AWQMP data collected at the Hwy 26 bridge site (RM 97.6) and the Deschutes River SRA site at the mouth (RM 0.1).

Although NO_3 concentrations become undetectable from spring into summer in the lower reaches of the river, the fact that heterocystous cyanobacteria are found throughout the length of the river seems counterintuitive. If the distribution of heterocystous taxa was favored solely by N-limitation, then we would have expected that other taxa would have out-competed them in the N-enriched reaches of the river. Although heterocystous cyanobacteria can fix atmospheric nitrogen, it is accomplished at considerable energy costs, so if inorganic nitrogen is available, its assimilation is preferable to acquiring nitrogen through fixation (Paerl 1990). Livingstone et al. (1984) showed that *Rivularia* exhibited high rates of nitrogen fixation in a stream in northern England, yet fixation still supplied only a small portion of *Rivularia*'s nitrogen requirements. Despite the presence of heterocystous cyanobacteria in the LDR, nitrogen remains the target nutrient for reducing the periphyton biomass in the LDR. In particular, the inorganic

components of nitrogen, NO_3 and NH_3, are specific forms that require reduction. Based on the water quality data collected during this study, achieving periods of lower available nitrogen likely will return the periphyton in the LDR to a state of extended nitrogen limitation.

While reducing NO_3 loading to rivers can reduce overall periphyton biomass, it can also increase the relative abundance of heterocystous cyanobacteria and diatoms. Researchers have identified target concentrations for defining when nitrogen causes dramatic increases in heterocystous taxa. The threshold for when a stream becomes N-limited appears to occur when nitrate concentrations fall below 0.055 to 0.075 mg/L (Grimm and Fisher 1986; Stancheva et al. 2013; Gillett et al. 2016;). Using these two thresholds, we observe the river location and number of times these thresholds were met (Figure 8-5). It's likely that the most critical periods of nutrient availability for determining periphyton abundance in the LDR are spring and summer. Seasonal concentrations of nitrate in the LDR show that concentrations in the spring meet these thresholds for much of the river, whereas concentrations in other seasons generally exceed these thresholds by a considerable margin (Figure 8-6).

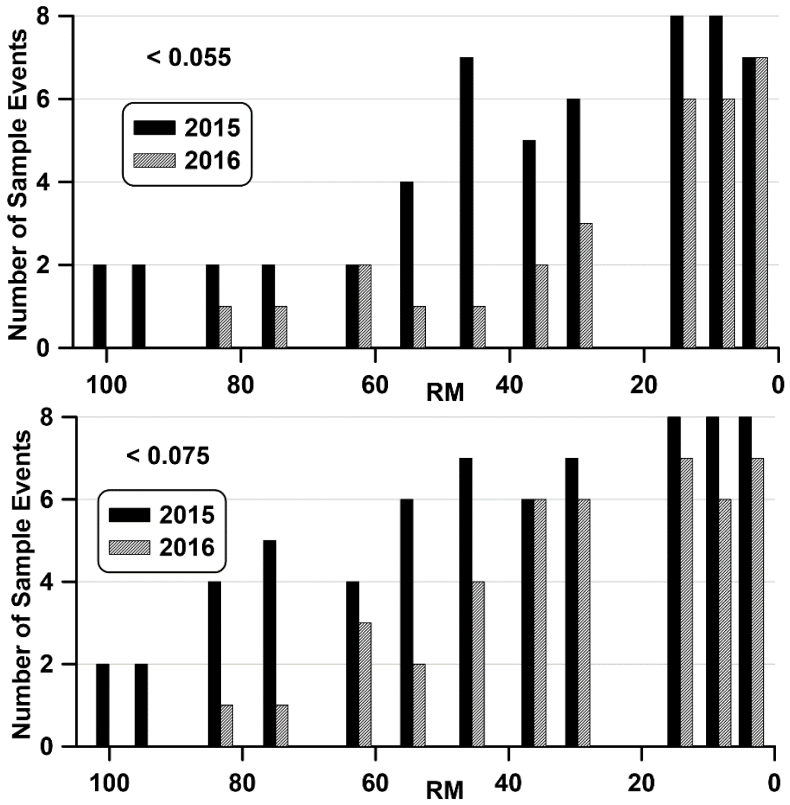

Figure 8-5. Number of sample events with concentrations reported at less than 0.055 mg/L *(top)* and 0.075 mg/L *(bottom)* for 2015 and 2016.

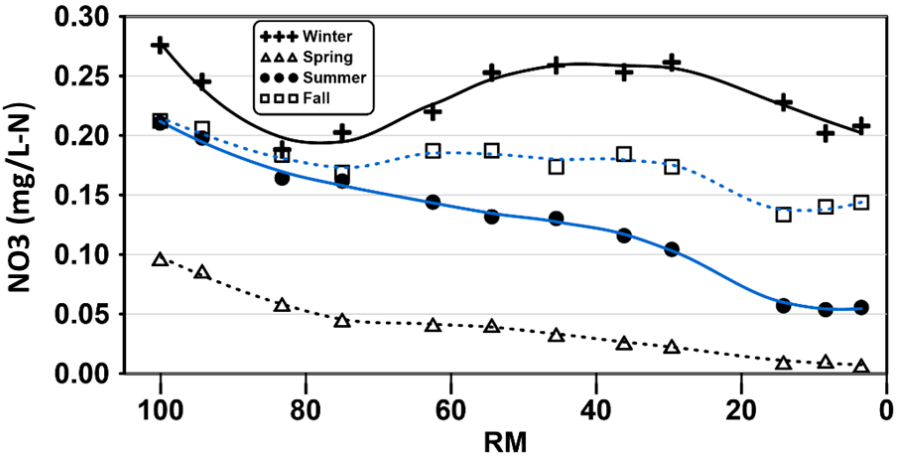

Figure 8-6. Average seasonal nitrate concentrations in the LDR for 2015–2016.

Concentrations of nitrate in the LDR, as shown Figure 8-6, show that there is no linear decline in NO_3 concentrations as might be expected if all the NO_3 inputs to the river were from the Project. Instead, we observe increases in NO_3, downstream of RM 80. Since concentrations of NH_3 are low in the river, we cannot attribute the increase in NO_3 to oxidation of NH_3. The sources of nitrate in the mid-reaches of the river are likely associated with inputs from tributaries draining agricultural land. The amount and type of cropland draining into the LDR show that there is approximately 55,000 acres of cropland in the catchments to the LDR, of which over 30,000 acres is irrigated (Table 8-1, Figure 8-7). Irrigated agriculture, which is generally more intensive (e.g., fertilizer application), and pasture, especially where livestock have access to streams, are expected to be greater sources of nutrients to the LDR.

Table 8-1. Cropland downstream of Pelton Round Butte based on 2016 satellite imagery.

Catchment	Ag type	Area (ac)	% Crop Type
East of ReReg Reservoir	Dryland	449	4.8
	Fallow/Idle Cropland	2350	24.9
	Irrigated	6643	70.4
Nena Creek	Dryland	110	100
Trout Creek	Dryland	2941	14.3
	Fallow/Idle Cropland	4454	21.7
	Irrigated	13121	64.0
Tygh Creek	Dryland	2346	43.9
	Fallow/Idle Cropland	1533	28.7
	Irrigated	1469	27.5
Wapinitia Creek	Dryland	2072	39.8
	Fallow/Idle Cropland	2296	44.1
	Irrigated	834	16.0
White River	Dryland	3510	24.2
	Fallow/Idle Cropland	2457	16.9
	Irrigated	8564	58.9

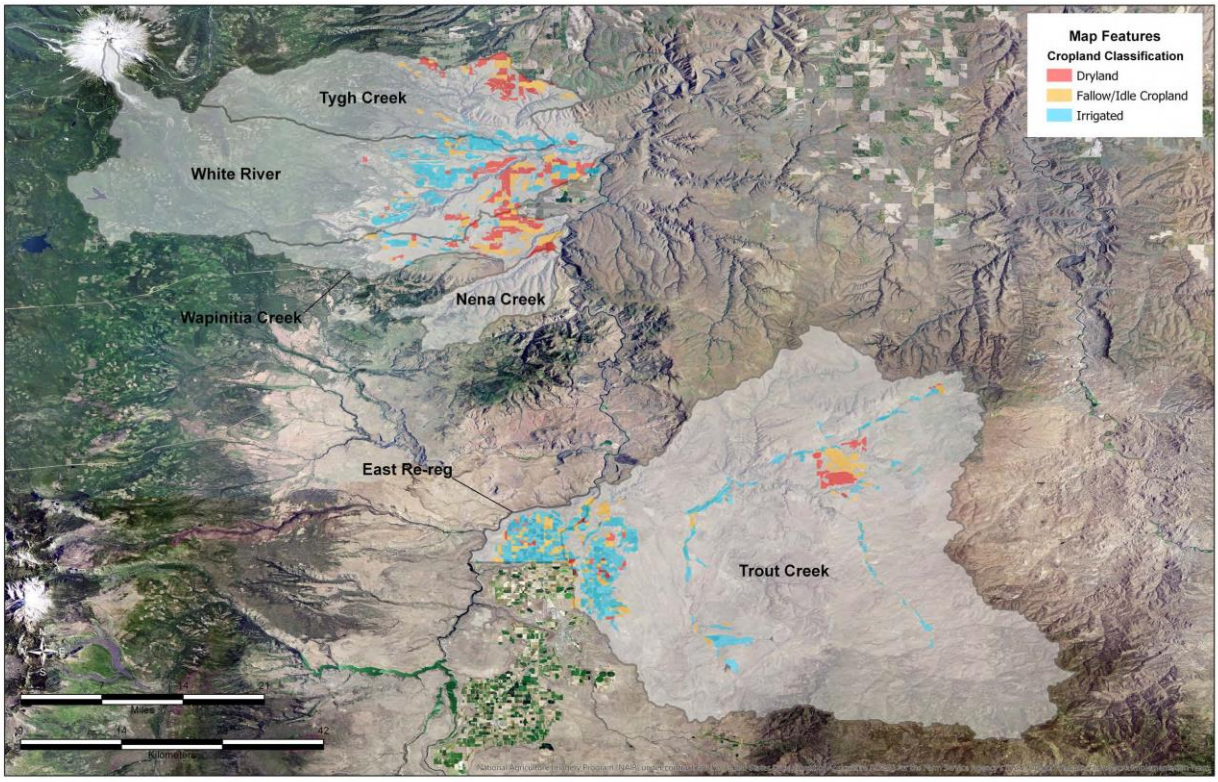

Figure 8-7. Distribution of cropland along the LDR based on satellite imagery from 2016.

8.4.3 Eutrophication

Characterizing eutrophication in rivers and streams has proven more challenging than in lakes, as noted by Dodds et al. (1998) and Dodds (2006). Streams exhibit longitudinal gradients and are subject to considerable hydrologic fluctuations. Stream hydraulics can be a critical factor affecting the expression of trophic properties and can override nutrient issues in some cases (Hilton et al. 2006). Most investigators would agree that reducing phosphorus is essential to reducing the trophic condition in lakes (Schindler et al. 2008, 2016; Carpenter 2008), either separately or in conjunction with nitrogen reduction (Xu et al. 2010; Lewis et al. 2011; Paerl et al. 2011).

However, the method to use to reduce eutrophy in streams and rivers is less clear. Most analyses of nutrient limitation and contributions to eutrophication in streams suggest that control of both N and P is essential for improving lotic systems (Dodds and Smith 2016; Lewis et al. 2011;

McDowell et al. 2009). This view also appears to be supported by Allan (1995), who noted a strong spatial pattern in nutrient limitation of streams in the United States, where eastern streams were typically P-limited and a moderate number of western streams were N-limited. However, none of those investigators make clear whether one nutrient should be favored over the other in treating the streams.

When evaluating eutrophication reduction strategies, it is important to consider what nutrients *can* be reduced. Under ideal circumstances, it may be desirable to reduce both N and P equally or to reduce P preferentially, but if natural features leave little flexibility around nutrient reduction, the choices become limited. Such is the case with the Deschutes River basin (see Section 2, Table 2-1), where natural phosphorus loading is high and as a result, opportunities for reducing phosphorus are limited. Although anthropogenic sources of phosphorus occur in the Crooked River, it is unlikely they contribute a sufficient quantity of P that can be reduced to achieve meaningful improvements in the LDR. In contrast, the Crooked River delivers over 80% of the NO_3 entering the Project. To better understand the potential outcomes associated with moderate nitrogen reductions without an equivalent phosphorus reduction we must examine other N-limited streams for evidence of possible outcomes for the LDR.

Data from streams in southern California offer some clues for what might happen if nitrogen were reduced in the LDR. The periphyton taxa in nitrogen-limited streams and rivers are variable, and Stancheva et al. (2013) showed that species of heterocystous cyanobacteria predominated in a wide range of nitrogen concentrations. *Nostoc verrucosum* was dominant at several sites with NO_3 concentrations less than 0.01 mg/L and reached its maximum relative biovolume (99.9 %) at NO_3 concentrations less than 0.0007 mg/L. In contrast, another heterocystous cyanobacteria, *Rivularia minutula*, reached its maximum relative biovolume (96.5%) at sites with NO_3 from 0.1 mg/L to 0.25 mg/L. Furthermore, *R. minutula* biovolume was positively correlated with NO_3 (Spearman rank $\rho = 0.82$, $P = 0.04$). It is likely that reducing available nitrogen could actually increase the proportion of N-fixing cyanobacteria and diatoms with cyanobacterium endosymbionts such as *Epithemia and Rhopalodia*. Note that both diatoms were present in the LDR, but at low densities. Stancheva et al. (2013) found that these two diatom taxa favored sites with relatively low concentrations of NO_3 (less than 0.075 mg/L) and

N:P greater than 15:1 (mass). Gillett et al. (2016) found that the percentage of N-fixing benthic taxa increased with decreasing NO_3 concentrations in the Klamath River and showed a dramatic increase in dominance once NO_3 concentrations approached DLs. However, the periphyton community composition in the Klamath River is radically different than that in the LDR. In the Klamath River, diatoms comprised 92.2% of the relative biovolume followed by cyanobacteria (7.0%) and green algae (< 1%). Comparable statistics for the LDR (using data from 2016) show that diatoms represent only 7.9% of the total biovolume with cyanobacteria representing 7.7% and green algae representing 84.3% in 2016. A reduction in NO_3 would likely result in a reduction of filamentous green algae such as *Cladophora* with some increase in heterocystous cyanobacteria.

It is tempting to use some of the same eutrophication metrics for both lakes and streams, which could lead to the conclusion that the presence of significant quantities of cyanobacteria is a sign of eutrophy. Although it is almost always true that the presence of cyanobacteria defines eutrophy in lakes, in rivers, it is more complicated. For example, some spring systems in the North Umpqua River in the Oregon Cascades are heavily dominated by cyanobacteria, particularly *Nostoc* (J. Eilers, unpublished data). The spring waters are cold, heavily enriched in phosphorus, and depleted in measurable inorganic nitrogen. The results of these studies show a wide a variety of periphyton community types exist in N-limited streams, making it difficult to identify a specific periphyton community that would occur in a specific stream without experimental evidence.

Dodds (2006) used periphyton chlorophyll instead of algae counts as a classification metric, in which periphyton chlorophyll values higher than 100 mg/m^2 represented streams considered to be eutrophic. Using that metric, four of the 12 sites in the LDR would have been considered eutrophic in 2015, with no particular longitudinal pattern. In 2016, all sites from RM 100 to RM 40 had chlorophyll values around 100 mg/m^2, with a peak (more than 250 mg/m^2) at Wreck Rapids (RM 36.2) and a decline to the mouth of the LDR. This variation in benthic chlorophyll in time and space highlights the difficulty in trying to classify an extended reach of a river that is subject to changing conditions.

Relatively little net uptake of phosphorus occurred from the ReReg Dam to the LDR's mouth, but there was a consistent net uptake of NO_3 ranging from about 0.10 mg/L to 0.20 mg/L NO_3-N from the Project to the mouth of the river. Although the reduction of phosphorus to the LDR would not be detrimental to water quality, the assimilation of nitrate data strongly suggests that reduction of periphyton in the LDR relying exclusively on nutrient reduction can only be achieved through decreasing nitrogen and specifically inorganic nitrogen. Although heterocystous cyanobacteria are present in the LDR, it is unlikely that they could fix enough nitrogen to offset any reductions in nitrogen that might be achieved. Thus, should nitrogen be reduced in the LDR resulting in an increase in heterocystous taxa, these species would be unable to fix enough nitrogen to replace the nitrogen reduced through management efforts.

In Section 0, nutrient concentrations in the LDR were compared to concentrations in several other rivers in Oregon. Those rivers exhibited a range of characteristics, some with strong similarities to the LDR's characteristics. For example, the Williamson River was identified as a system with apparent N-limitation, a characteristic that is not unique to a few isolated systems in Oregon but occurs around the globe. N-limitation has been reported in tributaries to the Euphrates River in Iraq (Hassan et al. 2017), the Amazon River (Richey et al. 1991), and tributaries to the River Rhine in Switzerland (Schanz and Juon 1983). Regions likely to host N-limited rivers include areas with abundant volcanic rocks, limestone, or dolomite, all rock types with high a P content (Krauskopf 1979). Many parts of the western United States have streams that are N-limited (Scott and Marcarelli 2012), particularly arid streams in the southwestern part of the country as reported by Grimm and Fisher (1986) for a stream in Arizona and by Stancheva et al. (2013) for 104 stream sites in southern California. Other areas of the United States also contain streams that are N-limited such as the Ozark Mountains in the south-central part of the country (Lohman et al. 1991). An example closer to Oregon is the Klamath River in California, where concentrations of NO_3 near the tailrace below Irongate Reservoir (RM 190) average slightly less than 0.2 mg/L, but approach levels near the DL (0.01 mg/L) by RM 59 and remain low to the mouth of the river (Gillett et al. 2016). That longitudinal pattern in NO_3 concentrations from the Klamath River is similar to the one observed in the LDR.

There appears to be a reasonably strong relationship between the distribution of heterocystous and non-heterocystous taxa in the LDR in association with longitudinal distribution of NO_3. Heterocystous taxa such as *Epithemia* and *Calothrix* are more abundant in the lower half of the LDR, whereas *Cladophora* abundance declines approaching the mouth of the LDR. Stancheva and Sheath (2016) noted that periphyton communities are affected not only by nitrogen and phosphorus, but also by flow regimes, light, temperature, grazing, substrate composition, and micronutrients. The most dramatic change in periphyton community composition in the LDR was associated with the change from 2016 to 2017 in which the abundance of *Cladophora* and other filamentous chlorophytes declined by an order of magnitude. The role of flow regimes is discussed Section 8.4.7 and the tentative assessment is that high flow events are equally or more important than nutrients in determining the composition and abundance of periphyton in the LDR. Note that flows and nutrient concentrations in the river are not independent. High flows can cause greater export of nutrients, particularly from tributaries to the LDR, whereas low flows have been associated with lower concentrations of NO_3 export from the Project.

In summary, the periphyton in the LDR is dominated by chlorophytes during years with low to normal discharge. Diatoms and cyanophytes represent a minor portion of the periphyton during these low to average discharge years. Unlike impoundments where dominance by cyanobacteria can typically be classified as eutrophic, rivers are more difficult to classify on the basis of periphyton communities. Biological communities in rivers respond not only to water chemistry, but also stream velocity, light, temperature, substrate, and grazing by macroinvertebrates. How these factors interact to produce a specific periphyton community type is not fully understood. For example, the Klamath River in California possess many similarities with the LDR, including a series of upstream impoundments, high phosphorus and high nitrate (below Irongate Dam). Despite these similarities, the periphyton community in the Klamath River is radically different than the LDR, thus illustrating the challenge in predicting periphyton communities in rivers. It appears that the most defensible criteria for characterizing the trophic condition of rivers at this state of our understanding is with the use of metrics such as periphyton chlorophyll. Using this metric, the LDR would most often be classified as mesotrophic to eutrophic.

8.4.4 Algal Community

Periphyton populations in the LDR have become a topic of considerable interest in recent years. This study documented filamentous chlorophytes as the dominant organisms associated with current periphyton in the river. Diatoms, which are often the dominant periphyton algae in rivers, were relatively unimportant on a biovolume basis in the LDR in 2015 and 2016. In summer 2017, diatoms represented nearly one third of the periphyton biovolume, but this was primarily because of the decline in abundance of the chlorophytes, rather than an increase in diatoms.

It is unknown at this time if the composition or abundance within the periphyton community in the LDR has changed over time because of issues with the historical dataset. During this study, we encountered three issues relating to taxonomic analysis of the algae and cyanobacteria data from the impoundments and the LDR. The first and most serious issue was the improper manner in which the periphyton in the earlier datasets were processed (Raymond et al. 1997; Kvam et al. 2001, 2002). The method of processing periphyton used by the taxonomist resulted in few filamentous taxa being reported and, as a result, very low biovolume of filamentous taxa. Both Raymond et al. (1997) and Kvam et al. (2001, 2002) used Aquatic Analysts for periphyton analyses, negating the value of the results from those studies. A review of the 2015 soft-bodied taxa reported by Aquatic Analysts found lack of agreement with three other laboratories that analyzed the same samples (Rhithron Associates, PhycoTech, and Georgia College). Consequently, the data from Aquatic Analysts were unsuitable for comparison with current periphyton samples in the LDR collected in this study.

Another issue was the significant differences in taxonomic results of phytoplankton and periphyton samples by current taxonomists. This issue is caused, in part, by the necessarily small subsamples used by professionals in algal taxonomy. Collected samples contain millions and perhaps billions of cells, but only 300–600 cells are counted to characterize a given sample. There is no obvious solution to the problem. It can be resolved only by using automated machine-based processing of samples, genetic analyses of samples or a light-based (pigment) approach.

Finally, using the current taxonomy for algae and particularly cyanobacteria in distinguishing among species with microscopy is a struggle. The diversity of algae and cyanobacteria is vast, and revisions and updates are continually being made to the various groups of organisms. That became apparent when attempting to compare algae taxonomy between samples from 30 years ago and samples collected for this study. The list of taxa has changed, in part, because species names have changed and not because the organisms present have changed. The problem is particularly acute with cyanobacteria because the state of the science is evolving rapidly. The prevailing method of algal identification is based on morphological features, which seems to be particularly troublesome for cyanobacteria because their cell/colony morphology is subject to change within a season.

The long-term solution might be to analyze taxa genetically, but that approach is still in development. Some of the most prominent taxa found in the impoundments and the LDR feature heavily in this discussion. The planktonic cyanobacterium formerly referred to as *Anabaena* is now identified by most taxonomists as *Dolichospermum.* That change in genus was promulgated by a revision of the group (cf. Komárek and Johansen 2014), which separated *Anabaena* and *Dolichospermum* based on habitat, retaining *Anabaena*, the older nomenclature, for the attached genera and assigning *Dolichospermum* as the planktonic form. However, some scientists in the field, particularly those who favor a more genetics-based approach to classifying cyanobacteria (Driscoll et al. 2018), do not support that distinction.

Challenges in taxonomy are not limited to cyanobacteria. Another important taxon in the Project is *Stephanodiscus niagarae*, a large centric diatom. The *Stephanodiscus* genus contains over 100 species and has been undergoing taxonomic revisions as well. The genus is morphologically variable and cells alter their degree of silicification based on environmental conditions (Stoermer et al. 1989; Theriot 1987; Jewson 1992). *S. niagarae* is described as a complex of related species comprised of "large, planktonic, morphologically variable species…" (Håkansson and Meyer 1994). Those characteristics lead to a considerable amount of uncertainty in classification of *Stephanodiscus* species that remains unresolved (Kociolek et al. 2014).

Regardless of the taxonomic issues associated with algal taxonomy, the periphyton data show that the LDR has high biomass of benthic algae. The chlorophyll values measured in the LDR periphyton are typically associated with productive waters. Classifications of stream trophic condition based on benthic biomass (as chlorophyll) show that many periphyton samples collected from the LDR would be considered mesotrophic to eutrophic waters (Table 8-2). The percentage of samples that would be classified as eutrophic waters varies considerably, depending on what threshold from Table 8-2 is selected as the criterion. The results show that the distributions of eutrophic sites are similar for 2015 and 2017, whereas for 2016 a greater percentage of sites would be considered eutrophic (Table 8-3). Several trophic classifications have been constructed based on concentrations of phosphorus and nitrogen (cf. Paul et al. 2017), but most of them are not applicable to the LDR because of the high concentrations of phosphorus derived from natural sources.

Table 8-2. Suggested values and ranges for maximum benthic biomass (as chlorophyll) levels to avoid problems for recreational and aesthetic use (Source: Dodds et al. 1998).

Maximum benthic biomass (mg chl/m^2)	**Comment**	**Reference**
50	Guidelines for New Zealand streams	McDowell et al. (2009)
55	Based on USGS NAWQA results from 976 streams in the US	Porter et al. (2008)
50-100	British Columbia Environment guideline	Nordin (1985)
100	Considered nuisance growth > 30% of time	Dodds (2006)
100-150	Based on 19 enrichment cases and surveys	Welch et al. (1988); Horner et al. (1983)
150	Guidelines for Clark Fork River, MT	Tristate Implementation Council (1996)
150-200	Based on perceived impairment	Welch et al. (1989)
200	Based on public perception for MT streams	Suplee et al. (2009)
200	Selected boundary based on Dodds et al. (1998)	Biggs (2000)

Notes: NAWQA = National Water-Quality Assessment; mg chl/m^2 = milligrams chlorophyll per meter squared.

Table 8-3. Percentage of periphyton samples from the LDR that would be classified as eutrophic based on a threshold.

Year	Chlorophyll Exceedance Threshold for Eutrophic Rivers (mg chl/m^2)		
	50	100	200
2015	45.5%	24.4%	7.3%
2016	65.4%	43.8%	22.2%
2017	46.4%	25.7%	7.1%

Note: mg chl/m^2 = milligrams chlorophyll per meter squared.

8.4.5 Cladophora

The periphyton community is highly variable by sample site, which would be expected because of the range of factors that affect periphyton communities, including water chemistry, current velocity, substrate type, depth, nearshore shading, and grazing by macroinvertebrates. Nevertheless, the major pattern that emerged was that the dominant periphyton taxa both temporally and spatially in 2015 and 2016 are filamentous chlorophytes. Filamentous green algae such as *Cladophora, Ulothrix*, and *Stigeoclonium* are highly visible ,are abundant largely in the spring and summer, and slough off as daylight declines towards the fall. *Cladophora* is widely distributed and is a common nuisance algae species reported in flowing waters (Dodds and Gudder 1992). It is considered to be a poor food source for macroinvertebrates, in part, because of its low content of amino acids (LaLonde et al. 1979), although when decaying, its utility as a food source increases. *Cladophora* can survive in N-limited waters by growing in close association with heterocystous taxa from which it acquires nitrogen (Whitton et al. 1986). Among the heterocystous epiphytes that grow on *Cladophora* are the cyanobacterium *Nostoc* and the diatom *Epithemia* (Bahls and Weber 1988). *Epithemia* was common in the LDR, whereas *Nostoc* was rare. *Cladophora* can also grow as an epiphyte on macrophytes such as *Elodea canadensis*, a taxa found throughout the LDR. These adaptations help to explain the widespread distribution of *Cladophora* and its success as a generalist. However, its long filaments make it vulnerable to high flow events which can either fragment the filaments or dislodge the plant entirely.

Periphyton limitation by nitrogen or phosphorus in the LDR as it relates to *Cladophora* is noteworthy because PO_4 is almost always abundant in the LDR, so any limitation would be associated with nitrogen (assuming metals are not limiting to periphyton). Concentrations of NO_3 leaving the Project are generally above 0.10 mg/L NO_3-N throughout this study and in the 1997 work (Raymond et al. 1998). However, rates of uptake resulted in concentrations of NO_3 approaching the DL in July 1997 and July 2015 and were near or less than 0.05 mg/L in much of the river below RM 80 in July 1997. These events would temporarily drive the NO_3:PO_4 ratio to values that are considered N-limiting (less than 7.2 based on mass). If the periphyton community is comprised of a high proportion of chlorophytes, then the apparent nitrogen-limitation would restrict growth of *Cladophora*. However, long-term NO_3 limitation would force cyanobacteria to fix atmospheric nitrogen, a far more energy-intensive biochemical pathway. If that is the case, then a strategy of targeting reduction of nitrogen to the LDR might be fruitful in reducing total periphyton biomass. At a minimum, it would likely reduce the biovolume of filamentous green algae such as *Cladophora*.

8.4.6 Turbidity

Turbidity in many rivers is strongly associated with input of erosional material. This can be true for the LDR, when high flow events in the basin contribute to turbid conditions in LBC. Additionally, high discharge events from tributaries to the LDR can affect turbidity levels in the river, particularly downstream of the White River during glacial melt from Mt. Hood. However, for much of the year, turbidity in the LDR is dominated by algal populations discharged from the impoundments. It gradually increases at the ReReg site (LDR01) from January into early spring. In mid-March to early April, turbidity increases dramatically, staying elevated for 4–6 weeks before slowly declining. Several factors appear to contribute to this increase in turbidity in the spring: (1) the increase in daylight and the stimulatory effect on phytoplankton in the impoundments; (2) flows through the surface intake at LBC increase to 100% of the flows from the impoundment in November and extending into May, increasing the opportunity for additional phytoplankton to be transported out of the system; and (3) a qualitative difference in phytoplankton populations throughout the year. In the spring, diatoms are dominant in the

impoundments and, because these algae have siliceous frustules (shells), they are much more likely to pass through the Project intact. In contrast, the dominant phytoplankton group in the summer is cyanobacteria, with cells that lack a strong cell membrane and seemingly are more likely to disintegrate as they pass through the turbines. However, a surprising number of intact cyanobacteria (*Dolichospermum/Anabaena*) cells were present in the seston, indicating that a significant number of cyanobacteria are passing through the turbines intact. The turbidity measured during the river float showed a slight tendency to increase turbidity downstream; however, the magnitude of the increase was small. The travel time in the river (about 33 hrs at typical summer flows) appears insufficient to allow for an increase in algae suspended in the water column to reproduce.

Algal pigments in the river present a more complex set of results. At ReReg site (LDR01), chlorophyll was measured with fluorescence using the ZAPS LiquID unit, with the AlgaeTorch, and using traditional laboratory analysis. The continuous measurements of chlorophyll from the ZAPS LiquID at ReReg site (LDR01) indicated that there were two major pulses in the spring—in April and in June—and one minor peak in October. The major peaks in pigments during the summer were associated with phycocyanin. The pigment data measured at the ReReg site (LDR01) using the AlgaeTorch appear to show the largest peaks in chlorophyll represented by total chlorophyll in June and October and a peak in blue-green algae in August. The analytical measurements of chlorophyll also showed a peak in June, but those data were sparse and insufficient to characterize temporal patterns well. The AlgaeTorch data provided the best opportunity to view longitudinal patterns in major pigments. The total chlorophyll spectrum showed a distinct peak in June and an even more pronounced peak in the fall. Only one set of samples were collected in April, and it is likely that the earlier peak was not captured in those samples. The total chlorophyll patterns appear to be well synchronized longitudinally and show little decline in magnitude downriver during the year. In contrast, the Total Chlorophyll spectrum showed a pronounced peak at ReReg site (LDR01) in August but exhibited considerable attenuation downstream. Presumably that pattern reflects a significant degradation of phycocyanin and related pigments during passage to the mouth of the river.

The turbidity in the LDR for much of the year is derived largely from biological sources, including algae released from the Project and, to a lesser extent, formerly attached algae that are dislodged from within the river. We observed a slight increase in turbidity downstream, which is consistent with that interpretation. As a result, it is likely that filter-feeding macroinvertebrates derive considerable resources from biologic suspended material. The major exception to that pattern is the summer discharge from the White River (RM 46.7), which drains from glaciers on Mt. Hood. It appears to be entirely suspended inorganic material, which can impact the river locally and, perhaps to some extent, to the LDR's mouth. In addition to suspended material, river transparency is also impacted by algal/cyanobacterial pigments. Chlorophyll concentrations are generally less than 15 µg/L, which is still relatively high for a river in the mountainous Pacific Northwest (PNW). Peak chlorophyll concentrations in the river were observed in October, which might be related to fall mixing in LBC and Lake Simtustus. Much of those pigments originate from the Project and decline downstream. Phycocyanin appears to degrade more rapidly than chlorophyll in the LDR.

8.4.7 Flow Regimes

There is a considerable body of literature on how streamflow affects periphyton in streams and rivers (Dodds 1991; Stevenson 1996a; Biggs 2000; Smolar-Žvant & Mikoš 2014; Poff & Schmidt 2016). Stream velocity affects which taxa can colonize the substrate and at what point algae become dislodged. Rivers with flows regulated by dams are noteworthy because of their capacity to stabilize flows and reduce natural variations in peak flows and low flows. The creation of flow regimes that minimize benthic restructuring that occurs with flood flows (e.g., Biggs 2000) can promote periphyton communities that deviate substantially from what might have occurred prior to streamflow regulation. Alteration of flow regimes can affect not only extremes in flow but also change the timing of flow releases. This section explores the relationship between the periphyton community and peak flows and the temporal distribution of those peak flows in the LDR, and the relationship between stream velocity and periphyton growth.

Although there is only three years of periphyton data available, the results offer some insight regarding how dams and flow regulation in the Deschutes basin may be affecting periphyton abundance and community composition in the LDR. There are seven major dams in the basin and several dozen smaller dams greater than 10 ft in height (OWRD, n.d.). Construction of the major dams began in the early 1920s with the completion of Ochoco, Crane Prairie and Crescent dams. The three impoundments exhibited considerable leakage, seldom held their design storage volume, and were later rebuilt (Crane Prairie 1940; Ochoco 1949; Crescent 1956). The remaining dams were constructed in the 1950s and 1960s with the last one being Round Butte Dam forming LBC in 1964 (Figure 8-8). The dams forming the Pelton Round Butte Project contribute to high total storage in the basin, but since these are operated as near-run-of-the-river impoundments, they provide relatively little active storage. Active storage represents that volume available for capturing and storing runoff and is most impactful in altering peak flows.

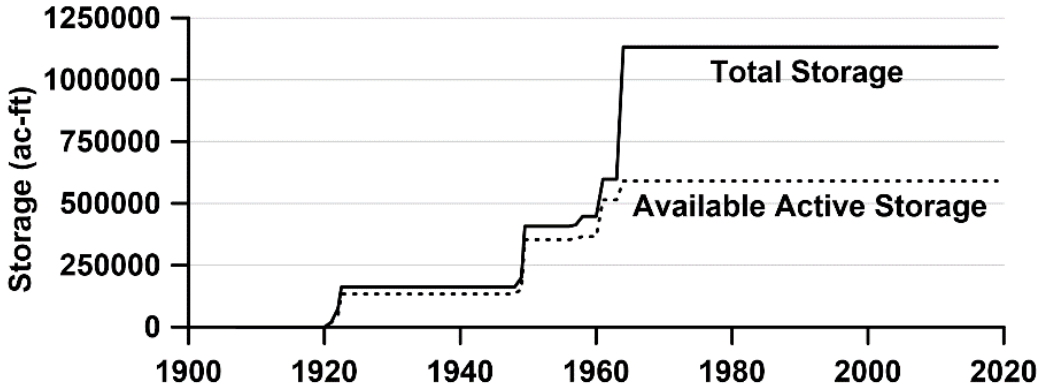

Figure 8-8. Cumulative storage behind major dams constructed in the Deschutes Basin.

Over 90 % of the active storage in the basin began to accumulate in 1949 which is a reasonable demarcation between a Deschutes River that was largely free-flowing to one which was dam-impacted; the difference in distributions is highly significant (K-S one-tailed test, p =0.011). Development of irrigation storage in the upper basin has the potential to greatly affect the hydrology of the LDR. Average annual flow in the LDR at Moody was greater (albeit, not significantly) between 1949–2017 (5,885 cfs, *se* = 104) than between 1907–1948 (pre-dam era) (5,645 cfs, *se* = 134), thus the difference in monthly distributions cannot be attributed to

differences in total precipitation between the two periods. It is evident that there has been a change in the proportion of peak flows by month between periods (Figure 8-9). The changes in timing of high flows to the LDR is also evident in average daily discharge between the two periods. The average daily flows for 1907–1948 shows the greatest daily average flows occur in mid-March and April (Figure 8-10). In contrast, flows for 1949–2017 are considerably greater in January and February than the pre-dam period.

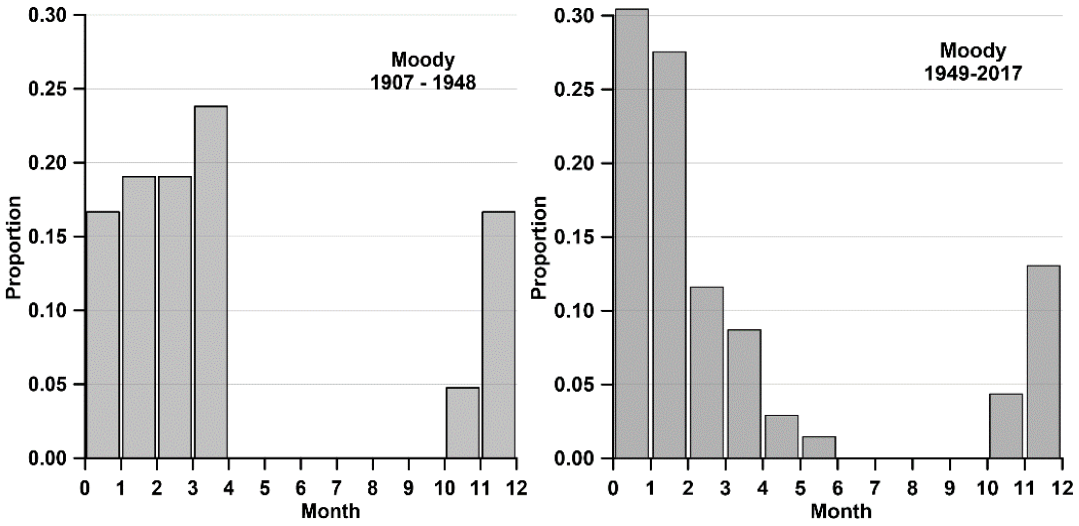

Figure 8-9. The proportions of monthly peak flows measured at Moody (USGS # 14103000) from 1907 to 2017.

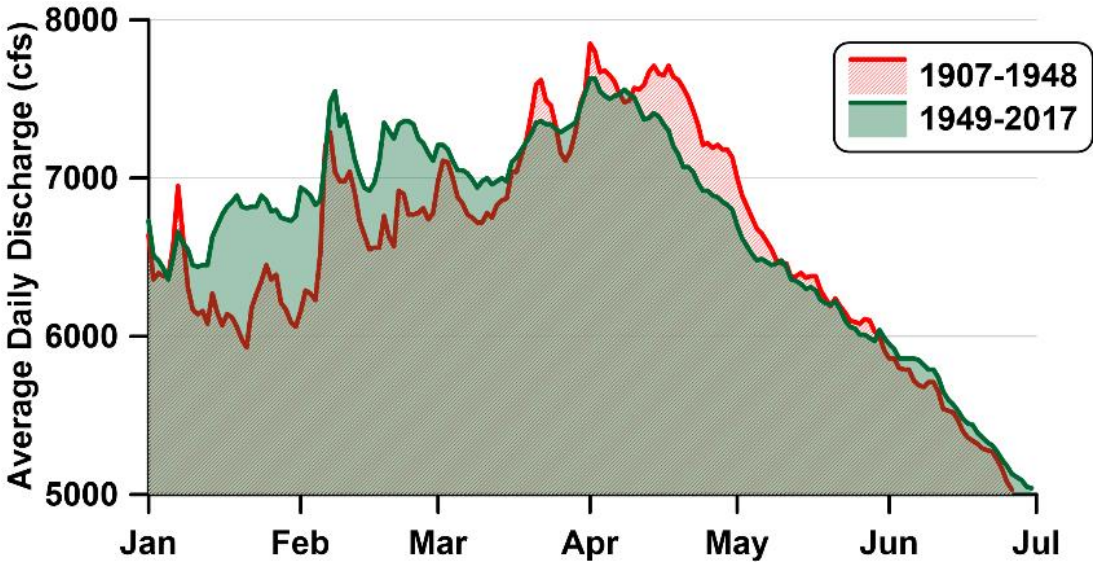

Figure 8-10. Average daily discharge at Moody for 1907–1948 and 1949–2017. Areas in red illustrate where 1907–1948 flows were greater than flows from 1949–2017 and areas in green show where flows from 1949–2017 are greater than those from 1907–1948.

The change in distribution of peak flows in the Deschutes River between the pre-dam and post-dam periods could have been caused by changes in timing of precipitation in the basin. We are unaware of any long-term estimates of precipitation that would allow for a direct examination of this question. The SNOTEL network was not initiated until the 1960s and long-term precipitation stations relevant to assessing precipitation in the basin are sparse. An alternative approach to assess the nature of the flows in the Deschutes River was conducted by examining flows in the John Day River using the site at McDonalds Ferry (USGS #14048000). We selected the John Day River for comparison with the LDR because the river is adjacent to the Deschutes basin, it is undammed, and there are long-term flow records for it. Both the Deschutes and John Day rivers exhibited greater mean annual flows (although not significantly different) from 1949–2017 compared to 1907–1948 [John Day River = 2,132 (+/-103) cfs) cfs compared to 1,941 (+/-132) and Deschutes River = 5,885 (+/-104) cfs compared to 5,645 (+/-134) cfs]. Peak monthly flows in the John Day River occurred in April during both periods, albeit with a noticeable shift in distribution. Nevertheless, peak monthly flows in the John Day River occurred 66.4% during spring in 1907-1948 compared to 63.4% of the time in spring during 1949-2017. These results suggest that much of the change in monthly peak flows in the Deschutes River is likely caused

by construction and operation of reservoirs in the basin and not temporal changes in precipitation between 1907–1948 and 1949–2017.

Between 1907–1948, the prevalence of peak flows in the Deschutes River at Moody occuring during April was statistically greater compared to 1949–2017 (Welch's test; F= 23.97, p = 0.0000) (Figure 8-11). Peak flows for the adjacent months of March and May were not significantly different for the two periods. In 2015, when the flow from the two undammed tributaries to the Deschutes River – the Metolius and Warm Springs Rivers – experienced high flows earlier in the year in January and February, the abundance of *Cladophora* in the LDR in 2015 remained high in the summer (Figure 8-12). In contrast, in 2017, both rivers experienced high flows in March, extending into April, and *Cladophora* biovolume decreased in the LDR. It is likely that if peak flows occur in the LDR in early spring (late March through April) after the biovolume of filamentous green algae increases (typically February through March), there is a greater likelihood of limiting the abundance of taxa such as *Cladophora* throughout the lower river for the remainder of the year.

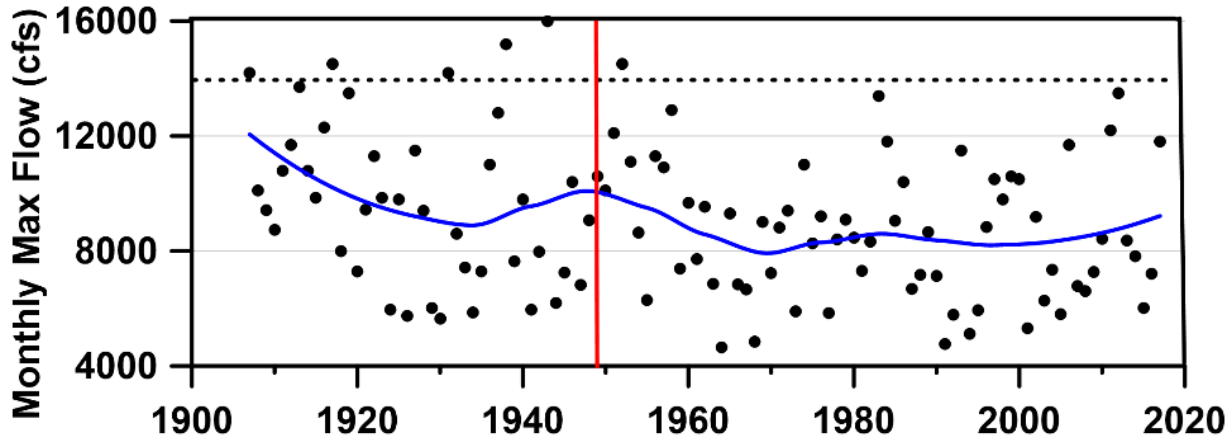

Figure 8-11. Peak streamflow at Moody during April from 1907–2017. The red vertical line separates a defined pre-dam period from the post-dam era. The blue line shows the LOESS fit of the monthly peak values. The dashed horizontal line at 14,000 cfs is provided as a frame of reference.

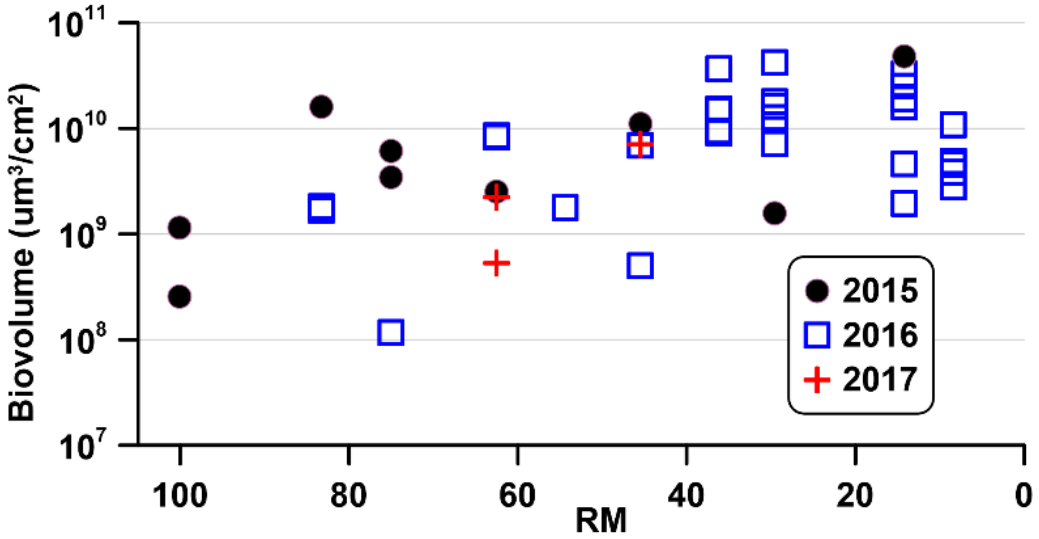

Figure 8-12. Biovolume of Cladophora during the summer from 2015 to 2017. Systematic sampling of periphyton was not initiated until August 2015.

The previous section discussed the discharge characteristics in the LDR. This section examines the relationship between discharge and stream velocity, which is the direct flow variable that impacts periphyton colonization and dislodgement from the substrate.

The LDR is a moderately fast-moving river. Typical travel time from the ReReg Dam to the mouth of the river is about 33 hr, yielding an average velocity of about 1.34 m/s (~ 3 miles per hour). Velocities such as this can be highly favorable to periphyton growth, assuming there are sufficient supplies of nutrients and light. The velocity experienced by the periphyton can be significantly less than this average velocity because bottom roughness contributes to turbulence and localized areas of decreased velocity. The effect of reduced velocity can intensify in shallow water adjacent to streambanks or gravel bars. However, so long as velocities remain above 0.15 m/s, periphyton can still experience "saturating velocities," in which a maximum supply of nutrients can still be achieved (Stevenson 1996a). Additionally, optimal velocity for nutrient supply to periphyton is highly species-dependent allowing for patchy distributions of periphyton community composition.

The amount of periphyton growth in streams is not only a function of nutrients and light, but also of time between high discharge events. High flow events scour the river bottom and remove

accumulated growths of periphyton (Biggs 2000). However, the annual variation in discharge for the LDR is extraordinarily small for a river of its size (Gannett et al. 2003). Relatively steady stream velocity makes it possible for extensive and intensive periphyton biomass to develop. The median flow for the Deschutes River at Moody is 5,230 cfs. The observations with the greatest discharge were made on December 23, 1964, when discharge reached 62,400 cfs, and on February 8, 1996, when it was 63,400 cfs. However, there are relatively few high flow events and only 67 days (out of 40,580 days extending back to WY1906) when flows at Moody exceeded 20,000 cfs.

At a discharge of 20,000 cfs (566 cm/s), the velocities are sufficient to begin moving cobble (Figure 8-13). This level of disturbance would likely dislodge a significant amount of periphyton as the cobbles were moved downstream contacting other rocks and exposing organic matter accumulated in the substrate. The significance of the 20,000-cfs threshold is that at that flow the modeled current velocity for the LDR approaches 2 m/s (6.56 feet per second) (Figure 8-14), which is sufficient to transport cobbles and cause substantial scraping of periphyton. Clearly, the effects would not be uniform down the river as local changes in slope and position of pools would affect the degree of disturbance.

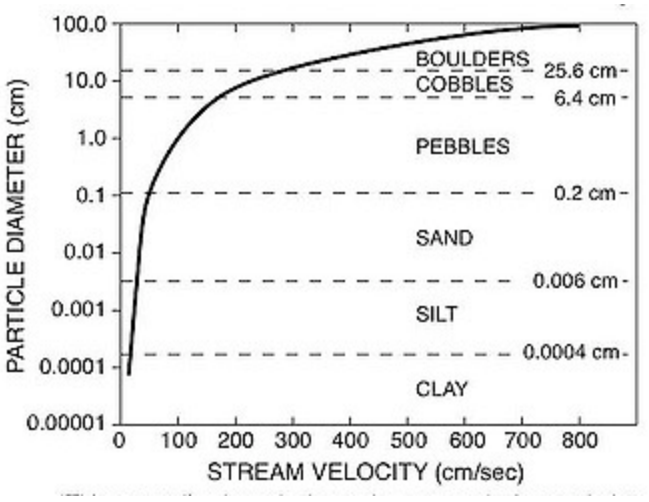

Figure 8-13. Generalized relationship between stream velocity and transport of particles of various diameters.

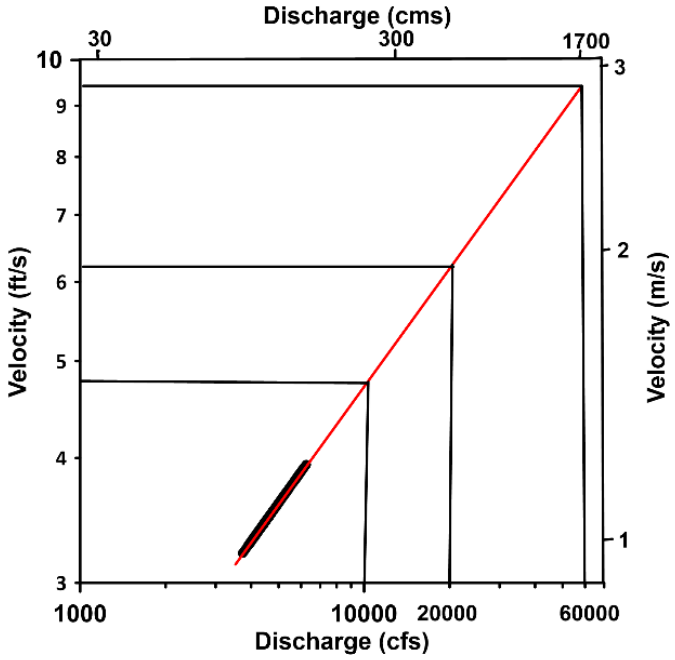

Figure 8-14. Stream velocity in the LDR based on QUAL2Kw model estimates at a specific discharge.

The most recent date on which flows exceeded 20,000 cfs in the LDR was January 1, 2006, over 11 years ago. [Note: Streamflow on the LDR at Moody (RM 1) reached 25,100 cfs on April 9, 2019, but monitoring for this study had concluded.] When we examine the PoR, the only other time with an interval between 20,000 cfs flow that was more than 11 years was during the Dust Bowl years (16 years). The median interval between flows greater than 20,000 cfs is 4 years and the mean is 5 years, so it is apparent that the LDR is currently experiencing a long interval between high flows. The field work conducted by Raymond et al. (1998) on the LDR was in 1997, 1 year after the largest flow recorded on the LDR. Because there were no comparable measurements collected on the LDR prior to the work in 1997, we have little means of determining the effect of the high flows in 1996 or the rate of probable recovery of the benthic habitat following the 1996 flood.

8.4.8 Pesticide Use

The LDR receives input from large agricultural sources, particularly from the Crooked River and extensive areas on the eastern shore of the Project downstream to Trout Creek. Pesticide use is

common in modern agriculture, but it is unclear what affect the pesticides might have on plankton communities in the Project impoundments and on periphyton in the LDR. We know from the ZAPS data that there is a strong FDOM signal from April to June at the ReReg site (LDR01), which occurs after peak flows (Figure 8-15). Significant use of pesticides began in the 1960s, appeared to peak in the 1980s, and has declined slightly (nationally) since then (Kellogg et al. 2000). Early pesticide use was dominated by insecticides, but as of 2000, herbicides accounted for about 70% of pesticide use in the United States. Although there is a strong FDOM signal in the LDR, it is a qualitative indicator of some type of fluorescent signal and is not specific to pesticides per se or any class of pesticides. However, the proximity of the Project to large areas of agricultural cropland increases the likelihood that some pesticides reach the LDR.

ODEQ began an intensive program to assess toxic chemical use and distribution in lakes and streams across the state starting in 2008. The field work for the Deschutes River basin was conducted in 2012 and revealed the presence of 7 currently used pesticides at 10 sites from a sampling of 19 locations (ODEQ 2015). None of the pesticides exceeded EPA aquatic life benchmarks or ODEQ criteria. The greatest number of pesticides detected occurred in spring and summer. Little is known regarding effects to algae at subtoxic levels or possible synergistic effects of multiple pesticides on aquatic life or periphyton. In early work on this topic, Lal (1984) noted the difficulty in assessing the actual toxicity of various pesticides to algae because of the variation investigators found in testing in different environments. Even when methodologies are standardized, it is difficult to assess algal response to a matrix of pesticides (cf. Hickman 1994). In more recent work, it was observed that different groups of periphyton respond differently to the herbicide metribuzin. Chlorophytes were greatly impacted by exposure to that herbicide and did not recover, whereas diatoms and cyanobacteria recovered well (Gustavson et al. 2003). It is becoming clear that individual groups of algae (and cyanobacteria) and species within groups have widely different sensitivities to specific herbicides and that the modes of action on organisms also vary greatly. These mechanisms include direct impairment of photosynthetic pathways and interference with uptake of nutrients (cf. Sabater et al. 2016).

In summary, several pesticides are present in the LDR and appear to be present at low concentrations. We are unaware of any direct effects of the pesticides on the periphyton community in the river, and there have been no studies to evaluate algae response to subacute concentrations.

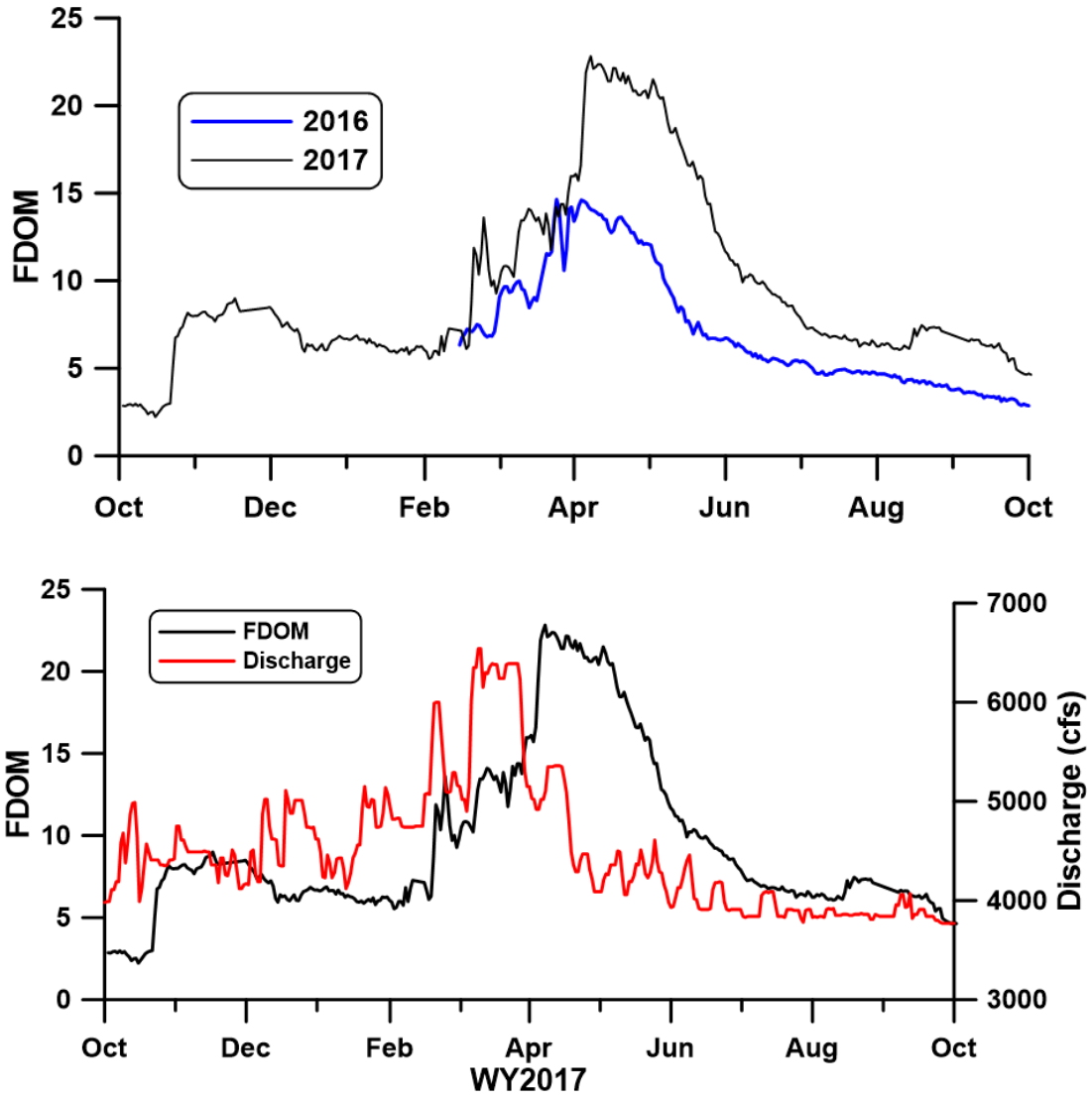

Figure 8-15. Measurements of FDOM at ReReg site (LDR01) using the ZAPS LiquID unit in WY2016–2017 (*top*) and a comparison of discharge at the ReReg site (LDR01) to FDOM measurements in WY2017 *(bottom)*.

8.4.9 Urbanization and Climate Change

The Deschutes River Basin is subject to other pressures related to anthropogenic activities. Population growth has been increasing substantially since the 1970s, with most of the growth occurring in Deschutes County (Figure 8-16). Urban growth likely will lead to more water consumption and increased runoff of nutrients, particularly to the Middle Deschutes.

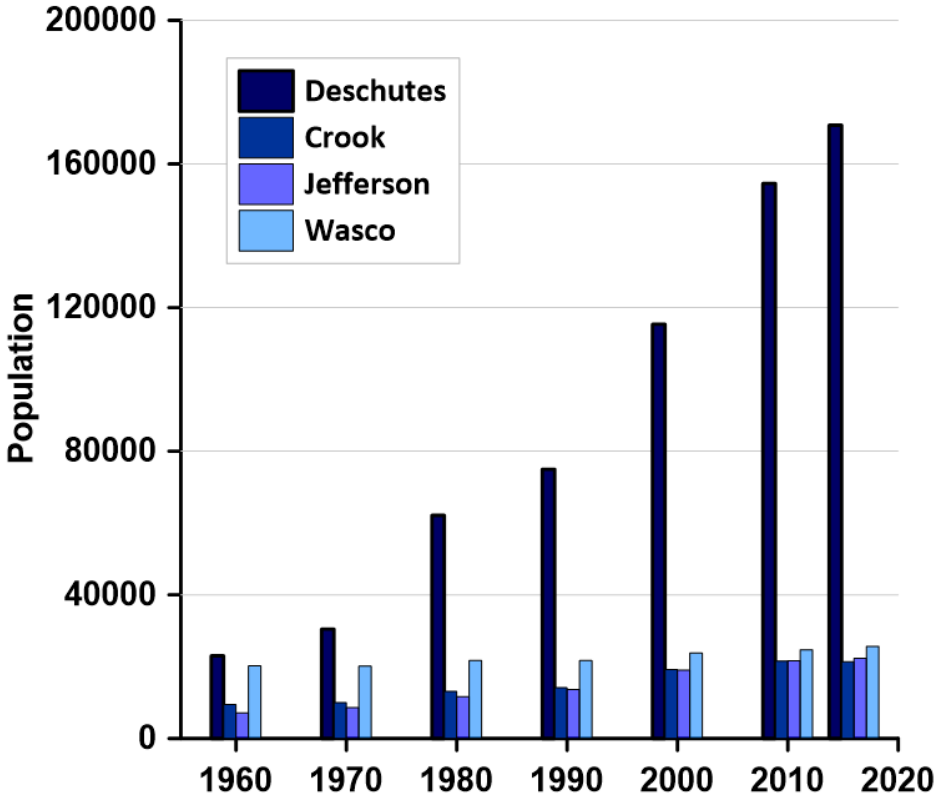

Figure 8-16. Population growth from 1960 to 2017 in the four primary counties bordering the Deschutes River.

It was noted earlier that changes in climate have already affected parts of the PNW by increasing air temperature (cf. Dalton et al. 2013). In addition to increase average annual air temperature, the Cascade Range has experienced a decreased snowpack (Mote et al. 2005; 2009; 2018). Forecasts for the region show increasing air temperature, decreasing streamflow, and a decrease in the snow:rainfall ratio of annual precipitation. Other changes in atmospheric chemistry include increases in CO_2 and nitrogen. CO_2 is important as a greenhouse gas, but it also

stimulates photosynthesis. Increased CO_2 concentrations in streams decrease pH and increase photosynthesis rates, although a greater impact might result from the response of terrestrial vegetation and the resulting changes in the chemistry of water delivered to streams (Brown et al. 2017). Emissions of other gases are also of concern. Galloway and Cowling (2002) provided an alert regarding global changes in nitrogen use, emissions, and deposition. The increased deposition of nitrogen apparently has already resulted in increased phytoplankton response in sensitive lakes in the northern hemisphere (Bergström and Jansson 2006). Emissions of reduced nitrogen (NH_x) associated with agriculture can have pronounced impacts on a local level (Sutton et al. 2008; Zbieranowski and Aherne 2013). The local effects of NH_x deposition are likely minor relative to delivery from aquatic sources in the Deschutes River basin. Similarly, effects of increasing CO_2 emissions on algal growth rates in the Project and LDR are expected to be minor relative to the effects of CO_2 on global and regional effects on air temperature. The effects of increased population growth in the basin were not evaluated in this study but could become a concern in the future.

8.5 Limitations of the Water Quality Monitoring Portion of the Study

Most ecological investigations generate new questions, and this study is no exception. In addition, there were aspects of lake and river ecology that could not be addressed in this study because of the focus on examining nutrient conditions, particularly in the LDR. Important aspects of lake and river ecology that could not be addressed include the following.

- Fisheries The potential effects of fisheries on water quality and the effect of water quality on fisheries are only briefly mentioned in the report. Changes in primary production in lakes and rivers can lead to significant changes in fish biomass and other effects on the aquatic community. Current fish populations are considered abundant in LBC (Terry Shrader, PGE, pers. comm., February 2019). It is conceivable that reductions in nutrients to the Project could result in reductions in fish biomass in the impoundments and/or the LDR. The other aspect of fisheries and water quality is the effect of fish biomass on water quality. Fish can affect water quality directly through excretion of nutrients, thus stimulating phytoplankton growth (Griffiths 2006; Eilers et al.

2011). Fish can indirectly affect water quality through predation on zooplankton which could result in decreased grazing of phytoplankton (Ekvall et al. 2014). These processes need not be mutually exclusive; for example, a large population of kokanee could produce a large amount of nutrient wastes and graze down the population of large cladocerans. Evaluation of these processes was beyond the scope of this study.

- River morphometry Its effect on periphyton distribution and water quality were not addressed. The LDR is largely a deep-run river with an average mid-channel depth of about 7 ft, although periphyton sampling was conducted at depths less than 2 ft. We have no data on what periphyton community exists in the deeper portion of the river, which occupies the majority of aquatic habitat. The decision to sample by wading into the river was based on the assumption that water was well-mixed in the river. Given the velocity of the water, this is likely a reasonable assumption for water quality with the exceptions of total suspended solids, which were not sampled. However, there is a strong likelihood that periphyton biovolume and community composition varies considerably with depth.
- River discharge Flows were relatively stable during the study. Maximum discharge at the River Mouth (LDR21) during the study period was 13,400 cfs (WY2017). The period between 2007 and 2017 did not include a major discharge event, arbitrarily characterized as 20,000 cfs at the River Mouth (LDR21). Historically, this is the second longest period without a major discharge event, exceeded only by the period from 1928 to 1942 during the Dust Bowl era. High discharge events in the LDR have occurred at an average interval of 5 years since 1906. High flow events are generally beneficial to stream systems because the high stream velocities can dislodge organic material imbedded in the substrate and can dislodge periphyton.
- Pesticides This study did not measure pesticides in the LDR, although the FDOM data suggest the presence of anthropogenic compounds with fluorescent properties are found in pesticides. Herbicides can directly affect the growth of algae, although some taxa such as cyanobacteria might be more resistant than other taxa to these exposures. The LDR receives considerable input from return irrigation flows, which could contain measurable pesticides. Periphyton communities could be indirectly affected by a change in

community composition of benthic invertebrates, particularly taxa that consume periphyton.

- Macroinvertebrate populations Macroinvertebrates have been studied in the LDR previously and no attempt was made to replicate those studies or to link the results of this water quality study to macroinvertebrate communities. We did not evaluate the distribution of invertebrate grazers or their possible relationship with the periphyton we sampled.
- Spatial variation of water quality in the impoundments This was not addressed in any detail in this study. Only two sites each were sampled in LBC and Lake Simtustus, and no sampling was conducted in the ReReg Reservoir. LBC has highly complex morphometry, which contributes to unique patterns in movement of water from the three tributaries. The spatial variations in water quality that exist in the two larger impoundments were inferred from the water quality modeling with CE-QUAL-W2 (W2).
- Algal toxins Algal toxins were not sampled in this study, although they represent a new and challenging factor to consider in managing water bodies throughout the world. Portions of LBC have been listed by the OHA in recent years as having high concentrations of the cyanotoxin, microcystin. It is unclear if this is a recent development associated with possible changes in species composition in the impoundments or reflects greater attention being paid to this issue.
- Sampling time Samples were collected during daytime hours, except for the 72-hr samplings in the LDR. Time of day is important in most aquatic systems because of the diurnal patterns of *in-situ* parameters such as pH and DO caused by oscillations in photosynthesis and respiration in the phytoplankton/periphyton community. It is reasonable to expect that there might be additional temporal changes in water quality associated with time of day. That is particularly true with a hydropower operation in which power generation can vary considerably with time of day.
- Macrophytes Aquatic vascular plants (aquatic weeds) were not sampled in this study of the LDR. The stable flow regime facilitates growth of macrophytes in zones with adequate substrate, sufficient light exposure, and generally low turbulence. The

macrophyte beds can generate high rates of localized photosynthetic activity, but also serve as substrate for epiphytic algae, especially epiphytic diatoms such as *Cocconeis*. *Elodea sp.* and *Ceratophyllum* sp.(?) were common macrophytes observed in patchy distributions throughout the river.

8.6 Summary of Major Findings Regarding Water Quality Monitoring

8.6.1 Tributaries to the Project

- All three major tributaries provide high concentrations of phosphorus to LBC. Many studies of eutrophication recommend targeting phosphorus alone, although more researchers are now recommending phosphorus reduction in combination with nitrogen. However, because the vast majority of phosphorus entering LBC is derived from natural weathering of basalt and other volcanic rocks, it is not feasible to substantially reduce the phosphorus load to the Project. One of the dilemmas facing eutrophication control in the Deschutes River basin is that the impoundments would likely benefit from a greater reduction of phosphorus, whereas the LDR would likely benefit from a greater reduction in nitrogen.
- Analysis of ODEQ AWQMP data indicates few trends in chemical constituents. pH appears to have increased in all three tributaries since 1960, but most of the increases occurred prior to 1990. It is unclear if changes in measurement technology are associated with the more recent increases and other apparent changes in the historical ODEQ data.
- Data from the USGS sites on the three tributaries show that all three sites have increased in temperature since the measurements became available starting in WY2007. The increases were minor for the Crooked and Metolius rivers, both dominated by spring inputs, but were substantial for the Middle Deschutes River. It is reasonable to assume that the small increases in water temperature in the Metolius and Crooked rivers could be caused by increasing air temperatures resulting from the changing climate; however, it is not clear what caused the recent large temperature increase at the USGS stream gage on the Deschutes River near Culver, OR (#14076500). Continued increases in tributary

temperature resulting from climate change can be expected to decrease the availability of cold water in the hypolimnion of LBC.

8.6.2 Lake Billy Chinook

- Only two samples sites were included in the monitoring program for LBC in this study. This allowed for comparison with previous studies where a site in Round Butte forebay was also sampled. However, because of the limited spatial distribution of the current study, any conclusions regarding water quality in areas other than the Crooked River arm of the impoundment should be viewed with caution. Statements of condition and changes described generally should be considered limited to the forebay and the portion of the reservoir up to the Common Pool (RES08).
- LBC is a eutrophic impoundment and the high levels of phytoplankton biomass result, in large part, from the naturally high concentrations of phosphorus in all three tributaries. Thermal stratification is intense in the upper several meters and gradually decreases with depth. There presently is no well-defined metalimnion. The waters from the Crooked River remain in the upper 12 m of the impoundment and cover the entire Crooked arm, several kilometers of the lower Metolius arm, and a small portion of the Deschutes arm. The position of the Crooked River water on the surface of LBC and the attractant flow created by the SWW cause the Crooked River inflow to move to the SWW and form a significant portion of the discharge downstream. The surface water is blended with water from the deep intake, which is still comprised largely of water from the Metolius arm. Historically, discharge during the warmer months was composed entirely of hypolimnetic water from the Metolius arm; Crooked River water remained isolated in the epilimnion during the warm months and moved throughout the surface waters of LBC.
- The epilimnion appears to concentrate some of the primary production, resulting in increased pH and supersaturated DO in the surface waters. The residence time of the epilimnion has decreased substantially with the installation of the SWW, but not enough to overcome the rate of phytoplankton reproduction. Pre-SWW, cold water from the Metolius River descended under the warmer overlying Crooked River water in the

Metolius arm and flowed directly to the hypolimnetic intake at Round Butte Dam. Some of that water now flows into a zone 20 m to 40 m deep in Round Butte forebay and extends up to the Common Pool. DO saturation values in the hypolimnion of LBC have decreased in late summer likely because of reduced withdrawal of hypolimnetic water that occurred prior to installation of the SWW. Because less hypolimnetic water is drawn from LBC under the current operating regime, the residence time of the hypolimnetic waters has increased, allowing greater opportunity for depletion of oxygen in the hypolimnion.

- Distribution of nutrients in LBC changed as a result of SWW operation. The only statistically significant change in TP was in the lower hypolimnion, where average TP values declined by 0.023 mg/L. During the study, PO_4 declined in all four depth zones of LBC post-SWW, but the only statistically significant decline occurred in the epilimnion, where PO_4 declined by 0.030 mg/L. NO_3 concentrations declined by 0.040 mg/L in the epilimnion and by 0.105 mg/L and 0.058 mg/L in the upper and lower hypolimnion, respectively. The metalimnion exhibited a nonsignificant increase in NO_3. The declines in epilimnetic PO_4 and NO_3 likely represent greater utilization of labile nutrients to support primary production. The decline in NO_3 in the hypolimnion likely reflects the decrease in supply of nitrogen (and subsequent nitrification) to the deep waters that occurred historically.
- It appears that measured analytical chlorophyll concentrations in the epilimnion of LBC increased nearly 50% post-SWW. Phytoplankton biovolume also appears to have increased. Phytoplankton community composition shows that centric diatoms, especially *Stephanodiscus* spp., remain abundant in the impoundment in spring and fall, with cyanobacteria dominant in the summer. Historically, the dominant cyanobacteria taxon was *Aphanizomenon flos-aquae*, whereas now it is *Anabaena/Dolichospermum*. The most abundant algal species present is *Stephanodiscus niagarae*, a centric diatom often transported intact through the Project and down the LDR.
- The current zooplankton community in LBC is dominated by rotifers, small, filter-feeding non-crustaceans. Large cladocerans and copepods are comparatively sparse. In

2006, the zooplankton community was dominated by the large crustaceans, with abundant populations of *Daphnia* spp. Changes of that kind are often associated with an increase in predation by planktivorous fish. The reduction in large daphnid species reduces grazing pressure on phytoplankton and an important food source for planktivorous fish. The data from 2006 were from a period when fish abundance in LBC was low and might not be typical of pre-SWW conditions. A study of fish and zooplankton populations in LBC by ODFW in 1996–1998 showed a zooplankton community similar to that found in this study, with relatively low densities of *Daphnia* and dominance by rotifers and copepods.

8.6.3 Lake Simtustus

- Only two sites were sampled in Lake Simtustus for this study, and most assessments of current conditions and changes over time are based on results from the Pelton forebay site (RES04). Additional sampling sites would allow for a more complete assessment of current conditions in Lake Simtustus.
- Although the water now discharged into Lake Simtustus is slightly warmer than it was prior to installation of the SWW, the mixing regime remains largely unchanged. The discharge from Round Butte Dam enters the hypolimnion of Lake Simtustus and moves to Pelton forebay, where the deep-water intake passes the water through to the ReReg Reservoir. The travel time through Lake Simtustus during summer flows is about 30 hr, whereas the epilimnion is stable for several months. The rapid travel time of water passing through the hypolimnion of Lake Simtustus minimizes changes in water quality during its transit to the ReReg Reservoir. Warm inflow from Willow Creek passes into the shallow epilimnion of Lake Simtustus and mixes throughout the surface waters.
- Concentrations of nutrients have changed in Lake Simtustus since the SWW was put into operation. Concentrations of TP declined by 0.036 mg/L ($p = 0.060$), and concentrations of PO_4 exhibited significant declines in the epilimnion and metalimnion. An increase in NO_3 throughout the water column was an unexpected change. The epilimnion and metalimnion showed large, significant increases (0.068 mg/L and 0.061 mg/L,

respectively), whereas the hypolimnion showed an increase of only 0.016 mg/L (ns). It is unclear if that change represents an increased rate of nitrification, a decreased rate of algal assimilation, or increased input of NO_3 to Lake Simtustus from tributaries and groundwater. An important source of nitrogen to Lake Simtustus is Willow Creek, where the median concentration of NO_3 exceeded 4 mg/L.

- As in LBC, the phytoplankton community in Lake Simtustus has abundant densities of the diatom *S. niagarae*. Whereas the summer phytoplankton community in LBC becomes dominated by cyanobacteria, *Dolichospermum* (*Anabaena*) population densities are relatively modest in Lake Simtustus. High concentrations of inorganic nitrogen such as those found in Lake Simtustus often suppress cyanobacteria by increasing the competitiveness of eukaryotes. A source for much of the nitrogen loading to the surface water in Lake Simtustus is Willow Creek, where NO_3 concentrations averaged over 4 mg/L. Willow Creek is also warm and its input to Lake Simtustus during the warmer months is confined to the epilimnion. The influx of NO_3 to the epilimnion of the impoundment provides a readily available source of nitrogen, which allows diatoms and green algae to outcompete cyanobacteria. Thus, the influx of NO_3 to Lake Simtustus suppresses—but does not totally eliminate—cyanobacteria. If the nitrogen load from Willow Creek were diminished, Lake Simtustus would experience a greater density of cyanobacteria towards site RES04 (Pelton forebay) during the summer. Both phytoplankton biovolume and chlorophyll concentrations declined in Lake Simtustus post-SWW, although transparency remained unchanged. It is unclear what mechanism or mechanisms were associated with the water quality changes observed in Lake Simtustus.
- The zooplankton community in Lake Simtustus appears to have become dominated by rotifers as has LBC. That change could be the result of a transfer of the zooplankton from LBC through the SWW. There are few data on fish community composition in Lake Simtustus to assess the possible role of fish in modifying the zooplankton community in the lake. Lake Simtustus prior to installation of the SWW had a kokanee fishery derived from movement of fish from LBC. Construction of the SWW included screening the turbines, which decreased fish mortality but also eliminated the kokanee fishery downstream. Lake Simtustus continues to be stocked with rainbow trout.

8.6.4 ReReg Dam Release

- The data show that the installation of the SWW has been successful in increasing the temperature of the release water to the LDR in the spring and late summer/early fall.
- The SWW combines surface and deep waters from LBC to achieve that goal; however, it alters other aspects of water quality, including causing increases in pH, DO, nutrients, and plankton to the LDR. pH values in the LDR have increased in addition to increases in DO saturation during the spring.
- A comparison of the water quality data collected in this study and data collected prior to the installation of the SWW shows that concentrations of nutrients released from the Project have also changed since the SWW was installed. Concentrations of TP in mid-summer more than doubled from July 1997 to July 2015 and 2016. Although PO_4 data are not available for 1997, it is likely that those concentrations increased by a similar margin. However, because the concentrations of phosphorus are naturally high in the basin, it is unclear if the increase in phosphorus has had any significant consequences in the LDR. Concentrations of NO_3 also increased by about twofold from May 1997 to 2016 and from July 1997 to July 2015–2017. NO_3 concentrations in September remained unchanged between 1997 and 2015–2017. The increases in NO_3 discharge likely increased primary production in the LDR.
- The Project currently releases high densities of phytoplankton at the ReReg Dam. No historical data exist against which to compare current data, but it is likely that the high phytoplankton densities represent a major increase over pre-SWW conditions because the historical release waters were derived from the hypolimnion in LBC. The dominant taxon represented in the release waters is *S. niagarae,* although there are a surprising number of intact cyanobacteria present in the water of the LDR derived from LBC.

8.6.5 Lower Deschutes River

- The LDR is warmer in the spring because of warmer discharge being released from LBC. Increased river temperatures promote a higher rate of metabolism for organisms and encourage increased periphyton growth.

- pH values appear to have increased slightly in the LDR based on comparing ODEQ AWQMP data to continuous 72-hr data collected in 1997. Based on the same data source, DO saturation also appears to have increased in the LDR.
- Concentrations of TP remain unchanged in the LDR based on the ODEQ AWQMP data; however, data collected in July 1997 compared with data from July 2015 and 2016 show a twofold increase in TP during July. The AWQMP data indicate that concentrations of PO_4 have exhibited a sharp decline at the mouth of the river since 2010 but show a slight increase at the Hwy 26 bridge site (RM 97.6). The data show a large increase in NO_3 at that site and a slightly smaller increase at the Deschutes River SRA site at the mouth (RM 0.1). In comparison with the 1997 data, NO_3 showed a twofold increase in May 2016 and July 2015 and 2016 at the ReReg Dam, and those increases remained throughout the length of the river in May and July 2016.
- The ratio of NO_3:PO_4 provides an indication of the relative deficiency of nitrogen to phosphorus in aquatic systems. Both nitrogen and phosphorus are abundant at the ReReg Dam; NO_3 decreases downstream whereas concentrations of phosphorus remain relatively high throughout the length of the river. These ratios indicate that the LDR experiences the greatest degree of nitrogen deficiency from winter to July (at all sites combined) and that the nitrogen deficiency increases steadily from the ReReg Dam to the mouth of the river. Phosphorus is seldom if ever limiting in the LDR. Nitrogen deficiency is not uncommon in western rivers such as the LDR.
- Considerable quantities of phytoplankton, mostly diatoms, are being transported from the Project to the LDR. Those algae, especially *S. niagarae*, are found in water samples from the river and embedded in periphyton throughout the length of the river. The historical periphyton data are inadequate to use in comparing against current periphyton communities, which were dominated by attached filamentous chlorophytes in 2015 and 2016. The most common chlorophyte is *Cladophora*, which is highly visible as long, filamentous growths. *Cladophora* requires an external source of inorganic nitrogen to proliferate. The community composition of periphyton changed greatly in summer 2017, largely because of a major decline in the distribution and abundance of *Cladophora*. The

decline in *Cladophora* appears to be associated with a high-flow event in the spring of 2017. Additional data are required to support this observation.

- Estimates of impairment of the LDR based on periphyton biomass (as chlorophyll) are highly dependent on the criterion selected for nuisance algae. At the lowest level used by others (50 mg chl/m^2), 46%–65% of the river samples would be considered from eutrophic waters. At the highest level (200 mg chl/m^2), 7%–22% of the samples would be considered to represent eutrophic waters. Using sample results from May through October would result in a high proportion of the samples being considered from eutrophic waters.
- The LDR has had an unusually stable flow regime over the past decade. The river has experienced the second longest interval without a major flushing flow (20,000 cfs at the mouth of the river). Long periods of stable flows favor periphyton growth. The last major flood event was in February 1996, with a peak discharge of 63,400 cfs at Moody (RM 1).

9 Water Quality Modeling in Project Reservoirs

Water quality in LBC is characterized by naturally high concentrations of phosphorus in the three principle tributaries, complex mixing patterns in the reservoir, and the presence of a variety of species of algae. Applying numerical models to these complex and possibly interrelated issues can make them easier to understand. Numerical models have enabled investigators to reproduce water quality conditions in the Project and apply those simulated conditions to the LDR. Although all models are simplifications of natural systems to some degree, they can help to isolate key factors in lake and river behavior and enable users to test how a water body might respond to changes in the system before implementing those changes.

9.1 CE-QUAL-W2 Model

W2 is a 2-D, laterally averaged hydrodynamic and water quality simulation model (Cole and Wells 2006). It is based on an accepted and well-established numerical strategy for simulated water temperature and water quality in deep, stratified reservoirs. It is worth noting, however, that water quality simulation does add challenges and uncertainties beyond those associated with water fluxes and temperatures. In an application of W2 to a reservoir in the Tualatin, OR, river system, the model successfully reproduced the phosphorus balance, correctly identified key sources and sinks of DO, and adequately assessed factors impacting phytoplankton growth (Rounds 2001.). But they concluded that the model failed to adequately predict pH, in part because of challenges associated with the prediction of phytoplankton growth.

A W2 model was first developed for the PRB system in 2014 to represent hydrodynamics and water temperature (Khangaonkar and Long 2014), and was then extended to include SWW operations at Round Butte Dam, as well as at both Lake Simtustus and the ReReg Reservoir (Xu and Khangaonkar 2015). In this study, the modeling team extended the existing W2 models to represent conditions in the reservoirs for the 3-year period of 2015, 2016, and 2017. In addition, the model was extended to fully account for water quality conditions throughout the system during the 3-year period. When possible, elements of the original modeling have been used directly and without modification.

W2 provides the option of including a wide variety of linked water quality components, many of which can include a user-defined number of subgroups. We included seven generic constituents to characterize water age, Cl^-, conductivity, Metolius River water, Deschutes River water, Crooked River water, and water introduced through the balance flows.

In addition, the model includes phosphate, NH_3, NO_3- NO_2, algae, zooplankton, DO, inorganic carbon, alkalinity, and both labile and refractory particulate and dissolved organic matter. The model also is capable of providing several other parameters, which are derived from the state variables. We included TOC, TN, TP, DO, and pH. Cole and Wells (2006) provides a detailed compilation of mathematics describing the interactions between water quality parameters.

9.2 Water Quality Modeling and Calibration

The focus of the modeling study was the water quality throughout the PRB system. In addition to water temperature, DO and pH were of special interest. Simulating those components requires a detailed kinetics model that includes nutrients and biology, elements that W2 includes. In this analysis, we compared key observations to model results, including DO and pH, but also conductivity, NO_3, ammonium, and P. A set of *in-situ* measurements of DO, pH, and conductivity are available as profiles at the Round Butte forebay (RES07) and the Common Pool (RES08) sites in LBC, and Pelton forebay (RES04) and the Mid-Lake site (RES25) in Lake Simtustus. Chemistry samples, as well as field data, for a variety of other parameters are also available throughout the system, although on a more limited basis. In addition, key water quality variables have also been observed in the tailraces of Round Butte, Pelton, and ReReg dams. This wide-ranging set of observations are compared against model results in a variety of different figures. In addition, the model includes a set of variables that do not correspond to available observations. In those cases, we include a similar set of figures outlining the model results, but without corresponding observed data, to more fully characterize the hydrodynamics, nutrient status, and biological activity that influence water quality. To organize the model evaluation, the report treats the three reservoirs separately, with a similar set of figures used to describe each one. The results are organized broadly into five primary categories (Table 9-1).

Table 9-1. A listing of key categories and parameters outlined in the report.

Category	Parameters
Temperature	Water temperature
Tracers	Conductivity and Cl^-: Deschutes, Metolius, Crooked, and balance flow tracers. The tracers indicate the proportion of water that originated from the different sources.
Nutrients	NO_3-N, ammonium-N, TN, TOC, phosphate.
DO and pH	DO and pH.
Biological components	Cyanobacteria, diatoms, zooplankton.

We developed separate models for each of the three impoundments, and for each, the figures include time series at multiple depths and in the tailraces. For LBC and Lake Simtustus, a set of detailed profile observations are also available. For those larger reservoirs, the analysis includes a detailed comparison of measured and modeled profiles, as well as a subset of profiles that more fully describe the modeled dynamics of selected state variables. Profiles are depicted in two ways: (1) as standard single-parameter, single-time profile of the value versus depth, and (2) as contour maps of depth versus time. The first depiction is useful to provide complete details, and the second depiction is useful as a quick summary of how each profile changes over time.

For this application, we followed general guidance provided by Cole and Wells (2006), who suggested that for a model like W2, results should be compared against all available data rather than separating observations into calibration and validation datasets. They state the following:

> "Ideally, calibration should involve multiple data sets encompassing as many variations and extremes as possible in the prototype. A model's ability to reproduce prototype behavior under a variety of conditions gives the modeler more confidence in the model's ability to accurately simulate the prototype under proposed conditions. To put it very simply, a model is a theory about behavior in the real world. A theory is continuously tested against all observed data, and, if it does not match the data, then the theory should either be modified or a new one developed that more closely agrees with observed data (Cole and Wells 2006)."

With those general ideas as a framework for the calibration process, we analyzed the model over a variety of dimensions over the full 3-year period of observations from 2015 through 2017. It is important to recognize, however, that the installation of the SWW might have resulted in changes to the LDR that exceed the variability seen from 2015 to 2017, when the SWW was fully operational. If we are looking to encompass "as many variations and extremes as possible in the prototype," calibration to conditions prior to the SWW installation would have been ideal. However, the data available to represent that time period are very limited and not sufficient to support the further calibration of the model. We did include a scenario (No SWW), which is discussed in Section 11, that was designed to mimic the release strategy prior to the SWW, with 100% of the water released from LBC at the bottom gate.

The challenge with any modeling exercise is to define a level of acceptability for calibration, so the calibrated model can be used in follow-on scenario analyses. For some elements of the system, guidance is clear on this point. Capturing surface elevations and simulating temperatures typically within about 1°C are good rules of thumb for W2 (Cole and Wells 2006). But for other water quality elements, particularly those that cannot be observed with great frequency, defining a final calibration is less clear. For that work, we primarily targeted the model to capture the magnitudes of observations and key trends in both time and space.

The goal for the temperature simulation was to end model adjustment when the absolute mean error (AME) was typically less than 1°C, a threshold suggested by (Cole and Wells, 2006).

$$AME = \frac{\sum_1^n |predicted - observed|}{n} \qquad \text{Equation 1}$$

We also include AME values for other variables when a reasonably large number of observations exist. This is generally the case for the *in-situ* profile measurements of conductivity, DO, and pH (see Table 9-2). A list of the key calibrated model parameters is included in Appendix F.

Table 9-2. Average AME values for locations in the Project with thermistor and profile observations. Individual AME values are included in individual figures.

Parameter	Location	Lake Billy Chinook	Lake Simtustus	ReReg Reservoir
Temperature (°C)	Tailrace	0.80	0.50	0.56
	In-lake thermistors	0.76	0.82	-
	Forebay	0.73	0.50	-
	Mid reservoir	0.72	0.86	-
Conductivity (µS/cm)	Forebay	13.16	12.31	-
	Mid reservoir	15.51	12.31	-
DO (mg/L)	Forebay	1.25	1.55	-
	Mid reservoir	1.30	2.24	-
	Tailrace	-	-	0.66
pH	Forebay	0.60	0.72	-
	Mid reservoir	0.56	0.61	-
	Tailrace	-	-	0.42

9.3 Data Sources

9.3.1 Geometry

W2 requires a 3-D bathymetric map, which is converted to a laterally averaged 2-D grid. In addition, it requires the locations of inflows and outflows. We used the geometry defined by Xu and Khangaonkar (2015) (reproduced for all three reservoirs in Appendix G).

9.3.2 Meteorological Data

Meteorological data from two external sites, as well as six sites operated and maintained by PGE, were compiled into a composite dataset for each of the three simulated reservoirs. Weather stations were used as appropriate based on their proximity to the simulated reservoir and availability of specific data elements. When possible, data collected by PGE was used directly. For dates and weather variables not collected by PGE, data were filled first from the AgriMet mrso weather station. Cloud cover data, not available at the reservoir stations or through AgriMet, were taken from the weather station at Redmond Airport.

9.3.3 Observed Data

Observed data was used in developing the W2 water quality model for two purposes: (1) to develop model boundary conditions such as climate data and tributary inflows (e.g., water flow, water temperature, and water quality); and (2) to represent simulated elements of the system, including evaluating the capacity of the model to capture observable system dynamics.

9.3.4 Tributary Flow Data

The primary tributaries in the system, the Deschutes, Metolius, and Crooked rivers, feed water into each of the three arms of LBC. The associated discharge data are collected by USGS at the Deschutes River near Culver, OR (#14076500); Metolius River near Grandview, OR (#14091500); and Crooked River below Opal Springs (#14087400). In addition to the primary inflows, a number of smaller streams also drain into the system. The largest of these, and the only ones that flow year-round, are Seekseequa and Willow creeks. Following analysis developed by Xu and Khangaonkar (2015), the modeling team set the discharge into Lake Simtustus from Seekseequa Creek to 0.07 cms. A set of observations was made in 2015 and 2016 in Willow Creek indicating an average discharge of 0.5 cms. We used that value, instead of the 1 cms from the earlier model.

9.3.5 Discharge from Reservoirs

PGE provided discharge from Round Butte Dam at a 1-minute timestep, with separate discharges from the upper and lower gates on the SWW. Those data were used to define the outflow from LBC and the inflow to Lake Simtustus. PGE also provided 1-minute time-step discharge from Pelton Dam, which was used in the modeling to define releases from Lake Simtustus and into the ReReg Reservoir. Discharge from the ReReg Reservoir was not collected directly. Instead, and following Xu and Khangaonkar (2015), stream discharge data collected by USGS at the Deschutes River at Madras (#14092500) were used to define outflows from the ReReg Reservoir. The USGS site is approximately 150 m from the tailrace.

9.3.6 Reservoir Stage Data

Modeling reservoir hydrodynamics require detailed inflow and outflow rates, but there is significant uncertainty in these measurements, other unmeasured flows from tributaries, as well as surface water to atmosphere exchange through evaporation and precipitation. Adjustments to exchange flows are typically required for the model to match measured reservoir surface water elevations. Following Xu and Khangaonkar (2015), we used surface water elevations in the three reservoirs to develop a set of balance flows that allowed the model to match the observed elevations.

9.4 Water Temperature Data

9.4.1 Tributary Data

The water temperature of large tributaries represents a key boundary condition that influences both the hydrodynamics and the temperatures in the reservoir model. USGS collects water temperature at the three primary tributary inflows, and those data were used as inputs to the model.

9.4.2 Discharge from Dams

Field personnel measured the temperature of water leaving LBC and Lake Simtustus throughout the Project timeframe. The data are not used as boundary conditions because the model simulates temperature throughout the system, given flow boundaries. Instead they are used in the model evaluation to more fully outline the capacity of the model to capture key features of the system. Similarly, USGS collects stream temperature at the Deschutes River at Madras gauging stations. Those data are also used in the model evaluation.

9.4.3 In-Reservoir Temperature Data

The field staff collected temperature data during the study period at a variety of different locations. The data were collected by a set of continuously recording thermistors in the reservoirs and include a set of profile measurements taken throughout the 3-year study period. The

modeling team used the data as evaluative endpoints to establish the capability of W2 to adequately capture temperature dynamics throughout the system.

9.5 Water Quality Data

9.5.1 Tributary Data

Field staff collected water quality data in each of the primary tributaries periodically during the first two years of the study period. In addition, ODEQ continuously collects water quality data in the major tributaries that is available for use. The ODEQ data were particularly useful in 2017, when PGE had stopped collecting tributary nutrient data. As with discharge and water temperature data in the tributaries, the water quality data are used as a boundary condition for the model. Temporal sampling of water quality was not high, and linear interpolation was used between sample points. The lack of data lead to an increase in uncertainty for the model results in 2017. No data on total inorganic carbon (TIC) were available for the tributaries, which led to some uncertainty in the carbonate cycling components of the model, including pH. We estimated TIC values for the tributaries based on observations of alkalinity and pH, but temporal variation in the incoming TIC was not available.

In addition to tributary water quality data, the model also requires water quality information for the balance flows calculated as positive. Without specifying balance flow chemistry, the model assumes a value for water quality parameters of 0. For some parameters, assuming small values is acceptable because the balance flows are typically small compared to tributary inflows or the volume of water in the system, and they do not exert a strong influence on the results. There are two situations, however, in which the balance flows can noticeably impact the water quality results. The first situation relates to the carbonate balance and the resulting pH equations. The balance uses TIC and alkalinity to infer pH, which is presented on a logarithmic scale. The logarithmic nature of the pH calculation means that it can be sensitive to small changes in either TIC or alkalinity. For these simulations, we assumed the balance flow chemistry was similar to that measured in the Metolius River, on the further assumption that the Metolius River is primarily comprised of groundwater and that the balance flows also represented groundwater. The balance flow values for TIC and alkalinity were then adjusted as part of the pH calibration.

The second situation in which the balance flow chemistry becomes important is if the balance flows are large compared to other flows in the system. Typically, that condition does not occur, but it did occur in winter of 2017 (Figure 9-1).

9.5.2 Discharge from Dams

Periodic water quality sampling in the tailraces is used as part of the evaluative procedure. As with the tributary samples, the temporal resolution of tailrace water quality sampling is relatively low.

9.5.3 In-Reservoir Water Quality Data

In-reservoir water quality samples were drawn at approximately monthly intervals during the spring, summer, and fall. These data are used to evaluate the modeled water quality. In addition to laboratory analyses, a set of profile measurements including DO, pH, and conductivity were also developed in LBC and Lake Simtustus.

9.6 Pelton Round Butte Model Development and Calibration

9.6.1 Model Setup

9.6.1.1 Input data and initial conditions

The initial water surface elevation (ELWS) for the PRB model was taken from observations and set to 480.54 m. Initial conditions for temperature and water quality variables were set to low values that did not vary with depth. The modeler took this conservative approach because no observed values were available for January 1, 2015. While this approach would be problematic for short-term simulations, in which initial conditions would be expected to impact results, for the 3-year simulations used in this study, the impact of reasonably correct initial conditions will influence model results only early in the simulation.

9.6.1.2 Meteorological inputs

When possible, meteorological data collected at the Round Butte weather station were used as input for the model. For those parameters or points in time when the Round Butte weather

station was down, data were taken from the Chinook Island station, then from the AgriMet mrso station, and, for cloud cover, daily average data from the Redmond Airport were used.

9.6.2 Model Calibration

9.6.2.1 Hydrology/ELWS/balance flows

Calibrating the model began with developing datasets designed to represent all the inflows to and outflows from the system. In most cases, because of the uncertainty in existing measurements and unmeasured flows, including evaporation, unmeasured tributaries, and groundwater exchange, additional estimates are required for the model to adequately capture observed reservoir elevations. Modelers used the water balance utility developed by Portland State University and the US Army Corps of Engineers to provide estimates of the balance flows. The process was originally developed for the 2013 W2 model, with balance flows updated to represent 2015–2017 (Xu and Khangaonkar 2015). Daily balance flows are outlined in Figure 9-1.

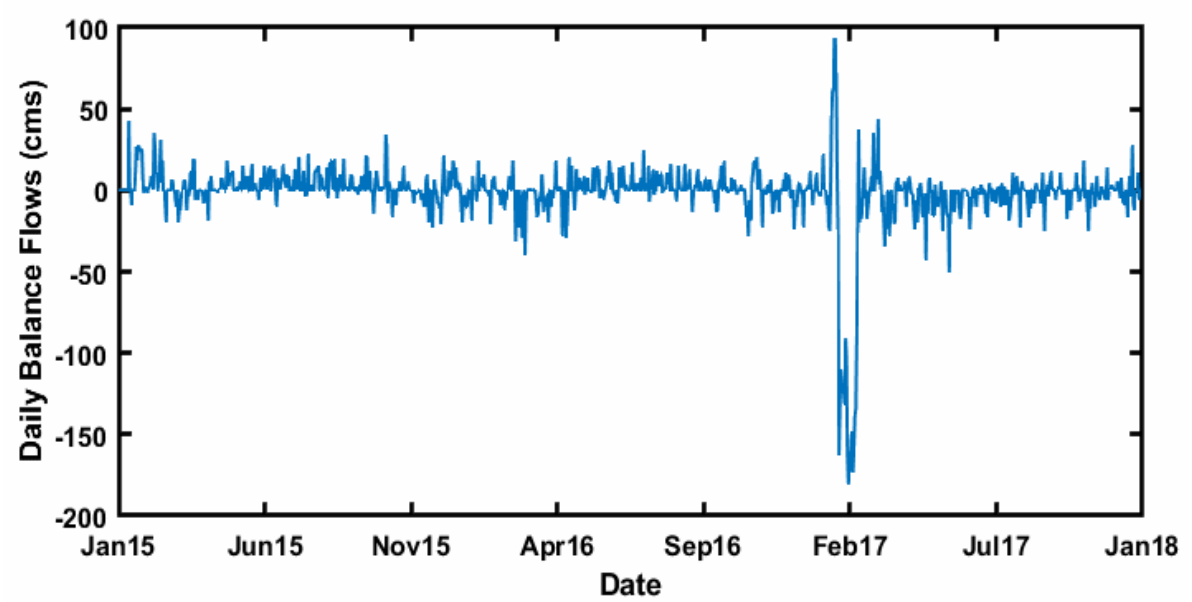

Figure 9-1. Daily balance flows for LBC.

The large negative balance flows during early winter 2017 (around Julian Day 775) represent the utility of ELWSs to ensure proper mass balance. For approximately 2 weeks during that period, discharge data from the dam were unavailable. The balance flow process was used to provide an estimate of the missing discharge values based on inflows and the observed changes in the ELWS of the reservoir. Surface elevations are well captured by the balanced model (Figure 9-2), with an AME of 0.19 m. Balance flows were added to each of the three arms in proportion to the average discharge in each arm over the 3-year simulation period (Table 9-3).

Table 9-3. Proportions used to allocate balance flows to the different arms.

	Crooked River	**Deschutes River**	**Metolius River**
Average daily discharge (cms)	43.10	25.19	44.08
Proportion	0.38	0.22	0.39

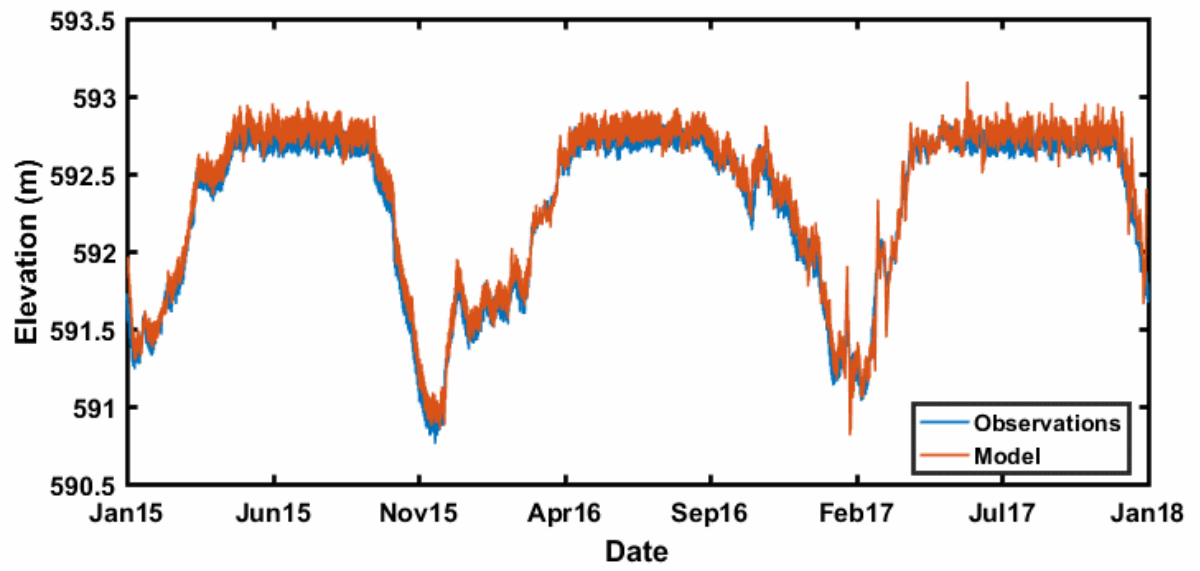

Figure 9-2. Simulated and observed reservoir ELWSs from January 1, 2015, to January 1, 2018.

9.6.2.2 Water temperature

Water temperature is sensitive to inflow temperatures, meteorological conditions, and water quality, which impacts light penetration depths. Models that incorporate temperature make use of these data, as well as a set of algorithmic parameterizations adjusted to allow simulated temperatures to match observations. Procedures outlined in Xu and Khangaonkar (2015) were followed for this model, including using the same set of model parameters. The primary difference was that meteorological data collect by PGE at Pelton Dam was used in place of the data from the AgriMet mrso site. Despite suggestions that such a change could influence the wind sheltering or shading parameters, that did not occur and those parameters were used in the model as suggested by Xu and Khangaonkar (2015). Tailrace temperatures, resulting from a mixture of water from the upper and lower gates, are acceptably captured with an AME of 0.76˚C (Figure 9-3). Time series of temperatures within the reservoir, at seven different depths, also show good model fits (Figure 9-4), with AME values all below 1˚C over the PoR. Profile temperatures also indicate close agreement between the model and the observations across a wide variety of different conditions (Figure 9-5).

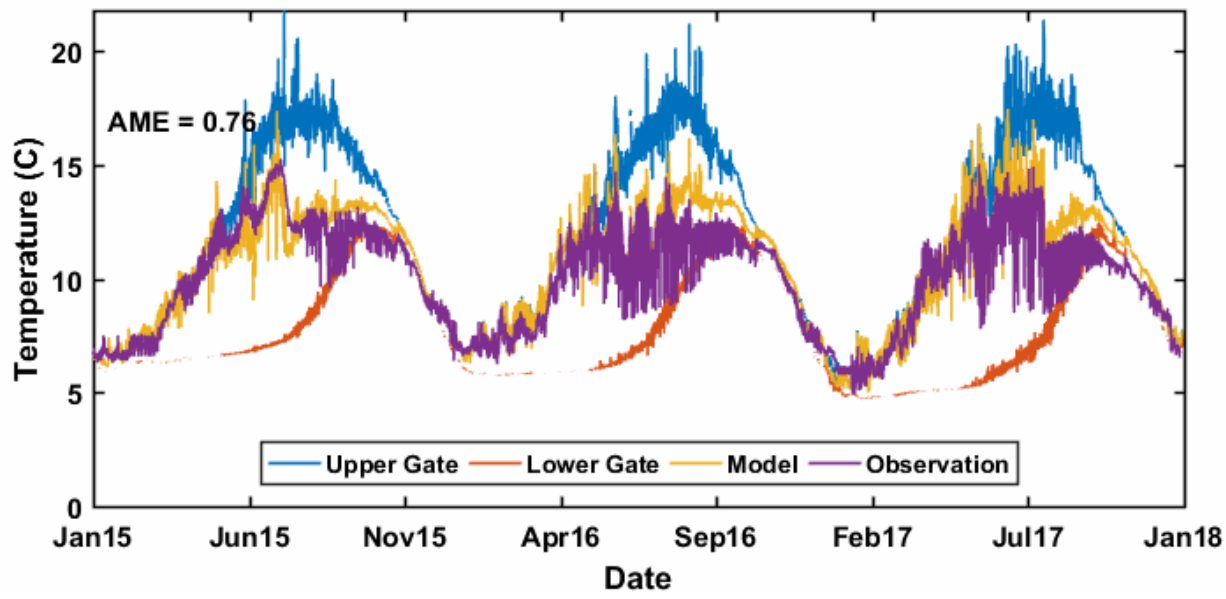

Figure 9-3. Simulated and observed water temperature at the outlet of LBC. Simulated temperatures at the upper and lower gates are included for reference.

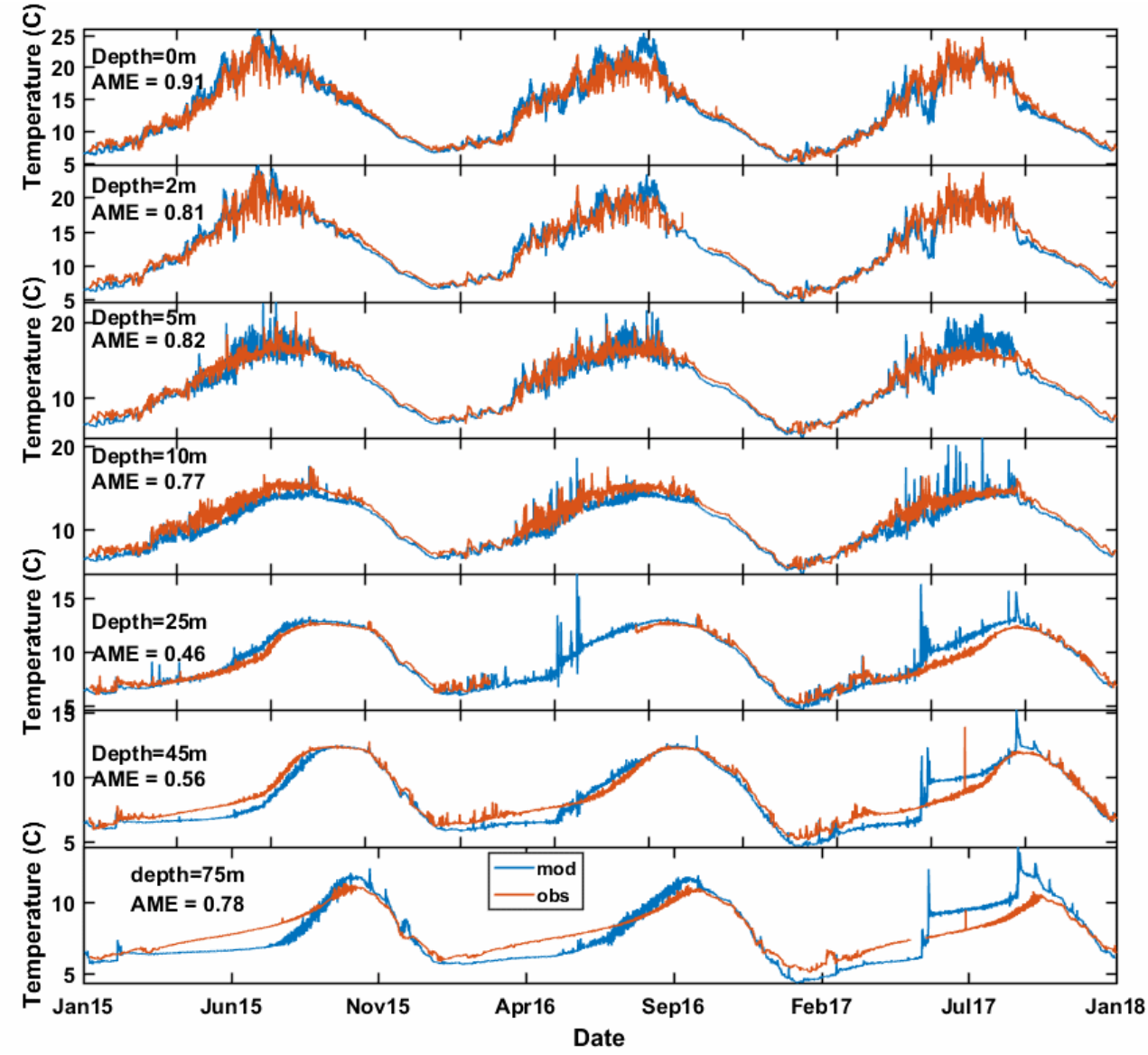

Figure 9-4. Simulated and observed water temperatures at different depths in LBC. Modeled spikes in temperature, particularly at 25 m, occur in part because they are captured at a depth below the surface.

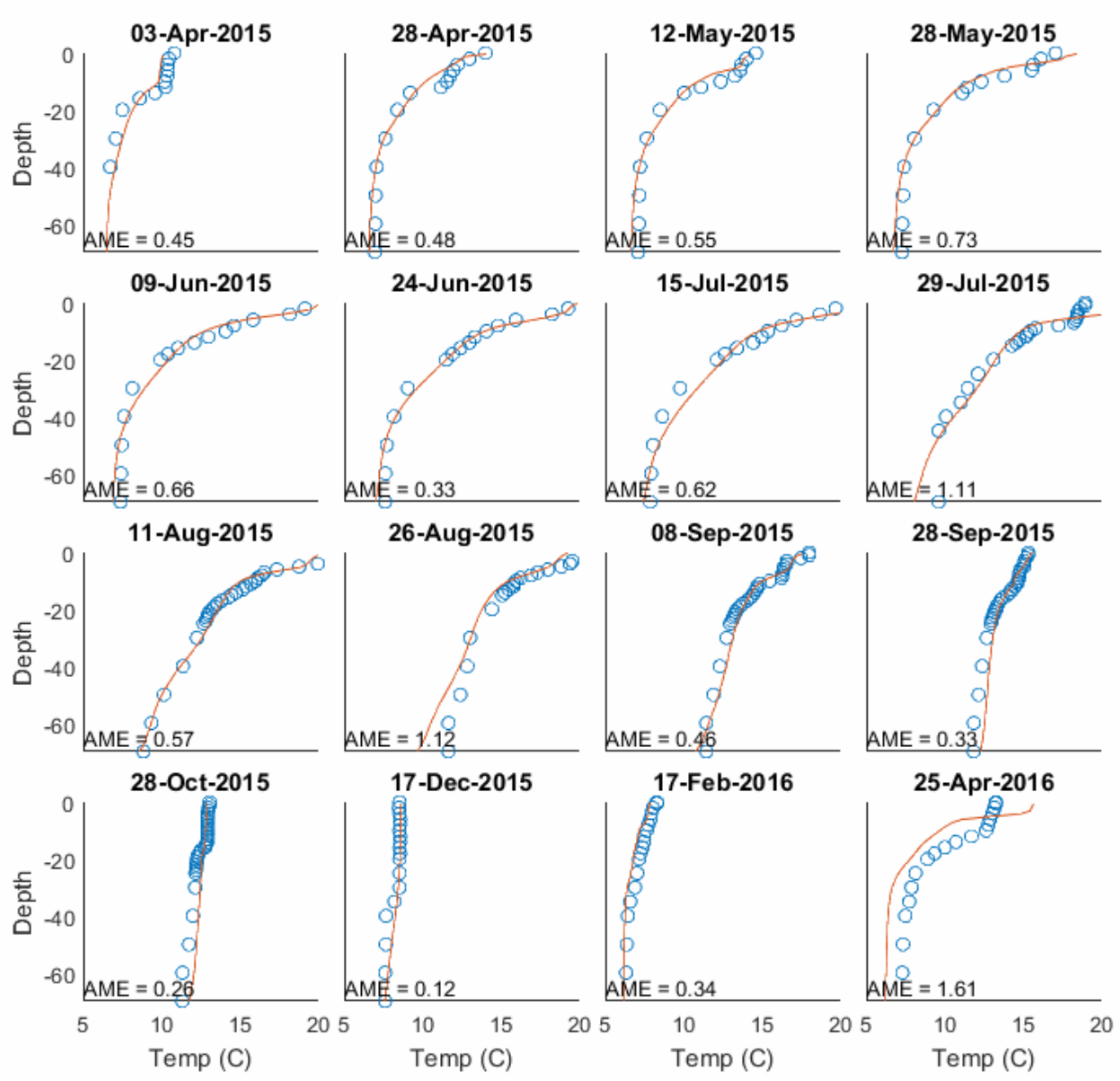

Figure 9-5. Observed temperature profiles (blue dots) and simulated temperature profiles (orange lines) at Round Butte forebay (RES07) (April 3, 2015–April 25, 2016). The units on the y-axis are meters below the surface.

As the ELWS changes, the model samples different model units. In some cases, particularly in the metalimnion in which vertical gradients can be large, the sampling of different model units can lead to relatively large changes in temperature, as seen at 25 m. The remaining profiles are outlined in Figure 9-6 to Figure 9-8.

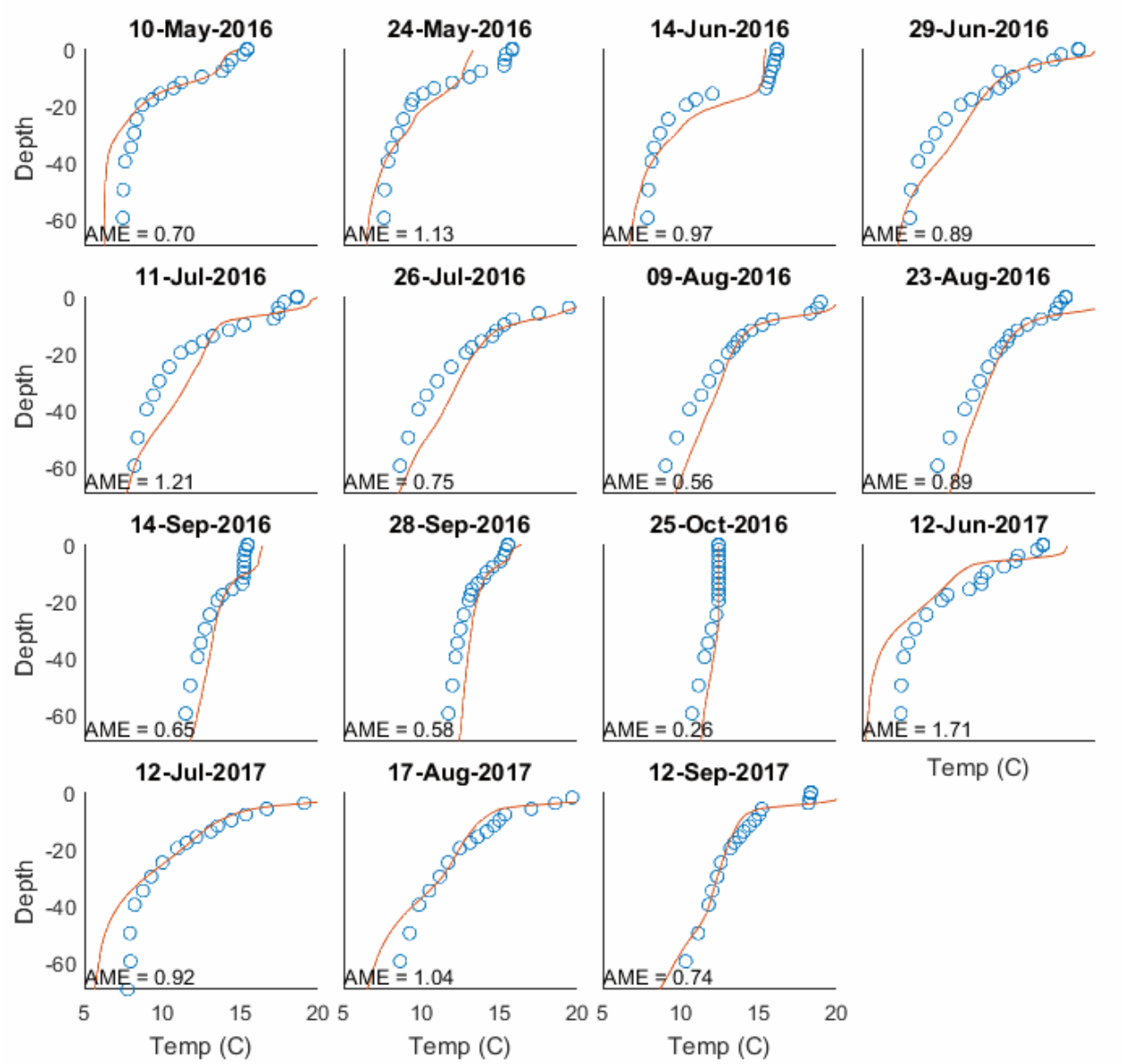

Figure 9-6. Observed temperature profiles (blue dots) and simulated temperature profiles (orange lines) at Round Butte forebay (RES07) (May 10, 2016–September 12, 2016). The units on the y-axis are meters below the surface. The negative values are included to indicate that it is a depth below the water surface.

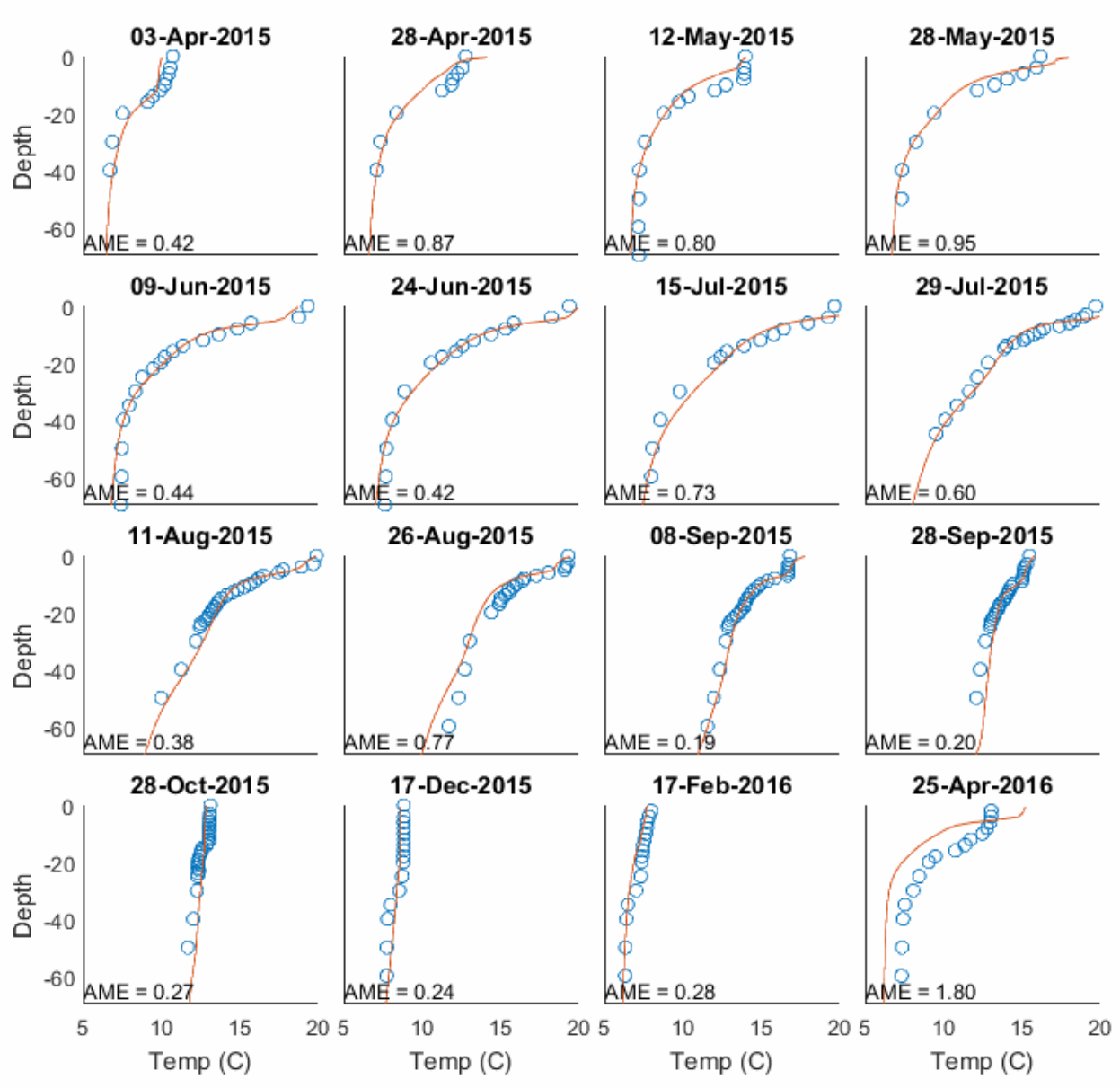

Figure 9-7. Observed temperature profiles (blue dots) and simulated temperature profiles (orange lines) at the Common Pool (RES08) (April 3, 2015–April 25, 2016). The units on the y-axis are meters below the surface.

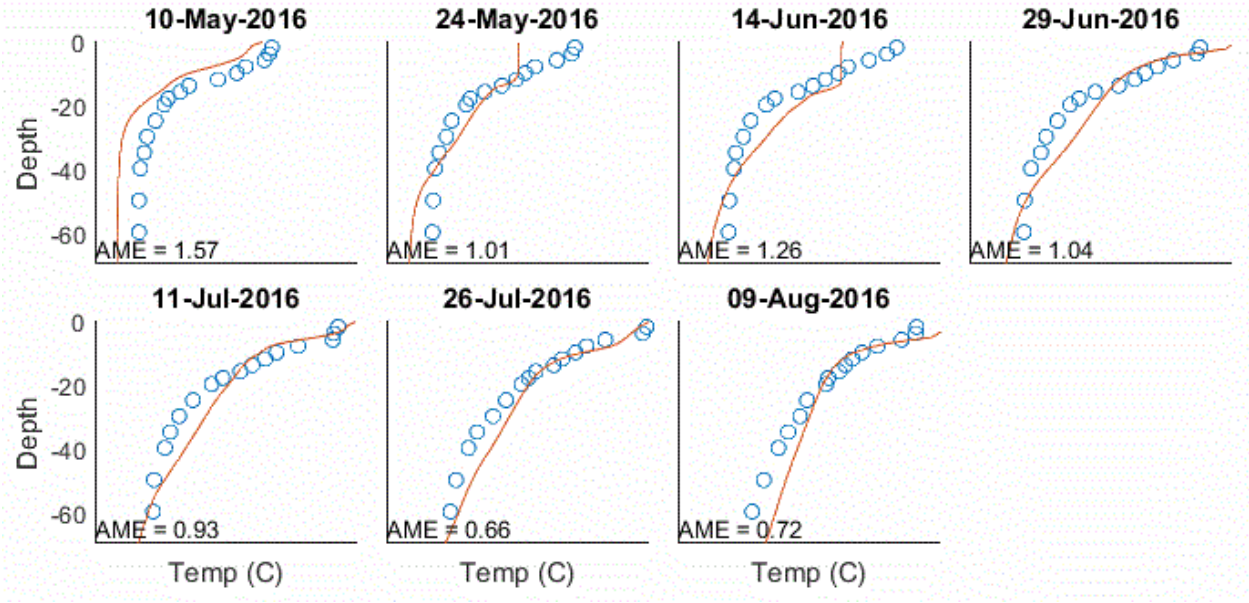

Figure 9-8. Observed temperature profiles (blue dots) and simulated temperature profiles (orange lines) at the Common Pool (RES08) (May 10, 2016–September 12, 2016). The units on the y-axis are meters below the surface. The negative values are included to indicate that it is a depth below the water surface.

9.6.2.3 Conservative tracers

Seven independent conservative tracers were included in the model to more accurately characterize how key sources of water mix in the reservoir and contribute to downstream reservoirs and the LDR. A set of four tracers was used to evaluate how water from the three tributaries and calibrated balance flows move through the system. The concentration of each tracer was set to a value of 1 mg/L in the source that it represented. The Deschutes River tracer was set to a value of 1 in the Deschutes branch water quality inflow, but the values for other river tracers were set to a value of 0. In the reservoir, mixing from all sources of water dilutes the value of each tracer and, because 1 is a maximum, the concentration of each tracer represents the proportion of the water that originated from each source. In addition, we included a tracer to provide the modeled age of the water and tracers to capture Cl^- and conductivity. Both Cl^- and conductivity were included in the observational strategy and provide useful conservative tracers for which we can evaluate model performance as it relates to mixing dynamics.

Results suggest residence time in the reservoir varies seasonally as a profile stratifies and de-stratifies, with the longest residence times occurring in the deeper water during the summer. The SWW draws most water from the surface and, along with the temperature-derived stratification, much of the hypolimnion is relatively isolated for the Round Butte forebay (RES07) and the Common Pool (RES08) (Figure 9-9 and Figure 9-10, respectively). Metolius River water tends to dominate in the deeper areas of the reservoir, primarily because it enters the system at a colder temperature. Crooked River water makes up a larger proportion of the epilimnion, for similar reasons. The model tracks the balance flows, much of which might be groundwater, but which also reflect other unmeasured sources and sinks. The somewhat larger amount of balance flow in the winter of 2017 is a result of missing flows from the lower gate during that period. This period is one example in which the balance flows clearly are not simply groundwater.

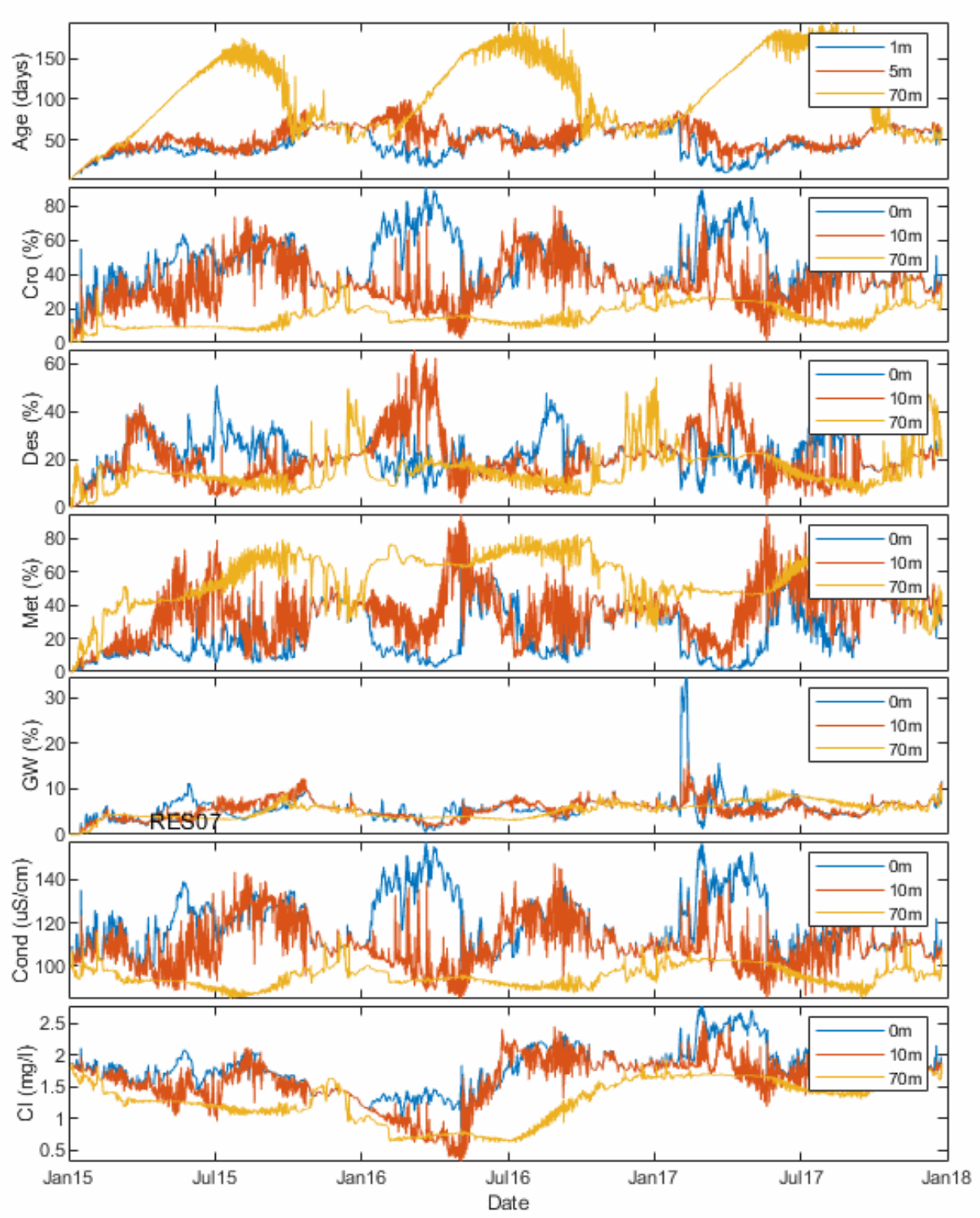

Figure 9-9. Simulated values at Round Butte forebay (RES07) showing the percentage of different water sources and estimated contribution of groundwater.

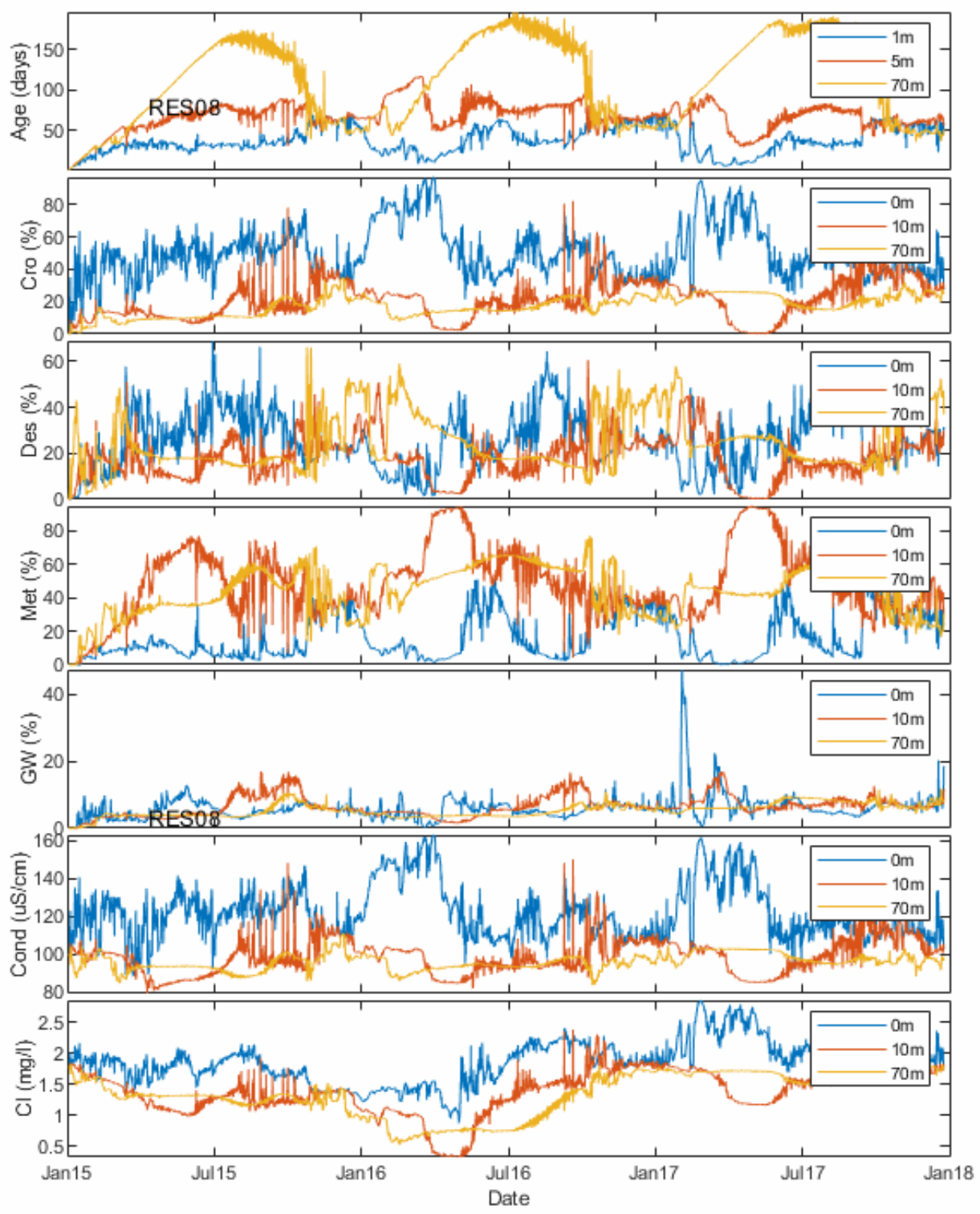

Figure 9-10. Simulated values at the Common Pool (RES08) showing the percentage of different water sources and estimated contribution of groundwater.

The profiles for each of the river tracers and residence times are provided in Appendix H. These results highlight the dominance of Metolius River water in the deeper parts of the reservoir and Crooked River water in the shallower areas.

Tailrace data represent the water leaving LBC just before it enters Lake Simtustus. The residence time of the tailrace indicates how long that water had been in LBC prior to its release. It varies from about 20 days to a maximum of about 120 days and reflects mixing dynamics in the reservoir, including stratification and the operation of the SWW. Conductivity is well approximated, indicating that mixing in LBC is adequately captured by the model. Contributions from the different tributaries to the tailrace water vary seasonally as a function of both stratification and the operation of the SWW (Figure 9-11).

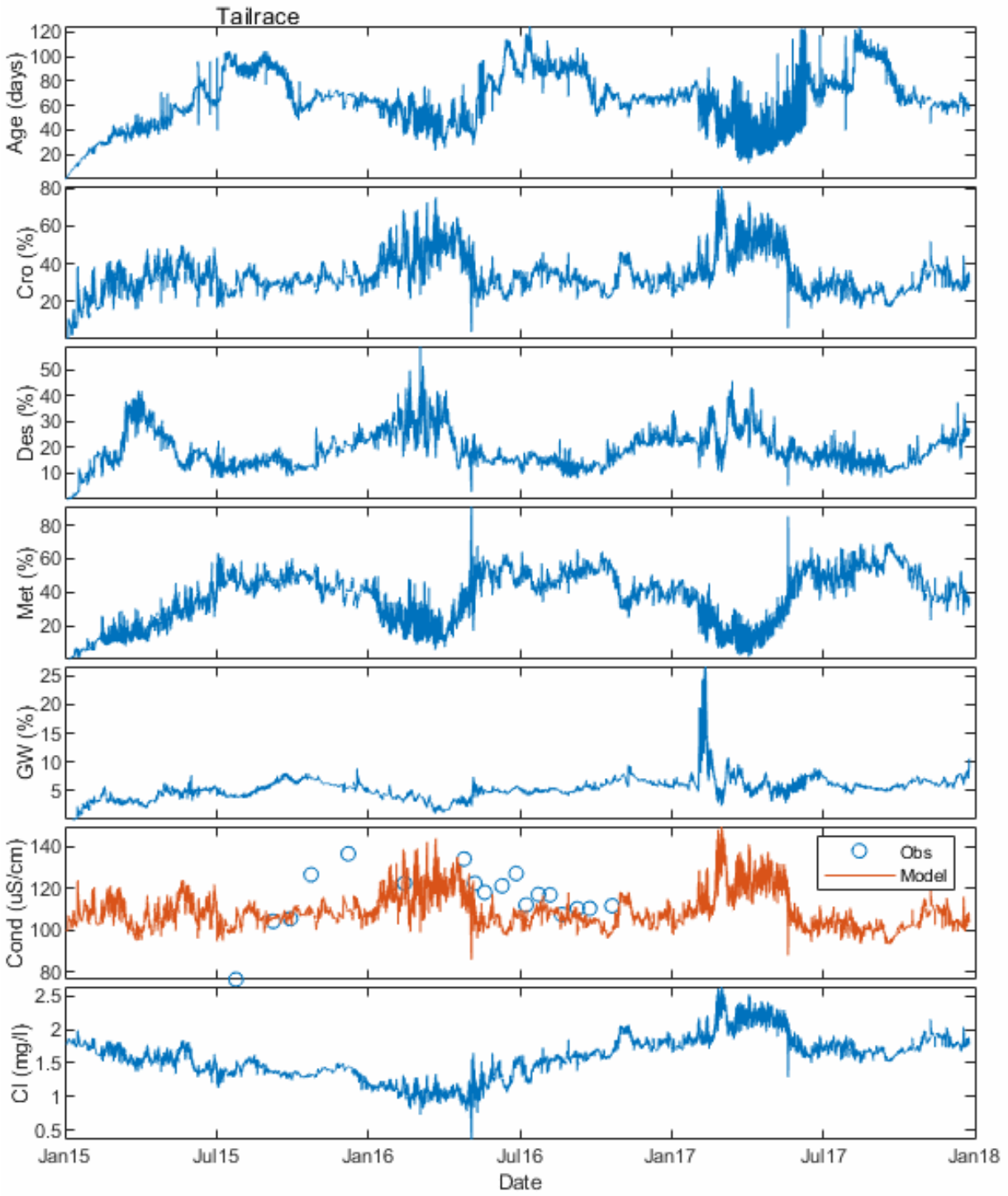

Figure 9-11. Simulated values at Round Butte tailrace showing the percentage of different water sources and estimated contribution of groundwater.

9.6.2.4 Nutrients

Nutrient dynamics govern biological production and originate primarily from tributary inflows, but also from cyanobacteria that can fix nitrogen. The model appears to capture the magnitude of nutrient concentrations and, with the relatively small number of samples used to characterize input from tributaries, the seasonal pattern is as close as can be expected.

The time-series comparisons for the Round Butte forebay (RES07) and the Common Pool (RES08) (Figure 9-12 and Figure 9-13, respectively) outline the capacity of the model to capture the general magnitudes of the observations. NO_3 appears at times to be underpredicted by the model during the winter and in the deeper areas of the reservoir, but the overall pattern of higher NO_3 concentrations with depth is well captured. During the summer periods, the model appears to underpredict nitrogen.

The prominent simulated peak in nutrients during the winter of 2015–2016 does not appear to match the relatively few measurements available during that time. The peak appears in the model results primarily because of two samples that showed high NO_3 and total N in the Crooked River during this period. This small set of samples was left in the modeling analysis because there was not a clear reason to drop them, but it is important to note that they clearly impact the results. This uncertainty supports the idea that complex water quality models, implemented in very dynamic systems, are strongly regulated by available input data. Nonetheless, the overall focus of this report is to document how the LDR might respond to changes in the LBC system. While this N peak during the winter of 2015 is not observed in the available measurements, it provides a useful test for more fully evaluating the impact of nutrients on the LDR. If there is a compelling reason to remove the two Crooked River N samples, the analysis can be rerun in the future.

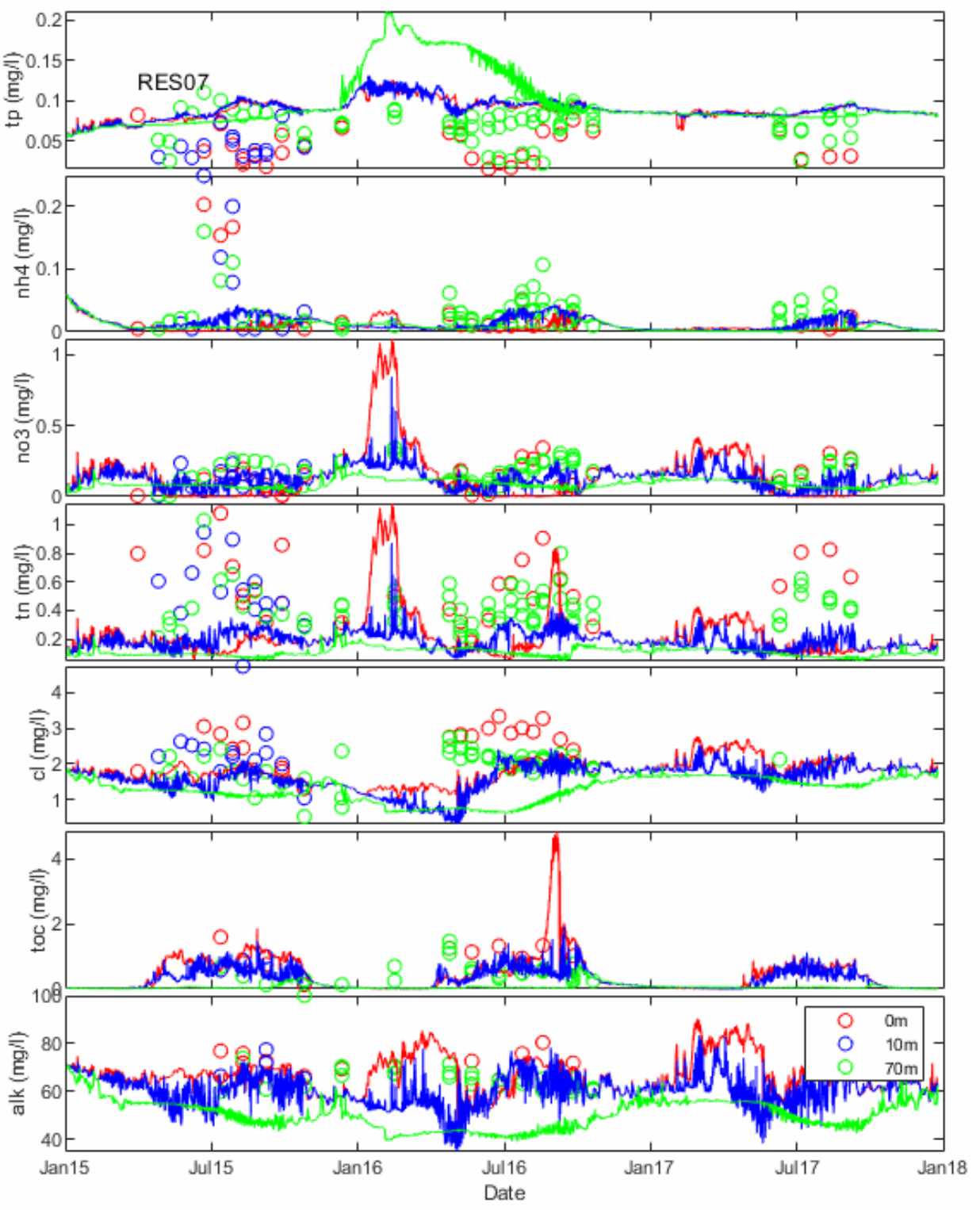

Figure 9-12. Simulated and observed nutrient dynamics at Round Butte forebay (RES07). Cl^- and alkalinity are included for reference.

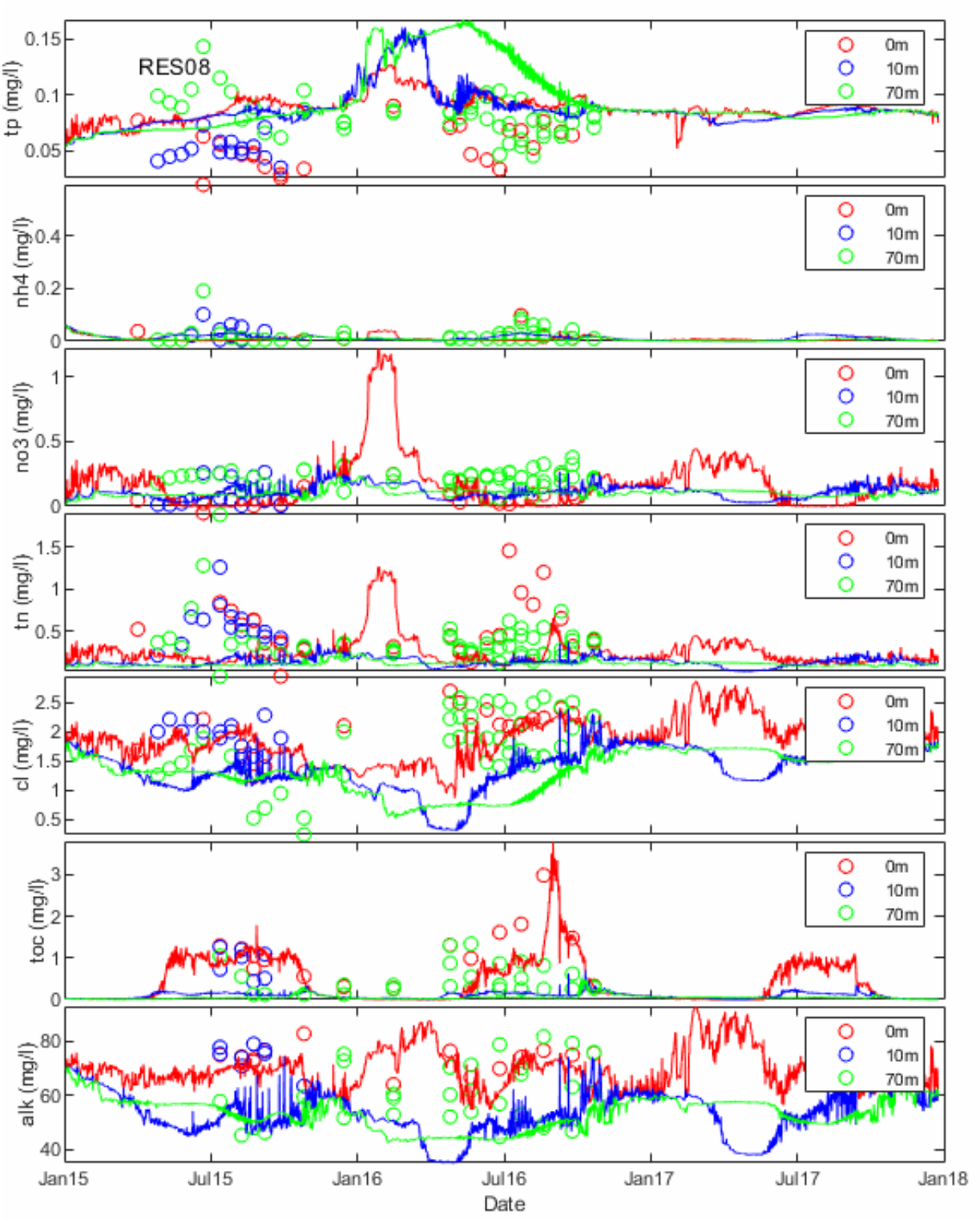

Figure 9-13. Simulated and observed nutrient dynamics at the Common Pool (RES08). Cl^- and alkalinity are included for reference.

Profiles of the nutrients are included for reference, although they are only for the Round Butte forebay (RES07) for the first 16 profile dates (Appendix H). Profiles are consistent with high summer biological activity, which tends to depress available nutrients through uptake in the warmer epilimnetic waters. During the winter, nitrogen arriving in the system from the tributaries collects in the reservoir and, with the much slower biological activity, concentrations increase.

Tailrace nutrient simulations are consistent with other time series and indicate that the model captures the general magnitude of the observations (Figure 9-14), but that nitrogen tends to be underpredicted during the summer period.

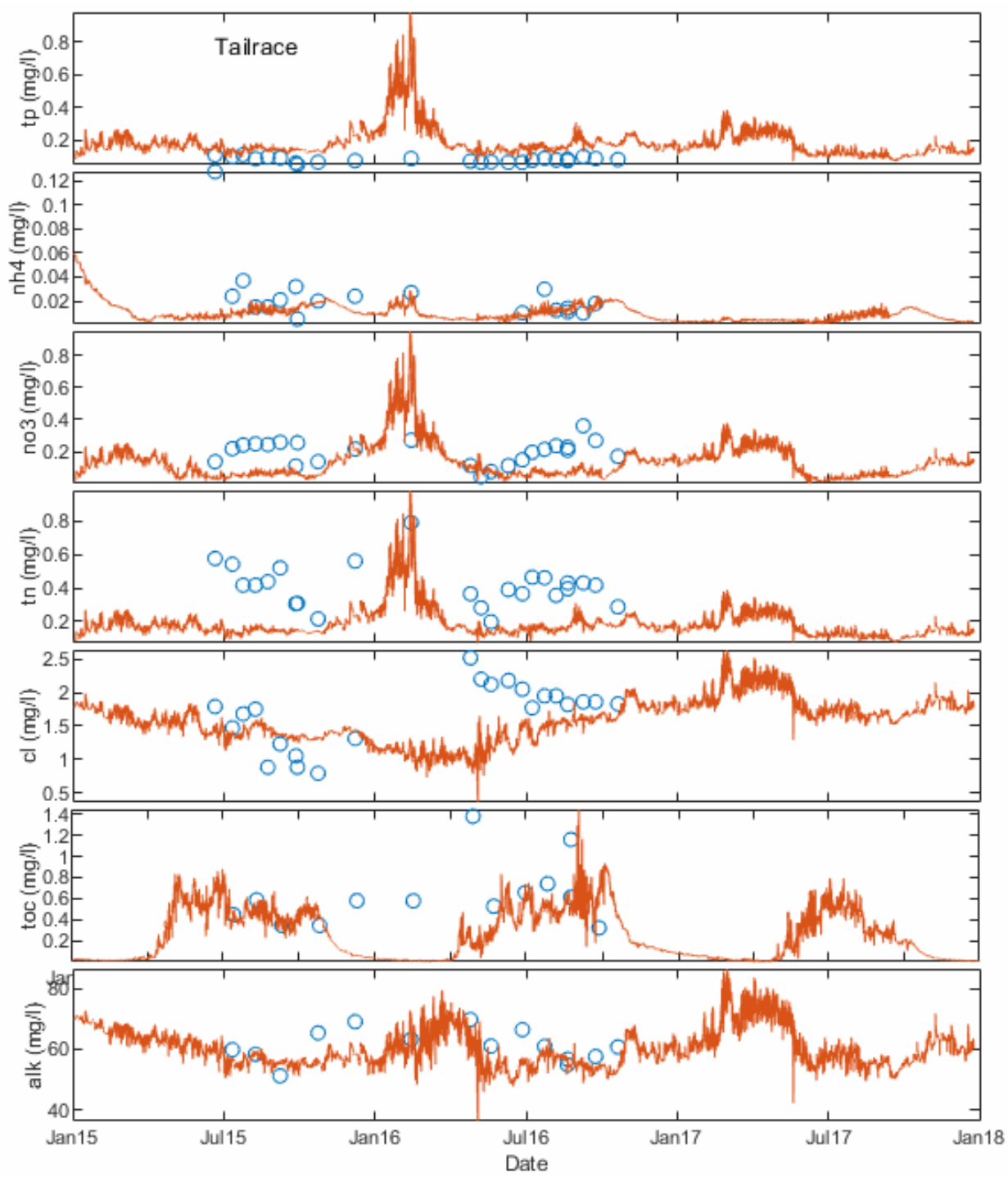

Figure 9-14. Simulated and observed nutrient dynamics in the Round Butte tailrace. Cl^- and alkalinity are included for reference.

9.6.3 Dissolved Oxygen and pH

DO and pH are useful water quality indicators because they are sensitive to biological productivity in the lake and are influenced by inflows from tributaries. Biological activity tends to dominate the signal during the warmer, active summer months.

The DO simulations depict a clear seasonal pattern, while water tends to be saturated during the winter period and to diverge during the growing season, with oversaturation in the epilimnion and undersaturation in the hypolimnion. The oversaturation is associated with algal growth and tends to spike in the late summer when cyanobacteria biovolume increases. pH follows a similar pattern (Figure 9-15 and Figure 9-16).

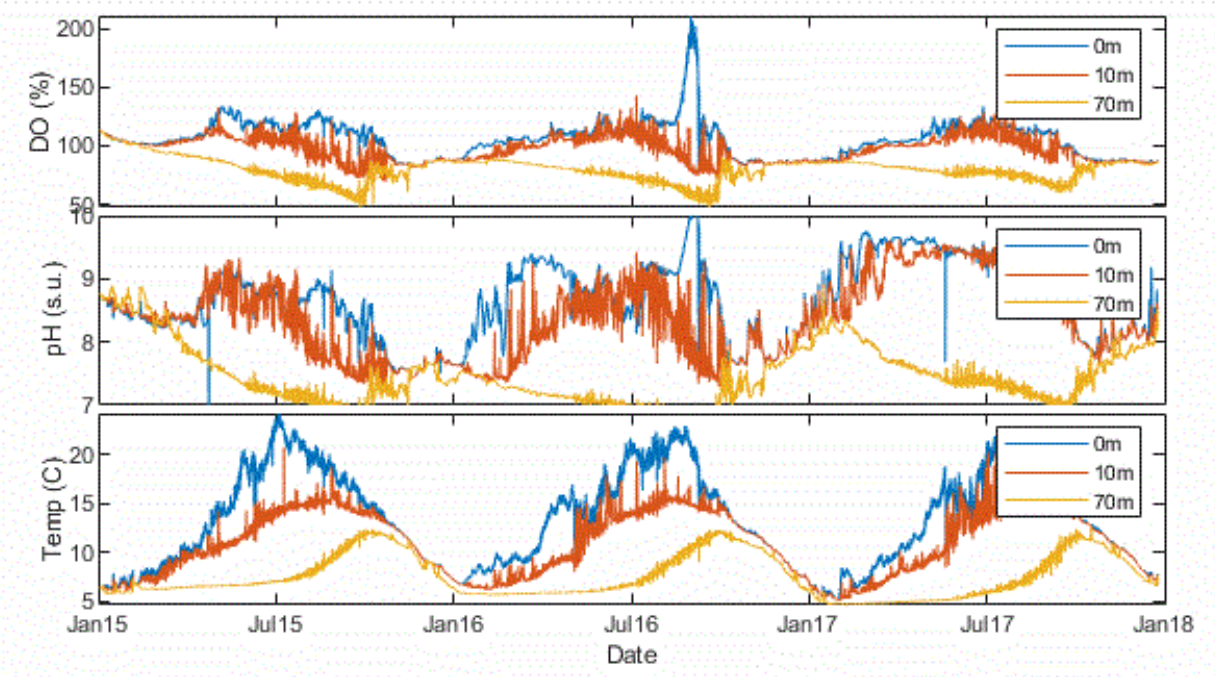

Figure 9-15. Simulated DO and pH dynamics at the Round Butte forebay (RES07). Simulated temperature is included for reference.

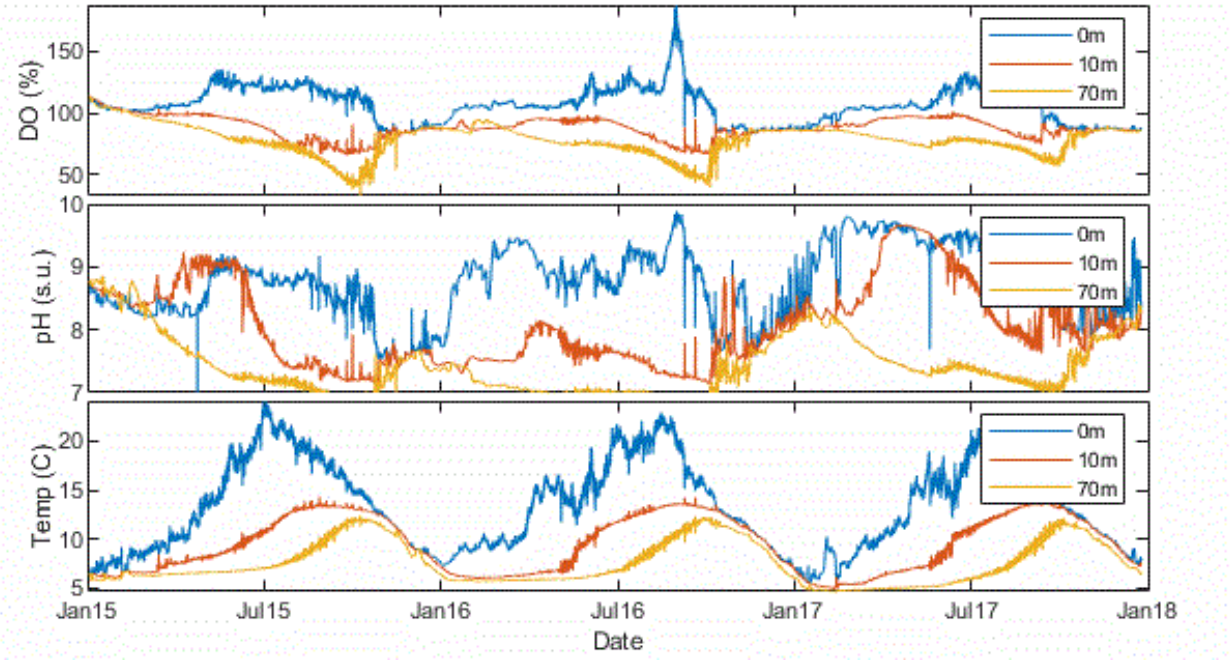

Figure 9-16. Simulated DO and pH dynamics at the Common Pool (RES08). Simulated temperature is included for reference.

Profiles of simulated and observed DO and pH are outlined in Appendix H. The model does not capture those active constituents as well as it captures water temperature or conductivity because they are influenced by a much more complex set of interactions. Nonetheless, the magnitudes and key seasonal patterns are well identified by the model. Contour maps indicate that the model successfully captures the pattern of higher values at the surface and lower values at depth during the warm period. Few measurements were collected during the winter, although the profiles indicate that, during that period, the model performs well. The pH for water in the hypolimnion is primarily influenced by the pH for the water in the tributaries. In cases in which the model and the observations diverge, it is likely that the simple estimated average values of TOC in each of the tributaries is insufficient to capture the seasonal pattern.

The model successfully captures the tailrace DO data and, while pH appears to be as much as 0.5 below the observations during some periods, the seasonal pattern of higher values in the warm period also is well captured by the model (Figure 9-17).

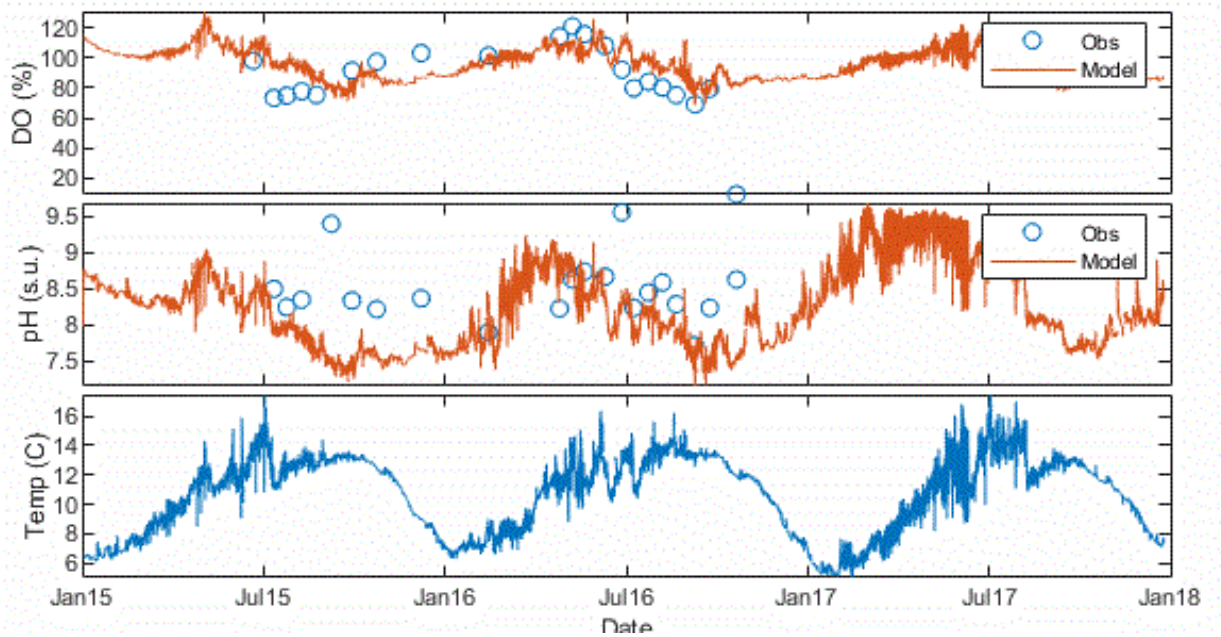

Figure 9-17. Simulated and observed pH and DO in the Round Butte tailrace. Water temperature is included for reference.

9.6.3.1 Biological components

The model is a simplification of the complex biological system in LBC, where we have tried to identify and parameterize key groups to capture the overall dynamics and responses to changing conditions. The model is comprised of two algal groups. The first group represents cyanobacteria and is parameterized to prefer warmer water and not to sink, and is simulated to have the capacity to fix N, setting the N half saturation value to 0, (as suggested by Cole and Wells 2006). The second group represents all other species, which tend to be dominated by the diatom, *Stephanodiscus*. Compared with the cyanobacteria, this group is simulated to prefer cooler water, is limited by the availability of N, and does sink. In addition, the model includes one zooplankton group.

Modeled time series capture the key features of the biological system, with production of algae and zooplankton during the warmer months. Cyanobacteria flourish in the late summer and are found primarily near the surface. Diatoms grow throughout the spring, summer, and winter and

are spread more fully through the water column (Figure 9-18 and Figure 9-19). Algae growth and the associated productivity increase DO and pH.

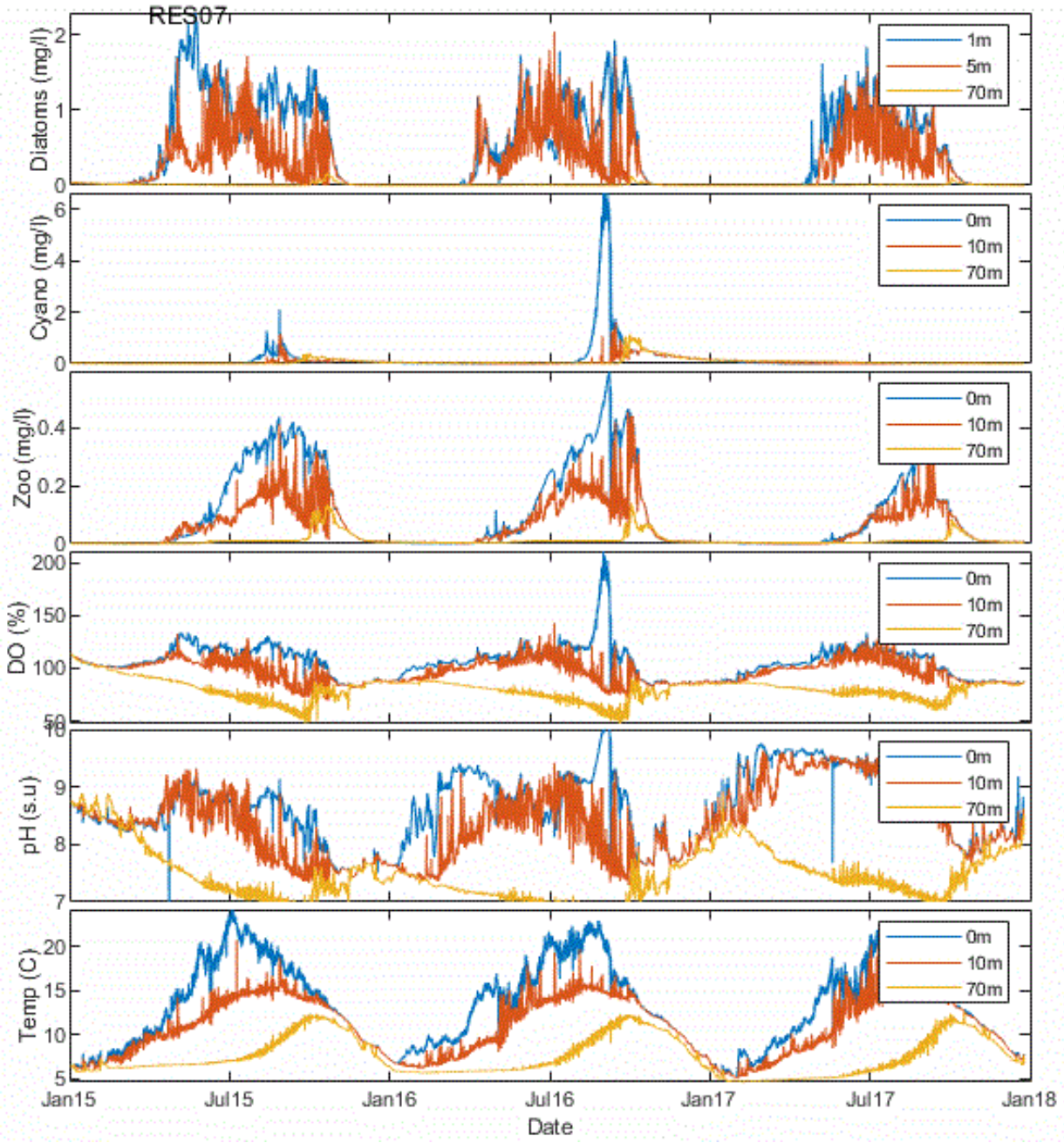

Figure 9-18. Simulated dynamics related to key biological components at Round Butte forebay (RES07).

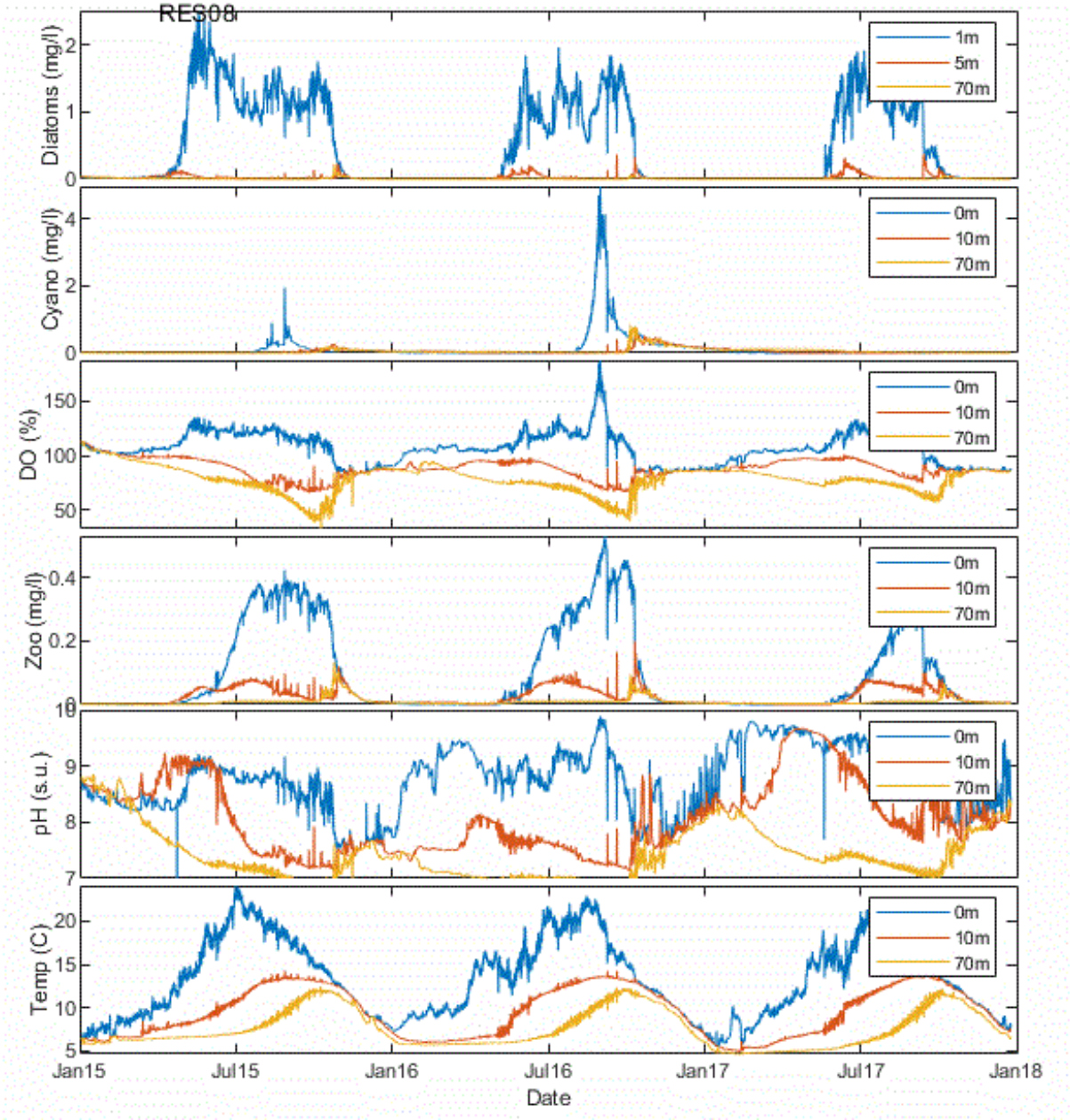

Figure 9-19. Simulated dynamics of the biological components of the system at the Common Pool (RES08).

As with other tailrace simulations, the model appears to successfully capture the biological components. This is particularly true of the seasonal pattern of growth and the relationship between biological production and elevated values of DO and pH (Figure 9-20). Algae and

zooplankton both occur in the tailrace in relatively high concentrations and are then exported to the upstream region of Lake Simtustus.

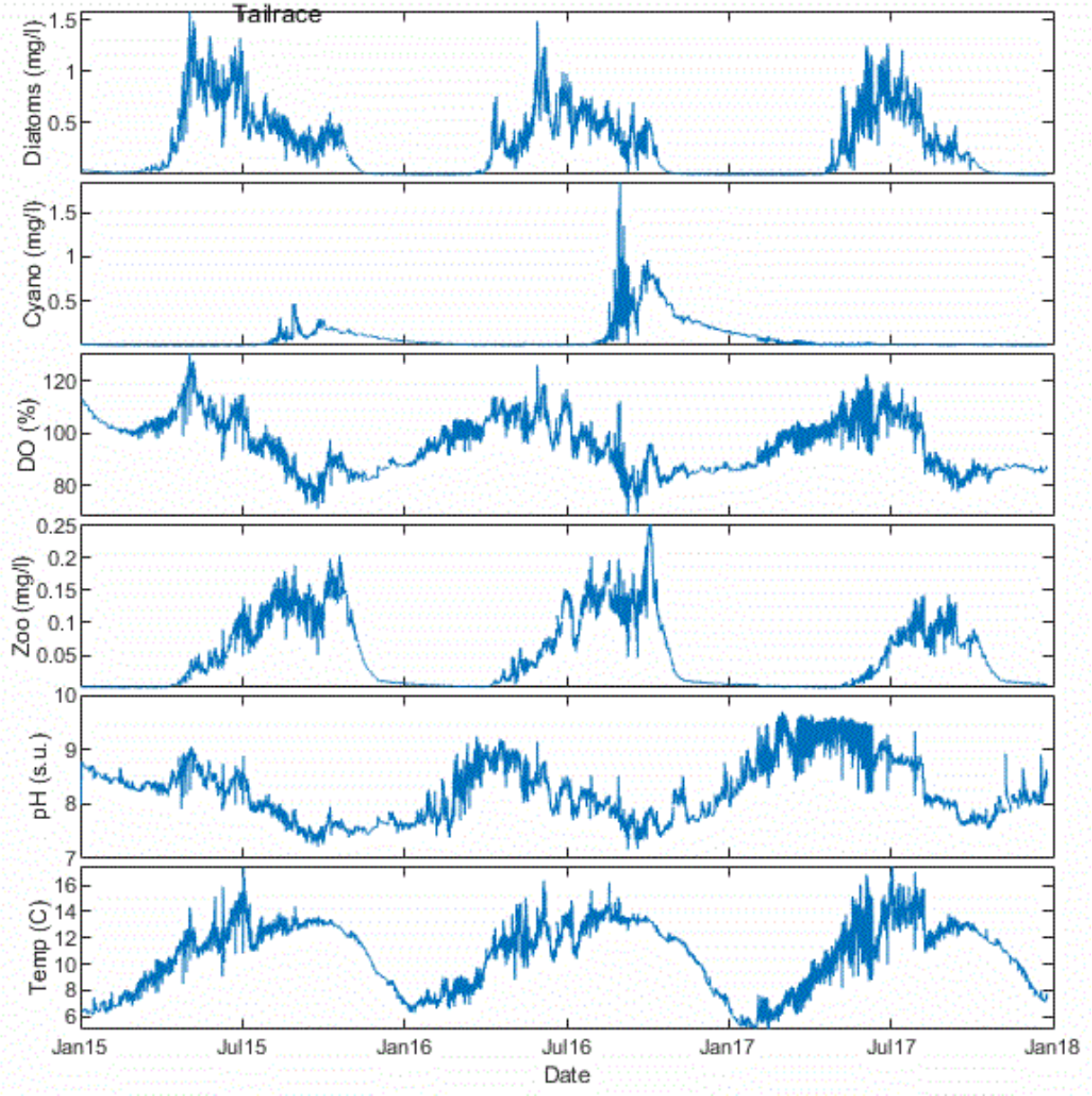

Figure 9-20. Dynamics outlining key features of the biological system in the Round Butte tailrace.

9.7 Lake Simtustus Model Development and Calibration

9.7.1 Model Setup

9.7.1.1 Input data and initial conditions

The initial ELWS for the Lake Simtustus model was taken from observations and set to 480.54 m. Initial conditions for temperature and water quality variables were set to low values that did not vary with depth. The modeler took the same conservative approach to this model as to the LBC model and for the same reason; No observed values were available for January 1, 2015. While this approach would be problematic for short-term simulations in which initial conditions would be expected to impact results for the three-year simulations in this study, the impact of estimated initial conditions will influence model results only early in the simulation.

9.7.1.2 Meteorological inputs

When possible, meteorological data collected at the Pelton weather station were used as input for the model. For those parameters or points in time when the Pelton weather station was down, data from the AgriMet mrso station were used. For cloud cover, daily average data from the Redmond Airport were used.

9.7.2 Model Calibration

9.7.2.1 Hydrology/ELWS/balance flows

As with the LBC model, the primary calibration strategy for the hydrology of the system involved using the balance utility to calculate missing flows necessary to capture the ELWSs given observed inflows and outflows. The balance flows (Figure 9-21) were added as a tributary near the bottom of the lake at segment 18 and resulted in an AME of 0.08 for daily values of simulated and observed ELWSs (Figure 9-22).

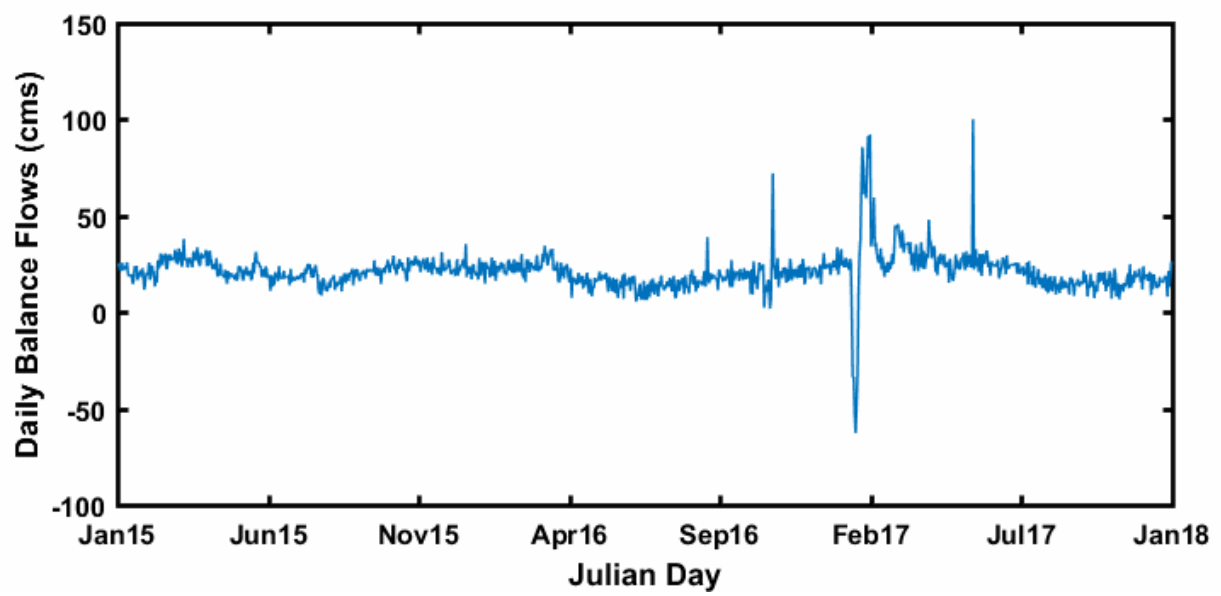

Figure 9-21. Daily balance flows for Lake Simtustus. The large spikes around February 2017 occurred because the outflow data were missing records during that period, leading to large calculated balance flows.

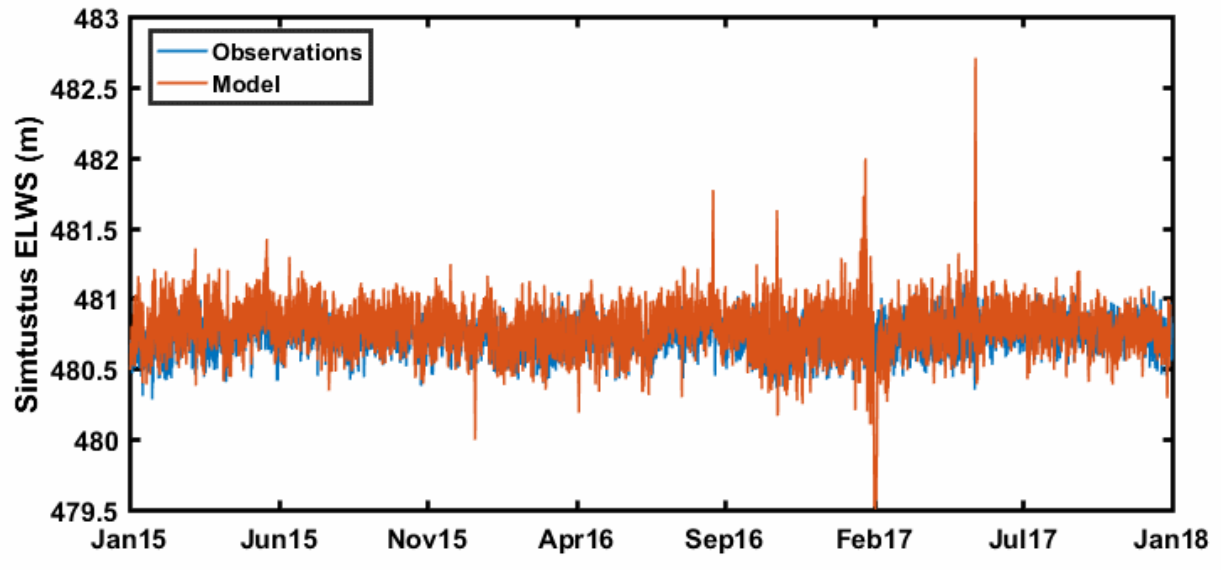

Figure 9-22. Observed and simulated hourly ELWS s for Lake Simtustus.

9.7.2.2 Water temperature

Water leaves the SWW at Round Butte Dam and enters Lake Simtustus. As previously noted, Lake Simtustus is a smaller body of water than LBC and because its volume is primarily derived from LBC, the condition of water entering from LBC impacts lake water quality substantially. Results indicate the model provides a reasonable approximation of dynamics in Lake Simtustus, successfully capturing water temperatures. This includes close agreement at a set of thermistors in the Pelton forebay (RES04) (Figure 9-23) as well as multiple profiles at Pelton forebay (RES04) (Figure 9-24 and Figure 9-25) and Mid-Lake site (RES25) (Figure 9-26 and Figure 9-27) taken throughout the simulation period of 2015–2017. Data from the Pelton tailrace temperature thermistor was not available during the first year of the simulation, but comparisons against data for the other two years are favorable, with an AME of 0.5°C (Figure 9-28). The spikes in the simulated temperature, particularly at 40 m, occur for three reasons: (1) the model samples the data as a depth below the surface and, as the surface elevation changes, sampling can move vertically between model cells(2) very large variations in flow exist, particularly at depth near the intakes; and (3) assumptions are made about balance flow temperatures that impact simulated temperature when balance flows are large. The three can combine to cause spikes in the output.

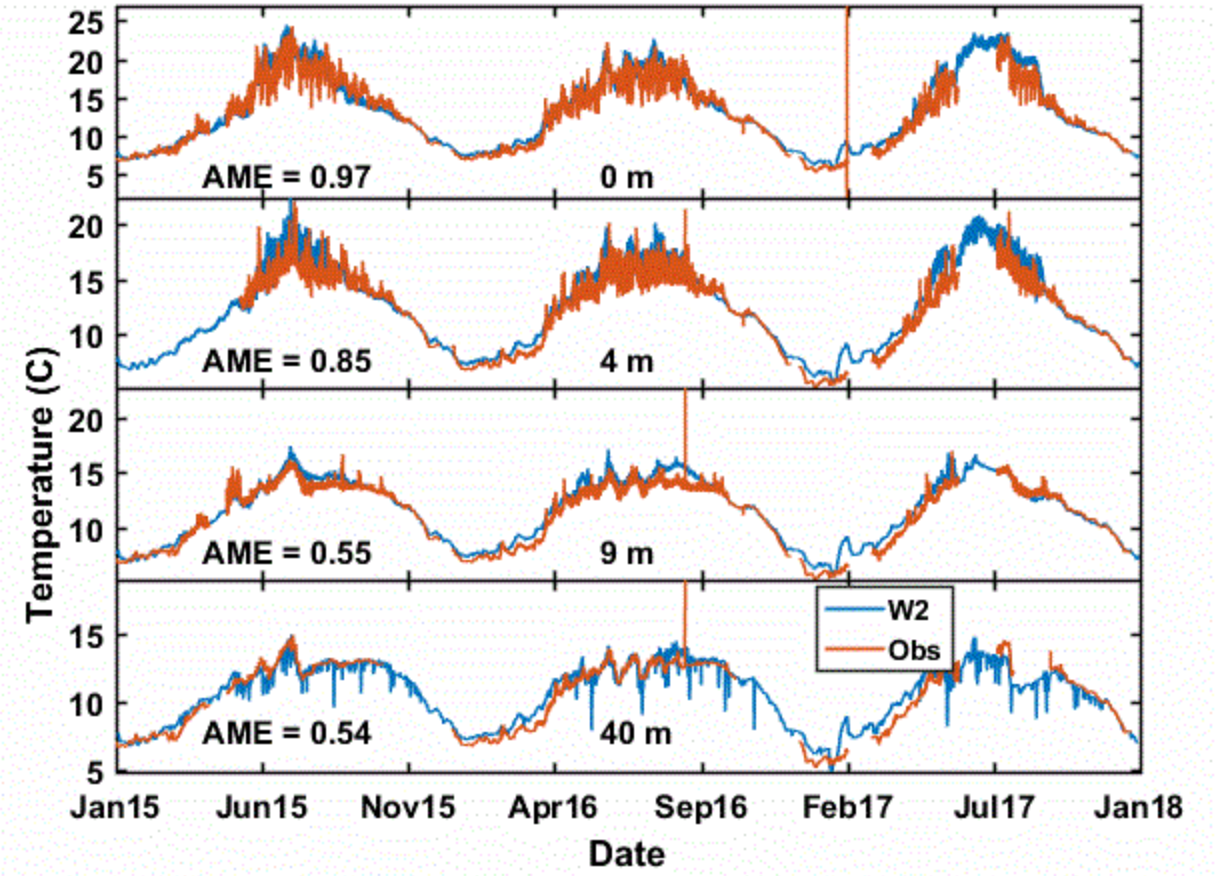

Figure 9-23. Simulated and observed temperature at Pelton forebay (RES04) at 0 m, 4 m, 9 m, and 40 m depth.

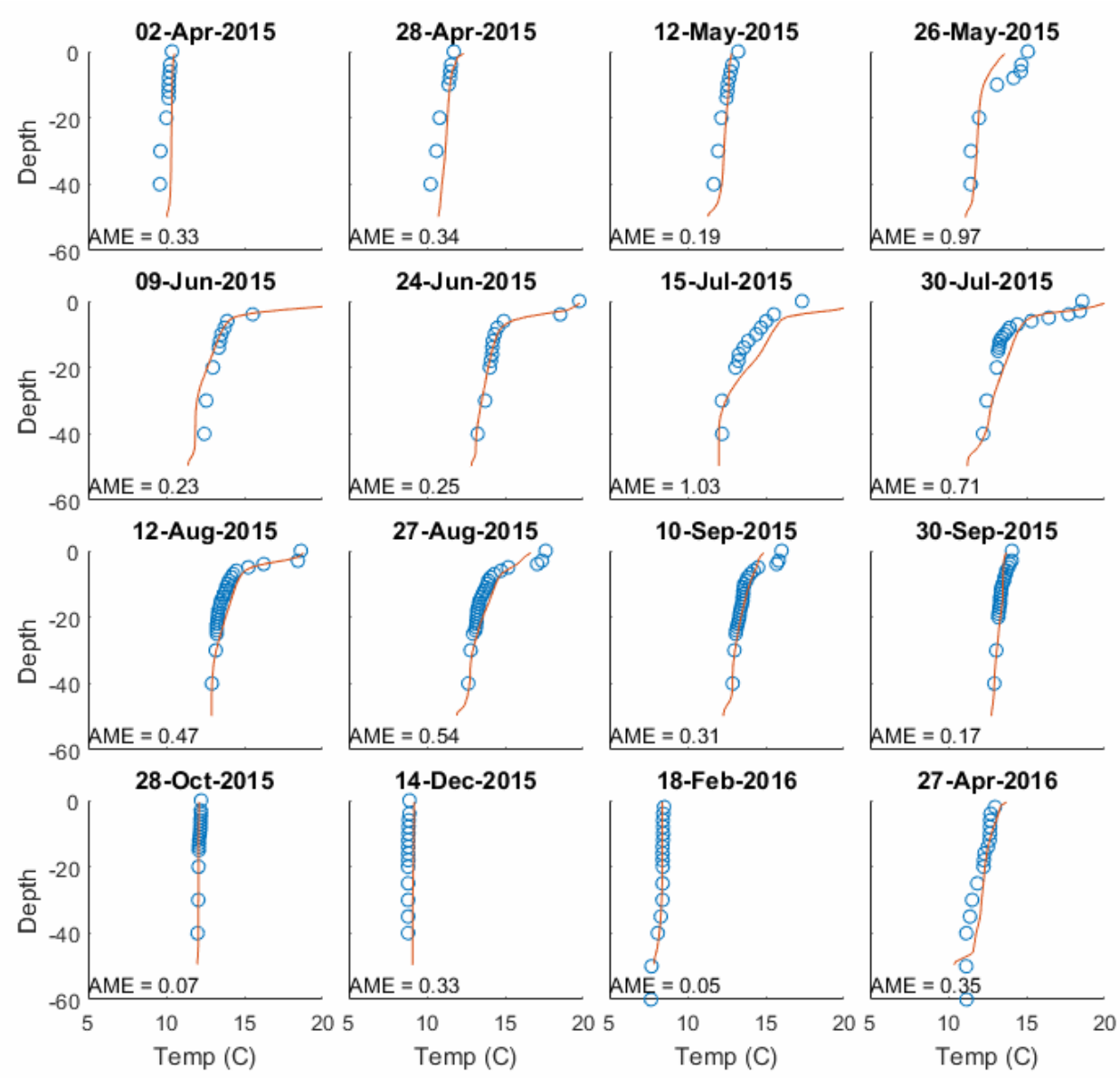

Figure 9-24. Simulated and observed water temperature profiles at the Common Pool (RES08) (April 2, 2015–April 27, 2016). The units on the y-axis are meters below the surface. The negative values are included to indicate that it is a depth below the water surface.

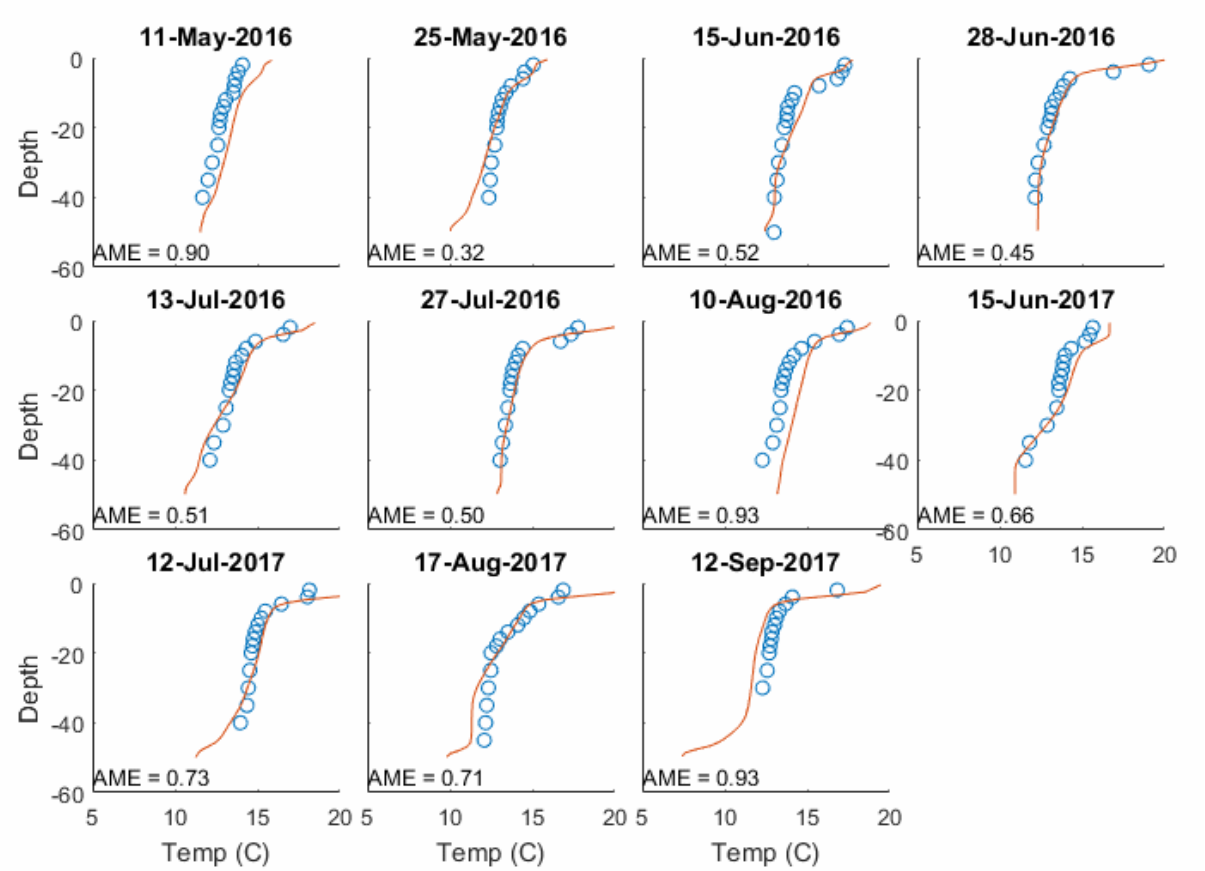

Figure 9-25. Simulated and observed water temperature profiles at the Common Pool (RES08) (May 11, 2016–September 12, 2017). The units on the y-axis are meters below the surface. The negative values are included to indicate that it is a depth below the water surface.

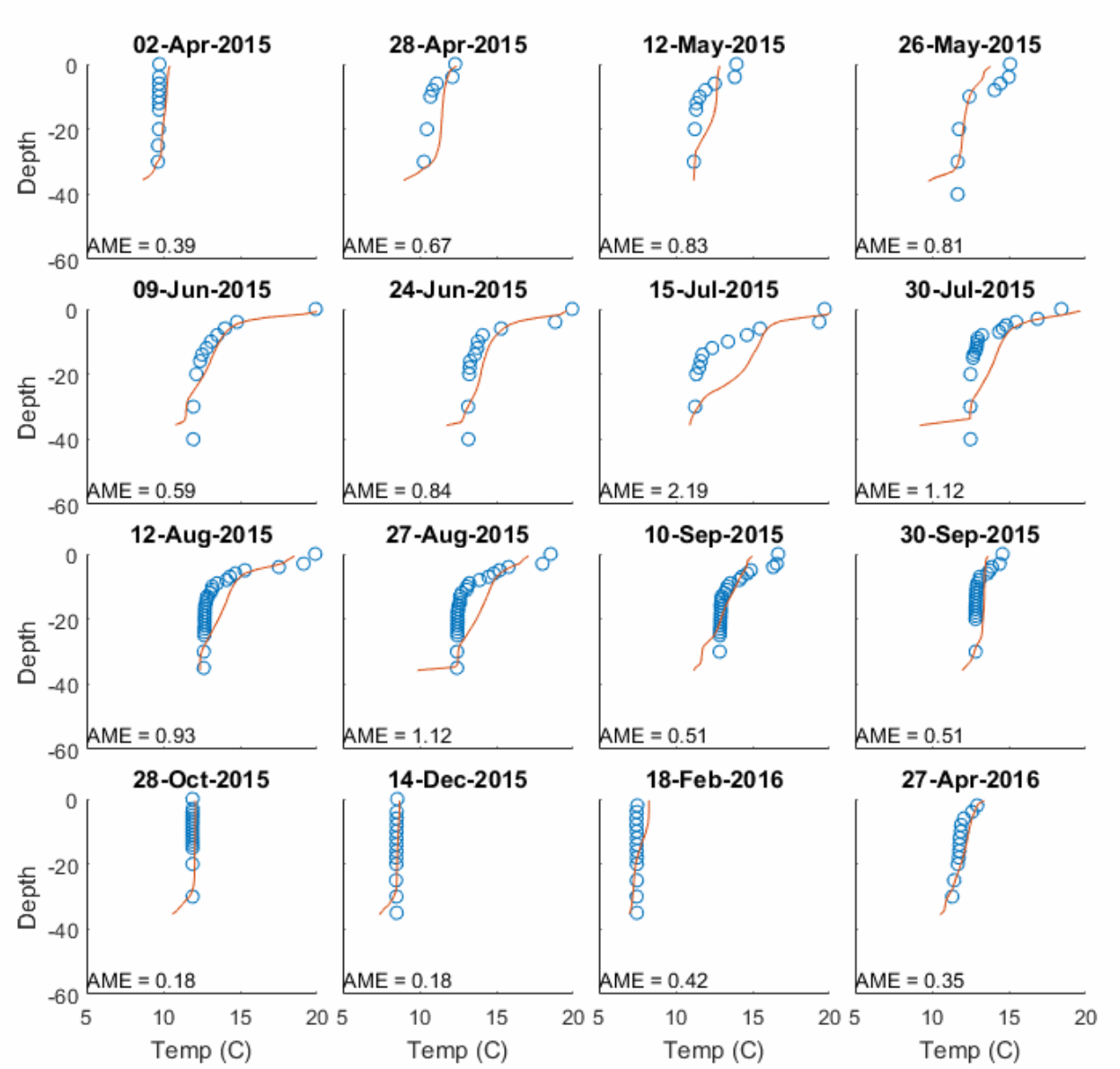

Figure 9-26. Simulated and observed water temperature profiles at the Mid-Lake site (RES25) (April 2, 2015–April 27, 2016). The units on the y-axis are meters below the surface. The negative values are included to indicate that it is a depth below the water surface.

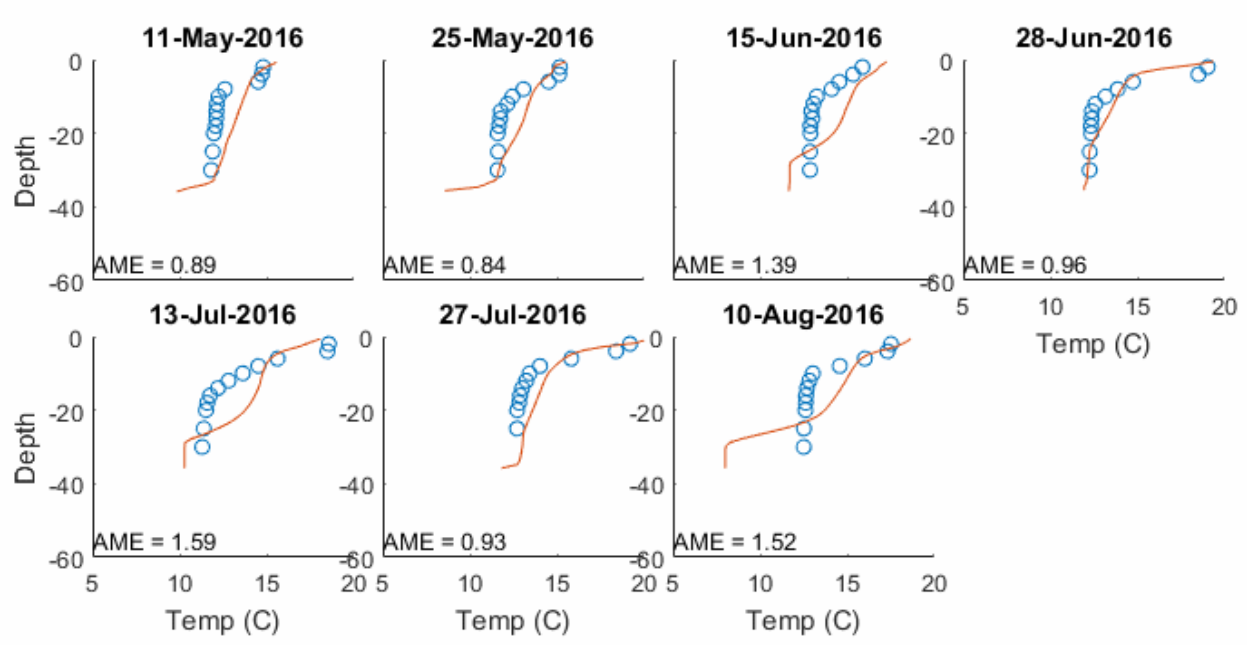

Figure 9-27. Simulated and observed water temperature profiles at the Mid-Lake site (RES25) (May 11, 2016–August 10, 2016). The units on the y-axis are meters below the surface. The negative values are included to indicate that it is a depth below the water surface.

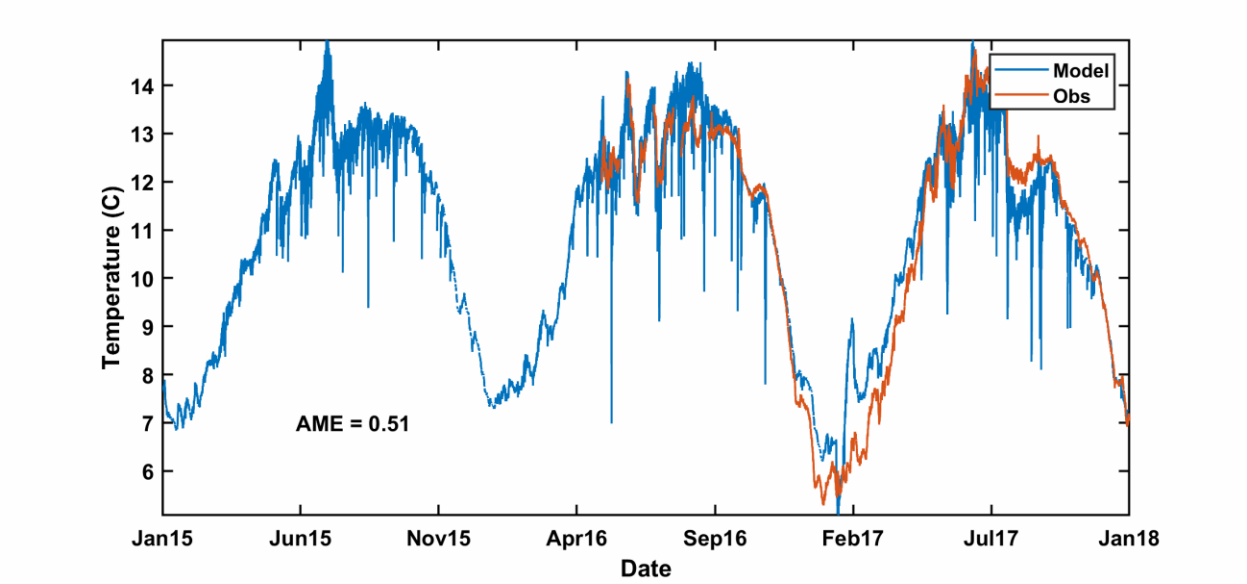

Figure 9-28. Simulated and observed water temperature profiles at the Pelton tailrace. The observed hourly discharge is included for reference. The spikes in simulated temperature occur primarily because of assumptions made about balance flow temperatures, which then impact simulated temperature when balance flows are large.

9.7.2.3 Conservative tracers

The tracers applied in the model are designed to track age and sources of water throughout the Project, not just within each reservoir. This definition of age is separate from the concept of residence time. As an example, the age of water in Lake Simtustus will always be older than in LBC because it represents an overall age of water within the PRB. Residence time is, however, much shorter in Lake Simtustus than in LBC. Similarly, the percentages of water from the three primary tributaries entering Lake Simtustus are equivalent to those leaving LBC. Age shows a peak of around 110 days in the late summer period, just prior to turnover in both LBC and Lake Simtustus (Figure 9-29).

It is a response to the stratification itself and is impacted by the operation of the SWW, which tends to result in older hypolimnetic water in LBC as it draws a majority of water from the surface. The tributary sources of water in Lake Simtustus respond similarly to the pattern of stratification and SWW operation, with an increase in Metolius River water as stratification develops in LBC, modulated by the operation of the gates on the SWW structure. The warmer water from the Deschutes and Crooked arms increases when the SWW is drawing primarily surface water and LBC is stratified.

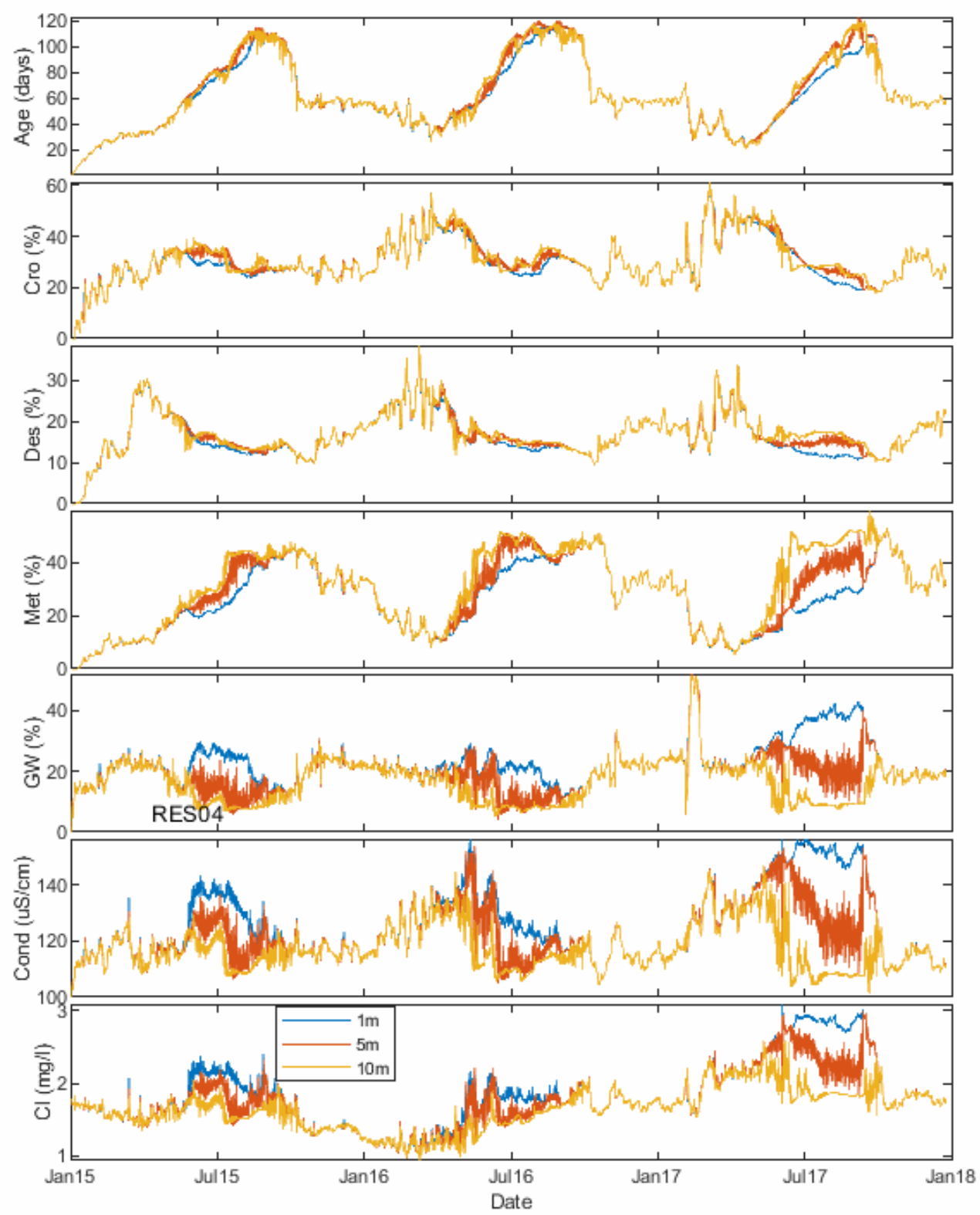

Figure 9-29. Simulated values at Pelton forebay (RES04).

Profiles of the overall project age of water in Lake Simtustus, as well as percentages of water from different sources, are outlined in Appendix H. This subset of profiles is useful for more fully evaluating the time series at different depths that are captured in Figure 9-30. Conductivity was not measured at the Mid-Lake site (RES25). The results suggest that the model captures conductivity well, indicating that interpretation of other conservative tracers—in particular, the percentages of water from the tributaries—are also well captured. Time series for each parameter at the Pelton tailrace are included in Figure 9-31. A set of observed conductivity values was collected in the tailrace.

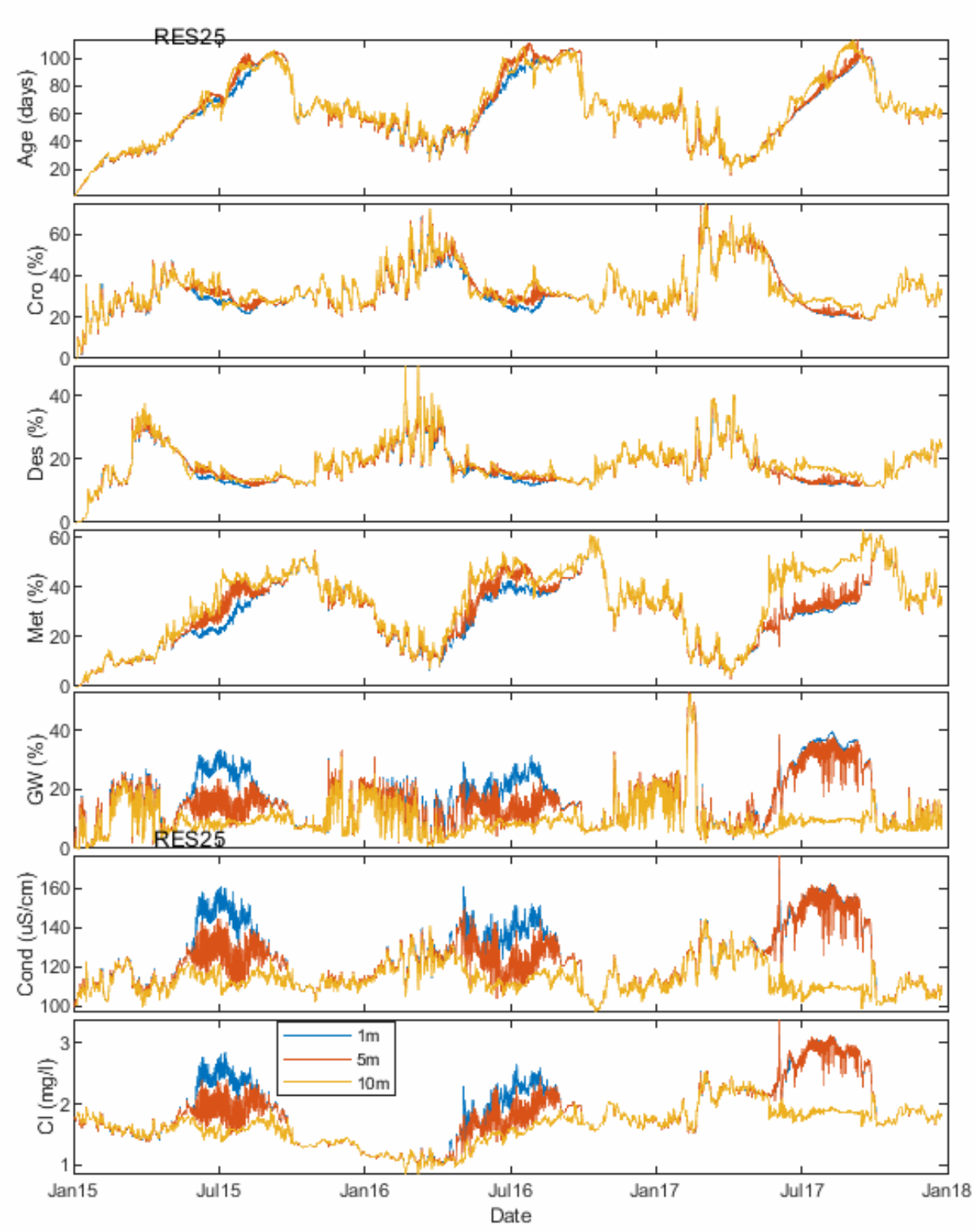

Figure 9-30. Simulated values at the Mid-Lake site (RES25).

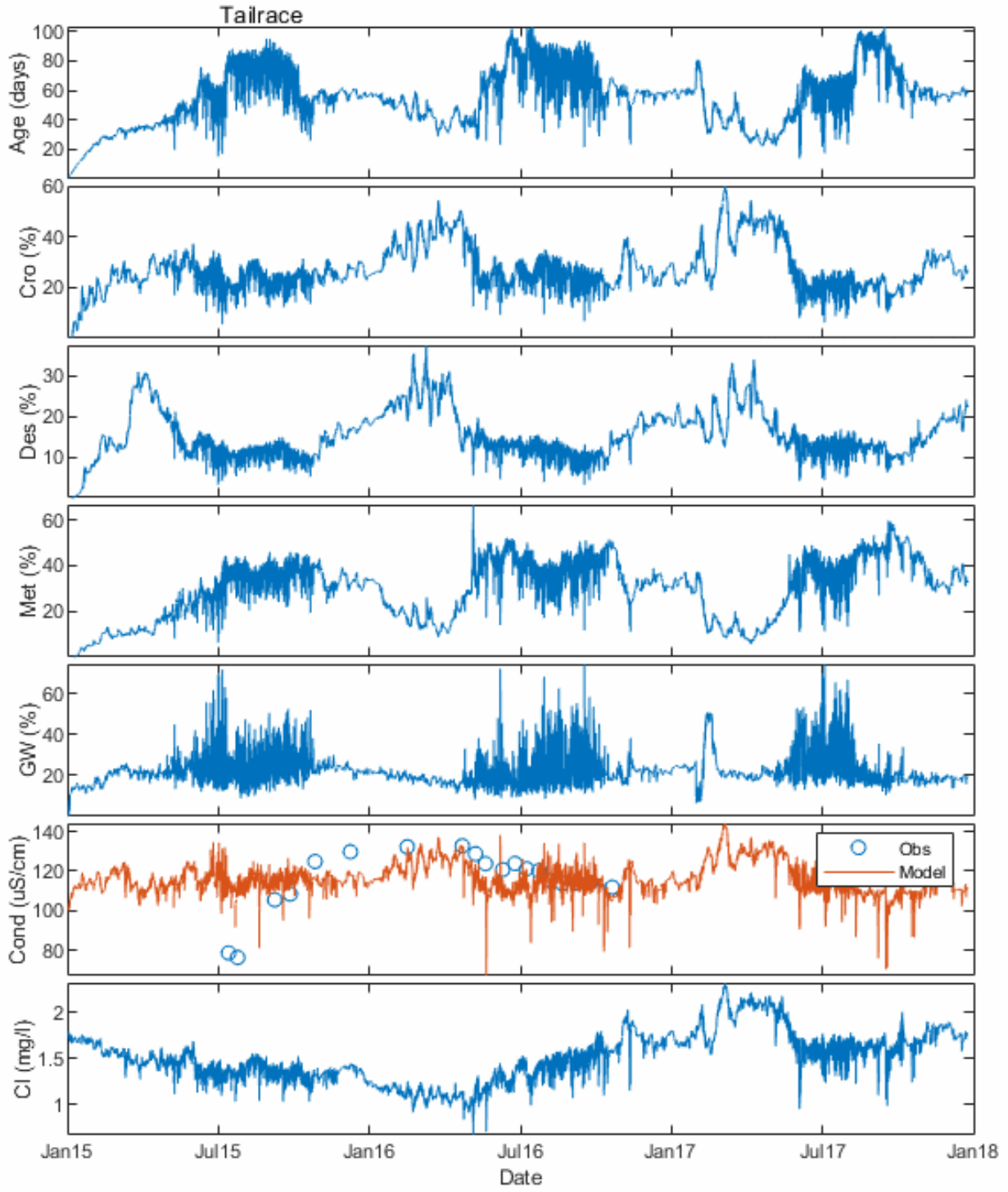

Figure 9-31. Simulated values at the Pelton tailrace. The spikes associated with groundwater (GW) occur because of variation in the balance flows.

9.7.2.4 Nutrients

Simulation of key nutrients in Lake Simtustus indicates a good fit with the available observations taken at the Pelton forebay (RES04) and Mid-Lake site (RES25). NO_3, ammonium, TOC, and TN show distinct peaks during the cooler, low-productivity periods, with higher peaks in the surface waters. A very large peak in nutrients was simulated to occur during the summer of 2017. The simulated peak occurs because the model overestimated a cyanobacteria bloom for that period (Figure 9-32 and Figure 9-33). The cyanobacteria can fix nitrogen and, in doing so, can contribute to the anomalously large simulated nutrient values. It is likely that the model produces this bloom because simulated surface water temperatures stayed high enough during the summer of 2017 to favor cyanobacteria growth. The fact that this bloom is not present in the observations is another indication of the limits of water quality models, particularly when applied to complex systems over long periods of time. In this case, a relatively minor modification to the temperature-dependent model governing cyanobacteria growth might have produced a smaller modeled bloom. That type of change, however, might have had different consequences in other elements of the model. While additional parameterization might improve the surface water N/algae components for modeling the summer of 2017, the increases in nutrients are predominately limited to the Lake Simtustus surface water and not exported downstream. Given that fact and the overall uncertainties associated with the modeling effort, we elected to leave them in the analysis.

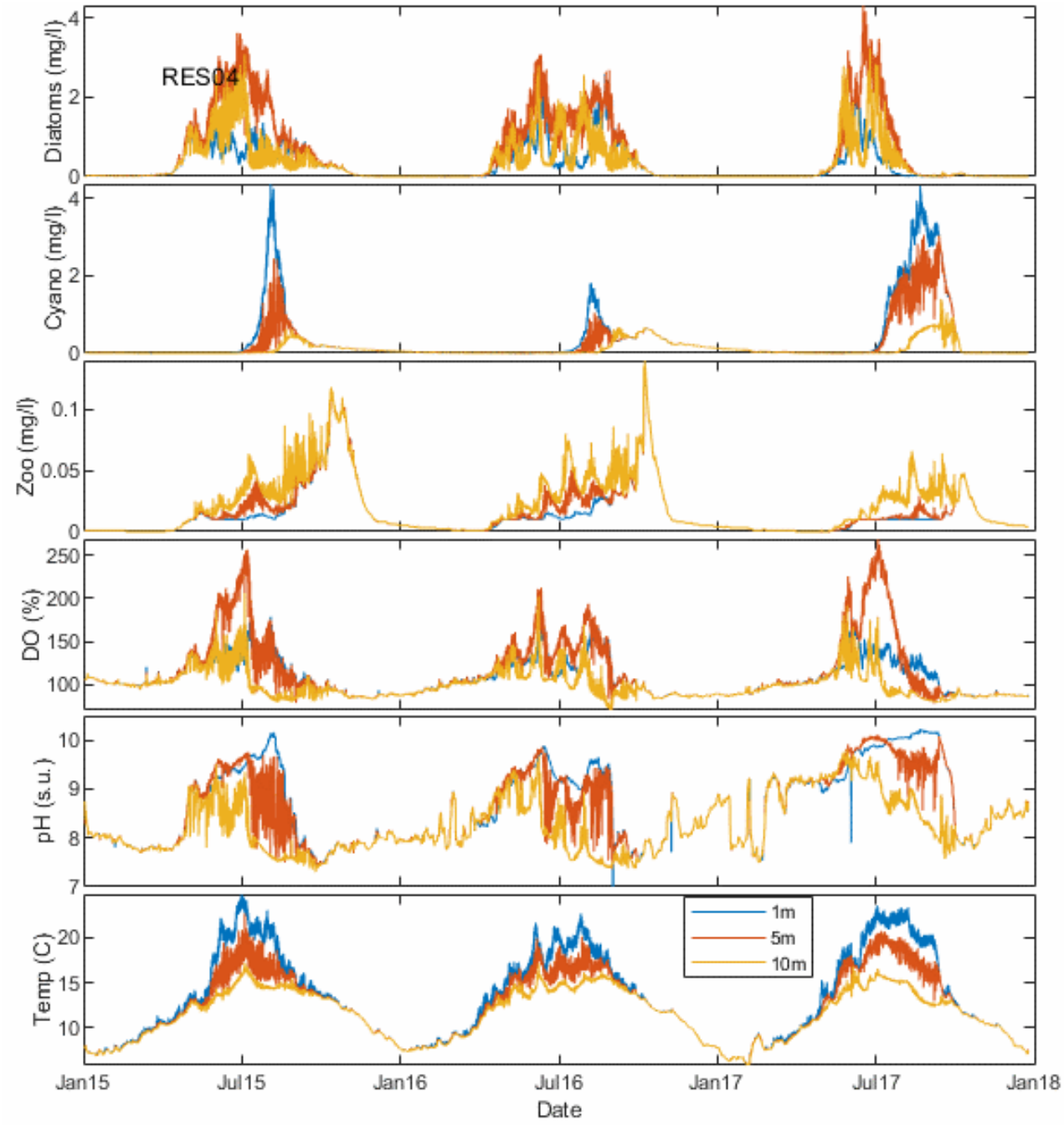

Figure 9-32. Simulated dynamics related to key biological components at Pelton forebay (RES04).

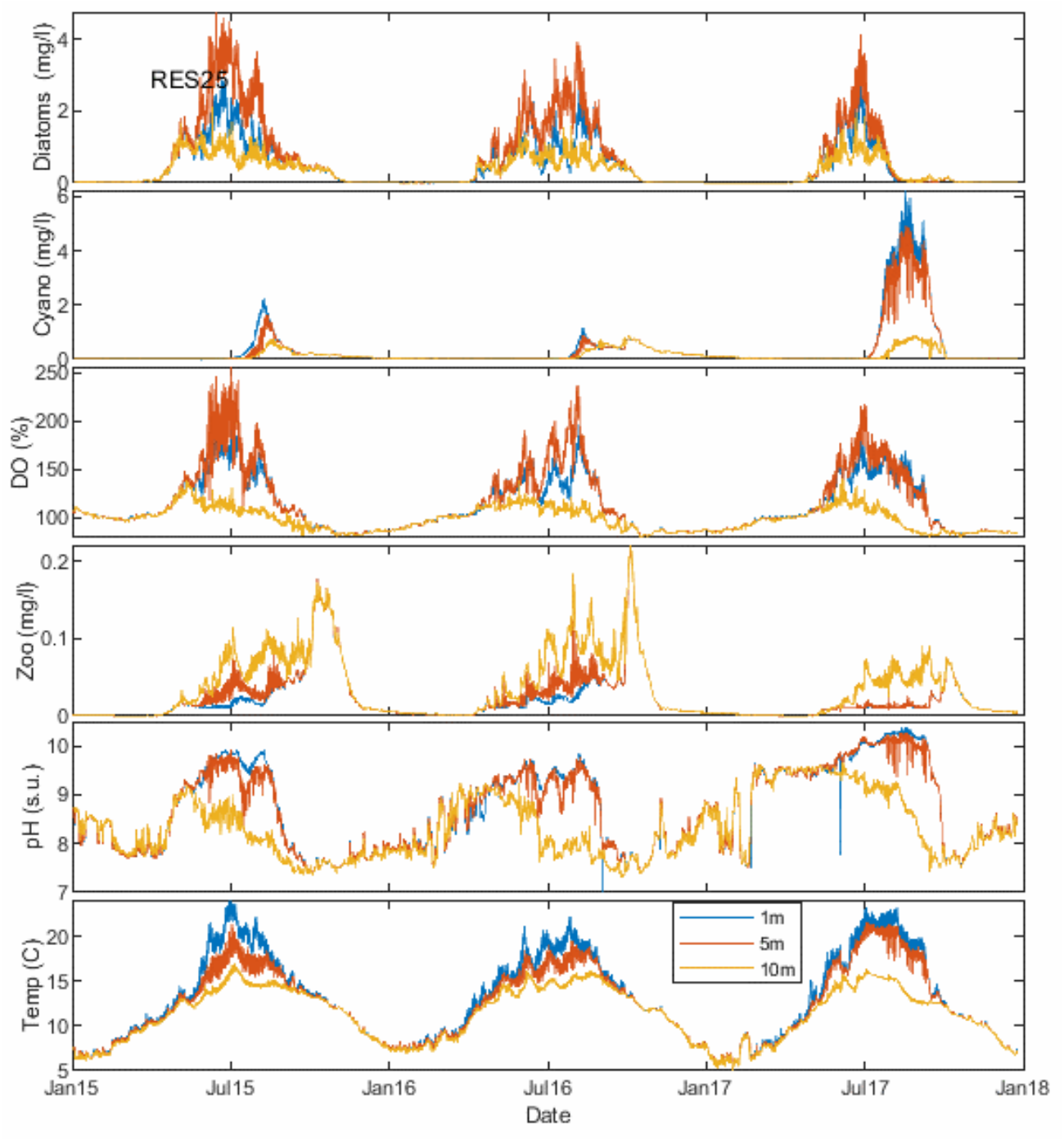

Figure 9-33. Simulated dynamics related to key biological components at Mid-Lake site (RES25).

TP shows a smaller seasonal change, likely because it is readily abundant because of the high concentrations in the tributaries and groundwater and does not tend to limit biological production (Figure 9-34 and Figure 9-35). Profiles of NO_3, ammonium, and PO4 are provided for a subset of times in Appendix H. Those profiles provide additional insight into the role of biological productivity, in which surface values tend to be depleted during the productive summer period. This pattern is modulated by mixing within the reservoir and some degree of photoinhibition, which can reduce algal growth at the surface during particularly warm periods of time. Tailrace time series are presented in Figure 9-36 and suggest that the model provides a close approximation of the nutrient contributions from Lake Simtustus to the ReReg Reservoir and that the overprediction of N is primarily limited to the surface water. The overprediction in the surface water does, however, lead to the highest TP and N values in the tailrace over the simulated 3-year period.

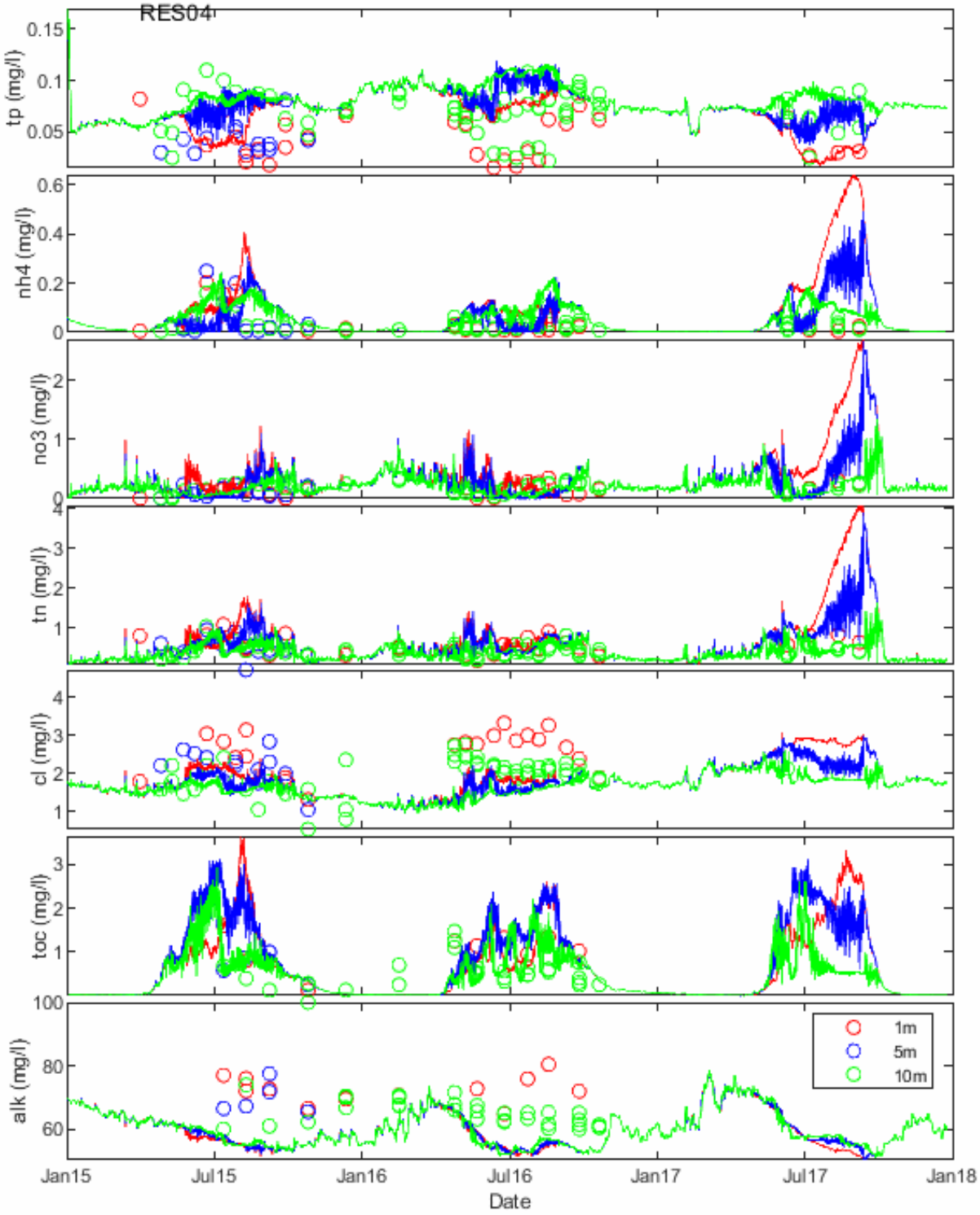

Figure 9-34. Simulated and observed nutrient dynamics at Pelton forebay (RES04). Cl^- and alkalinity are included for reference.

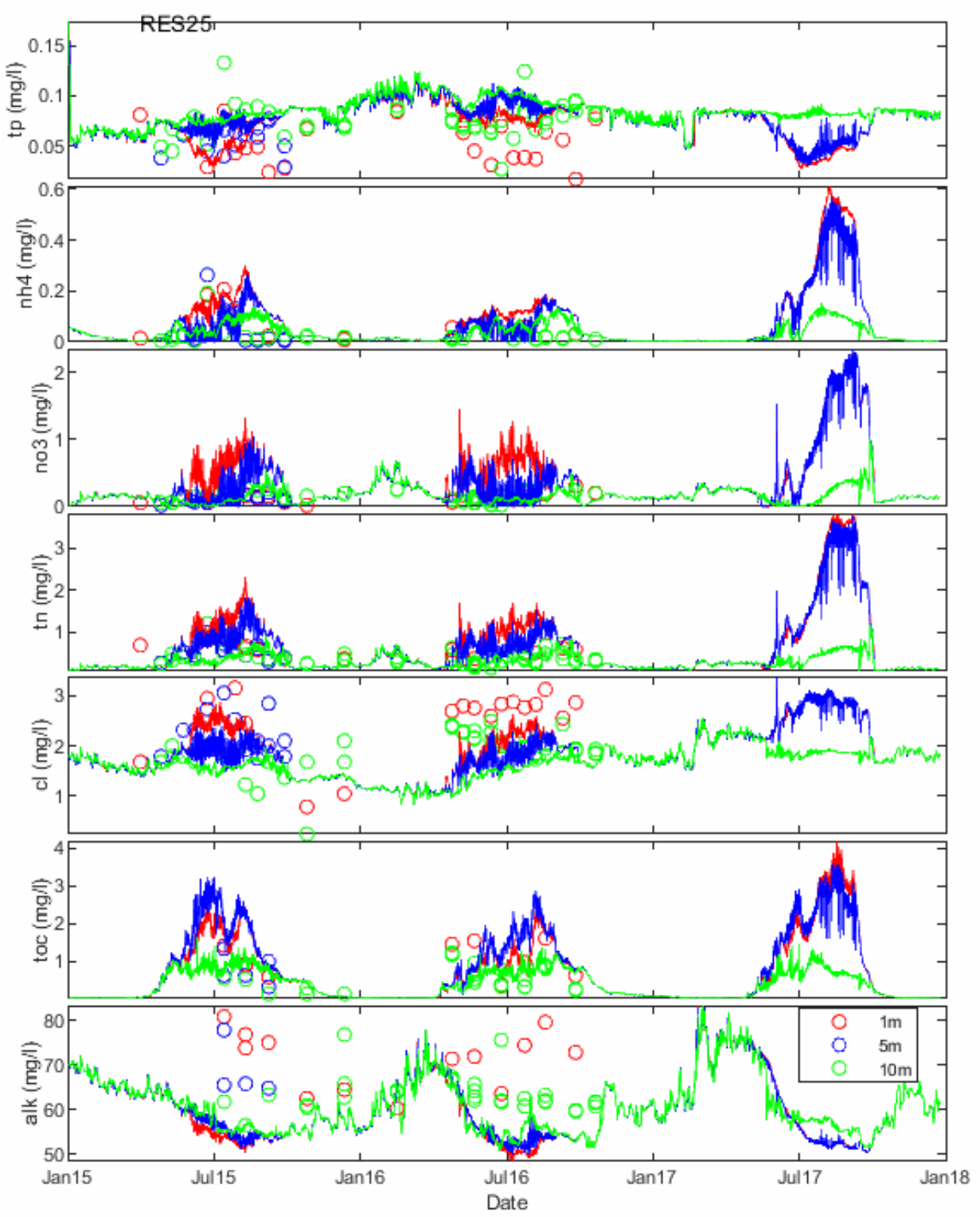

Figure 9-35. Simulated and observed nutrient dynamics at the Mid-Lake site (RES25). Cl^- and alkalinity are included for reference.

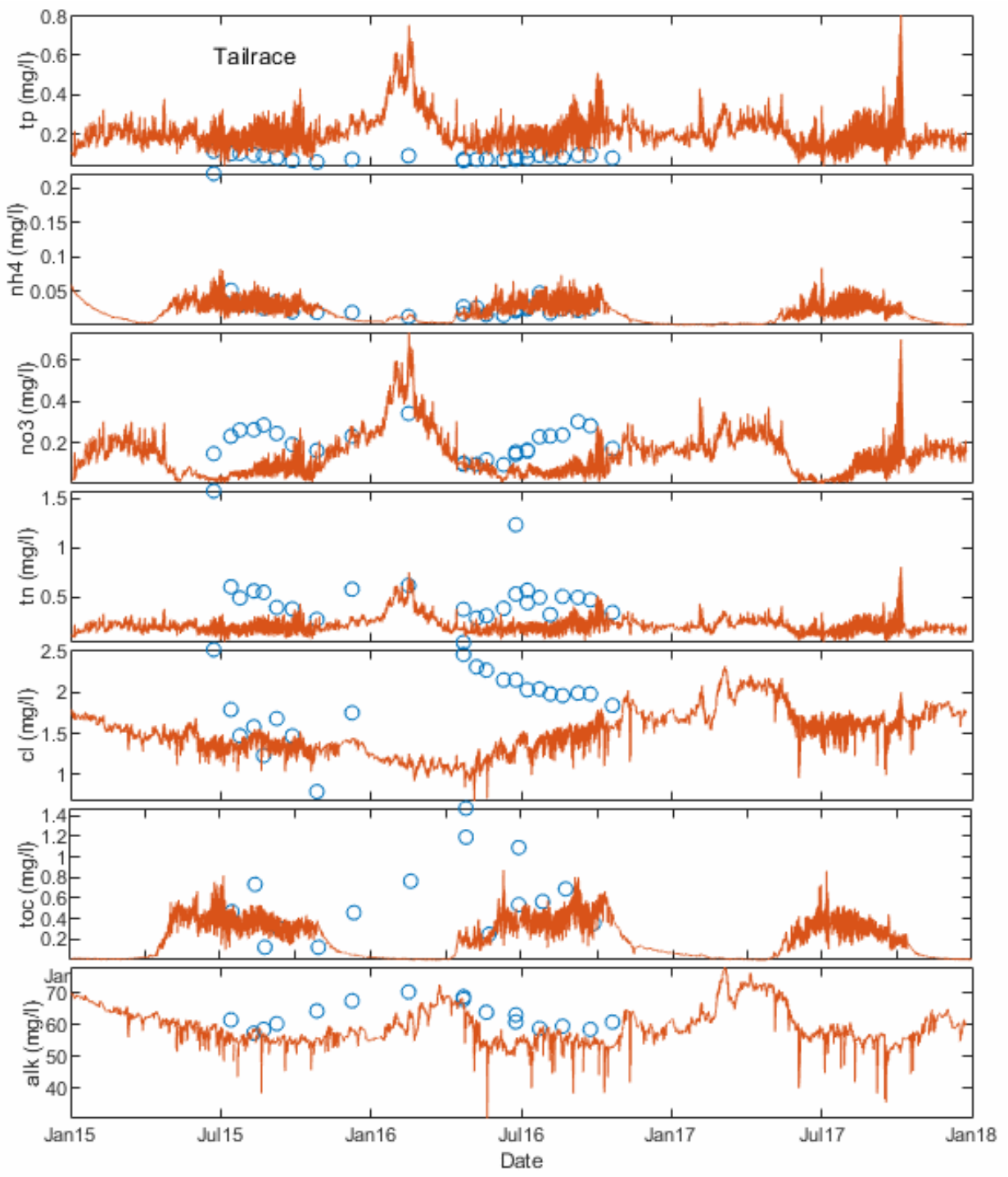

Figure 9-36. Simulated and observed nutrient dynamics in the Pelton tailrace. Cl^- and alkalinity are included for reference.

9.7.2.5 Dissolved Oxygen and pH

pH and DO in Lake Simtustus follow a familiar pattern, with summertime primary production elevating the levels of both during the warm summer months (Figure 9-37 and Figure 9-38). The reservoir stratifies during the summer, with much of the water entering from LBC remaining at the bottom of the reservoir as it moves toward the bottom gate at Pelton Dam, leading to pH values at depth that more closely resemble those in the Round Butte tailrace.

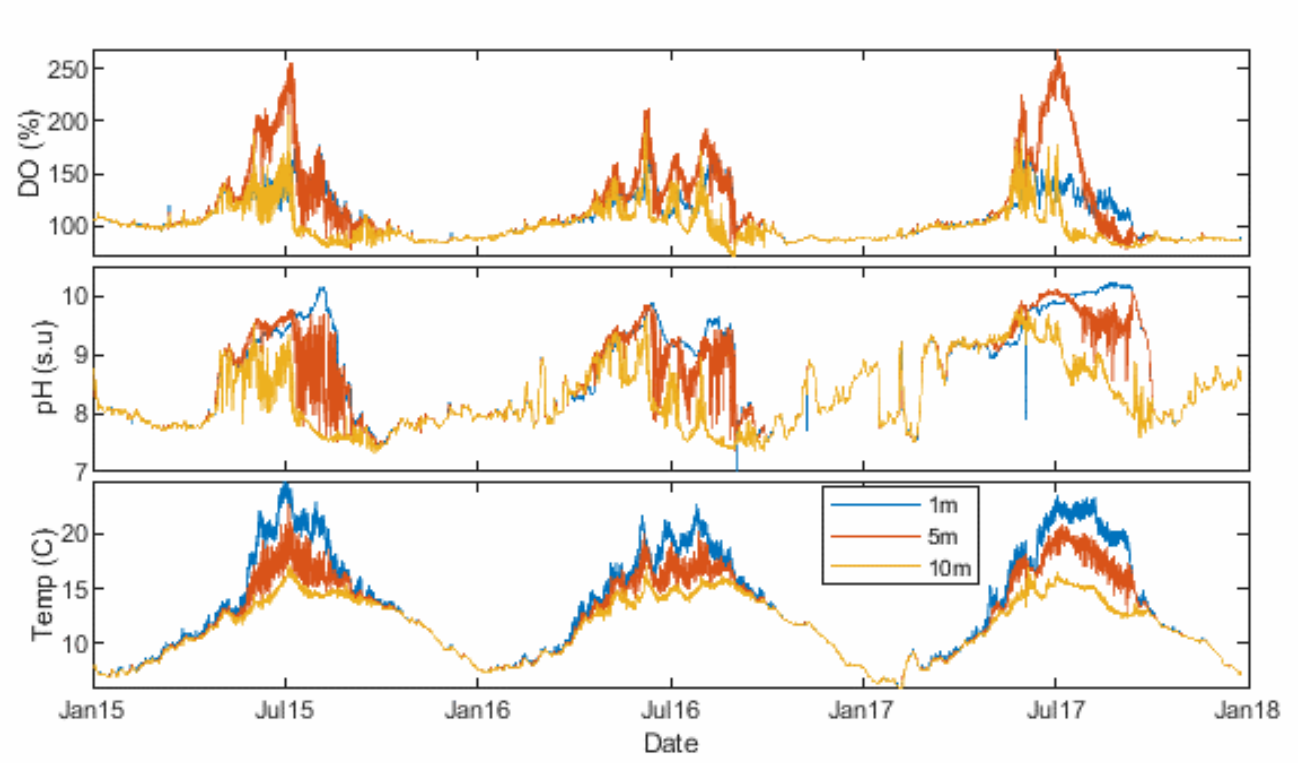

Figure 9-37. Simulated DO and pH dynamics at Pelton forebay (RES04). Simulated temperature is included for reference.

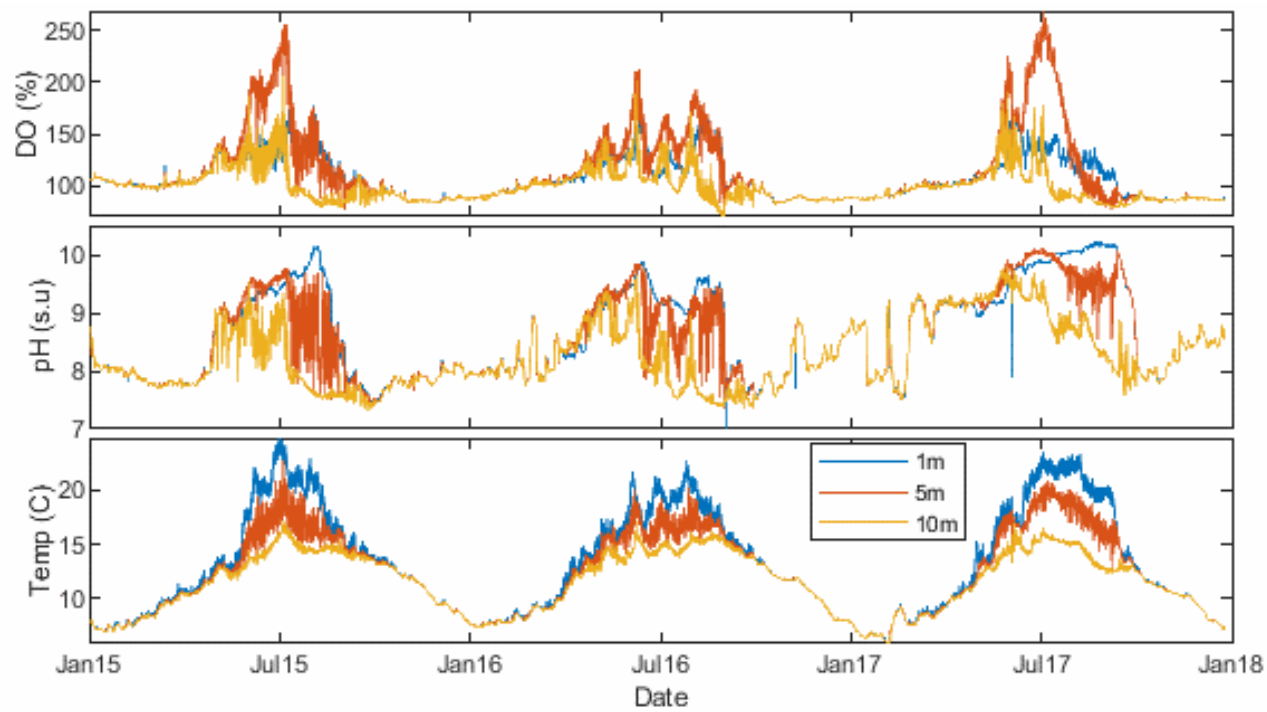

Figure 9-38. Simulated DO and pH dynamics at the Mid-Lake site (RES25). Simulated temperature is included for reference.

The comparative contour plots of measured and modeled results outlining DO and pH dynamics provide additional visual evidence that the model captures key features of the system through time, in particular the summer increases in DO and pH (Appendix H). The individual profiles of DO and pH are also included to more fully outline changes in depth at specific points in time.

The Pelton tailrace data indicate an acceptable relationship between measured and modeled DO and pH (Figure 9-39). The unmeasured flows are an average of approximately 25 cms in Lake Simtustus, and the assumed concentrations of TIC and alkalinity in unmeasured flows influence pH, particularly in the tailrace, because they are added to the bottom of the reservoir and so are more directly connected to the outlet structure (Figure 9-21). The unknown values of TIC and alkalinity in the unmeasured flows were adjusted based on these observations.

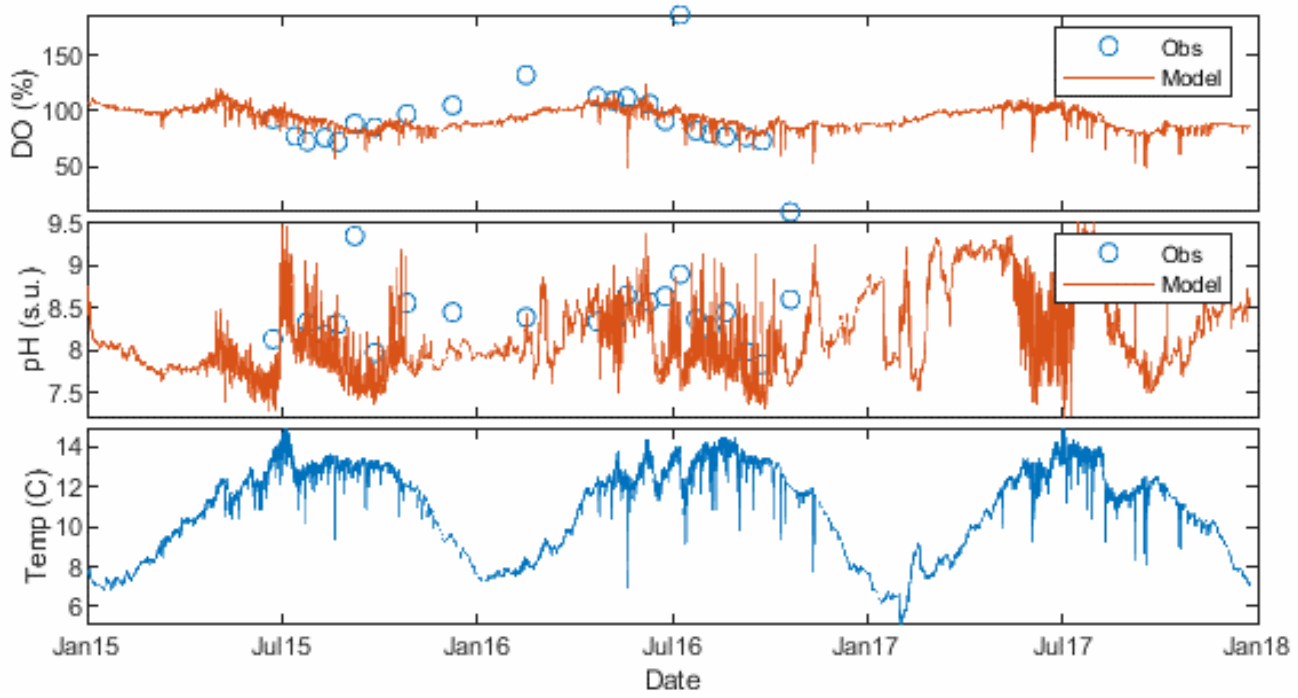

Figure 9-39. Simulated and observed pH and DO in the Pelton tailrace. Water temperature is included for reference.

9.7.2.6 Biological components

The simulated biological activity in Lake Simtustus follows a pattern similar to the pattern in LBC, with both algal groups and zooplankton increasing during the warmer seasons. Figure 9-32 and Figure 9-33 outline those dynamics at Pelton forebay (RES04) and the Mid-Lake site (RES25). Note that diatoms appear during the summer, gradually giving way to cyanobacteria, both followed by zooplankton, increasing along with their primary food source. Also note the large peaks in cyanobacteria during the summer of 2017. The large peaks are not borne out by the data but, as discussed in Section 9.7.2.4, were left in the model and are used to provide a wider range of inputs into the scenario analysis.

Appendix H provides a subset of the available profiles. Those profiles outline the progression of the algae and zooplankton over time and with depth. The primary patterns are the increase in each during the warmer period, primarily in the warmer water near the surface. Zooplankton show an increase in the mid-depths, primarily because they are inhibited by the very warm surface water and can feed on detritus, which follows the biological production and slowly sinks

through the water column, particularly during the late summer and fall, after significant blooms. As noted earlier, a large concentration of both algae and zooplankton are exported from LBC into Lake Simtustus. A portion of these are entrained in water that moves through the lake's hypolimnion in response to the bottom release at Pelton Dam. These additions contribute to the elevated concentrations of algae and zooplankton in the deeper waters of Lake Simtustus (Figure 9-32 and Figure 9-33) as well as in the Pelton tailrace (Figure 9-40). The tailrace data for the biological components at Pelton Dam are also outlined.

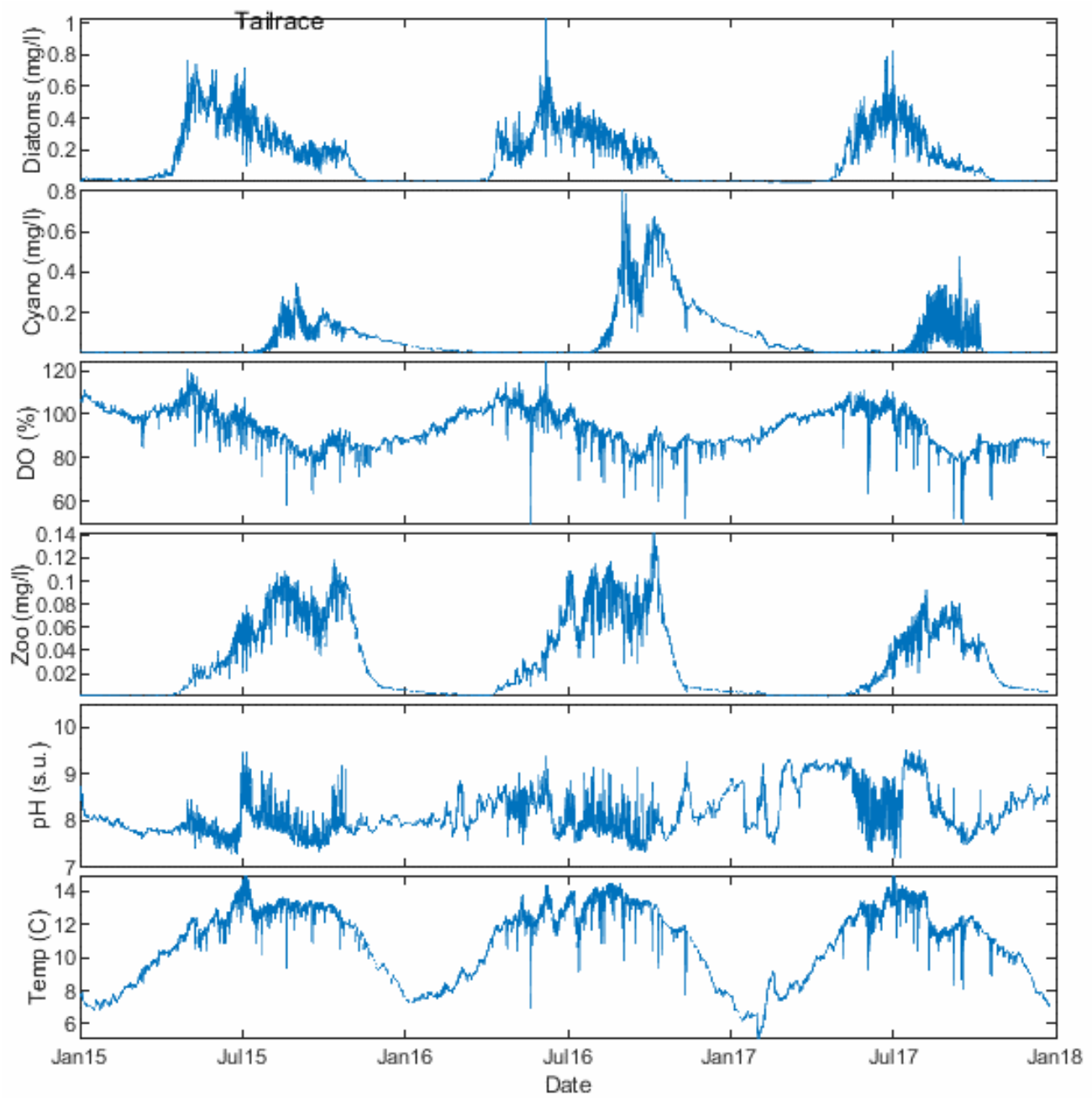

Figure 9-40. Simulated biological components in the Pelton tailrace. Temperature and pH are included for reference.

9.8 ReReg Reservoir Model Development and Calibration

9.8.1 Model Setup

9.8.1.1 Input data and initial conditions

The initial ELWS for the ReReg Reservoir model was taken from observations and set to 434.06m. As with the models for the other reservoirs, initial conditions for temperature and water quality variables were set to low values that did not vary with depth.

9.8.1.2 Meteorological inputs

When possible, meteorological data collected at the Pelton weather station were used as input for the model. For those parameters or points in time when the Pelton weather station was down, data from the AgriMet mrso station were used and, for cloud cover, daily average data from the Redmond Airport were used. This dataset was also used to drive the Lake Simtustus model.

9.8.2 Model Calibration

9.8.2.1 Hydrology/ELWS/balance flows

The process for developing the hydrology calibration at the ReReg Reservoir was similar to the one outlined by Xu and Khangaonkar (2015), as well as the process used in this study for the other reservoirs. The resulting ELWSs are outlined in Figure 9-41, and the calculated balance flows are shown in Figure 9-42. The AME for the daily ELWSs, comparing the modeled results to the observations, is 0.86 m. The AME for the ReReg Reservoir is higher than the AME either for LBC (0.1 m) or Lake Simtustus (0.08m) because, as a reregulating reservoir, its ELWS is much more dynamic that the ELWSs the other two.

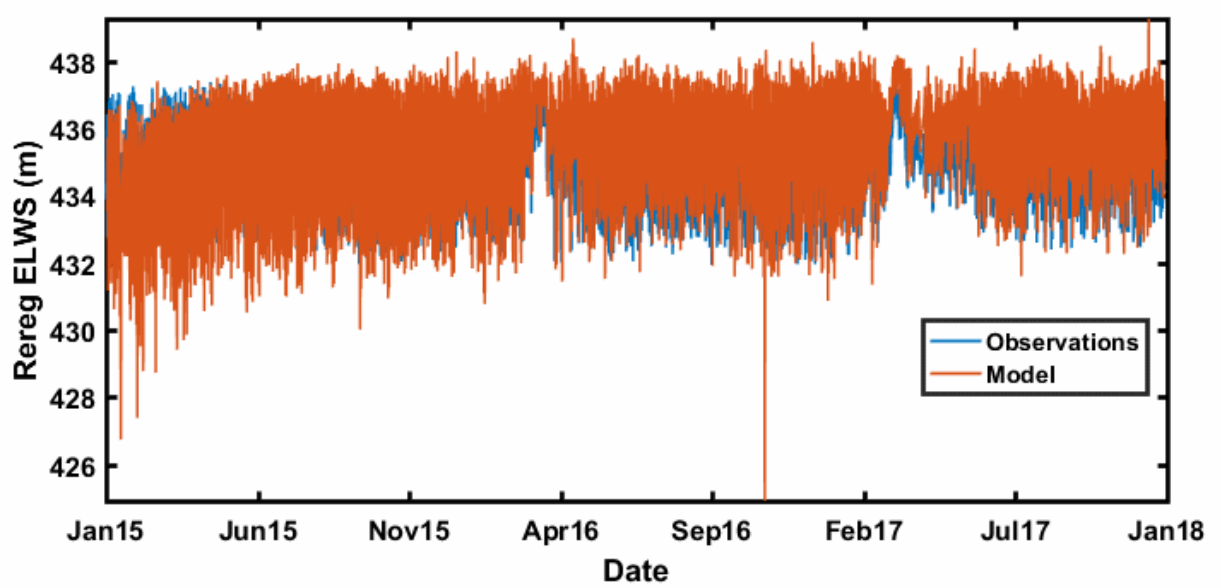

Figure 9-41. Simulated and observed elevation at the ReReg Reservoir.

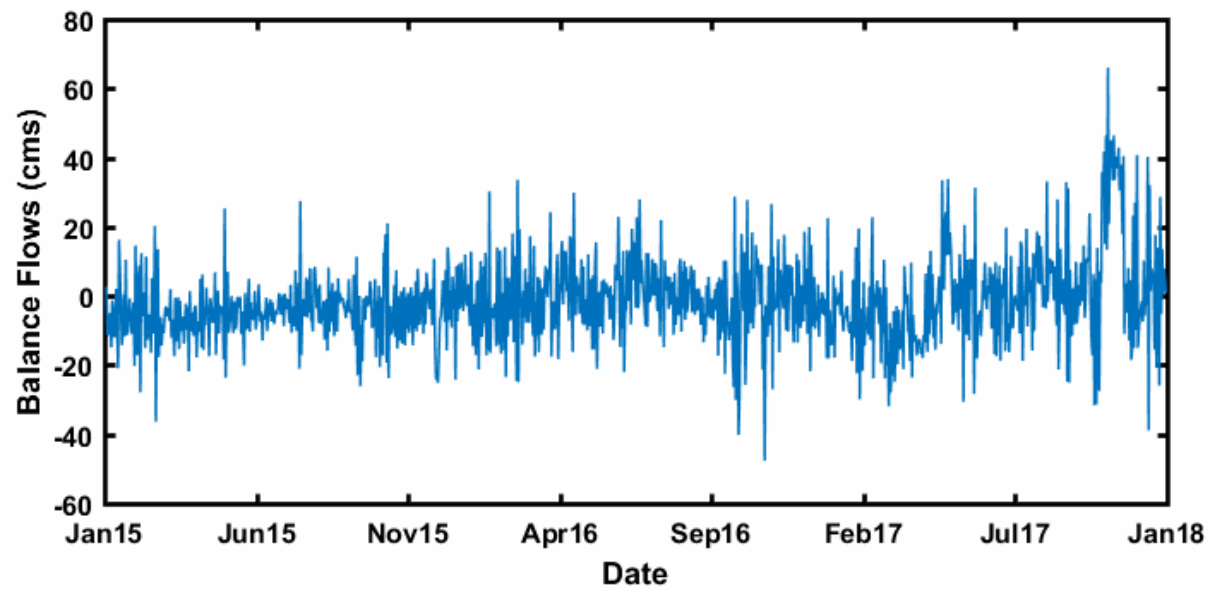

Figure 9-42. Calculated daily balance flows needed to capture observed surface elevations at the ReReg Reservoir.

9.8.2.2 Water temperature

Because of the very short residence times at the ReReg Reservoir, the focus of the report is on the tailrace data at the ReReg site (LDR01). The time series of simulated and observed water temperatures indicate that the model adequately captures the observations with an overall AME of 0.49°C (Figure 9-43).

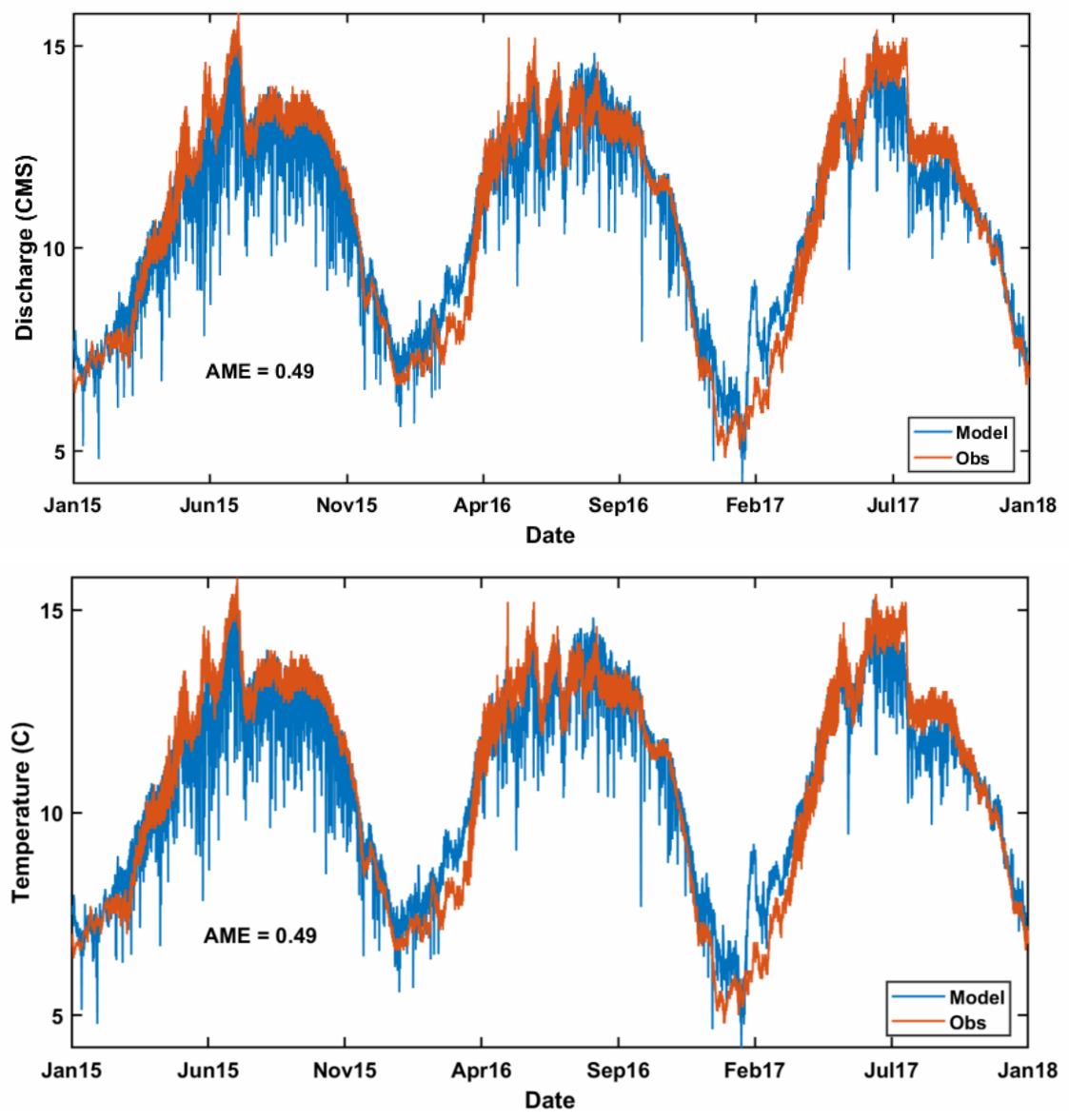

Figure 9-43. Simulated and observed temperatures downstream of the ReReg Reservoir. Spikes in the simulated temperatures occur primarily because of spikes in the balance flows. The spikes develop when the assumed temperature of the balance flows is different than the reservoir temperatures and when balance flows are large.

9.8.2.3 Conservative tracers

Tracers from the ReReg tailrace closely approximate those from the Pelton tailrace (Figure 9-44). This is an unsurprising result given the very short residence time of water in the ReReg Reservoir.

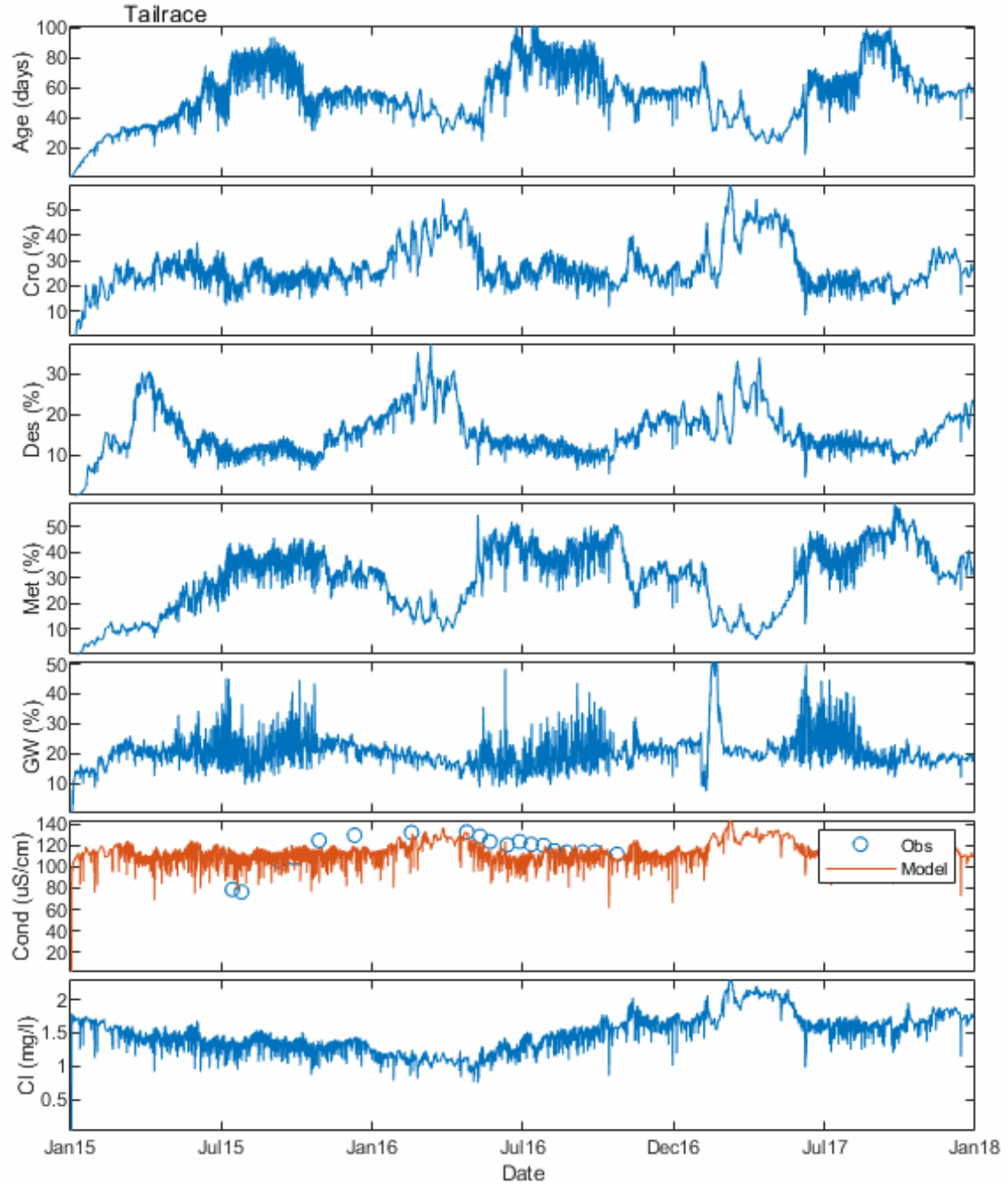

Figure 9-44. Simulated values for conservative tracers in the ReReg tailrace.

9.8.2.4 Nutrients

The model captures the magnitudes of observed nutrient data at the ReReg tailrace (Figure 9-45). The pattern of the dynamics is consistent with the observed pattern in other locations in the Project. Given the short residence time in the ReReg Reservoir, the water quality looks very similar to the water quality in the Pelton tailrace. As with LBC and Lake Simtustus, summer NO_3 values are underpredicted by the model.

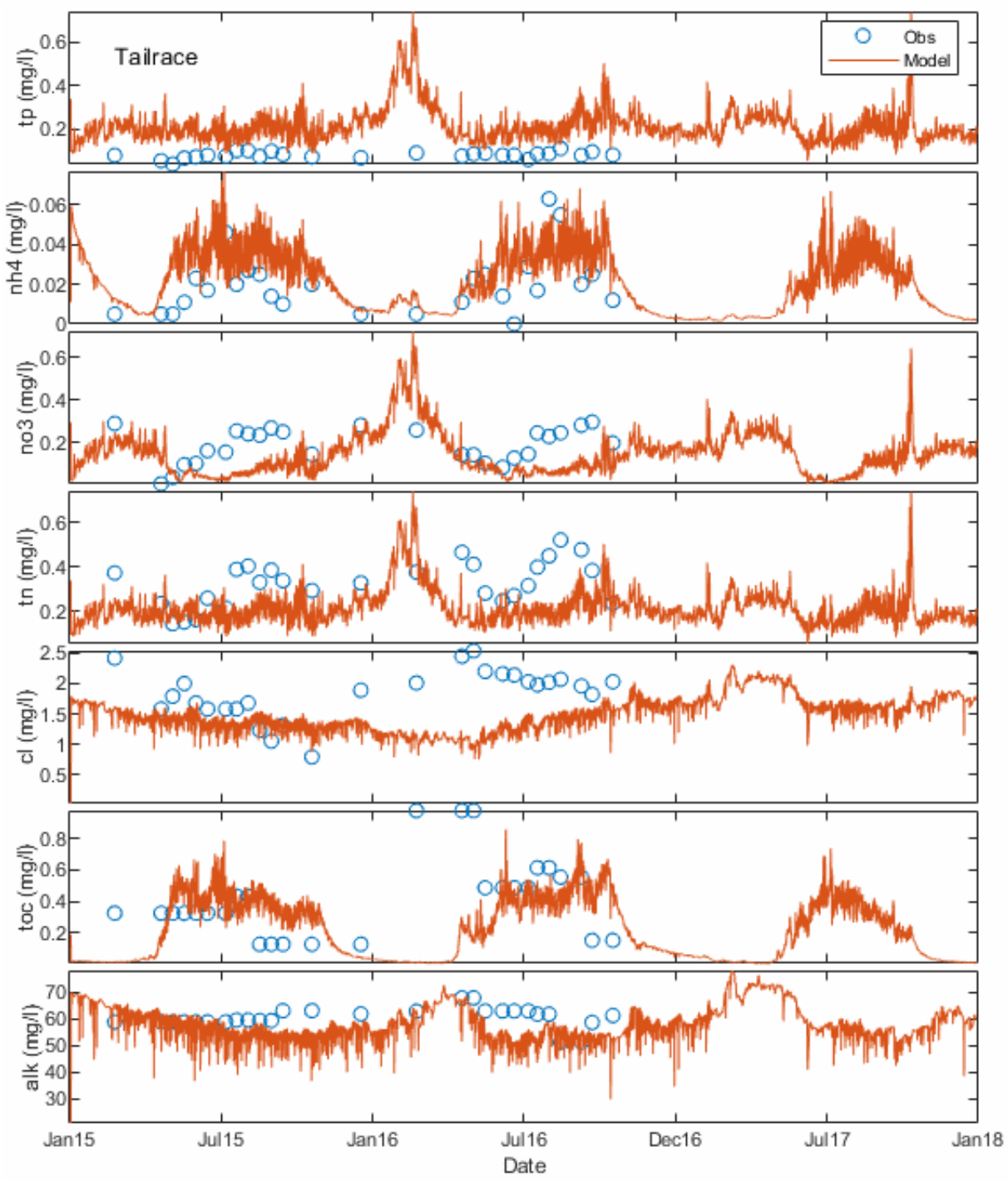

Figure 9-45. Simulated and observed nutrient dynamics in the ReReg tailrace. Cl^- and alkalinity are included for reference.

9.9.2.5 Dissolved Oxygen and pH

The simulated DO and pH tailrace time series at the ReReg Dam are similar to those at the Pelton Dam (Figure 9-46). DO is very closely approximated and pH values fall within the range of the observations, which outline a range from 7 to 10.

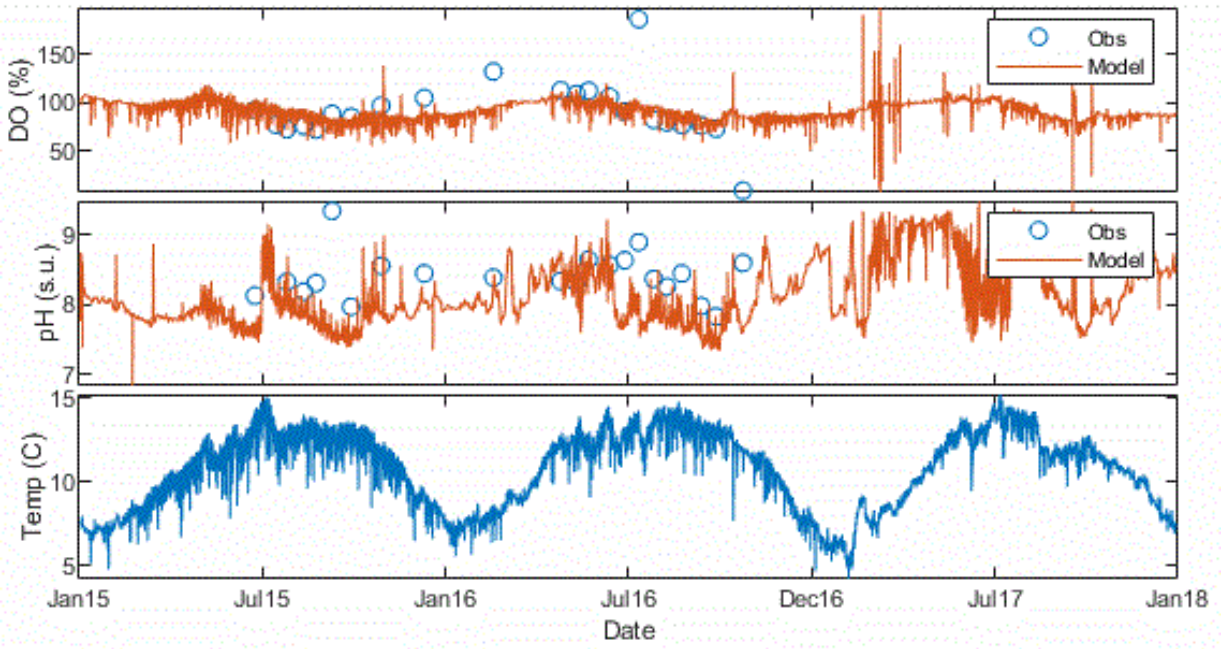

Figure 9-46. Simulated and observed DO and pH dynamics in the ReReg Reservoir tailrace. Simulated temperature is included for reference.

9.8.2.5 Biological components

As with other parameters, the biological components in the ReReg tailrace are similar to those simulated for the Pelton tailrace (Figure 9-47). The short residence time in the ReReg Reservoir explains this pattern and suggests that in-pool transformations at the ReReg Reservoir do not strongly influence the condition of the water leaving the system.

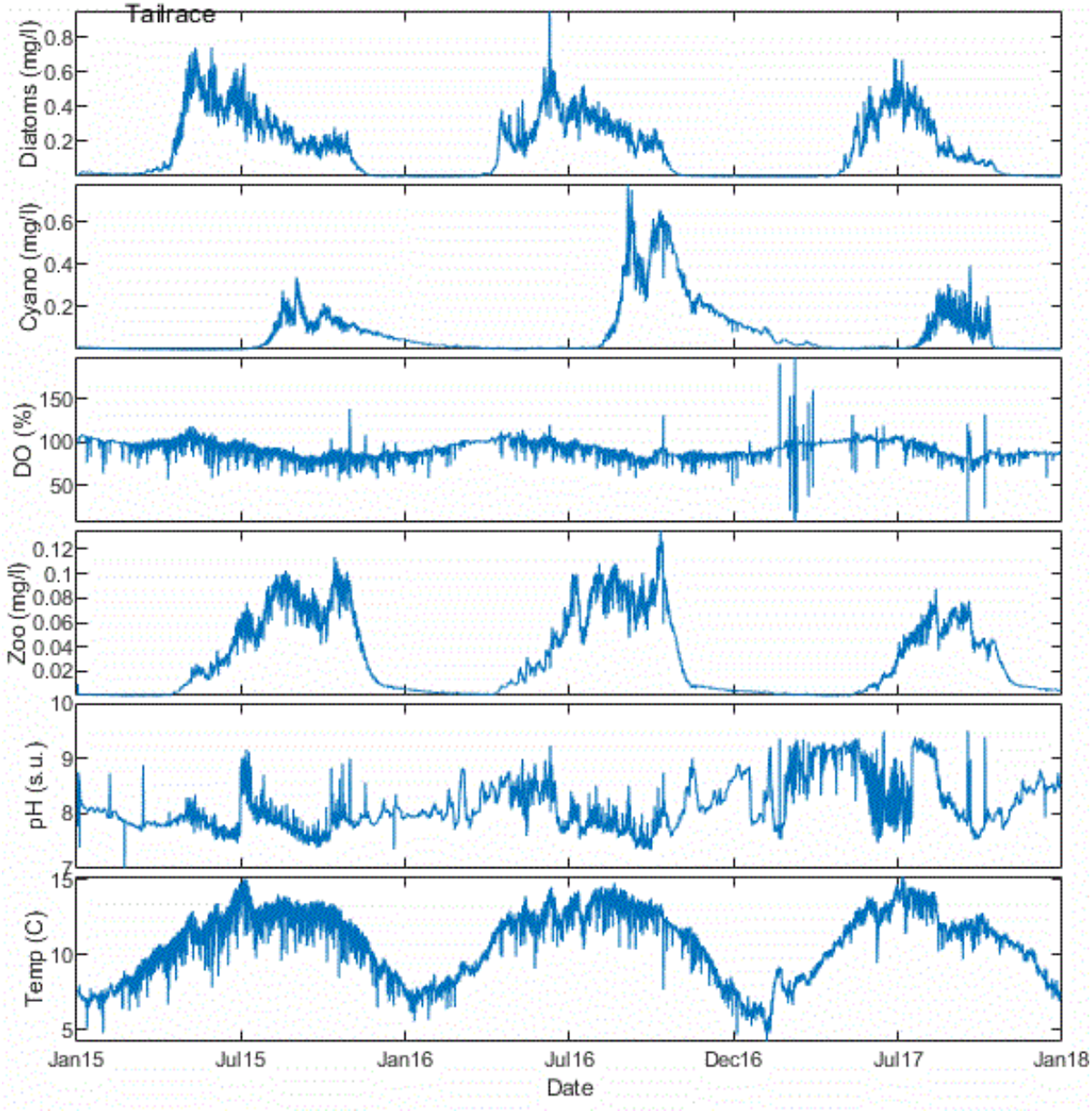

Figure 9-47. Tailrace time series for biological components in the ReReg Reservoir.

9.9 Conclusions

A hydrodynamic and water quality model of the PRB complex was developed for this study and calibrated to data collected during the period from 2015 through 2017. The model has been demonstrated to capture observed ELWSs, water temperatures, and a variety of water quality parameters.

In developing the water quality models, some of the limitations associated with modeling complex water quality interactions in complex systems clearly emerged. Most prominent are challenges associated with simulating multiple algal groups. We limited the algae groups to just two, but even then, complex interactions between nutrient availability, water temperature, and algal production dynamics led to some clear overpredictions of algal growth, especially of cyanobacteria. Those overpredictions led to some overprediction of nutrient availability and have implications for the 2Kw simulations in the LDR. This is mostly the case in the summer of 2017, when a large cyanobacteria bloom was simulated to occur in Lake Simtustus. Models of environmental systems will always include uncertainties, but we have used the best available data in an attempt to constrain them. For the W2 model, ELWSs and water temperature are better constrained by physics and mass balance than by the more complex water quality components. That is evident in these results. These uncertainties produce a larger range of variation in exported algae and nutrients than is typically seen in the LDR, suggesting that the results for summer 2017 represent a condition that has not existed previously but could exist under a future condition. Given this, it was maintained as part of the further scenario analysis in both the PRB and the LDR.

The model was developed to support the evaluation of a series of scenarios incorporating different potential future conditions. The goal behind the scenarios was to evaluate how the reservoir water temperature and water quality might change and how those changes might propagate through the LDR. Section 10 describes the model of the LDR. Section 11 combines the W2 reservoir modeling with the 2Kw river model to evaluate a set of scenarios that explore how changes in climate and management might impact water quality in both PRB and the LDR.

10 Water Quality Modeling in the Lower Deschutes River

10.1 Introduction

This section discusses the development and calibration of a 2Kw model to simulate water quality conditions in the LDR. The model was developed to provide some predictive capacity around the water quality in the LDR, specifically to evaluate how changes in conditions at the ReReg Dam might impact the river. Like all environmental models, 2Kw is built on a set of broad simplifications to capture the dynamics of natural systems. It is designed to help isolate key factors in lake and river behavior and allow users to test how a water body might respond to changes in the system before those changes are implemented. In some cases, the simplifications needed to produce the model limit the analysis that can be developed using it. Some of the limitations of 2Kw are apparent in this modeling and are highlighted as they arise.

10.2 Study Area

The LDR emerges from the Project, flowing in a northerly direction for 100.1 mi (161 km) before discharging into the Columbia River. Details outlining its hydrology, morphology, and observed water quality are included in sections 2 and 6 of this report.

10.3 Background

Huntington et al. evaluated water temperature in the LDR in 1999. They used the Stream Network Temperature (SNTEMP) model (Bartholow 1991) to simulate the impact of the Project on temperature in the LDR, finding that the impact varied by season and that, while the influence of the Project did extend throughout the 100-mi river, it attenuated as the water moved through the river. They noted the following:

> Our simulations suggest that, during the period modeled, PRB decreased river temperature from late May to early August, increased them until about mid-December, then decreased them again until mid-May….The SNTEMP simulations suggest that immediately below PRB, weekly mean temperature were elevated by an average of approximately 0.7°C (range +.2°C to +1.5°C) from early August to mid-December and reduced by an average of about 1.7°C (range -0.2°C to -3.5°C) during the remainder of

> the annual cycle. Downstream at Colorado Rapids, 4.0 mi. above the river's mouth, the estimated PRB effect from the same periods was to raise temperature by an average of about 0.5C (range -0.1°C to +1.0°C) and to decrease them by approximately 0.6°C (range -0.1°C to -1.7°C) (Huntington et al. 1999).

This work was instrumental in establishing estimates of a naturalized stream temperature regime in the LDR and in providing some early predictive capacity related to the impact of the Project on the river. The work was limited, however, by the time and space scales over which the model could be run. Specifically, the model inputs, including climate variables, stream flows, and stream temperatures, were input as weekly average values and then compared against weekly average values of simulated stream temperature. In the years since Huntington et al. (1999) developed their work, modeling technologies have improved to the point at which diel simulations are typically expected. The capacity to capture subhourly scale dynamics might be important for a variety of reasons, in particular because short-term exposure to relatively high water temperatures could be deleterious to stream biota. Simulations of average weekly temperatures might not provide those details. In addition, it has been recognized that canyon conditions in the LDR play a key role in the heating of the river water that occurs as it moves downstream. These conditions might vary over a wide range as the sun rises and sets and as subdaily meteorological events move through the region. A model that captures the dynamic influence of shading in the canyon provides additional details that help to more accurately capture mechanisms related to the temperature dynamics in the LDR. And finally, the SNTEMP model includes only water temperature. To capture water quality dynamics in the river, a more complete modeling platform is needed.

The model outlined in this section was developed to simulate diel temperature and water quality dynamics in the LDR. The work is underpinned by the robust, multiyear data collection described in previous sections.

10.4 QUAL2Kw Model

2Kw is a 1-D river temperature and water quality model available in the public domain. It includes a diel heat budget and water quality kinetics model, along with a steady-state hydraulic

model that simulates steady, nonuniform water flows. The model is an updated version of QUAL2E, the well-known river water quality model (Brown and Barnwell 1987), and it simulates the fate and transport of key water quality pollutants (Table 10-1).

Table 10-1. State variables captured by the 2Kw modeling framework.

Variable	Units
Temperature	°C
Conductivity	µmhos
Inorganic suspended solids	mg D/L
DO	mg O2/L
Slow-reacting CBOD	mg O2/L
Fast-reacting CBOD	mg O2/L
Organic nitrogen	µg N/L
NH_3 nitrogen	µg N/L
NO_3 nitrogen	µg N/L
Organic phosphorus	µg P/L
Inorganic phosphorus	µg P/L
Phytoplankton	µg A/L
Detritus	mg D/L
Pathogen	cfu/100 mL
Alkalinity	mg $CaCO_3$/L
TOC	mole/L
Bottom algae biomass	g D/m^2
Bottom algae nitrogen	mg N/m^2
Bottom algae phosphorus	mg P/m^2

Notes: µg = micrograms; µmhos = micromhos; CBOD = carbonaceous biochemical oxygen demand; cfu = colony forming units; mg/L ≡ g/m^3; D = dry weight; A = chlorophyll a.

The model uses Microsoft Excel as its user interface, with model algorithms written in Fortran 95 and invoked as an executable by the Excel interface. Key algorithms that make up the model are included in Chapra et al. (2012).

10.5 Data Sources

10.5.1 Climate Data

Previous analyses of the LDR have generally relied on air temperature data from weather stations at the Redmond Airport and in Madras near the LDR but located above the river canyon. We suspected that those sites underestimated maximum air temperatures in the canyon. A comparison of the air temperature from Pelton Dam showed the canyon site was consistently warmer than the nearby AgriMet mrso station (Figure 10-1). To provide more accurate air temperature data for the LDR, field staff installed weather stations at three sites in the canyon: Moody, Buckhollow Creek, and Pelton Dam. An additional weather station was added to the ReReg Dam in September 2016. The weather stations were equipped with Onset Computer weather stations (model U30-NRC) with sensors for air temperature, relative humidity, wind speed, wind direction, and photosynthetically active radiation (PAR). Data collected at 15-minute intervals were used in the 2Kw model.

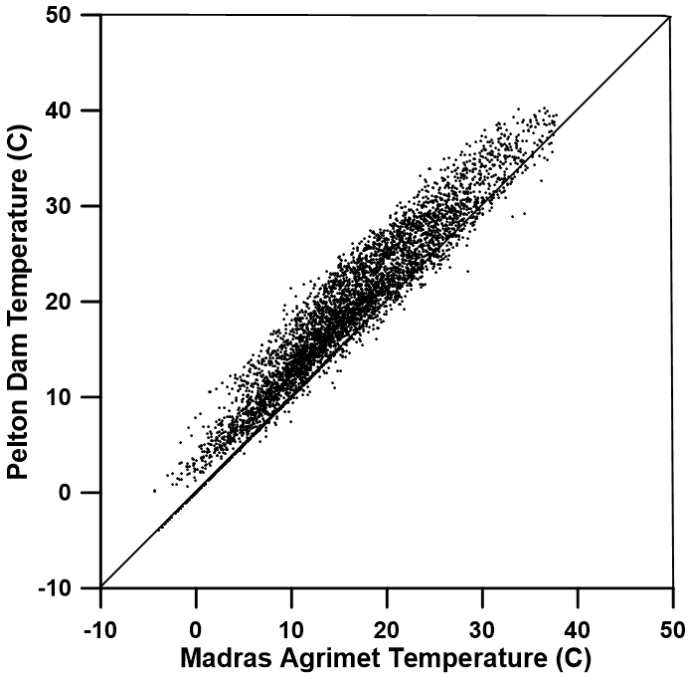

Figure 10-1. Comparison of air temperature at Pelton Dam and the Madras AgriMet mrso station.

10.5.2 Discharge Data

Discharge in the LDR is measured at two sites by USGS: Madras (#14092500) site immediately downstream of the ReReg Dam at RM 100 and above the mouth at Moody (#14103000). The Moody site has operated since 1897, and the Madras site has operated since 1923. Tributary flows to the LDR measured by USGS include Shitike Creek (#14093000, RM 97.6), Beaver Creek (#14097100), and Warm Springs River (#14097100, RM 84.3). Historical data are available for the White River from USGS (#14101500, RM 46.7), which operated the site from 1917 to 1990; those data were supplemented by measurements collected by field staff. Streamflow measurements have been continuously measured at Trout Creek by OWRD (#14095255, RM 88.5). Field staff also recorded supplemental stream discharge measurements at Dry Creek.

10.5.3 Water Quality Data

Field staff began to collect water quality data in February 2015. Those efforts consisted of monthly sampling during the cooler months (February–April; October–November) and biweekly sampling through the warmer months (May–September) of 2016. Monthly water quality sampling continued from June through September of 2017.

Water quality sampling at the designated monitoring fixed sites consisted of collecting water samples for analysis of a variety of analytes (See Section 3, Table 3-4). Water samples were also collected for analysis of algal community composition and abundance and zooplankton community composition. Nine rocks collected at each site were scraped for periphyton (5-cm delimiter), which were analyzed for community composition and abundance. Sonde measurements were collected at each site for temperature, pH, DO, conductivity, and turbidity using a YSI 6920 unit (substitutions of other models occurred in some instances). Chlorophyll *a* and cyanobacteria were measured *in-situ* using an AlgaeTorch.

Water temperature was continuously measured at several locations using an Onset Computer Pro v2 data logger (model U22-001) programmed at 15-minute intervals. The monthly and biweekly sampling was supplemented by 72-hr deployments of YSI 6920 sondes and collection of water

samples multiple times during the deployment. The sites included in these more intensive deployments were Trout Creek campground (RM 88.5), Harpham Flats (RM 55.8), Buckhollow Creek (RM 42.7), and near the mouth of the LDR (RM 0.5).

These fixed-site measurements were supplemented by a float of the river July 15–21, 2016. A raft was equipped with an In-Situ sonde that measured temperature, pH, DO, conductivity, and turbidity. An Onset Computer DO logger (model U26-001) was also added to the continuous measurements. Spot measurements were made of chlorophyll *a* and cyanobacteria with the AlgaeTorch. The raft was also equipped with an Onset Computer weather station to continuously record air temperature, wind speed, and solar radiation. The position of the raft was recorded with a Lowrance DGPS, and depth to substrate was measured with a Lowrance HDS-7 Gen 2 echosounder.

10.6 Model Setup

The river modeling portion of the Water Quality Study focused on the spring, summer, and early fall periods during which warmer water develops throughout the system. The modeling was based on the timeframe of April 1 into October of each year, with the last day of the simulation being defined based upon the availability of input data. This resulted in two separate simulations (one for 2015 and one for 2016) that each ran for 213 days. A third simulation was developed using the 2017 data. Results from the third simulation are included as part of the scenario analysis in Section 11.

2Kw is based on a numerical solution to the heat balance and individual mass balance for each of the water quality state variables. Continuous simulations for the LDR were developed using the Euler numerical solution procedure that was stable across the study period at a timestep of approximately one and one-half minute. Data were collected and processed every 3 hr to accommodate the storage limitation of the Excel-based interface, which was reached at shorter timesteps. In addition, a third simulation was developed for a 12-day period in July 2016 that encompassed the more detailed 4-day river float data collection. The collected data included a longitudinal profile of temperature and water quality parameters taken during the 4-day float, as well as hourly observations of water quality parameters at five sites along the LDR. Given the

shorter time period (12 days versus 213 days), the model run over this period was sampled every hour. This more detailed simulation was used as an additional verification step.

10.6.1 Geometry and Ttools

2Kw is a 1-D model that allows for a user-defined number of segments to characterize a study area. The number of segments in the model represents a balance between the overall length of the system, the level of detail, and numerical considerations.

Ttools is an ArcGIS extension, developed at Washington Department of Energy to generate 2Kw geometries and shade inputs. The input data required by Ttools includes near stream topography, vegetation height, and linear datasets representing right and left banks as well as the stream centerline. From these inputs, Ttools produces the physical characterization for each reach, including slope, width, and a detailed hourly calculation of effective shading from both vegetation and topography.

The topographic data used to support the development of the model inputs was based on LiDAR data provided by the Oregon Department of Geology and Mineral Industries (DOGAMI) that covered the entire LDR. These data were developed primarily to represent the stream and near-stream topography and do not always capture enough of the canyon environment to support the complete shading calculations. To accommodate this, we mosaicked the LiDAR data with standard 10-m Digital Elevation Model data to ensure complete topographic shade calculations. The required linear features (i.e., right bank, left bank, and stream centerline) were digitized from a combination of the LiDAR data and satellite imagery. Vegetation height was derived from the LiDAR data. Figure 10-2 is a representation of the LiDAR-derived slope of the LDR from the Project to the Columbia River.

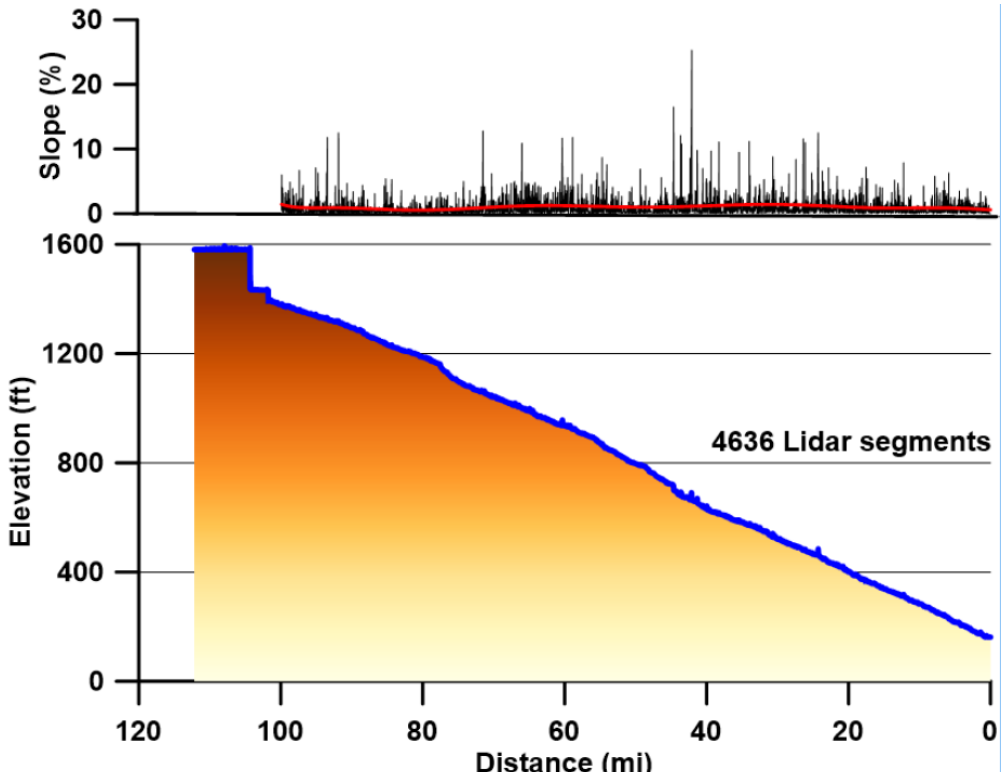

Figure 10-2. A longitudinal profile derived from LiDAR data representing the LDR. The two vertical drops at RM ~95 and RM 100.1 represent Pelton Dam and the ReReg Dam, respectively.

10.6.2 Model Input Data

Ttools was used to generate an input grid of 800 m resolution, which resulted in a total of 204 individual segments to capture the dynamics along the 100.1-mi LDR. The four maps are shown in Figure 10-3, which spans four pages.

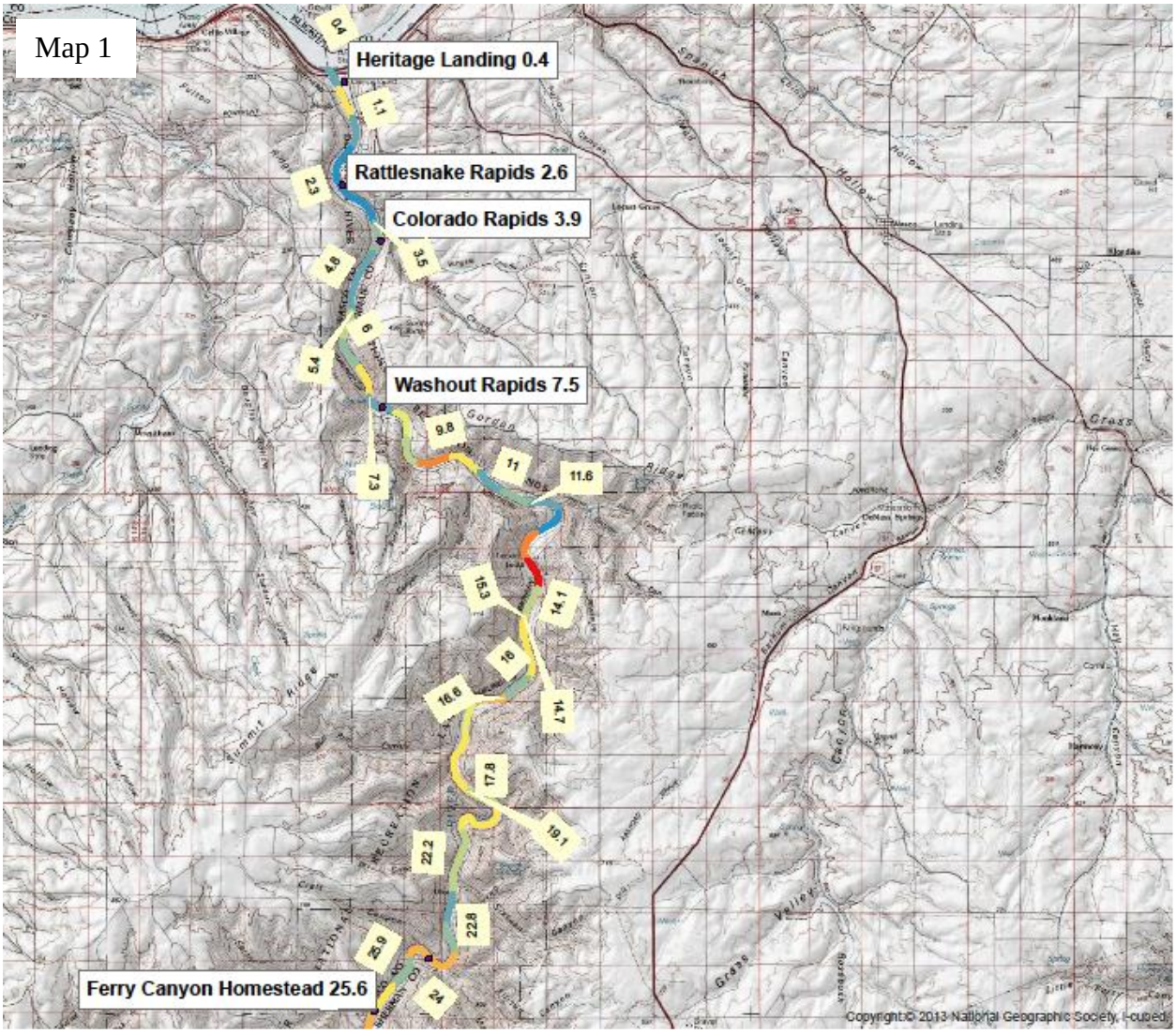
Map 1
Heritage Landing 0.4
Rattlesnake Rapids 2.6
Colorado Rapids 3.9
Washout Rapids 7.5
Ferry Canyon Homestead 25.6
0.4
1.1
2.3
3.5
4.8
5.4
6
7.3
9.8
11
11.6
15.3
14.1
16
16.6
14.7
17.8
19.1
22.2
22.8
25.9
24
Copyright © 2013 National Geographic Society, i-cubed

Map 2

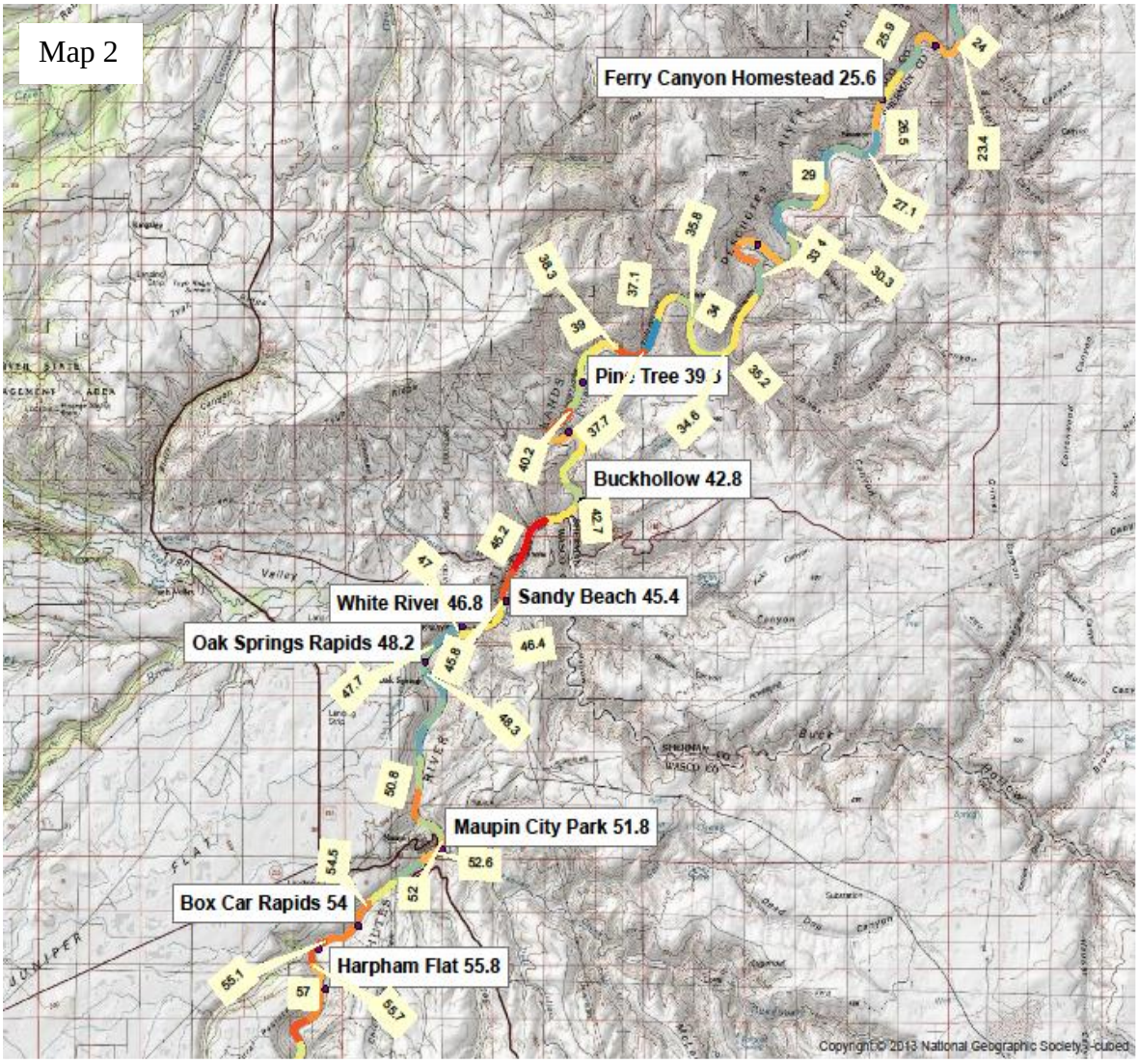
Ferry Canyon Homestead 25.6
Pine Tree 39.3
Buckhollow 42.8
White River 46.8
Sandy Beach 45.4
Oak Springs Rapids 48.2
Maupin City Park 51.8
Box Car Rapids 54
Harpham Flat 55.8
Copyright© 2013 National Geographic Society, i-cubed

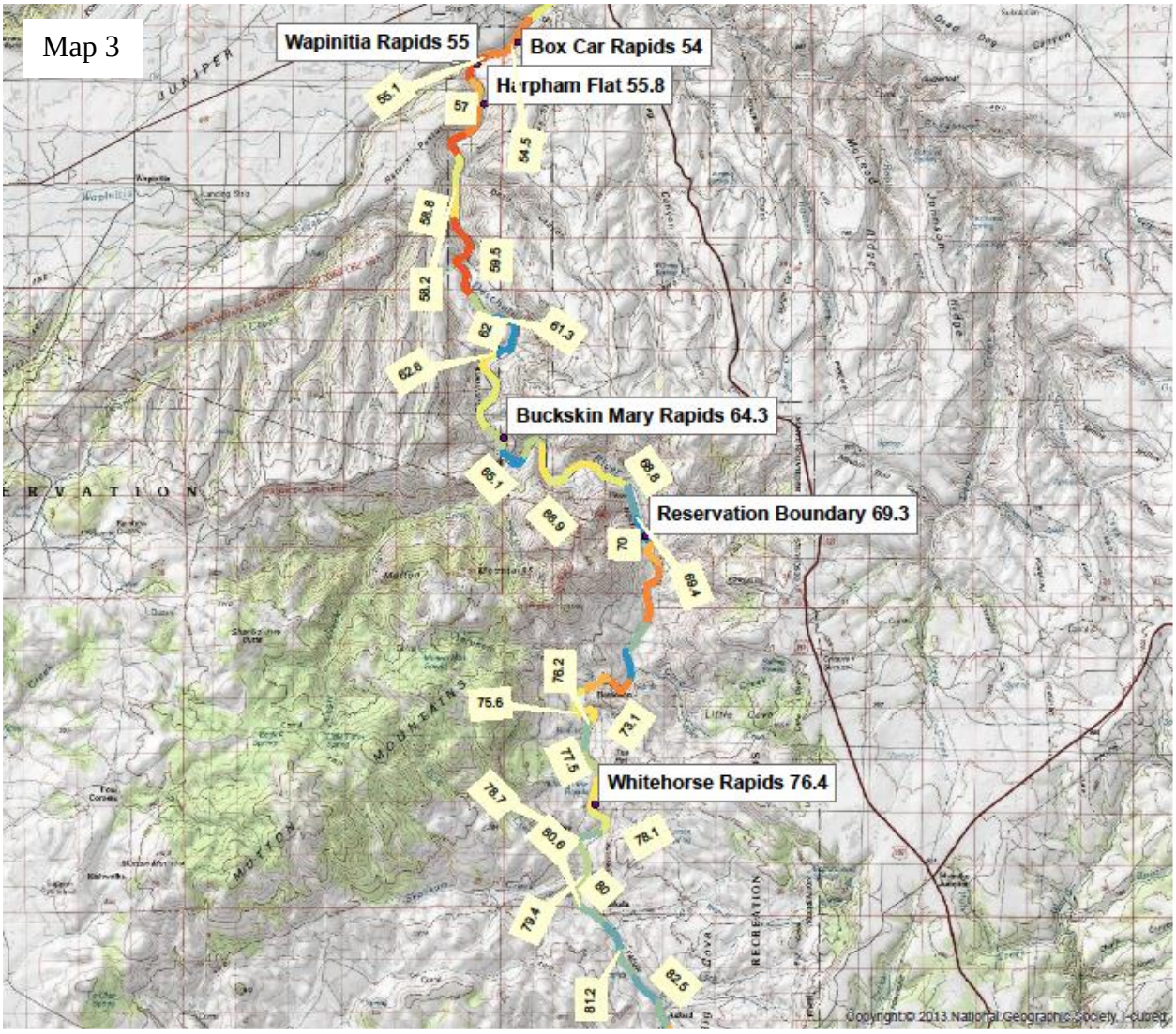
Map 3
Wapinitia Rapids 55
Box Car Rapids 54
Harpham Flat 55.8
Buckskin Mary Rapids 64.3
Reservation Boundary 69.3
Whitehorse Rapids 76.4
56.1
57
54.5
58.8
59.5
59.2
62
61.3
62.8
65.1
68.9
68.8
70
69.4
76.2
75.6
73.1
77.5
78.7
80.6
78.1
80
79.4
81.2
82.5
Copyright© 2013 National Geographic Society, i-cubed

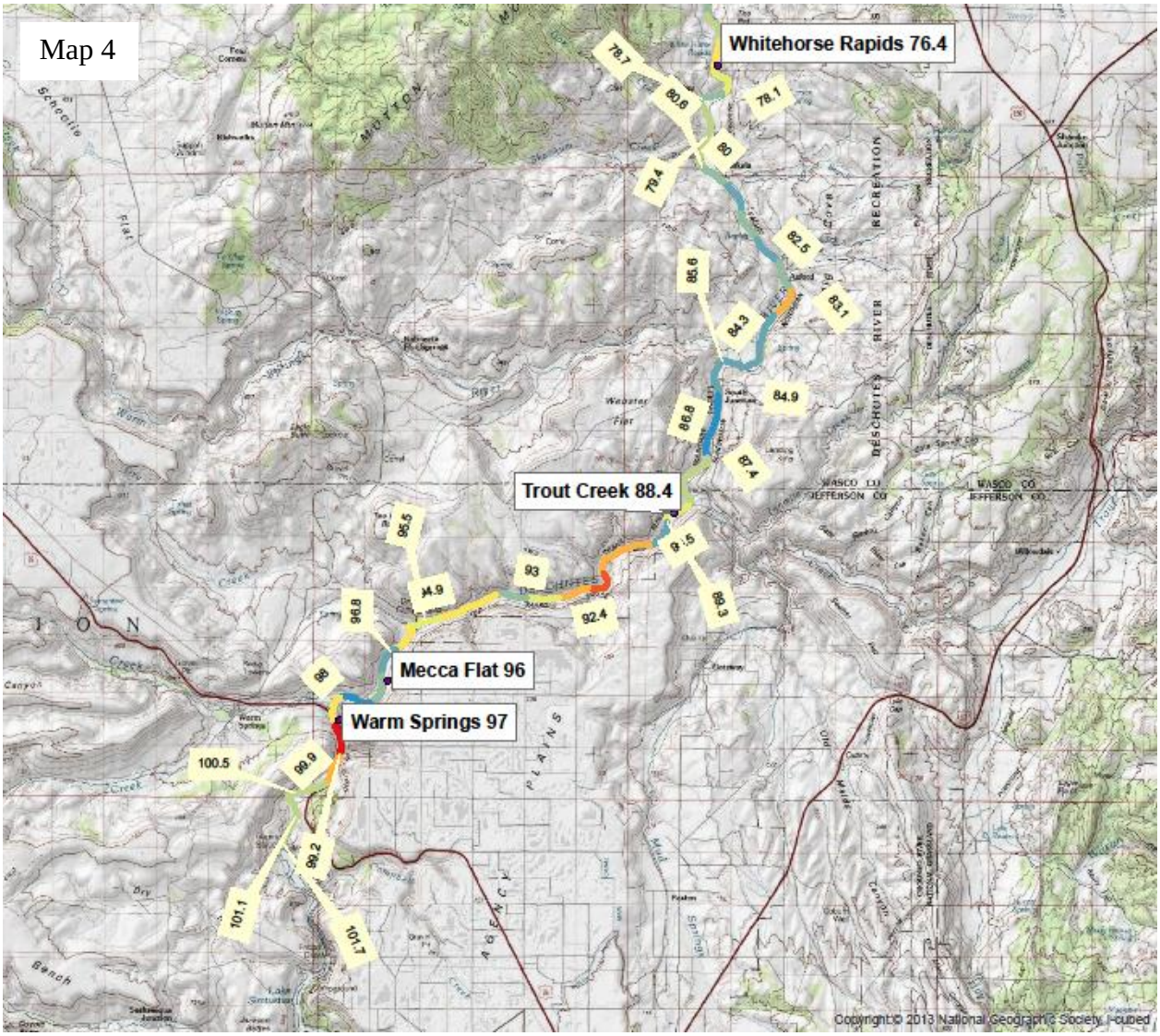

Figure 10-3. These maps depict each of the 204 individual model segments, as implemented by Ttools. The river mile for each segment is shown. The color of each segment represents the average gradient: blue represents shallow gradient, yellow and green represent mid-range gradient, and red represents steep gradient.

10.6.3 Effective Shade

For each modeled segment, the shading algorithm produces an estimate of effective shade for each hour of each day in the simulation. This calculation includes the position of the sun as it changes seasonally and diurnally, as well as shading related to topography and vegetation. Figure 10-4 depicts the shade calculations for each hour of the day on January 28, 2015. Calculations for effective shade vary spatially as a function of the depth and orientation of the canyon. The segments outlined on the two bottom panels are in steeper canyons and, throughout that winter day, the period of time during which they were entirely unshaded was shorter than for the segments outlined in the upper two panels, both of which are in more open areas of the river. Given the wide variety of canyon depths and river orientations, this level of detail, particularly related to topographic shading, is an important component of the water temperature model.

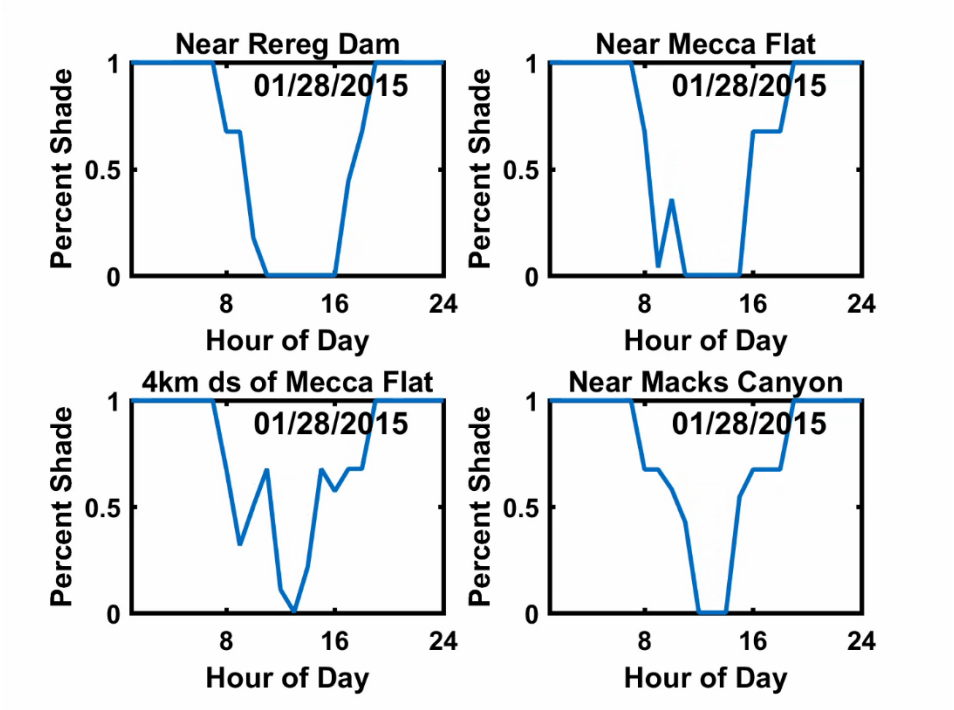

Figure 10-4. Effective shade for one day at four locations.

10.6.4 Boundary Conditions

Like all numerical models, 2Kw requires a set of boundary conditions related to simulated quantities. When possible, the boundary conditions comprise measured quantities, but when measurements are not available, the boundary conditions are either inferred from literature values or calibrated. Table 10-2 lists key boundary conditions, and Table 10-3 provides mapping between the water quality inputs required by 2Kw and available data sources.

Table 10-2. Key boundary conditions developed as input for the 2015 and 2016 2Kw models.

Type	2Kw Spreadsheet	Measurement Frequency	Source(s)
Climate	Air temperature, solar radiation, wind speed	Every 15 minutes	PGE weather stations
Climate	Dew point temperature	Every 15 minutes	Calculated from PGE weather station, air temp, and humidity
Hydrology	Headwater - flow	Every 30 minutes	USGS Madras gage
Hydrology	Continuous sources	Hourly	OWRD Oak Springs gage
Hydrology	Continuous sources	Occasional samples	PGE flow measurements at Shitike Creek, Warm Springs River, Trout Creek, and White River
Temperature	Headwater - temperature	Every 30 minutes	USGS Madras gage
Temperature	Continuous sources	Infrequent samples	PGE measurements at Shitike Creek, Warm Springs River, Trout Creek, and White River
Water Quality	Conductivity, Inorganic solids, DO, CBODslow, Organic nitrogen, Ammonium-nitrogen, NO_3-nitrogen, Organic phosphorus, PO_4, Phytoplankton, Alkalinity, pH	Infrequent Samples. See Table 10-3	PGE field sampling

Table 10-3. Mapping between required 2Kw water quality variables and available data.

Required by 2Kw	Required Unit	Source of Data
Conductivity	µS/cm 25°C	Conductivity measurements
Inorganic solids	mgD/L	Assumed to be zero
DO	mg/L	DO (mg/L) measurements
CBODslow	mgO_2/L	Average 2015 measured BOD5
CBODfast	mgO_2/L	Assumed to be zero
Organic nitrogen	µgN/L	Total nitrogen measurements – ammonium + NO_3
Ammonium-nitrogen	µgN/L	Ammonium measurements
NO_3-nitrogen	µgN/L	NO_3 measurements
Organic phosphorus	µgP/L	Total Phosphorus – PO_4 measurements
Inorganic phosphorus	µgP/L	PO_4
Phytoplankton	µgA/L	Assumed to be 100 µgA/L
Detritus (POM)	mgD/L	Assumed to be zero
Pathogen	cfu/100 mL	Assumed to be zero
Generic constituent	user defined	Cl^- measurements
Alkalinity	$mgCaCO_3/L$	Alkalinity measurements
pH	s.u.	pH measurements

Notes: POM = particulate organic matter; µgA/L = micrograms chlorophyll a per liter; mgD/L = milligrams dry mass per liter. Field/lab data were linearly interpolated to hourly values.

10.7 Model Analysis

The goal behind model analysis was to establish that the simulation captured key features of the hydrology and water quality in the LDR. This is done through model calibration, in which parameters are adjusted to produce model outputs that reproduce observations, and through model verification, in which the model is run over a different set of conditions, but with the calibrated parameter set. The verification step is useful in establishing that the calibrated model is robust, providing useful simulations during conditions over which it was not calibrated.

As with any model, 2Kw is a simplification of reality, designed to capture key features of the water quantity and quality in riverine systems. It is important to recognize the simplified nature of the model, especially when limitations impact its ability to provide predictive outcomes. A key limitation of 2Kw is that it is a 1-D model. It can estimate how quantities move across multiple grid cells, but it assumes that within each grid cell, quantities are fully mixed across a

rectangular cross section. That leads to challenges, for example, in the simulation of periphyton, which will establish in shallow areas, but not necessarily in deeper sections where light penetration might be limited. Within each grid cell, the model does not distinguish different depths. There is a single, average depth from which light limitation is calculated. With the LDR's large flows, the average cell depths can be large and result in a model that is not well suited to simulating periphyton dynamics. To properly simulate quantities such as periphyton, which are defined by changes across the channel cross section, a 2-D model is required.

10.7.1 Hydrology

We used flow data from the USGS Madras (#14092500) and Moody (#14103000) gages, along with spot measurements at larger tributaries collected during the study period, to develop the hydrological model calibration. Following procedures outlined in the model documentation, we developed an overall hourly flow balance to estimate all unmeasured losses of stream flow between the Madras and Moody gauges. These calculated unmeasured losses were then input into the model as groundwater contributions. The model results are outlined in Figure 10-5.

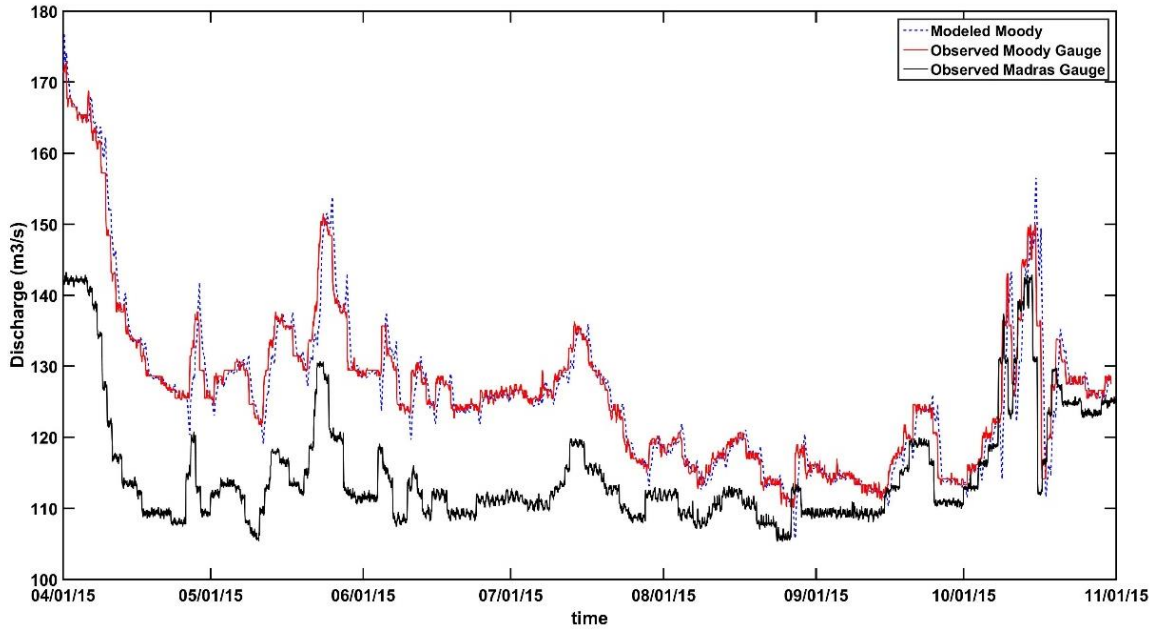

Figure 10-5. Comparison of observed stream discharge at Moody (RM 1) and Madras (RM 100), with simulated stream discharge at Moody for the 2015 study period. Simulated discharge at Madras is not shown because the observations are used as the upper flow boundary condition.

10.7.2 Water Temperature

The model implements a detailed heat budget for each segment, simulating water temperature from it. One of the primary unknown boundary conditions in applications of 2Kw is the temperature of diffuse groundwater inflows. Following suggestions from the 2Kw user's manual, we used the groundwater temperature as the primary calibration variable.

10.7.2.1 Calibration

The data collected during 2015 were used to develop the model calibration, for which the goal was the same as for the W2 calibration: to end model adjustment when the AME was less than 1^{o}C, a threshold suggested by Cole and Wells (2006) (See Section 9.2, Equation 1).

Hourly temperature data at five locations and across the full spring/summer/fall period were used in the calibration. Typically, temperature simulations focus calibration statistics on either 7-day running maximum values or on daily minimum and maximum temperature. Using diel data presents a more challenging test of the model because it includes the timing of changes in temperature throughout the daily cycle.

Results from the calibration are presented in Table 10-4, where both diel AME and AME values associated with both the 7-day running maximum and 7-day running minimum temperatures are included. In all cases, AME values are less than 1^{o}C. The diel results are presented as time series in Figure 10-6 for each of the five sites. In addition, the individual sites are represented in Appendix H, Figures 61-70. Both versions are provided to facilitate comparisons across sites and at a particular location.

Table 10-4. River temperature (°C) AME values for the diel data, 7-day running maximums, and 7-day running minimums for each of five locations within the LDR during 2015.

Site	Diel AME	7-day max AME	7-day min AME
Dry Creek	0.51	0.33	0.13
Nena	0.92	0.32	0.45
Sandy Beach	0.74	0.47	0.64
Macks Canyon	0.95	0.45	0.57
Moody	0.98	0.60	0.50

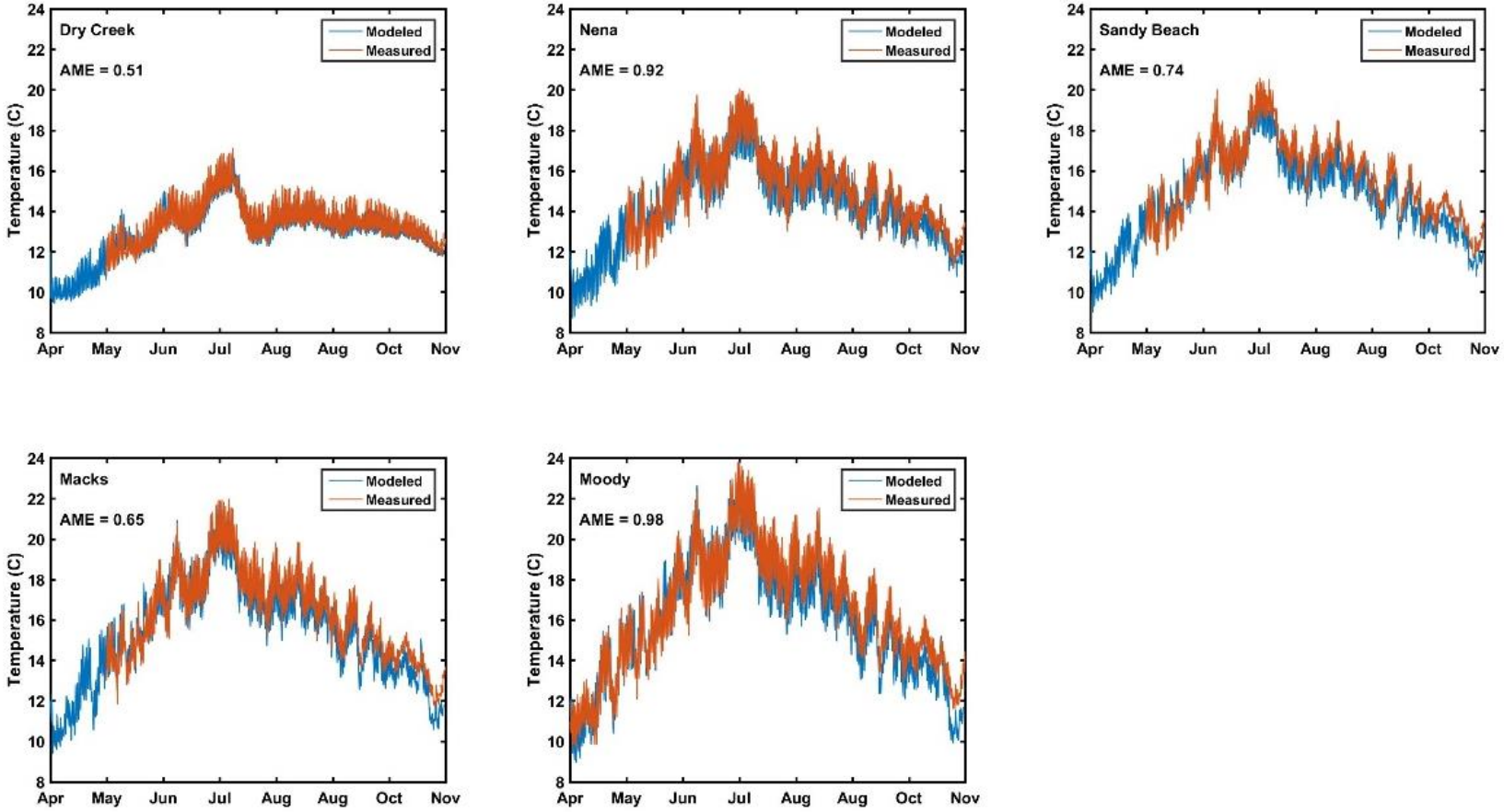

Figure 10-6. Diel time series of measured versus modeled temperature for the five locations in the LDR during summer 2015. Data collection at the first four sites did not start until May 1. The station at Moody (RM 1) is operated by USGS and runs continuously.

Model validation is a process that involves running a previously calibrated model over a new set of data. It is an effort to evaluate how well a calibrated model can capture conditions that are different from those that defined the calibration period. Validation is a useful test, particularly when the model will be used to simulate scenarios that adjust conditions that define the calibration period. In this case, we applied the model calibrated to the 2015 data to the 2016 period. As with the calibration, the goal was to describe a model in which the AME for each station, calculated based on the diel data, was less than 1°C. Results indicate that AME values are less than 1°C for all data and across the measurement period during given conditions in 2016 (Table 10-5). As with the calibration period, time series including diel data and weekly running averages are presented in a set of figures (Figure 10-7). These results provide added confidence that the model captures key dynamics defining water temperature in the LDR and a basis for proceeding with scenario analysis.

Table 10-5. River temperature (°C) AME values during model validation for the diel data, 7-day running maximums, and 7-day running minimums for the five locations within the LDR during 2016.

Site	Diel AME	7-day min AME	7-day max AME
Dry Creek	0.14	0.15	0.10
Nena	0.53	0.46	0.39
Sandy Beach	0.49	0.38	0.29
Macks Canyon	0.53	0.43	0.32
Moody	0.78	0.83	0.47

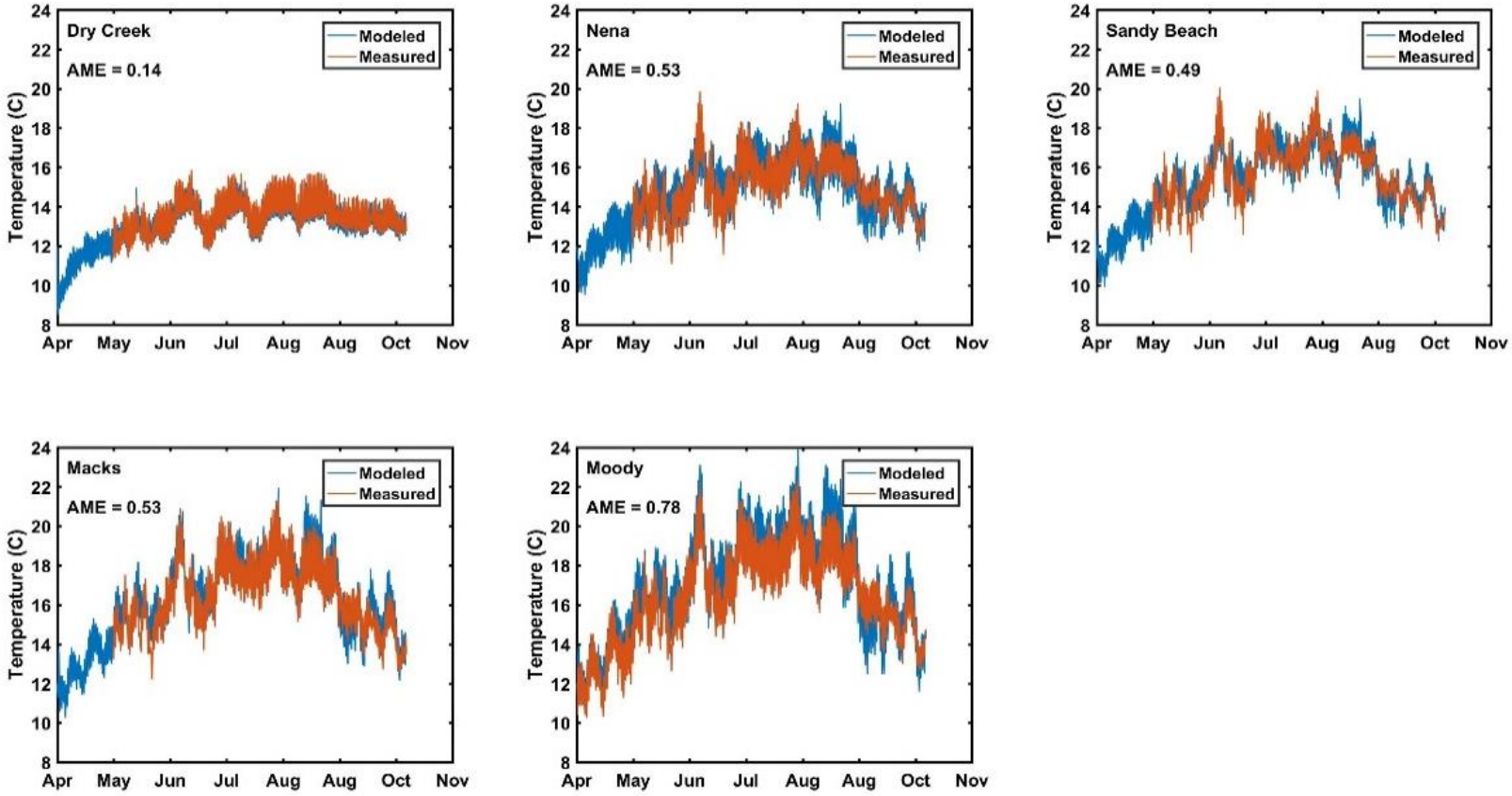

Figure 10-7. Hourly time series of measured versus modeled temperature at the five locations in the LDR during summer 2016.

10.7.2.2 Short term simulations and longitudinal profile

Water temperature and water quality models are typically evaluated from a Eulerian perspective, in which data are collected at static locations, recording observations of water as it flows downstream. In locations like the LDR–where release temperatures vary diurnally; warm, dry daytime conditions result in significant heating of the water as it moves through the canyon; and the water experiences multiple diurnal cycles before it leaves the system (the travel time of water from the ReReg Dam to the mouth of the LDR is approximately 30–36 hr) – it is also useful to observe conditions as water moves through the system. This Lagrangian perspective can be approximated by floating instruments with the current.

During the period from July 18 to July 24, 2016, instruments recording temperature, pH, conductivity, and DO were floated longitudinally through the LDR, beginning at the ReReg Dam and ending at Moody. These data, which combine a Lagrangian perspective (when moving) with a Eulerian perspective (when static, typically during the overnight period), were used to further verify that the 2Kw model adequately captured relevant dynamics in the LDR.

More fully outlined in Figure 10-8, comparisons of a variety of temperature observations against model results indicate that the model captures the diurnal pattern of temperature as well as the longitudinal profile as it heats and cools during the diurnal period. Of interest are subfigures B2 and C, which compare the observed longitudinal temperature data against the modeled longitudinal profile. This unique set of observations indicates that the temperature portion of the model performs well, even at locations where continuous temperature is unavailable. An animated version of this figure and similar figures is available on PGE's website at portlandgeneral.com/waterquality.

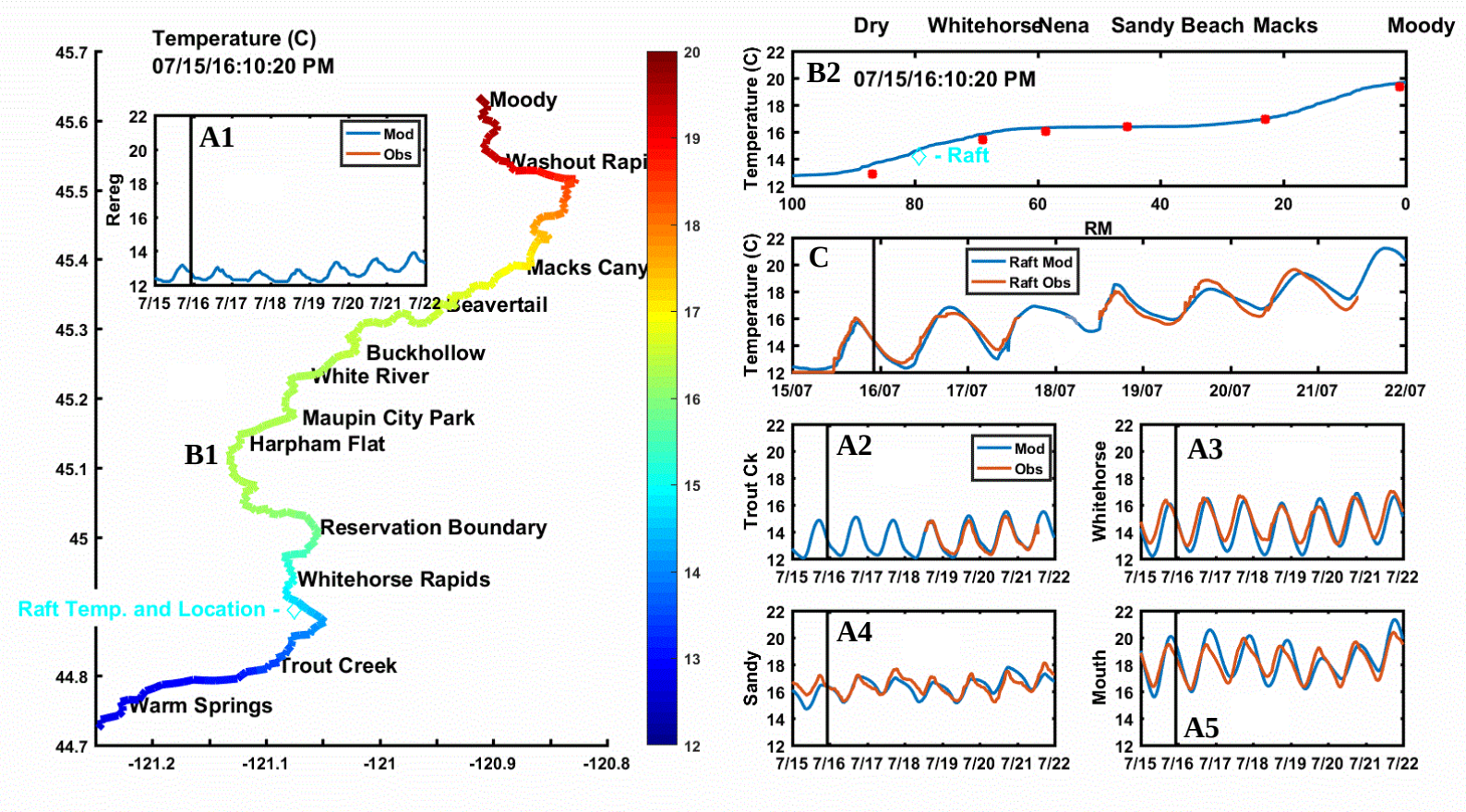

Figure 10-8. Combined Eulerian and Lagrangian viewpoints of simulated and observed temperature dynamics in the LDR. Plots labeled A1–A4 represent time series data of observations (*in orange*) and model results (*in blue*) at individual locations in the system. The vertical black line in each of the plots defines the point in time where the B and C snapshot figures were taken. Plots B1 and B2 outline the temperature at a particular moment in time for all locations in the LDR. The red dots in B2 are the observations at that point in time, at different gauged locations on the river. The colors in B1 represent the water temperature at a single point in time. Plot C represents the floating (Lagrangian) temperature observations in orange, with the modeled observations at each point in time and space in blue. Note that the two periods of time when the observations (*orange*) disappear correspond to gaps in the observed data. An animated version of this figure is available on PGE's website at portlandgeneral.com/waterquality.

10.7.3 Water Quality Model

A complete 2Kw water quality model for the LDR was developed using a manual calibration procedure and comparing available water quality data to model results. The goal behind the calibration was to reproduce key features from the observations, including diurnal variations (for pH and DO, which were measured *in situ*), trends in the longitudinal profile, and seasonal trends. To accomplish this, we systematically varied model parameters within suggested ranges as provided in the model documentation. Except for the DO reaeration coefficient, which was adjusted at Sherars Falls, all water quality parameters were assumed to be constant throughout the LDR. The final calibrated model parameters are outlined in Appendix I. As with the water temperature model, calibrations were developed using 2015 data and the calibrated parameter set was then run using the 2016 dataset as a further evaluation step.

The water quality model includes biologically active constituents (DO, pH, NO_3-nitrogen, ammonium-nitrogen, TN, TP, algae, and periphyton) and inactive constituents (alkalinity, Cl^-, and conductivity). The biologically active constituents display diurnal variations as well as seasonal changes. For most parameters, observations are limited to grab samples, which do not capture the diurnal variability. Nonetheless, comparing modeled parameters against these observations establishes that the model does capture key features of the water quality dynamics in the LDR. A select set of subhourly observations for DO and pH are outlined to more fully characterize the capacity of the model to reproduce the diurnal variation.

The simulation of nutrients and water quality is a more challenging and uncertain endeavor than the simulation of water temperature alone for the following reasons:

- Water quality dynamics are more complicated with a wide variety of mutually dependent state variables defined, in part, by temperature-dependent rates. These models typically rely on calibrated parameters that are typically difficult to measure.
- Water quality observations are typically more difficult and/or expensive to develop and, because of this, observed time series are generally not as detailed as they are for temperature. The sparser datasets contain less information than their continuous

counterparts. That said, the use of available water quality observations is a key component in water quality simulation, given uncertainties in how to parameterize these complex systems.

Despite these well-known challenges, the simulation of in-stream water quality provides a useful mechanism to more fully understand how systems may respond to future changes in boundary conditions and internal states.

10.7.3.1 Dissolved Oxygen and pH

DO represents a key element of water quality in the LDR. It is influenced primarily by the turbulent nature of the river, especially across steeper sections that include riffles and rapids, which keep DO levels near saturation. In addition, algae and periphyton contribute DO to the water through photosynthesis, and, during periods of high biological activity, DO can become supersaturated. Respiration and decomposition of organic matter consume oxygen as both sediment oxygen demand and BOD. In modeling DO, we used the Churchill reaeration subroutine (Churchill et al. 1962), following guidance provided in Pelletier et al. (2006). The model appears to reasonably capture DO dynamics throughout the system (Figure 10-9, Figure 10-10, and Figure 10-11). Key features of the DO dynamics include a pronounced summer reduction of DO from the Project. The depression is likely associated with increased oxygen demand in the reservoirs as they become more productive with increased summer light and temperatures. The increase in production results in an accumulation of decaying biomass that sinks through the water column, which leads to increases in oxygen demand with depth and associated decreases in tailrace DO. Additionally, as the tailrace water warms through the summer, the temperature dependence of DO saturation can also contribute to lower DO concentrations. The depleted summer tailrace DO is quickly reintroduced into the water as it moves down the LDR, through a combination of atmospheric equilibration and biological production.

A second element of the DO pattern is the large diurnal swings in modeled DO. These swings are a function of biological activity in the system, with elevated DO during the daylight hours

when both algae and periphyton are active, and depressed levels at night when biological activity stops.

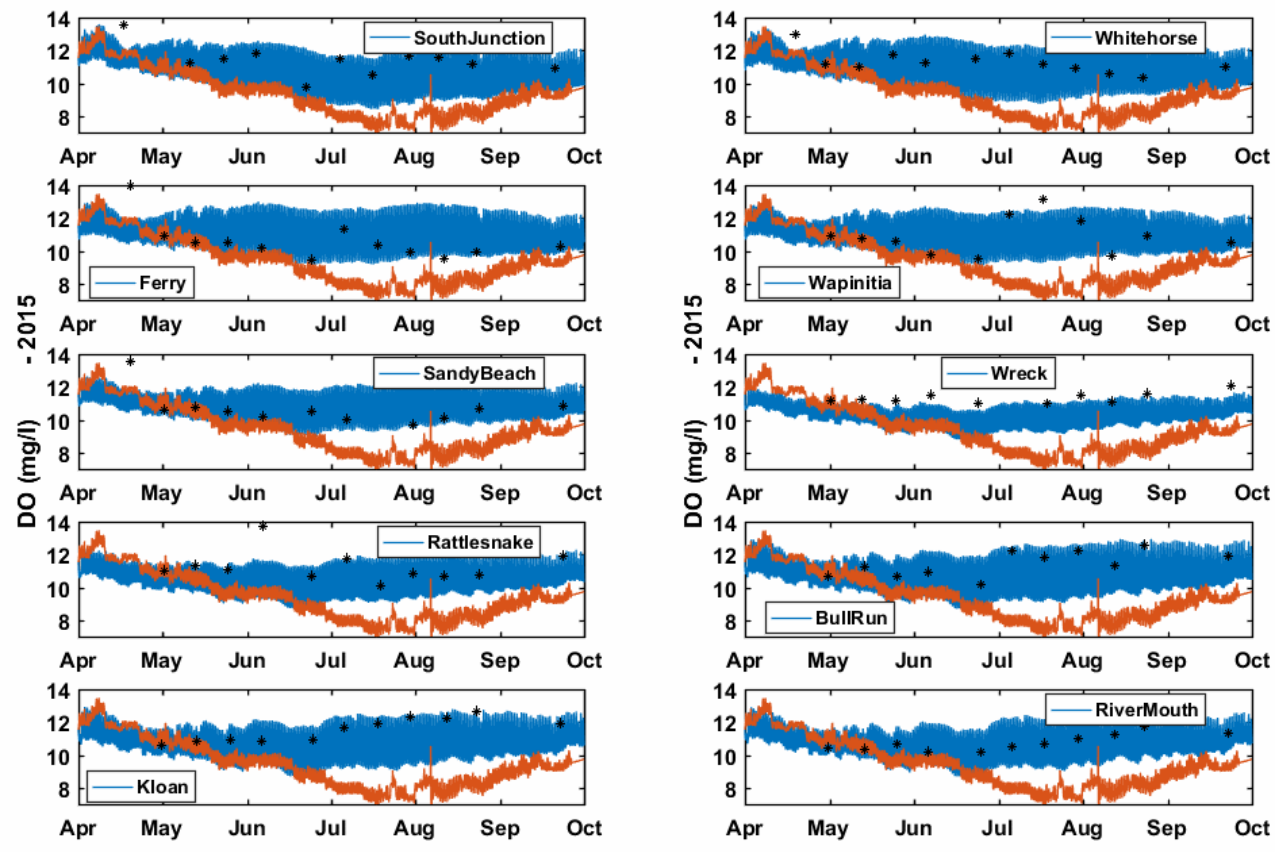

Figure 10-9. Simulated and observed DO during 2015. The black dots represent observations, the blue line represents simulated DO, and the orange line represents the upstream DO boundary condition (included for reference).

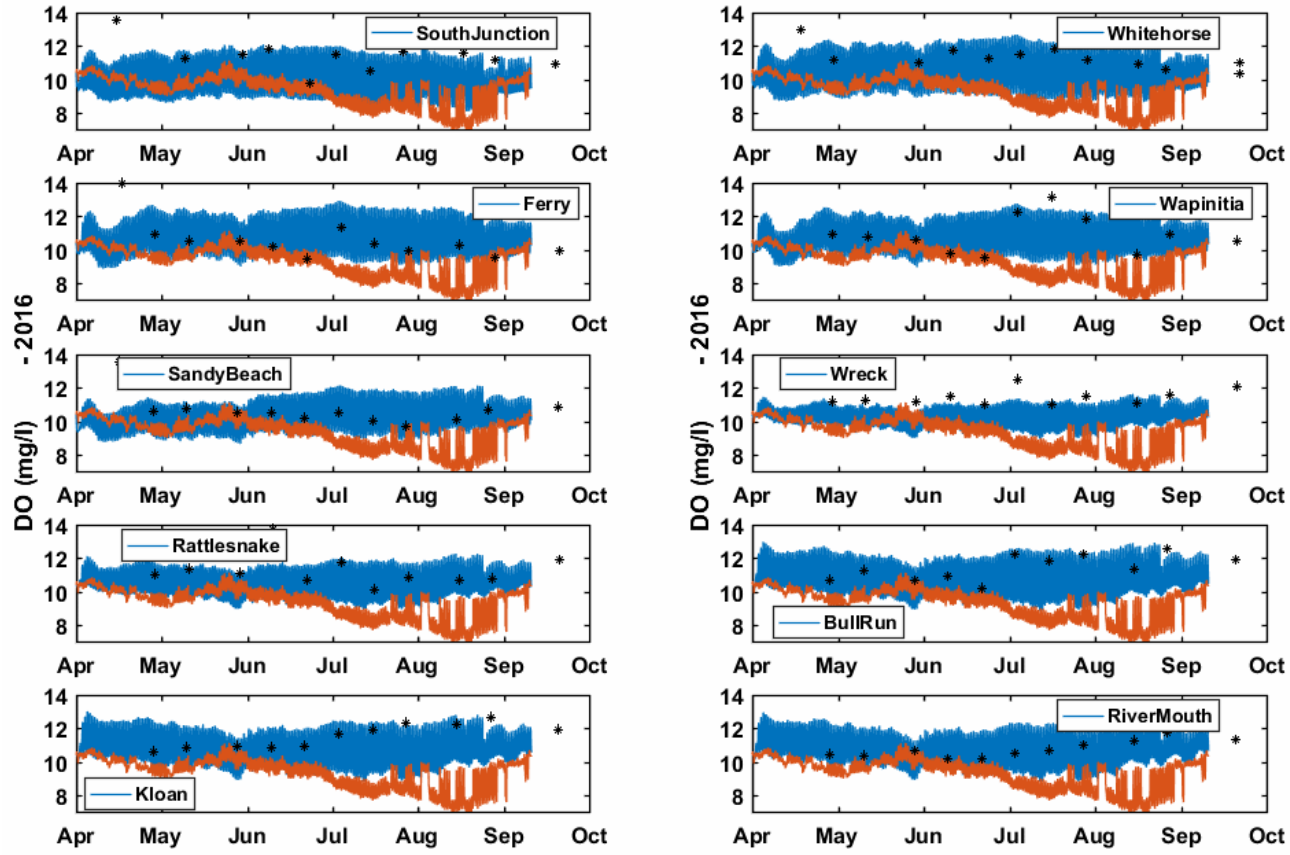

Figure 10-10. Simulated and observed DO during 2016. The black dots represent observations, the blue line represents simulated DO, and the orange line represents the upstream DO boundary condition (included for reference).

The diurnal pattern is not evident in the observed grab samples, but the short period over which continuous DO measurements were made suggest that the model reasonably captures the pattern (Figure 10-11).

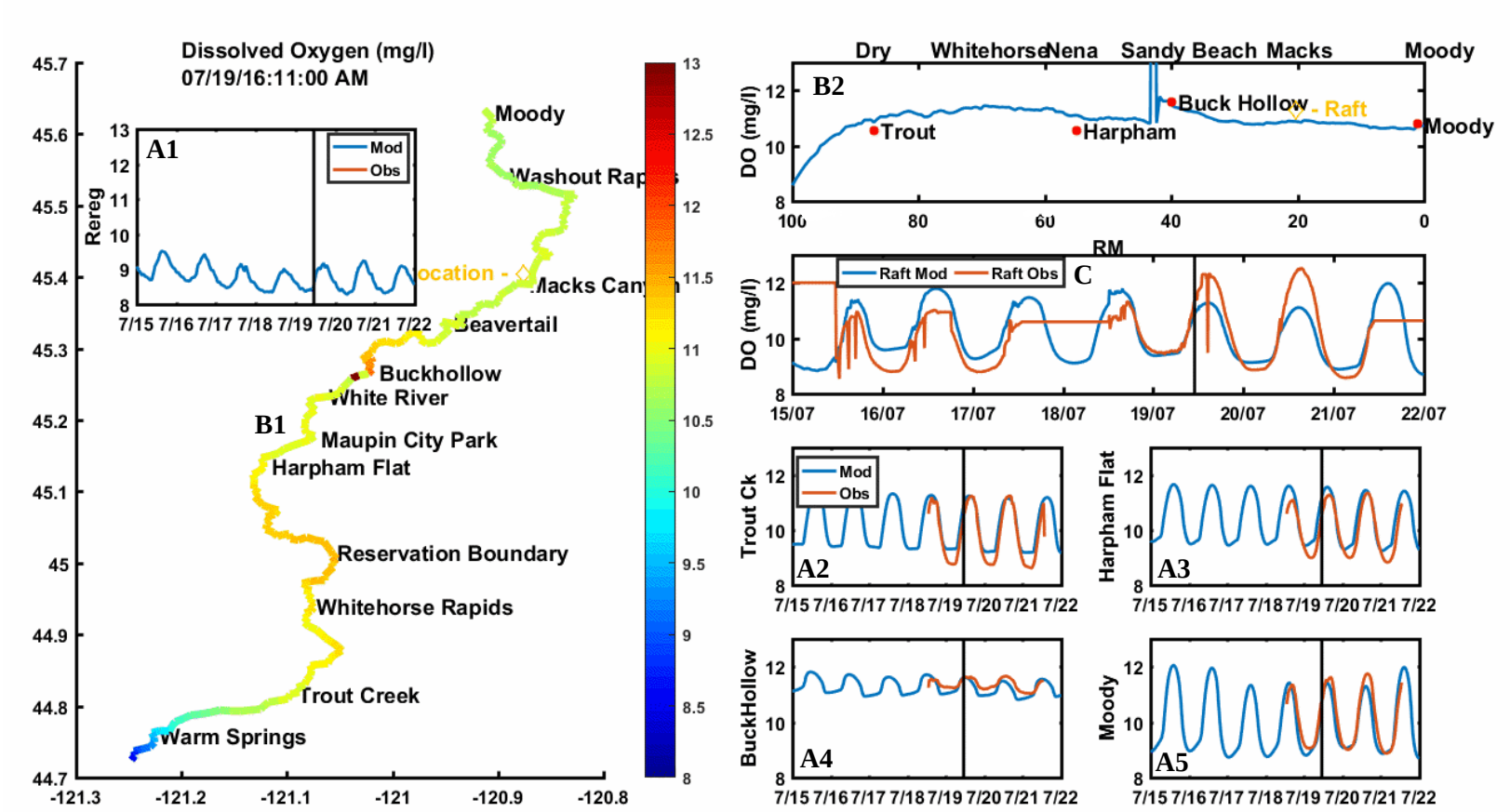

Figure 10-11. Combined Eulerian and Lagrangian viewpoints of simulated and observed DO dynamics in the LDR. Plots labeled A1–A4 represent time series data of observations (*in orange*) and model results (*in blue*) at individual locations in the system. The vertical black line in each plot defines the point in time where the B and C snapshot figures were taken. Plots B1 and B2 outline the DO at a particular moment in time for all locations in the LDR. The red dots in B2 are the observations at that point in time, at different gauged locations on the river. The colors in B1 represent the DO at a single point in time. Plot C represents the floating (Lagrangian) DO observations in orange, with the modeled observations at each point in time and space in blue. Note that the two periods of time when the observations (*orange*) disappear correspond to gaps in the observed data. An animated version of this figure is available on PGE's website at portlandgeneral.com/waterquality.

The pH of the LDR is primarily a function of biological activity in the river and the alkalinity, pH, and algae entering the river from the reservoirs and the LDR tributaries. Similar to DO, pH shows a pronounced diurnal pattern as biological activity cycles on and off each day (Figure 10-12, Figure 10-13, and Figure 10-14). Observed pH values are typically found within the diurnal variation captured by the model, although in some areas, particularly from Sandy Beach to Rattlesnake, the model appears to overestimate pH values, particularly during the verification period in 2016. The overestimation is likely a result of complex hydrodynamics in and around Sherars Falls, which are not well captured by the 1-D hydrologic model in 2Kw. In both years, observed pH is captured accurately by the model at both Kloan Rapids (LDR20) and the River Mouth (LDR21). The short-term simulations outline the longitudinal pattern in pH and further suggests that the model reasonably captures pH at most locations (Figure 10-14).

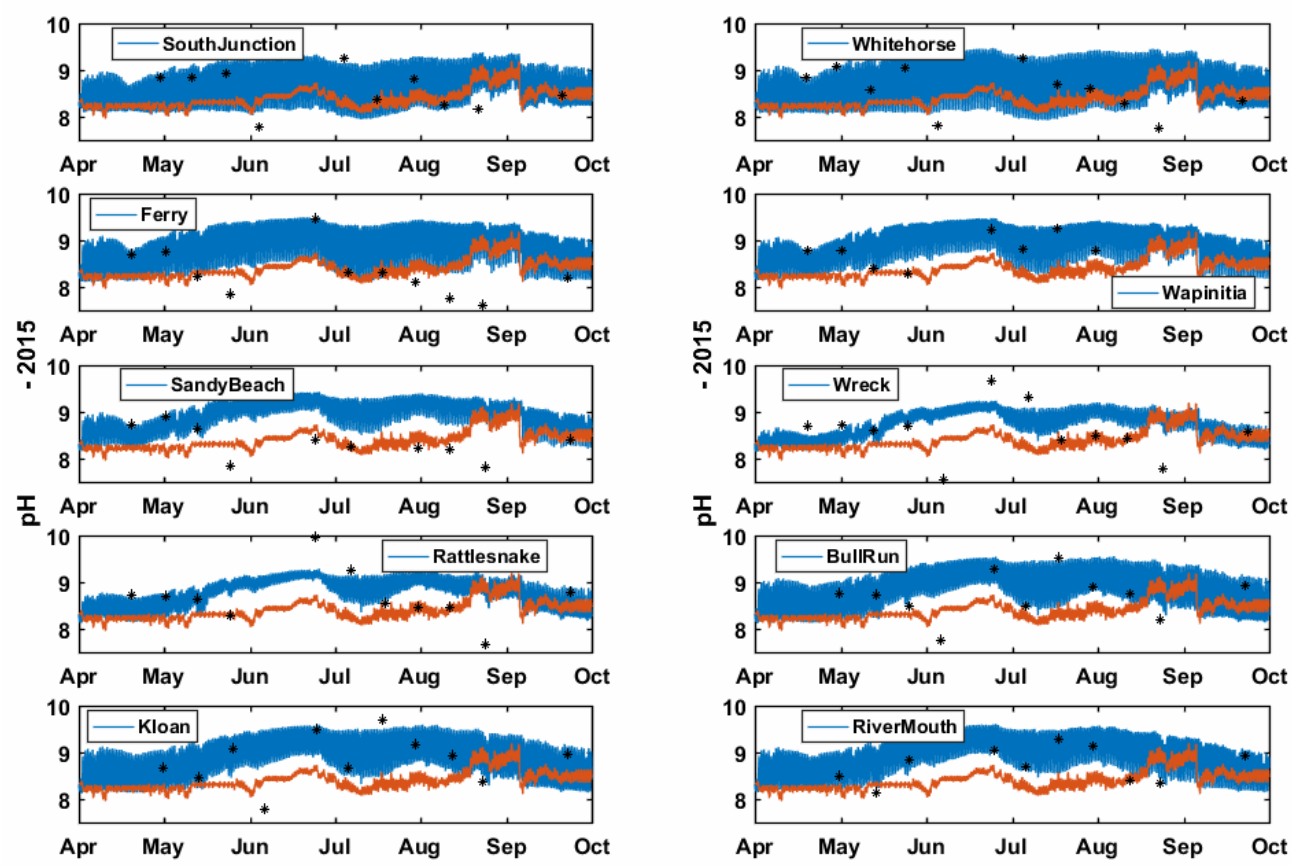

Figure 10-12. Simulated and observed pH during 2015. The black dots represent observations, the blue line represents simulated pH, and the orange line represents the upstream pH boundary condition (included for reference).

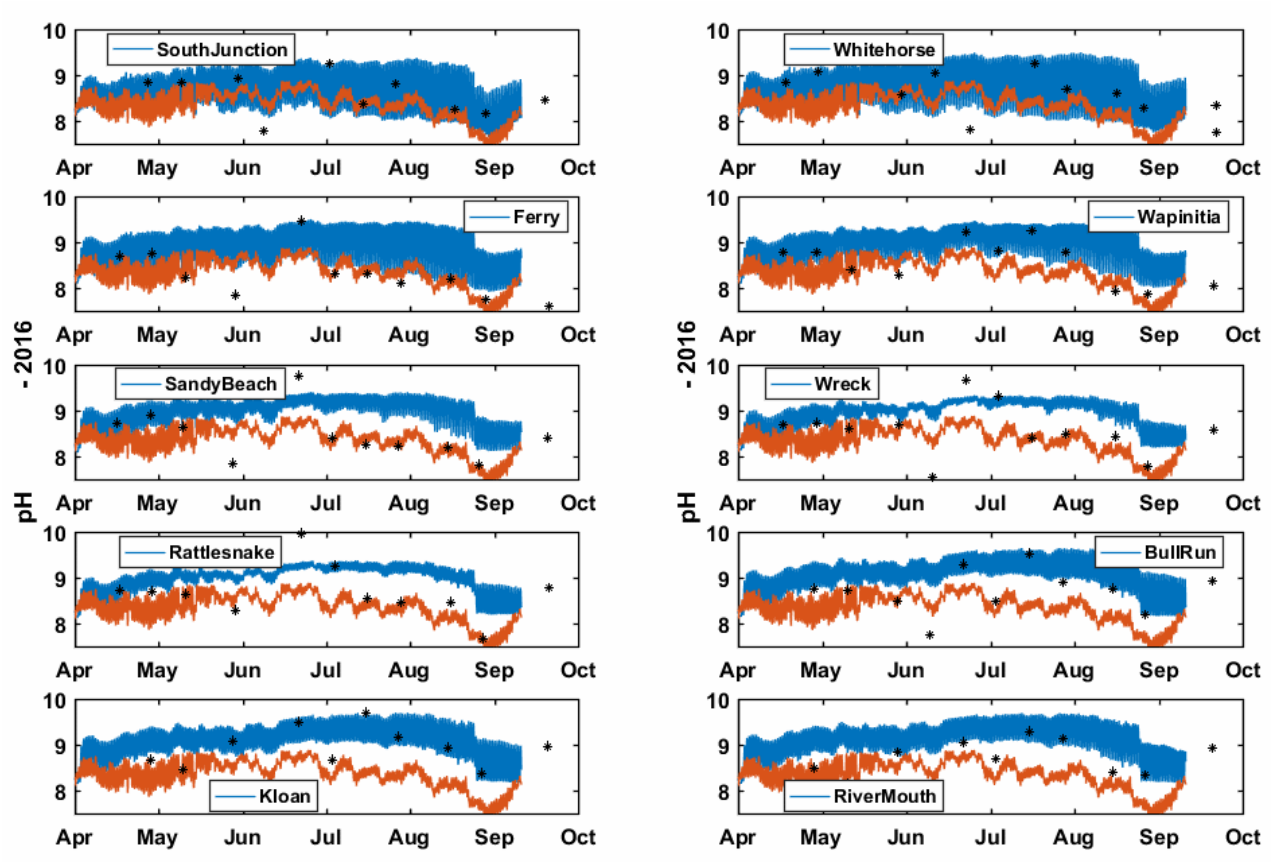

Figure 10-13. Simulated and observed pH during 2016. The black dots represent observations, the blue line represents simulated pH, and the orange line represents the upstream pH boundary condition (included for reference).

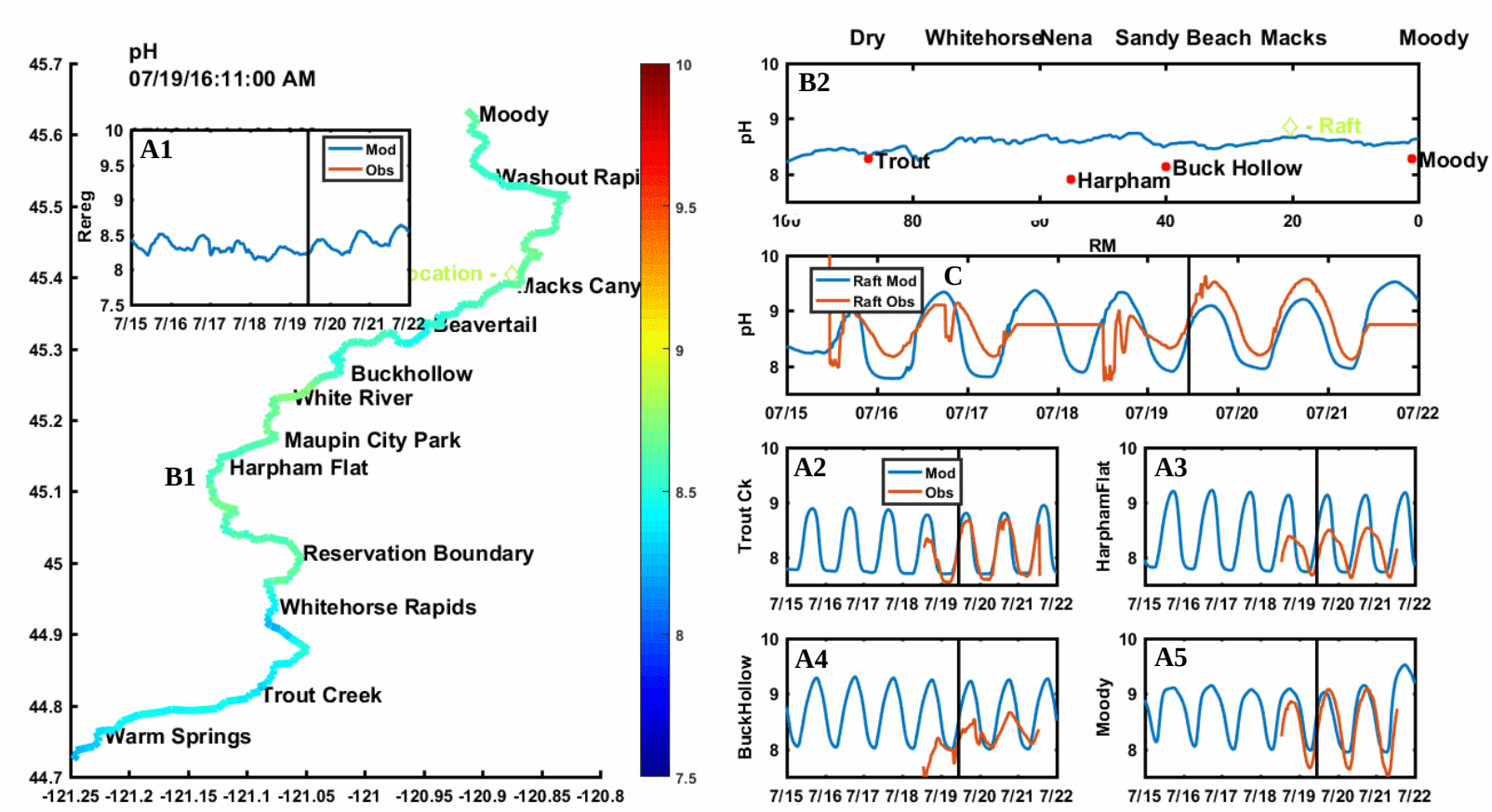

Figure 10-14. Combined Eulerian and Lagrangian viewpoints of simulated and observed pH dynamics in the LDR. Plots labeled A1–A4 represent time series data of observations (*in orange*) and model results (*in blue*) at individual locations in the system. The vertical black line in each plot defines the point in time where the B and C snapshot figures were taken. Plots B1 and B2 outline the pH at a particular moment in time for all locations in the LDR. The red dots in B2 are the observations at that point in time, at different gauged locations on the river. The colors in B1 represent the pH at a single point in time. Plot C represents the floating (Lagrangian) pH observations in orange, with the modeled observations at each point in time and space in blue. Note that the two periods of time when the observations (*orange*) disappear correspond to gaps in the observed data. An animated version of this figure is available on PGE's website at portlandgeneral.com/waterquality.

10.7.3.2 Nitrogen and Phosphorus

Nitrogen and phosphorus are the primary nutrients that exert control on biological production in the LDR. Primary sources for both are the various tributaries to the LDR and the Project. The 2Kw model simulates the primary exchange pathways for both nutrients, including biological exchange between live biological components, particulate organic matter, and inorganic forms of each nutrient. The primary observational data for nutrients includes NO_3, ammonium, TN, and TP. While the model uses NH_3-N as input, we present results for ammonium-N, as it tends to be higher at pH values typically found in the LDR.

NO_3 is characterized by an increase over the summer periods, evident across all observation points (Figure 10-15 and Figure 10-16). In addition, the NO_3 values tend to decrease in the downstream direction. The increase in NO_3 over the summer period is primarily driven by discharge of NO_3 from LBC, where NO_3 increases with reservoir productivity. As water moves through the LDR, NO_3 is assimilated through biological activity, leading to decreases in the downstream direction.

NH_3 concentrations are lower than NO_3 concentrations, primarily because the highly oxygenated riverine environment supports the oxidation of NH_3 to NO_3 through nitrification. The overall pattern suggests an increase in NH_3 concentrations over the summer period, similar to NO_3. This pattern and the low concentrations are reasonably captured by the model (Figure 10-17 and Figure 10-18).

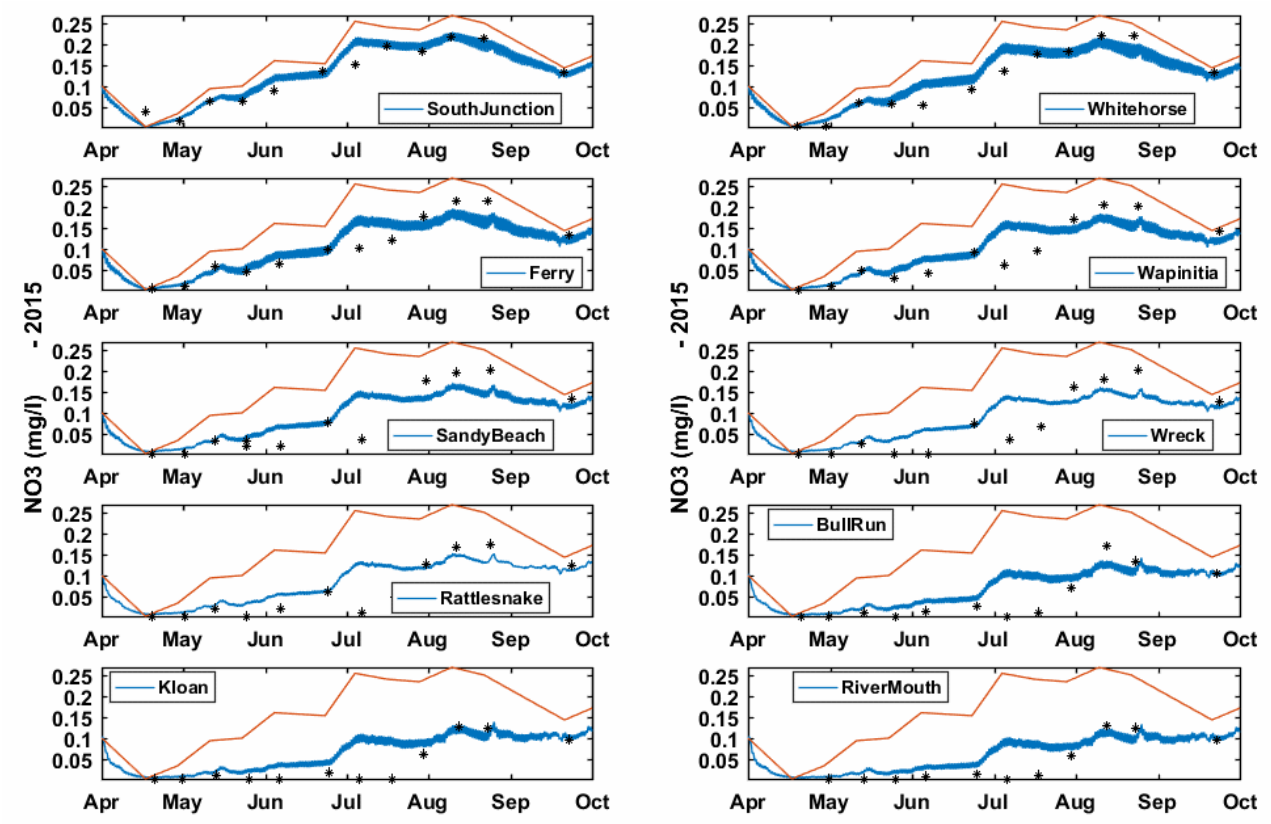

Figure 10-15. Simulated and observed NO_3 during 2015. The black dots represent observations, the blue line represents simulated NO_3, and the orange line represents the upstream NO_3 boundary condition (included for reference).

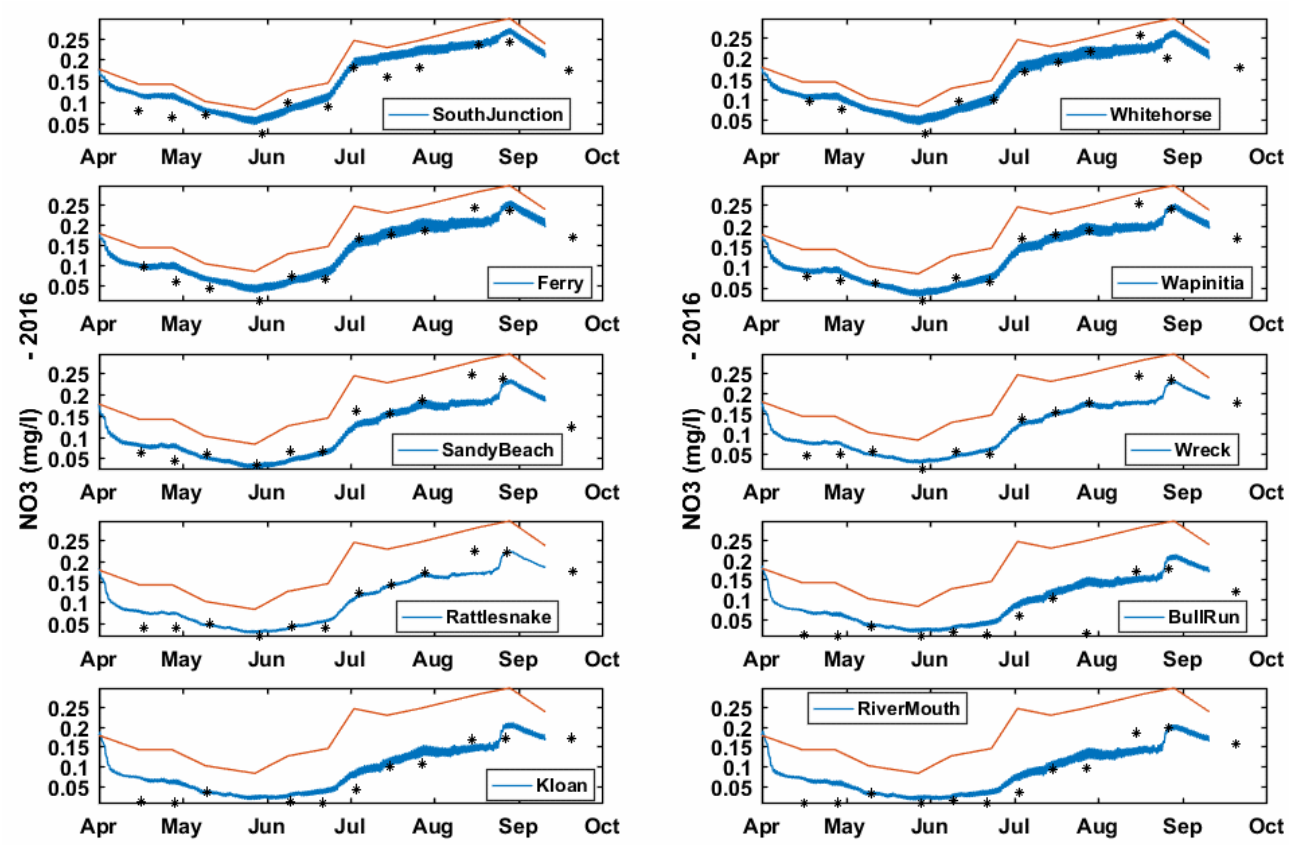

Figure 10-16. Simulated and observed NO_3 during 2016. The black dots represent observations, the blue line represents simulated NO_3, and the orange line represents the upstream NO_3 boundary condition (included for reference).

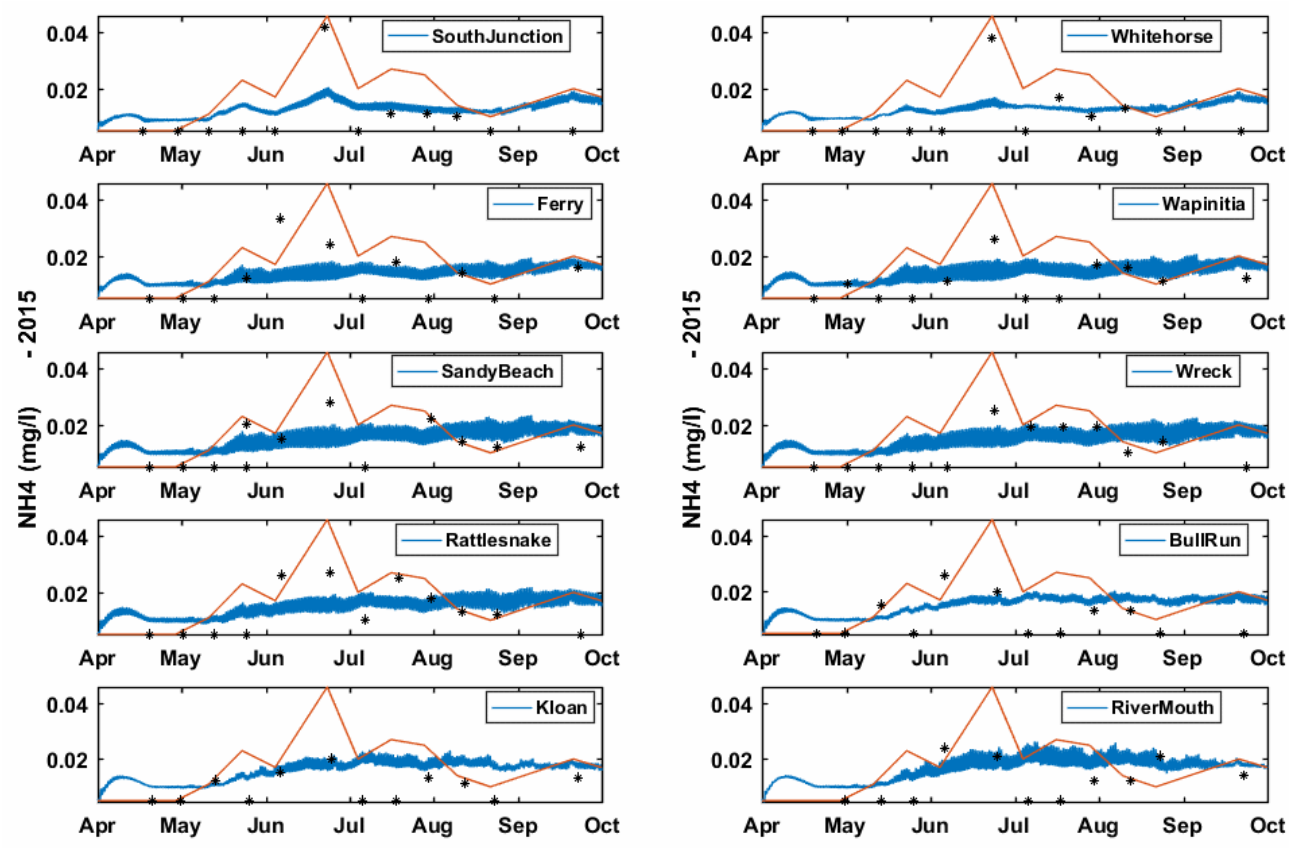

Figure 10-17. Simulated and observed ammonium during 2015. The black dots represent observations, the blue line represents simulated ammonium, and the orange line represents the upstream ammonium boundary condition (included for reference).

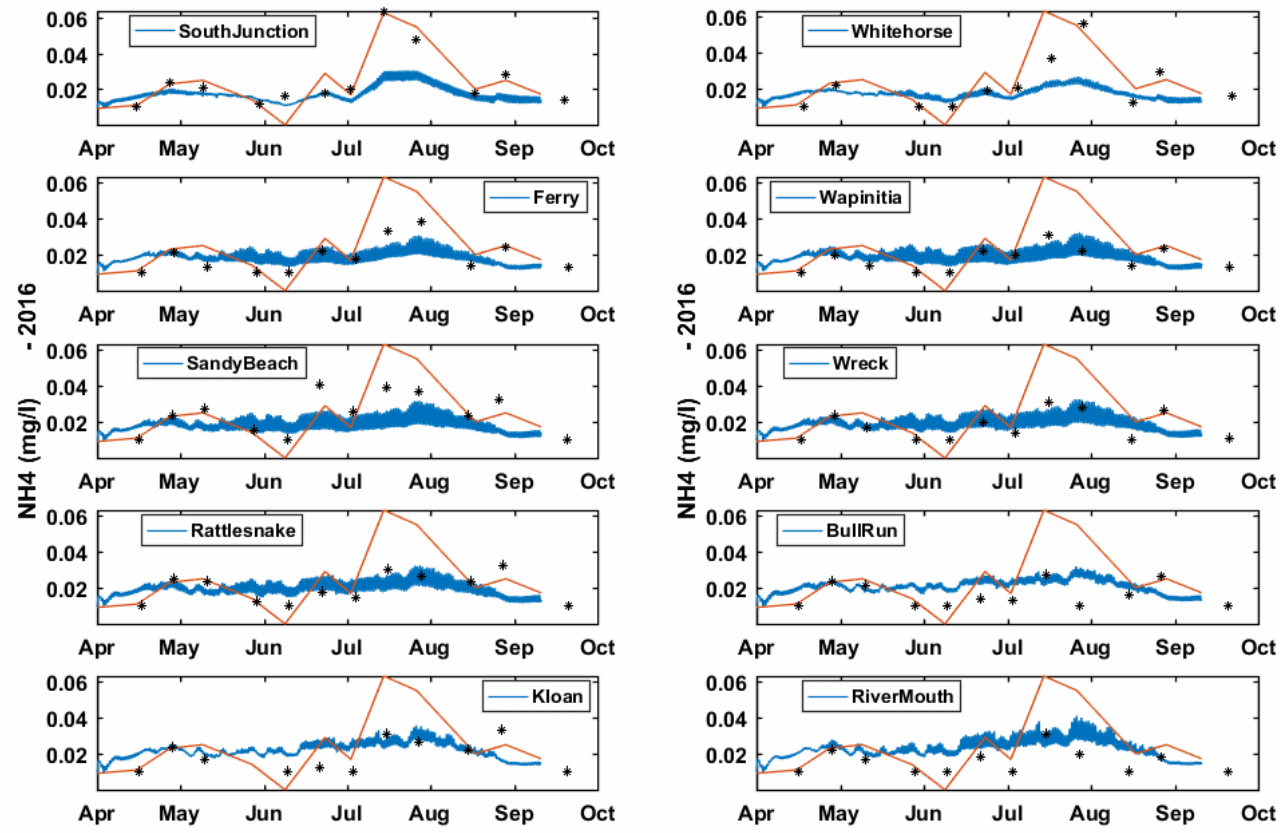

Figure 10-18. Simulated and observed ammonium during 2016. The black dots represent observations, the blue line represents simulated ammonium, and the orange line represents the upstream ammonium boundary condition (included for reference).

TN in the 2Kw model represents the sum of all nitrogen in NO_3, NH_3, and organic nitrogen and in algae. The model captures both the magnitude and evolution of TN throughout the system, which, given good approximations for both NO_3 and NH_3, suggests that organic nitrogen is also well simulated (Figure 10-19 and Figure 10-20). Organic nitrogen increases as plants (algae and periphyton) die and decreases through hydrolysis and particulate settling, although settling is not relevant in a fast-moving river like the LDR.

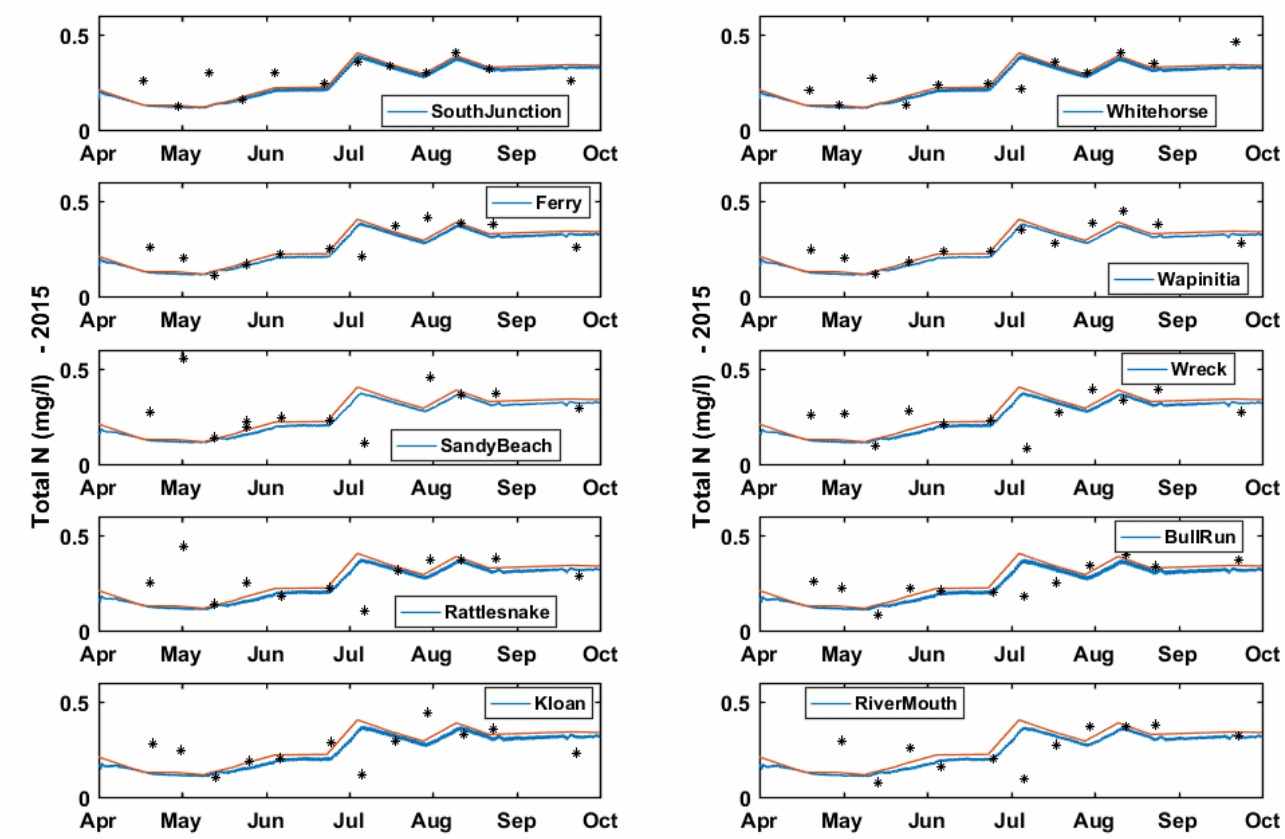

Figure 10-19. Simulated and observed TN during 2015. The black dots represent observations, the blue line represents simulated TN, and the orange line represents the upstream TN boundary condition (included for reference).

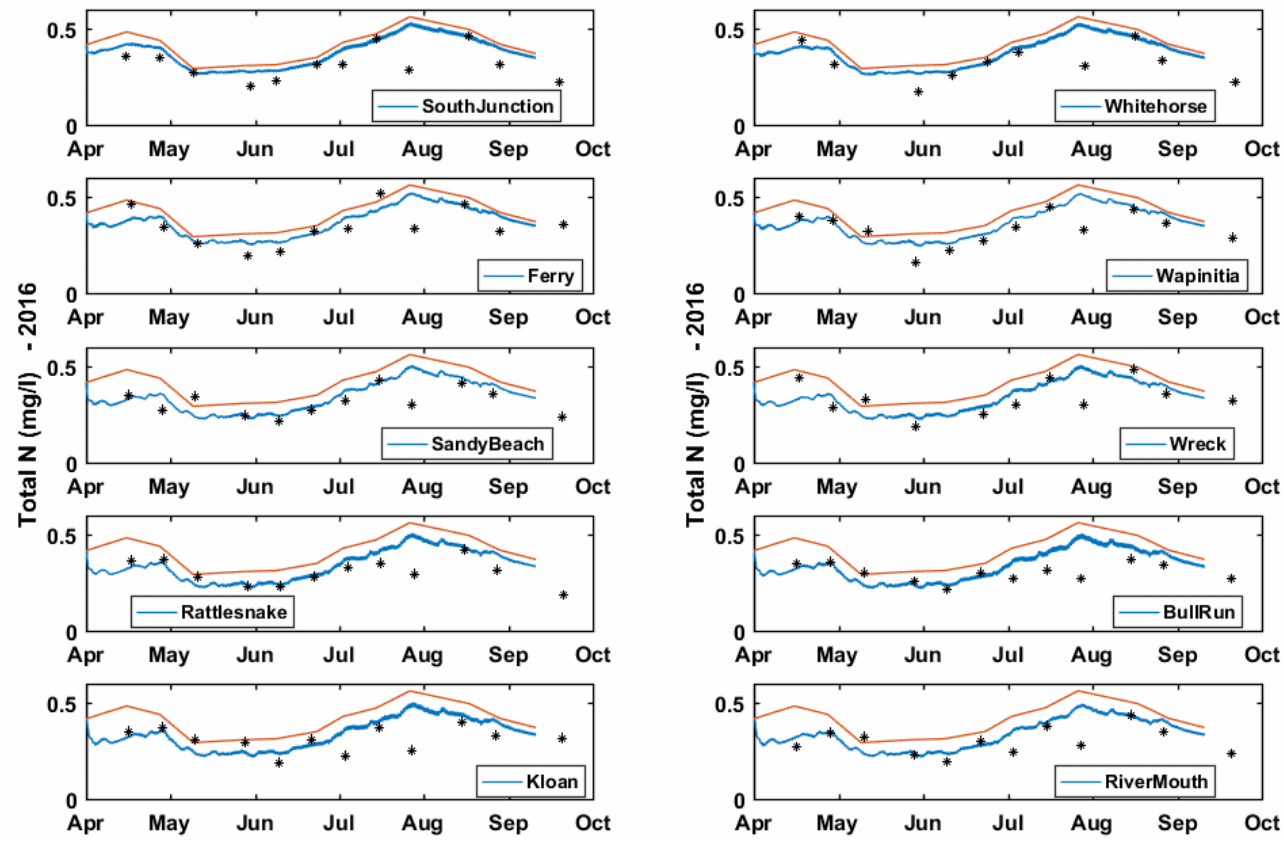

Figure 10-20. Simulated and observed TN during 2016. The black dots represent observations, the blue line represents simulated TN, and the orange line represents the upstream TN boundary condition (included for reference).

Phosphorus is a key biological nutrient but, because the LDR is a nitrogen-limited system, it exists in abundance and concentrations tend to be similar throughout the system. As with nitrogen, phosphorus does increase throughout the summer period as a function of increased biological activity. The model reproduces observed phosphorus, both in space and time (Figure 10-21 and Figure 10-22).

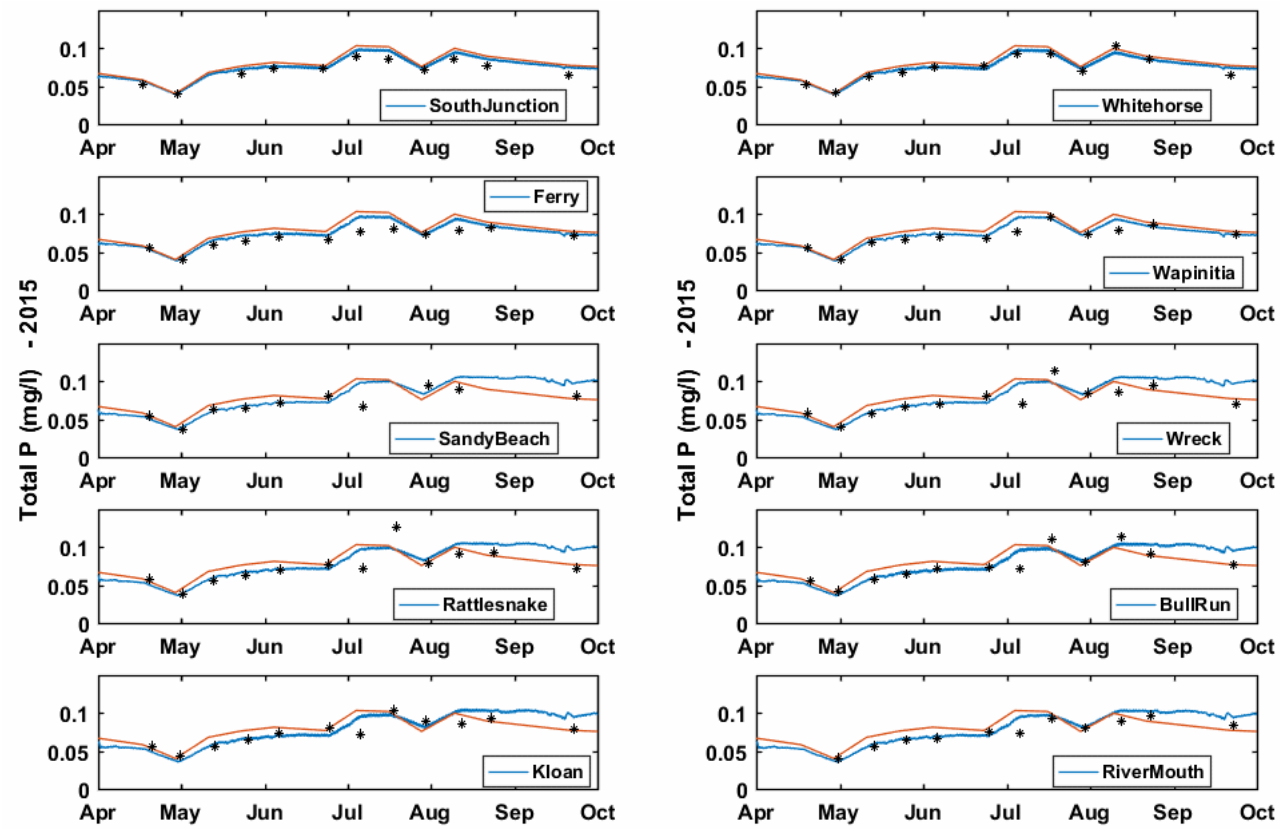

Figure 10-21. Simulated and observed TP during 2015. The black dots represent observations, the blue line represents simulated TP, and the orange line represents the upstream TP boundary condition (included for reference).

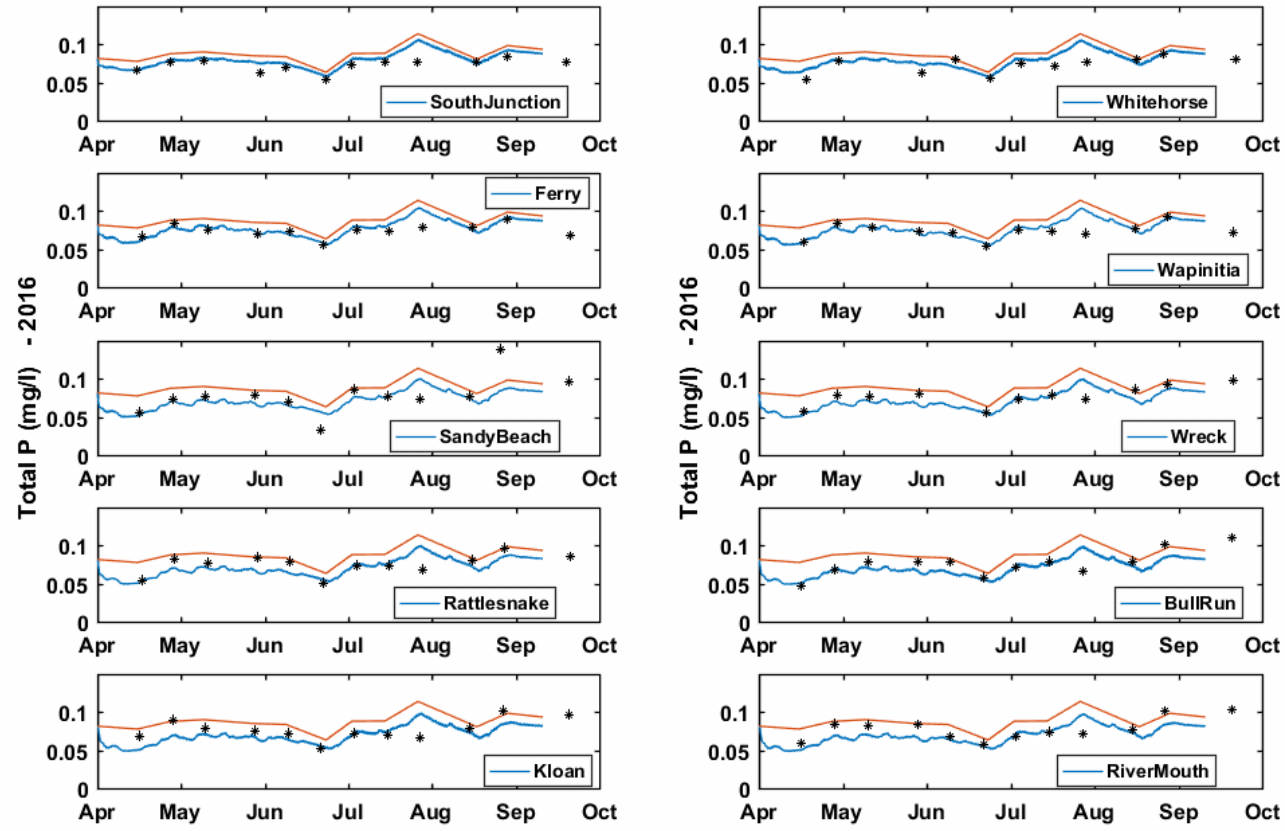

Figure 10-22. Simulated and observed TP during 2016. The black dots represent observations, the blue line represents simulated TP, and the orange line represents the upstream TP boundary condition (included for reference).

10.7.3.3 Conductivity, alkalinity, and chloride

The 2Kw model treats conductivity (Figure 10-23 and Figure 10-24), Cl^- (Figure 10-25 and Figure 10-26), and alkalinity (Figure 10-27 and Figure 10-28) all as conservative quantities. The conservative nature of the quantities suggests they are useful in establishing that the transport components of the model (separate from the biological components) are reasonably well captured. In almost all cases, both observations and model results bear out the conservative nature of these quantities. The exception occurred in the summer of 2016, when a continuous record of conductivity at the ReReg Dam was available. In that case, there were two observation periods in and around July 2016 during which model results diverge from the observations by around 20 µS/cm. Given the success of the model throughout 2015 and 2016, these differences likely are related to calibration issues associated with the continuous conductivity measurements.

The large difference in continuous conductivity at the ReReg site (LDR01) and observed conductivity at Whitehorse (LDR07) lends further credence to this explanation (Figure 10-23 and Figure 10-24).

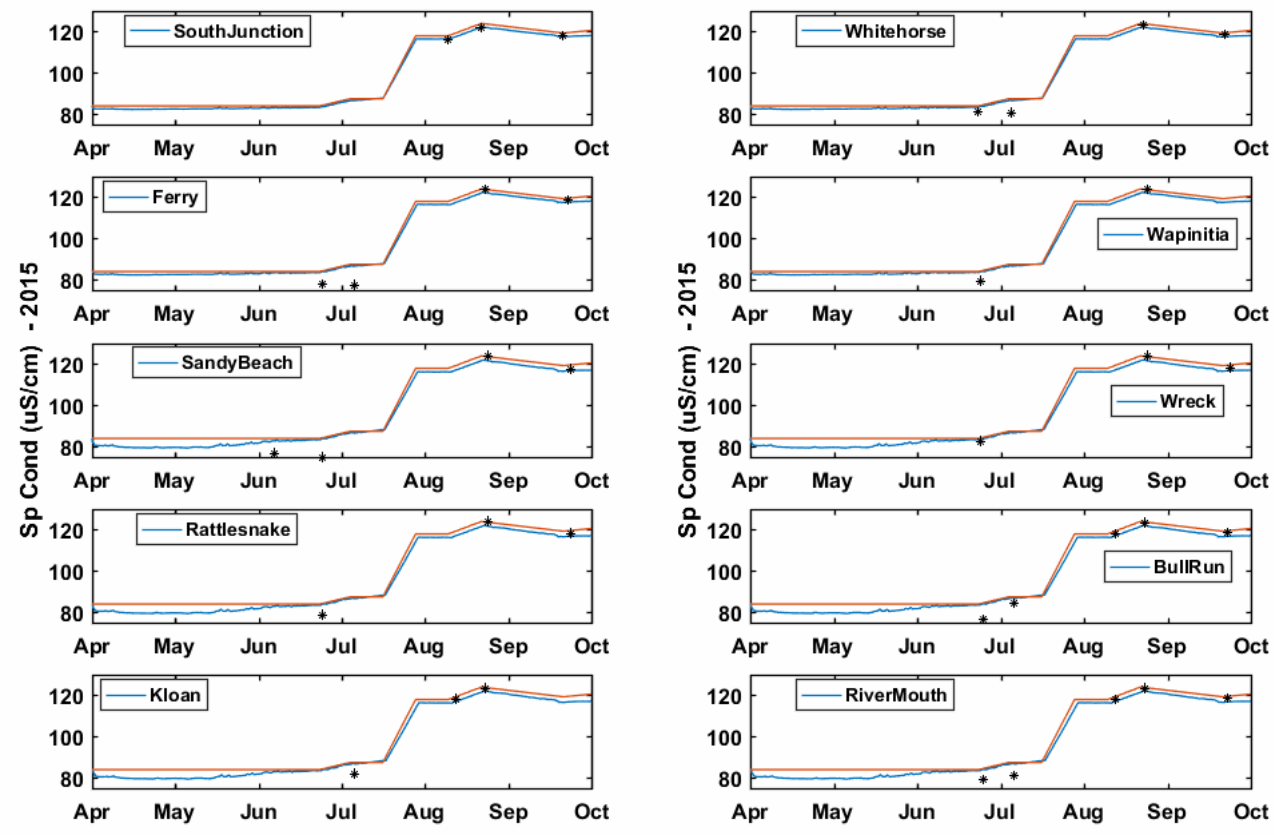

Figure 10-23. Simulated and observed conductivity during 2015. The black dots represent observations, the blue line represents simulated conductivity, and the orange line represents the upstream conductivity boundary condition. The boundary condition is included for reference.

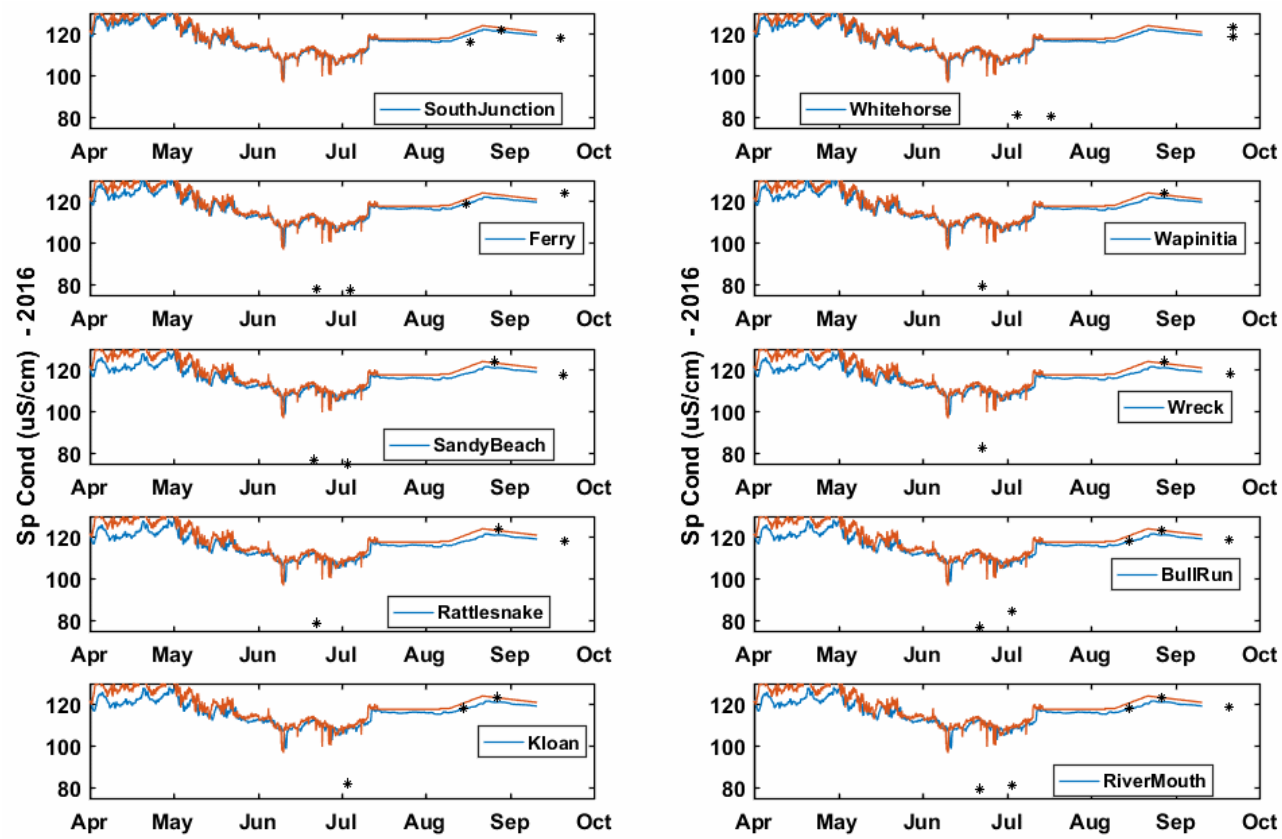

Figure 10-24. Simulated and observed conductivity during 2016. The black dots represent observations, the blue line represents simulated conductivity, and the orange line represents the upstream conductivity boundary condition (included for reference). From April through mid-July, a continuous conductivity record is available at the ReReg Dam. That continuous record was used as model input during the period of time for which it was available.

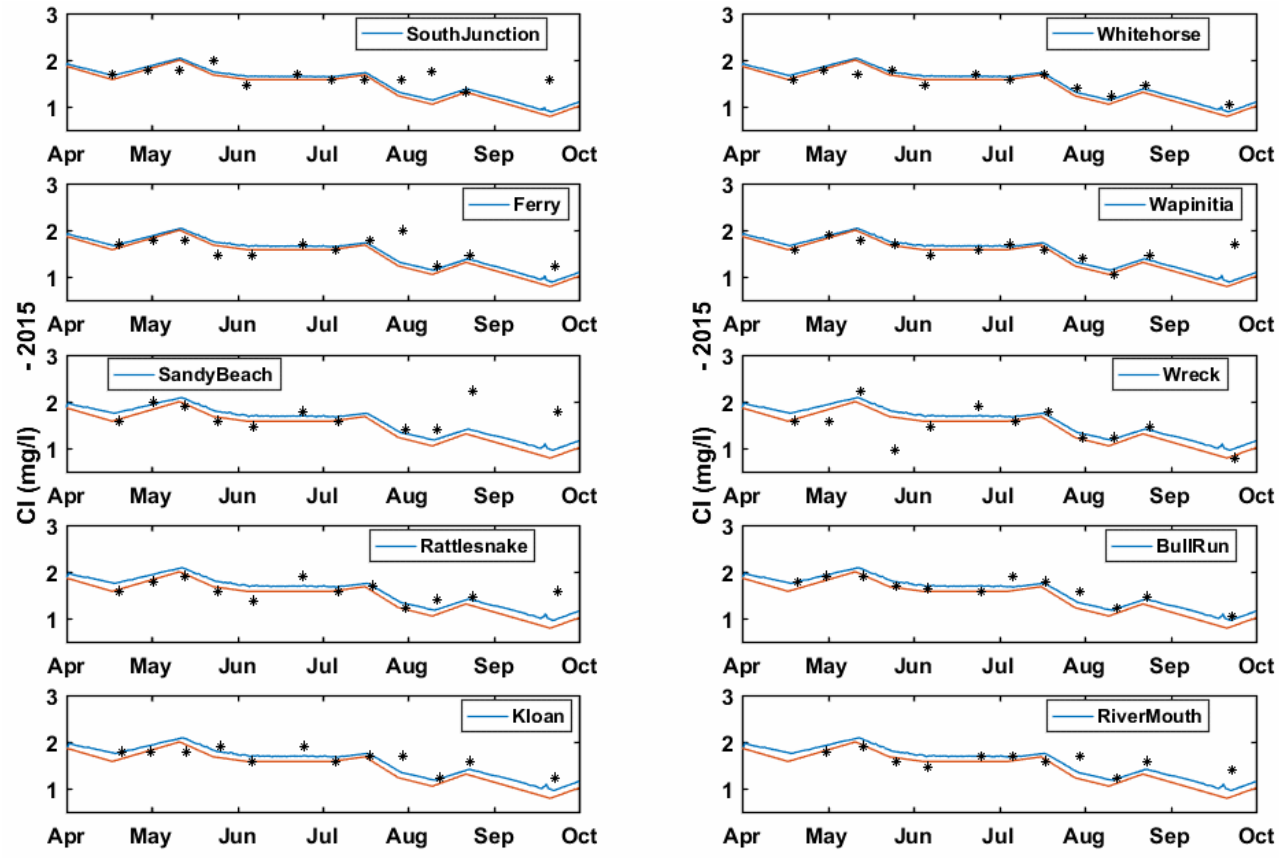

Figure 10-25. Simulated and observed Cl^- during 2015. The black dots represent observations, the blue line represents simulated Cl^-, and the orange line represents the upstream Cl^- boundary condition (included for reference).

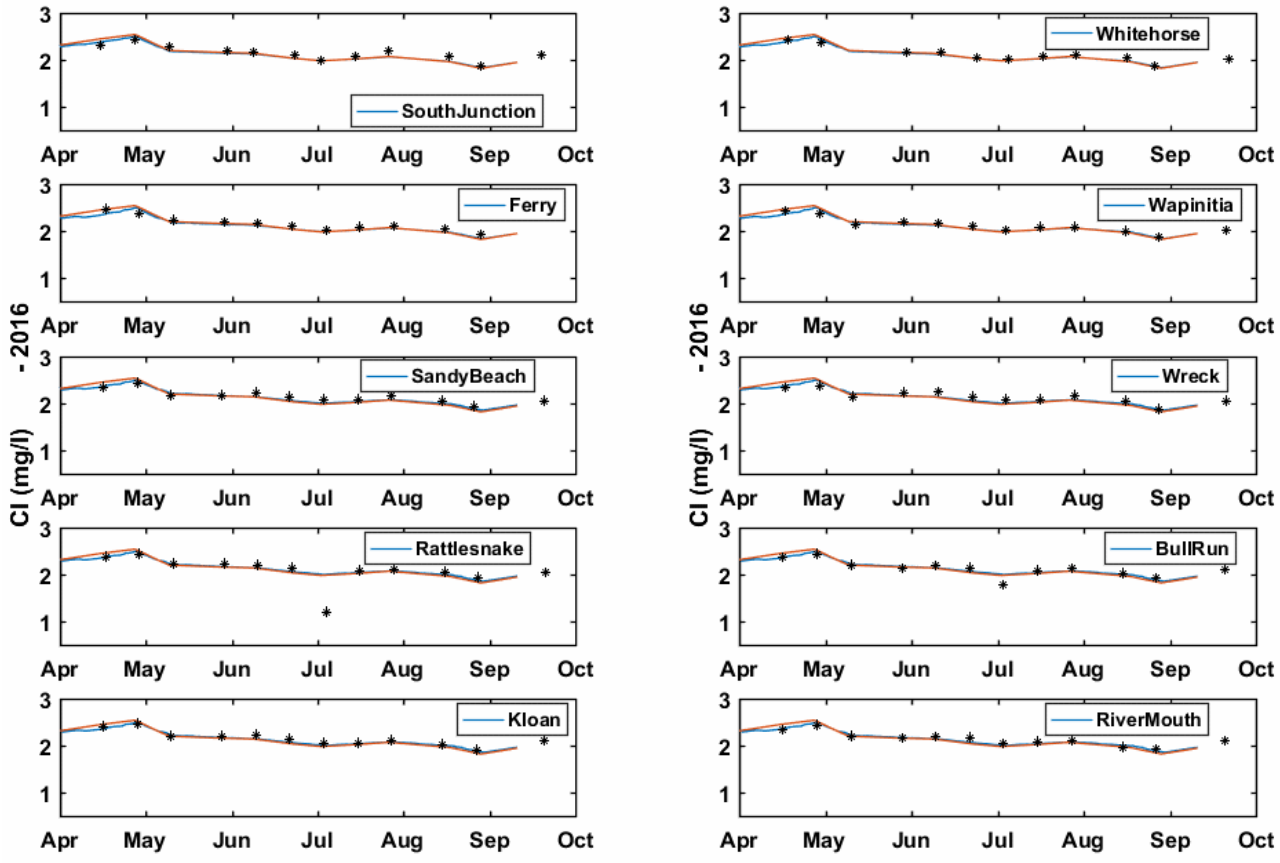

Figure 10-26. Simulated and observed Cl^- during 2016. The black dots represent observations, the blue line represents simulated Cl^-, and the orange line represents the upstream Cl^- boundary condition (included for reference).

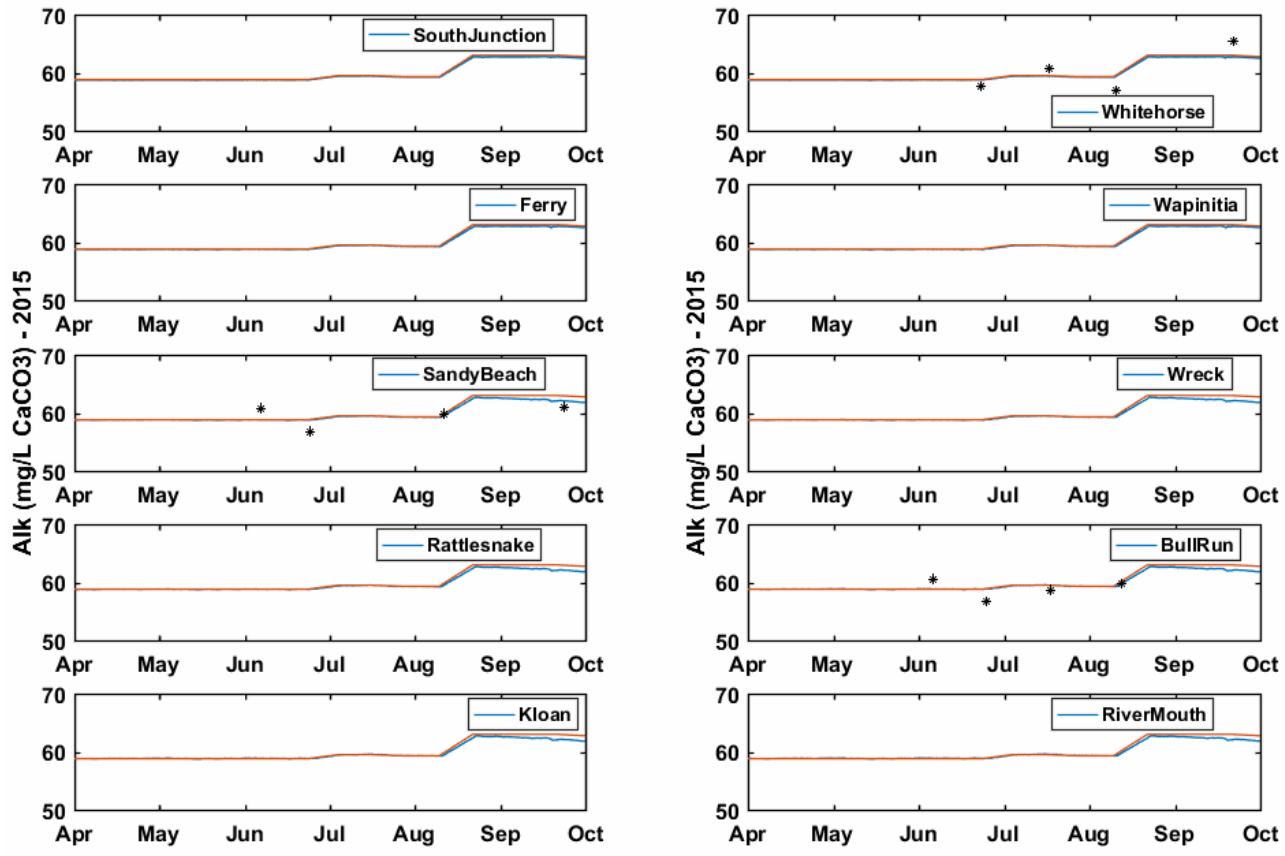

Figure 10-27. Simulated and observed alkalinity during 2015. The black dots represent observations, the blue line represents simulated alkalinity, and the orange line represents the upstream alkalinity boundary condition (included for reference).

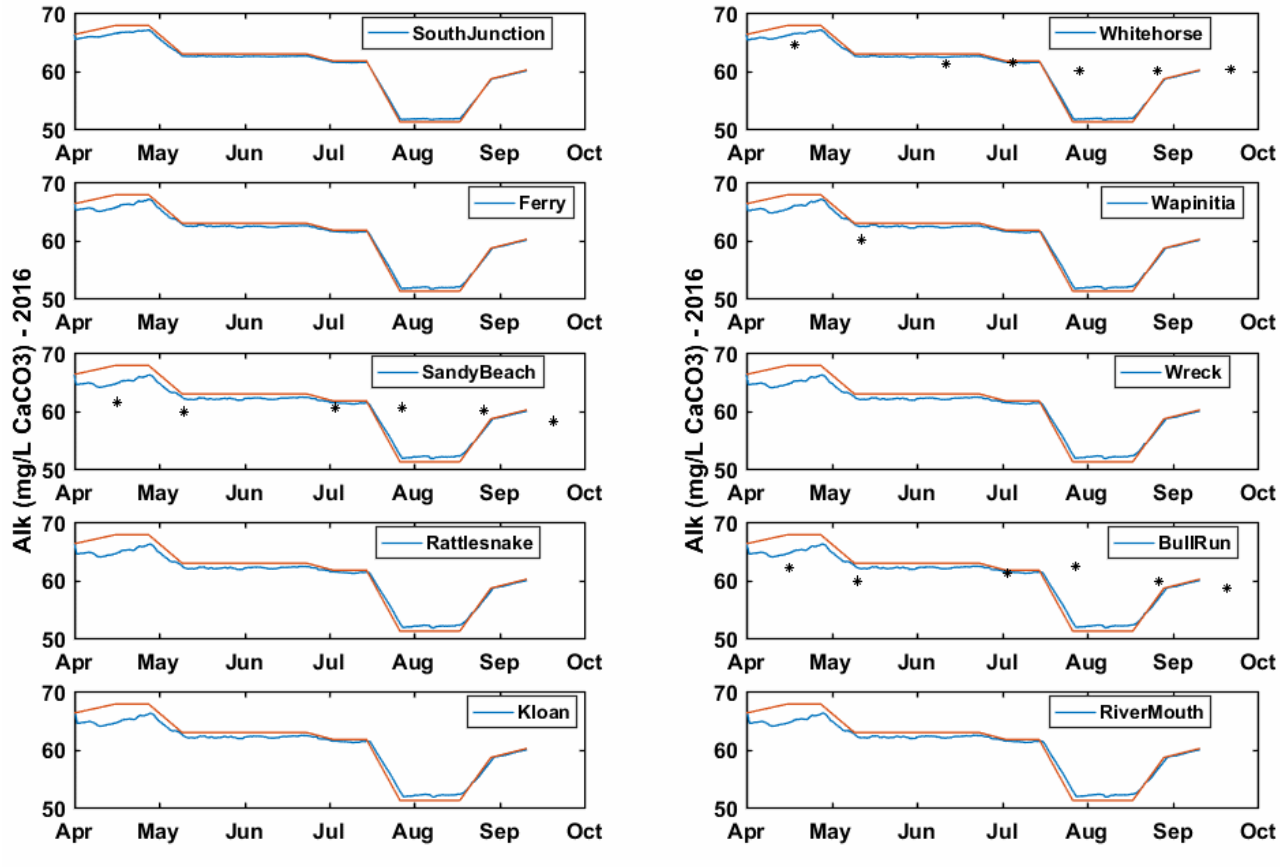

Figure 10-28. Simulated and observed alkalinity during 2016. The black dots represent observations, the blue line represents simulated alkalinity, and the orange line represents the upstream alkalinity boundary condition (included for reference).

10.7.3.4 Phytoplankton and Periphyton

Modeled and observed phytoplankton dynamics are outlined in Figure 10-29 and Figure 10-30. Results indicate that the model provides an adequate simulation of phytoplankton development throughout the LDR. An important feature of the results (both observed and modeled) is that the magnitude of the algal biomass at the ReReg Dam moves through the LDR without much change. That behavior is attributable to the short residence times in the LDR. At around 1½ days, the residence time leaves two full-sun periods of growth, at most.

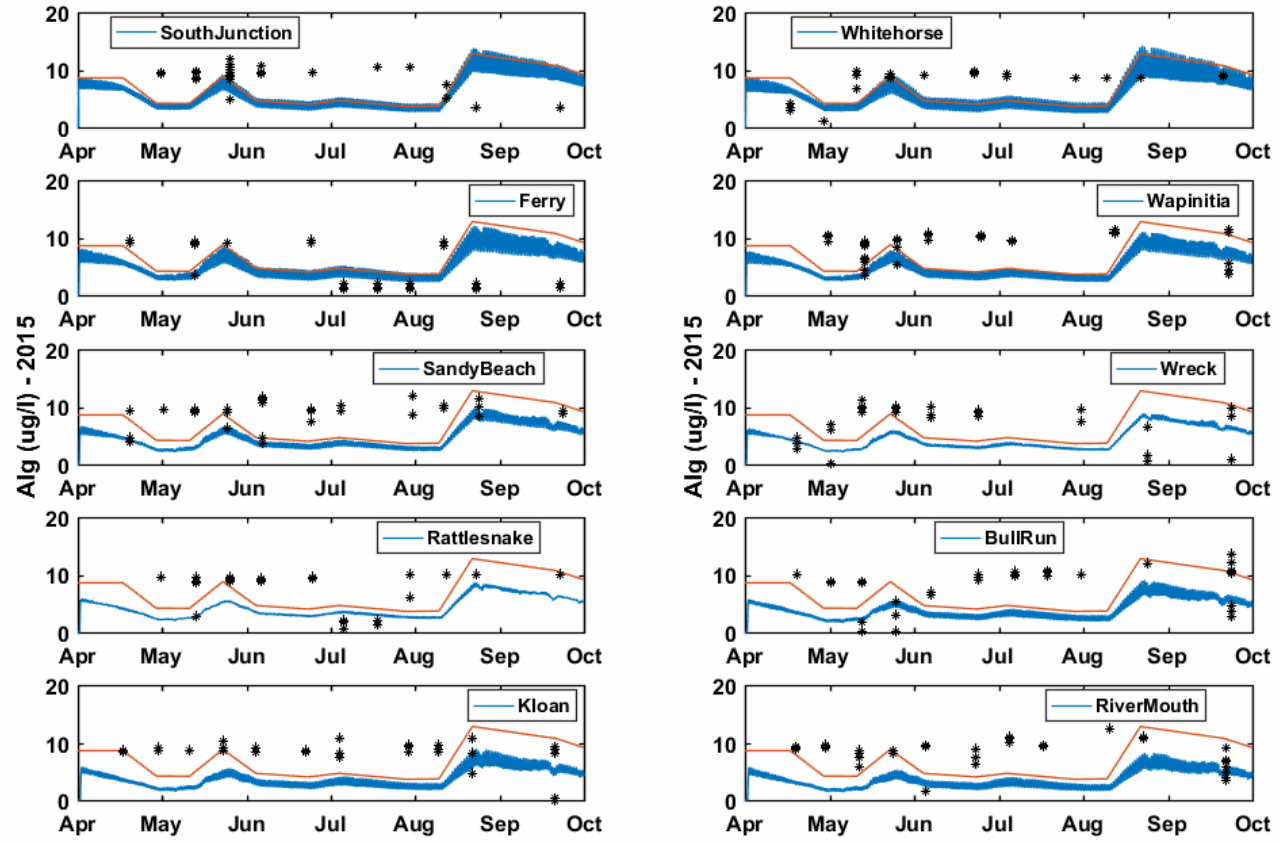

Figure 10-29. Simulated and observed phytoplankton during 2015. The black dots represent observations, the blue line represents simulated phytoplankton, and the orange line represents the upstream phytoplankton boundary condition (included for reference).

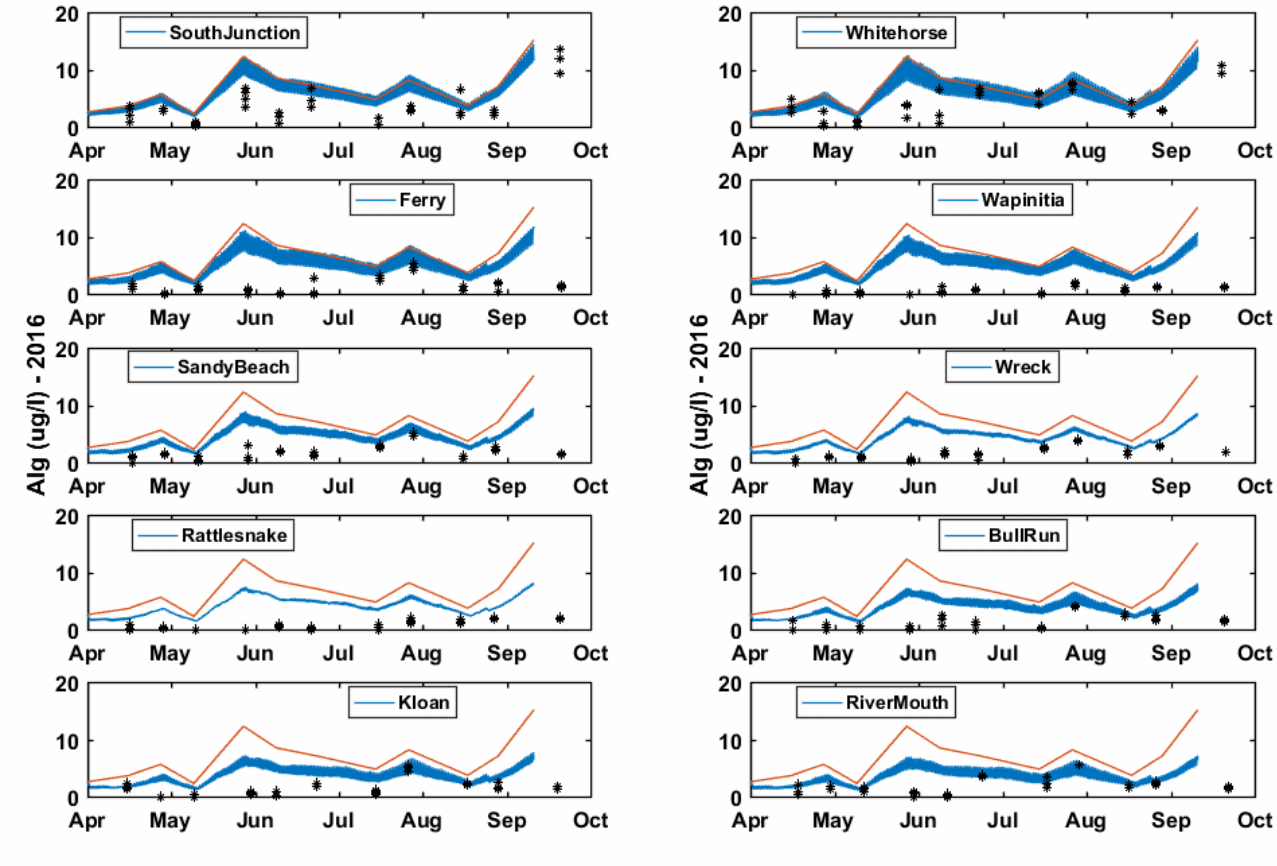

Figure 10-30. Simulated and observed phytoplankton during 2016. The black dots represent observations, the blue line represents simulated phytoplankton, and the orange line represents the upstream phytoplankton boundary condition (included for reference).

As noted earlier, the simulation of periphyton dynamics in a large river using a 1-D model is limited somewhat because the model does not capture the range in water depths or velocities found in the river cross section. The periphyton model relies on the maximum light penetration depth to drive growth, which further limits the utility of an average depth. Additionally, periphyton sampling is limited to a small set of locations with wadable depths, so that sampled periphyton biomass will tend to occur where light penetration reaches the bottom and where periphyton will tend to be more abundant. With these challenges, the periphyton model is one area in which limitations of the model algorithms might impact the model's capacity to fully capture all relevant dynamics. Nonetheless, the important feature is that the model does include periphyton growth and its interaction with the water quality variables. While it will not capture

all of the spatial variability of periphyton growth, it does appear to adequately approximate the general magnitude of observed periphyton dynamics (Figure 10-31 and Figure 10-32),

Elements of the periphyton model, particularly those associated with scour during high-discharge events, were developed based on observations from a single, much smaller watershed located in the Swiss Alps (Uehlinger et al. 1996). The difference in scales between the empirical dataset on which the model was based and the LDR are not necessarily unusual but could impact the model's capacity to simulate the effect of high flows on scouring. A newly developed extension of the 2Kw periphyton model has been developed to more realistically represent variable cross sections in large rivers (Flynn et al., 2013). That set of algorithms is not currently included in the 2Kw model, although future modeling efforts in the LDR could benefit from incorporating this model or one like it into the effort. Section 11 explores the ability of the 2Kw model, as set up for this study, to simulate flushing flows and regrowth dynamics.

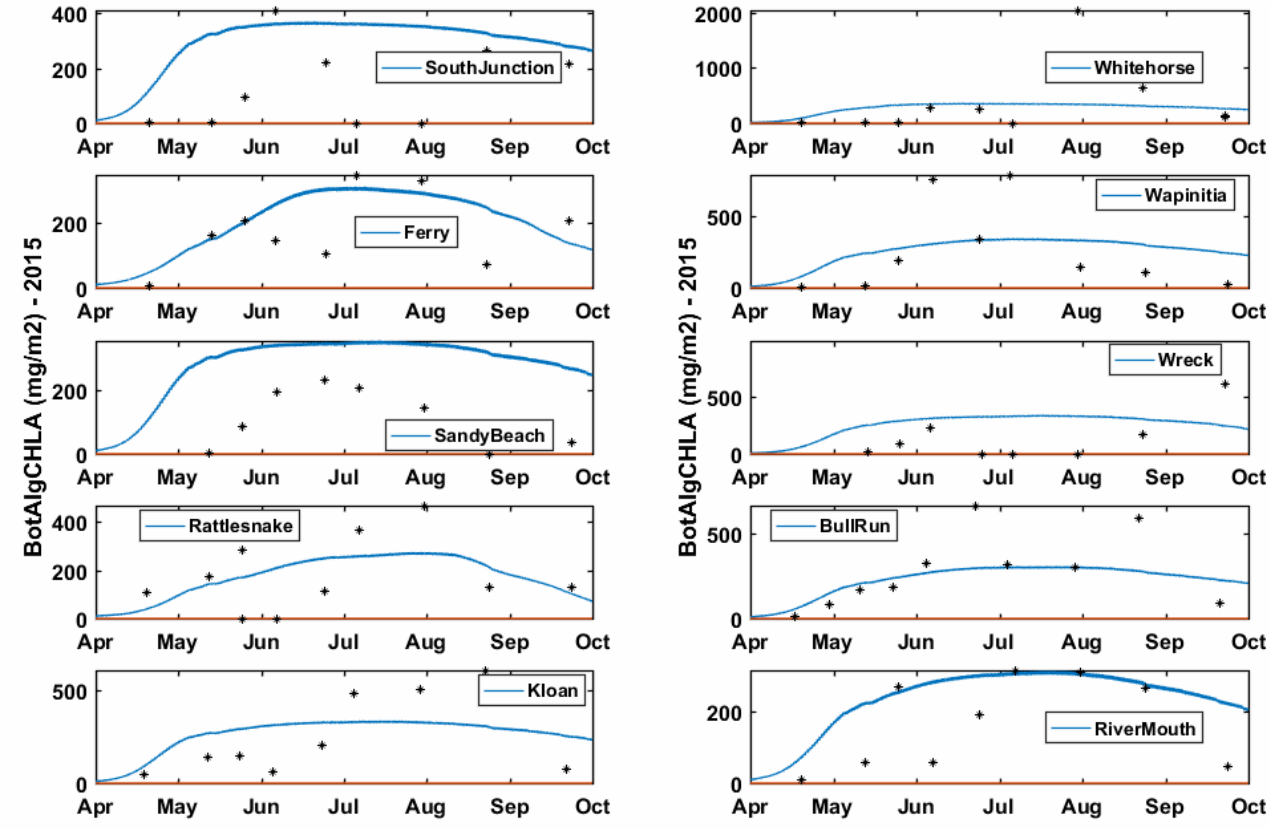

Figure 10-31. Simulated and observed periphyton (as chlorophyll *a*) during 2015. The black dots represent observations, and the blue line represents simulated periphyton.

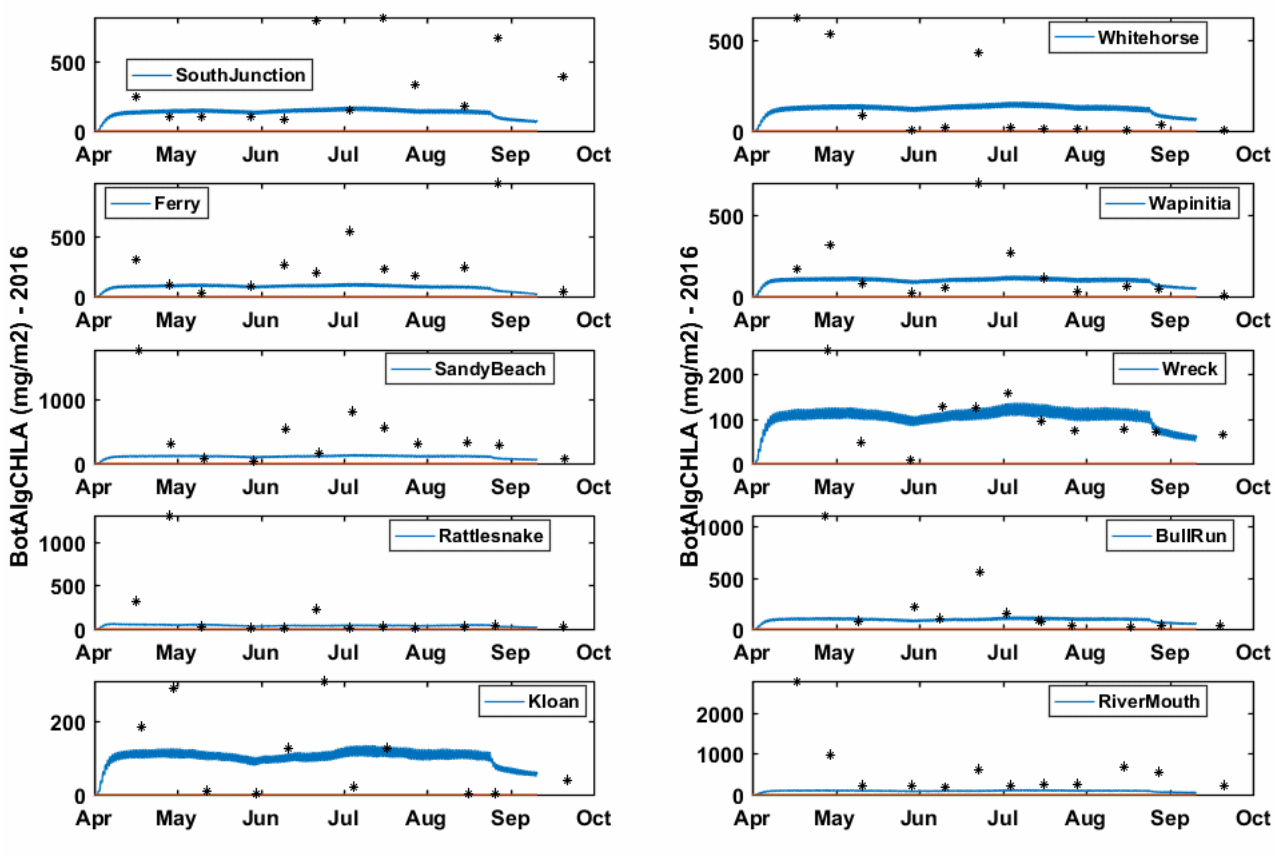

Figure 10-32. Simulated and observed periphyton (as chlorophyll *a*) during 2016. The black dots represent observations, and the blue line represents simulated periphyton.

10.8 Conclusions

A 1-D hydrology and water quality model was developed to represent the LDR. Data collected during 2015 was used to calibrate the model and data from 2016 was used to provide further evaluation of the model's consistency with available data sources. In addition, a third model representing the spring, summer, and fall of 2017 has also been developed. That model will be used, with the 2016 model, in Section 11 to provide the basis for a scenario analysis in the LDR.

11 Scenario Analysis: Integrated Modeling of Project Reservoirs and the Lower Deschutes River

A primary objective for developing the W2 and 2Kw models for the Project and the LDR was to explore how potential changes in watershed management, climate, and Project operations may influence water quality in the LDR. To accomplish this, we specified a set of scenarios and developed a set of linked W2/2Kw model runs to capture key parameters defining those scenarios. In most cases, the parameters for the calibrated model were used, along with modified boundary conditions that reflected scenario intent. The exception to this approach was allowing the maximum periphyton growth rate to vary as a mechanism to incorporate scenario-specific changes into the species composition of periphyton.

The scenario definitions fall into three general categories:

- Applying different water release blends from the SWW.
- Altering reservoir management, including the installation of an epilimnetic curtain and reducing tributary nutrient concentrations.
- Exploring potential climate changes to long-term water temperatures and water quality.

Table 11-1 summarizes the assumptions behind each of the scenario definitions.

The key objectives of analyzing the scenarios are to evaluate water quality changes associated with Project operations changes and to explore the role of future climate on water quality. This study does not consider the impact of water quality changes on other trophic levels such as resident and anadromous fish and macroinvertebrates or the costs of scenario strategies, FERC license constraints, policy impacts, or recreational impacts. The scenario analysis is designed to provide a mechanism for quantifying water temperature and water quality in the system and determining how they might respond to changes expressed in the scenarios, not to advocate for any particular management strategy.

Table 11-1. Key assumptions behind the scenario definitions.

Scenario	Assumption
Baseline	Scenario results are compared against the calibrated model results from 2015–2017. Calibrated results are used as the baseline.
SWW 100/40	100% surface withdrawal from Mar 15 to June 15; 40% surface withdrawal, 60% bottom withdrawal for remainder of the year.
SWW 40	40% surface withdrawal, 60% bottom withdrawal year-round
No SWW	100% bottom withdrawal all year to mimic pre-SWW
Night Blend	100% surface withdrawal from 9 p.m. to 4 a.m. from Mar 15 to Jun 15; 40% surface withdrawal, 60% bottom withdrawal during remaining hours.
NO_3 Decrease	75% reduction of NO_3 and NH_4 in the inflow from the Crooked River and Willow Creek; SWW operation is the same as in the baseline.
N and P Reduction	50% reduction of PO_4, NO_3, and NH_4 from the Crooked River; SWW operation is the same as in the baseline
Curtain	Algae barrier installed in Round Butte forebay from Jun 15 to Sep 15.
Cold Flush	Continuous 60% bottom, 40% surface withdrawals from Jul 20 to Jul 25, 2015.
Flushing Flow	10,000 cfs flows from Apr 28 to 30.
Future Climate	Multiple climate change scenarios for 2039–2041 and 2089–2091.
Future Tributary Temperature	Estimates of tributary summer water temperature for 2040 and 2080.

Six key parameters are presented in the analysis of the scenarios: water temperature, pH, DO, conductivity, NO_3 and algae. A single zooplankton group was also included as a simulated state variable in the W2 model but have been left out of the scenario analysis for clarity. Phosphorous simulations were also left out of most scenario analyses as phosphorous is abundant throughout the system and does not appear to limit production. That result is explored in the N/P watershed reduction scenario, which includes an analysis of phosphorus.

A set of standard plots was developed for each scenario that includes daily time series across the simulation period comparing scenario and baseline (current conditions) results. The calibrated models outlined in sections 9 and 10 are used as the baseline. Using this approach focuses the

analysis on the change in water quality associated with each of the scenarios, with reference to the calibrated models.

For the reservoirs, time series from two key locations are included for each scenario. The locations are in the surface waters of Round Butte forebay and at the ReReg Dam tailrace. We also developed boxplots comparing the six parameters in the Round Butte, Pelton, and ReReg tailraces for each season (winter is defined as January, February, March; spring as April, May, June; summer as July, August, September; and fall as October, November, December). In cases in which the box-plots were not instructive, we have excluded them. Additionally, other targeted figures and tables were included as needed to more clearly outline key features of the different scenarios.

For the LDR, time-series plots and longitudinal profiles are used to show comparisons of the scenarios to the baseline results. The figures focus on time series at RM 96 (5 river miles downstream of ReReg Dam) and RM 1 (Moody), with time snapshot longitudinal profiles to provide a wider spatial context for the analysis. Our scenario analysis focuses on the 2016 and 2017 models; however, for some scenarios, conditions in 2015 were of interest, so we have included the calibration model as the basis for analyzing those scenarios. Conditions in 2015 were of particular interest in the Flushing Flow scenario because it had been proposed as a possible water quality management strategy during the warm dry summer of 2015.

Section 11.1 describes model limitations. Sections 11.2 through 11.12 describe each of the scenarios and present its simulated impacts on water quality variables. Section 11.13 evaluates the statistical significance between mean water quality values for each scenario and the baseline. Sections 11.14 and 11.15 describe the conclusions of the scenario analysis and areas for future research, respectively.

11.1 Model Limitations

We relied on the fact that the foundations of both models incorporate enough detail that the simulated changes associated with each scenario can provide meaningful feedback on how those changes might affect water quality. This report describes the limitations and shortcomings associated with the models that might impact their ability to forecast change. In cases in which

the temporal or spatial aggregation of the models appears to affect their ability to forecast change, we suggest undertaking smaller scale and more detailed reach-level observational studies to more fully evaluate potential water quality in the LDR. This suggestion is particularly relevant to developing the predictive capacity related to periphyton growth and development. The 2Kw model assumes that periphyton can be properly characterized with a 1-D model, but that assumption begins to break down with a river system as large as the LDR, in which we expect wide variation in periphyton density across the channel cross section and within each of the 800-m model segments. Recent work has proposed a more disaggregated periphyton model to better capture dynamics in large rivers (Flynn et al., 2013), but that model has not yet been included in the 2Kw framework. Despite the potential shortcomings associated with its scale, the periphyton model does capture magnitudes of attached algae densities (in Section 10). The key role of attached algae in regulating water quality in the LDR is further demonstrated in Section 11.8.

The W2 model allows for multiple algal groups. We included two: the first representing diatoms and the second representing cyanobacteria. However, the 2Kw model can accommodate only a single group, so the diatoms and cyanobacteria output from the W2 models was summed as a single group of algae for input into the 2Kw model. If a scenario results in differentiation between diatoms and cyanobacteria, we included some disaggregated analysis within the W2 model results. But, because of limitations in the 2Kw model, those disaggregated algae cannot be propagated through to the LDR.

While no calibration of the 2Kw model was developed based on pre-SWW conditions, the analysis in Section 7 indicated that pre-SWW periphyton densities were lower than post-SWW. This was based on several lines of reasoning. First, measurements of pH and DO from this study compared with the Raymond et al. (1998) data and examination of the ODEQ AWQMP showed that both parameters are greater in the current study. Increases in pH and DO would be consistent with increases in periphyton biomass. Second, the 1994–1996 and current study data showed an increase in summer nitrate concentrations in the LDR. Additional nitrate would make it possible for periphyton biomass to increase. Third, spring water temperatures increased because of the operation of the SWW. Periphyton growth rates would be expected to increase

with increases in temperature. None of these factors individually are proof that periphyton has increased in the LDR, but collectively they provide a coherent explanation.

An effective strategy for simulating the impact of a change in the distribution of species would be to include multiple periphyton groups in the model. In that way, as conditions favored one group over another, the model might directly capture the evolving species composition. The 2Kw development group is currently working to expand the model to incorporate multiple groupings (Greg Pelletier, pers. comm., April 14, 2019), those additions were not available at the time of this study. Because the available version of the model cannot capture a change in species distribution, the only other option was to include some between-scenario modification of model parameters. Recognizing that the periphyton model was calibrated to capture conditions in 2015 justifies this approach because it adequately represents the distribution of periphyton species that existed during that period. When simulating periods of time during which we observed that the species distribution was different than those in the calibration period, we anticipated that the parameterization needed to be adjusted. The primary challenge was that there is no clear basis for defining the parameter variability.

As an initial mechanism to accommodate a change in the periphyton species distribution, we made the simplifying assumption that the maximum periphyton growth rate is different for different species distributions and that it varies with the difference between the baseline and scenario temperatures at the ReReg tailrace.

In the zero order periphyton model used in this study, the maximum growth rate is defined in units of $gD/m^2/d$ (grams dry weight per meter squared per day). A low value of the growth rate (taken as the minimum recommended value of 50 $gD/m^2/d$) was associated with the temperature difference in the No SWW scenario.

The high growth rate value (100 $gD/m^2/d$) was developed from the 2Kw model calibration based on conditions in 2015. The simple linear relationship defined by these two points (Figure 11-1) was used to estimate the maximum growth rate for each of the scenarios (Table 11-2).

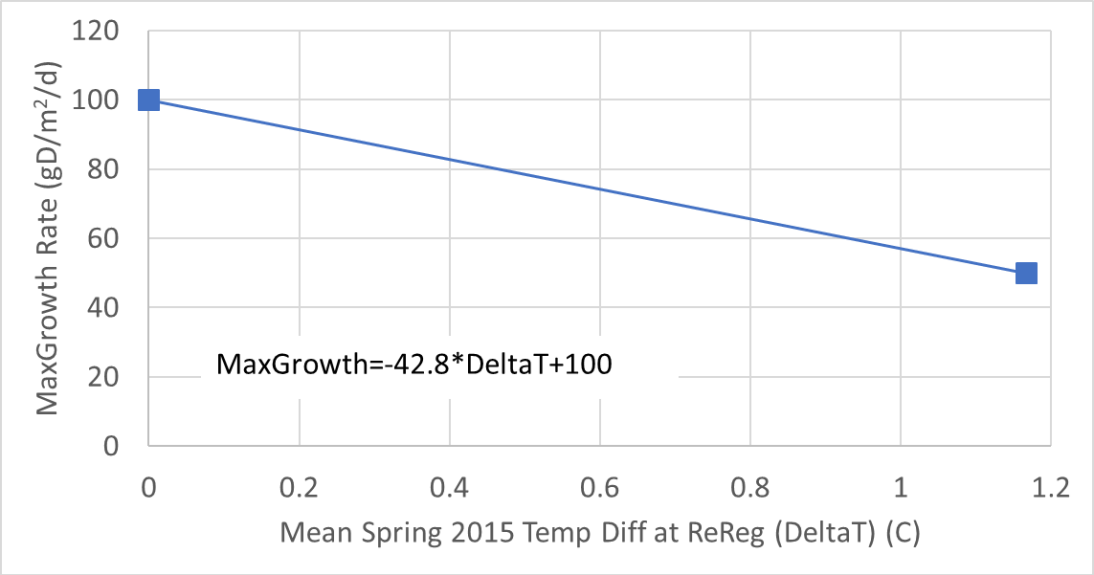

Figure 11-1. A simple assumed relationship between maximum growth rate and the difference between average spring temperatures at ReReg site (LDR01).

Table 11-2. Estimated temperature differences and maximum periphyton growth rate parameter. The maximum growth rate was calculated using the relationship outlined in Figure 11-1.

Scenario	Mean Water Temperature Difference (Baseline-Scenario) in Spring 2015	Max Growth Rate
SWW 100/40	-0.229	109.81
SWW 40	0.738	68.34
No SWW	1.166	49.98
Night Blend	0.594	74.55
Curtain 20ft	0.055	97.66
Curtain 40ft	0.106	95.43
Curtain 50ft	0.164	92.95
Curtain 60ft	0.178	92.37
NO_3 Reduction	0.012	99.48
N and P Reduction	0.012	99.48
Cold Flush	0.024	98.97
Future Climate	-0.800	134.30
Flushing Flow	0.0	100.0
2040	-0.004	100.19
2080	-0.027	101.14

Summer NO_3 concentrations in the ReReg tailrace are an important component of the study, where elevated export of NO_3 from LBC might alter water quality in the LDR. As noted in Section 9, the W2 model underestimates the export of N during the baseline period. A brief analysis of the scenarios indicates that the underestimate of NO_3 is also present in each of the scenarios (Figure 11-2). Because of the important nature of available N (primarily NO_3) in potentially limiting production in the LDR, the model-to-model connection between the reservoir and LDR simulation was adjusted to include observed NO_3 where the modeled reservoir simulations resulted in low NO_3 export. When modeled NO_3 exported from the reservoir system was below observed values, the inflows of NO_3 were elevated to match the observations. An exception to this rule was made for the NO_3 Decrease scenario, which explored reductions of NO_3 input into the reservoir system. That scenario resulted in low export of NO_3 to the LDR (Figure 11-2) compared to the baseline and that modeled low NO_3 was not adjusted.

This technique limits the capacity of the linked model to capture some impacts of scenario-based changes in NO_3 load to the LDR, but also accommodates a more realistic representation of the availability of NO_3 at the headwaters of the LDR. Model refinements in future work could base the NO_3 adjustment on relative differences between each scenario and the baseline or focus on further refinement of the W2 calibration to more fully capture NO_3 export during the summer periods.

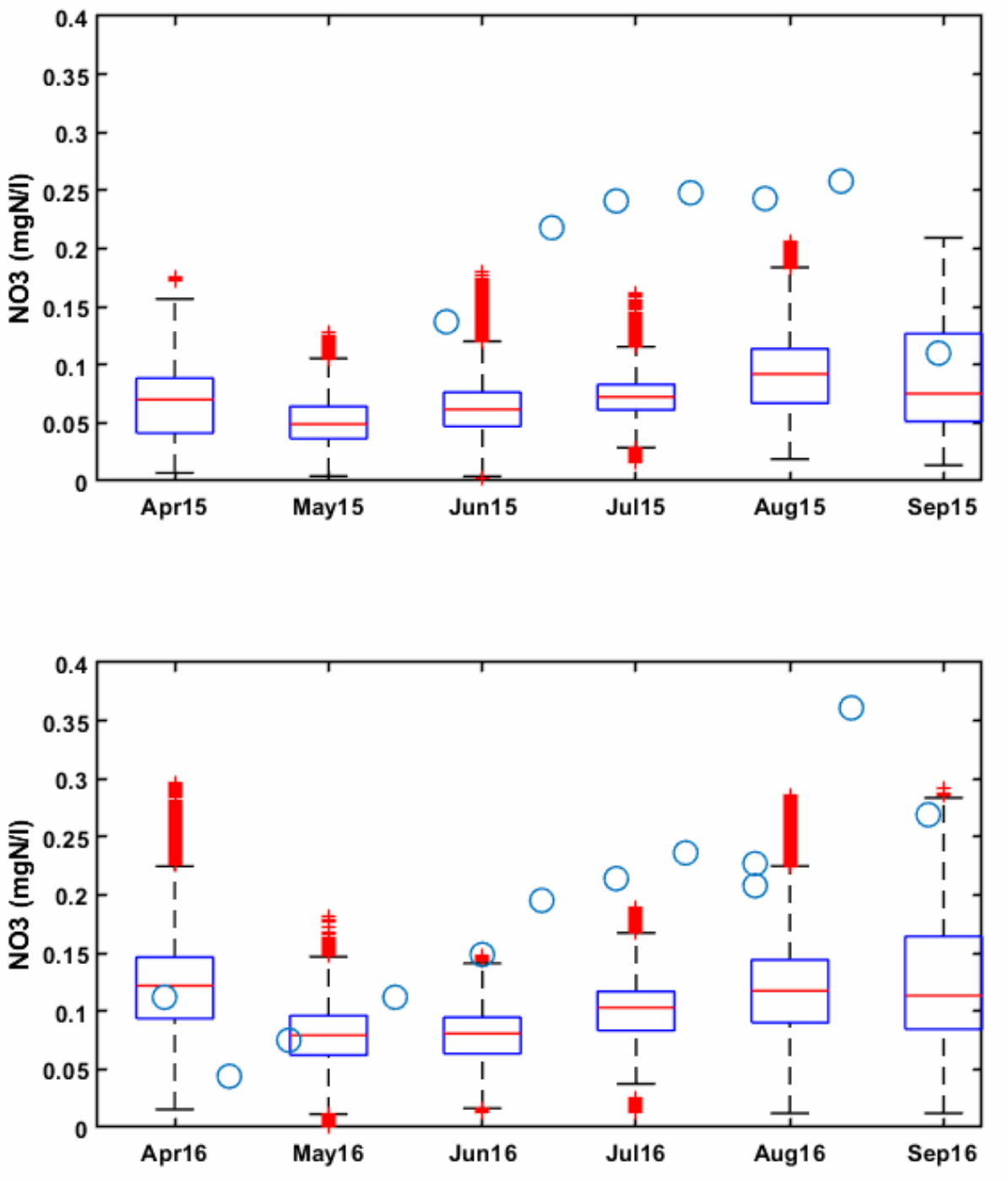

Figure 11-2. NO_3 concentration in the ReReg tailrace from April–September 2015 (*top*) and 2016 (*bottom*). All the values for all scenarios are included as monthly boxplots. Observed data are included as blue dots. The figure demonstrates the summertime underprediction of NO_3 as consistent across all scenarios.

11.2 SWW 100/40 Scenario

The SWW 100/40 scenario was run from 2015 to 2017 to explore the effect year-round maximum bottom withdrawal (except during fish passage season) would have on water quality in the LDR. It is designed to evaluate the impacts of operating the SWW with 100% of water drawn from the upper gate between March 15 and June 15, which is the time of year when the majority of salmon and steelhead smolts are moving downstream through LBC and benefit the most from surface flows (Pyper 2016). Maximum surface withdrawals at the SWW maximize fish capture at the collection facility. At all other times of the year (June 16–March 14), the upper gate operates at 40% and the bottom gates operate at 60% to maximize bottom water discharge into the LDR.

The gate flows defined for this scenario are shown in Figure 11-3. The scenario results in periods of large differences in gate flows when compared with the baseline, but those differences occur primarily in the winter, when the baseline shows most of the water being released from the upper gate. During much of that period, the reservoir is not stratified, so the differences in temperature and water quality in the surface water of LBC are minor (Figure 11-4).

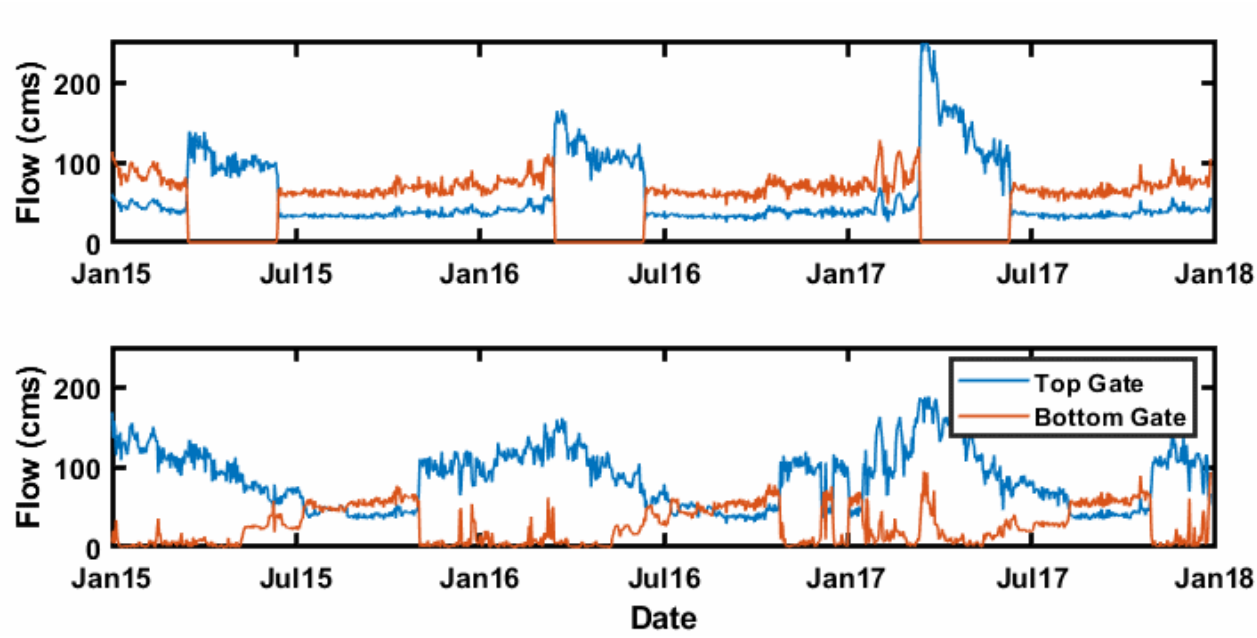

Figure 11-3. Gate flows for the SWW100/40 scenario with 100% surface withdrawals during the spring and 60% bottom release the rest of the year. The *top* figure shows scenario conditions. and the *bottom* figure shows baseline conditions.

This scenario is simulated to have mixed impacts on temperatures of LBC surface water during the early summer period. There is a very small reduction in mean daily surface temperature in 2015 and 2016, and a more prominent reduction in the summer of 2017. That reduction occurs because more surface water is exported from the reservoirs from March 15 through June 15 because of the modifications in the gate flows. This increase in surface water export from LBC removes an elevated proportion of the warming spring surface water compared to the baseline. The loss of the warmer surface water appears to result in the somewhat cooler surface temperatures, at least for some years. This result is noteworthy because the modest reduction in surface temperature largely limits the simulated cyanobacteria bloom that occurred in the baseline model during summer 2017 and is carried on, impacting the downstream model components (Figure 11-4).

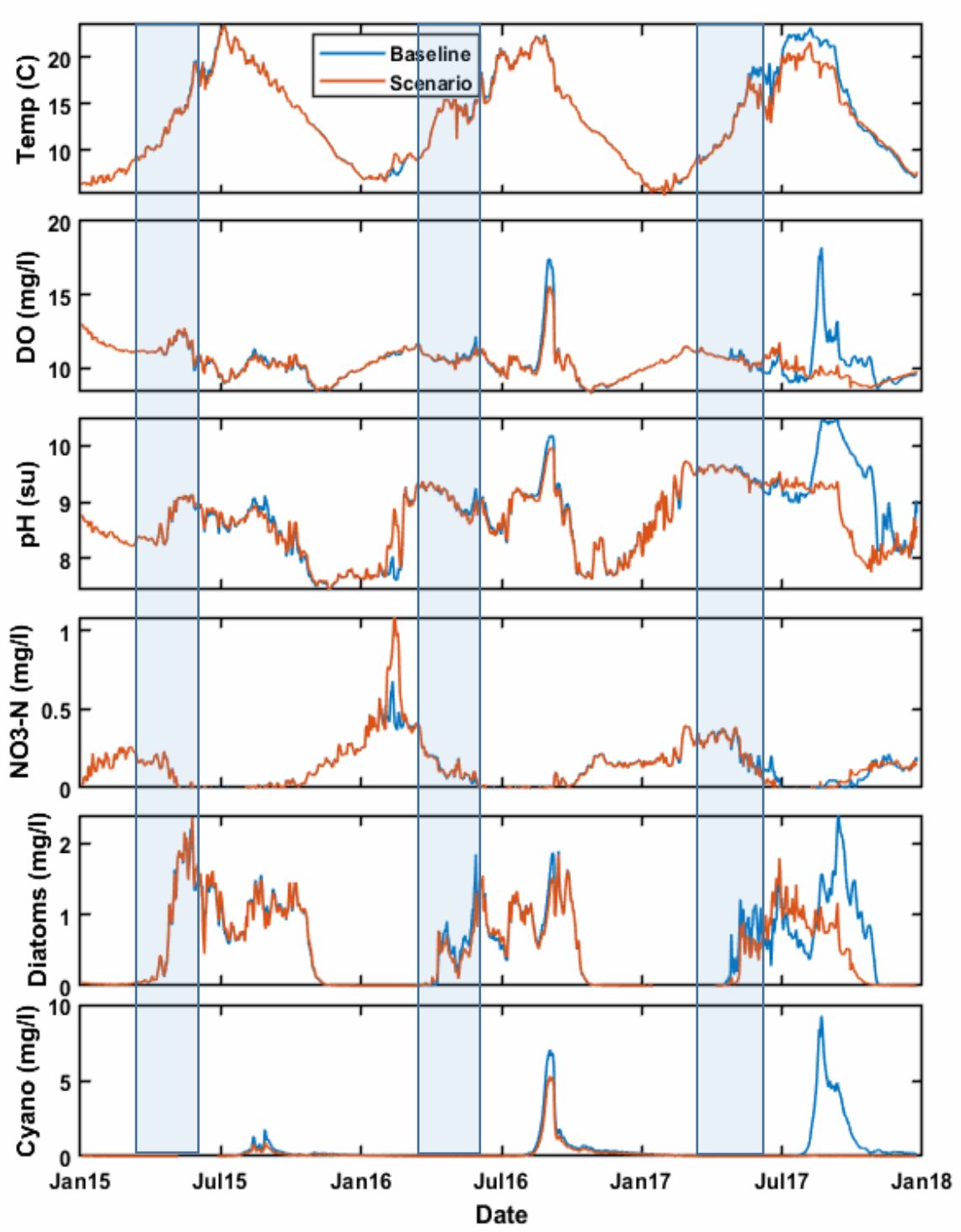

Figure 11-4. Time series of daily model results for the SWW100/40 scenario in the surface water of Round Butte forebay (RES07). Baseline condition results are in blue, and scenario results are in orange. Approximate periods when the bottom release is zero are outlined in the three blue boxes.

Phytoplankton growth in LBC was not affected nearly as much in 2016 as it was in 2017, most likely because of the temperature dependence of the kinetic equations used to represent phytoplankton growth and development. It remains uncertain as to why 2015 and 2016 are simulated to experience less surface cooling than 2017.

The tailraces of the reservoirs show a somewhat elevated spring temperature, likely because of the additional surface water released from LBC during the spring periods (Figure 11-5). The full daily time series at the ReReg tailrace suggest that the elevated temperatures lead to somewhat elevated pH values during the spring when bottom releases are low (Figure 11-6). However, pH decreases as the summer progresses and bottom withdrawal from the SWW is maximized at 60%. This change leads to lower DO and pH values in the ReReg tailrace and, additionally, reduced export of algae into the LDR during the period when operations are different than the baseline (Figure 11-6).

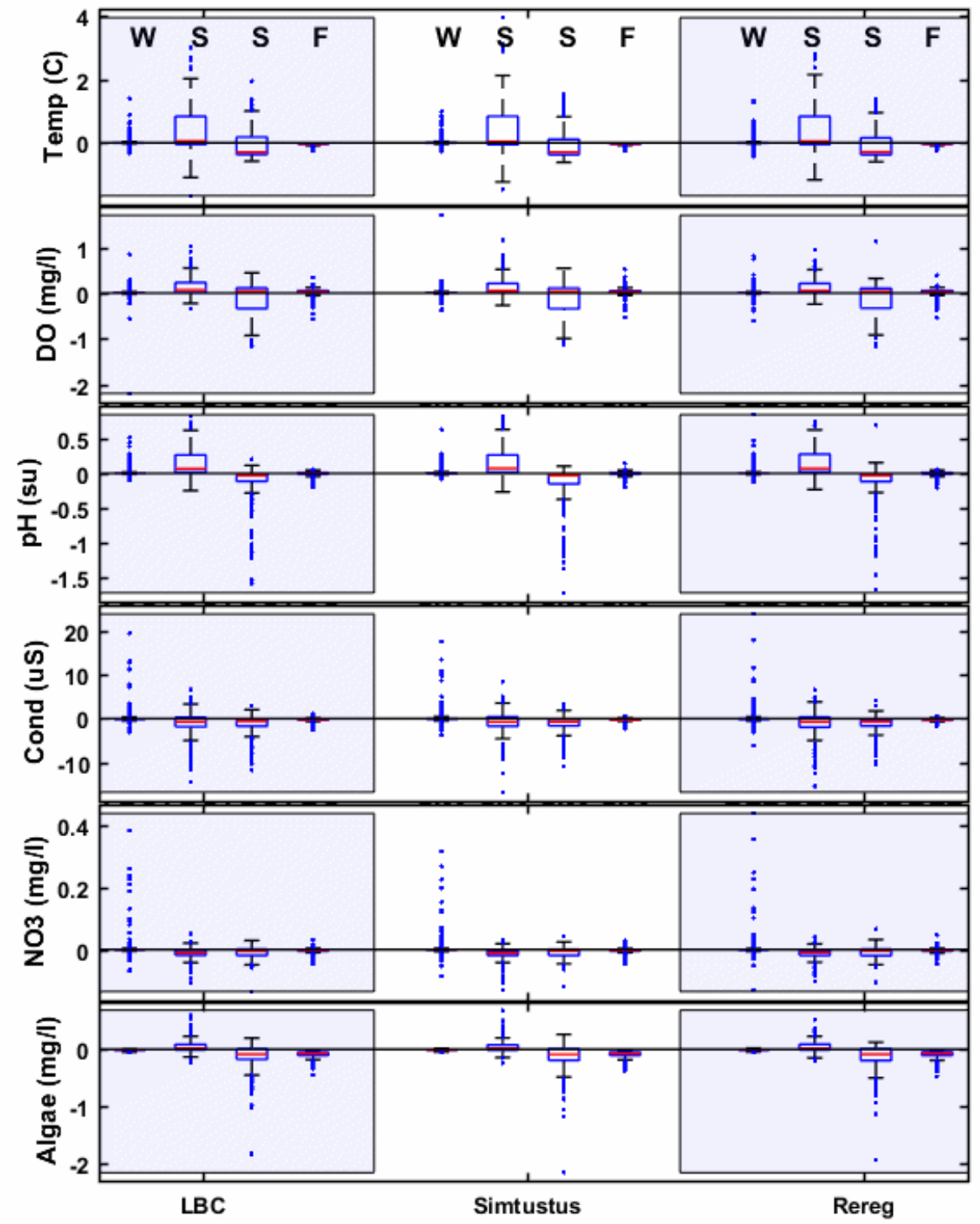

Figure 11-5. A comparison of the differences between baseline and SWW100/40 scenario daily values in the tailraces of the reservoirs across four seasons. Positive values indicate the scenario value was larger than baseline. Seasons are shown in order of winter (W), spring (S), summer (S), and fall (F).

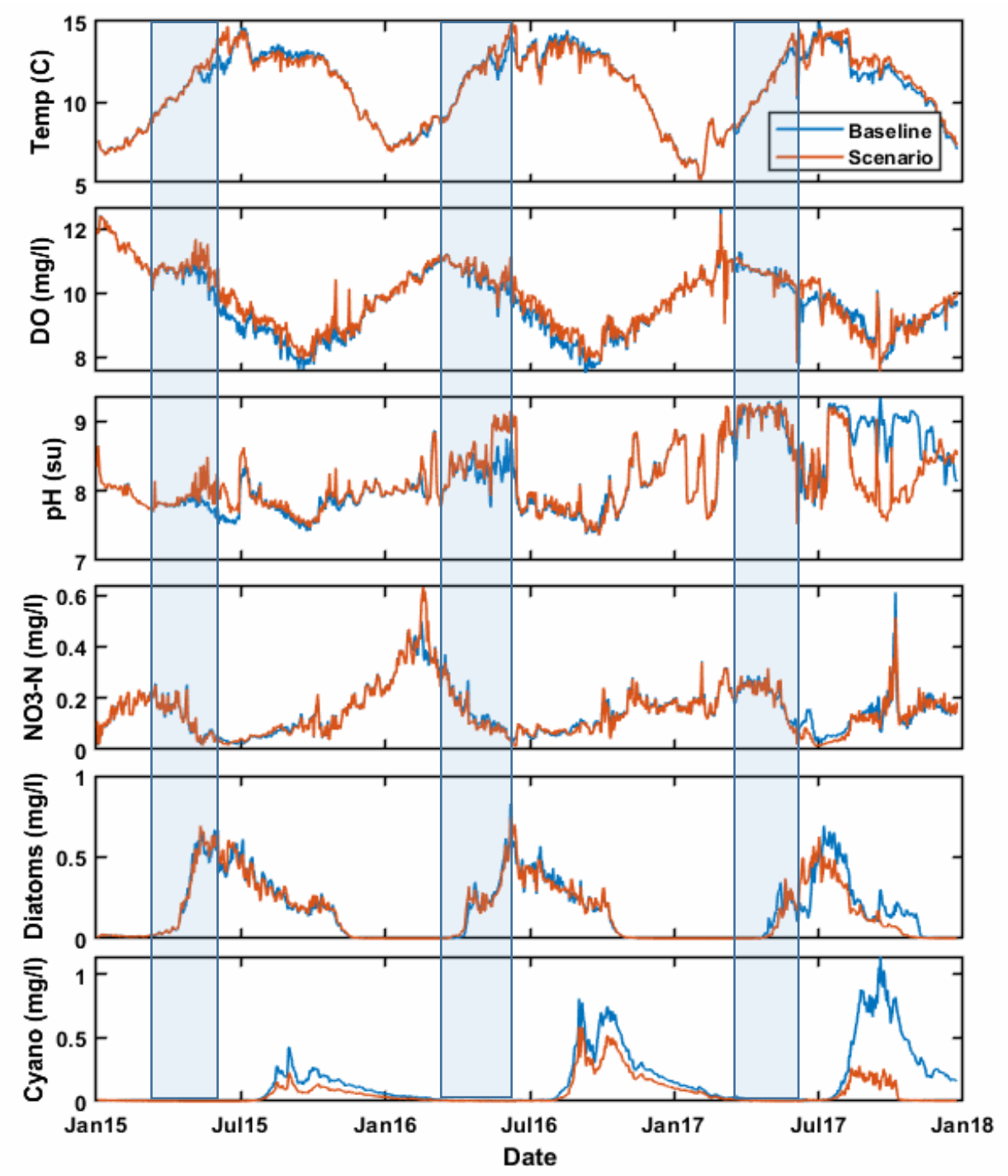

Figure 11-6. Time series of daily model results in the ReReg tailrace for the SWW100/40 scenario. Baseline condition results are in blue and scenario results are in orange. Approximate periods when the bottom release is zero are outlined in the three blue boxes.

However, these changes have a modest impact on the LDR. At RM 96, the warmer water released from LBC during the fish collection period is evident in the model results, as are higher values of both pH and DO (Figure 11-7). At Moody, the differences are smaller, as heating and primary production that occurs during the approximately 33-hr river residence time acts to increase both temperature and pH (Figure 11-8).

Longitudinal profiles outline how the changes in the temperature of the water released into the LDR propagate through the canyon (Figure 11-9). The profiles supplement the temporally variable results depicted in the time series figures to fill in the spatial gap between RM 96 and RM 1. The profiles do not capture much of the temporal variability and should be interpreted in conjunction with the time series. Profile results indicate that the small increase in water temperature does carry through the LDR during the period over which it is released. Small increases in DO appear to move through the system as well, until Sherars Falls (RM 44), where mixing appears to reset DO closer to the saturation value. By contrast, during 2016, pH was elevated in the ReReg tailrace water and moved through the full 100 mi to Moody. During 2017, pH at the ReReg tailrace was not elevated as part of the scenario and a pH value similar to the baseline propagated through the LDR and was evident at Moody. The scenario appears to have minor impacts on NO_3, phytoplankton, and periphyton.

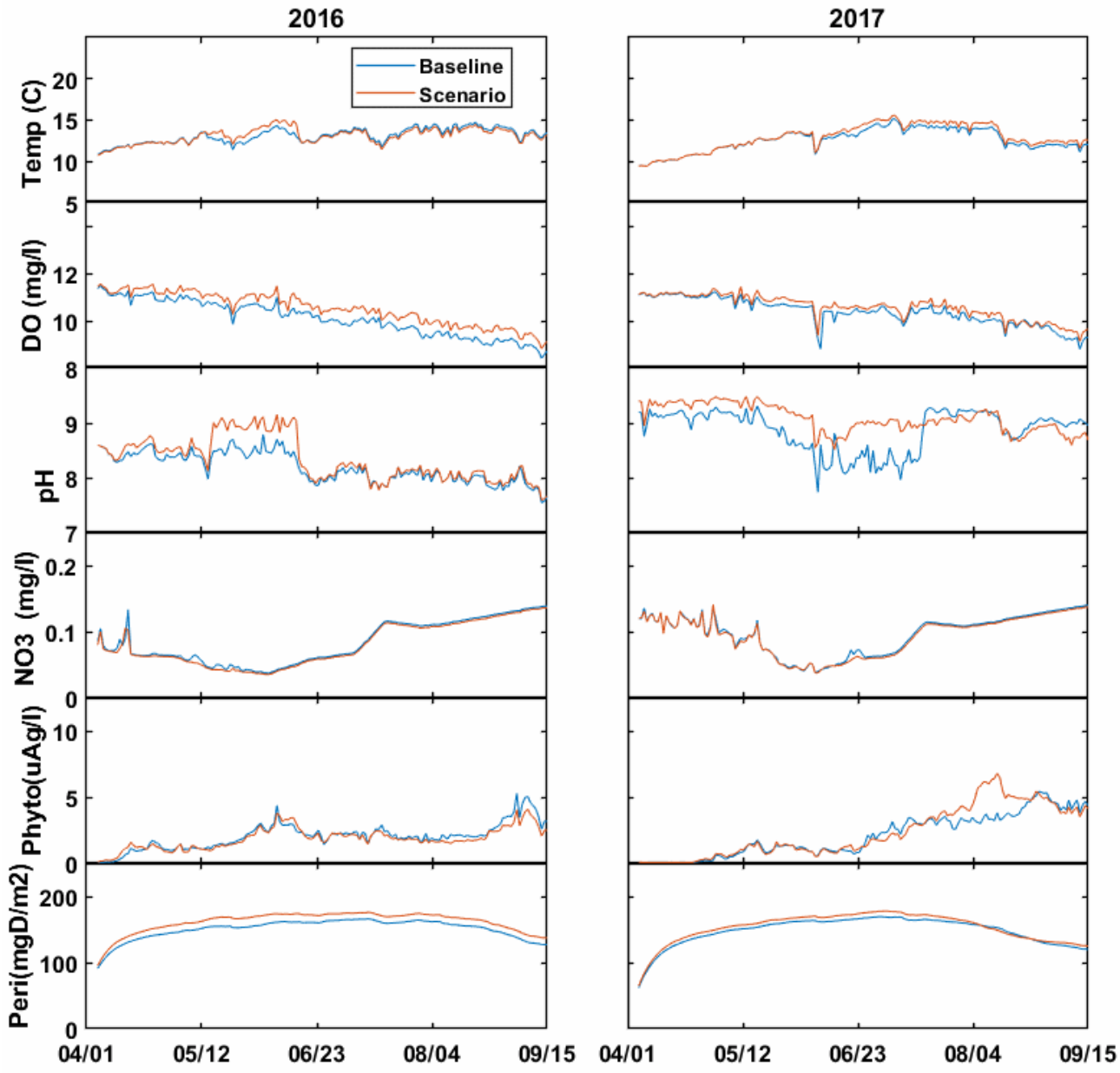

Figure 11-7. A comparison of daily results at RM 96 on the LDR for the SWW100/40 scenario. This figure shows the period between April 1 and September 15.

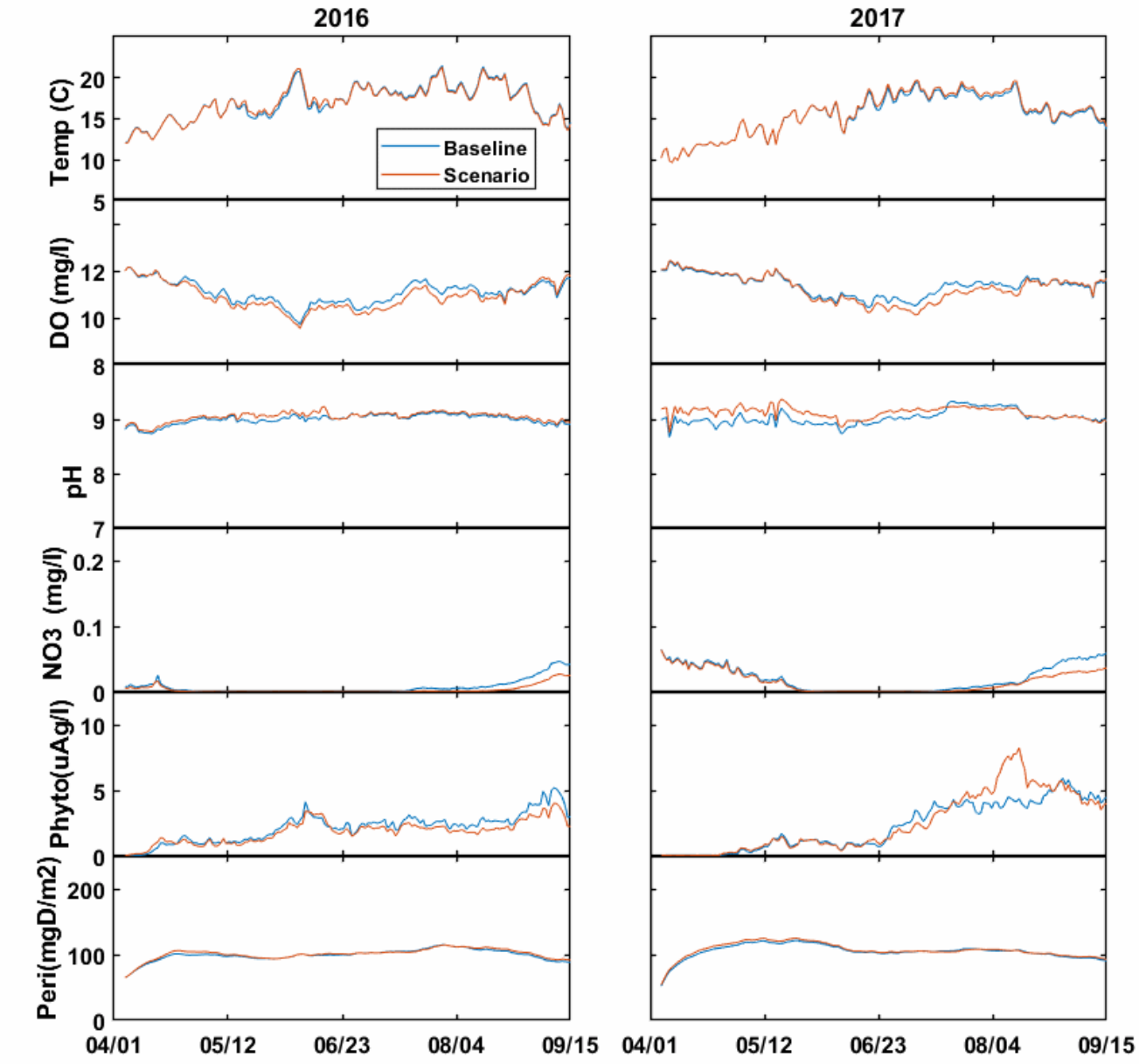

Figure 11-8. A comparison of daily results at Moody (RM 1) on the LDR for the SWW100/40 scenario. This figure shows the period between April 1 and September 15.

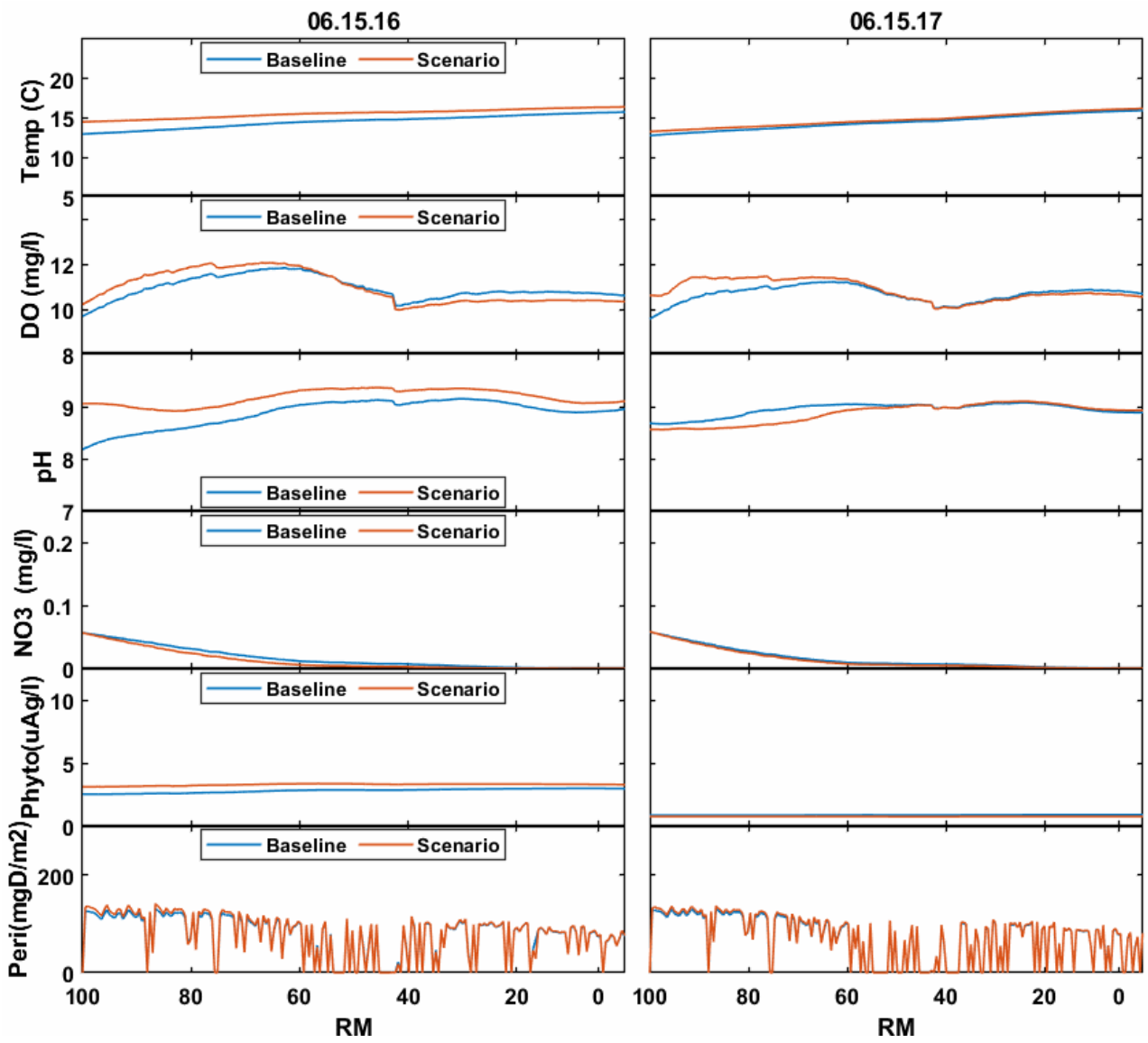

Figure 11-9. Water quality profiles from immediately below ReReg Dam to the LDR mouth for the SWW 100/40 scenario. These profiles were taken on June 15 of 2016 and 2017 and represent daily average values.

11.3 SWW 40 Scenario

The SWW 40 scenario assumes the SWW draws 40% of its water from the surface and 60% from the bottom gate at all times during the year (Figure 11-10). This scenario is similar to the SWW 100/40 scenario in that it maximizes hypolimnetic withdrawals and minimizes surface water withdrawals. However, since this ratio is applied year-round, fish passage from March 15 through June 15 would be negatively affected because decreased surface water withdrawals in LBC means less surface flow into Round Butte forebay to attract downstream-migrating fish into the fish collection facility at the SWW (Pyper 2016).

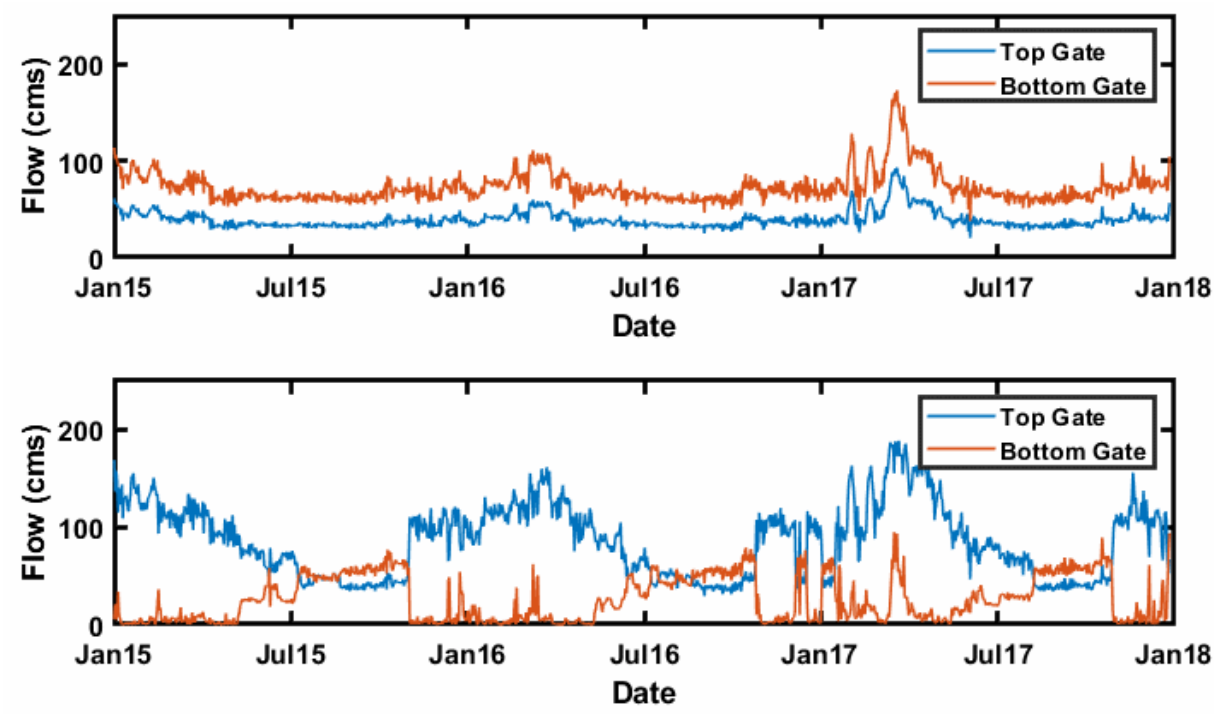

Figure 11-10. Gate flows for the SWW 40 scenario. This scenario applies 40% surface withdrawal and 60% bottom withdrawal year-round. The *top* figure shows the scenario gate flows, and the *bottom* figure shows the baseline gate flows.

The model results indicate that in LBC, SWW 40 operation led to somewhat elevated temperatures in the surface waters during the spring and summer in 2016 and 2017 (Figure 11-11). These elevated temperatures were caused by retaining warmer surface water in the reservoir as a side effect of drawing more water from the lower gate. Conditions in 2016

resulted in the warmer surface water leading to an earlier bloom of algae and, along with the early peak, associated increases in pH and DO. Changes from the baseline scenario compared to model years 2015 and 2017 are minimal.

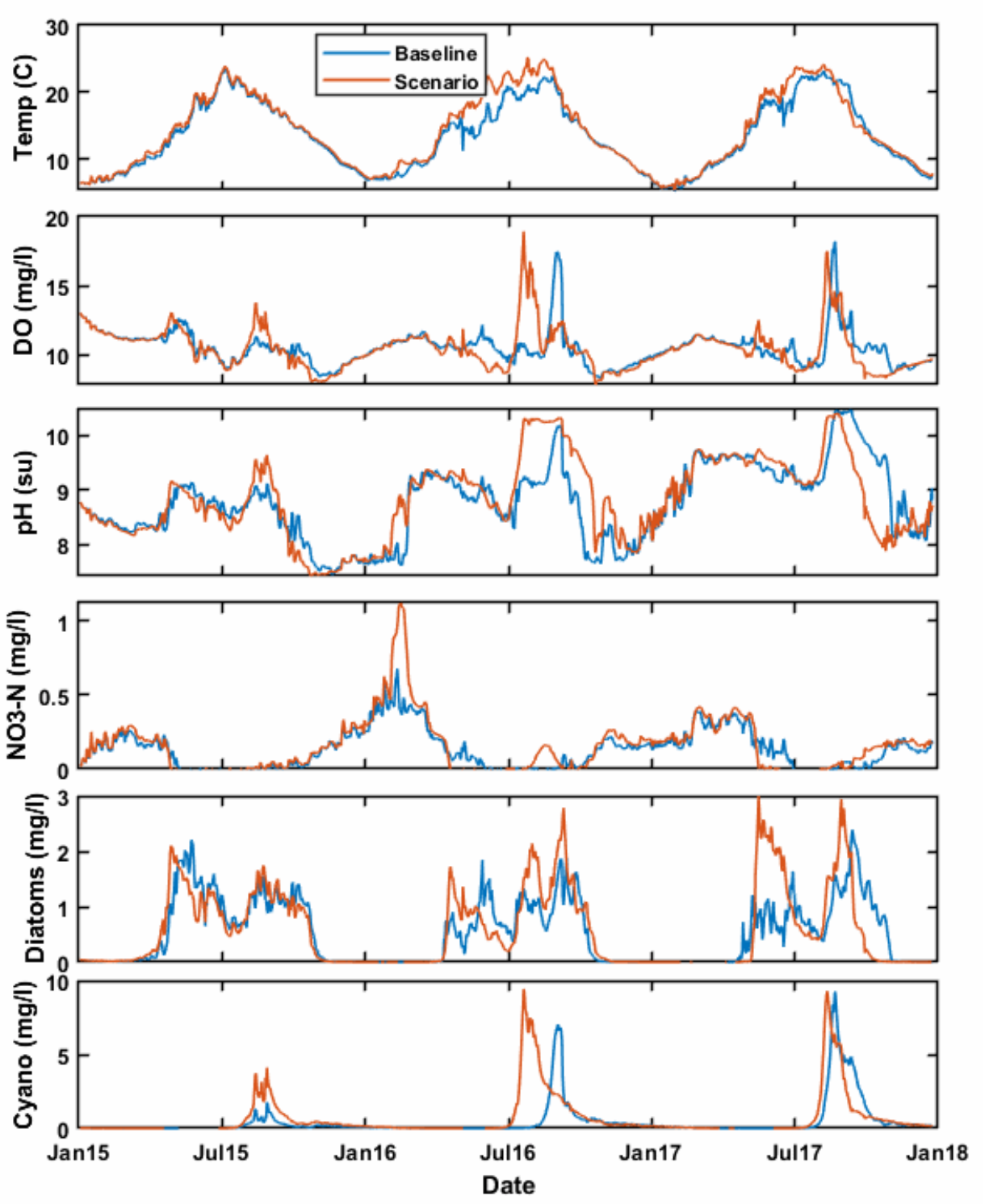

Figure 11-11. Time series of daily model results for the SWW40 scenario in the surface water of Round Butte forebay (RES07). Baseline condition results are shown in blue, and SWW40 scenario results are shown in orange.

The seasonal boxplots of the tailrace waters in the three reservoirs indicate that spring temperatures will decrease while summer temperatures will increase moderately under scenario conditions (Figure 11-12). Cooler spring temperatures are likely to lead to reduced biological activity, with reductions in the pH and DO of the water exported to the LDR during the spring and early summer. However, moving more of the colder bottom water into the river early in the year leaves less of it in the reservoirs during the summer months, which results in warmer water with elevated algae concentrations being released during the later summer period (Figure 11-13). This is particularly evident in model years 2015 and 2016. For model year 2017, the baseline model describes an especially high cyanobacteria growth rate, which appears to overshadow any impact on the tailrace water under the scenario conditions.

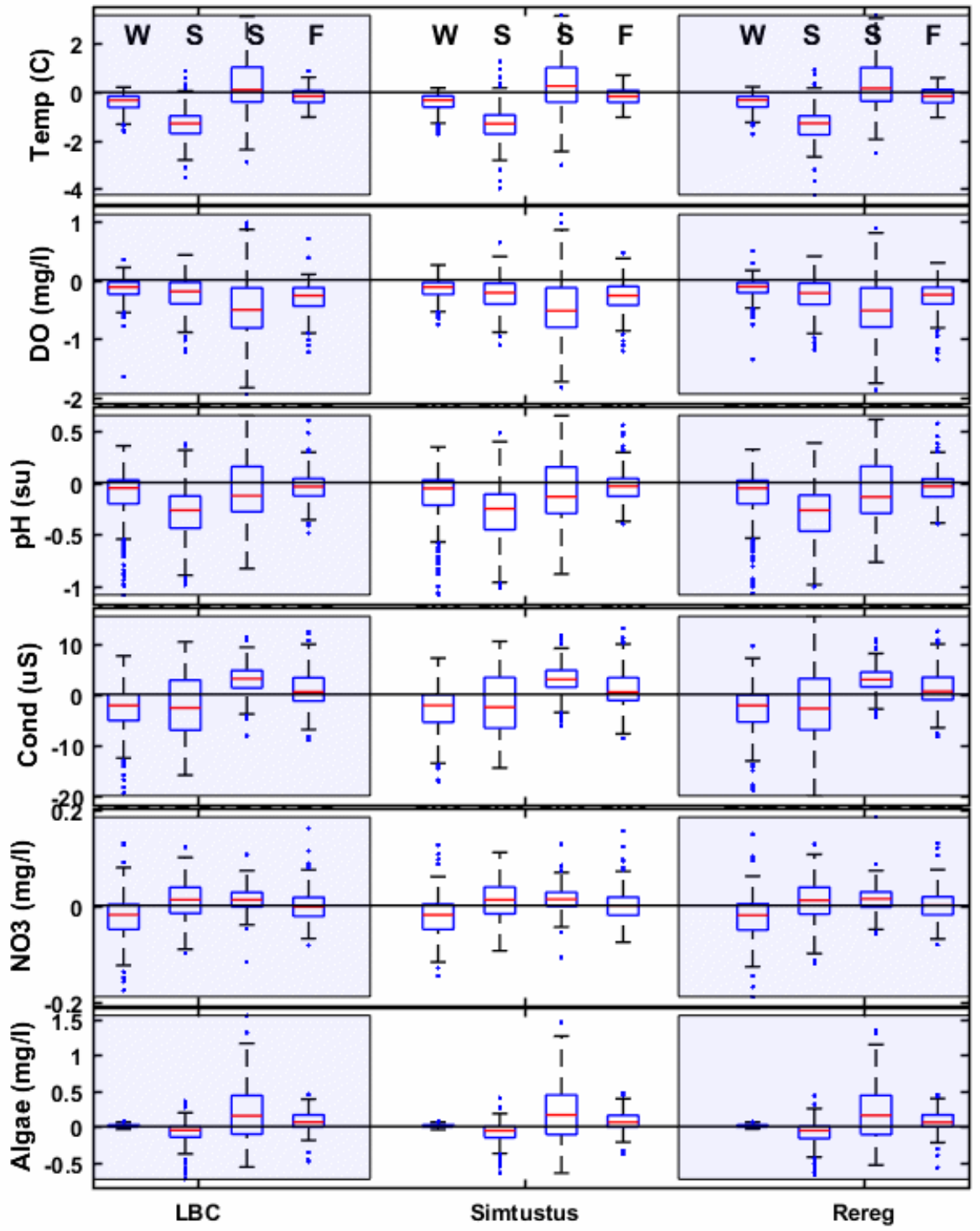

Figure 11-12. A comparison of the difference between baseline and SWW40 scenario daily values in the tailraces of the reservoirs across four seasons. Positive values indicate that the scenario value was larger than the baseline value. Seasons are shown in order of winter (W), spring (S), summer (S), and fall (F).

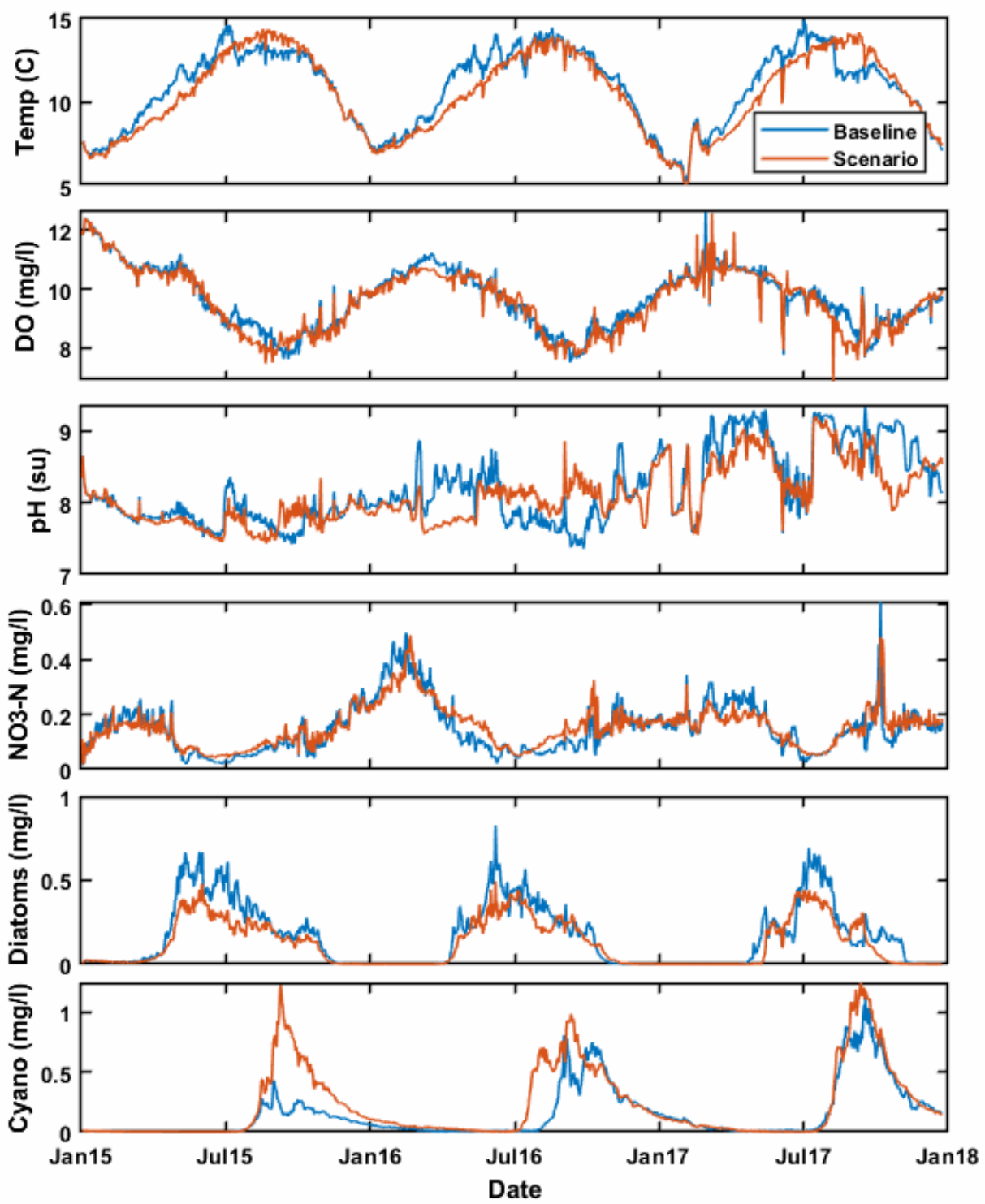

Figure 11-13. Time series of daily model results at ReReg tailrace for the SWW40 scenario. Baseline condition results are shown in blue, and scenario results are shown in orange.

The pattern of cooler spring and moderately warmer late summer water temperatures at the ReReg tailrace appears to continue through the LDR. Figure 11-14 represents conditions at RM 96, and Figure 11-15 represents conditions near Moody (RM 1). Near the ReReg Dam, the lower spring temperatures lead to early spring reductions in pH and overall reductions in periphyton development. The scenario does not appear to differ from the baseline for DO, phytoplankton, and NO_3 (Figure 11-14).

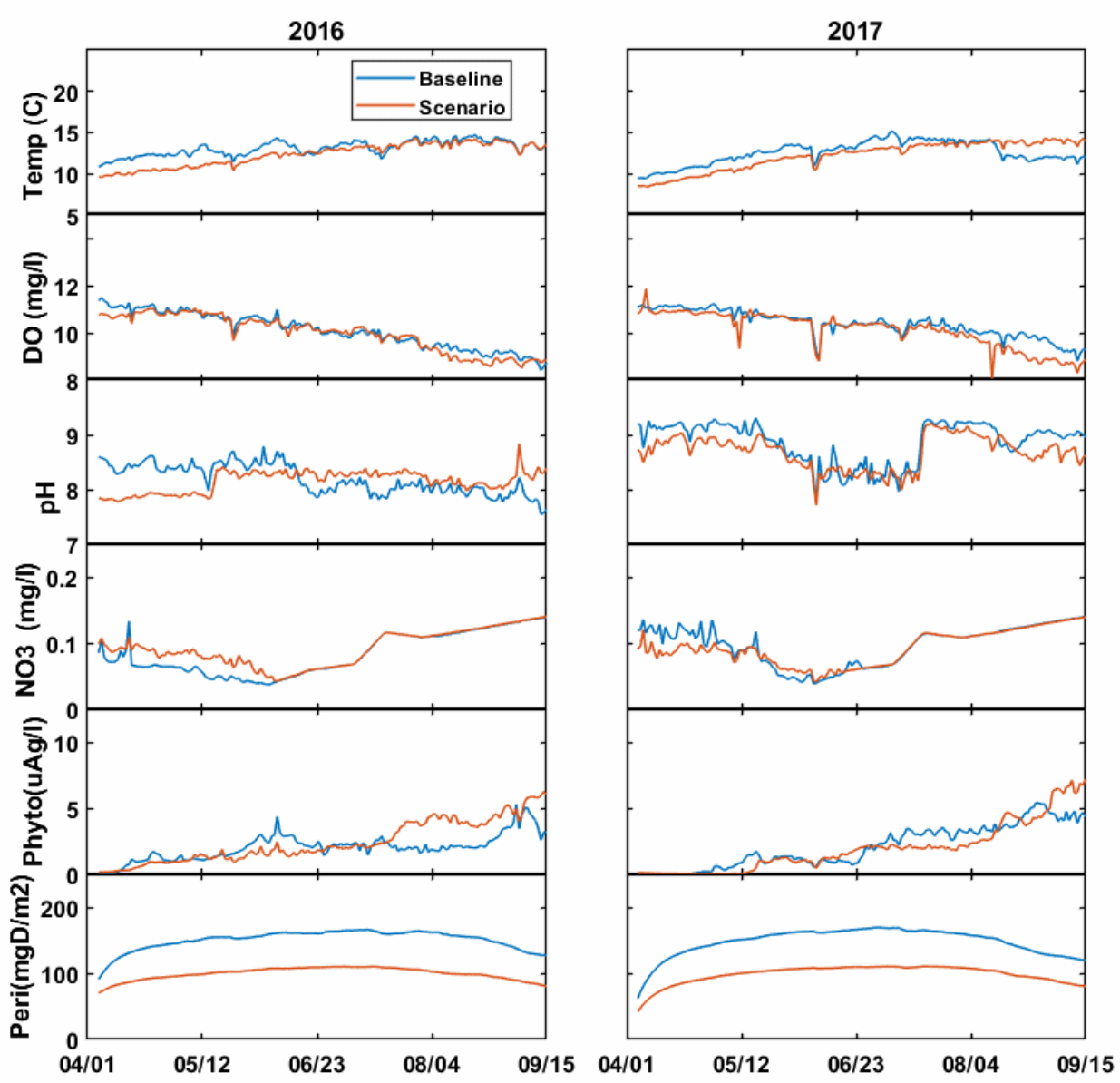

Figure 11-14. A comparison of daily results at RM 96 on the LDR for the SWW40 scenario.

The results at Moody (Figure 11-15) are consistent with those near the ReReg Dam at RM 96, although the reductions in biological productivity lead to slightly elevated values for NO_3. The fact that NO_3 appears to increase at Moody under the scenario suggests that the simulated decreases in periphyton (which results in excess NO_3) outweigh the impact on water quality of the increases in phytoplankton development (which would tend to reduce NO_3), particularly those occurring late in the summer. The model capturing a reduction in pH values at Moody is consistent with this line of reasoning. These reductions occur primarily in response to the reduction in periphyton development.

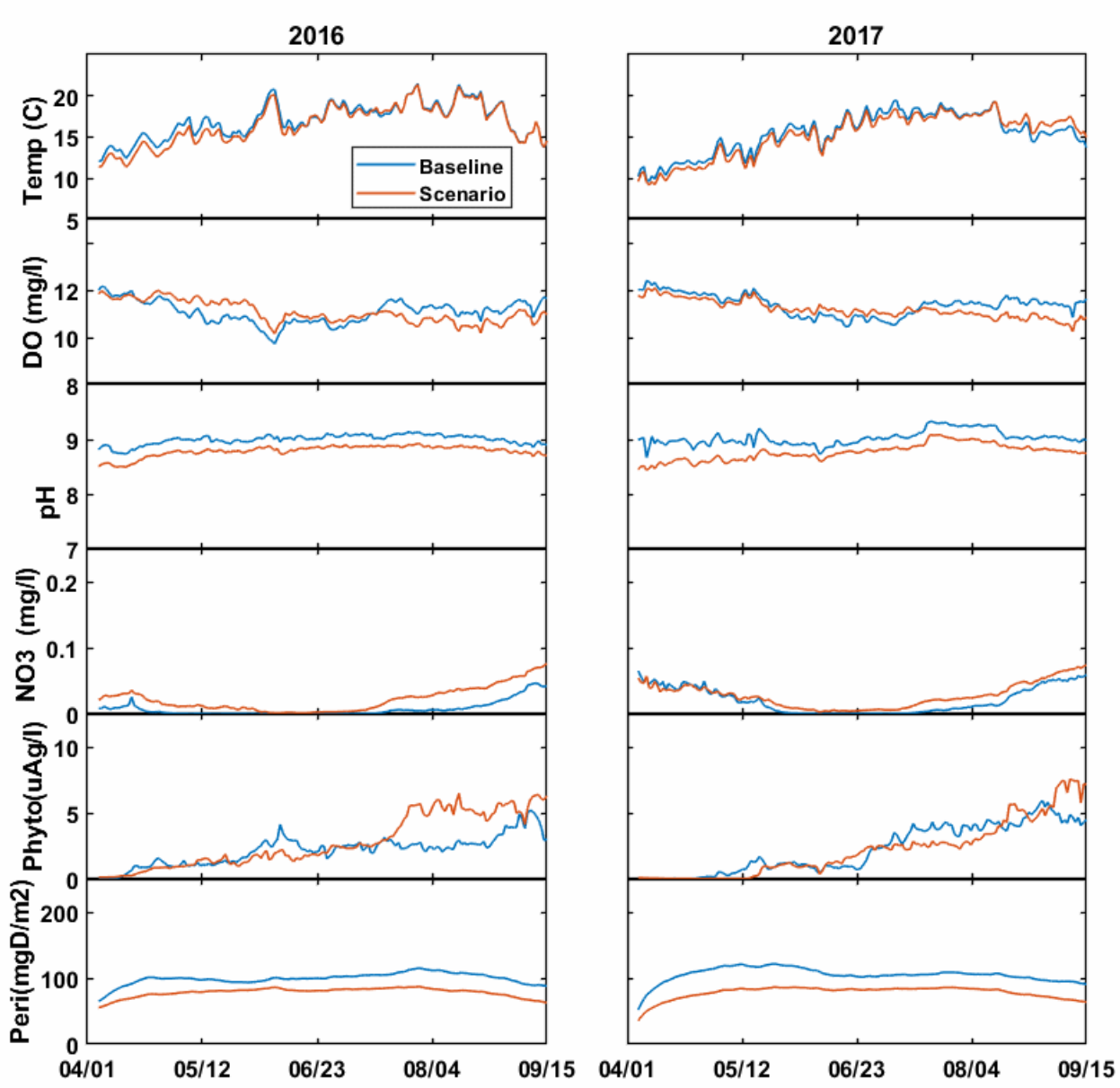

Figure 11-15. A comparison of daily results at Moody (RM 1) on the LDR for the SWW40 scenario.

A set of longitudinal profiles from May 16 in 2016 and 2017 depict a pattern similar to the baseline scenario (Figure 11-16). May 16 was selected to represent conditions during the period in which the scenario results in the largest differences in temperature compared to the baseline. The longitudinal profiles represent a snapshot in time and supplement the time series shown in

Figure 11-15. They are useful both in comparing how the scenario results compare against the baseline spatially and in depicting the spatial pattern of the variables. In 2016, the water warms as it flows from ReReg tailrace to Moody; however, in 2017, warming is not apparent. This is because weather conditions during the period from which the profiles were taken were relatively cool. The result highlights the fact that, while daily profiles usefully outline changes across the entire 100-mi LDR, they capture only a small component of temporal variability and should be interpreted along with the time series.

In model year 2016, profiles indicate that DO increases initially paralleled baseline increases but returned to near-baseline levels in the area near Sherars Falls (RM 44). The turbulence at Sherars Falls brings water passing over it back to saturation, from the supersaturated conditions that developed upstream. This pattern of near-saturated DO near the falls exists during the calibration and was also noted during the 72-hr continuous surveys. pH increases in model year 2016 but decreases along the profile in 2017 (again due to cooler meteorological conditions around the day the profile represents). NO_3 is taken up through biological production as the water moves downstream and, therefore, decreases as water moves from the ReReg Dam to Moody. Phytoplankton does not show much variation spatially, likely because of the relatively short residence time in the LDR. The periphyton profile indicates that the scenario results in a decline in periphyton development across the system.

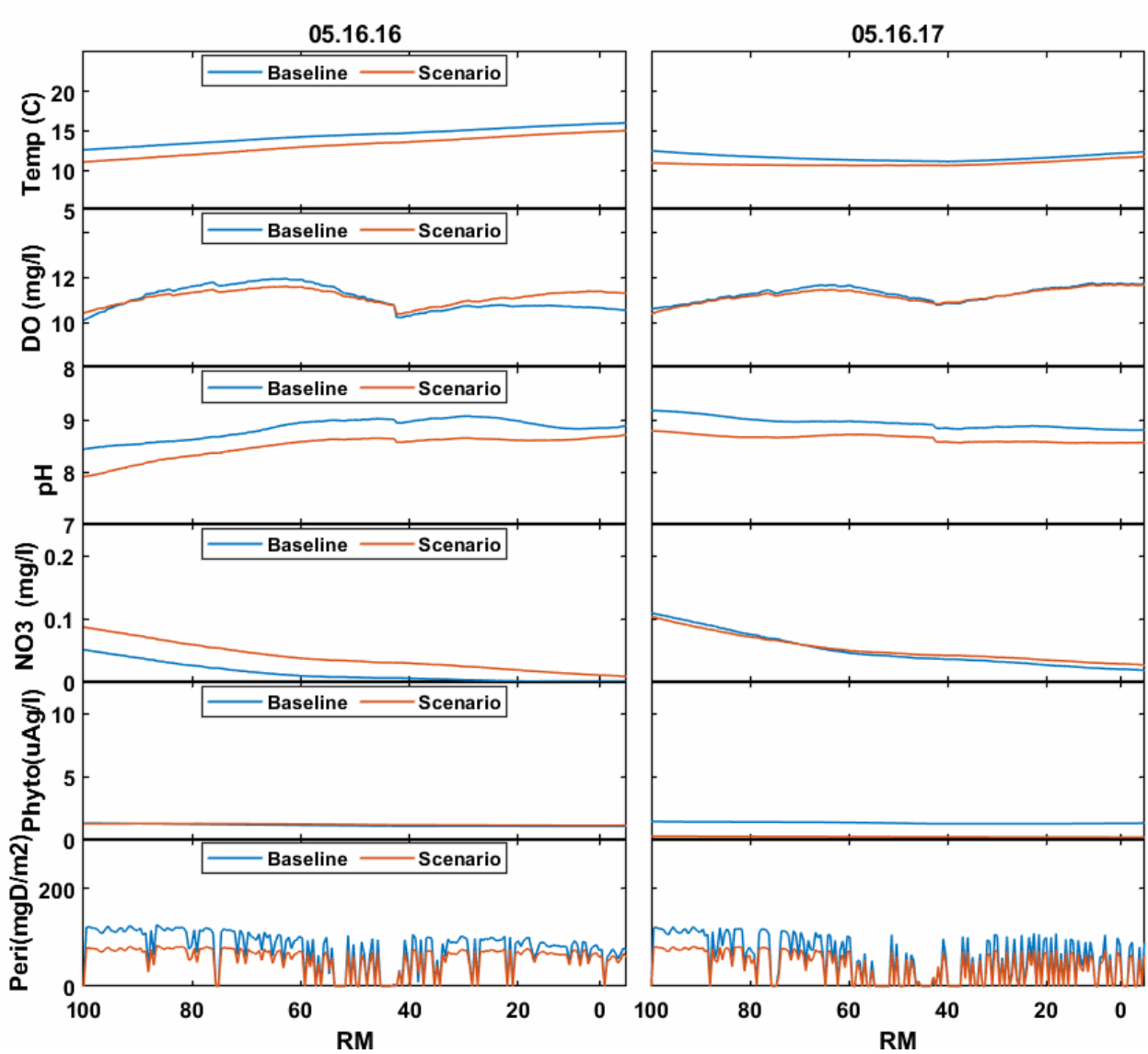

Figure 11-16. Water quality profiles from immediately below ReReg Dam at RM 100.1 to the LDR mouth at RM 0. These profiles were taken on May 16 of 2016 and 2017 and represent daily average values.

11.4 No SWW Scenario

The No SWW scenario evaluates how conditions would have developed during 2015–2017 if the SWW had not been constructed. Prior to installation of the SWW, all water from LBC was released from the bottom gate (Figure 11-17). This scenario is not designed to result in a

possible outcome because the No SWW scenario cannot be implemented using the SWW as constructed. However, this scenario was intended to bracket the full range of responses the river could experience. Furthermore, the No SWW scenario conditions do not reflect the original intention behind the SWW, which was to introduce surface flows to better facilitate fish capture in LBC and provide a temperature regime in the LDR that more closely mimics a natural temperature regime in the river.

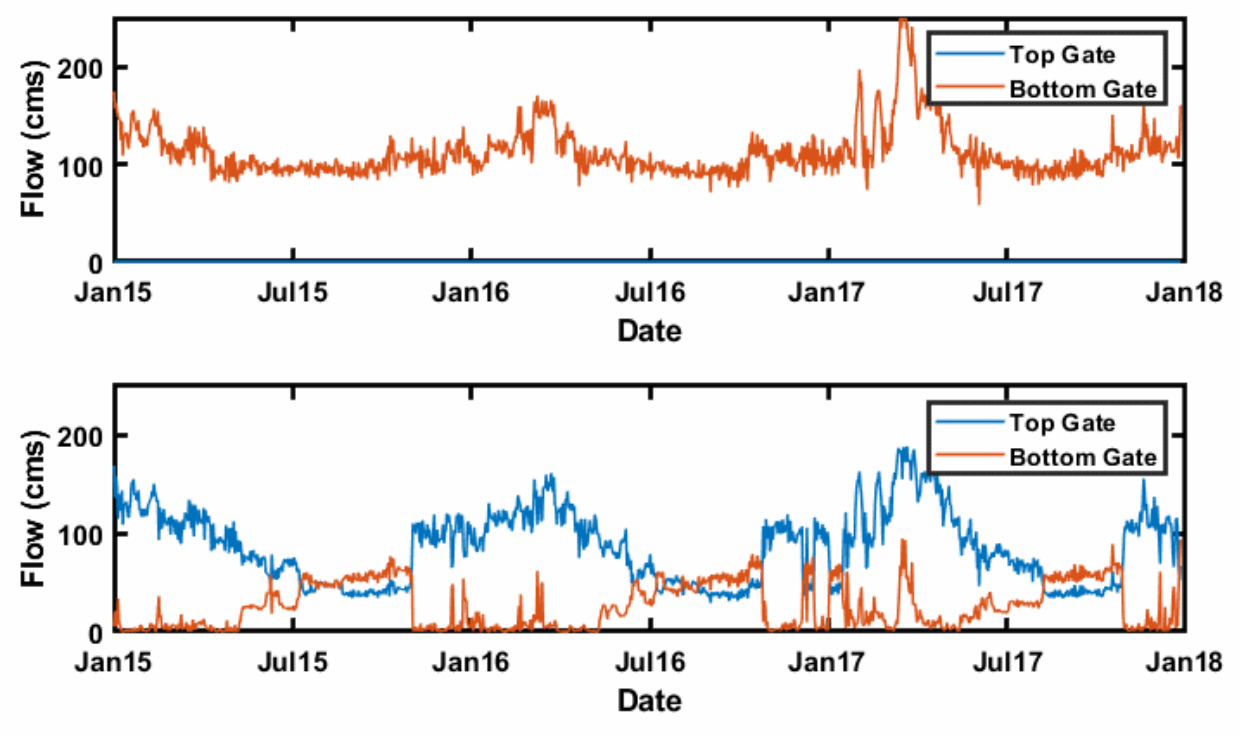

Figure 11-17. Gate flows for the No SWW scenario assuming 100% bottom water withdrawal. The *top* figure shows the scenario gate flows, and the *bottom* figure shows the baseline gate flows.

The results of the No SWW scenario suggest surface water temperatures and productivity increase in the spring and summer in LBC (Figure 11-18). The increase in productivity is characterized by an increase in algal concentrations, along with increases in both pH and NO_3. A portion of the elevated NO_3 appears to be related to increases in cyanobacteria. These changes in the surface water of LBC occur under the scenario because 100% of the water leaving LBC is drawn from the lower gate. This leaves warmer, more productive water in the epilimnion.

The increases in LBC surface water temperature coincides with decreased temperature in the tailraces during the winter and spring periods (Figure 11-19). Both the increase at the surface and the decrease in the tailrace are caused by cooler hypolimnetic water being released from LBC during the winter and spring, leaving warmer, more productive water in the epilimnion. The model suggests that the increase in epilimnetic production provides potential for increased algal export to the LDR (Figure 11-20). In this case, some of the increased cyanobacteria become entrained within water released from Round Butte forebay (RES07). Unlike cyanobacteria, the diatoms do not appear to increase in LBC surface water under the scenario and, therefore, do not appear elevated in the ReReg tailrace.

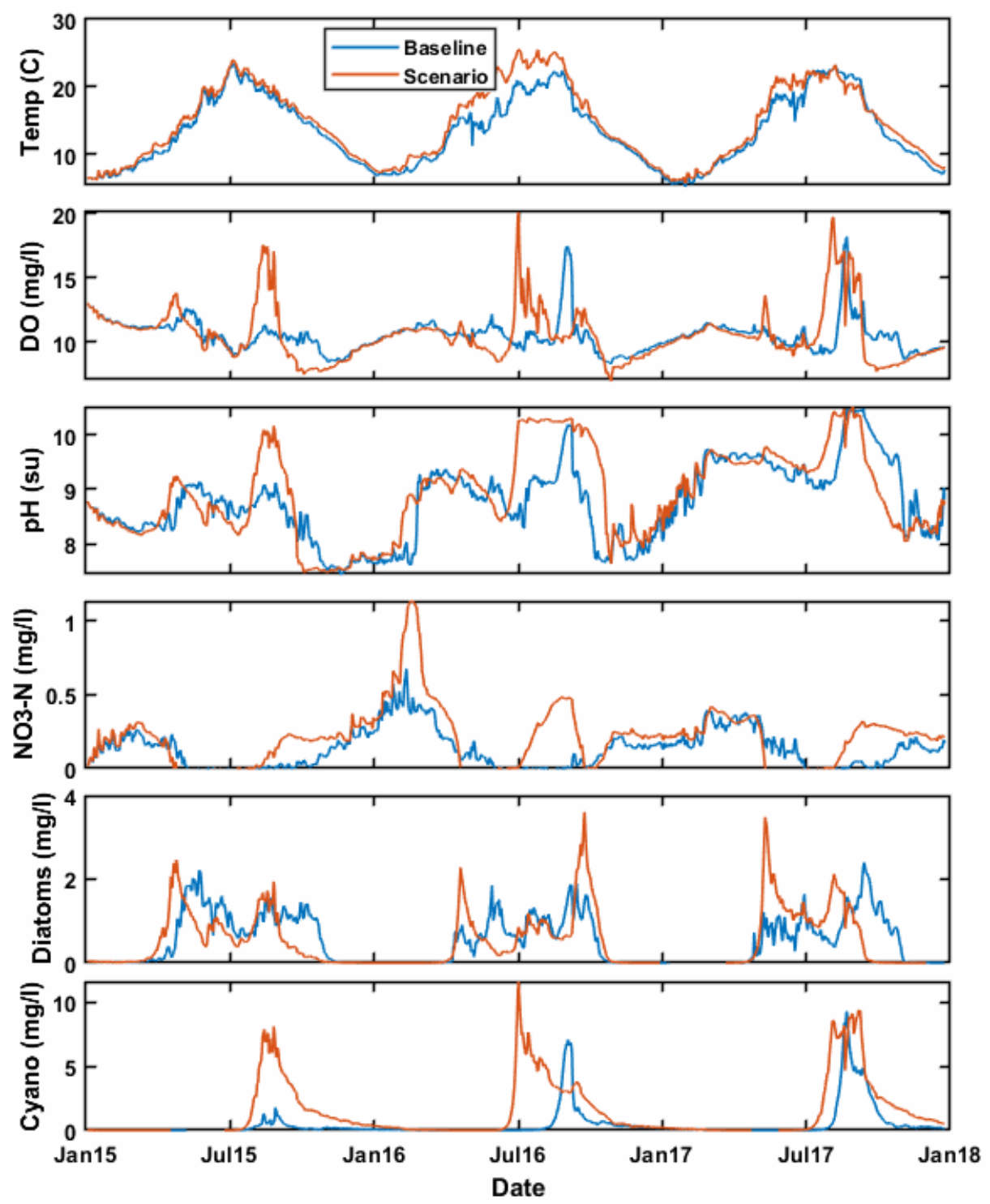

Figure 11-18. Time series of daily model results for the No SWW scenario in the surface water of Round Butte forebay (RES07). Baseline condition results are shown in blue, and scenario results are shown in orange.

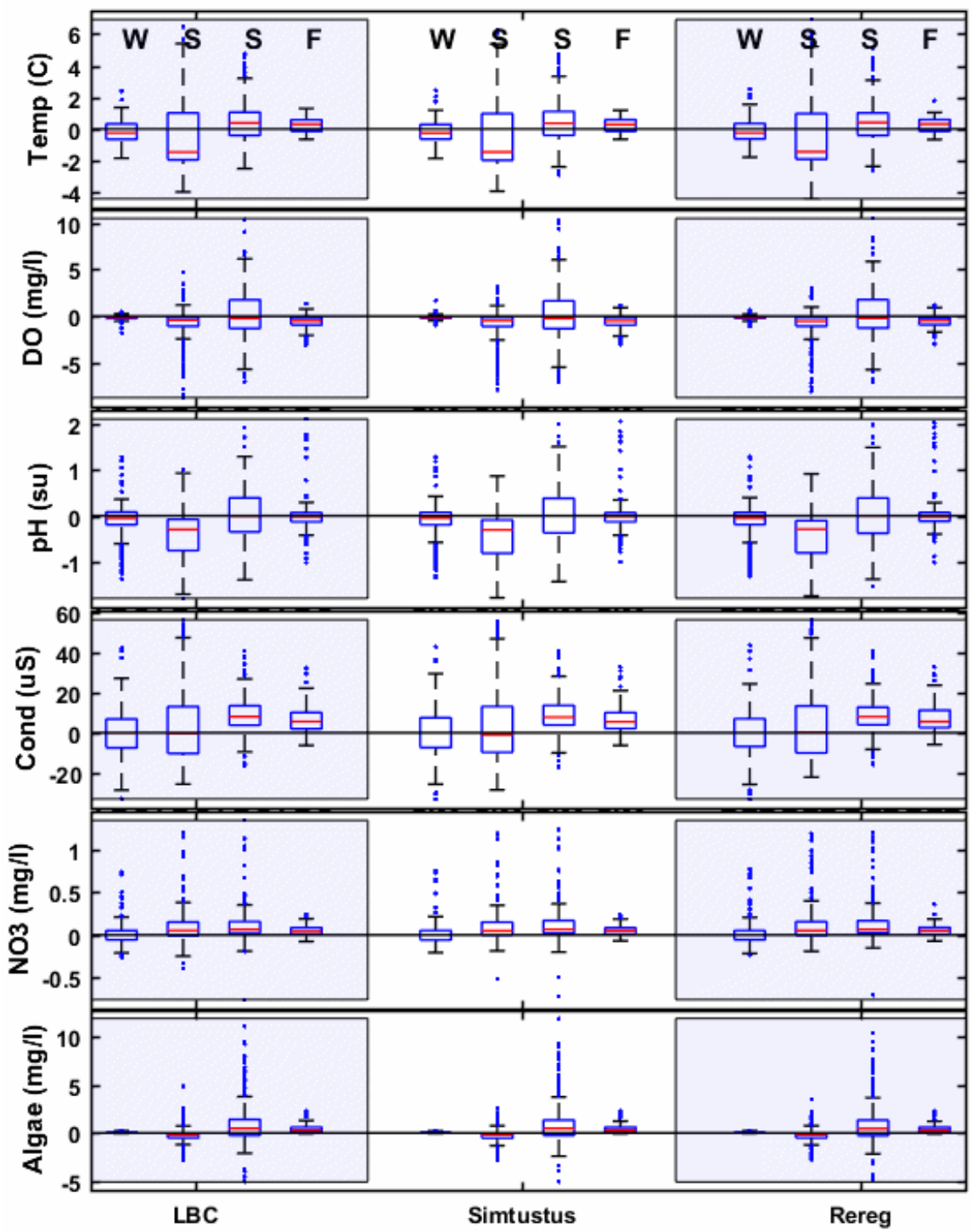

Figure 11-19. A comparison of the differences between baseline and No SWW scenario daily values in the tailraces of the reservoirs across four seasons. Positive values indicate that the scenario value was larger than baseline values. Seasons are shown in order of winter (W), spring (S), summer (S), and fall (F).

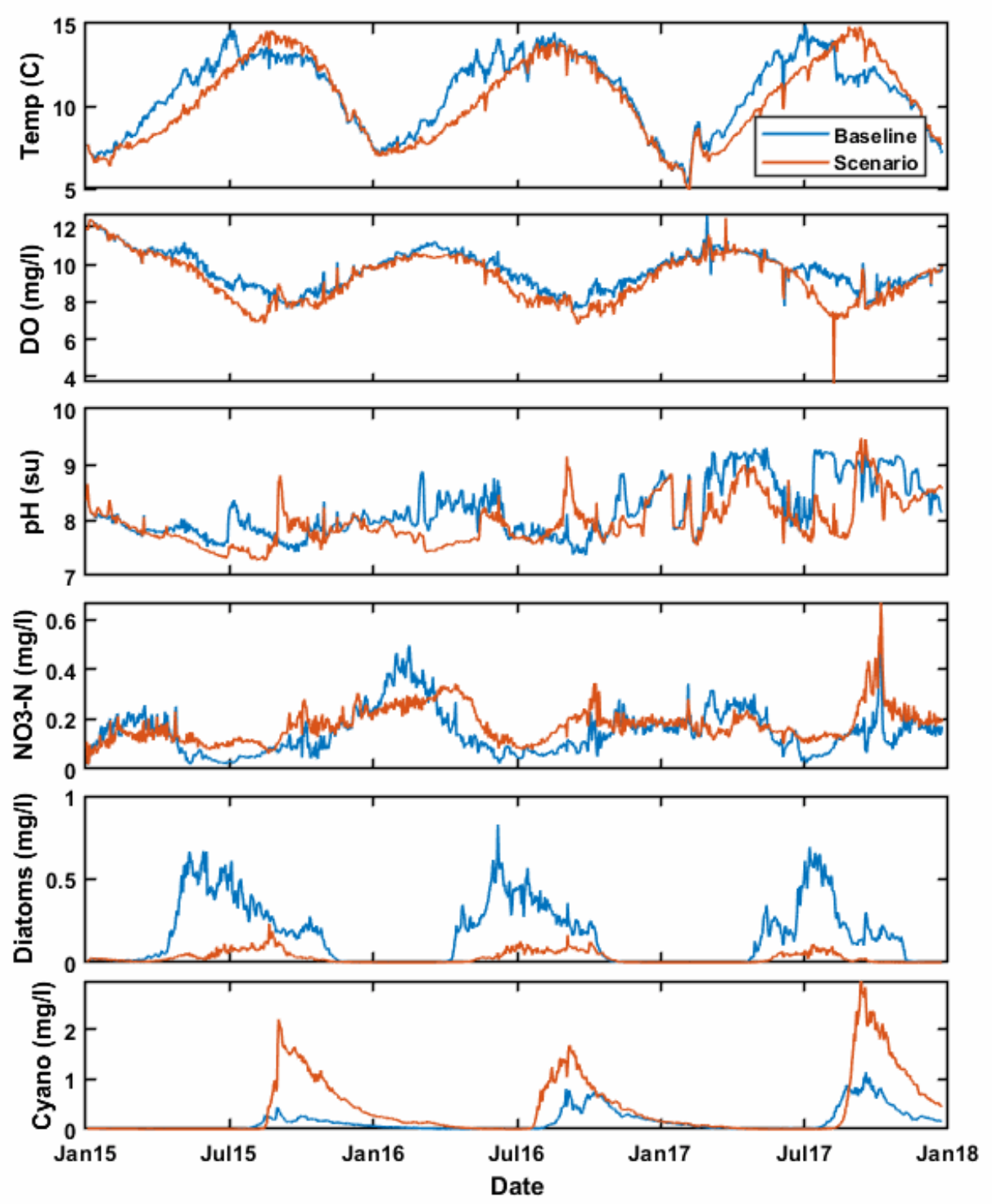

Figure 11-20. Time series of daily model results in ReReg tailrace for the No SWW scenario. Baseline condition results are shown in blue, and scenario results are shown in orange.

The patterns in the LDR are similar to those outlined for RM 96 (Figure 11-21) and Moody (RM 1) (Figure 11-22). DO and pH values are lower for scenario conditions than for the baseline, although scenario pH does increase during the late summer. The late-summer pH increase appears to have been caused by an increased export of cyanobacteria, which flourished during the warmer surface water conditions associated with scenario conditions. The effect of the scenario is also seen with the periphyton, which decrease under scenario conditions, likely because of lower water temperatures in the spring and early summer.

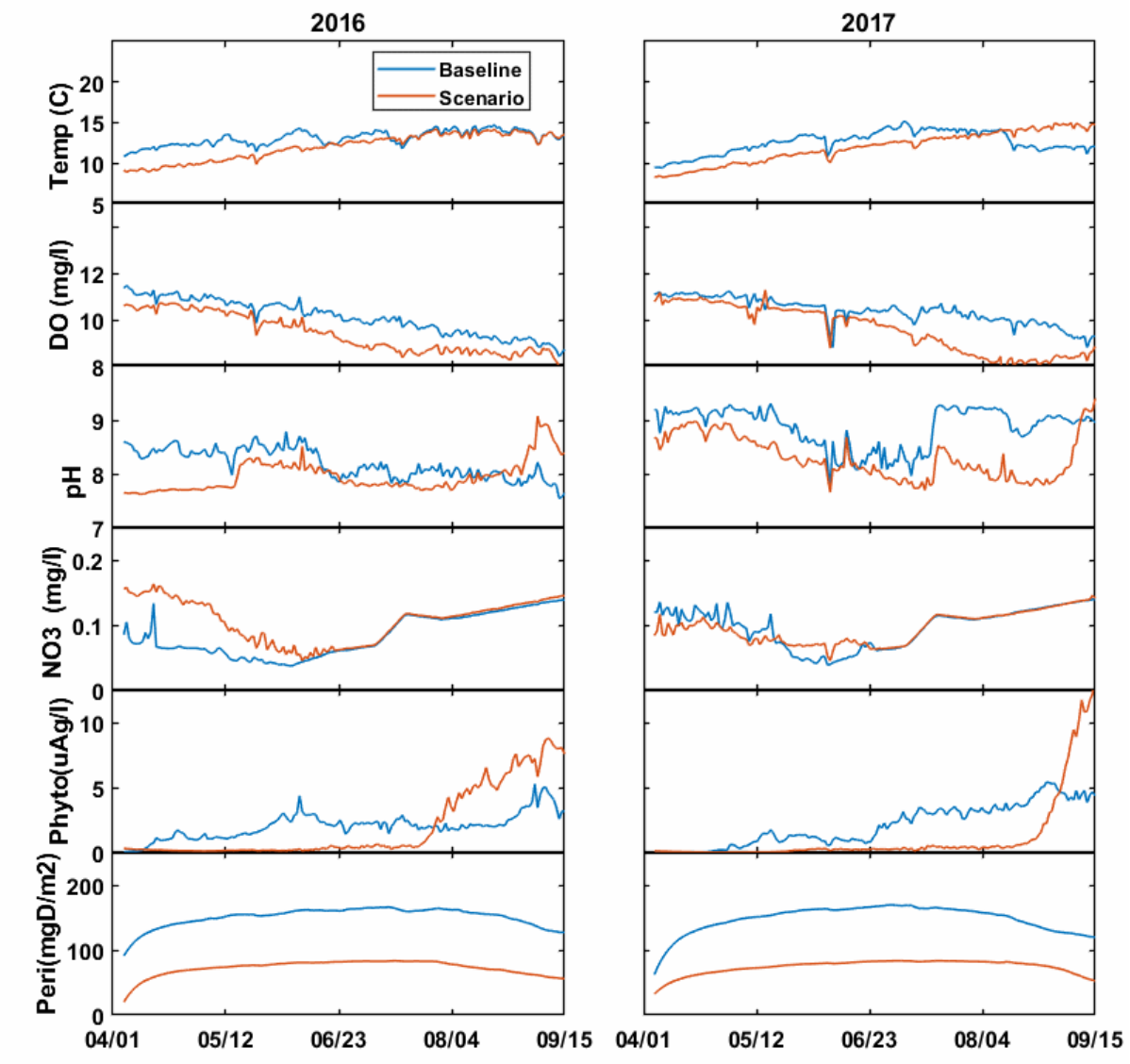

Figure 11-21. A comparison of daily results at RM 96 on the LDR for the No SWW scenario. Data from 2015 were used for calibration so are not displayed.

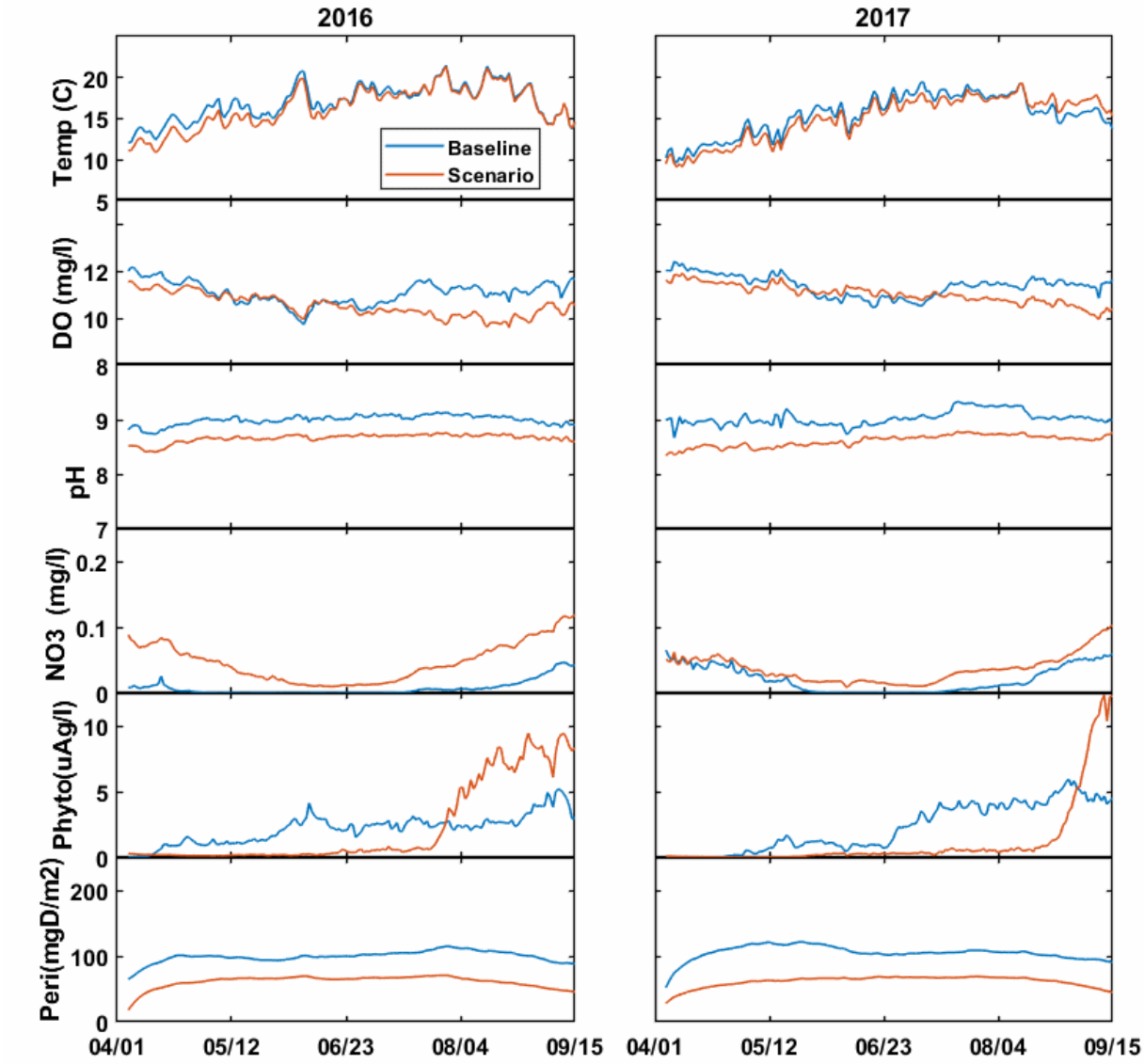

Figure 11-22. A comparison of daily results at Moody (RM 1) on the LDR for the No SWW scenario. 2015 data were used for calibration so are not displayed.

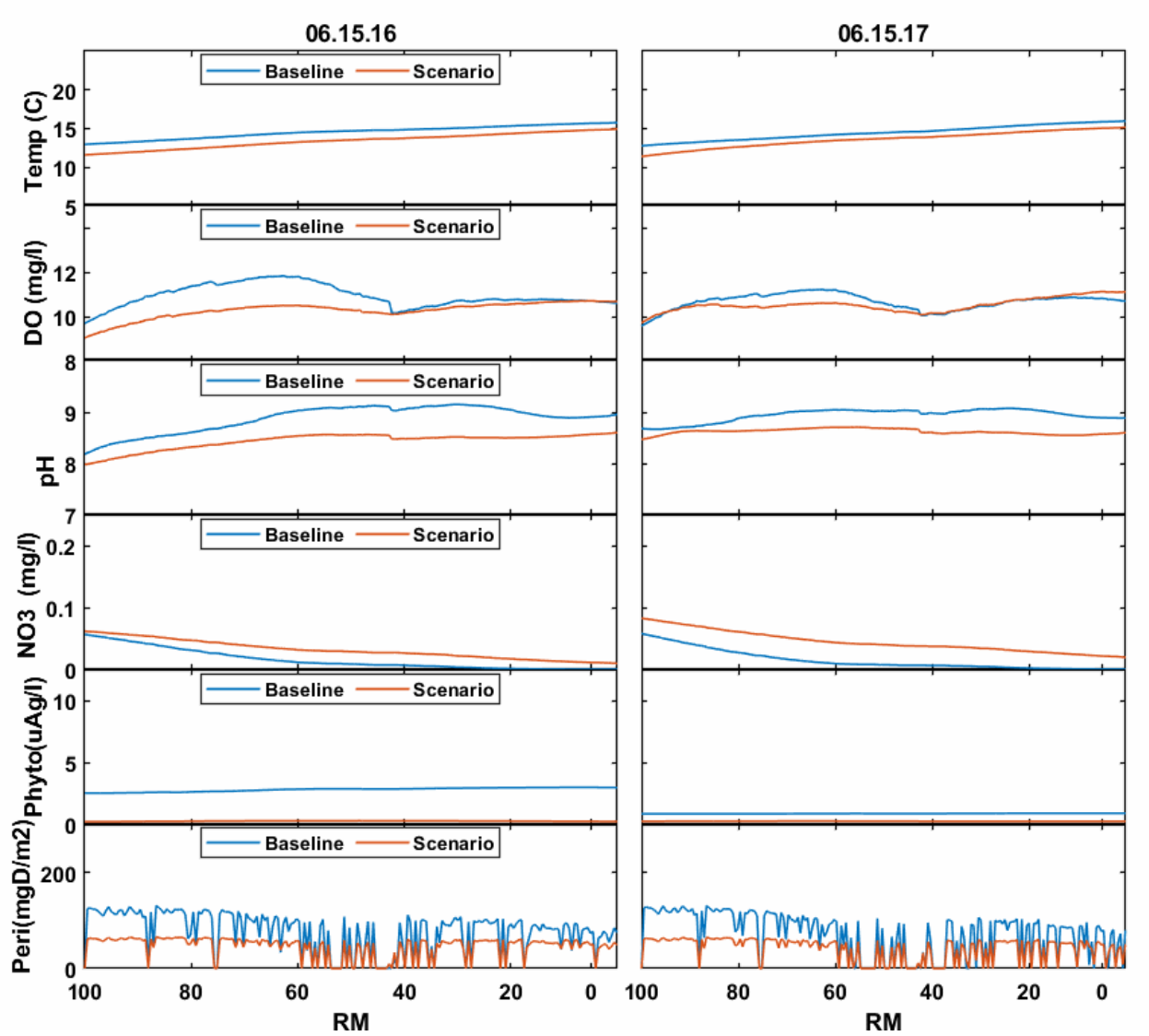

Figure 11-23. Longitudinal water quality profiles for the No SWW scenario, from ReReg Dam (RM 100.1) to the LDR mouth (RM 0). These profiles were taken on June 15 of 2016 and 2017.

11.5 Night Blend Scenario

The Night Blend scenario evaluates a condition in which, during the primary fish migration period from March 15 to June 15, the SWW operates with 100% surface water withdrawals during the night and 40% surface water withdrawals during the day. During the rest of the year, gate flows are the same as baseline conditions. "Night" was defined as the hours from 9 p.m. to

4 a.m. This scenario was explored in response to a previous study (Pyper 2016), which found that fish benefit from high surface flows during that time period.

As outlined in sections 11.2 through 11.4, modifying the operation of the SWW changes the mixing dynamics in LBC, which influences the temperature and productivity of the water moving through Lake Simtustus, the ReReg Reservoir, and the LDR. The Night Blend scenario explores a similar dynamic, and the projected results are similar. In this scenario, more water is released from the bottom gate than in baseline conditions (Figure 11-24). A set of water temperature profiles from the Round Butte forebay (RES07) describe this response (Figure 11-25). The increase in water released through the lower gate leaves less cold water in LBC and warmer water at the surface (Figure 11-26). Warmer surface water results in an increase in productivity in the surface water.

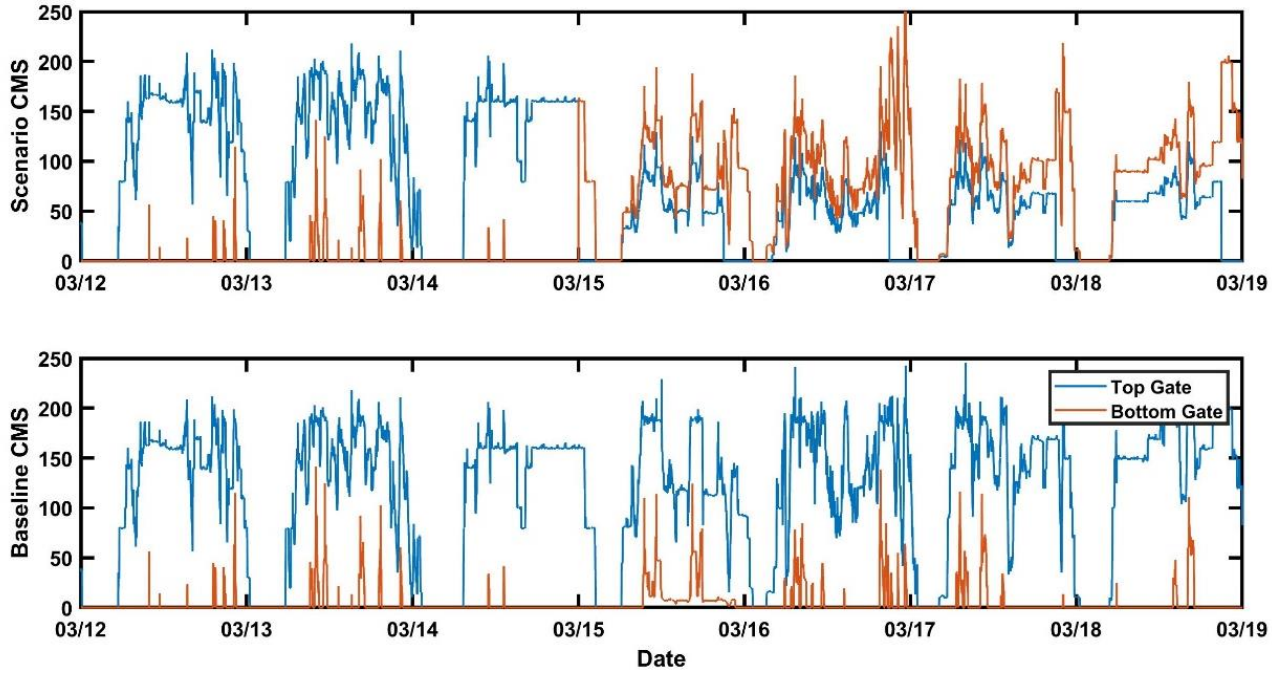

Figure 11-24. Gate flows associated with the Night Blend scenario. A subset of 7 days is included to more fully outline changes in the daily operation of the SWW under this scenario (*top*). Note that before March 15, the flows are the same as in baseline conditions (*bottom*).

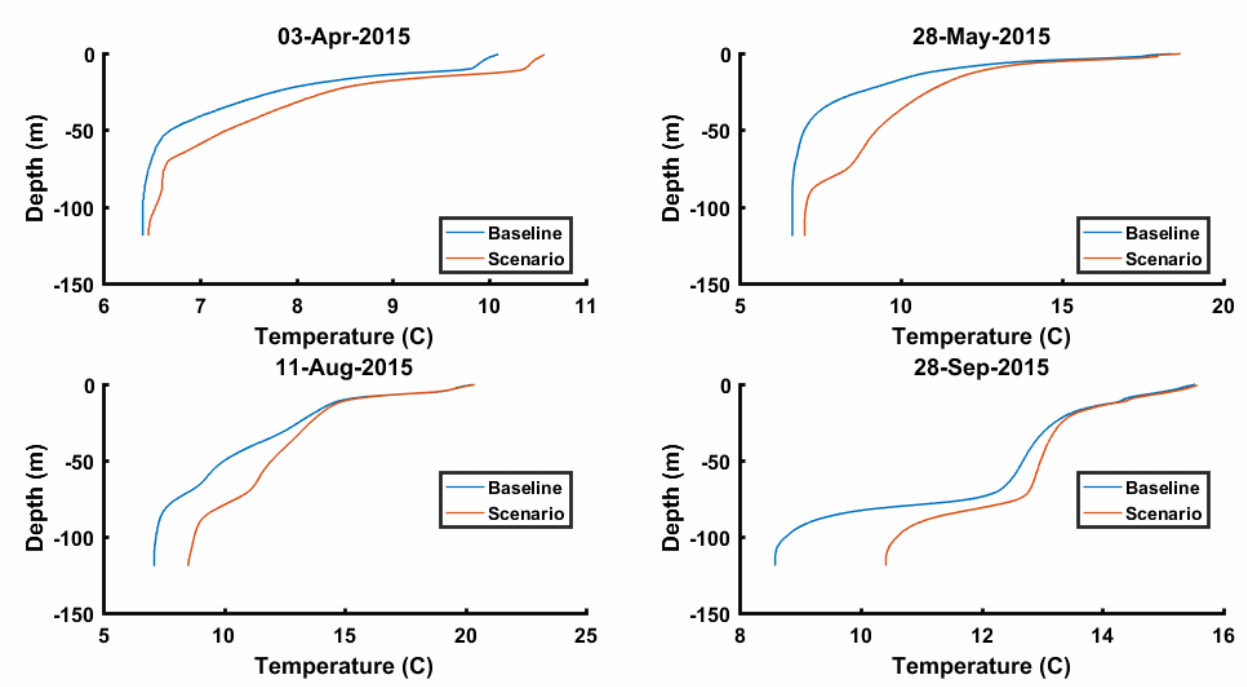

Figure 11-25. Temperature profiles (°C) comparing results for the Night Blend scenario to the baseline in Round Butte forebay (RES07). The scenario results in more cold water being released from LBC, which leaves less cold water in the reservoir. This results in an increase in temperature across the profile depth.

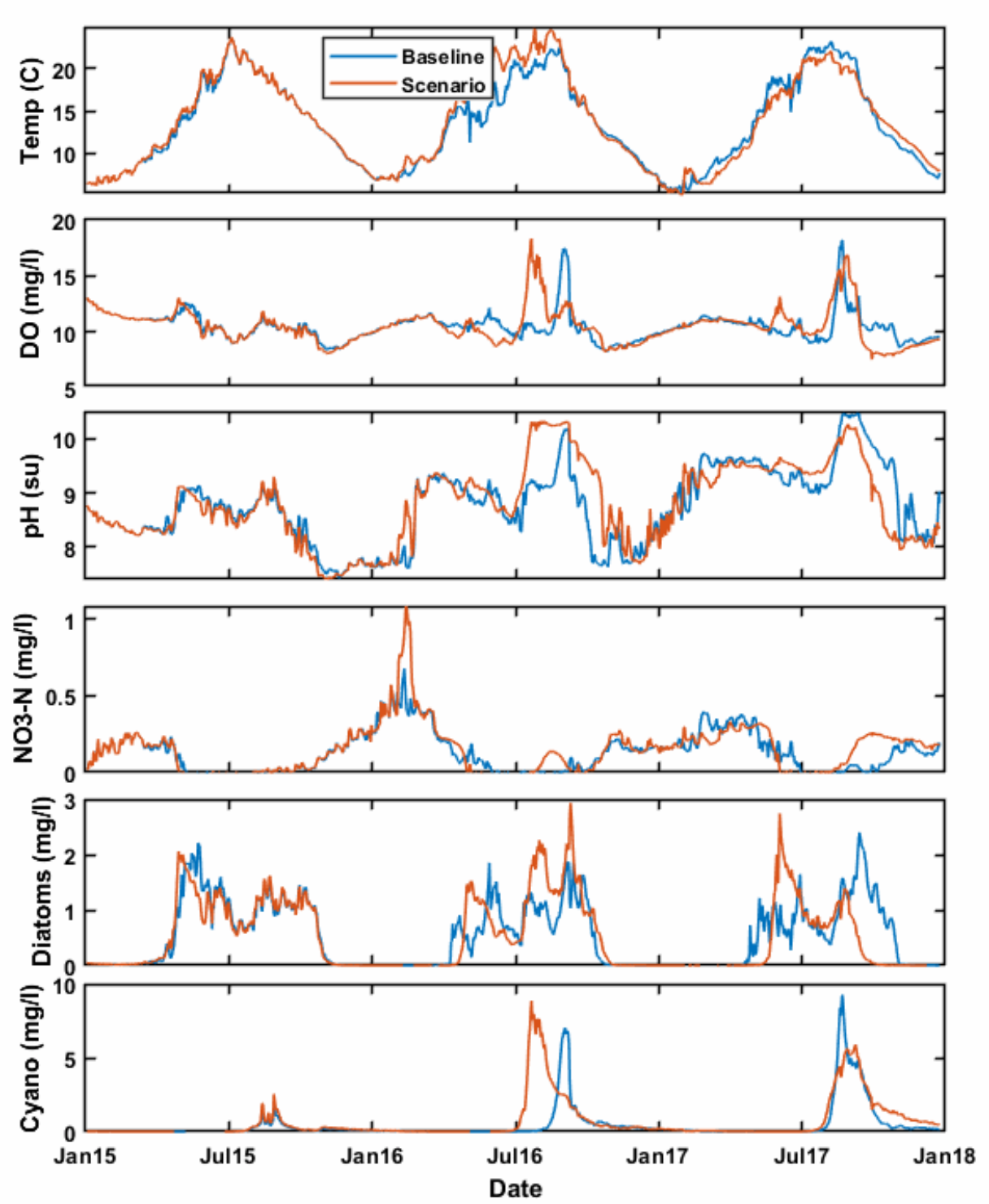

Figure 11-26. Time series of daily model results for the Night Blend scenario in the surface water of Round Butte forebay (RES07). Baseline condition results are shown in blue, and scenario results are shown in orange.

Night Blend scenario conditions impact Round Butte tailrace temperatures and water quality (Figure 11-27), resulting in cooler tailrace water in the spring and early summer, and warmer tailrace water in the late summer, as cold water in LBC is consumed. This pattern of change might have a critical effect on the LDR fall Chinook. This thermal pattern holds as the tailrace water from LBC moves through Lake Simtustus and the ReReg Reservoir, showing a pattern similar to that in the ReReg tailrace (Figure 11-28). Thermal conditions within the tailraces of the three reservoirs are shown in the seasonal boxplots (Figure 11-29).

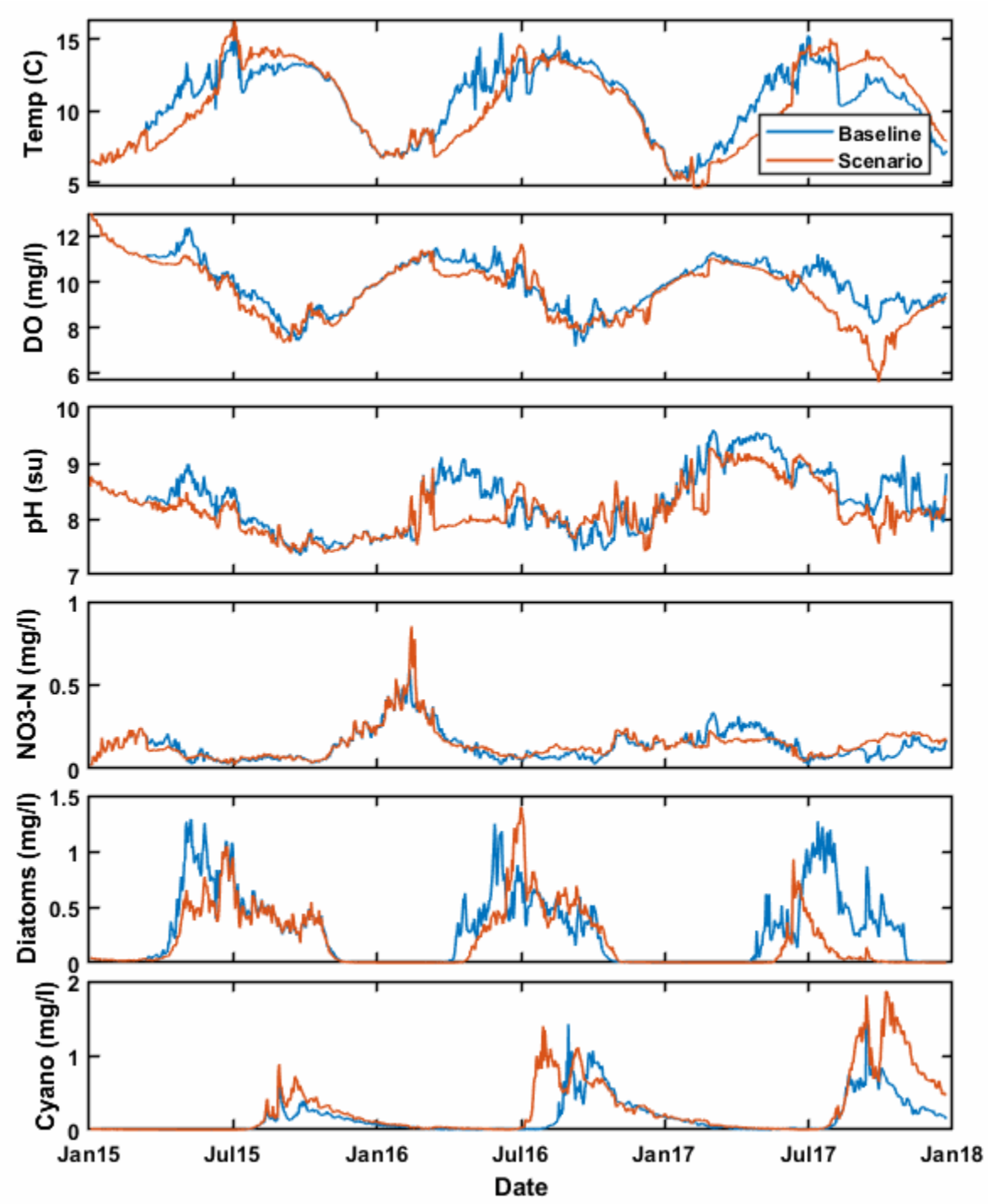

Figure 11-27. Time series of daily model results in the Round Butte tailrace with the baseline results in blue and the Night Blend scenario results in orange.

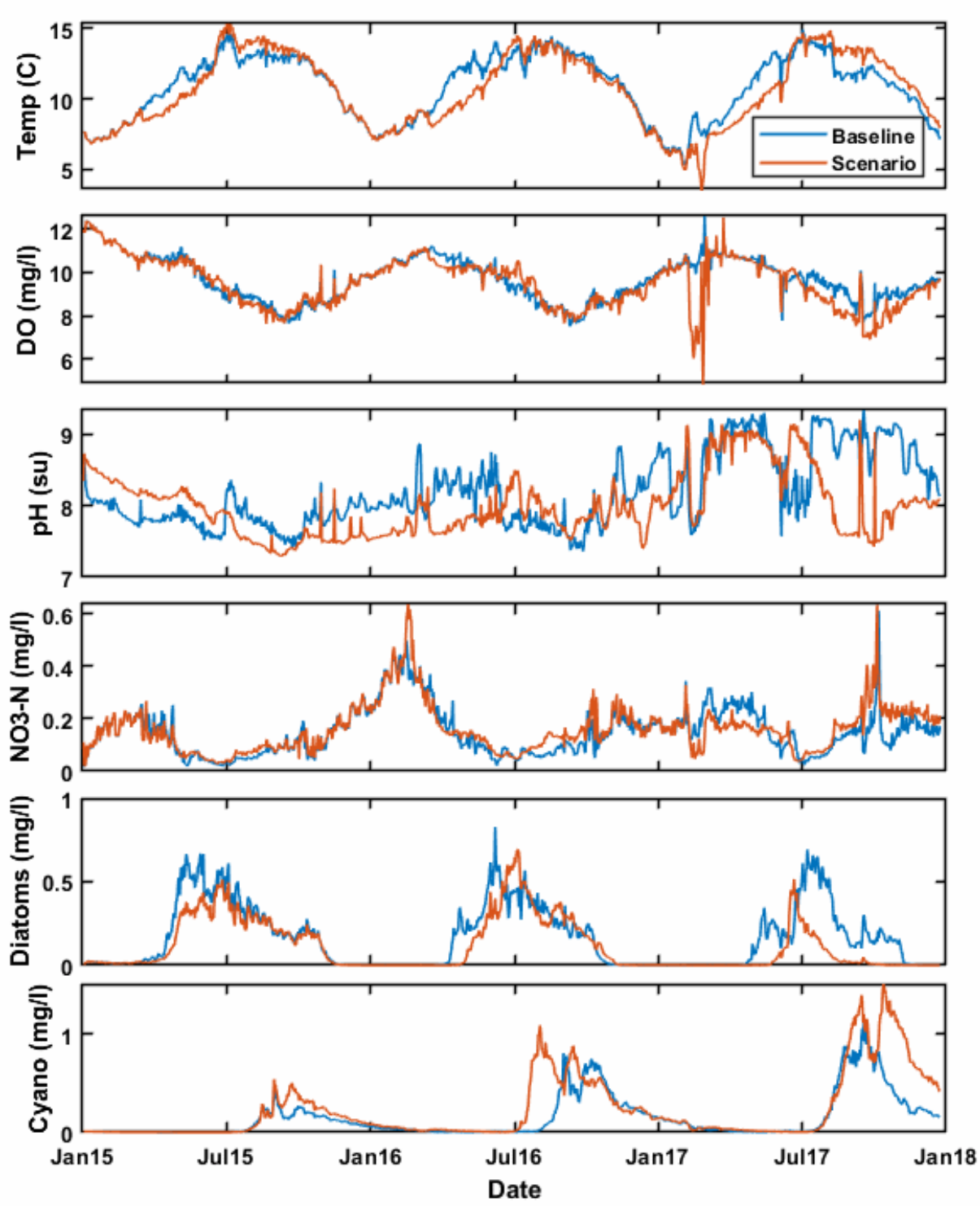

Figure 11-28. Time series of daily model results in the ReReg tailrace, with the baseline results in blue and the Night Blend scenario results in orange.

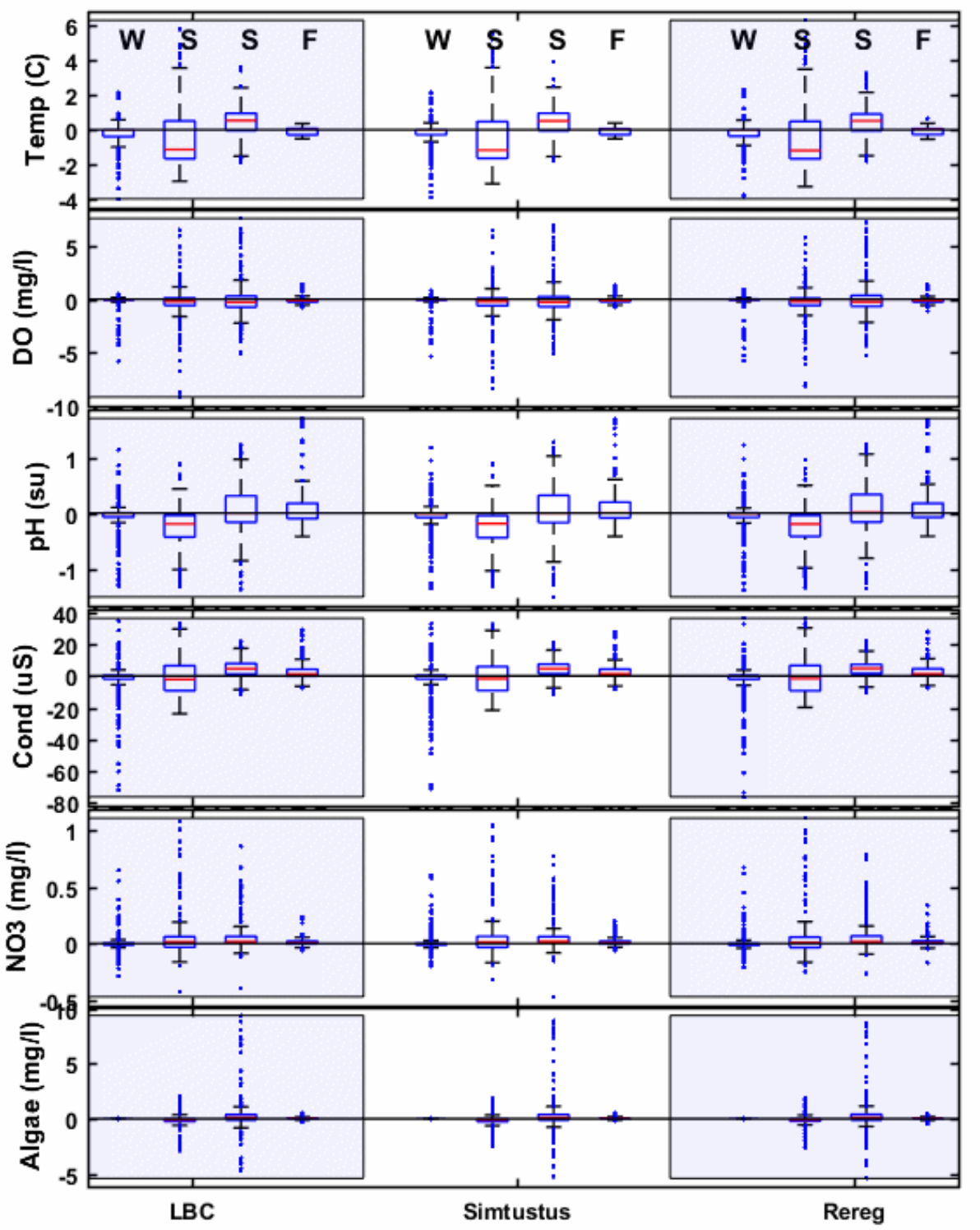

Figure 11-29. A comparison of the differences between baseline and scenario daily values across four seasons in the reservoirs. Positive values indicate that the scenario value was larger than baseline value.

In the LDR, the cooler spring and early summer conditions at the ReReg tailrace lead to cooler and less productive conditions throughout the LDR (Figure 11-30). Conditions in model year 2016 led to warmer and more productive late summer conditions at Moody (Figure 11-31, *left*). Note the increases in late summer algae, pH, and periphyton. However, in model year 2017, the cooler early season conditions did not result in more productive late-season conditions (Figure 11-31, *right*). The differences between the two years highlight the dynamic nature of the system and likely results from an interaction between climate, the scenario release assumptions, and mixing dynamics in LBC.

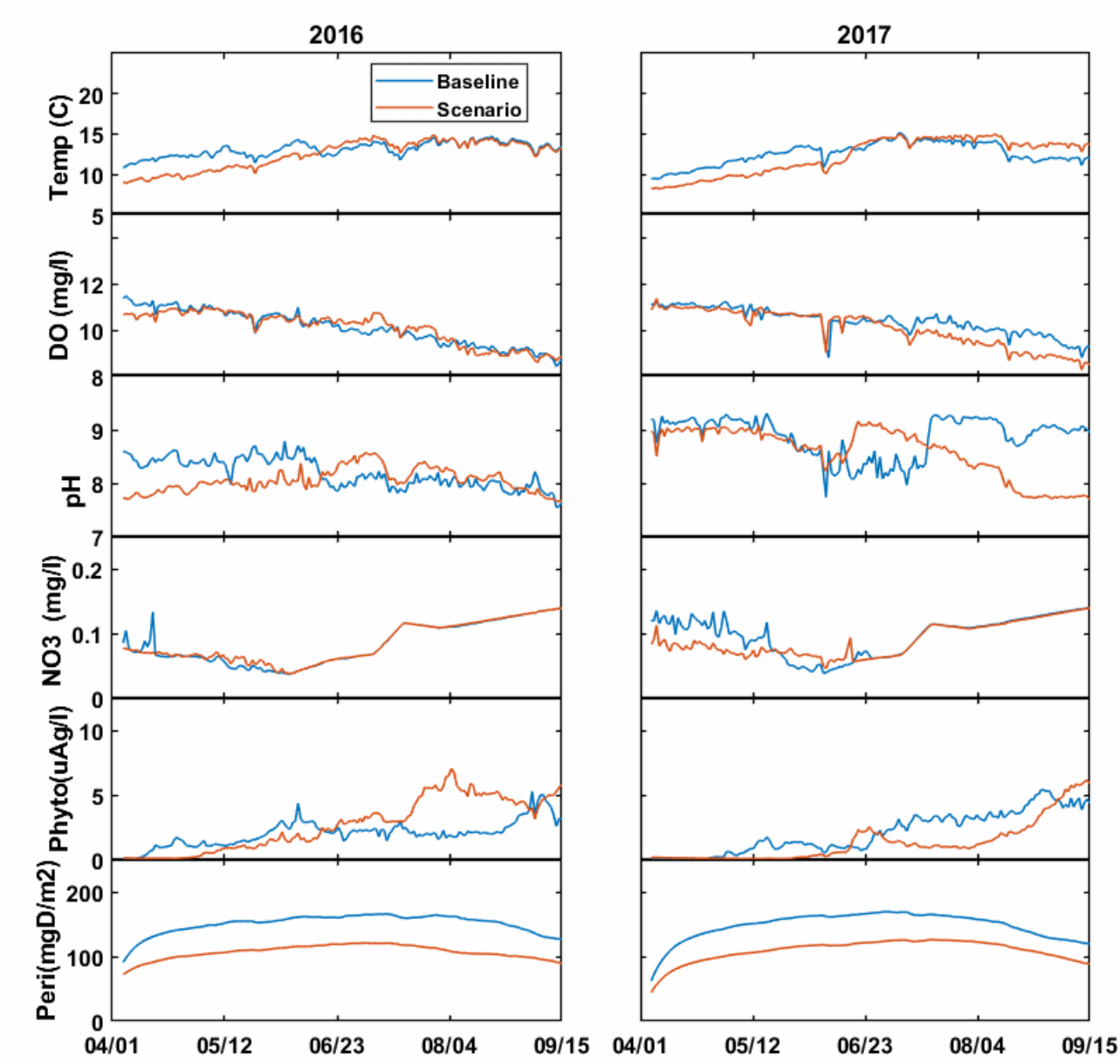

Figure 11-30. A comparison of daily results for the Night Blend scenario and the baseline at RM 96.

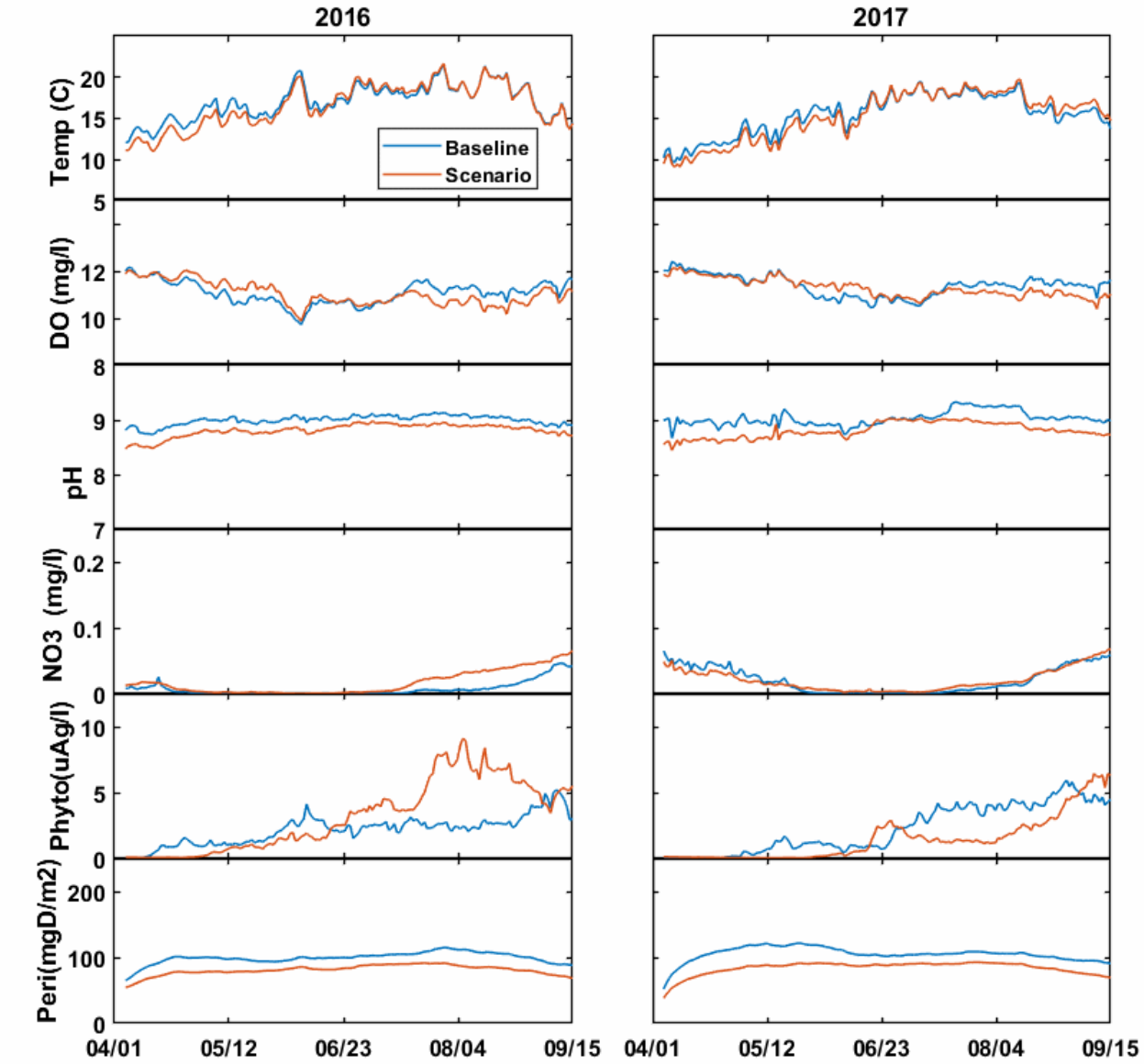

Figure 11-31. A comparison of daily results for the Night Blend scenario and the baseline on the LDR at Moody (RM 1).

11.6 NO_3 Decrease Scenario

The NO_3 Decrease scenario assumes a 75% reduction in NO_3 from the Crooked and Deschutes rivers and Willow Creek, with the goal of exploring how watershed-derived nutrient additions impact water quality. We chose a 75% reduction because it roughly approximates the magnitude of the difference in NO_3 concentrations between the Metolius and Crooked rivers.

These reductions in nutrient concentrations were incorporated into the LBC model inputs, then run through the three reservoirs to produce input for the LDR model. In this scenario, we focus the analysis exclusively on the LDR results.

The reductions in NO_3 export to the LDR result in changes throughout the river system. At RM 96, near the ReReg tailrace, the most obvious differences between the scenario and the baseline are the NO_3 concentrations, not surprising given the scenario definition. These decreases in NO_3 are associated with decreases in the algal biomass as well as periphyton development. pH and DO show minor responses at RM 96 (Figure 11-32). Further downstream, at the mouth of the LDR, comparable reductions in NO_3, algal biomass, and periphyton are simulated (Figure 11-33). The changes in pH and DO are more pronounced than at RM 96, primarily because of reduced primary production throughout the LDR, given the reduction in available nutrients. The potential impacts of these changes on macroinvertebrate and piscine communities are outside the scope of this investigation.

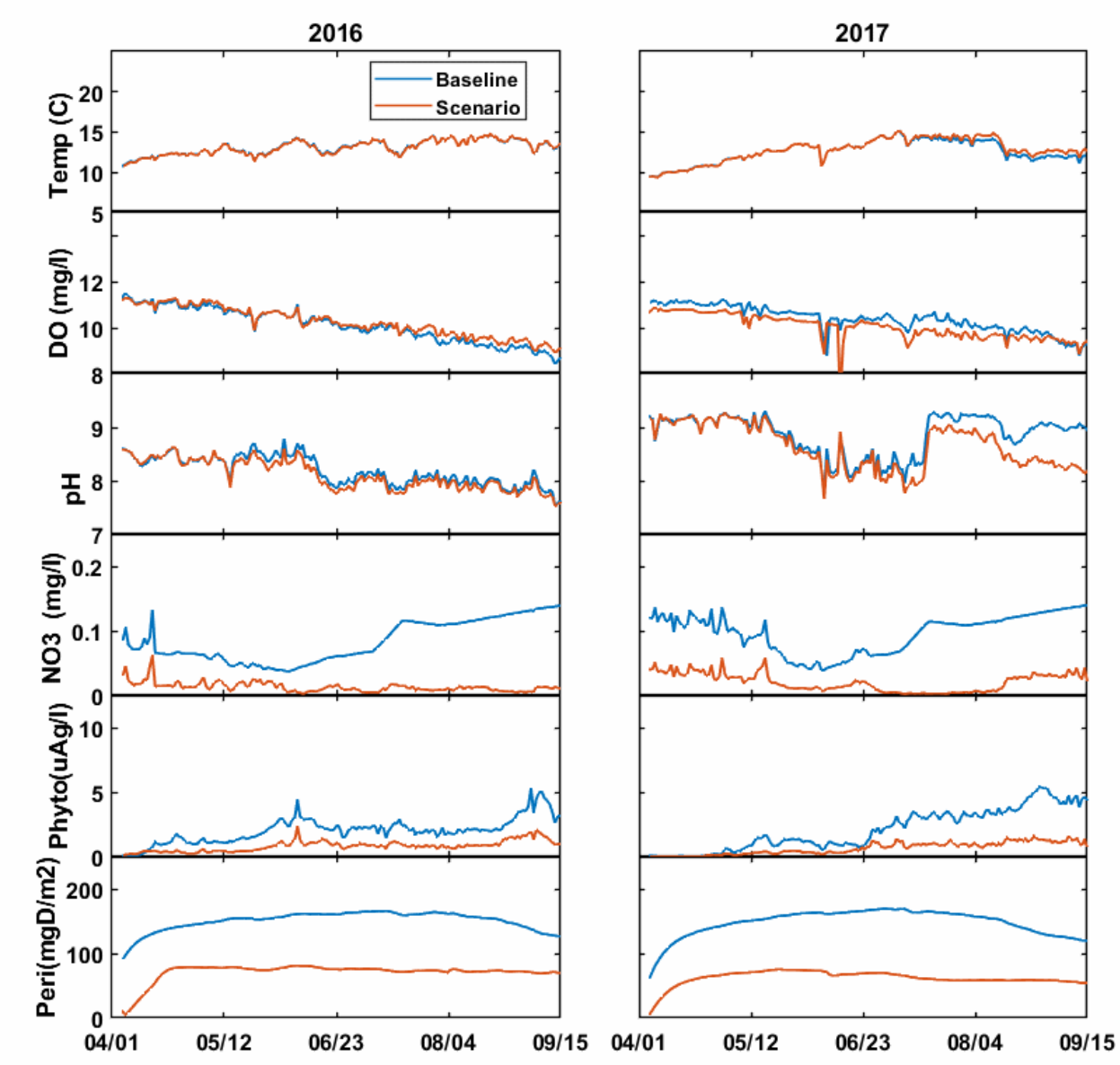

Figure 11-32. A comparison of daily results at RM 96 on the LDR for the NO_3 Decrease scenario.

.

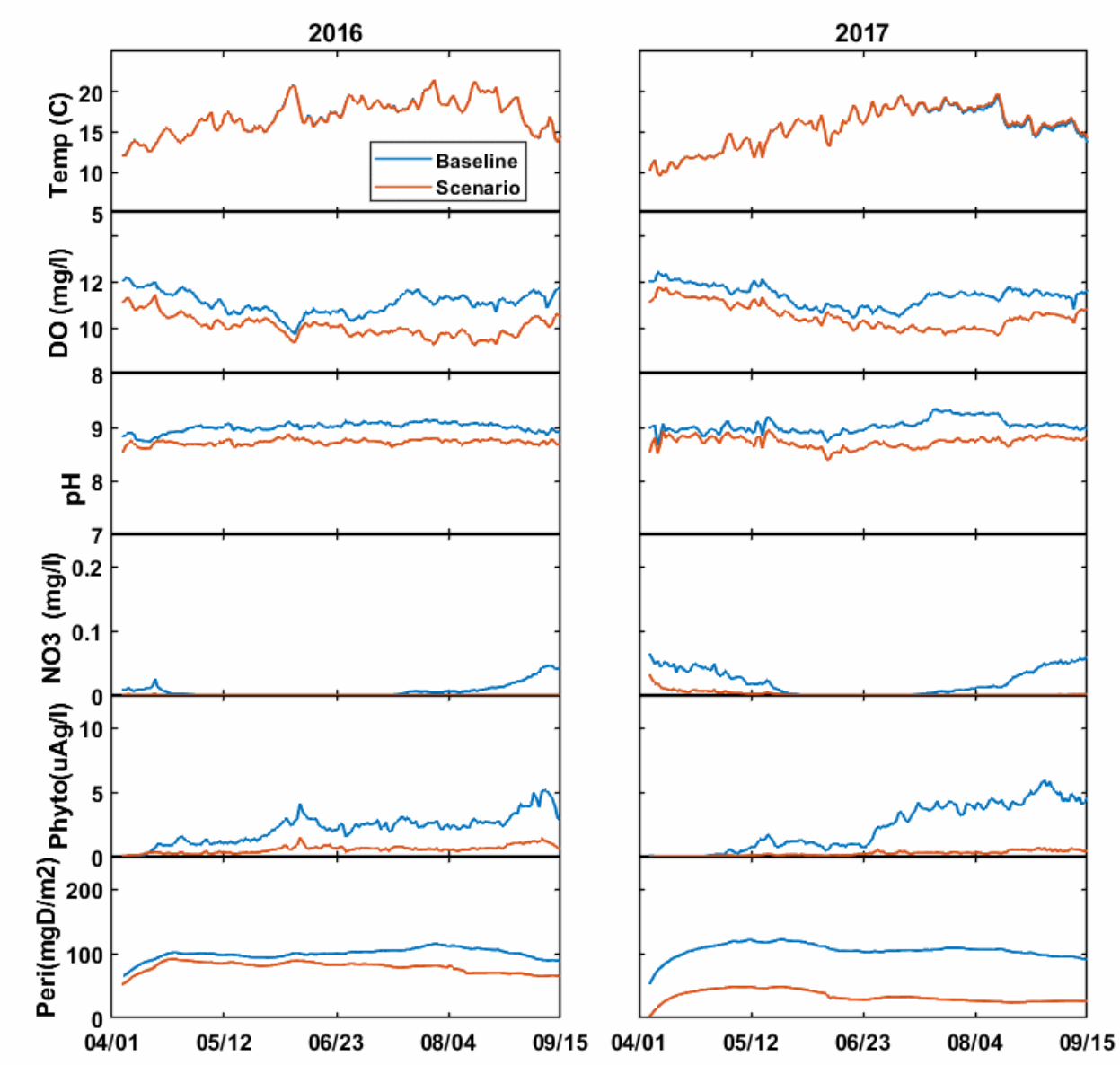

Figure 11-33. A comparison of daily results at Moody (RM 1) on the LDR for the NO_3 Decrease scenario.

11.7 Nitrogen and Phosphorus Decrease Scenario

We developed a second watershed nutrient reduction scenario to explore the impact of reductions in both nitrogen and phosphorus. The scenario assumes that the concentrations of both were reduced by 50% in the Crooked River inflow to LBC. As with the NO_3 Decrease scenario, the results from the reservoir models were used to drive the LDR models, but the analysis focuses only on the LDR. This scenario was developed to complement the NO_3 Decrease scenario by reducing both key nutrients and more fully describing the contribution of each to primary production in the LDR.

In most ways, the results from this scenario mimic those from the NO_3 Decrease scenario, with the imposed reductions in nutrient levels driving reductions in pH, phytoplankton, and periphyton density. Figure 11-34 and Figure 11-35 outline results from RM 96 and Moody (RM 1), respectively. Note in the figures that DO has been replaced with PO_4 to demonstrate that both nitrogen and phosphorus were reduced.

While patterns are similar to those from the NO_3 Decrease scenario, the magnitude of the changes are notably smaller, likely because of the modeled sensitivity to available nitrogen. In this scenario, nitrogen from the Crooked River was reduced by 50% while, in the NO_3 Decrease scenario, it was reduced by 75%, effectively elevating the export of nitrogen in this scenario. That difference appears to impact periphyton and phytoplankton development, which in turn impacts other indicators of primary production (e.g., pH). While phosphorus was also reduced in this scenario, those reductions do not appear to impact results because available phosphorus concentrations (characterized by PO_4) remain high enough that nitrogen remains the primary nutrient limitation.

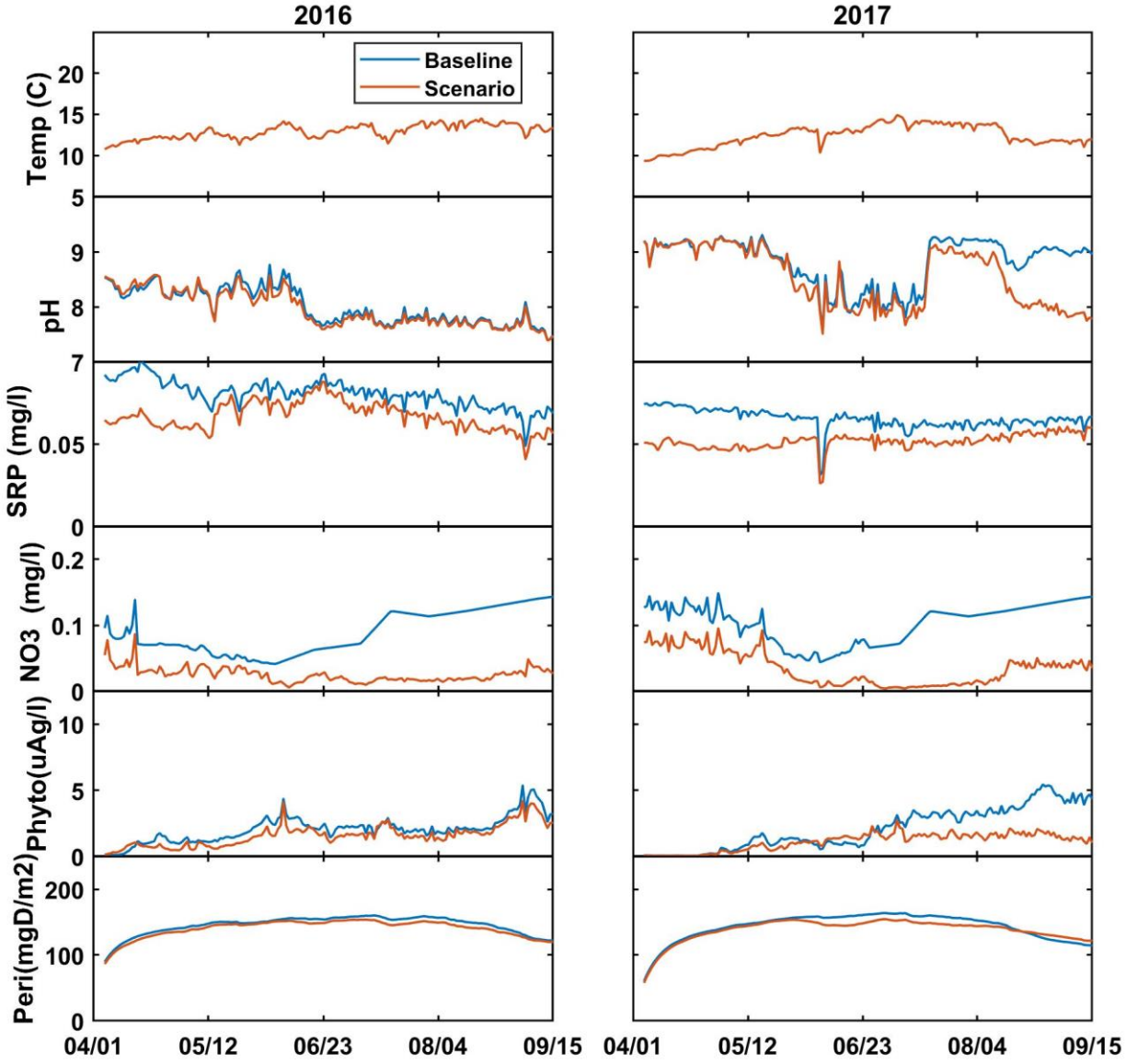

Figure 11-34. A comparison of daily results at RM 96 on the LDR for the Nitrogen and Phosphorus Decrease scenario.

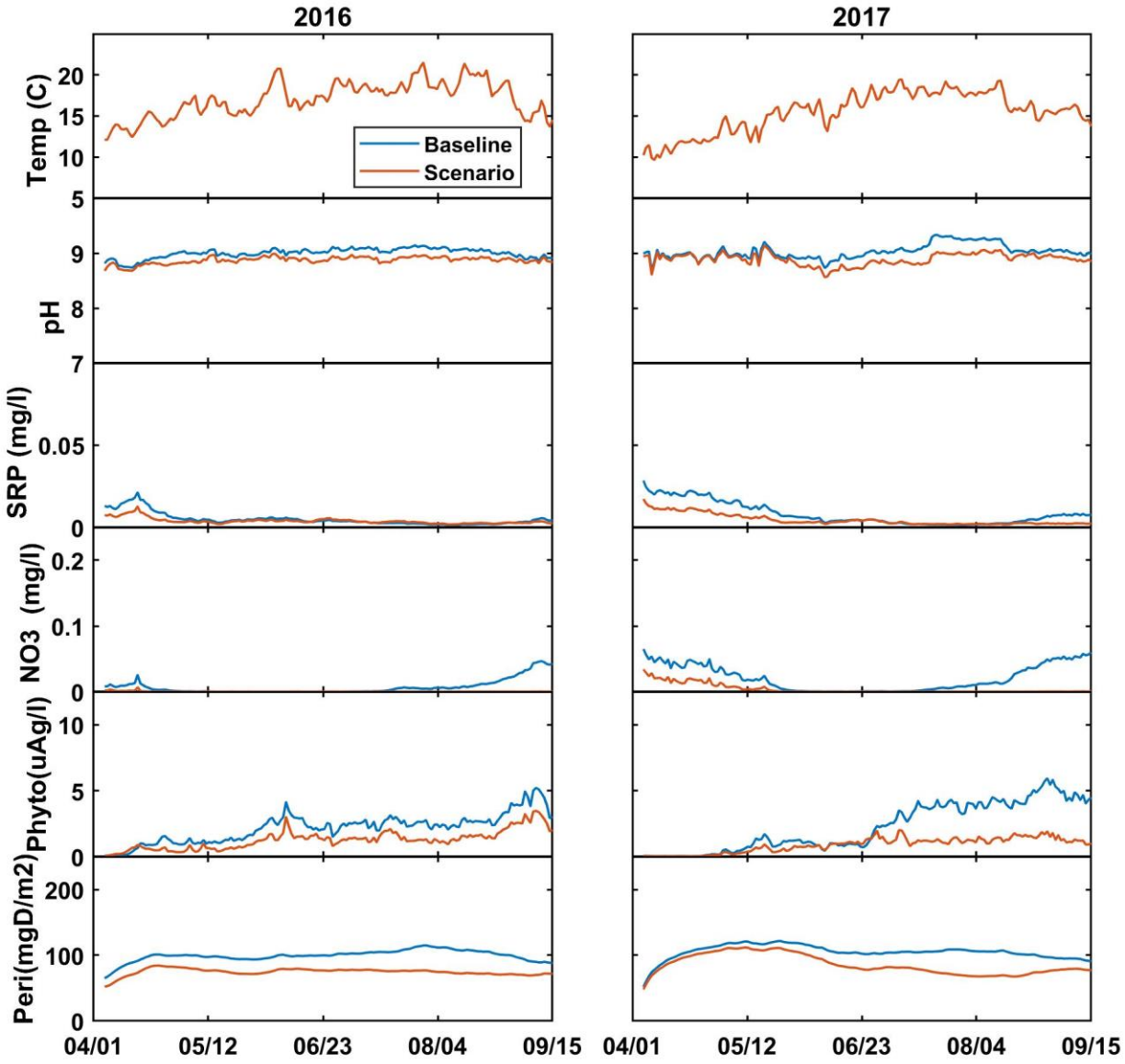

Figure 11-35. A comparison of daily results at Moody (RM 1) on the LDR for the Nitrogen and Phosphorus Decrease scenario.

To more fully explore the relative roles of limiting factors, Figure 11-36 outlines how water temperature, light, nitrogen, phosphorus, and carbon contribute to periphyton limitation. The most limiting factor is the availability of light, while the impact of water temperature decreases as temperatures warm, and carbon is overabundant and not limiting at any point (the value is 1.0

at all times). In the baseline model, nitrogen and phosphorus make a very similar contribution to the overall model limitation, but under the Nitrogen and Phosphorus Decrease scenario, the nitrogen limitation increases significantly, while the phosphorus limitation remains similar to that in the baseline. This indicates that the system is more sensitive to changes in nitrogen than it is to changes in phosphorus, a result that supports the theory that phosphorus is abundant relative to stoichiometric requirements and that it is nitrogen that acts as the primary nutrient limitation.

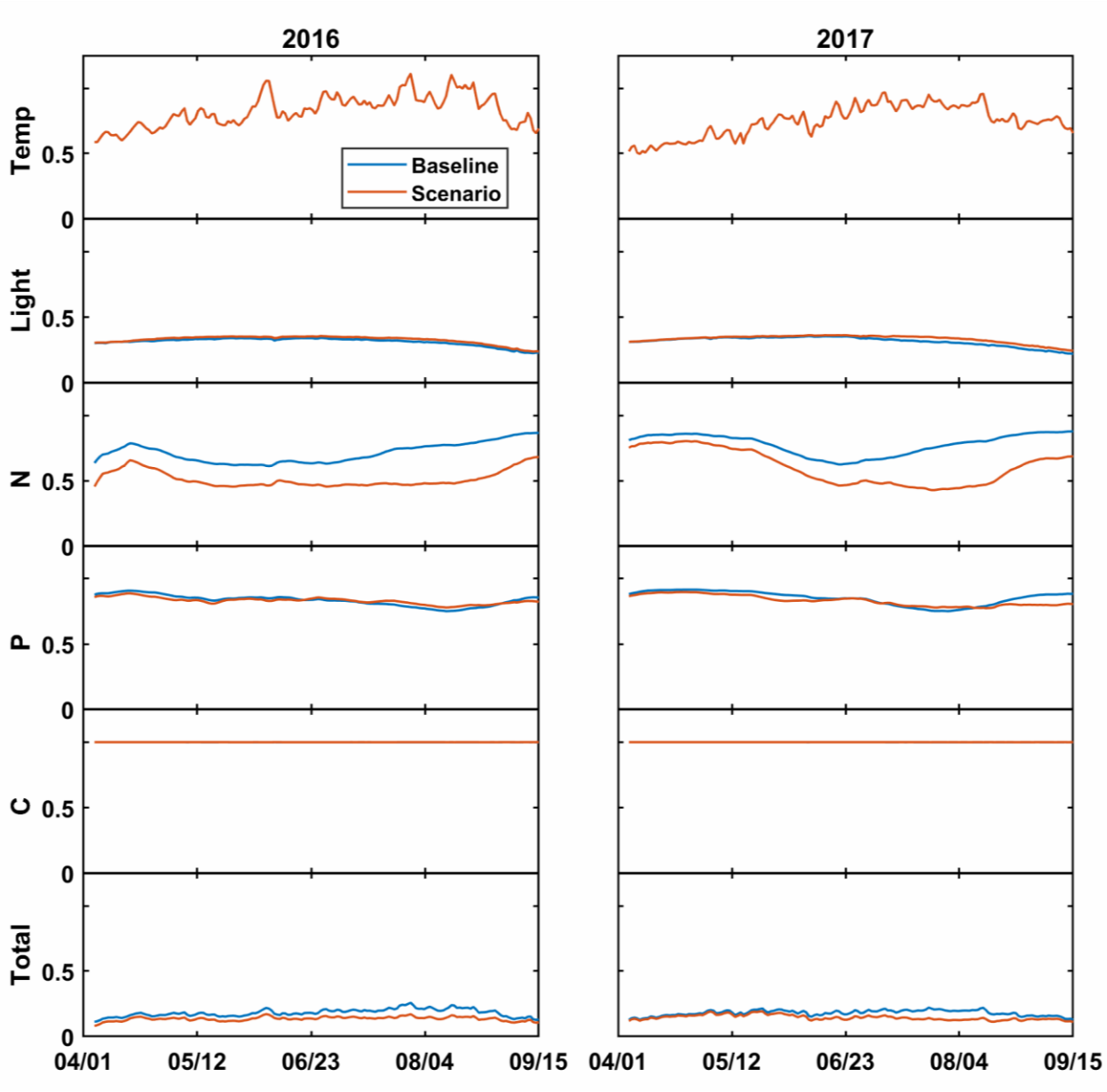

Figure 11-36. A time series figure outlining the proportion of total periphyton growth limitation attributed to each limiting variable. These results represent the LDR at Moody (RM 1). A value of 1 indicates no limitation, while a value of 0 indicates complete limitation.

11.8 Curtain Scenario

This scenario explores the impact of the installation of a curtain across LBC at a location in the Round Butte forebay (RES07). The curtain is intended to keep algae from moving through the SWW and into Lake Simtustus. A W2 scenario was developed to evaluate the potential impacts

of this strategy. The scenario condition assumes the curtain is installed in the forebay, at a location between 250 m and 500 m from the SWW. The analysis includes a variety of curtain depths. It is simulated as a skimmer weir taken from Cole and Wells (2006) and is operational from June 16 to September 15 (Figure 11-37). This operational window was chosen to limit the curtain's impact on fish passage (March 15–June 15). To simulate the yearly installation and removal of the curtain, the W2 model was paused to allow for parameter changes, and then restarted with the updated presence/absence of the curtain.

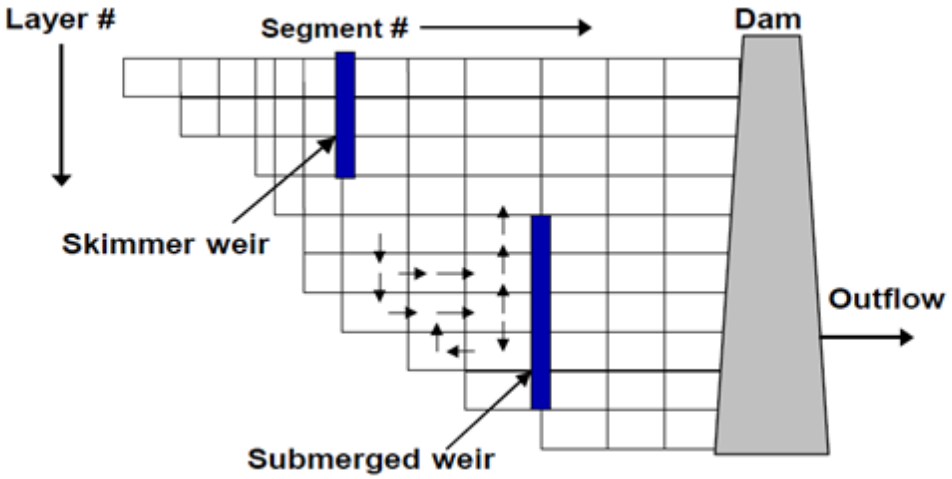

Figure 11-37. The curtain is represented as a skimmer weir in the Curtain scenario (*Source*: Cole and Wells, 2006).

We evaluated three curtain depths at 20-m intervals between 20 m and 60 m. The purpose of the curtain is to hold algae, which tend to collect in the warmer, lighter water near the surface. Both observation and simulation indicate that algae are present at depths over 30 m, suggesting that the curtain might need to be at least that deep. Another factor that might be relevant is the seiche that develops during windy periods, which might result in a deeper epilimnion, allowing algae and other water quality components to move under the curtain.

Three time-series plots were developed to explore the impact of the various curtain depths. We looked at water quality in the surface waters in the Common Pool (RES08), Round Butte forebay

(RES07), and ReReg tailrace, which also describes the water that would be introduced into the LDR.

All the curtain options appear to successfully isolate the surface intake from much of the epilimnetic water in LBC. The curtains appear to accomplish this by physically blocking the warmer surface water from entering the intake. The isolation leads to lower water temperatures in the forebay and at the ReReg tailrace during the period when the curtains are in place. In most cases, the deepest curtain provides the greatest isolation, which, in turn, results in the largest decreases in forebay and tailrace temperatures. DO and pH also tend to be lower near the intakes, and the export of early season diatoms is significantly reduced by the curtain. The cyanobacteria show some increase in the forebay in model year 2015, but the 2016 and 2017 results indicate that late summer blooms of cyanobacteria are effectively kept out of the forebay (Figure 11-38).

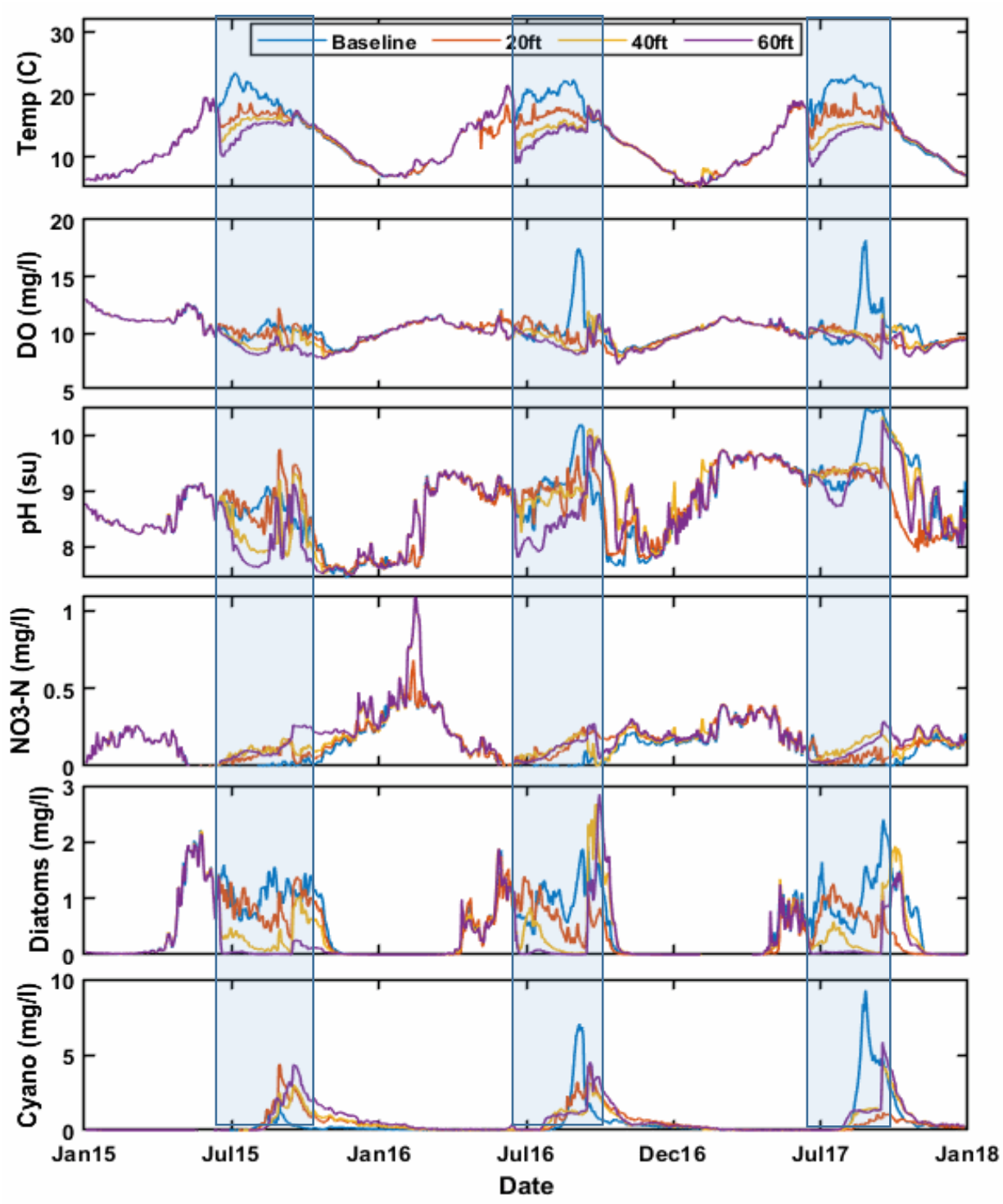

Figure 11-38. Time series of daily model results in the surface water in the Round Butte forebay (RES07) for the Curtain scenario. Four curtain depths are compared against the baseline model (no curtain). The blue boxes indicate the approximate times when the curtains were in place.

The increase in cyanobacteria in the forebay during the 2015 model year with the curtains in place appears to be related to the fact that cyanobacteria are distributed throughout the well-mixed epilimnion during this period. Figure 11-39 shows a cross section from Round Butte Dam through the Crooked River arm during at a point (August 18, 2016) when the 40-ft curtain was in place. The diatoms are scarce at this time late in the summer but are successfully kept from the forebay by the curtain. There are also much less cyanobacteria present in the forebay than on the other side of the curtain. However, the cyanobacteria are abundant, and mixed throughout the epilimnion. These conditions result in a situation where some cyanobacteria are pushed under the curtain by currents developed by gate operations and through wind-driven seiche development, so at least at this point in time, the curtain reduces cyanobacteria export but does not eliminate it.

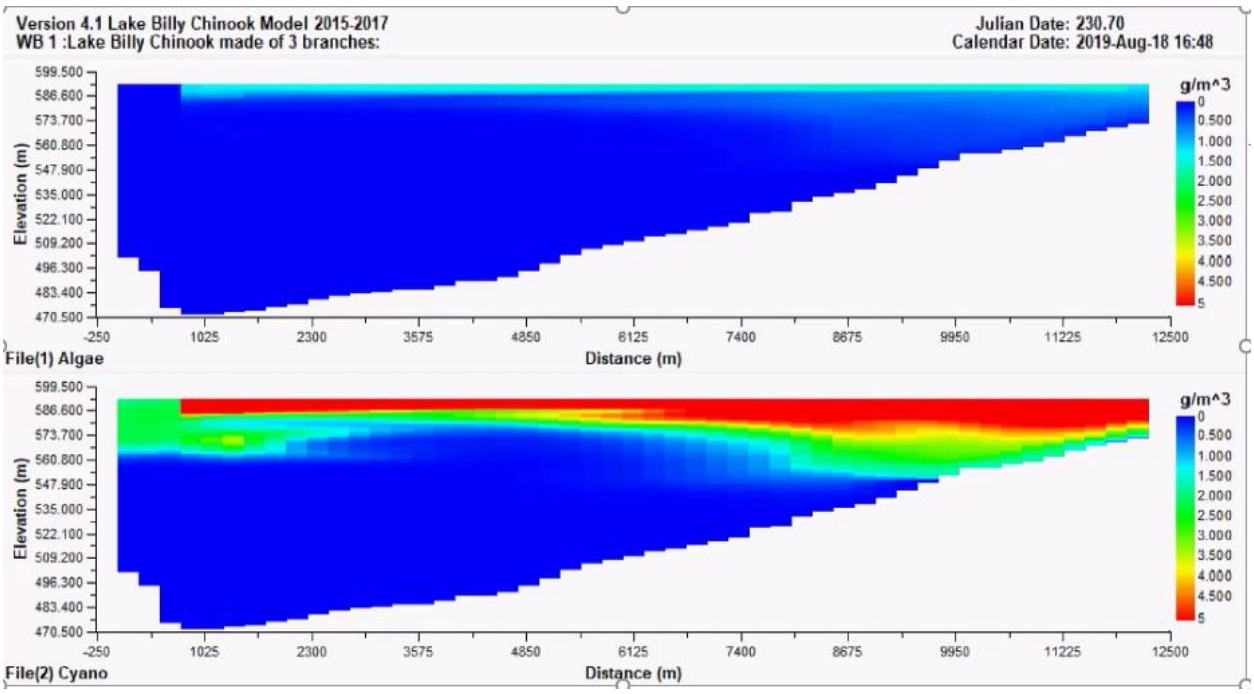

Figure 11-39. A set of cross sections representing algal concentrations in LBC with a 40-ft curtain in place for the Curtain scenario. Diatoms are shown on the *top*, and cyanobacteria are shown on the *bottom*.

Conditions in the Common Pool (RES08) reflect the fact that the curtains result in the export of less warm surface water LBC. Reduced surface water export in turn results in warmer water remaining in the reservoir. This water tends to be more productive, and has higher DO and pH, and increased concentrations of algae. Surface water temperatures also tend to be warmer, particularly in the 2016 and 2017 model years (Figure 11-40). The changes in surface temperature and low NO_3 favor cyanobacteria over diatoms, and cyanobacteria abundance is, in fact, increased in these areas of the reservoir when compared against the baseline model.

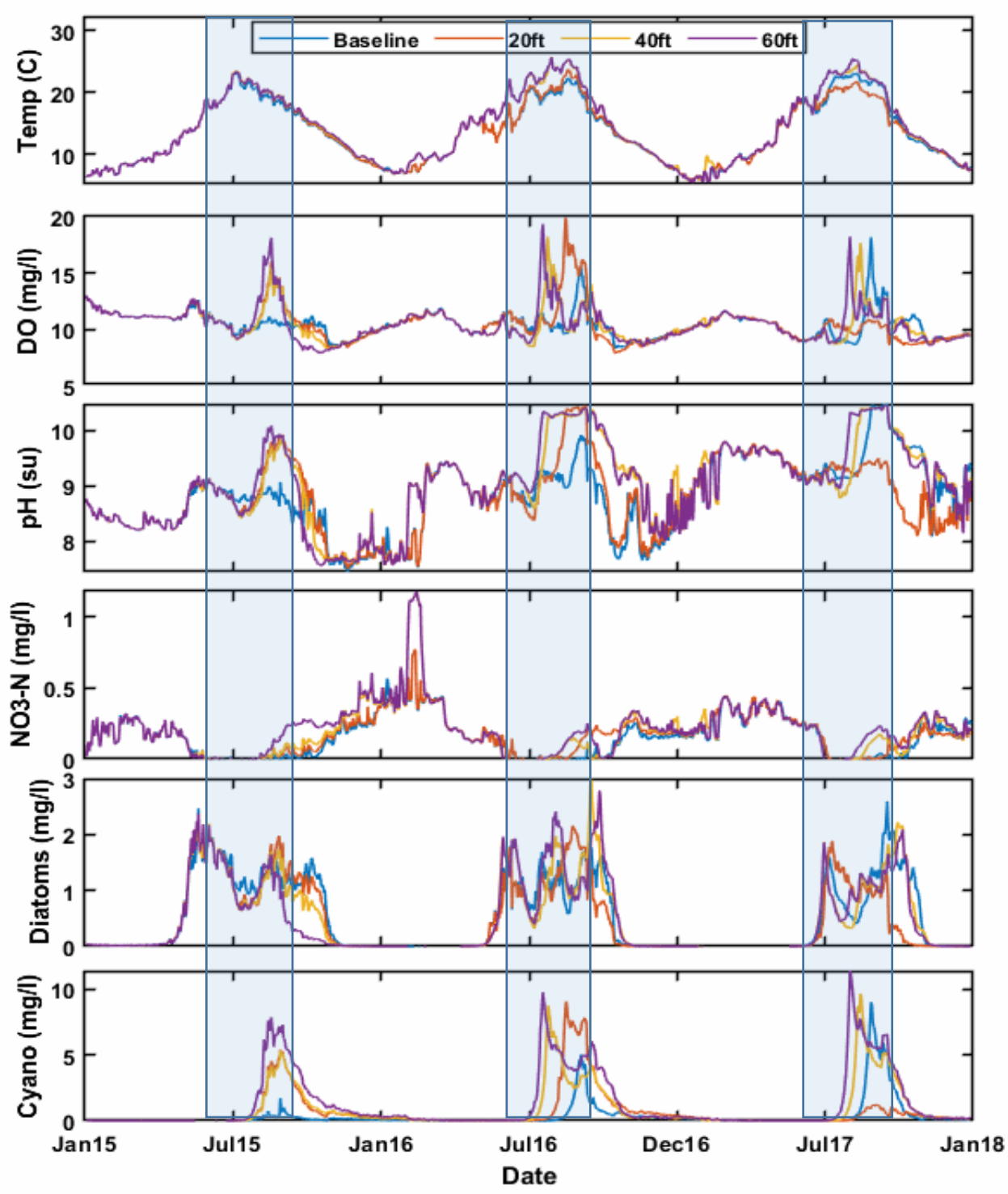

Figure 11-40. Time series of daily model results in the surface water of LBC in the Common Pool (RES08) for the Curtain scenario. Four different curtain depths are compared against the baseline model (no curtain). The blue boxes represent the approximate times when the curtains were in place.

The water in the ReReg tailrace with curtains in place is best characterized as a muted version of the changes in the Round Butte forebay (RES07) (Figure 11-41). The water is cooler and diatom export is clearly decreased, again primarily because the diatom peak tends to occur before the curtains are in place, so abundance is low during the periods when the curtains are installed. Cyanobacteria export appears to increase, primarily because some epilimnetic water can move under the curtain in LBC. While at least some portion of the cyanobacteria grouping will tend to float (following guidance from the model developers, the cyanobacteria sinking rate is set to 0 meters to capture the floating behavior), the model indicates that mixing associated with the withdrawals and wind-generated seiches acts against the tendency to float, moving a portion of the cyanobacteria throughout the epilimnion of LBC. The increased amount of cyanobacteria in the Common Pool (RES08) results is associated with an increase of cyanobacteria in the forebay, which in turn leads to an increase in export from ReReg Dam. The changes in DO and pH at the ReReg tailrace are variable, though they tend to increase during periods when cyanobacteria abundance is elevated. NO_3 is typically somewhat elevated in the tailrace with the curtains in place.

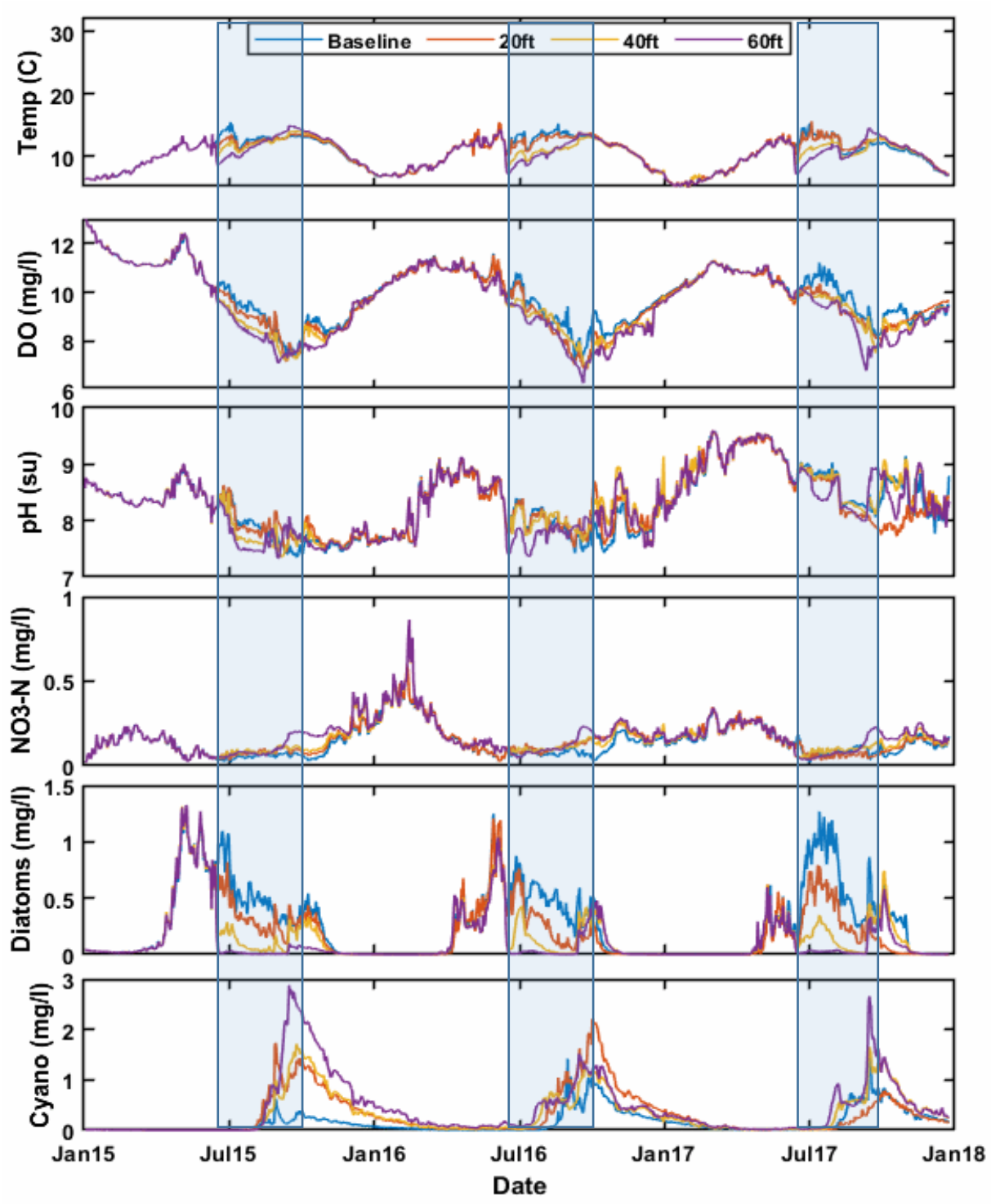

Figure 11-41. Time series of daily model results in the ReReg tailrace for the Curtain scenario. Four different curtain depths are compared against the baseline model (no curtain). The blue boxes represent the approximate times when the curtains were in place.

The 2Kw model of the LDR indicates that the curtain's impact on the ReReg tailrace water is passed throughout the LDR. To outline these changes, two time-series plots are presented. These figures outline water quality in the river during the time when the curtain is in place (June 15–September 15 in 2016 and 2017). At RM 96, water quality in the river is similar to that at the ReReg tailrace (Figure 11-42). Of the six water quality variables evaluated, water temperature shows the clearest impact because cooler water is released when the curtain is in place, regardless of curtain depth, although the deepest curtain (60 ft) shows the largest temperature decline. Results for other variables are more complicated, but it appears generally that the impact of curtain installation in model year 2017 is more significant than the one in 2016. This result relates to the very large cyanobacteria bloom that was simulated to occur in LBC during the summer of 2017. The curtain appears to have a greater effect in 2017 than in years that were less productive (e.g., 2016). In 2017, DO is similar across the summer period and pH shows declines relative to the baseline, particularly later in the summer season. Since the 2Kw model does not allow for multiple algae groups, the diatoms and cyanobacteria that are simulated to be exported from PRB by the W2 models were added together to represent total algae for the LDR modeling. In model year 2017, the curtains tend to limit export of algae into the LDR, and the declines are evident from modeling results at RM 96 (Figure 11-42).

In model year 2016, while the water temperature was lower with the curtain installed in LBC, the response for other parameters is variable at both RM 96 (Figure 11-42) and Moody (Figure 11-43). DO, pH, and phytoplankton do not vary significantly as compared to the baseline. NO_3 appears largely unchanged.

In all cases, periphyton growth appears only minimally impacted by the Curtain scenario conditions. Results at Moody are outlined in Figure 11-43 and are muted versions of the results described for the ReReg tailrace.

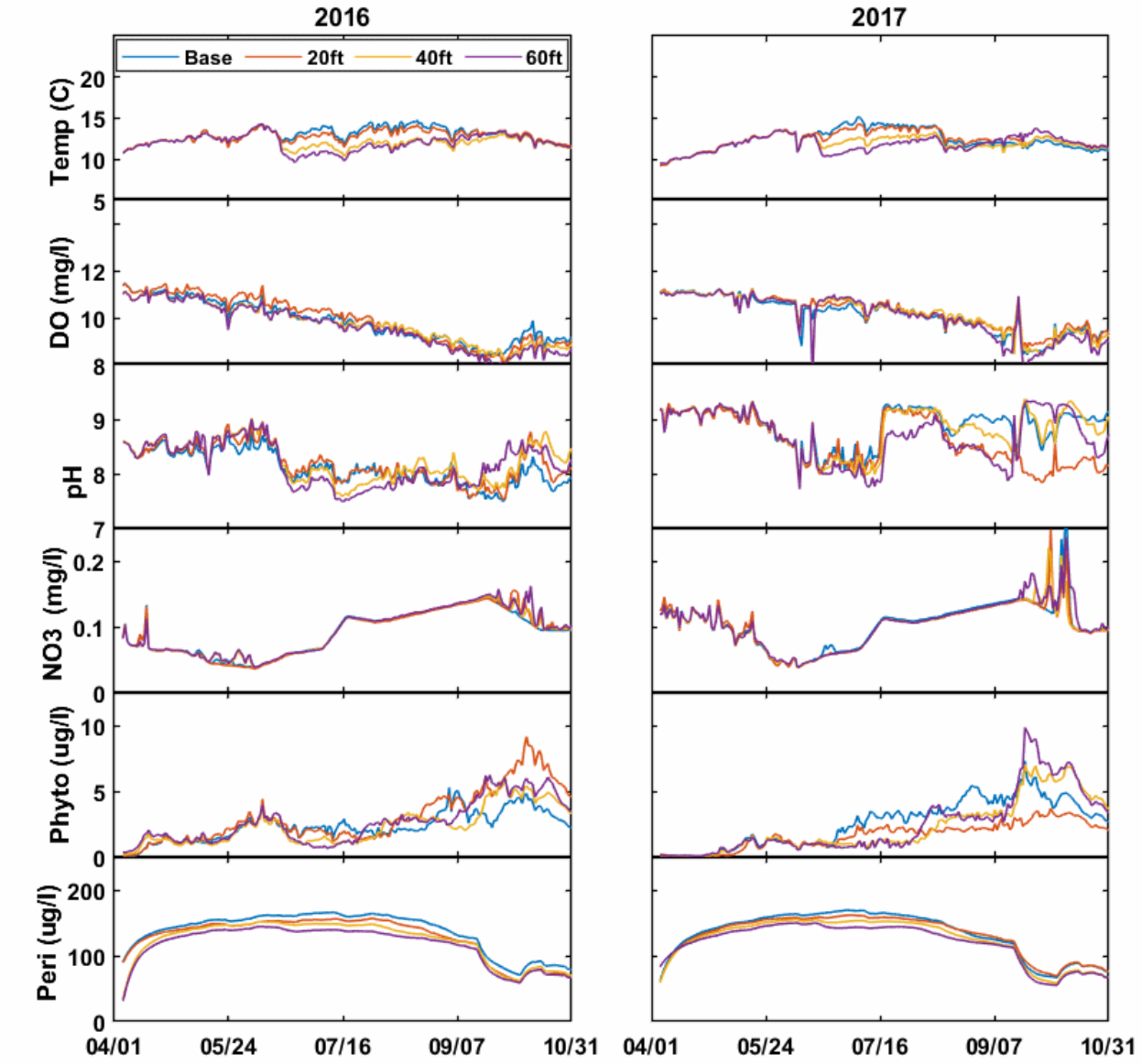

Figure 11-42. A comparison of daily results for the Curtain scenario at RM 96 on the LDR.

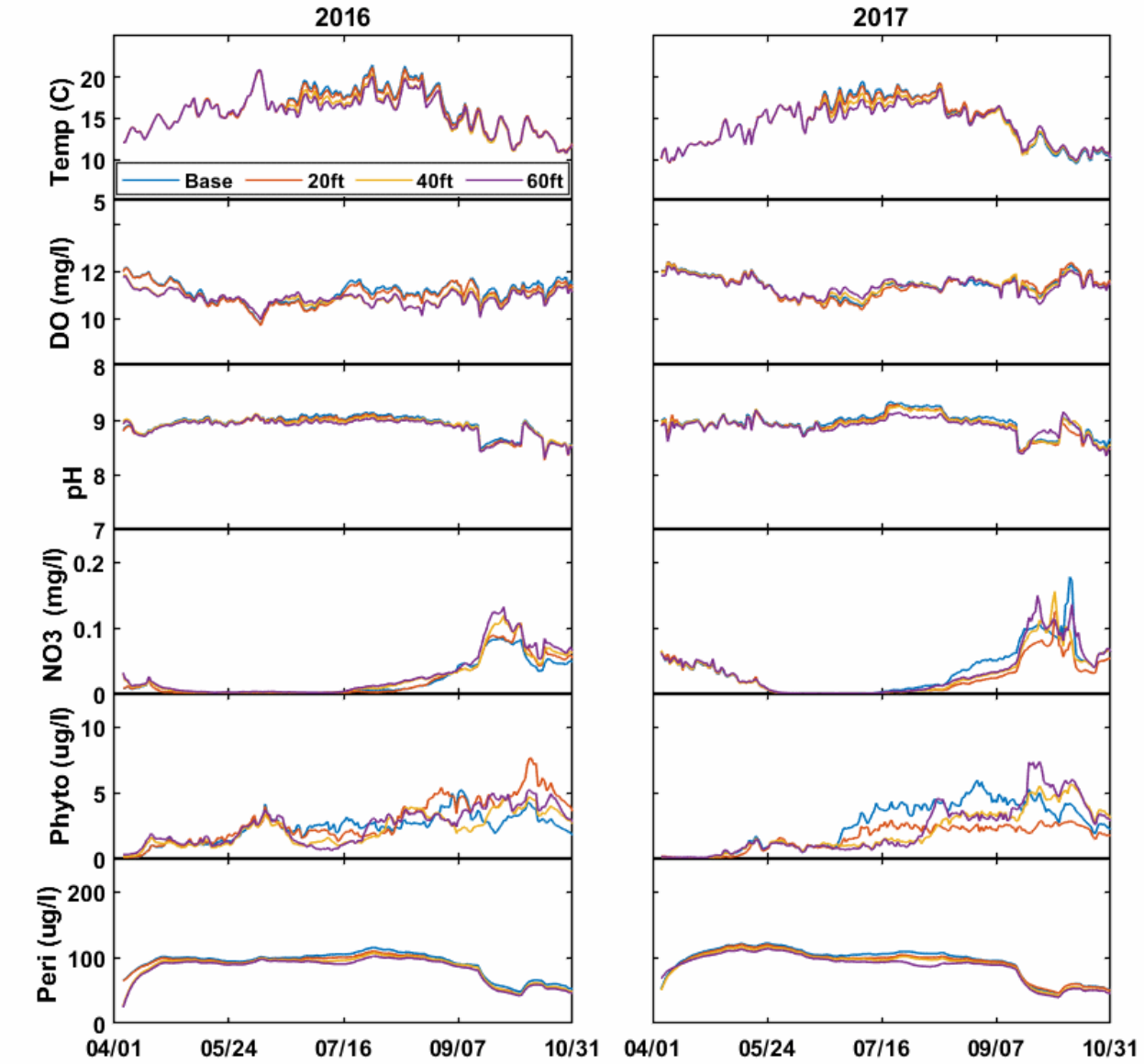

Figure 11-43. A comparison of daily results for the Curtain scenario on the LDR at Moody (RM 1).

Overall, the results suggest that the installation of a curtain could result in lower water temperatures leaving LBC during the period when the curtain is in place and these lower release temperatures would have the potential to reduce the amount of cool water available in LBC later in the year. A curtain will hold back epilimnetic water in LBC during the summer, which has the potential to warm and become more productive than it would without the curtain in place

(baseline conditions). The effect of this warm, productive water at RM 96 is expressed as elevated pH and phytoplankton concentrations for some of the curtains in the periods just after the curtain is removed (Figure 11-41).

The most noteworthy aspect of the results for this scenario is that the modeled response depends on curtain depth and climate conditions. The deepest curtain (60 ft) produces some of the largest late-summer pH and phytoplankton values, while the shallower curtains result in less dramatic effects. While not conclusive, the model results appear to indicate that a shallower curtain might allow for portions of the epilimnion to move under the curtain and into the intakes. This export of a portion of the epilimnion reduces the heating of the surface waters, which in turn minimizes the impact of removing the curtains in late summer. At the same time, the shallower curtain still reduces the amount of surface water entering the intakes during the period during which it is in place. The variation in curtain depth results highlights that additional calculations are needed to more fully quantify the potential implications of curtain placement. More detailed assessment with W2 might be useful, although it is likely that a more complex 3-D hydrodynamic model would be required to quantify the ways in which different curtain depths might interact with the vertical profiles in the impoundment. A 3-D model would be useful in assessing how horizontal flows associated with the gate release in the forebay change with the curtain depths. By evaluating a series of curtain depths with the 2-D W2 model, we have quantified how interactions between the gates and potential curtain installations could impact water quality in the impoundment and in the LDR. A 3-D analysis would be useful prior to the installation of a curtain to fully evaluate the details of the hydrodynamics in the forebay without the limitations introduced in the 2-D assumption.

11.9 Cold Flush Scenario

A Cold Flush scenario was developed to evaluate the impact of a warm-season release of colder hypolimnetic water. It was developed specifically to reflect conditions in 2015, when river flow was low, air temperature was high, and water temperature at the mouth of the LDR was over 20°C. During that period, releasing a short-term flush of cold water from the Project was considered to reduce water temperature downstream. In this scenario, we use the modeled

system to evaluate whether such a flush of cooler water would have any lasting impact on water temperature and quality in the LDR under conditions such as those observed in 2015. We modeled SWW operations with 60% bottom withdrawal for July 20–25, 2015, which corresponded to the time period of exceptionally warm conditions that occurred that year. For the rest of the year, the SWW operations are unchanged from 2015 conditions (Figure 11-44). While the analysis was originally conceived to address conditions that occurred in 2015, we also included the cold flush during the summer of 2016. The additional year was included to evaluate the potential implications of a cold flush during another period of time.

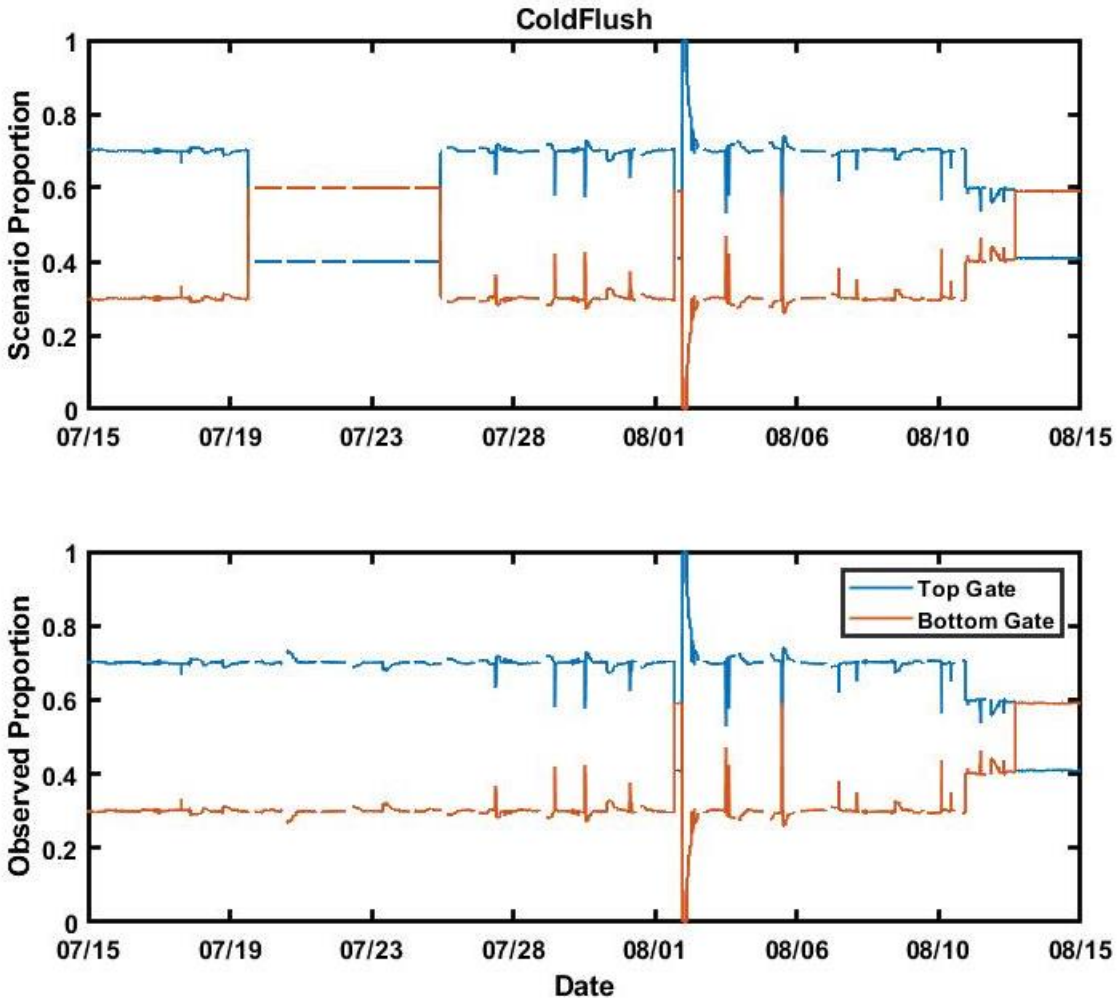

Figure 11-44. Gate flows for the Cold Flush scenario. The figure represents the proportion of the total flow drawn from each of the gates around July 20-25, 2015, when operations were changed under the scenario. The top figure shows scenario conditions, and the bottom figure shows baseline conditions.

The release of cooler hypolimnetic water does not appear to have any marked impact on the surface temperature in Round Butte forebay (RES07) (Figure 11-45, *bottom*), suggesting that a short-term release of cooler water during that period would not have resulted in significant changes to the surface temperature of LBC. Water temperature in the Round Butte tailrace is impacted by the short-term change in the release strategy, with about a 2°C drop in daily average temperature over the 6 days of modified operation (Figure 11-45, *top*). Once the cold flush ends on July 25, the temperature at Round Butte returns to baseline conditions. These results suggest that a cold flush would have a minor impact on the capacity of the Project to provide cold water in the late summer. Note, however, that this finding is limited to the specific time period and release strategy. Longer releases of cold water, or releases at different times of the year or under different weather conditions could produce different results, which were not evaluated in this scenario.

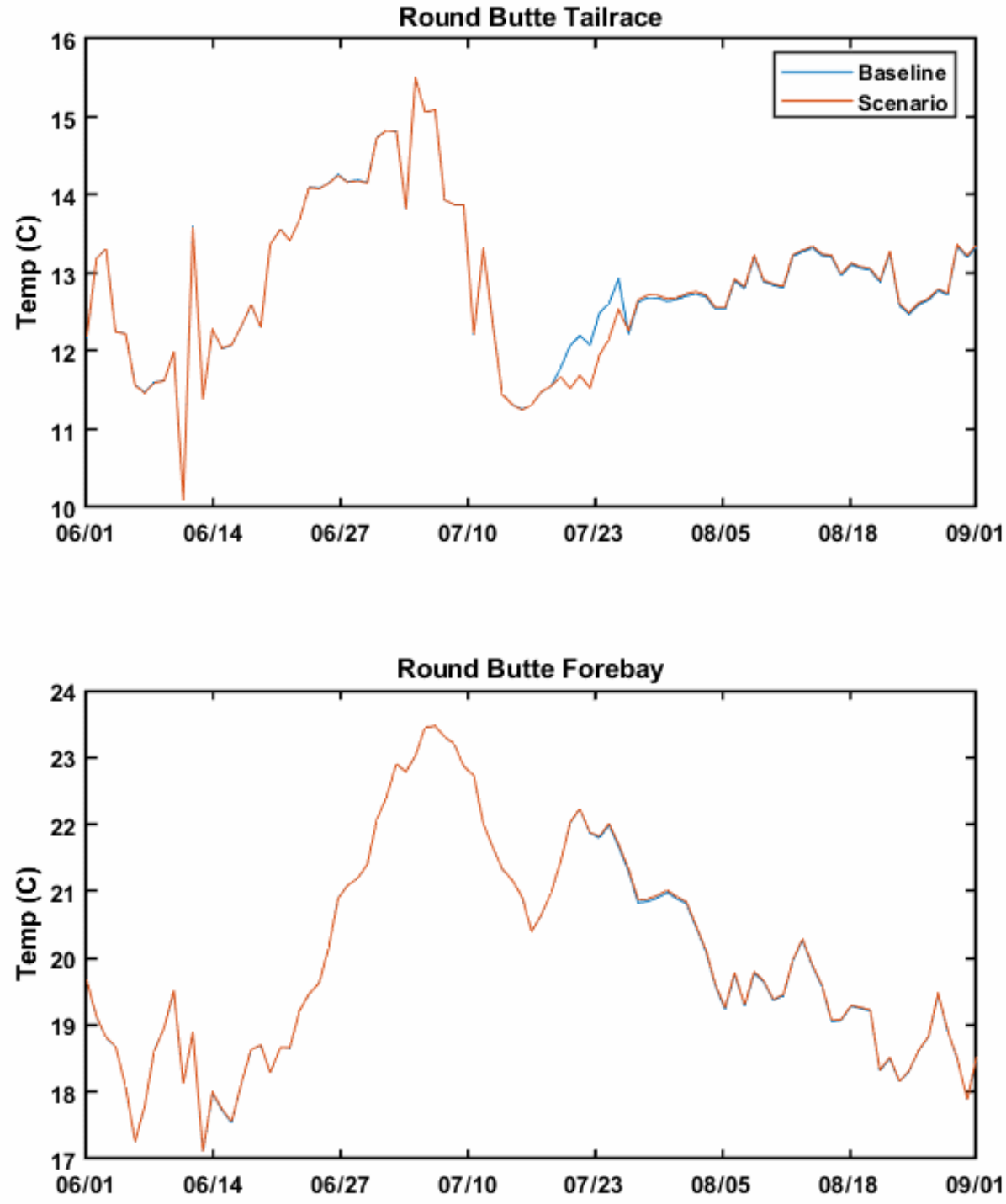

Figure 11-45. Time series of daily modeled water temperature in the surface water of Round Butte forebay (RES07) and Round Butte tailrace for summer 2015 for the Cold Flush scenario. Baseline condition results are shown in blue, and scenario results are shown in orange.

Because of the short-term changes in the tailrace temperature, the 2Kw model was used to project the impact of the change on the LDR. Results suggest that the short-term cold-water release had no clear impact on the LDR at RM 96 (Figure 11-46). While a small decrease in water temperature might occur during the short-term release period, the model indicates it would be minor and would not persist in the days after the release. The finding also suggests that, at least under the conditions evaluated, the short-term release of hypolimnetic water would not have changed downstream conditions to any measurable degree. Future research could expand on this analysis to examine different conditions. For example, the tailrace temperature during July 1–5, 2015, was around 15°C, compared to around 12°C for the scenario timeframe of July 20–25 (Figure 11-45). The infusion of colder water might be more consequential if the tailrace temperature was higher. In any case, results suggest that (1) the effect on river temperature at the mouth of the LDR would be extremely short term, (2) the effect at the mouth would be muted by heating in the canyon, and (3) the cold flush could, in certain years, affect availability of cold water later in the season.

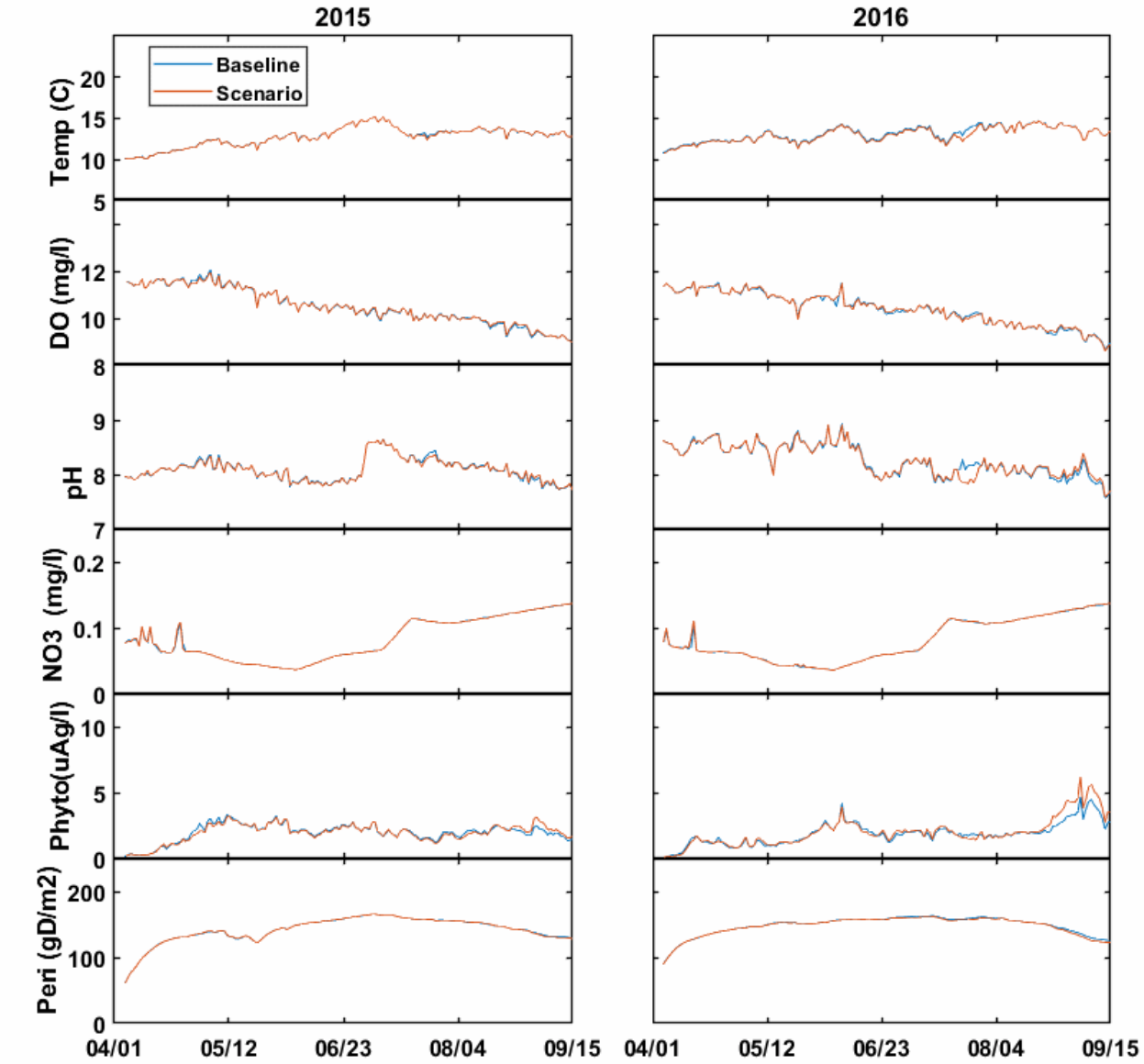

Figure 11-46. Daily time series representing key water quality variables for the Cold Flush scenario at RM 96 on the LDR. Baseline condition results are shown in blue and scenario results are shown in orange.

11.10 Flushing Flow Scenario

The Flushing Flow scenario was developed to explore the degree to which a large flow might scour the river bed. It follows from the discussion in Section 7.2, focused on the low peak flows in the Deschutes River basin in recent years and the potential effect of periodic large flows in

removing large amounts of attached periphyton. In this scenario, a 2-day, 10,000-cfs event was imposed at the headwater (RM 100) in the 2Kw model, occurring between April 28 and April 30.

For this scenario, the model parameter defined as "critical flow for catastrophic scour" was set to 250 cms from April 28 to 30. This rate is lower than a flushing flow of 10,000 cfs (about 283 cms) but higher than most flows during the remaining simulation period. In early April of 2017, discharge from the ReReg tailrace approached 250 cms, with a peak of 244 cms on April 1.

The catastrophic scour rate was set to its maximum suggested value, and we assumed that flows were sufficient to completely scour the bed. The parameterization was developed to induce scouring flows, letting the sensitivity analysis evaluate how recovery of periphyton proceeds and the impact of reduced periphyton on other water quality components. This parameterization differs from the one included in the baseline (and all other scenarios) in that scouring events in the baseline models was defined using a velocity threshold of 2 m/s, rather than the discharge threshold imposed as part of this scenario. This change was made to accommodate the flow-based definition of the scenario. To ensure that comparisons to the baseline relate to the flushing flow and not to the difference in parameterization, results presented here include a baseline model that uses the same flow-based threshold.

The modeling results suggest that periphyton might recover quickly from a scouring event (Figure 11-47 at RM 96 and Figure 11-48 at Moody). During the modeled 2-day high flow event, periphyton was removed at both locations, as was expected. In 2017, the early season high-flow values (which occur before the imposed flushing flow) approximate the flushing flow magnitude and result in large early-season reductions in periphyton. In both locations and throughout the LDR, the removal of periphyton does not appear to significantly impact other water quality variables (Figure 11-49). In the 2016 simulation, it appears to result because the periphyton regrowth dynamics are fast, with the periphyton rebounding to baseline levels within 1 month of the flushing flow. During the period of regrowth, pH and DO are modified, but those differences are minimized once the periphyton reaches baseline levels. In 2017, the scenario results are similar to those in the baseline because, as noted earlier, a large flow event in early April resulted in discharge values that were close to the "'catastrophic" threshold, which led to

the removal of most of the periphyton prior to the onset of the flushing flows. With little periphyton available, the flushing flows had only a minor impact.

The flushing flows are an upstream boundary condition in the LDR model; consequently, the W2 models for the reservoirs were not part of the analysis, which limits the scenario's potential to evaluate changes in the LDR. Specifically, this scenario does not evaluate whether the flushing flow significantly reduces the amount of cold water left in LBC or violates any regulatory FERC requirements governing operations in the reservoir.

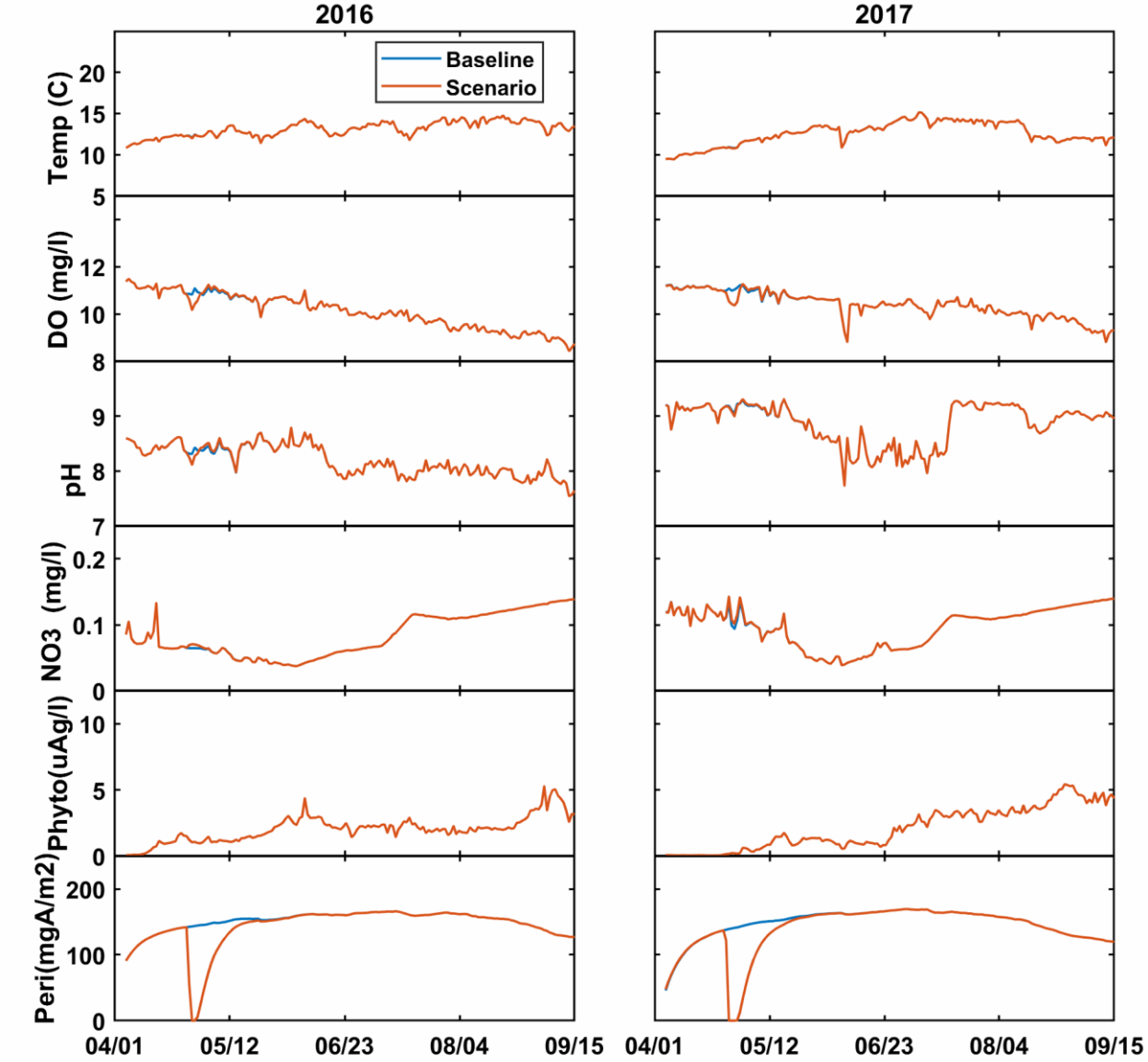

Figure 11-47. Average daily results of the Flushing Flow scenario at RM 96 on the LDR. In this scenario, a large flushing flow was imposed from April 28 to 30. Discharges from the Project were assumed to be 10,000 cfs for the 2-day period. Baseline condition results are shown in blue, and scenario condition results are shown in orange.

.

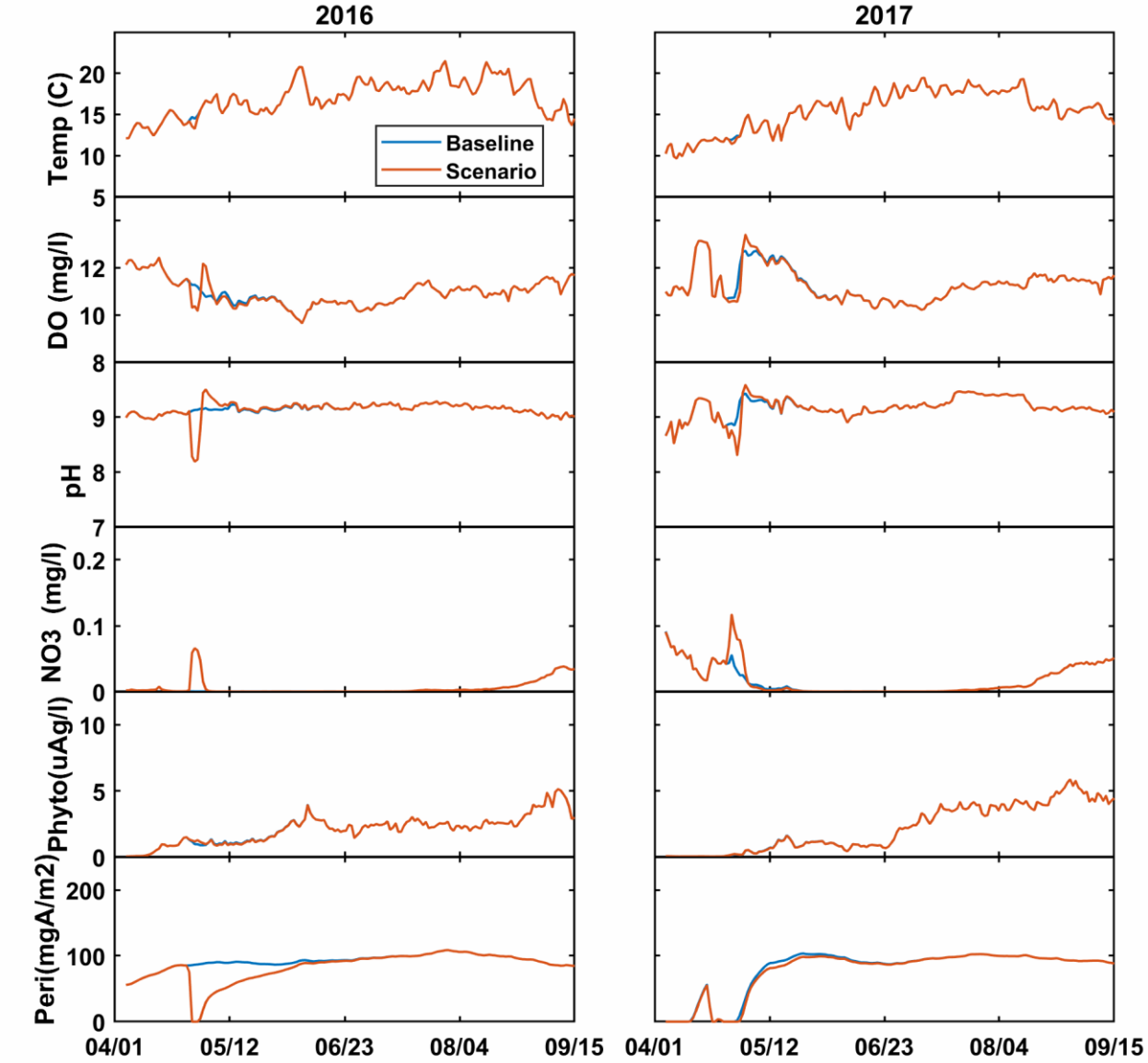

Figure 11-48. Average daily results of the Flushing Flow scenario at Moody (RM 1) on the LDR. In this scenario, a large flushing flow was imposed from April 28 to 30. Discharges from the Project were assumed to be 10,000 cfs for the 2-day period. Baseline condition results are shown in blue, and scenario results are shown in orange.

Model dynamics suggest that periphyton would regrow within a relatively short timeframe of less than 30 days. This result serves to define the minor changes in water quality associated with the scenario and would benefit from an observational study documenting the impact of flushing

flows on periphyton in the LDR *and* the trajectory of regrowth. Because those data are unavailable at this time, we can indicate only that it is consistent with the model algorithms and is supported by other 2Kw modeling work developed in the Yellowstone River in Montana (Flynn et al., 2013). They document a similar regrowth pattern for periphyton at a similar discharge to the LDR.

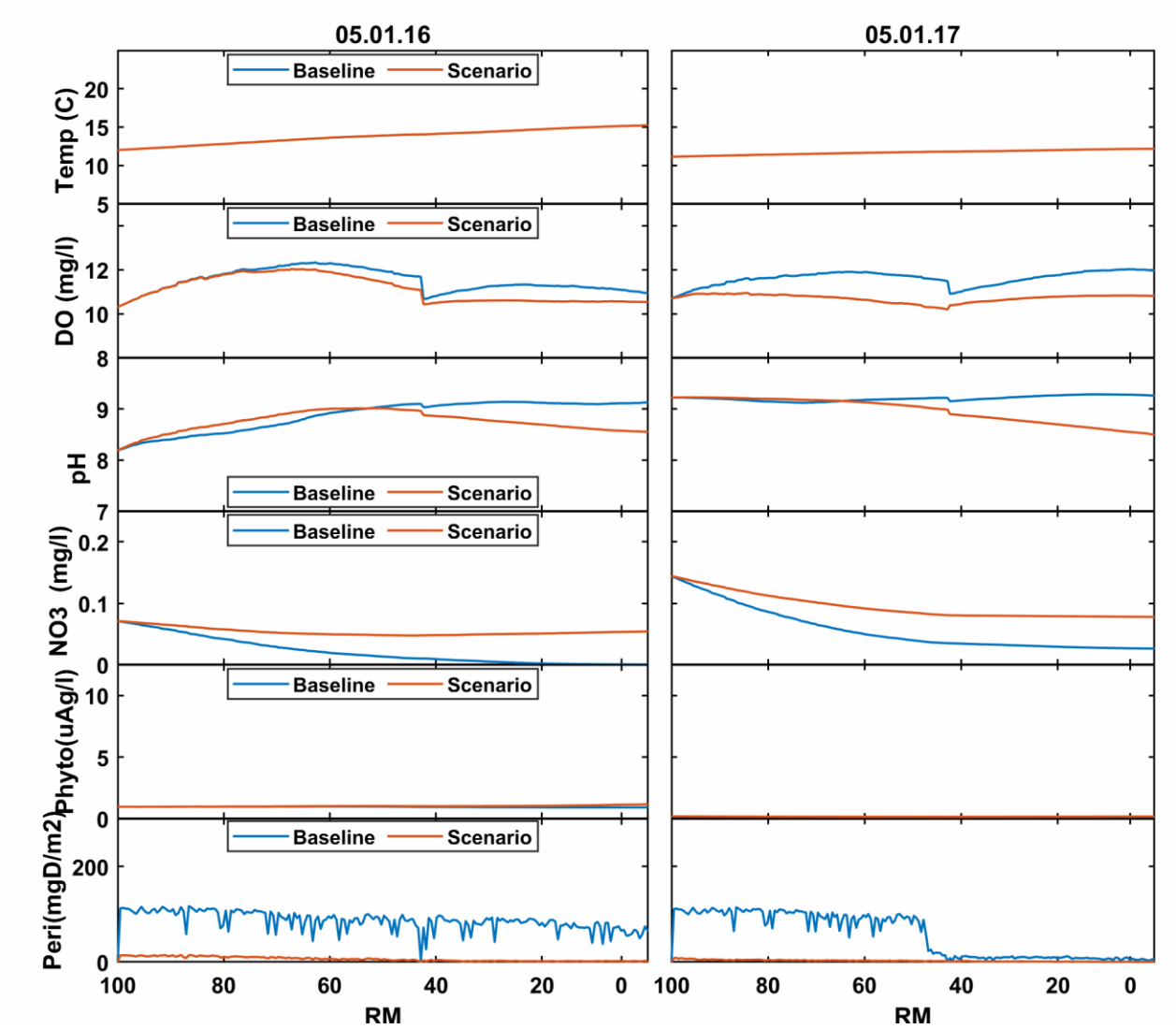

Figure 11-49. Longitudinal profiles of model results from ReReg Dam (RM 100.1) to the LDR's mouth (RM 0). These profiles were taken on May 1 of 2016 and 2017, just after the flushing flow, and represent average values for the day.

To more fully explore the potential implications of periphyton growth for the water quality of the LDR, a set of model sensitivity runs were developed with minimal periphyton by setting the maximum growth rate to 10 $gD/m^2/d$ (compared with a baseline value of 100 $gD/m^2/d$). The reduced growth rate results in lower periphyton densities, which is useful for quantifying the role of periphyton in affecting water quality in the LDR (Figure 11-50 and Figure 11-51). These sensitivity analyses are included only to supplement the Flushing Flow scenario and to more fully explore the role periphyton plays in the water quality of the LDR system.

The reduced periphyton density results in decreased productivity, which leads to direct reductions in DO and pH. Additionally, more NO_3 is available in the system as a result of the decreased periphyton production. The phytoplankton also increase in response to reduced competition for the available nutrients. The phytoplankton are unable to take full advantage of the extra nitrogen, however, probably because of the short residence time in the system. The excess nutrients, here reflected as NO_3, result in the elevated concentration at Moody.

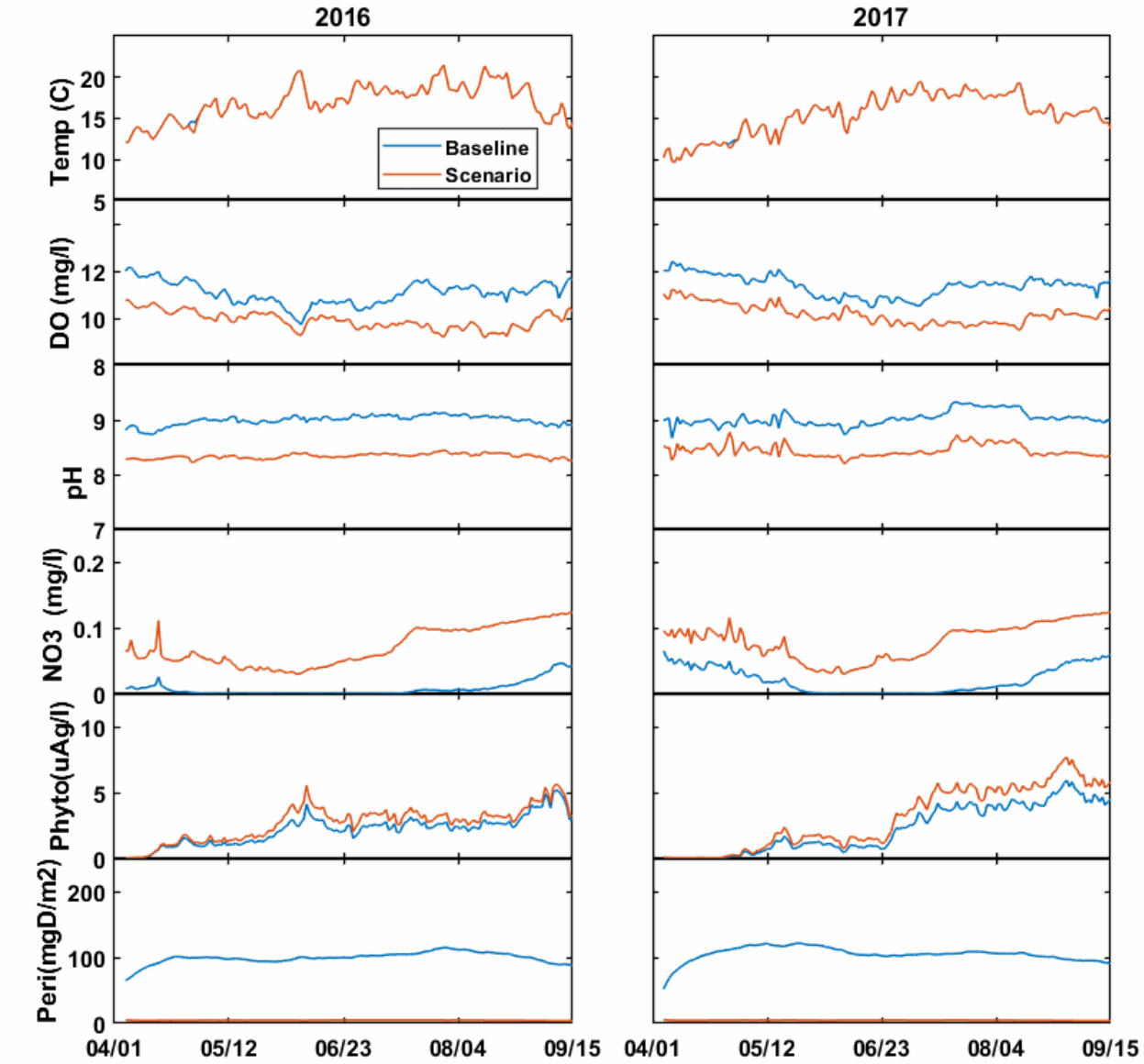

Figure 11-50. Results from a sensitivity run that included limited periphyton development. These time series represent conditions at Moody (RM 1) and are included to help outline the role of periphyton in the water quality of system.

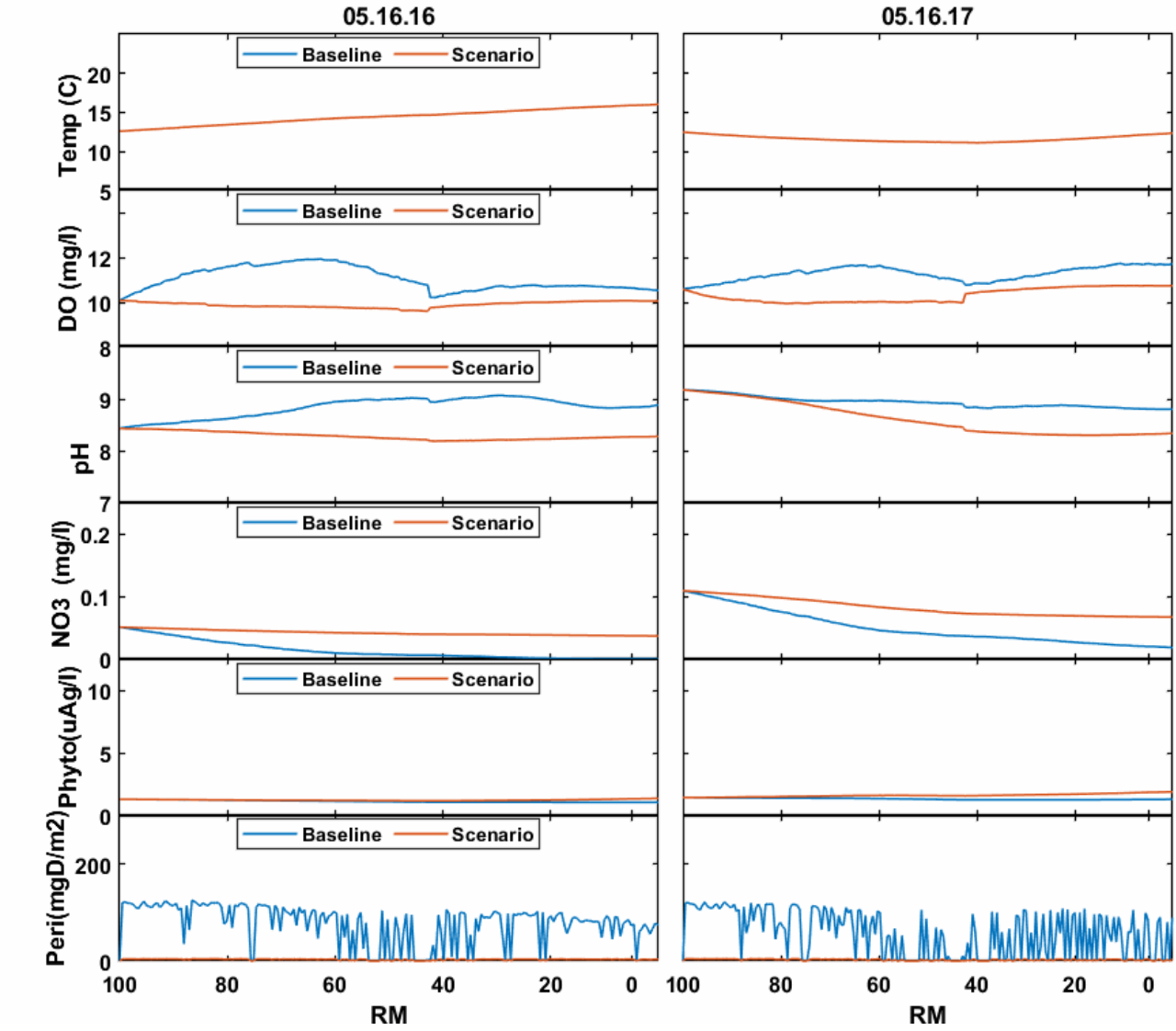

Figure 11-51. Daily average values for a simple model run with limited periphyton development from ReReg Dam (RM 100.1) to the LDR's mouth (RM 0). These profiles were taken on May 16 of 2016 and 2017.

11.11 Future Climate Scenario

The Future Climate scenario was developed to evaluate the potential impact of future climate on temperature and water quality at the Project. The development of this scenario was complicated by the need to characterize uncertain future climate conditions. Our solution to this issue was to make use of future climate conditions developed from downscaled Global Climate Model

(GCM) data using the Multivariate Adaptive Constructed Analogs approach (Abatzoglou and Brown, 2012). The downscaled climate data were downloaded from Climatology Lab (n.d.) for the coordinates for Round Butte Dam. We relied on a study by Vano et al. (2015) that outlines the capability of different models to capture climate in the PNW and, as suggested there, initially developed climate projections from the Geophysical Fluid Dynamics Laboratory model and the Hadley Center Global Environment model (HadGEM) for Reference Concentration Pathway (RCP) 4.5 and 8.5. Climate modelers use the RCPs to characterize climate boundary conditions by specifying sets of assumptions regarding the trajectory of atmospheric chemistry development (van Vuuren et al., 2014). While the definitions of the RCPs are quite detailed, broadly speaking, RCP 4.5 assumes long-term stabilization of atmospheric chemistry, while RCP 8.5 is characterized by continued increases in greenhouse gas emissions. RCP 8.5 tends to produce a warmer future climate than RCP 4.5 To document some key elements of these scenarios, daily values of downscaled GCM air temperatures, taken from the coordinates of Round Butte Dam and summarized as yearly means, are presented in Figure 11-52.

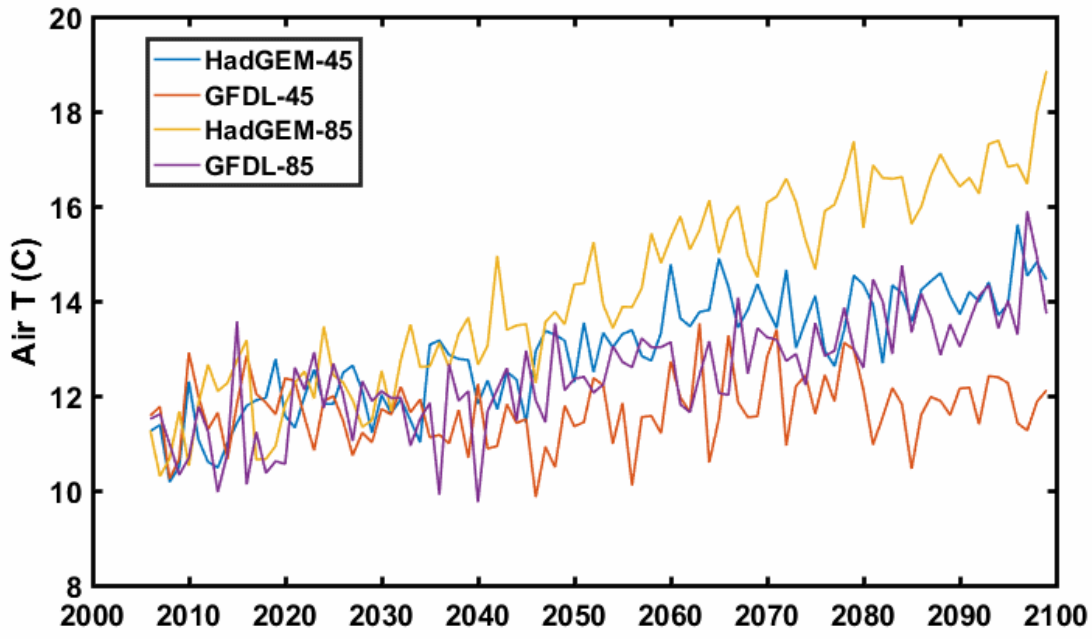

Figure 11-52. Projected mean yearly air temperatures for the area around Round Butte Dam from 2006 to 2099. Different models and RCPs result in a wide variety of different potential climate trajectories (Source: van Vuuren et al., 2014).

Our goal in this analysis was to evaluate the potential for relatively warm climate conditions to impact water quality in the reservoirs and LDR. We selected a particularly warm period/climate model from those outlined in Figure 11-52: HadGEM 8.5 during the 3-year period from 2089 to 2091.

After identifying downscaled GCM data over a 3-year period of interest (again, where we purposely selected a warm period from the warmest RCP), we determined how to include the downscaled GCM data in the W2 model, considering that W2 requires diurnal, not daily, data. We used the GCM data for daily minimum and maximum temperature and humidity, as well as average daily incoming shortwave radiation. Wind speed, wind direction, and cloudiness are not available from the GCM output, so we represented those variables with daily average values from the Pelton weather station for the years 2015–2017. The mixing of downscaled GCM data with actual observations certainly can lead to some internal inconsistencies. For example, the mixed dataset might include a very warm summer day (defined by GCM temperature) with clouds (defined in the observations). Nonetheless, the mixed climate dataset does provide an initial mechanism to evaluate the potential impacts of future climate on water quality. For simplicity, we refer to 2015–2017 in the analysis that follows. It is important to remember, however, that air temperature, humidity, and radiation were taken from a warm 3-year period as simulated by HadGEM 8.5.

As noted previously, climate projections are available only as daily values, rather than the hourly values used in W2 and 2Kw calibration. For that reason, a second version of the baseline W2 model was also developed using daily climate as a mechanism to reasonably compare simulated future conditions to the baseline under this scenario.

Results indicate that average daily values of water temperature appear consistently higher in Round Butte forebay (RES07) surface water under the Future Climate scenario (Figure 11-53). These warmer conditions lead to longer periods of elevated productivity in the reservoir, evident in the pH, DO, and algal response time series (Figure 11-53). A similar pattern is outlined in the seasonal boxplot summaries (Figure 11-54).

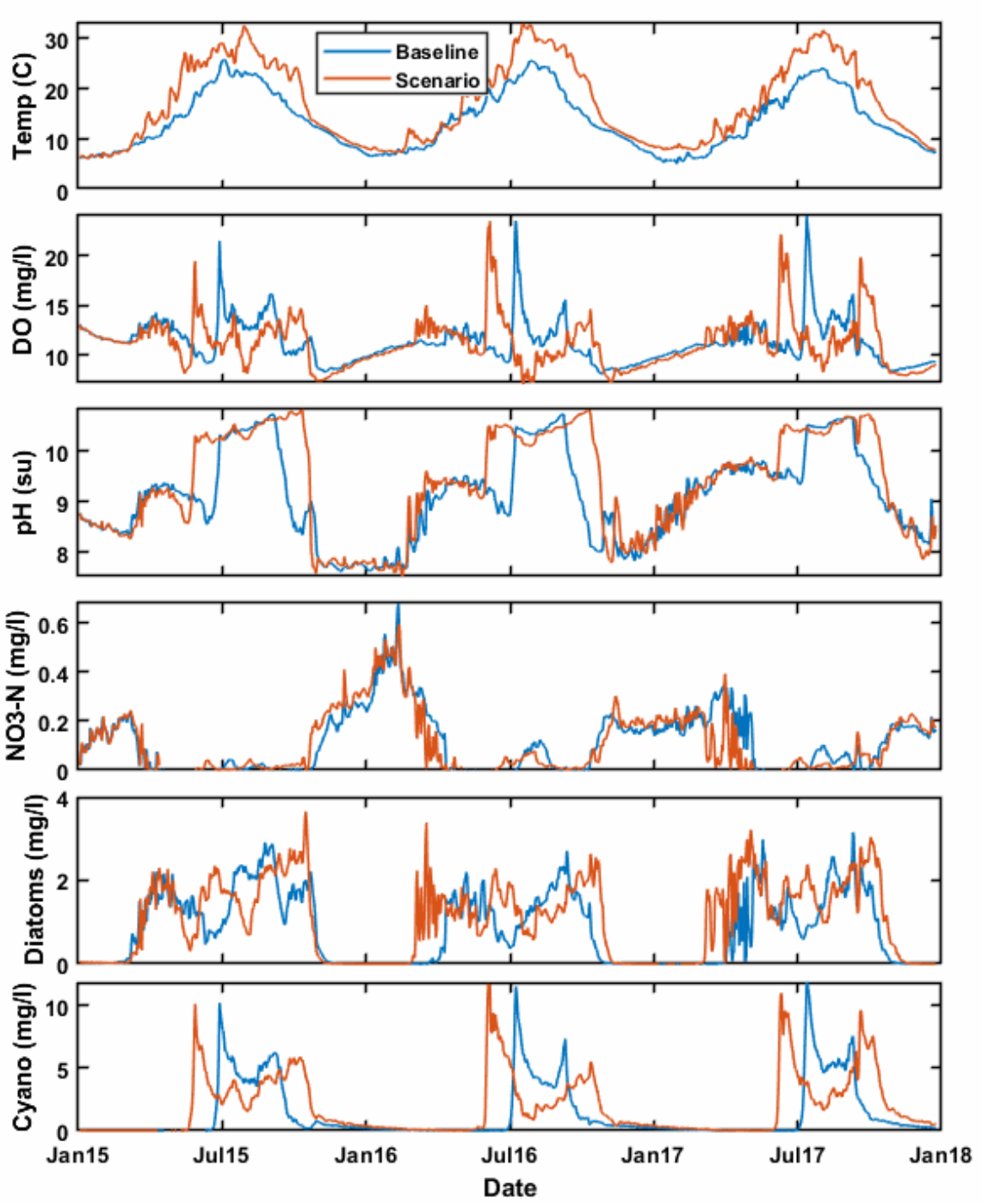

Figure 11-53. Time series of daily model results for the HadGEM 8.5 climate scenario in the surface water of Round Butte forebay (RES07). Baseline condition results are shown in blue, and scenario results are shown in orange. Note that the horizontal axis labels indicate years 2015–2018, but this includes the mixed climate dataset with elements from the HadGEM 8.5 model taken from years 2089-2091.

The tailrace time series at the ReReg Reservoir indicates that the elevated air temperatures led to increased temperatures throughout the system, including in the deeper areas of the reservoir, with elevated productivity projected in the tailrace water through the summer periods (Figure 11-55).

The projected changes in the ReReg tailrace waters influence the LDR, with projected increases in water temperature throughout the system, as evidenced by the time series at Moody (Figure 11-56). The changes to water quality are predicted to be minor, although the impact might have been muted by using average daily data rather than the hourly data under which 2Kw is designed to operate. Further analysis focused on the disaggregation of the daily data to provide a more realistic diurnal pattern is needed before these results can be considered reliable.

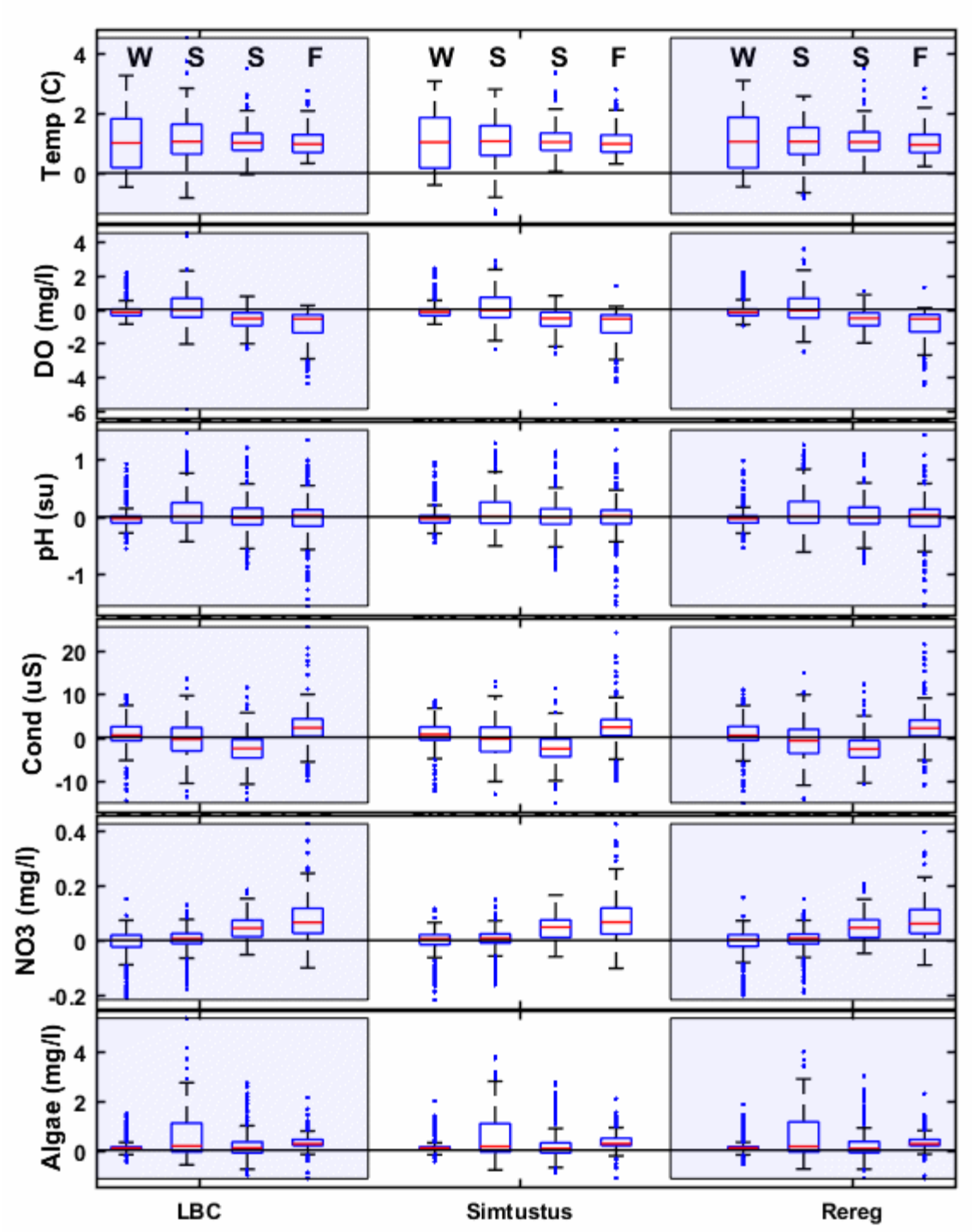

Figure 11-54. A comparison of the differences between the baseline and HadGEM 8.5 scenario daily values in the tailraces of the reservoirs across four seasons. Positive values indicate that the scenario value was larger than baseline. Seasons are shown in order of winter (W), spring (S), summer (S), and fall (F).

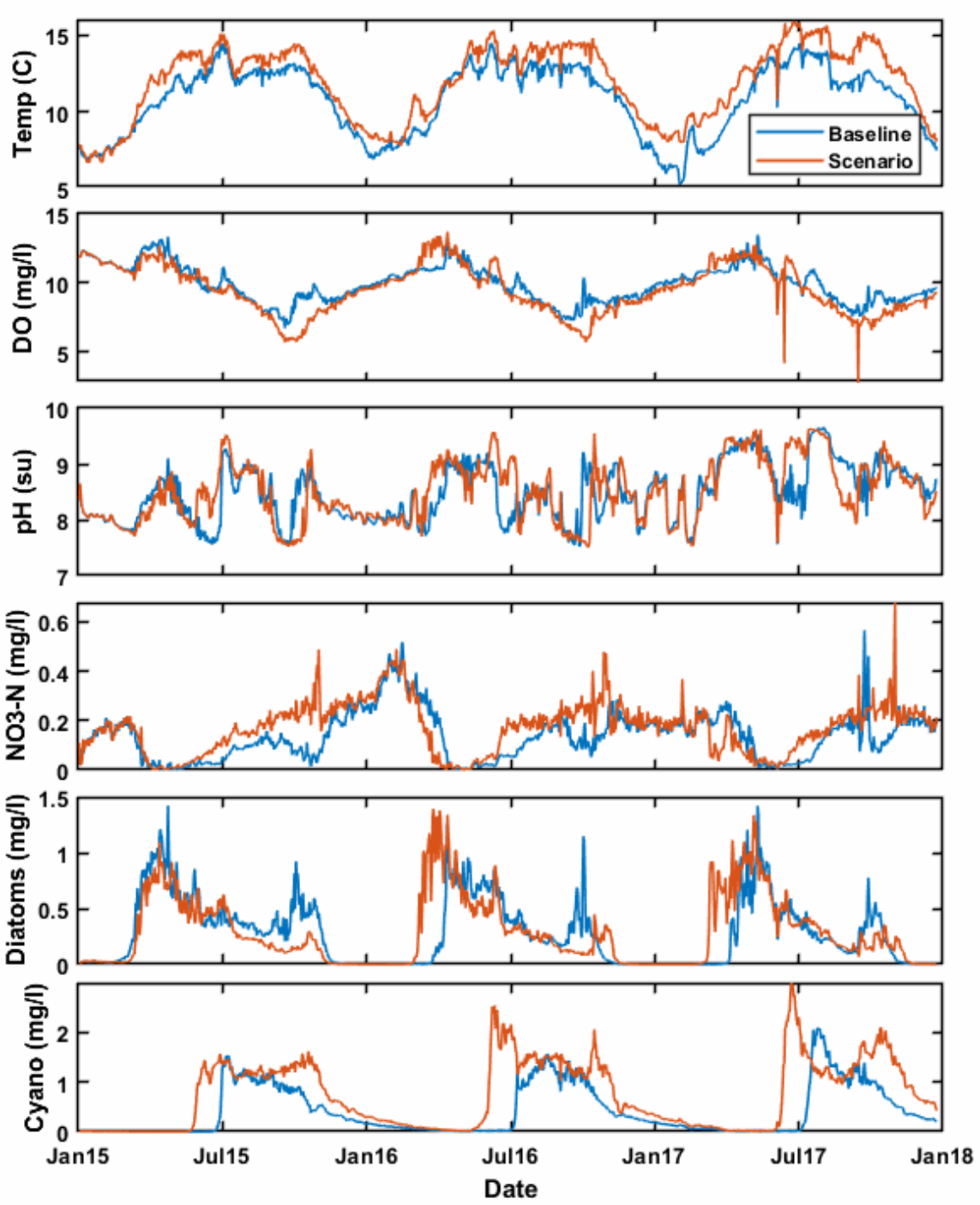

Figure 11-55. Time series of daily model results in for the HadGEM RCP 8.5 (years 2089–2091) climate scenario at ReReg tailrace. Baseline condition results are shown in blue, and scenario results are shown in orange. Note that the horizontal axis labels indicate years 2015–2018, but this includes the mixed climate dataset with elements from the HadGEM 8.5 model taken from years 2089–2091.

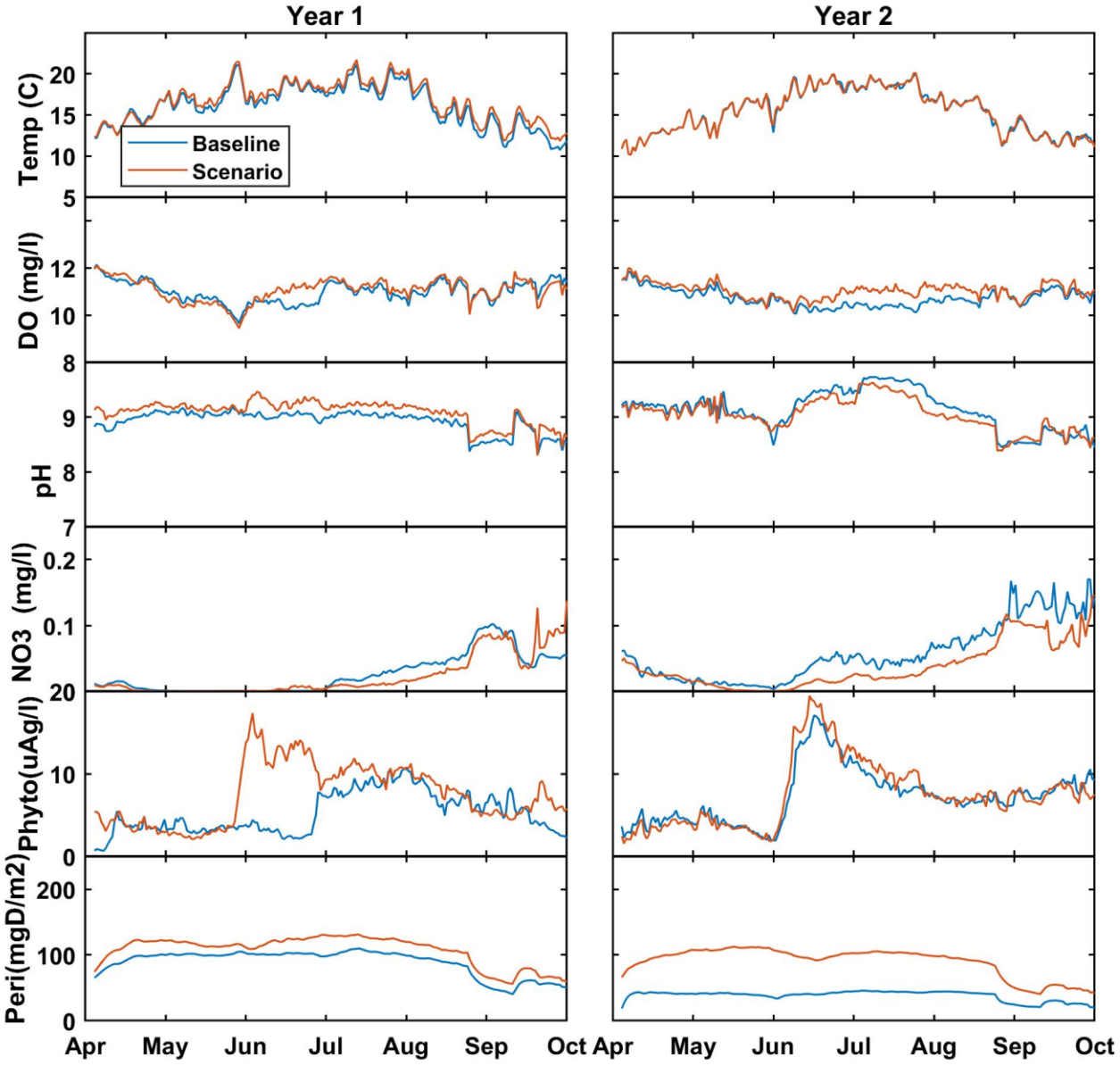

Figure 11-56. A comparison of daily results at Moody (RM 1) on the LDR from the HadGEM 8.5 scenario. Note that the figure headings indicate years 2016 and 2017, but this includes the mixed climate dataset with elements from the HadGEM 8.5 model take from years 2089–2091.

11.12 Future Tributary Temperature Scenario

This scenario is designed to explore how changes in tributary water temperature might influence water temperature and quality in the reservoirs and the LDR. As with the Future Climate scenario, it is difficult to adequately define future water temperatures, particularly at the subdaily timescale required by W2. We rely on stream temperature forecasts developed by Isaak et al. (2017) for sites corresponding to the inflows to LBC: the Crooked, Deschutes, and Metolius rivers. The available forecasts are defined by Isaak et al. (2017) as average monthly water temperatures during the months of June–September. To include these data in W2, we applied the monthly change in temperature to the existing hourly water temperature data at the three locations (Figure 11-57). The stream temperature projections from Isaak et al., 2017 were developed only for the summer period (Table 11-3). Projected temperature changes for other months of the year are unavailable. Given the lack of input data available, we assumed water temperatures outside the summer months to be the same as the baseline conditions. Isaak et al. (2017) projected stream temperatures for two years—2040 and 2080—and we used both projections by developing two different model scenarios. The first scenario applies the projected 2040 temperature changes to the 3-year baseline inflow temperatures, and the second scenario applies the 2080 temperature changes (Figure 11-57). The two scenarios are compared together against the baseline model results.

Table 11-3. A summary of the monthly stream temperatures for 2040 and 2080 taken from Isaak et al. (2017). Temperature deltas are the difference between projected monthly means and current monthly means.

Month	Tributary	Temp. current (°C)	Temp. delta 2040 (°C)	Temp. delta 2080 (°C)	Difference between scenarios
June	Crooked	14.10	1.47	2.55	1.08
July		14.36	1.67	2.64	0.97
Aug		14.38	1.42	2.37	0.95
Sept		13.60	0.88	1.55	0.67
June	Deschutes	13.97	1.46	2.54	1.08
July		15.00	1.68	2.66	0.98
Aug		15.01	1.43	2.39	0.96
Sept		13.18	0.87	1.54	0.67
June	Metolius	7.25	1.34	2.33	0.99
July		9.67	1.57	2.48	0.91
Aug		9.83	1.35	2.24	0.89
Sept		8.65	0.82	1.45	0.63
Average		12.41	1.33	2.28	0.89

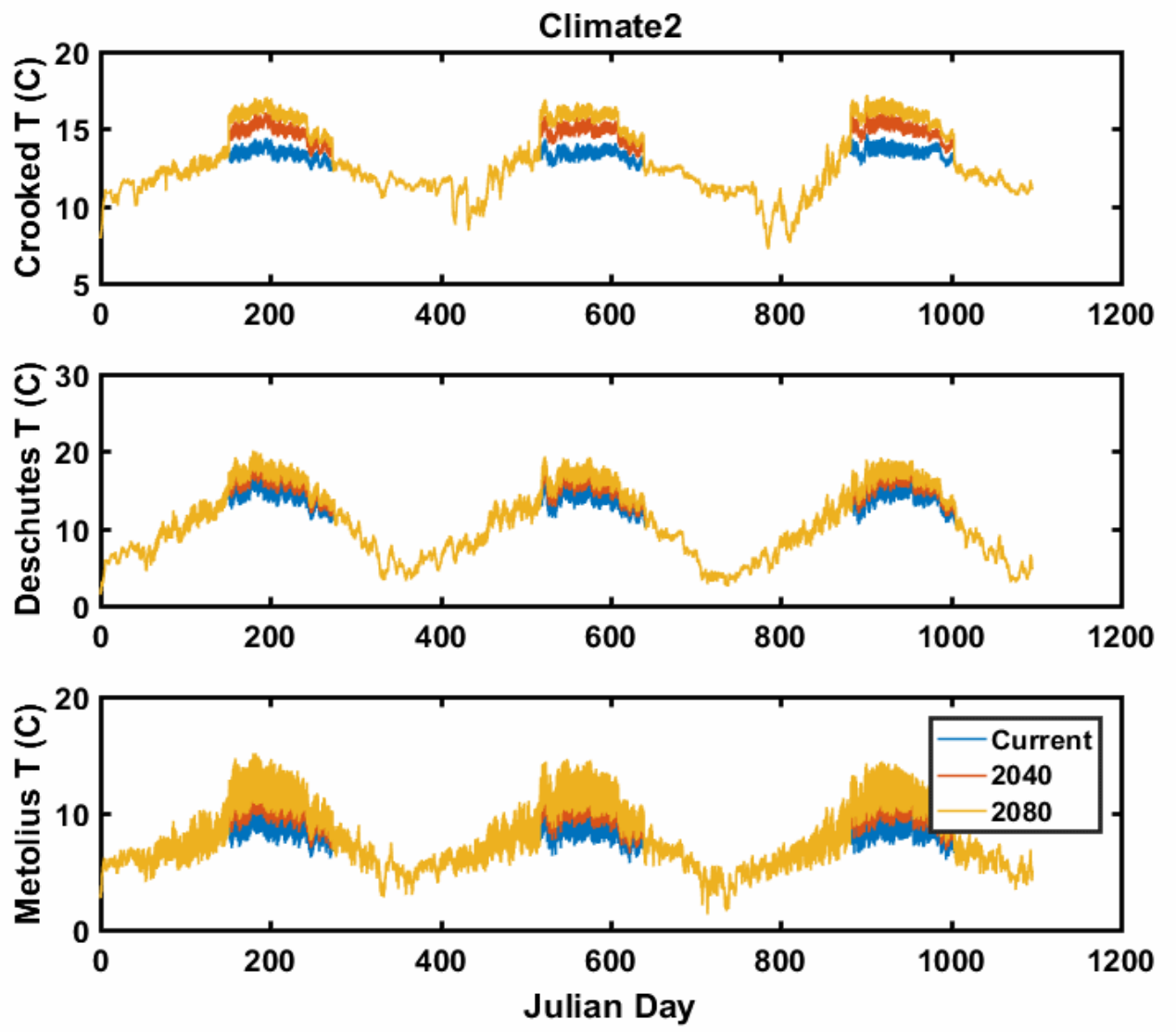

Figure 11-57. Hourly baseline water temperatures with the Isaak et al. (2017) projected temperature delta applied during the summer months. Note the y-axis for the Deschutes River differs from the other two tributaries. These data are one element of the meteorological dataset used to drive the models under the two Future Tributary Temperature scenarios.

Increased temperatures of the incoming water from the three tributaries result in elevated surface water temperatures in LBC (Figure 11-58). While the 2080 tributary temperature increases are higher than the 2040 increases, the increases in LBC surface water temperatures are similar. We believe that this occurs because the difference between the projected 2040 and 2080 tributary temperature averages is small compared to the amount of heating in the surface water (about

0.9℃ compared to a 6℃ and 12℃ increase in LBC surface water temperature). Regardless of the cause, the increased surface water temperature in both years leads to increased productivity and associated increases in algal biomass, pH, and DO in LBC surface water during the summer (Figure 11-58).

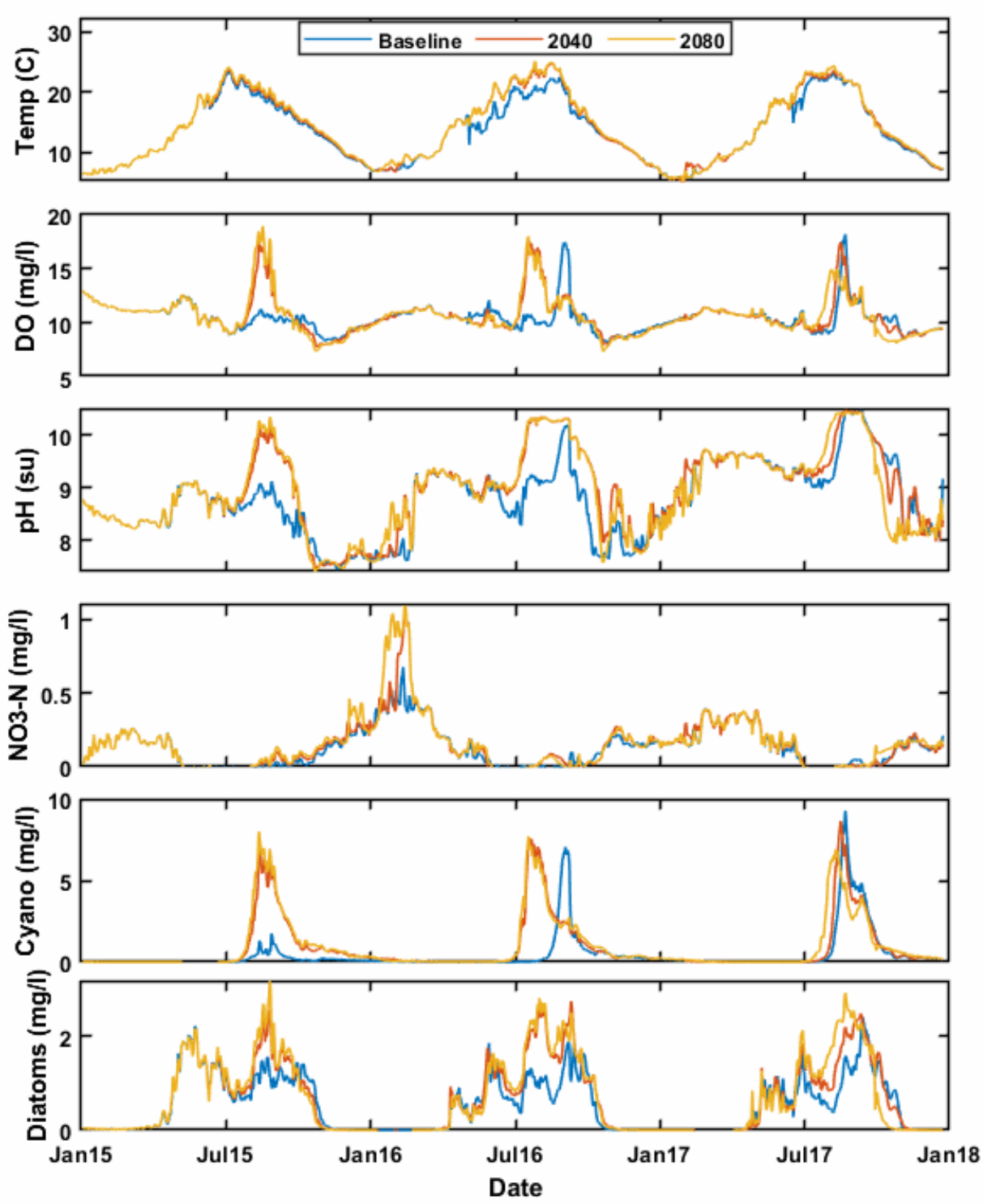

Figure 11-58. Time series of daily model results of the 2040 and 2080 Future Tributary Temperature scenarios in the surface water of Round Butte forebay (RES07).

The effect on water temperature in the tailraces is muted by the SWW as it mixes water from the surface with cooler, hypolimnetic water from Round Butte forebay (RES07) (Figure 11-59). Further downstream, the moderately warmer tailrace discharge influences water temperature and quality in the LDR, although projected impacts are minor (Figure 11-60 below ReReg and Figure 11-61 at Moody). The simulations indicate an increase in algae production in the LDR in both 2016 and 2017. These increases in LDR phytoplankton occur because of the simulated increases in export from LBC during the period (Figure 11-59).

This study did not include a scenario combining projections of both meteorological conditions and tributary temperatures, although such an analysis might provide additional insight into the potential impact of climate change on the Project and the LDR. The scenario analysis could benefit from the development of water temperature models for the three LBC tributaries, which would facilitate the production of future tributary water temperatures in conjunction with future projections of climate.

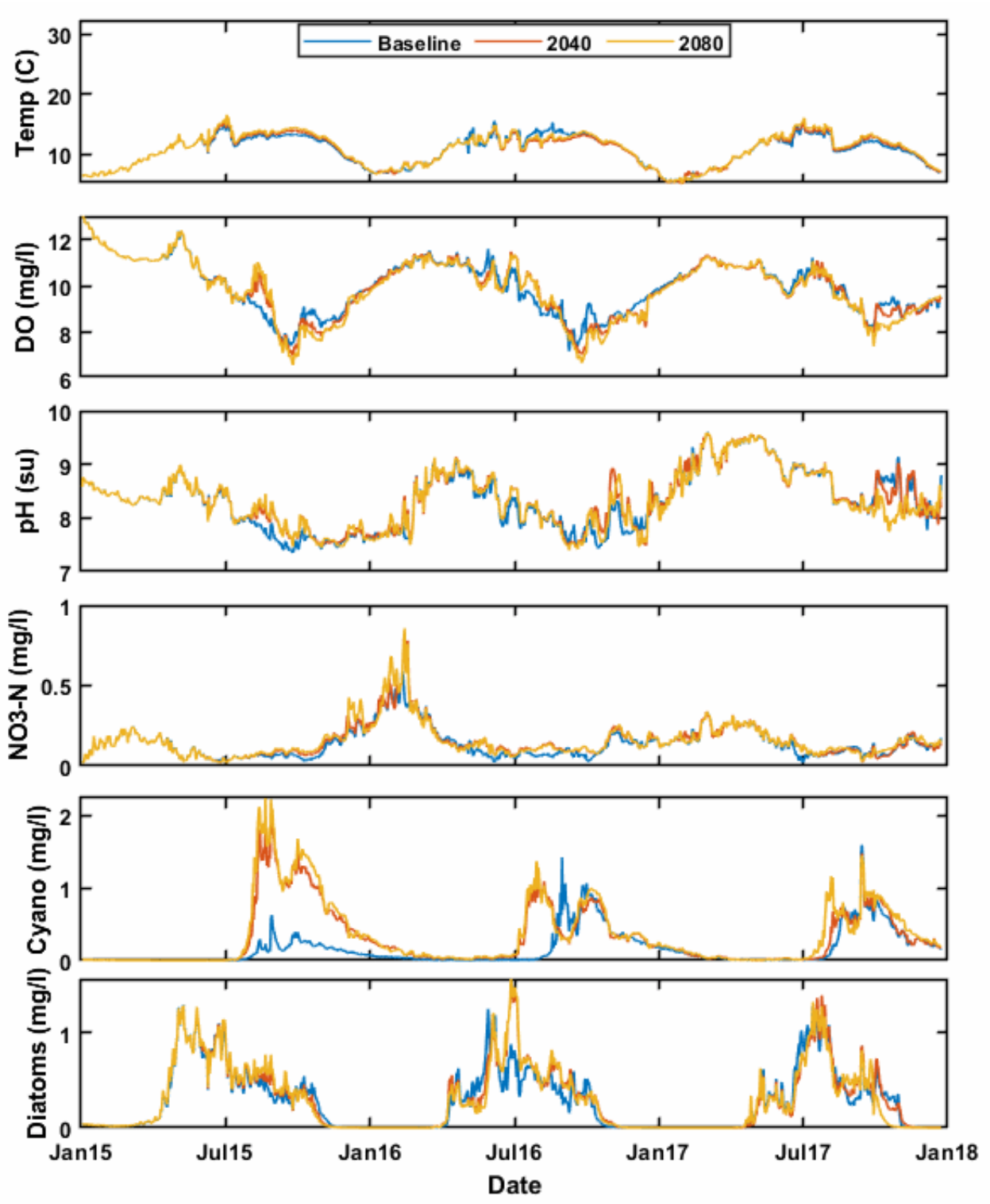

Figure 11-59. Time series of daily model results for the 2040 and 2080 Future Tributary Temperature scenarios in the tailrace water of the ReReg Reservoir.

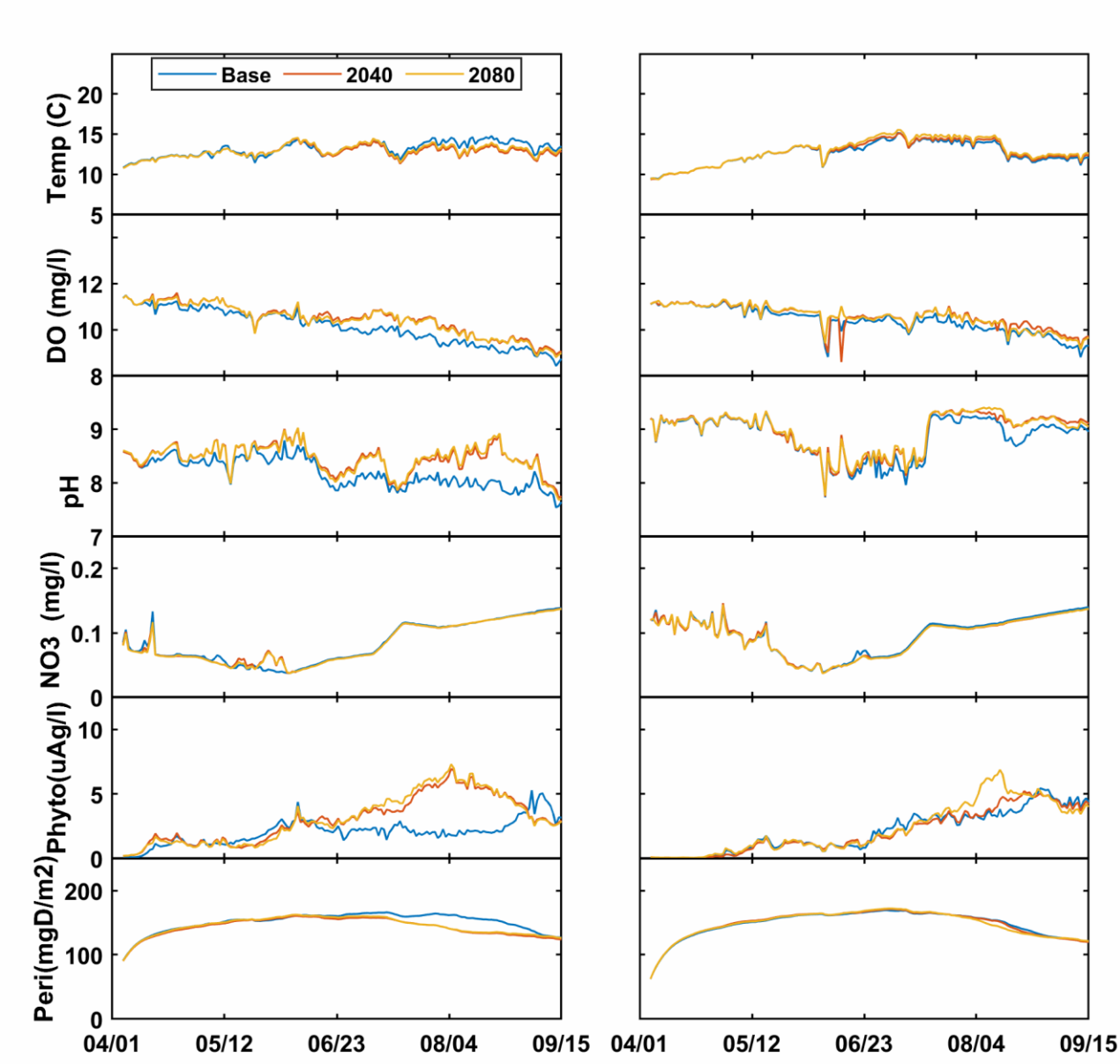

Figure 11-60. A comparison of daily results from the 2040 and 2080 Future Tributary Temperature scenarios on the LDR at RM 96.

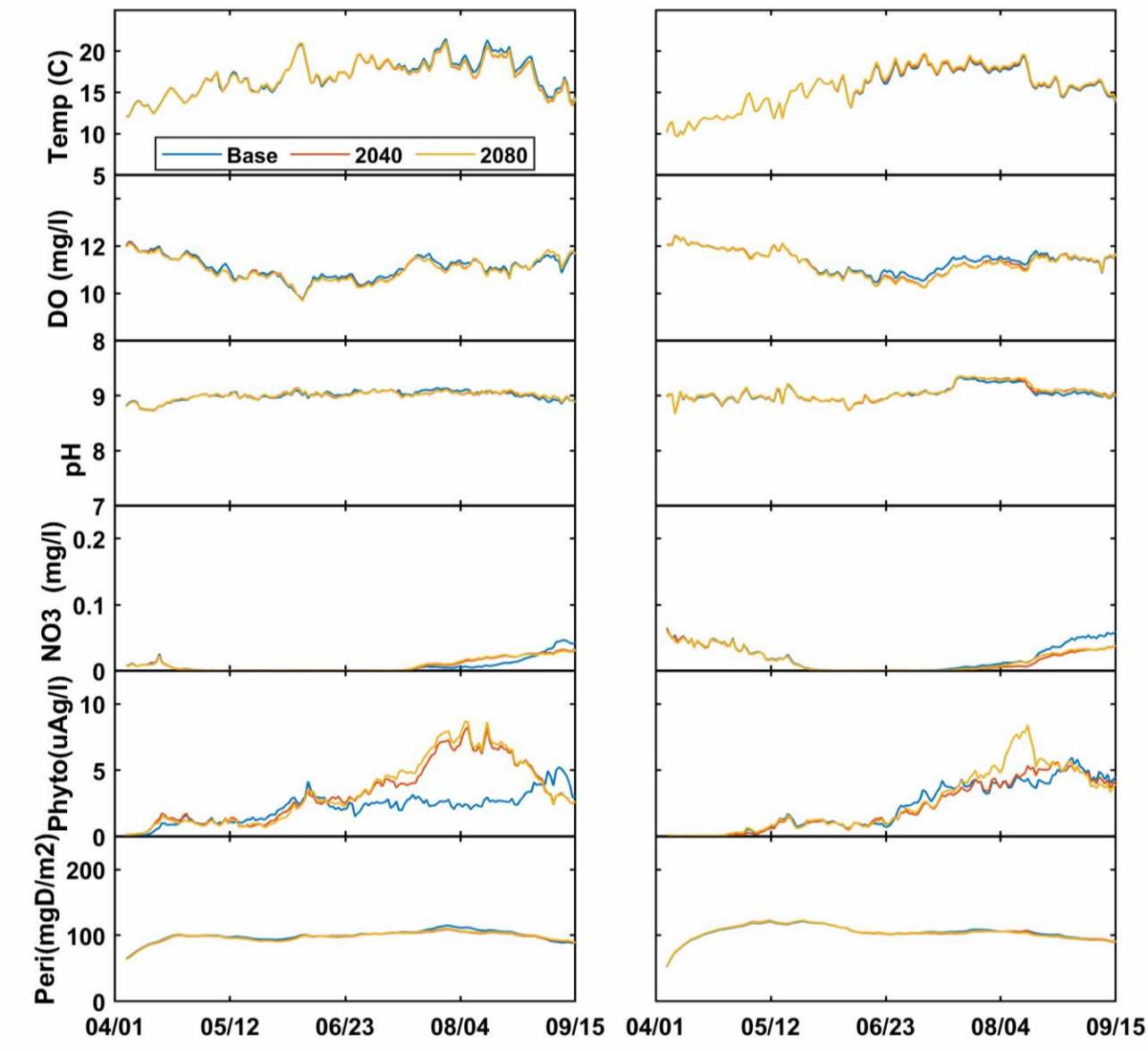

Figure 11-61. A comparison of daily results from the 2040 and 2080 Future Tributary Temperature scenarios on the LDR at Moody (RM 1).

11.13 Statistical Comparison of Scenario Results

Simulations of temperature and water quality dynamics in the impoundments and LDR can be characterized in many ways. Doing so concisely is challenging because of the wide variety of linked quantities, which can vary over time and space and at different scales. The time series and boxplots presented in sections 11-2 through 11-12 provide a means to understand key

features of the changes between scenarios through time, and elements of the spatial variation were presented in reservoir and river cross sections. This section presents statistical comparisons of the results across the different scenarios. These comparisons complement the details presented in sections 11.2 through 11.12 and offer a mechanism to outline how different scenarios compare to each other and the baseline. The modeling included only water quality effects of the different scenario definitions. Other important dynamics, including fisheries, regulation, recreation, and economics, are not reflected in these results. In this sense, these comparisons represent one piece of a complicated puzzle.

We have developed the comparisons as one-way analysis of variance (ANOVA) statistics, testing the hypothesis that the means of the baseline results do not differ from the means of the results of each of the scenarios. Table 11-4 presents a statistical summary of the model results at RM 96. Boxplots outlining all the data used in developing the statistics are presented in Figure 11-62. We focused the statistical comparisons on the upstream side of the LDR (at RM 96) because observations and previous results indicate that the largest differences between scenarios exist at that location, although we also provide a summary of the simulated conditions at Moody (RM 1) for reference (Figure 11-63).

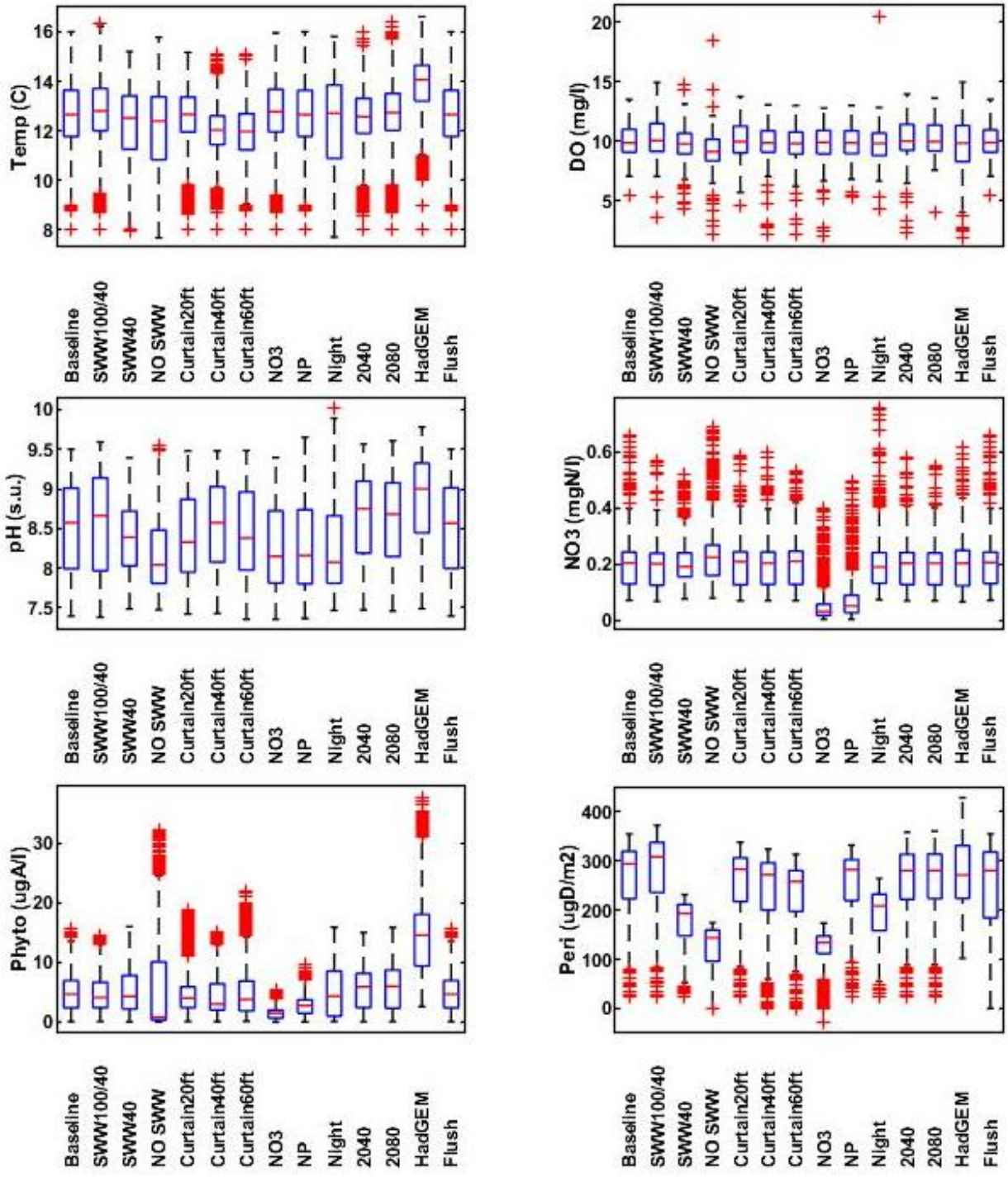

Figure 11-62. Boxplots presenting the subdaily modeled data from RM 96 used in developing the statistical tests. On each box, the central mark indicates the median, and the bottom and top edges of the box indicate the 25th and 75th percentiles, respectively. The whiskers extend to the most extreme data points not considered outliers, and the outliers are plotted individually using the '+' symbol.

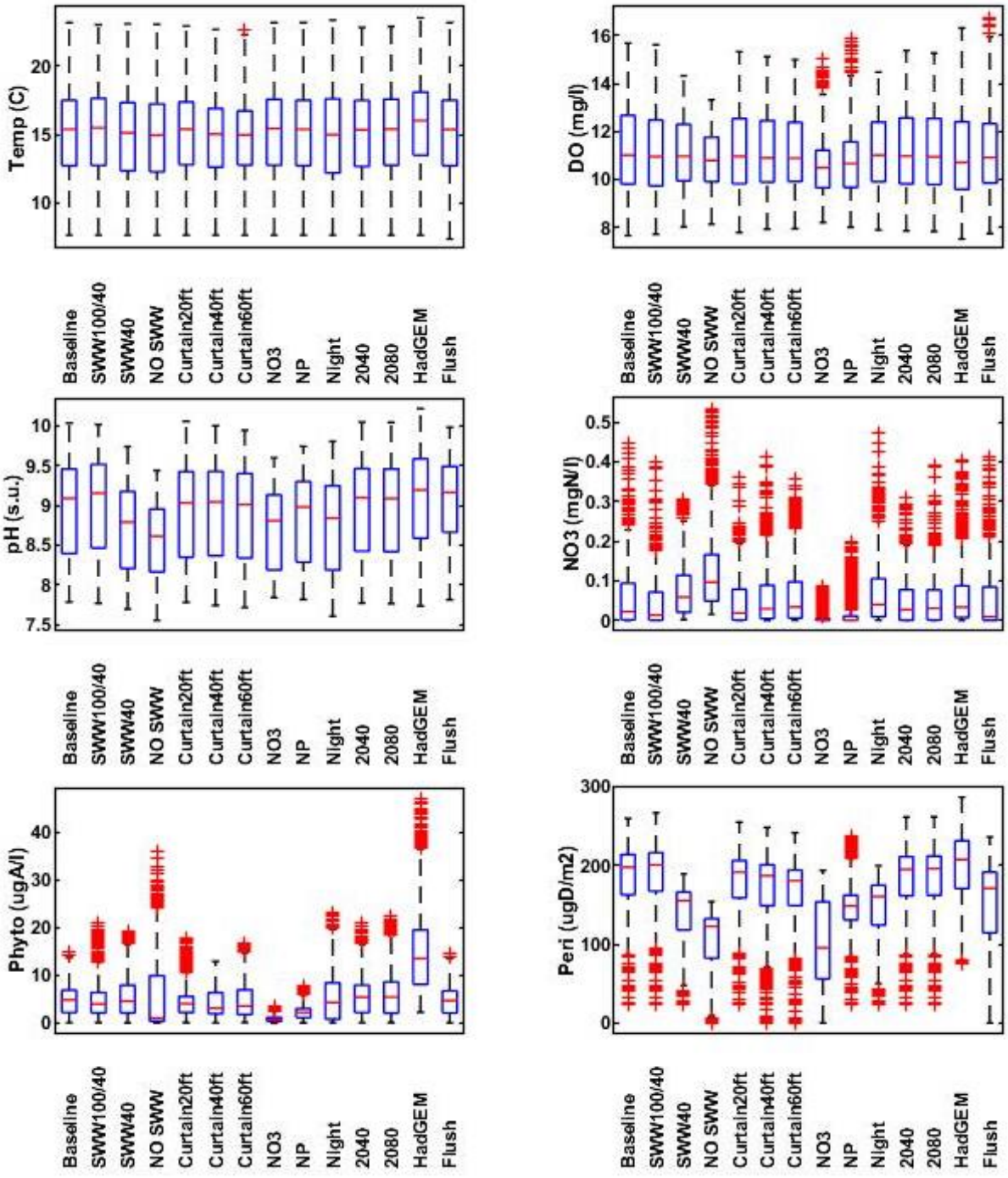

Figure 11-63. Boxplots presenting statistical summaries of the subdaily modeled data at Moody (RM 1). On each box, the central mark indicates the median, and the bottom and top edges of the box indicate the 25th and 75th percentiles, respectively. The whiskers extend to the most extreme data points not considered outliers, and the outliers are plotted individually using the '+' symbol.

Table 11-4. Summary statistics for the subdaily model results from each scenario. Results from 2Kw simulations in 2016 and 2017 were used as the basis for the statistics. All statistics presented in the table were derived from RM 96.

Scenario	Statistic	Temp (°C)	DO (mg/L)	pH (s.u.)	NO_3 (mg/L)	Phyto-plankton (mg A/L)	Periphyton (µgA/m2)
Baseline	Min	8.00	5.39	7.40	0.071	0.07	23.82
	Max	16.00	13.50	9.50	0.661	15.54	354.31
	Mean	12.63	10.00	8.49	0.194	4.86	267.20
	Std	1.27	1.21	0.58	0.069	3.01	66.49
SWW 100/40	Min	8.00	3.56	7.38	0.068	0.10	23.82
	Max	16.32	14.94	9.59	0.566	14.51	371.99
	Mean	12.81	10.26	8.56	0.189	4.75	281.57
	Std	1.32	1.34	0.62	0.066	3.18	70.08
SWW 40	Min	7.92	4.36	7.49	0.077	0.05	23.84
	Max	15.21	14.70	9.39	0.522	16.03	230.97
	Mean	12.22	9.82	8.39	0.199	5.11	177.44
	Std	1.54	1.07	0.42	0.061	3.71	43.21
No SWW	Min	7.68	2.21	7.48	0.080	0.04	0.00
	Max	15.78	18.51	9.55	0.690	32.26	174.30
	Mean	12.06	9.27	8.18	0.222	5.54	128.57
	Std	1.75	1.11	0.45	0.077	7.42	38.74
Curtain 20 ft	Min	8.00	4.63	7.42	0.070	0.10	23.82
	Max	15.17	13.76	9.48	0.588	18.89	337.62
	Mean	12.57	10.10	8.40	0.193	4.66	256.94
	Std	1.11	1.29	0.53	0.069	3.53	64.09
Curtain 40 ft	Min	8.00	2.18	7.43	0.071	0.08	0.00
	Max	15.08	13.06	9.48	0.597	15.14	323.45
	Mean	12.00	9.99	8.53	0.194	4.56	244.38
	Std	0.95	1.17	0.54	0.067	3.47	67.01
Curtain 60 ft	Min	8.00	2.22	7.36	0.071	0.15	0.00
	Max	15.08	13.00	9.48	0.534	21.86	313.03
	Mean	11.92	9.87	8.44	0.197	5.01	233.79
	Std	1.09	1.22	0.56	0.071	4.03	61.63
NO_3 Decrease	Min	8.00	1.98	7.35	0.004	0.02	0.0
	Max	15.96	12.78	9.39	0.401	5.51	173.07
	Mean	12.74	9.95	8.27	0.044	1.44	124.50

Scenario	Statistic	Temp (°C)	DO (mg/L)	pH (s.u.)	NO_3 (mg/L)	Phyto-plankton (mg A/L)	Periphyton (µgA/m2)
	Std	1.28	1.17	0.54	0.042	0.89	31.92
Nitrogen and Phosphorous Reduction	Min	8.00	5.33	7.37	0.004	0.05	23.82
	Max	16.00	13.01	9.65	0.496	9.74	331.56
	Mean	12.63	9.96	8.28	0.066	2.77	259.50
	Std	1.27	1.19	0.55	0.057	1.75	56.88
Night Blend	Min	7.71	4.25	7.47	0.074	0.12	23.84
	Max	15.81	20.47	10.03	0.758	15.90	264.09
	Mean	12.31	9.79	8.23	0.193	5.06	193.62
	Std	1.90	1.18	0.50	0.071	4.23	48.43
Future Tributary Temperature 2040	Min	8.00	2.36	7.47	0.070	0.06	23.82
	Max	16.00	13.95	9.56	0.582	15.03	357.86
	Mean	12.56	10.21	8.65	0.192	5.63	261.17
	Std	1.20	1.28	0.52	0.066	3.49	65.26
Future Tributary Temperature 2080	Min	8.00	4.05	7.46	0.070	0.10	23.82
	Max	16.44	13.62	9.61	0.550	15.87	360.21
	Mean	12.74	10.16	8.61	0.191	5.89	262.14
	Std	1.27	1.29	0.54	0.065	3.78	65.09
Future Climate (HadGEM)	Min	8.00	1.89	7.49	0.066	2.62	101.66
	Max	16.62	14.96	9.78	0.617	37.62	427.86
	Mean	13.86	9.93	8.85	0.189	14.67	270.96
	Std	1.22	1.92	0.58	0.078	6.36	76.75
Flushing Flow	Min	8.00	5.39	7.40	0.071	0.07	0.00
	Max	16.00	13.50	9.50	0.661	15.54	354.31
	Mean	12.63	9.99	8.49	0.194	4.86	254.24
	Std	1.27	1.20	0.58	0.069	3.01	79.36

Radar plots are used as a first strategy to highlight differences between mean values (Figure 11-64). These plots outline the difference between the means of each scenario and the baseline, so that a negative value indicates that the mean declined under the scenario. Results indicate that the SWW 100, No SWW, Night Blend, and the deeper curtains scenarios reduce the mean water temperature exported from PRB into the LDR.

Mean values of DO appear largely unchanged, although the No SWW and Night Blend scenarios result in reductions. Mean values of pH are reduced for the No SWW, Night Blend, and NO_3 Decrease scenarios and show increases for the SWW100/40 and one of the Future Climate scenarios. Mean NO_3 values are largely unchanged by the scenarios, except by the NO_3 Decrease scenario. This result is consistent with the scenario design, which targeted reductions in N export from PRB to the LDR.

The patterns for mean algae concentration and periphyton abundance are similar, with reduced means for the SWW100/40, No SWW, Night Blend, and NO_3 Decrease scenarios. These reductions in biomass result in reduced productivity and contribute to the reductions seen for pH and DO.

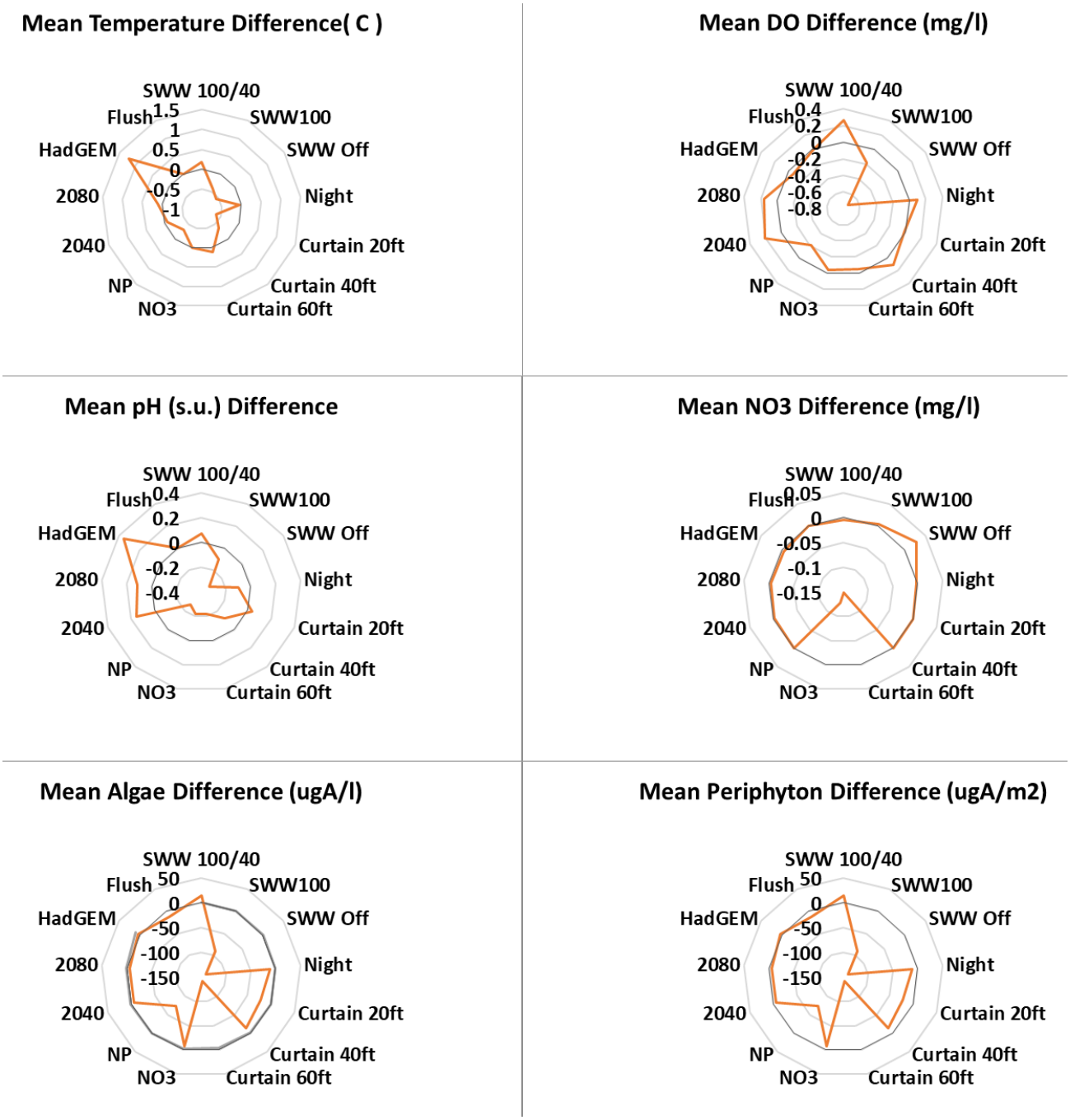

Figure 11-64. Radar plots outlining the differences in mean values between the scenarios and baseline model. A value of 0 (darker gray circle) indicates no difference between scenario and baseline means. Negative values indicate that the scenario was less than the baseline.

Of the different scenarios that incorporate the modification of the SWW operational standard, the No SWW and SWW40 scenarios represent conditions that are inconsistent with current operating rules. SWW 100/40 and Night Blend involve SWW operation that is more similar to the current strategy, but these scenarios present noticeably different modeled responses, with the Night Blend scenario appearing similar to those for No SWW and SWW40.

The primary difference between the Night Blend and SWW 100/40 scenarios is that, in the Night Blend scenario and during the spring migration period, surface water is released during the cooler evening hours, with the addition of some colder water from the bottom gate during the daylight hours. In SWW 100/40, 100% of the water is released from the surface during all times of the day during the migration period. The reduction of surface water release during the spring period for the Night Blend scenario helps to explain why the scenario results appear more like those for the No SWW scenario. But the timing of the changes in the gate releases plays a key role as well.

Water that is released during the evening hours tends to cool as it moves through the cooler canyon conditions that exist at night, and water that is released during the daylight period tends to warm as it moves through a warmer canyon (Figure 11-65).

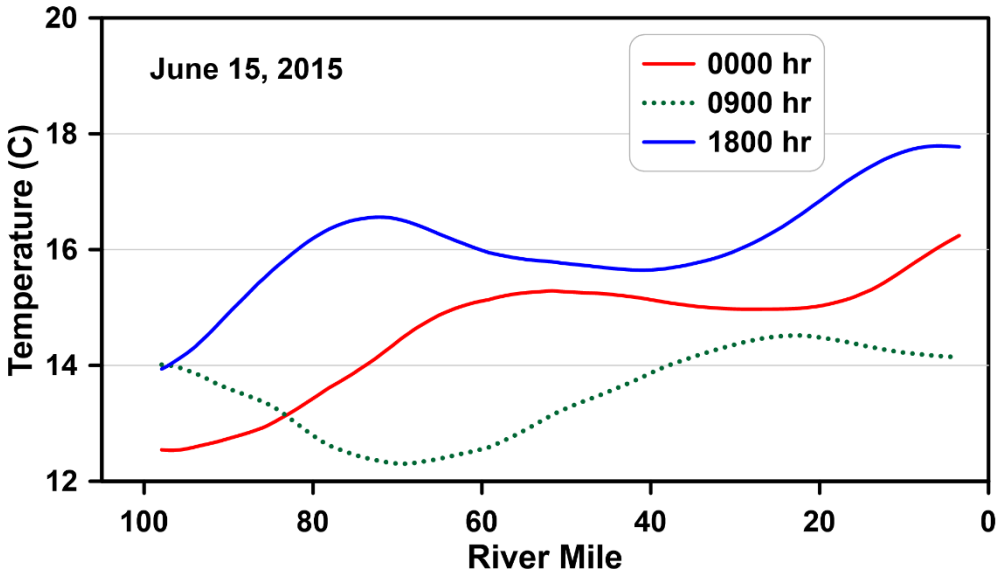

Figure 11-65. Longitudinal profiles of water temperature taken at three different points in time on June 15, 2015.

Because it takes around 33 hr for the water to move from ReReg tailrace to the mouth of the LDR, water released at night tends to be cooler than water released during the day, simply because it will have experienced more cool hours in the LDR canyon. By releasing warm surface water at night, along with cooler blends during the day, the Night Blend scenario appears to minimize canyon heating as compared to other blending strategies and approximates the differences in spring water temperatures at Moody associated with the No SWW and SWW 100/40 scenarios, but with potentially less of an impact on the fish collection strategy.

The one-way ANOVA results indicate whether a scenario resulted in statistically significant differences in the mean values when compared with the baseline (Figure 11-66, Figure 11-67, Figure 11-68, Figure 11-69, Figure 11-70, and Figure 11-71). These figures outline lower and upper limits for 95% confidence intervals for the true mean difference of each scenario and parameter and are developed for model results at RM 96. When the p-values are very small, indicating that the mean difference is significant, the symbol is in red. When no difference is detected, the symbol is green. The confidence interval is represented as the horizontal line through each point.

These results are consistent with the radar plots and outline statistically significant (p=0.05) differences between means. A key outcome of these results is that the scenarios tend to produce statistically significant differences in mean values, indicating that the system is sensitive to many of the scenario variables explored in the study. The tests are limited to evaluating the significance of each difference between mean values.

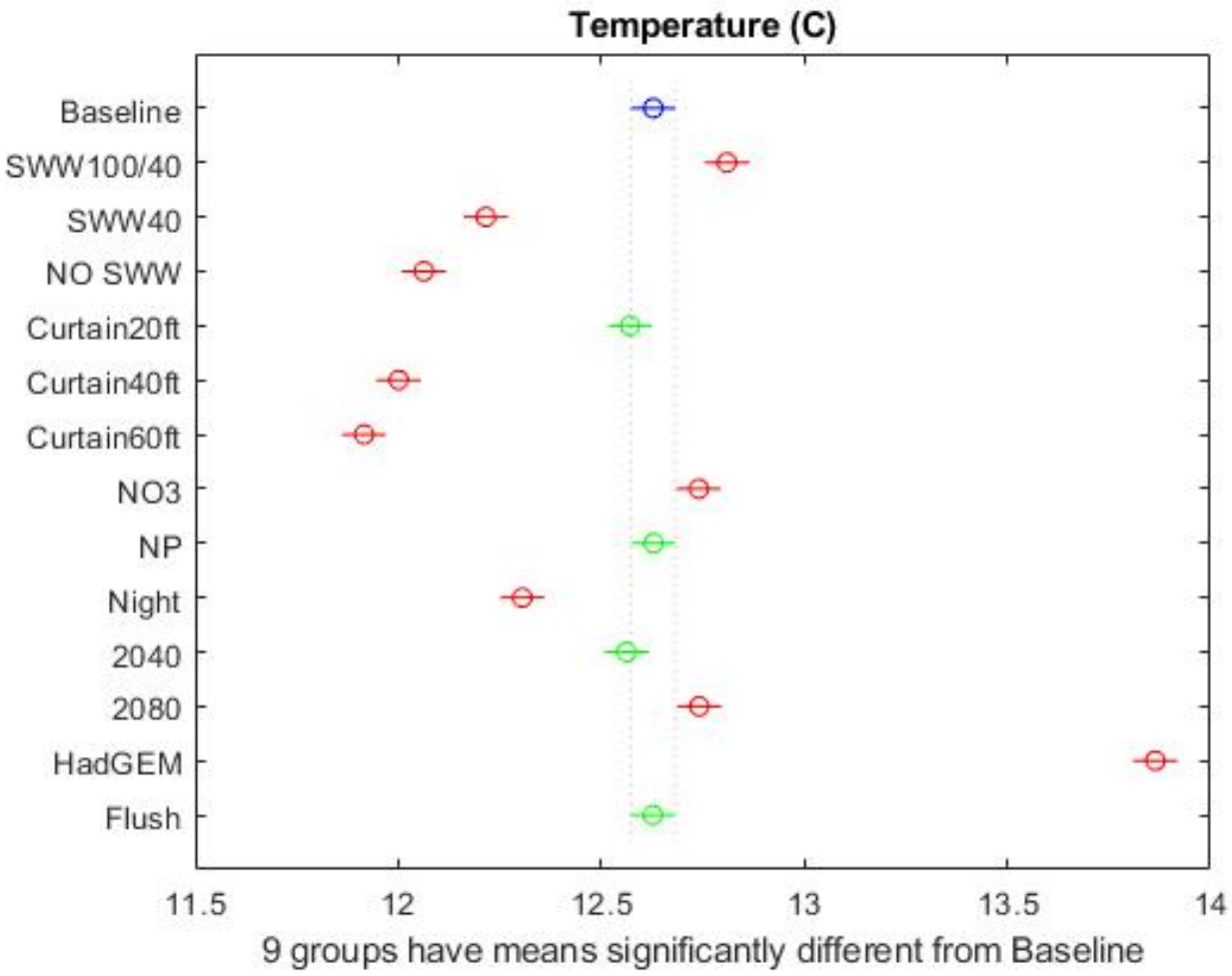

Figure 11-66. Mean water temperature and comparison intervals for each scenario and the baseline. Red indicates a statistically significant difference between scenario and baseline; green indicates no statistically significant difference. Modeled data were taken from simulation results at RM 96.

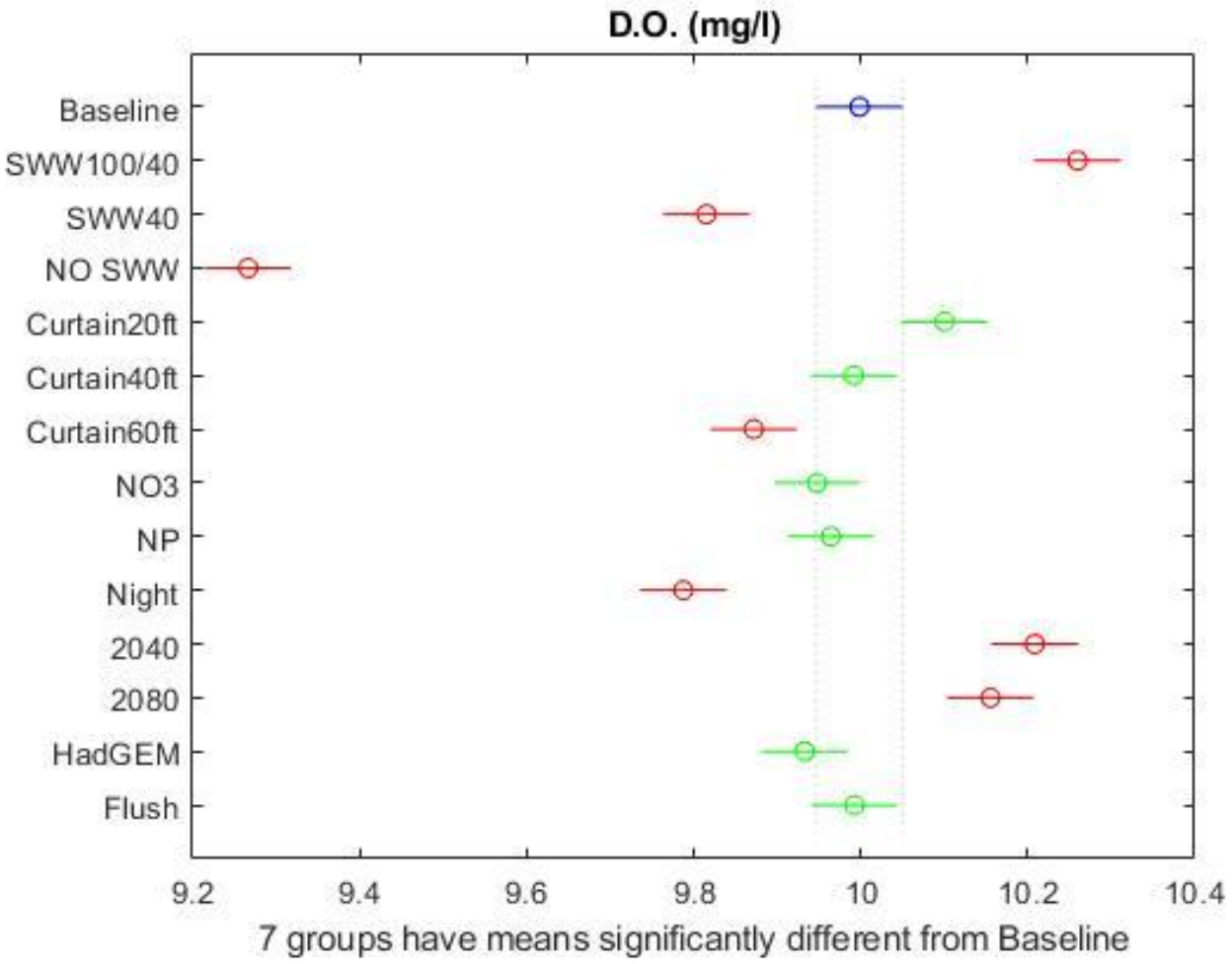

Figure 11-67. Mean DO concentrations and comparison intervals for each scenario and the baseline. Red indicates a statistically significant difference between scenario and baseline; green indicates no statistically significant difference. Modeled data were taken from simulation results at RM 96.

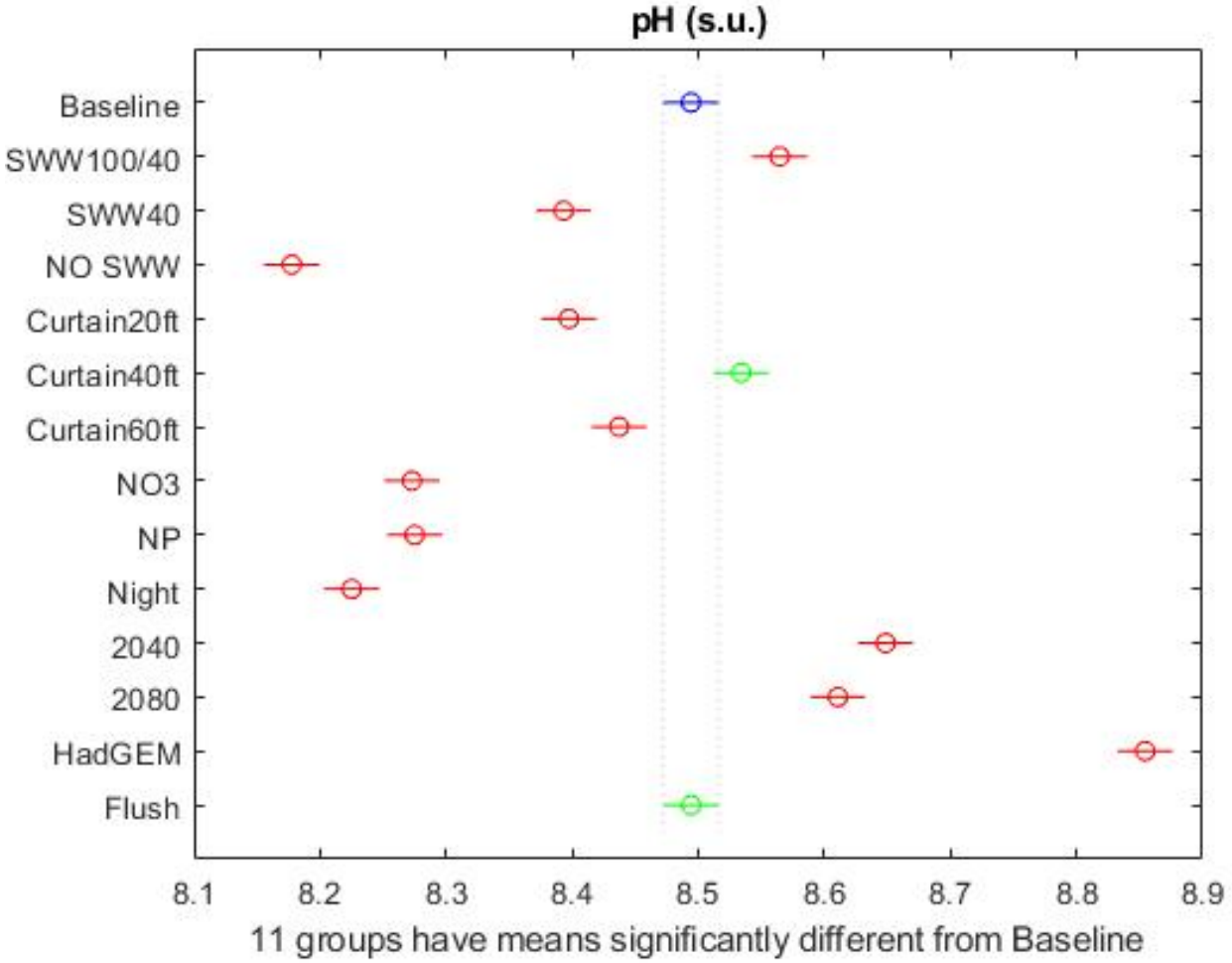

Figure 11-68. Mean pH values and comparison intervals for each scenario and the baseline. Red indicates a statistically significant difference between scenario and baseline; green indicates no statistically significant difference. Modeled data were taken from simulation results at RM 96.

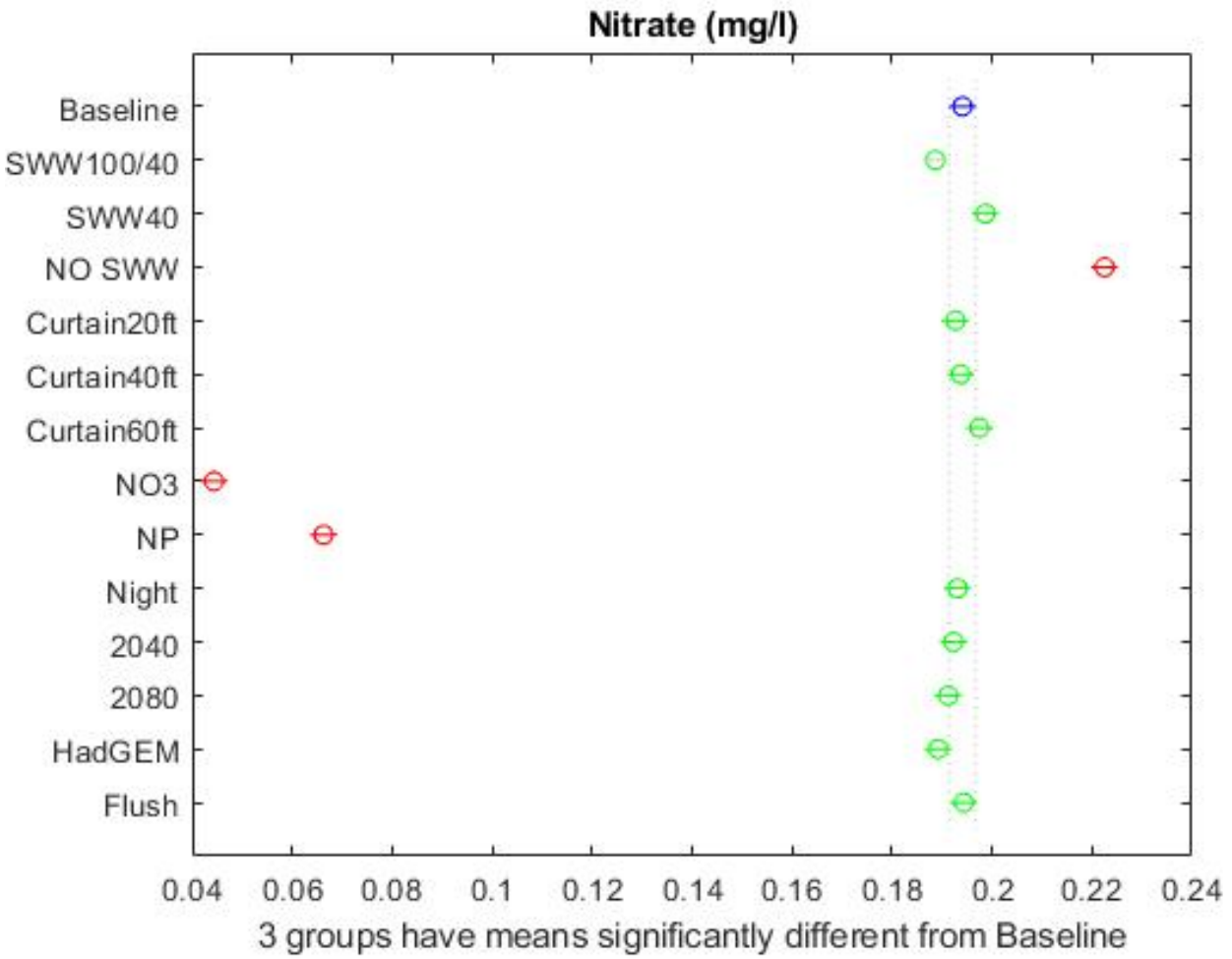

Figure 11-69. Mean NO_3 concentrations and comparison intervals for each scenario and the baseline. Red indicates a statistically significant difference between scenario and baseline; green indicates no statistically significant difference. Modeled data were taken from simulation results at RM 96.

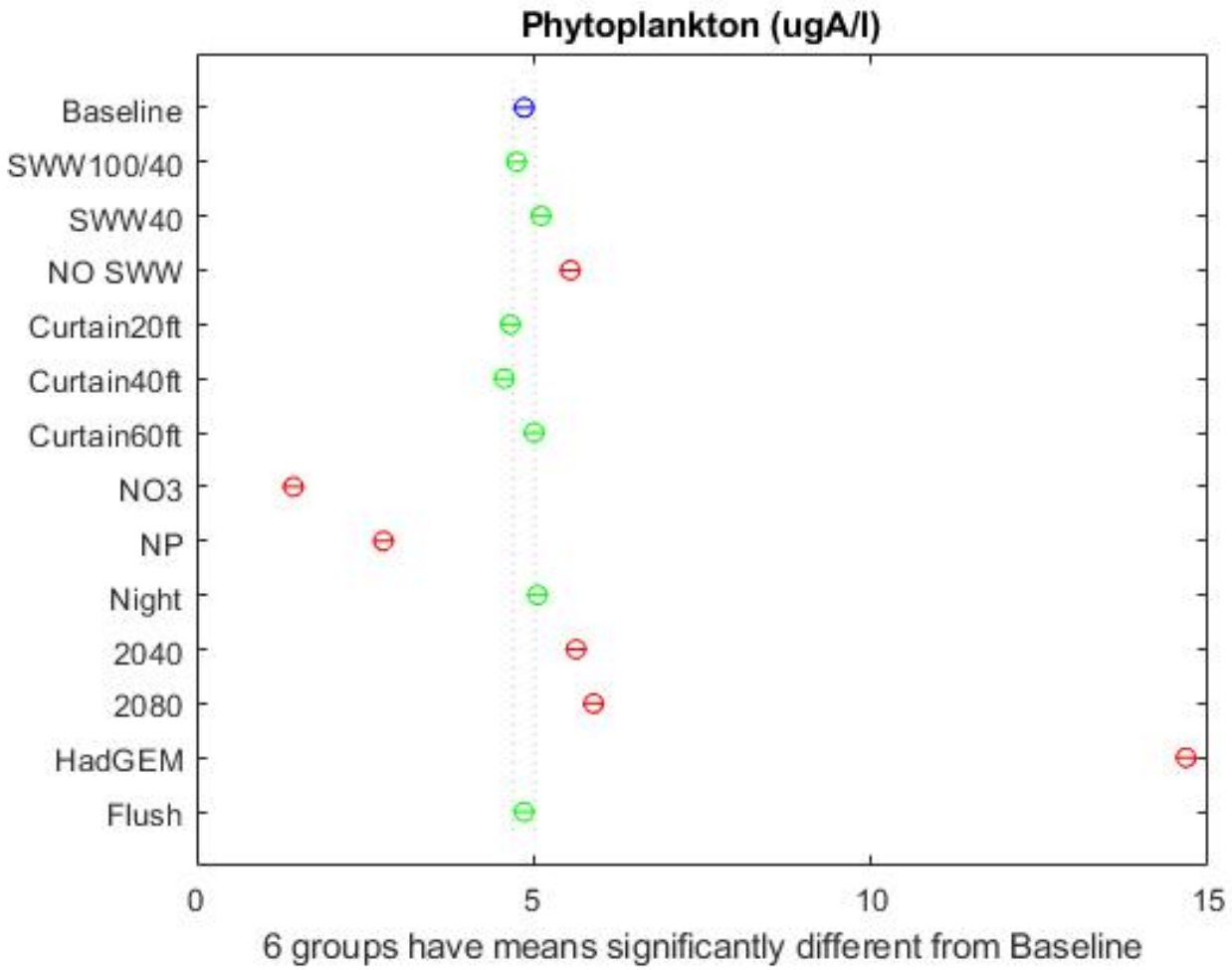

Figure 11-70. Mean phytoplankton concentrations and comparison intervals for each scenario and the baseline. Red indicates a statistically significant difference between scenario and baseline; green indicates no statistically significant difference. Modeled data were taken from simulation results at RM 96.

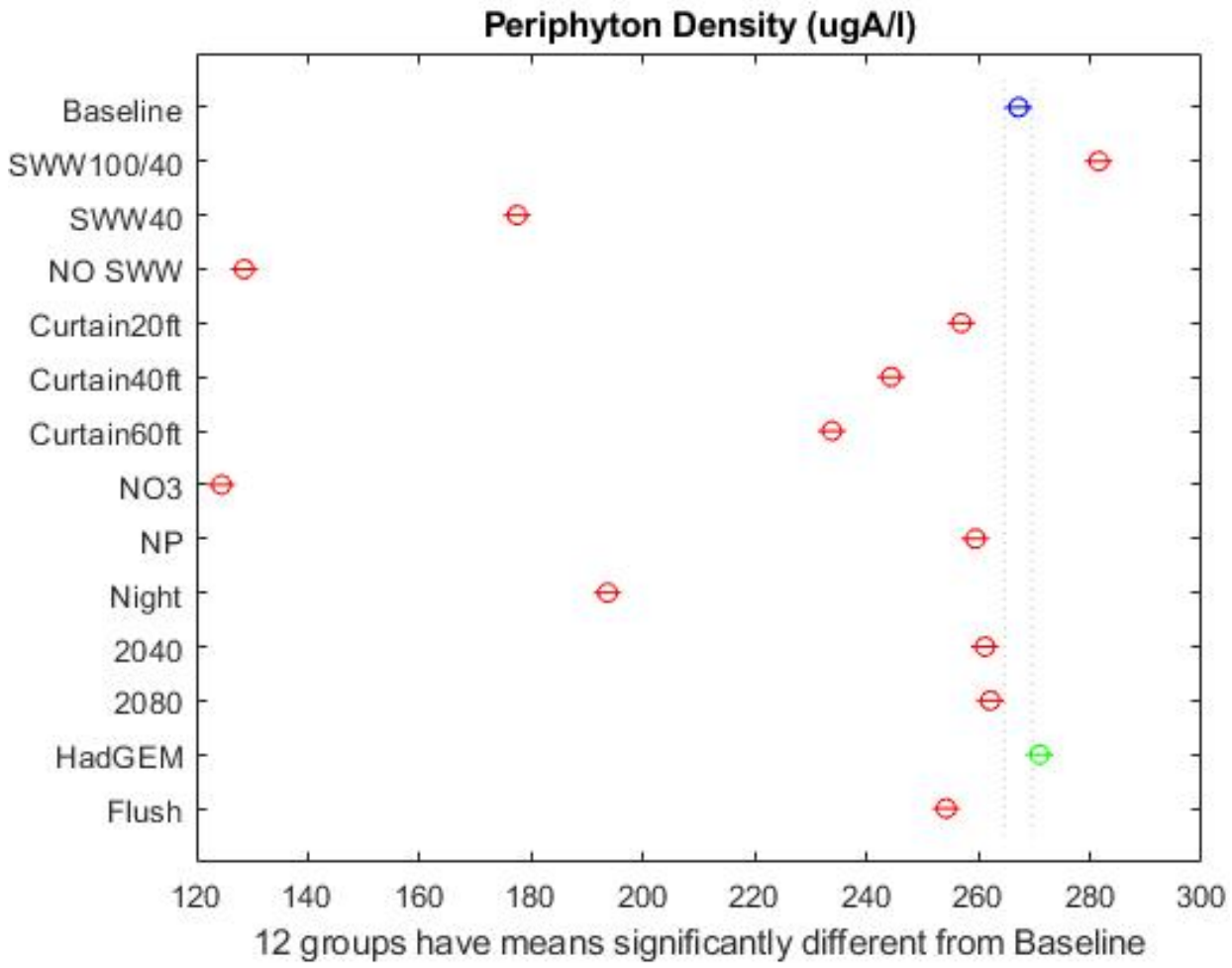

Figure 11-71. Mean periphyton densities and comparison intervals for each scenario and the baseline. Red indicates a statistically significant difference between scenario and baseline; green indicates no statistically significant difference. Modeled data were taken from simulation results at RM 96.

11.14 Scenarios Conclusion

The calibrated W2 reservoir model and 2Kw river model were linked and scenarios developed to explore potential influences on water temperature and quality in the LDR. Our modeling results are consistent with many observations of the system outlined in sections 9 and 10. Project operations can be modified to induce changes within the Project, and those changes can be passed through to the LDR, impacting water quality throughout the system. The cooler water at the bottom of LBC should be considered a finite resource that could become increasingly scarce

during the late summer, particularly when release strategies consume it before the warmer weather subsides. We attempted to quantify this limitation by modeling current operational scenarios in the context of future climate and tributary temperature predictions. The wide variability in simulated future climate complicated the analysis, and future research could explore a wider range of possibilities. Nonetheless, it will continue to be challenging to maintain enough cool water through the summer months if tributary water temperatures increase as average global climate becomes warmer.

Reductions in nitrogen entering the system, particularly from the Crooked River and Willow Creek, could improve water quality in the reservoir system and in the LDR. The simulations in the impoundments separated diatoms from cyanobacteria and, under both nutrient reduction scenarios, both phytoplankton groups declined in concentration. Cyanobacteria are not entirely reliant on NO_3/ammonium as a source of nitrogen because of their capacity to use nitrogen through fixation. As only two sites were monitored in LBC and, with the spatial variability in impoundment water chemistry, it is not possible to definitively predict the consequences of a reduction of specific nutrient from the tributaries. However, because the LDR is nitrogen-limited, it is likely that a reduction of NO_3 would reduce periphyton biomass in the river. This concept is addressed in greater detail in Section 12.

Two scenarios were developed to explore the potential impact of short-term releases of water from LBC. The first was intended to evaluate the impact of a cool-water release during a heat wave to test the possibility that such a release could be effective during only the very hottest periods and might require a significantly longer period of cold-water release than was evaluated in this study. Our evaluation targeted a specific set of days in July 2015, and the cold-water release did not appear to have measurable impacts in the LDR. However, it is important to note that the period we used did not correspond to the height of the heat wave, and further exploration over a wider range of conditions could be instructive.

The second short-term release strategy focused on large flushing flows. We wanted to explore the degree to which an extremely large, sudden release in the spring might remove established periphyton in the LDR, thereby improving water quality during the following summer. In this

case, the 1-D 2Kw was unable to fully evaluate the impact. The model indicated that periphyton were effectively eliminated by the flushing flow, but simulated regrowth was surprisingly fast.

We also simulated a change in operations that would release water at night during critical periods of the year. This scenario is intended to explore an operational change to promote an attractant flow to the SWW at night. This approach was thought to be more effective at attracting migrating smolt. It has the effect of reducing downstream temperatures and appears likely to reduce periphyton growth, pH, and DO saturation in the LDR.

Installing a retractable algae-retaining curtain in LBC might have a positive influence on water quality in the LDR during the period in which it is in place. Our modeling indicated the curtain would isolate the water near the intakes from the rest of the surface water, causing the SWW to effectively pull cooler, less productive water from below the bottom of the curtain. We explored several different curtain depths and, while all appear to have similar influence, the deeper curtains might be more effective in terms of reducing the temperature of water released through the SWW. It should be noted, however, that the surface water on the upstream side of the curtain can be expected to be warmer and more productive than it would be otherwise. When the curtains are pulled up to allow for fish passage, this warmer surface water would quickly move through the system, impacting water quality in the LDR.

Our modeling is consistent with the observation that in general, releases of colder water will likely reduce growth rates of periphyton in the LDR, and releases of water from deeper in LBC will likely reduce the transport of phytoplankton downstream. This result occurs because the model algorithms directly tie periphyton growth rate to water temperature and nutrient availability. Nonetheless, the capacity of the model to quantify the degree of reduction is useful. Phosphorus is naturally abundant throughout the Deschutes River basin; only in the Crooked River are concentrations of phosphorus significantly elevated above natural background levels. Even if the anthropogenic phosphorus inputs from the Crooked River could be eliminated, the Project impoundments would likely still be subject to algal/cyanobacterial blooms. This finding is corroborated by observations in other central Oregon impoundments that receive only background levels of phosphorus and yet still experiencing algal blooms. While phosphorus is

naturally high, nitrogen in the tributaries is derived largely from anthropogenic sources. It is unclear what impact reducing nitrogen loading to LBC would have because the sampling design for this complex reservoir was not intended to fully characterize the spatial variability in water quality. However, because phosphorus is naturally abundant throughout the Deschutes River basin, it may be difficult to control. Consequently, algal growth in the impoundments and the LDR are best controlled by reducing inputs of nitrogen to the system.

We also found that while operational changes can positively impact water quality in the LDR, the impact is constrained by the availability of cooler water in LBC during the warm summer months and by regulatory requirements imposed by the current FERC license. The cooler water is a finite resource and, depending on release strategies and future climate conditions, may become scarce during the late summer.

11.15 Areas for Future Research

11.15.1 Data Collection

Water quality modeling depends first and foremost on water quality data. The modeling effort was based on a well-developed set of water quality data but, nonetheless, could always be improved by additional data collection. In particular, TIC and alkalinity data are quite limited. Additionally, while the monthly timestep chemistry data collection is an important component of the study, shorter interval collection periods would more completely characterize the temporal variability. More frequent data collection could corroborate our assumption of a linear interpolation between available data points.

Periphyton growth rates represented in the 2Kw model have a high degree of uncertainty, which affects the predicted rate of periphyton regrowth following a major flushing event. While other modeling research corroborated the simulated periphyton growth rates, observational studies could be conducted to more clearly determine periphyton growth kinetics in the LDR. With better input data, more detailed studies using 2-D models may better explore these dynamics.

11.15.2 Modeling

Much of the modeling output displays current and forecasted water quality at the surface, while other important changes are taking place lower in the water column of the impoundments. Some of the model scenarios forecasts, including those associated with climate change, were based a daily average time-step input. However, the model is capable of incorporating finer resolution temporal data that would likely exhibit higher daily maximum temperatures than currently displayed. Full assessment of model performance should consider those additional model outputs.

The 2Kw model used for the LDR currently accommodates only a single algal group. It would be useful to expand that definition to allow for modeled differentiation between diatoms and cyanobacteria.

Two climate change scenarios, one for meteorological conditions and another for tributary water temperature, were explored separately in this study. A more comprehensive analysis would combine stream temperature estimates with projections of future climate and integrate them into W2/2Kw simulations. Ideally this combined scenario would also be more temporally detailed than those employed here as well, covering year-round conditions instead of only summer months.

The curtain simulations indicated complex interactions between the movement of water toward the LBC gates and the curtain. While the results of this study clearly suggest that curtains could effectively isolate the intakes from some epilimnetic water, more sophisticated 3-D hydrodynamic modeling is needed to optimize curtain depths.

12 Study Conclusions

12.1 Overview

This study was designed to inform the Licensees of the current water quality conditions in the LDR and to explore how potential changes in Project operations, watershed management, and climate might influence water quality in the LDR. However, in working and becoming more familiar with this complex system, more issues arose than could be fully resolved. Specifically, examining changes in water quality was greatly limited by the available data from the period before the SWW was introduced. Additionally, while the model forecasts offer insight into how the Project and the LDR might respond to changes in Project operations and external forcing factors like climate and hydrology, the models are comparatively simple representations of complex systems and their results should be viewed with a degree of skepticism. Despite these limitations in the science and circumstances, several valuable conclusions can be drawn from the study.

12.2 Current Status

12.2.1 Water Quality Status in the Tributaries to Lake Billy Chinook

The available data for the three tributaries to LBC show a wide range of physical and chemical properties. Discharge from the Crooked and Metolius rivers are similar, each contributing almost 40% to the total inflow compared to the Deschutes River, which provides slightly more than 20% of the inflow. On average, the Crooked River is the warmest of the three rivers, although the Deschutes River exhibits a higher maximum summer temperature. The Metolius River is cooler and, therefore, denser and prone to sink to the deeper portions of LBC. Conductivity values, which reflect total dissolved ions, were lowest in the Metolius River and highest in the Crooked River. These differences allow the movement of the tributary inflow to be traced through LBC. Concentrations of TP and PO_4 were high in all three tributaries, but the rivers differed greatly in their nitrogen inputs. The concentrations of NO_3 in the Crooked River were elevated and accounted for over 86% of the NO_3 input to LBC. With the exception of some phosphorus from

the Crooked River, phosphorus inputs to LBC are primarily derived from natural sources. By contrast, NO_3 inputs are derived almost entirely from anthropogenic sources.

Major Finding *The Crooked River is a major source of nutrients to LBC, especially of inorganic nitrogen. The Middle Deschutes River also inputs significant nutrient loads to LBC.*

12.2.2 Water Quality Status in the Impoundments

LBC and Lake Simtustus were sampled at two locations during the study; no samples were collected from the ReReg Reservoir. pH data in the surface waters approached 9.5 during the summer, and the DO saturation exceeded 120% all three summers. The surface waters in LBC are enriched in nitrogen and phosphorus, largely from inflow from the Crooked River, whose flow can be traced from the confluence with LBC to Round Butte forebay. These concentrations are low in the surface waters (1 m) during June and July but increase during other seasons. Concentrations of nitrogen and phosphorus are abundant at most depths in the reservoir. LBC is a highly productive (eutrophic) reservoir with high densities of phytoplankton. The dominant phytoplankton taxon is a large, centric diatom, *Stephanodiscus niagarae*, which is present in a wide variety of habitats, but usually is abundant in these densities only when there are high concentrations of nitrogen and phosphorus. During the summer, the dominant phytoplankton species is the cyanobacterium *Dolichospermum* (*Anabaena*), the presence of which is also indicative of eutrophic waters. The phytoplankton-rich surface waters are exported downstream through the SWW, passing through Lake Simtustus relatively unchanged and into the LDR.

Lake Simtustus is significantly different than LBC, in part, because it only has a single primary inflow – Round Butte tailrace. The relatively cool water discharged from Round Butte Dam passes into the hypolimnion of Lake Simtustus (when the lake is stratified) and moves through the reservoir in about 30 hr. In contrast, the surface waters in Lake Simtustus become isolated during the warmer months and receive no further input other than inflow from Willow Creek. Discharge from Willow Creek is low, the concentrations of NO_3 are high (minimizing cyanobacteria blooms in Lake Simtustus), and the inflow water temperature is warm. Lake Simtustus is somewhat less productive than LBC and has less dense phytoplankton populations,

lower levels of chlorophyll, and greater transparency. Consequently, Lake Simtustus has lower levels of surface pH and DO saturation.

Major Finding *Both LBC and Lake Simtustus are highly productive systems, although LBC is the more productive of the two. The surface waters in LBC contain high densities of diatoms and cyanobacteria (during the summer) that are available for transport downstream through the SWW.*

12.2.3 Water Quality Status in the Lower Deschutes River

The LDR has high concentrations of nitrogen and phosphorus. Both total phosphorus and PO_4 concentrations exhibit little change throughout the length of the river, thus showing little net uptake of phosphorus. Phosphorus is assimilated and recycled through the system, but the magnitude of the net uptake is minor relative to its availability. In contrast, NO_3 concentrations show a substantial decline from the ReReg Dam to the mouth of the river, indicating considerable net uptake of nitrogen. The total reduction of NO_3 throughout the length of the LDR can range from 0.10 mg/L to 0.20 mg/L. In some months, concentrations of NO_3 decline close to the DL (0.01 mg/L) toward the mouth of the river, suggesting strong nitrogen limitation.

The LDR contains considerable seston (suspended algae) and periphyton (attached algae). The seston consists of diatoms, especially *S. niagarae*, and cyanobacteria, largely *Dolichospermum* (*Anabaena*), transported from LBC. The periphyton in 2015 and 2016 was largely dominated by *Cladophora*. Cyanophyte and diatom abundance was comparatively low in the LDR during this period. . The importance of nitrogen to the LDR is illustrated by conditions in the Metolius River, which is considered one of the highest quality rivers in the state and supplies about 40% of the inflow to LBC. The Metolius River has concentrations of total phosphorous around 0.07 mg/L and concentrations of PO_4 around 0.06 mg/L; these values are similar to values observed in the other two tributaries. However, in comparison to the Crooked River, the Metolius River has little periphyton biomass because it has no measurable NO_3, whereas the Crooked River has concentrations of NO_3 around 0.4 mg/L. Similarly, the Williamson River in southern Oregon also has high concentrations of PO_4 (about 0.06 mg/L) and low concentrations of NO_3 (near DLs). Like the Metolius, it is considered a high-quality river. Factors that affect periphyton

community composition, location, and abundance include light availability, temperature, current velocity, substrate and suppression by grazers. However, among the nutrients, nitrate reduction (and when present, ammonia) has the greatest potential for control.

Major Finding *Although phosphorus is highly available throughout the LDR, nitrogen uptake is substantial, indicating that nitrogen is sometimes the limiting nutrient. Therefore, a reduction in NO_3 may be needed to reduce the periphyton biomass in the LDR. The periphyton population in the LDR was dominated by filamentous green algae in 2015 and 2016. These algae require an external source of nitrogen. The composition of the seston is dominated by the centric diatom, S. niagarae, with some contributions of cyanobacteria, both of which are derived from the surface withdrawal in LBC.*

The periphyton community in the LDR was dominated by filamentous green algae in 2015 and 2016. The dominant genus was *Cladophora*, a taxon often associated with highly productive waters. However, *Cladophora* abundance and distribution was greatly diminished in summer 2017, following high flows in spring 2017. *Cladophora* is subject to being dislodged at high stream velocities, and it is conceivable that the high flows in 2017 dislodged *Cladophora* and other filamentous green algae but had little impact on the abundance or distribution of cyanophytes and diatoms. An examination of nutrient concentrations in the LDR showed that NO_3 concentrations in the river in summer 2017 were greater than previous years. *Cladophora* and other green algae require an external source of nitrogen; therefore, river chemistry in 2017 should have favored chlorophytes. Although there is currently insufficient data to support the hypothesis that elevated spring flows caused a change in periphyton between years, this pattern should be monitored for repeat events to assess the possible relationship between river flows and periphyton community composition.

Major Finding *The periphyton community composition exhibited a large change from one dominated by chlorophytes in 2015 and 2016 to one with comparable levels of periphyton biovolume among the three major phyla in summer 2017. This change may have been caused by high river flows in spring 2017, which dislodged filamentous green algae. This pattern needs to*

be examined with data from subsequent years to assess if there is a relationship between maximum river discharge and periphyton community composition.

12.3 Historical Changes in Water Quality

12.3.1 Water Quality Changes in the Major Tributaries to Lake Billy Chinook

The three tributaries to LBC exhibited temperature increases at the USGS tributary gauging stations during the available PoR (2006–2017). The largest temperature increase was associated with the Middle Deschutes River site. The temperature data from this relatively brief period is insufficient from which to draw a conclusion about the cause of the increases, although it should be noted that these increases are consistent with temperature increases observed in the region. Forecasts for the region indicate a distinct possibility of further increased air temperature as well as decreased annual precipitation.

The only water quality data available to examine for trends in water quality for the three tributaries were from ODEQ AWQMP. The data for the Crooked River has shown considerable variation throughout the PoR, whereas the data for the Metolius and Deschutes rivers were relatively stable. The only variable that showed a trend for all three rivers was pH, which displayed an increase of about 0.5 pH units from 1960 to present.

Major Finding *Possible increases in water temperature are the major concern for the tributaries to the Project. Forecasts for the region indicate that these increases in water temperature are likely to continue into the foreseeable future.*

12.3.2 Water Quality Changes in the Reservoirs

Primary production in LBC appears to have increased, at least at the Round Butte forebay site, based on measured increases in pH and DO saturation. Historical pH in the surface waters seldom approached 9.0 (data from 1994–1996), whereas it now occasionally exceeds 9.5. Concentrations of phosphorus and nitrogen have either stayed unchanged or declined, depending on the depth of the sample. TP showed a statistically significant decline in the lower hypolimnion, PO_4 showed a significant decline in the epilimnion, and NO_3 showed significant

declines in both the upper hypolimnion and lower hypolimnion. Some of these changes (e.g., the decline of PO_4 in the epilimnion) likely represent changes associated with increased primary production, whereas those deeper in the water column likely represent changes in mixing patterns in the reservoir. There was a 48% increase in epilimnetic chlorophyll in LBC between 1994–1996 and 2015–2017, a fact that supports the apparent increase in primary production. Also, the phytoplankton appear to have changed somewhat between 2006 and the present study. Centric diatoms are still an important component of the phytoplankton, but cyanobacteria appear to have shifted from dominance by *Aphanizomenon* to *Dolichospermum* (*Anabaena*). The cyanobacteria also could be becoming more abundant earlier in the summer than in historical observations.

Although the hypolimnion in Lake Simtustus is now warmer because of the addition of the SWW and blending of surface water, few other major changes have occurred in the water quality of Lake Simtustus. The chlorophyll concentrations did show a 54% decline between 1994–1996 and the present study, but the transparency did not increase as might be expected.

Major Finding *Primary production increased in the surface waters of LBC at the Round Butte forebay and declined in the epilimnion of Lake Simtustus. The increase in primary production of LBC was accompanied by an earlier onset of cyanobacteria and a change from Aphanizomenon to Dolichospermum (Anabaena). Note that any conclusions regarding changes in LBC are restricted to the Round Butte forebay (RES07) and the Common Pool (RES08), the two sampling sites in the study. LBC is a large, complex reservoir and a more comprehensive study of the impoundment is required to assess impoundment-wide changes.*

12.3.3 Water Quality Changes in the Lower Deschutes River

Although the data are somewhat limited, both pH and DO appear to have increased in the LDR since 1997. Concentrations of both NO_3 and TP from the ReReg Dam to the mouth of the LDR during May and September appeared to remain consistent between 1997 and this study, but the July concentrations were substantially higher during this study. The water quality data collected by ODEQ at the Hwy 26 bridge (RM 97.6) and the mouth of the LDR (RM 0.1) show a gradual annual increase in NO_3 concentrations throughout the PoR, although the April-to-September

values exhibit a more noticeable increase in recent years. The largest recent increase in NO_3 occurred at the Hwy 26 bridge site (RM 97.6). Since 2010, concentrations of PO_4 have exhibited a slight increase at the Hwy 26 bridge site (RM 97.6), but there was a significant decline at the mouth of the LDR (RM 0.1). TP and BOD_5 show little or no change between pre- and post-SWW at the two monitoring locations. Unfortunately, a flaw in the analysis of the historical periphyton data collected in 1997 prevented us from comparing periphyton communities between the two periods.

Major Finding *Concentrations of NO_3 have likely increased in the LDR as indicated by the data collected along the length of the river in 1997 and in the long-term data collected by ODEQ. Increased NO_3 would allow for increased biomass of periphyton, but we lack the data to corroborate that hypothesis.*

12.4 Model Development and Calibration of the Pelton Round Butte Reservoirs

A hydrodynamic and water quality model of the PRB complex was developed and calibrated to data collected during the period from 2015–2017. The model has been demonstrated to capture observed surface water elevations, water temperatures, and a variety of water quality parameters.

As we developed the water quality models, some of the limitations associated with modeling complex water quality interactions in complex systems clearly emerged. Most prominent are challenges associated with simulating multiple algal groups. We limited the algae groups to just two, but even then, complex interactions between nutrient availability, water temperature, and algal production dynamics led to some clear overpredictions of algal growth, particularly of cyanobacteria. Models of environmental systems will always include uncertainties and, in this study, we have used the best available data to try to constrain them. For the W2 model, surface water levels and water temperature are better constrained by physics and mass balance than the more complex water quality components.

The model tends to underpredict NO_3-N in LBC, typically by 0.1 mg/L–0.2 mg/l during the summer months. This modeled underprediction likely results from elevated primary production, which uses the available N (NO_3 and NH_3). To achieve the high values of pH and DO

concentrations observed in LBC, the model increases its utilization of NH_3 and NO_3, resulting in an underprediction of NO_3.

Major Finding *The W2 model adequately captures the surface and temperature dynamics throughout the PRB system, and key features of the system's water quality, including the highly productive summers, are well represented by the model results. However, nutrient and biological processes are more complicated and, therefore, more uncertain and are not as closely approximated by the model. Note that any reference to model performance in LBC is limited to the Round Butte forebay (RES07) and the lower portion of the Crooked River arm. A more comprehensive assessment of other portions of LBC would require a more spatially comprehensive monitoring program.*

12.5 Model Development and Calibration of the Lower Deschutes River

A 1-D hydrology and water quality model was developed to represent the LDR. Data collected during 2015 was used to calibrate the model and data from 2016 was used to provide further evaluation of the model's consistency with available data sources. In addition, a third model representing the spring, summer, and fall of 2017 was also developed.

Calibration and evaluation of the LDR model indicated that it provides acceptable simulation of stream discharge and water temperature throughout the system, with AME values of less than 1°C for locations with continuous temperature observations. Water quality results also compared well against observations, although with fewer available observations, the work relies on visual inspection rather than calculated error statistics.

A limitation in the use of the 2Kw model is that it only allows for the inclusion of a single groupings to represent floating algae and periphyton. This simplification makes it difficult to capture potential differences associated with changes in the species distribution; in particular, changes in growth rates that might be associated with moving from diatom to cyanobacterial prevalence. While the available data is unable to clearly indicate a change in periphyton densities or distribution of species, Section 7 outlined observations that suggest that such a change may have occurred. Given that 2Kw is limited to a single species grouping, this type of

response was not directly captured by the model. As an initial strategy to explore such a change, we allowed the maximum growth rate of the single periphyton group to vary as a function of water temperature. This virtual experiment approach provides an initial mechanism to explore changes associated with the evolving biological system, but could be improved by better periphyton data and the capacity for the model to capture multiple periphyton species in the model.

Major Finding *Water temperature, stream discharge, diurnal DO, and pH were well captured by the calibrated 2Kw model. As with the reservoir modeling, comparison of the modeled results of the biological system against observations suggest additional uncertainty associated with the water quality simulations. The model formulation for the biological components could be expanded to better capture dynamics that appear to define the LDR.*

12.6 Scenario Analysis

The overall goal of the model-based scenario analysis was to explore how potential changes in Project operations, watershed management, and climate might influence water quality in the LDR. The calibrated W2 reservoir model and 2Kw river model were linked to explore the impact of potential changes to water temperatures and water quality throughout the Project and LDR. To explore these potential impacts, we developed a set of scenarios. The operation of the SWW could be modified to induce changes to water quality in the Project and throughout the LDR system. However, the cooler water in the reservoir should be considered a finite resource, which for warmer summers and depending on release strategies, may be become scarce during the later summer. We attempted to quantify this by incorporating predictions of future climate and tributary temperature, although those simulations were challenged by the wide variability in simulated future climate. Nonetheless, the challenge associated with maintaining this volume of cool water will continue and may become more significant if tributary temperatures increase.

Major Finding *Scenario variables, including climate inputs, watershed nutrient inputs, and Project operations have statistically significant influences on the water temperature and water quality of both the reservoirs and the LDR. The capacity to modify water quality through reservoir management is limited by climate and watershed nutrient contributions. However, the*

existing model and available data are not sufficient to provide definitive guidance regarding optimal management techniques and would need to account for factors not addressed in this analysis. These factors include fish passage at Round Butte, LDR and reservoir fisheries, and LDR macroinvertebrates as well as compliance with CWA Section 401 and FERC license regulations.

12.7 Recommendations

12.7.1 Nutrient Reduction

LBC and Lake Simtustus are highly productive reservoirs, a fact that may facilitate high biomass of fish. Unfortunately, it also causes dense blooms of algae and cyanobacteria, an undesirable situation, as cyanobacteria are a poor food source for zooplankton, which in turn serve as a major food source for kokanee. Additionally, high concentrations of nutrients, particularly in LBC, are transported downstream to the LDR further promoting growth of periphyton. Recent literature indicates that the best strategy for reducing eutrophication in a system such as LBC is a dual approach that reduces both nitrogen and phosphorus. However, most of the phosphorus entering LBC is derived from natural weathering. The greatest opportunity for reducing phosphorus inputs to LBC is through reduction of anthropogenic sources in the Crooked River basin. The vast majority of NO_3 inputs are also derived from the Crooked River, likely from irrigation return flow associated with crop production. Several methods are available for treatment of return irrigation flow, including distribution of the return flow through constructed or existing wetlands to encourage assimilation of inorganic nitrogen and PO_4 by wetland plants. A reduction in nutrients in LBC will reduce their presence in Lake Simtustus, although there will remain considerable irrigation return flow from Willow Creek. However, removing this source would likely increase the probability that the upstream reach of the reservoir would experience increased cyanobacteria blooms because a reduction in available nitrogen would increase the competitive advantage of cyanobacteria over non-heterocystous taxa.

The data on the LDR show that reducing nitrogen will have a greater effect in reducing periphyton biovolume compared to reducing phosphorus. The mats of filamentous green algae such as *Cladophora* are dependent on available inorganic nitrogen for growth, and their

abundance will likely be reduced if nitrogen is limited. Therefore, one can expect that reducing the nitrogen concentrations in the LDR will promote longer reaches with nitrogen-limitation and will move the periphyton community to one with a lower density of total biovolume.

12.7.2 Operational Considerations

The SWW system was designed to improve smolt attraction and provide Project operators with some degree of control over the thermal profile of discharge to the LDR. In the years since installation, the SWW has proven successful in attracting smolts to be collected for transport downstream, but it is also responsible for increased transport of algae and cyanobacteria to the LDR, which contribute to the primary production of the LDR. The greater the degree to which algae transport to the LDR can be reduced, the more likely there will be a positive effect by increasing water clarity and possibly reducing periphyton biovolume.

The SWW provides Project operators control of the water temperature released to the LDR, which allows them to achieve a temperature regime that more closely mimics natural temperature conditions in the river and facilitates salmonid growth and survival. The more natural seasonal river temperatures also result in higher rates of metabolism for all organisms, including algae and cyanobacteria, and promotes species shifts in periphyton community composition.

It may be possible to improve water quality in the LDR by altering the operational profile of the SWW, but it is important to preserve the smolt-attraction flows at critical times, especially March 15 to June 15. A more effective means of reducing transport of algae downstream might be to install a Hypalon barrier during periods when smolt collection is minimal. This type of barrier can be effective, particularly in minimizing the transport of cyanobacteria, which tend to remain buoyant and high in the water column. However, a more detailed assessment with a complex 3-D hydrodynamic model is necessary to better understand the effectiveness of the barrier at different depths and the effect it would have on water quality in the LBC. Model simulations suggest that installing a Hypalon current might increase phytoplankton abundance in LBC.

Prior to the construction of a number of dams in the Deschutes River basin, 1907–1948, peak flows in the spring were greater than in 1949–2017. Additionally, the current distribution of peak flows more typically occurs in the winter, whereas 1907–1948 peak flows occurred more frequently in spring. This apparent change in the magnitude and timing of peak flows in the river is coincident with the onset of climate change, which includes reduced snowpack in the Cascades. The reduction of peak spring flows may be increasing the likelihood that filamentous green algae become dominant in the river. Peak flows in late March or April approaching 20,000 cfs at the mouth appear to satisfy the removal of most of the *Cladophora*. However, the ability to achieve flows of that magnitude at the mouth may require significant tributary input given the regulatory and safety concerns immediately below the Project. More precise work on the contributions of dam construction and operation and climate change is needed to establish their role in changes in flows for the LDR.

12.7.3 Research Considerations

This monitoring and modeling study identified areas of uncertainty that cannot be resolved without further research:

- The periphyton community in the LDR is highly variable among years. Developing a better understanding of the autecology of some of these taxa such as *Cladophora* could yield important information for better managing conditions in the river.
- The monitoring design employed in this study sampled the substrate to a depth only slightly greater than 2 ft, although the LDR is considerably deeper. Further study regarding the extent of periphyton growth in the deeper portions of the river channel is warranted.
- The monitoring program for the LDR did not address the biomass of vascular plants (aquatic weeds). This was done, in part, because no historical observations exist of vascular plants for comparison. However, a complete assessment of plant growth would include vascular plants in the sampling program. An entirely different sampling design would be required to capture the patchy distribution and abundance of vascular plants.

- The ZAPS LiquID unit identified a peak period during spring runoff when values of FDOM were relatively high. FDOM is highly specific to complex organic compounds often associated with pesticides and related chemicals, although high molecular weight natural organic degradation products can also contribute to high FDOM values. Targeted research might identify specific compounds present in the LDR and their potential relationship to upstream sources.
- With increased attention focused on water quality in the Crooked River and efforts in place to improve it, a monitoring program could be helpful in documenting possible changes in nutrient export to LBC from the river.
- The 2015–2017 monitoring program focused on concentrations of nutrients throughout the system. However, it did not include any evaluation of the cycling of nutrients in the impoundments or the LDR. Nutrient cycling is often investigated using naturally occurring isotopes that allow for measuring fluxes from water to algae to invertebrates and vertebrates. The internal nutrient cycles associated with the large biomass of planktivorous fish might be an important consideration in the overall productivity of LBC.
- The reduction of NO_3 and, to a lesser extent, other nutrients to the Project could result in unanticipated biological responses in the lakes and the LDR. Limnocorrals and other test chambers such as artificial streams could be used in localized portions of the reservoirs and the LDR to help further the understanding of these processes.
- The dramatic decrease in abundance of filamentous chlorophytes in summer 2017 followed a spring with the greatest discharge observed since before 2015. It is unclear if these elevated spring flows were responsible for the decrease in *Cladophora*, although no other mechanism appears to explain the change in periphyton. Continued observation of periphyton in the LDR should continue to determine how the periphyton community changes in association with elevated spring discharge.
- The three tributaries to LBC appear to exhibit increases in water temperature and recent forecasts predict increases in the mean annual air temperature for the region. The Project operates under a temperature plan developed in 1997, before there was a widespread

realization that the climate was changing. Consideration should be given to evaluating how the Project might be operated differently under a scenario of decreasing availability of cold water in LBC.

13 Acknowledgments

This study was funded by Portland General Electric and the Confederated Tribes of the Warm Springs Reservation of Oregon through a contract to MaxDepth Aquatics, Inc. The project manager for PGE was Erica Amt, who facilitated all aspects of this work. We thank PGE staff at the Madras office for collecting data for this study, including Lori Campbell, Katherine Smith, Elayne Barclay, Leah Hough, and Nathan Stotts. Benn Eilers, MaxDepth Aquatics, Inc., provided support for the study, including data acquisition during the river float and data processing of LiDAR data, hydroacoustic data, and other spatial datasets. Jeff Hogle, CTWS, graciously provided data on fish populations in LBC. Dan Brown and Bonnie Lamb, ODEQ, kindly provided AWQMP and other data related to the Project. We appreciate comments provided by external technical reviewers.

14 Literature Cited

Abatzoglou, J.T., Brown, T.J. 2012. A comparison of statistical downscaling methods suited for wildfire applications. Int. J. Climatol. 32, 772–780.

Allan, J.D. 1995. *Stream Ecology: Structure and Function of Running Waters*. Kluwer Academic Publishers Dordrecht, Netherhlands. 388 pp.

American Public Health Association. 1998. Standard Methods for the Examination of Water and Wastewater. 20th Edition.

Bahls, L.L. and E.E. Weber. 1988. Ecology and distribution in Montana of *Epithemia sorex* Kütz., a common nitrogen-fixing diatom. *Proc. Mont. Acad. Sci.* 48:15-20.

Bartholow, J.M., 1991. A modeling assessment of the thermal regime for an urban sport fishery. Environ. Manage. 15, 833–845.

bbe Moldaenke. AlgaeTorch chlorophyll and cyanobacteria measurement instrument. *https://www.bbe-moldaenke.de/en/products/chlorophyll/details/algaetorch.html*

Bergström, A-K. and M. Jansson. 2006. Atmospheric nitrogen deposition has caused nitrogen enrichment and eutrophication of lakes in the northern hemisphere. *Global Change.* 12:635-643.

Biggs, B.J.F. and P. Gerbeaux. 1993. Periphyton development in relation to macro-scale (geology) and micro-scale (velocity) limiters in two gravel-bed rivers, New Zealand. *New Zealand Journal of Marine and Freshwater Research*. 27: 39-53.

Biggs, B.J.E. 2000. Eutrophication of streams and rivers: dissolved nutrient-chlorophyll relationships for benthic algae. *J. North Amer. Benthological Soc.* 19:17-31.

Brown, L.C., Barnwell, T.O., 1987. The enhanced stream water quality models QUAL2E and QUAL2E-UNCAS: Documentation and user manual. US Environmental Protection Agency. Office of Research and Development. Environmental Research Laboratory.

Brown, T-R., E. Low-Décarie, R.W. Pillsbury, G.A. Fox and K.M. Scott. 2017. The effects of elevated atmospheric CO_2 on freshwater periphyton in a temperate stream. *Hydrobiologia*. 794:333-346.

Bunting, L., P.R. Leavitt, V. Hall, C.E. Gibson, and E.J. McGee. 2005. Nitrogen degradation of water quality in a phosphorus-saturated catchment: The case of Lough Neagh, Northern Ireland. *Verh. Int.Verein. Limnol.* 29:1005-1008.

Caldwell, R.R. and M. Truini. 1997. Ground-water and water chemistry data for the Upper Deschutes Basin, Oregon. USGS Open-File Report 97-197. 77 pp.

Canfield, D.E., S.B. Linda, and L.M. Hodgson. 1985. Chlorophyll-biomass-nutrient relationships for natural assemblages of Florida phytoplankton. *J. Amer. Wat. Resourc. Assoc.* 21: 381-391.

Cao, Y., N. Zhang, J. Sun and W. Li. 2019. Responses of periphyton on non-plant substrates to different macrophytes under various nitrogen concentrations: A mesocosm study. Aquatic Botany. 154:53-59.

Carpenter, S.R. 2008. Phosphorus control is critical to mitigating eutrophication. *Proc. Nat. Acad. Sci*. 105:1139-11040.

Chapra, S.C., Pelletier, G.J. and Tao, H. 2012. QUAL2K: A Modeling Framework for Simulating River and Stream Water Quality, Version 2.12: Documentation and User's Manual. Civil and Environmental Engineering Dept., Tufts University, Medford, MA.

Chételat, J., F.R. Pick, A. Morin, and P.B. Hamilton. 1999. Periphyton biomass and community composition in rivers of different nutrient status. *Can. J. Fish. Aquat. Sci.* 56:560-569.

Churchill, M., Elmore, Buckingham, 1962. The prediction of stream reaeration rates. J. Sanit. Eng. 88, 1–46.

Climatology Lab. No Date. Multivariate Adaptive Constructed Analogs. Retrieved from *http://www.climatologylab.org/maca.html*.

Cole, T.M., Wells, S.A., 2006. CE-QUAL-W2: A two-dimensional, laterally averaged, hydrodynamic and water quality model, version 3.5.

Conley, D.J., H. Paerl, R. W. Howarth, D.F. Boesch, S.P. Seitzinger, K.E. Havens, C. Lancelot and G.E. Likens. 2009. Controlling eutrophication: nitrogen and phosphorus. *Science.* 323:1014-1015.

Cotner, J.B. 2016. Nitrogen is not a "House of Cards". Response to Schindler et al. 2016. "Reducing Phosphorus to Curb Lake Eutrophication is a Success". *Environ. Sci. & Technol.* 50: 8924.

Dalton, M.M, P.W. Mote, and A.K. Snover (eds). 2013. Climate Change in the Pacific Northwest: Implications for our Landscapes, Waters, and Communities. Island Press. Washington, D.C. 230 pp.

Deschutes Basin Board of Control. 2016. Settlement Fact Sheet: Oregon Spotted Frog. October 28, 2016. Retrieved from *http://dbbcirrigation.com/projects/news/settlement-agreement-fact-sheet-oregon-spotted-frog/*.

Dodds, W.K. and D.A. Gudder. 1992. The ecology of *Cladophora*. *J. Phycol* .28:415-427.

Dodds, W.K., J.J. Jones, and E.B. Welch. 1998. Suggested classification of stream trophic state: Distributions of temperate stream types by chlorophyll, total nitrogen, and phosphorus. *Water Research.* 32:1455-1462.

Dodds, W.K. 2006. Eutrophication and trophic state in rivers and streams. *Limnology & Oceanography.* 51:671-680.

Dodds, W.K. and V.H. Smith. 2016. Nitrogen, phosphorus, and eutrophication in streams. *Inland Waters.* 6:155-164.

DOGAM (Oregon Department of Geology and Mineral Industries. No Date. Lidar. Retrieved from https://www.oregongeology.org/lidar/

Driscoll, C.B. and others. 2018. A closely-related clade of globally distributed bloom-forming cyanobacteria within the Nostocales. *Harmful Algae.* 77:93-107.

Eilers, J.M., R. Raymond and B. Eilers. 2003. Lemolo Lake, Oregon: monitoring and modeling water quality. A report to PacifiCorp. JC Headwaters, Inc. Bend, OR

Eilers, J.M., B.J. Eilers, R. Sweets, and A. St. Amand. 2005. An analysis of current and historic conditions in Lava Lake in support of a TMDL nutrient loading assessment. Report to the Upper Deschutes Watershed Council. MaxDepth Aquatics, Inc. Bend OR. 60 pp.

Eilers, J.M., H.A. Truemper, L.S. Jackson, B.J. Eilers, and D.W. Loomis. 2011. Eradication of an invasive cyprinid (*Gila bicolor*) to achieve water quality goals in Diamond Lake, Oregon (USA). *J. Lake & Reservoir Mgmt.* 27:194-204.

Eilers, J.M., K. Vache, B. Eilers, R. Sweets, and J. Cornett. 2016. Assessing the chemical and biological resilience of lakes in the Cascade Range to acidic deposition. *Wat Air Soil Pollut.* 227:432.

Ekvall, M.K., P. Urrutia-Cordero, and L-A. Hansson. 2014. Linking cascading effects of fish predation and zooplankton grazing to reduced cyanobacterial biomass and toxin levels following biomanipulation. *PLOS One.* 9:e112956.

Feminella, J.W. and C.P. Hawkins. 1995. Interactions between stream herbivores and periphyton: A quantitative analysis of past experiments. *J. North Amer. Benth. Soc.* 14:465-509.

Finlay, K., A. Patoine, D.B. Donald, M. Bogard, and P.R. Leavitt. 2010. Experimental evidence that pollution with urea can degrade water quality in phosphorus-rich lakes of the Northern Great Plains. Limnol & Oceangr. 55:1213-1230.

Flynn, K.F., Chapra, S.C., Suplee, M.W., 2013. Modeling the lateral variation of bottom-attached algae in rivers. Ecological Modelling 267, 11–25.

Fulton, R.S. III. 1988. Grazing on filamentous algae by herbivorous zooplankton. *Freshwater Biology*. https://doi.org/10.1111/j.1365-2427.1988.tb00450.x

Galloway, J.N. and E.B. Cowling. 2002. Reactive nitrogen and the world: 200 years of change. Ambio. 31:64-71.

Gannett, M.W., K.E. Lite, Jr., D.S. Morgan and C.A. Collins. 2001. Ground-water hydrology of the Upper Deschutes Basin, Oregon. USGS Water-Resources Investigation Report 2000-4162. 74 pp.

Gannett, M.W., M. Manga, and K.E. Lite, Jr. 2003. Groundwater hydrology of the Upper Deschutes Basin and its influence on streamflow. In A Peculiar River: Geology, Geomorphology, and Hydrology of the Deschutes River, Oregon, ed. J.E. O'Connor and G. E. Grant., pp 31-50. American Geophysical Union. Washington, DC.

Gillett, N. D., Y. Pan, J.E. Asarian and J. Kann. 2016. Spatial and temporal variability of river periphyton below a hypereutrophic lake and a series of dams. *Science of the Total Environment.* 541:1382-1392.

Goldman, J.C. and E.J. Carpenter. 1974. A kinetic approach to the effect of temperature on algal growth. *Limnol. Oceanogr.* 19:756-766.

Grabowska, M. and H. Mazur-Marzec. 2016. The influence of hydrological conditions on phytoplankton community structure and cyanopeptide concentration in dammed lowland river. *Environ. Monit. Assess.* 188: 488.

Griffiths, D. 2006. The direct contribution of fish to lake phosphorus. *Ecology of Freshwater Fish.* 15:86-95.

Grimm, N.B. and S.G. Fisher. 1986. Nitrogen limitation in a Sonoran Desert stream. J. N. Am. Benthol. Soc. 5:2-15.

Gustavson, K., F. Møhlenberg, and L. Schlüter. 2003. Effects of exposure duration of herbicides on natural stream periphyton communities and recovery. *Archives of Environmental Contamination and Toxicology.* 45: 48-58.

Håkansson, H. and B. Meyer. 1994. A comparative study of species in the *Stephanodiscus niagarae*-complex and a description of *S. heterostylus* sp. nov. *Diatom Research*. 9:65-85.

Hassan, F.M, J.M. Salman and S. Al-Nasrawi. 2017. Community structure of benthic algae in a lotic ecosystem, Karbala Province – Iraq. *Baghdad Science Journal.* 14:692-706.

Hawes, I, and R. Smith. 1993. Effect of localized nutrient enrichment on the shallow epilithic periphyton of oligotrophic Lake Taupo, New Zealand. *New Zealand Journal of Marine and Freshwater Research.* 27:365-372.

Hickman, C.W. 1994. Pesticide chemistry and toxicity to algae. *In* Advances in Limnology. L.C. Rai, J.P. Gaur, and C.J. Soeder (eds). Archiv für Hydrobiologie Heft 42. Chap. 8 pp. 206-234.

Hilton, J., M. O'Hare, M. J. Bowes and J.I. Jones. 2006. How green is my river? A new paradigm of eutrophication in rivers. *Science of the Total Environment.* 365:66-83.

Horner, R.R., E.B. Welch, and R.B. Venestra. 1983. Development of nuisance periphytic algae in laboratory streams in relation to enrichment and velocity. *In* R.G. *Wetzel (ed). 1983. Periphyton of Freshwater Ecosystems. Proceedings of the First International Workshop on Periphyton of Freshwater Ecosystems. Växjö, Sweden, 14-17 September 1982. Dr. W. Junk Publishers. The Hague.*

Huntington, , C.W., T. Hardin, and R. Raymond. 1999. Water temperature in the Lower Deschutes River, Oregon. Consultant report to Portland General Electric. Portland, OR.

Isaak, D.J., Wenger, S.J., Peterson, E.E., Ver Hoef, J.M., Nagel, D.E., Luce, C.H., Hostetler, S.W., Dunham, J.B., Roper, B.B., Wollrab, S.P., 2017. The NorWeST summer stream

temperature model and scenarios for the western US: A crowd-sourced database and new geospatial tools foster a user community and predict broad climate warming of rivers and streams. Water Resour. Res. 53, 9181–9205. Related Website: *https://www.fs.fed.us/rm/boise/AWAE/projects/NorWeST.html*

Jewson, D.H. 1992. Life cycle of a *Stephanodiscus* sp. (Bacillariophyta). *J. Phycol.* 28: 856-866.

Johnson, D.M., R.R. Petersen, D.R. Lycan, J.W. Sweet, M.E. Neuhaus and A.L. Schaedel. 1985. Atlas of Oregon Lakes. Oregon State University Press., Corvallis, OR. 317 pp.

Kellogg, R.L., R. Nehring, A. Grube, D.W. Goss and S. Plotkin. 2000. Environmental indicators of pesticide leaching and runoff from farm fields. Presentation at "Conference on Agricultural Productivity: Data, Methods, and Measures." March 9-10, 2000, Washington, D.C.

Khangaonkar, T., Long, W., 2014. Temperature and Water-Quality Model of Lake Billy Chinook - Upgrade to CE-QUAL-W2. (No. PNNL-ACT-10016). Pacific Northwest National Laboratory, Richland, WA.

Kociolek, J.P., E.C. Theriot, D.M. Williams, M. Julius, E.F. Stoermer, and J.C. Kingston. 2014. Centric and araphid diatoms. *In* J.D. Wehr, R.G. Sheath, and J.P Kociolek (eds). Freshwater Algae of North America. Academic Press., New York. Chap. 15, pp. 653-708.

Komárek, J. and J.R. Johansen. 2014. Filamentous cyanobacteria. *In* J.D. Wehr, R.G. Sheath, and J.P Kociolek (eds). Freshwater Algae of North America. Academic Press., New York. Chap. 4, pp. 135-235.

Krauskopf., K.B. 1979. Introduction to Geochemistry. McGraw-Hill Book Company, New York. 617 pp.

Kvam, B., D. Reiser, and C. Eakin. 2001. Lower Deschutes River macroinvertebrate and periphyton monitoring report – Fall 1999 and Spring 2000 Sampling. R2 Resource Consultants report to Portland General Electric and the Confederated Tribes of the Warm Springs Reservation of Oregon.

Kvam, B., D. Reiser, and C. Eakin. 2002. Lower Deschutes River macroinvertebrate and periphyton monitoring report – Spring 2000/2001 and Fall 1999/2001 Sampling. R2 Resource Consultants report to Portland General Electric and the Confederated Tribes of the Warm Springs Reservation of Oregon.

Lal, S. 1984. Effects of insecticide on algae. *In* R. Lal (ed). Insecticide Microbiology. Springer, Berlin. Chapter 9. Pp 203-235.

LaLonde, R.T., C.D. Morris, C.F. Wong, L.C. Gardner, D.J. Eckert, D.R. King, and R.H. Zimmerman. 1979. Response of *Aedes triseriatus* larvae to fatty acids of *Cladophora*. *J. Chem. Ecol*. 5:371-381.

Lewis, W.M., W.A. Wurtsbaugh and H.W. Paerl. 2011. Rationale for control of anthropogenic nitrogen and phosphorus to reduce eutrophication of inland waters. *Environ. Sci. & Technol.* 45:10300-10305.Livingstone, D., A. Pentecost, and B.A. Whitton. 1984. Diel

variations in nitrogen and carbon dioxide fixation by the blue-green alga *Rivularia* in an upland stream. *Phycologia*. 23: 125-133.

Lohman, K., J.R. Jones, C.B. Daniel. 1991. Experimental evidence for nitrogen limitation in a northern Ozark stream. J. *N. Amer. Benthol. Soc*. (*Freshwater Science)*. 10:14-23.

Manga, M. 1997. A model for discharge in spring-dominated streams and implications for the transmissivity and recharge of quaternary volcanics in the Oregon Cascades. *Wat. Resour. Res.* 33:1813-1822.

McDowell, R.W., S.T. Larned and D.J. Houlbrook. 2009. Nitrogen and phosphorus in New Zealand stream and rivers: control and impact of eutrophication and the influence of land management. *New Zealand Journal of Marine and Freshwater*. 43:985-995.

Mote, P.W., A.F. Hamlet, M. P. Clark and D.P. Lettenmaier. 2005. Declining mountain snowpack in western North America. *Am. Met. Soc.* January:39-49.

Mote, P.W., M. Clark and A.F. Hamlet. 2009. Variability and trends in mountain snowpack in western North America.

Mote, P.W., S. Li, D.P. Lettenmaier and R. Engel. 2018. Dramatic declines in snowpack in the western US. *Climate and Atmospheric Sciences.* 1:2; doi:10.1038/s41612-018-0012-1.

MRSO. Madras, Oregon AgriMet Weather Station. Retrieved from *https://www.usbr.gov/pn/agrimet/agrimetmap/mrsoda.html*.

Mueller, A-M., D. Degan. 2017. Hydroacoustic evaluation of the limnetic fish population in Lake Billy Chinook, Oregon. Population size and distribution. Report prepared for Confederated Tribes of the Warm Springs. Warm Springs, Oregon. Aquacoustics, Inc., Sterling, Alaska.

Mulholland, P. 1996. Role in nutrient cycling in streams. In R.J. Stevenson, M.L. Bothwell and R.L. Lowe (eds). 1996. Algal Ecology: Freshwater Benthic Ecosystems.

NLCD (National Land Cover Database). 2011. Retrieved from *https://www.mrlc.gov/data/legends/national-land-cover-database-2011-nlcd2011.*

Nordin, R.N. 1985. Water quality criteria for nutrients and algae (technical appendix). Water Quality Unit, Resource Quality Section. Water Management Branch, B.C. Ministry of Environment, Victoria.

NRCS (Natural Resources Conservation Services). No Date. HOGG PASS SNOTEL Data. Retrieved from *https://www.nrcs.usda.gov/wps/portal/nrcs/detail/or/snow/products/?cid=nrcs142p2_046298*

NREL (National Renewable Energy Laboratory). 2017. https://www.nrel.gov/gis/images/state-level-resource-maps/dni/Oregon-DNI-2017-01.jpg

O'Connor, J.E. and G.E. Grant (eds). 2003. A Peculiar River: Geology, Geomorphology, and Hydrology of the Deschutes River, Oregon. Water Science and Applications 7. American Geophysical Union. Washington, D.C. 239 pp.

Omernik, J.M. 1977. Nonpoint source stream nutrient level relationships: A nationwide study. EPA-600/3-77-105.

ODEQ. 2012. Water Quality Assessment - Oregon's 2012 Integrated Report Assessment Database and 303(d) List. Retrieved from https://www.deq.state.or.us/wq/assessment/rpt2012/search.asp.

ODEQ. 2015. *Basin Summary Reports; Supplement to the Statewide Water Quality Assessments Report*. DEQ15-LAB-0065-TR. Ver. 1.1. 124 pp.

ODEQ AWQMP. No Date. Water Quality Monitoring Data. Retrieved from *https://www.oregon.gov/deq/wq/Pages/WQdata.aspx.*

OWRD (Oregon Water Resources Department). No. Date. Dam Inventory Query. Retrieved from *https://apps.wrd.state.or.us/apps/misc/dam_inventory/*

Otten, T.G., J.R. Crosswell, S. Mackey and T.W. Dreher. 2015. Application of molecular tools for microbial source tracking and public health risk assessment of a *Microcystis* bloom traversing 300 km of the Klamath River. *Harmful Algae*. 46: 71-81.

Paerl, H.W. 1990. Physiological ecology and regulation of N_2 fixation in natural waters. *In* K.C. Marshall (ed). Advances in Microbial Ecology. Vol 11. Plenum Press, New York. Chap. 8, Pp 305-344.

Paerl, H.W. and J. Huisman. 2008. Blooms like it hot. *Science.* 320:57-58.

Paerl, H.W., H. Xu, M.J. McCarthy, G. Zhu, B. Qin, Y. Li, and W. Gardner. 2011. Controlling harmful cyanobacterial blooms in a hyper-eutrophic lake (Lake Taihu, China): The need for a dual nutrient (N& P) management strategy. *Water Research.* 45:1973-1983.

Paerl, H.W. and V.J. Paul. 2012. Climate change: Links to global expansion of harmful cyanobacteria. *Water Research.* 46:1349-1363.

Paul, M.J., B. Walsh, J. Oliver and D. Thomas. 2017. Algal indicators in streams: A review of their application in water quality management of nutrient pollution. Report to EPA. Research Triangle Park. #822B17002. 44pp.

Pelletier, G.J., Chapra, S.C., Tao, H., 2006. QUAL2Kw–A framework for modeling water quality in streams and rivers using a genetic algorithm for calibration. Environmental Modelling & Software 21, 419–425.

Poff, L. and J.C. Schmidt. 2016. How dams can go with the flow. *Science.* 353:1099-1100.

Pohl, K.A., K.S. Hadley and K.B. Arabas. 2002. A 545-year drought reconstruction for central Oregon. *Physical Geography*. 23: *https://doi.org/10.2747/0272-3646.23.4.302*.

Porter, S.D., D.K. Mueller, N.E. Spahr, M. D. Munn and N.H. Dubrovsky. 2008. Efficacy of algal metrics for assessing nutrient and organic enrichment in flowing waters. *Freshwater Biology*. 53:1036-1054.

Pyper, B. 2016. Effect of Flow on Downstream Passage of PIT-tagged Juvenile Chinook and Steelhead at Round Butte Dam, Madras, Oregon. Portland General Electric. Portland, OR.

Raven, J.A. and R.J. Geider. 1988. Temperature and algal growth. *New Phycol.* 110:441-461.

Raymond, R.B., J.M. Eilers, K.B. Vache, and J.W. Sweet. 1997. *Limnology of Lake Billy Chinook and Lake Simtustus, Oregon*. 1997 Final Report to Portland General Electric. E&S Environmental Chemistry, Inc. Corvallis, OR.

Raymond, R.B., J.M. Eilers, J.A. Bernert, and K.B. Vache. 1998. *Lower Deschutes River Studies: Water Quality and Biota*. 1997 Final Report to Portland General Electric. E&S Environmental Chemistry, Inc. Corvallis, OR.

Redfield, A.C. 1958. The biological control of chemical factors in the environment. *Amer. Sci.* 46:205-222.

Reynolds, C.S. 1984. The Ecology of Freshwater Phytoplankton. Cambridge University Press. 384 pp.

Reynolds, C. 2006. Ecology of Phytoplankton. Cambridge University Press. New York. 535 pp.

Richey, J.E., R.L. Victoria, E. Salati and B.R. Forsberg. 1991. The biogeochemistry of a major river system: the Amazon case study. Chap 3 *In* E.T. Degens, S. Kempe and J.E. Richey (eds). Biogeochemistry of Major World Rivers. Scientific Committee on Problems of the Environment (SCOPE 42). John Wiley & Sons. New York. Pp 57-74.

Robarts, R.D. and T. Zohary. 1987. Temperature effects on photosynthetic capacity, respiration, and growth rates of bloom-forming cyanobacteria. *New Zealand Journal of Marine and Freshwater Research.* 21:391-399.

Rounds, S.A., 2001. Modeling water quality in the Tualatin River, in: Geological Survey Water-Resources Investigations Report 01–4041.

Sabater, S., J. Artigas, N. Corcoll, L. Prola, X. Timoner, and E. Tornés. 2016. Ecophysiology of river algae. *In* O. Necchi Jr. River Algae. Springer, New York. Chapter 9. Pp 197-217.

Schanz, E. and H. Juon. 1983. Two different methods of evaluating nutrient limitation of periphyton bioassays using water from the Rhine River and eight of its tributaries. *Hydrobiologia*. 102:187-195.

Schindler, D.W., R.E. Hecky, D.L. Findlay, M.P. Stainton, R.B Parker, M.J. Paterson, K.G. Beaty, M. Lyng and S.E.M. Kasian. 2008. Eutrophication of lakes cannot be controlled by reducing nitrogen input: Results of a 37-year whole-ecosystem experiment. *Proc. Nat. Acad. Sci.* 105:11254-11258.

Schindler, D.W., S.R. Carpenter, S.C. Chapra, R.E. Hecky and D.M. Orihel. 2016. Reducing phosphorus to curb lake eutrophication is a success. *Environ. Sci & Technol.* 50:8923-8929.

Scott, J.T. and A.M. Marcarelli. 2012. Cyanobacteria in Freshwater Benthic Environments. *In* B.A. Whitton (ed). Ecology of Cyanobacteria II: Their Diversity in Space and Time. Springer. New York. Chap 9. Pp 271-289.

Scott, J.T. and M.J. McCarthy. 2010. Nitrogen fixation may not balance the nitrogen pool in lakes over timescales relevant to eutrophication management. *Limnol & Oceanogr.* 55:1265-1270.

Shatwell, T. and J. Köhler. 2019. Decreased nitrogen loading controls summer cyanobacterial blooms without promoting nitrogen-fixing taxa: Long-term response of a shallow lake. *Limnol. Oceangr.* 64:S166-S178.Sigee, D.C. 2005. Freshwater Microbiology. John Wiley & Sons, Ltd. New York. 524 pp.

Singh, S.P. and P. Singh. 2015. Effect of temperature and light on the growth of algae species: A review. *Renewable and Sustainable Energy Reviews.* 50:431-444.

Smolar-Žvanut, N. and M. Mikoš. 2014. The impact of flow regulation by hydropower dams on the periphyton community in the Soca River, Slovenia. *Hydrological Sciences Journal.* 59:1032-1045.

Snyder, L., J.D. Potter and W.H. McDowell. 2018. An evaluation of nitrate, FDOM, and turbidity sensors in New Hampshire streams. *Water Resources Research*. https:/doi.org/10.1002/2017WR020678.

Sokal, R.R. and F.J. Rohlf. 1981. Biometry. W.H. Freeman and Company. San Francisco. 859 pp.

Stancheva, R., R.G. Sheath, B.A Read, K.D. McArthur, C. Schroepfer, J.P. Kociolek, and A.E. Fetscher. 2013. Nitrogen-fixing cyanobacteria (free-living and diatom endosymbionts): their use in southern California stream bioassessment. *Hydrobiologia*. 720:111-127.

Stancheva, R. and R.G. Sheath. 2016. Benthic soft-bodied algae as bioindicators of stream water quality. Knowledge and Management of Aquatic Ecosystems. 417:15.

Steinman, A.D. 1996. Effects of grazers on freshwater benthic algae. *In* R.J. Stevenson, M.L. Bothwell, and R.L. Lowe (eds). Algal Ecology: Freshwater Benthic Ecosystems. Academic Press, NY. Pp. 341-374.

Stevenson, R.J. 1996a. The stimulation and drag of current. Chap. 11 *In* Stevenson, R.J., M.L. Bothwell and R.L. Lowe (eds). Algal Ecology: Freshwater Benthic Ecosystems. Academic Press. New York. Pp. 321-340.

Stevenson, R.J., M.L. Bothwell and R.L. Lowe (eds). 1996b. Algal Ecology: Freshwater Benthic Ecosystems. Academic Press. New York. 753 pp.

Stoermer, E.F., G. Emmert, and C.L. Schelske. 1989. Morphological variation of *Stephanodiscus niagarae* Ehrenb. (Bacilliophyta) in a Lake Ontario sediment core. *J. Paleolimnology*. 2:227-236.

Stoermer, E.F. and J.J. Elser. 2002. Ecological Stoichiometry: the Biology of Elements from Molecules to the Biosphere. Princeton University Press. Princeton. 439 pp.

Sullivan, T.J., C.T. Driscoll, J.M. Eilers, and D.H. Landers. 1988. Evaluation of the role of sea salt inputs in the long-term acidification of coastal New England lakes. *Environ. Sci. Technol.* 22:185-190.

Suplee, M.W., V. Watson, M. Teply and H. McKee. 2009. How green is too green? Public opinion of what constitutes undesirable algae levels in streams. *J. Amer. Water Works Assoc.* 45:123-140.

Sutton, M., S. Reis and S. Baker (eds). 2008. Atmospheric Ammonia: Detecting Emission changes and environmental Impacts. Results of an Expert Workshop under the Convention on Long-Range Transboundary Air Pollution. Springer. Berlin.

Theriot, E. 1987. Principal component analysis and taxonomic interpretation of environmentally related variation in silicification in *Stephanodiscus* (Bacillariophyta). *British Phycological Journal.* 22:359-373.

Thiesfeld, S.L., J.C. Kern, A.R. Dale, M.W. Chilcote and M.A. Buckman. 1999. Lake Billy Chinook sockeye salmon and kokanee research study 1996-1998. Contract completion report by Oregon Department of Fish and Wildlife. Pelton Round Butte Hydroelectric Project. FERC No. 2030. 154 pp.

Tristate Implementation Council. 1996. Clark Fork River voluntary nutrient reduction program. Nutrient Target Subcommittee draft report. Montana Department of Environmental Quality, Helena, MT.

USGS. No Date. USGS Current Water Data for the Nation. Retrieved from *https://waterdata.usgs.gov/nwis/rt*,

USGS. 2015. Davis Lake Volcanic Field Retrieved from *https://volcanoes.usgs.gov/volcanoes/davis_lake/*.

Uehlinger, U., Bührer, H., Reichert, P., 1996. Periphyton dynamics in a floodprone prealpine river: evaluation of significant processes by modelling. Freshwater Biology 36, 249–263.

van Vuuren, D.P., E. Kriegler, B.C. O'Neill, K.L. Ebi, K. Riahi, T.R. Carter, J. Edmonds, S. Hallegatte, T. Kram, R. Mathur, and H. Winkler. 2014. A new scenario framework for Climate Change Research: scenario matrix architecture. Clim. Change. 122:373–386. *https://doi.org/10.1007/s10584-013-0906-1*.

Vano, J.A., J.B. Kim, D.E. Rupp, and P.W. Mote. 2015. Selecting climate change scenarios using impact-relevant sensitivities. Geophys. Res. Lett. 42:5516–5525.

Wehr, J.D., R.G. Sheath, and J.P. Kociolek. 2015. Freshwater Algae of North America. Academic Press, Amsterdam. 1050 pp.

Welch, E.B., J.M. Jacoby, R.R. Horner, and M.R. Seeley. 1988. Nuisance biomass levels of periphytic algae in streams. Hydrobiologia. 157:161-168.

Welch, E.B., R.R. Horner, and C.R. Patmont. 1989. Prediction of nuisance periphyton biomass: a management approach. Water Research. 23:401-405.

Wetzel, R.G. 2001. *Limnology: Lake and River Ecosystems*. Academic Press, New York.

Whitton, B.A., T.M. Khoja and I.A. Arif. 1986. Water chemistry and algal vegetation of streams in the Asir Mountains, Saudi Arabia. *Hydrobiologia*. 133:97-106.

Whitton, B.A., and P. Mateo. 2012. Rivulariaceae. *In* B.A. Whitton (ed). Ecology of Cyanobacteria II: Their Diversity in Space and Time. Springer. New York. Chap 22. Pp 561-591.

Whyte, J.N.C. 1987. Biochemical composition and energy content of six species of phytoplankton used in mariculture of bivalves. *Aquaculture.* 60:231-241.

Williamson, C.R. 2001. Copepoda. *In* J.H. Thorp and A.P. Covich (eds). *Ecology and Classification of North American Freshwater Invertebrates.* Academic Press, New York. Pp. 915-954.

Williamson, N., T. Kobayshi, D. Outhet, and L.C. Bowling. 2018. Survival of cyanobacteria in rivers following their release in water from large headwater reservoirs. *Harmful Algae.* 75:1-15.

Xu, W., Khangaonkar, T., 2015. Temperature model of the Pelton Round Butte hydroelectric project reservoirs (No. PNNL-25094). Pacific Northwest National Laboratory.

Xu, H., H. Paerl, B. Qin, G. Zhu, and G. Gao. 2010. Nitrogen and phosphorus inputs control phytoplankton growth in eutrophic Lake Taihu, China. *Limnology & Oceanography*. 55:420-432.

Yonkofski, C., W. Xu, and T. Khangaonkar. 2016. Hydrogeologic review of the Pelton Round Butte Hydroelectric Project waterbodies and potential thermal impacts of groundwater discharge. Pacific Northwest National Laboratory. PNNL-25541.

Yu, Q., Y, Chen, Z. Liu, N. van de Giesen and D. Zhu. 2015. The influence of a eutrophic lake to the river downstream: spatiotemporal algal composition changes and the driving factors. *Water*. 2015:2184-2201.

Zbieranowski, A.L. and J. Aherne. 2013. Ambient concentrations of atmospheric ammonia, nitrogen dioxide and nitric acid in an intensive agricultural region. *Atmospheric Environment.* 70:289-299.